UNIVERSITY OF SOUTHAMPTON

FACULTY OF ENGINEERING, SCIENCE & MATHEMATICS

School of Civil Engineering and the Environment

Protection and Management of Marine Areas in the Mediterranean Sea: Applications of Satellite Remote Sensing

by

Marta Manca Zeichen

Thesis for the degree of Doctor of Philosophy

MAY 2010

Graduate School of
Civil Engineering and the Environment

This PhD dissertation by

Marta Manca Zeichen

has been produced under the supervision of the following persons:

Supervisor/s

Dr. Pete Shaw

Prof. Ian Robinson

To my inspiring muse, my mother Ginevra and to my father, the poet Valentino Zeichen, whose perception of time goes far beyond the span of my studies.

Circular-linear time

Despite the circularity
of astronomical cycles
and the fruits of the earth,
the ancestors invented
linear historical time
straightening the circular one
of seasonal agriculture,
observing the small plants
which grew higgledy-piggledy
until some chances set the seeds
ranked one after another;
shoots in barely crooked rows
as seen in our kitchen gardens.

Man planted numbers
Without knowing numeration
And learned to count them
when they were still unknown,
he fixed the whole figure
with symbols in stone.

Valentino Zeichen

Zeichen V., 2006. *Neomarziale.* ñLo Specchioò Ed. Arnoldo Mondadori, Milano, pp. 148.

UNIVERSITY OF SOUTHAMPTON

ABSTRACT

FACULTY OF ENGINEERING, SCIENCE & MATHEMATICS
SCHOOL OF CIVIL ENGINEERING AND THE ENVIRONMENT

Doctor of Philosophy

PROTECTION AND MANAGEMENT OF MARINE AREAS IN THE MEDITERRANEAN SEA: APPLICATIONS OF SATELLITE REMOTE SENSING

by
Marta Manca Zeichen

Marine Protected Areas (MPAs) are recognised globally as effective tools for protecting valuable and vulnerable marine ecosystems (habitats, species and communities), maintaining the biological diversity, and safeguarding the associated historical and cultural resources. MPAs accommodate local communities and regulate the different uses of the sea, fostering more sustainable use of marine resources. Moreover, MPAs are increasingly being used as environmental laboratories, enabling a greater scientific understanding of marine systems. In the Mediterranean Sea about a hundred of MPAs have been designated during the last decades, all but one of which are in coastal areas.

This study develops a new way of using RS techniques tailored for the monitoring and management of Mediterranean MPAs. The advance in satellite Remote Sensing (RS) technologies has made possible to look at the MPAs not only by means of discrete *in situ* surveys but rather on the basis of a ñsynopticò and repeated view. The primary aim of this thesis was to establish how the satellite sensors can be successfully used and whether RS provides reliable tools for monitoring and managing Mediterranean MPAs. The study aimed specifically at describing and identifying, by means of passive remote sensors, the spatial and temporal scale of the bio-physical processes occurring in Mediterranean MPAs. Observations retrieved by ocean colour and thermal infra-red sensors, for a range of MPA study sites, were used to depict system functioning by the analysis of the prevailing spatial and temporal variations of the geophysical parameters and biophysical conditions. The seasonal variations of the ecological indicators (i.e. phytoplankton blooms and thermal trends) were analysed over various MPAs located in different regions of the Mediterranean basin, and different bio-optical algorithms were tested in a coastal MPA. The short-term and long-term monitoring (interannual) of the ecological indicators is key to elucidating trends and modifications in the biogeochemical balance of the basin possibly caused by environmental changes which could potentially affect the MPAôs resilience. Consequently it is now possible to monitor MPAs easily and at low cost, by integrating RS with the traditional sampling methodologies to work towards safeguarding of valuable marine habitats and species. RS should be considered as key tool that fosters the ecosystem-based management.

LIST OF TABLES

LIST OF FIGURES

DECLARATION OF AUTORSHIP

I, MARTA MANCA ZEICHEN

Declare that the thesis entitled

Protection and Management of Marine Areas in the Mediterranean Sea: Applications of satellite Remote Sensing

and the work presented in the thesis are both my own, and have been generated by me as the result of my own original research. I confirm that:

- This work was done wholly or mainly while in candidature for a research degree at this University;
- Where any part of this thesis has previously been submitted for a degree or any other qualification at this University or any other institution, this has been clearly stated;
- Where I have consulted the published work of others, this is always clearly attributed;
- Where I have quoted from the work of others, the source is always given. With the exception of such quotations, this thesis is entirely my own work;
- I have acknowledged all main sources of help;
- Where the thesis is based on work done by myself jointly with others, I have made clear exactly what was done by others and what I have contributed myself;
- Parts of this work have been published as:

M. Manca Zeichen, M.G. Finoia, M. Locritani, N. Ruggeri, L. Tunesi, G.P. Gasparini, M. Bassetti, V. Grandi, R. Cattaneo-Vietti and P. Povero, 2008. A preliminary analysis of *in situ* and remotely sensed environmental variables in the coastal region of the Portofino Marine Protected Area. *Chemistry and Ecology*, 24, S1: 57–66.

Signed:
Date: 21.05.2010

ACKNOWLEDGEMENTS

Firstly I would like to thank my supervisors Dr. Pete Shaw for his patience, encouragement and support and Prof. Ian Robinson for his excellent advices. I feel immense gratitude to both my supervisors who in different ways helped me to understand the Philosophy underneath the PhD thesis and helped me immensely in reviewing the manuscript.
I am very grateful to Dr. Silvestro Greco for having supported financially the first years of this PhD.
I feel immense gratitude to Dr. Maria Grazia Finoia who helped me with statistical analyses and to interpret critically the results obtained.
I would like to thank Dr. Dave Poulter and Dr. Vittorio Barale for having provided the archive of the NASA ocean colour images.
I also wish to thank the European Space Agency (ESA) and the German Aerospace Centre (DLR) for having supplied the ocean colour and thermal images respectively.
Other people deserve a big "thank you" for their fundamental help during my work: Dr. F. Pascucci and S. Donfrancesco.
I also wish to thank Dr. G. P. Gasparini, Prof. P. Povero and Dr. L. Tunesi for having provided the *in situ* data.
A big “thank you“ also goes to A. Annunziatellis for his providential help at the final stage of the thesis.
I wish to thank my family for the encouragement that has been vital to the completion of this thesis.
Finally I would like to thank my beloved Arnaldo who encouraged me and sustained me continuously throughout the development of the thesis.

LIST OF ACRONYMS

a	Absorbance
ACCOBAMS	Agreement on the Conservation of Cetaceans of the Black Sea, Mediterranean Sea and contiguous Atlantic area
AVHRR	Advanced Very High Resolution Radiometer
b_b	Backscatter coefficients
BW	Bottom Water
c	Beam attenuation coefficient
CASI	Compact Airborne Spectrographic Imager
CBD	Convention on Biological Diversity
CDOM	Coloured Dissolved Organic Matter
Chl	Chlorophyll-like Pigment concentration
CNPPA	Commission on Natural Parks and Protected Areas
CNR	National Research Council
CZCS	Coastal Zone Color Scanner
DIP.TE.RIS	Department for the Study of the Territory and its Resources
DLR	Deutsche Zentrum fur Lüft und Raumfahrt
DN	Digital number
EC	European Commission
E-Distances	Energy-distances
EEC	European Economic Community
EEZ	Exclusive Economic Zones
EO	Earth Observation
EOWEB	Earth Observation Data Service
ESA	European Space Agency
E-statistic	Energy statistic
ETM	Landsat Enhanced Thematic Mapper
EU	European Union
EuroGOOS	European Global Ocean Observing System
GMES	Global Monitoring for Environment and Security
HDF	Hierarchical Data Format
HRPT	High Resolution Picture Transmission
ICZM	Integrated Coastal Zone Management
IOPs	Inherent Optical Properties
IUCN	International Union for Conservation of Nature
L1A	Level 1A
L2	Level 2
L4	Level 4
Lw (λ)	Water Leaving Radiances
LwN(λ)	Normalised Water Leaving Radiance
LAC	Local Area Coverage
LIW	Levantine Intermediate Water
LTER	Long Term Ecological Research Network Site
MAW	Modified Atlantic Water
MCSST	Multichannel Sea Surface Temperature
MER_FR	MERIS Full Resolution
MER_RR	MERIS Reduced Resolution
MERIS	Medium Resolution Imaging Spectrometer
MERSEA	Marine Environment and Security for the European Area

MFS	Mediterranean ocean Forecasting System
MFSPP	Mediterranean Forecasting System Pilot Project
MFSTEP	Mediterranean Forecasting System Towards Environmental Predictions
MNRs	Marine Nature Reserves
MODIS	Moderate Resolution Imaging Spectroradiometer
MOON	Mediterranean Operational Oceanography Network
MPAs	Marine Protected Areas
NASA	National Aeronautics and Space Administration
NGOs	Non-governmental organizations
NOAA	National Oceanic and Atmospheric Administration
NOCS	National Oceanography Centre, Southampton
NRC	National Research Council
PC1	First Principal Component
PC2	Second Principal Component
PCA	Principal Component Analysis
RS	Remote Sensing
SAR	Synthetic Aperture Radar
SeaDAS	SeaWiFS Data Analysis System
SeaWIFS	Sea-viewing Wide Field-of-view Sensor
SD	Standard deviation
SPAMI	Specially Protected Areas of Mediterranean Interest
SST	Sea Surface Temperature
UNEP	United Nations Environment Programme
UNCLOS	United Nations Convention on the Law of the Sea
UNCED	United Nation Conference on the Environment and Development
UNFCCC	United Nations Framework Convention on Climate Change
UTM	Universal Transverse Mercator
VHRR	Very High Resolution Radiometer
W	Week
WCC	West Corsica Current
WCPA	World Commission on Protected Areas
WMDW	Western Mediterranean Deep Water
WIW	Winter Intermediate Water
WWF	World Wide Fund for Nature

CHAPTER 1

BACKGROUND AND CONTEXT TO THE STUDY

1.1 INTRODUCTION

Marine Protected Areas (MPAs) are recognised as vital tools for accomplishing a broad spectrum of objectives. MPAs are increasingly being used to protect key habitats and threatened species, manage fisheries, enable greater scientific understanding of marine systems, in addition MPAs accommodate local communities and nature-based tourism or recreational users. Moreover, MPAs serve as valuable anchors for the large-scale conservation of the biosphere, and as such they may contribute to securing the future of marine conservation (Agardy, 1994).

MPAs are an integral component of environmental conservation and restoration. It could be stated that "fully marine reserves are a powerful tool for marine conservation and management" (Palumbi, 2001). Individual MPAs have now been shown to be critically important in achieving conservation of species, biological communities, and habitats. First, research within MPAs can serve an inventorying function, giving us a view of what is there and in what condition. Inventorying and assessment can take place through developing species lists, conducting distribution/abundance surveys, measuring water quality, mapping biological communities, and measuring physical attributes such as water temperature, salinity, turbidity, and testing for the presence of pollutants. Secondly, MPA-based research can indicate trends in populations of organisms, environmental quality, and ecosystem health. Thirdly, MPA-based research can give us an indication of how well MPAs are achieving their management goals. Fourthly, individual MPAs play a very important role in scientific research, by providing invaluable sites for conducting controlled studies.

According to Davis *et al*., (1990) "Given the increasing demand for information on the status of biological diversity, many are realising the need for improved information systems". The advance in technologies, in particular those related to spatial analysis such as Remote Sensing (RS), has made possible the monitoring of MPAs not only by

long-established *in situ* surveys but rather on the basis of a "synoptic" and broad-scale view of the marine area. Consequently it is now possible to monitor easily and at low cost marine areas which require preservation of high biodiversity and/or consequently threatened ecosystems. MPA-based research and, in particular, research on applications of RS could yield information not only about individual sites but also about large marine ecosystems as a whole.

1.2 RESEARCH PERSPECTIVE

1.2.1 General Aims

The primary aim of this thesis is to develop a new way of using RS, establishing how it can be used and determining its reliability and effectiveness as a tool in monitoring and managing established Mediterranean MPAs. This aim implies the development of a new methodology tailored to the MPAs to provide answers to the following questions:

- How can we better observe MPAs in order to enhance their protection?
- Can RS tools be successful in monitoring and managing MPAs?

The thesis will be developed in three experimental chapters which aim to describe, by means of different remote sensors, (1) bio-physical processes occurring within the MPA test sites and (2) oceanographic features essential for sustaining the system. The bio-physical conditions that persist across MPAs will thus be identified.

1.2.2 Specific Aims

The three central experimental chapters aim at first describing, by means of passive remote sensors, bio-physical processes occurring in the MPA test sites and oceanographic features that sustain the system. Thus identifying what bio-physical conditions persist along the selected Mediterranean MPAs. The specific aims of each experimental section are as follows.

The aims of **chapter 3** were primarily to investigate the seasonal trend of the biophysical variables in the study sites to understand the system functioning and to characterise the MPAs considered, by:

1. Assessing the spatial and temporal scale of the phenomena to be investigated in order to sort the appropriate spatial and temporal resolution of the Earth Observation (EO) sensors.
2. Analysing the geophysical parameters retrieved by the passive remote sensors such as the concentration chlorophyll-like pigments (*chl*) and the Sea Surface Temperature (SST skin).
3. Detecting upwelling regions, phytoplankton blooms, SST skin variability and thermal trends in the MPAs investigated.
4. Depicting the system functioning by the analysis of the trends of the biophysical processes.

The aims of **chapter 4** were to observe and quantify the spatial and temporal patterns of a recurrent algal bloom in a pelagic MPA. In particular by assessing the geophysical parameter *chl* as marker of algal biomass, its seasonal and interannual pattern. Finally characterising and monitoring the status and the bio-physical trend of the pelagic MPA considered.

Chapter 5 aimed to set up a multidisciplinary system as a means to monitor and, further, manage a relatively small coastal marine protected area. This aim was addressed by the large scale analysis of the geophysical parameters detected by remote sensors such as *chl* and SST skin identifying the transient dynamical phenomena that are rarely detectable only by means of *in situ* sampling. To this end, the use of optical and thermal remote sensed observations was coupled with *in situ* measurements in order to investigate bio-physical processes which occurred in the coastal zone.

1.3 THESIS OUTLINE

The present thesis comprises six chapters.

Chapter 1 discusses and reviews the history, criteria as well as technical approaches to the protection of marine areas and in particular marine biodiversity, MPAs and Sanctuaries. Further sections of this chapter on the Mediterranean marine system focus on its biodiversity and anthropogenic impact, and the protection of Mediterranean MPAs and Mediterranean Sanctuaries. This chapter also describes the potential applications of remote sensing in observing marine systems and in particular its usefulness in monitoring MPAs.

Chapter 2 illustrates in details the rationale for selecting the particular Mediterranean MPAs considered in this study, highlighting their characteristics in terms of physical and biological features. Moreover, this chapter focuses on the methodological approach chosen to the monitoring of Mediterranean MPAs. This section describes the rationale for selecting specific remote sensors as primary tools for monitoring Mediterranean MPAs. A description of the optical and thermal remote sensors used, focusing on the issue of the spatial resolution, is provided. Limitations related to the use of particular ocean colour algorithms are considered.

Chapter 3 illustrates the role and the purpose of remote sensing in the context of MPAs highlighting in particular how the geophysical variables retrieved by EO satellites supply a clear description of the biophysical processes occurring in the proximity of MPAs. Ocean colour and SST skin maps were analysed for a year for each of the MPAs under investigation. The results of this spatial analysis allowed formulation of a comparison among the MPAs selected and provided a basis on which to understand and explain in what extent they differ.

Chapter 4 focuses on the temporal analysis of the system considering as case study an open sea Mediterranean MPA. A long time series of ocean colour observations was analysed in order to monitor the concentration of *chl* and to document its spatial and temporal as well as seasonal and interannual variability within the open sea MPA. The

chl surface patterns were used to trace and monitor the seasonal phytoplankton bloom events recurring every year in the study site. Historical series were also used to investigate the trend of *chl* within the open sea MPA.

Chapter 5 focuses on the use of a new ocean colour sensor in investigating coastal MPA waters. *Chl* maps were processed using two types of different algorithms specific to coastal and pelagic areas. This chapter investigates the problem of algorithms selection by correlating ocean colour data with data collected by profilers within MPA waters. The analysis allowed validation of the algorithms used for this particular MPA.

Chapter 6 illustrates the conclusions of the thesis providing a description of the achieved objectives and of the level of remote sensing applications. In particular this section focuses on the value of remote sensing in serving the process of monitoring MPAs. The implications for the Mediterranean MPAs are also discussed through the evaluation of the experimental work conducted.

1.4 PROTECTION OF MARINE AREAS

Early attempts to tackle seriously the problem of degrading marine ecosystems by the global community started in 1950s. The first Regional Seas Programme was later established by the Governing Council of the United Nations Environment Program (UNEP) in 1972. In particular, its primary aim was to protect the marine environment from pollution and overexploitation (Kelleher and Bleakely, 1994).

In 1975 the International Union for Conservation of Nature **(**IUCN) called for a conference on Marine Protected Areas in Tokyo. In particular, this conference reported the degrading state of the global marine environment and called for the establishment of a system of Marine Protected Areas (MPAs) which should have encompassed examples of global marine ecosystems. This conference was followed by the III World Congress on National Parks organised in 1982 in Bali, Indonesia, by the IUCN Commission on Natural Parks and Protected Areas (CNPPA) (Gubbay, 1995; Ticco, 1995; NRC, 2001). The Bali Action Plan pointed out the strategic importance of incorporating the MPAs

into a global network of protected areas. This congress produced the key publication *Marine and Coastal Protected Areas: A guide for Planners and Managers* (Salm and Clark, 1984) which highlighted the main reasons for MPA selection and designation, stressing ecological, bio geographical and scientific importance.

The primary goal of marine conservation and management is (Kelleher and Bleakely, 1994):

> *"To provide for the protection, restoration, wise use, understanding and enjoyment of the marine heritage of the world in perpetuity through the creation of a global, representative system of marine protected areas and through the management, in accordance with the principles of the World Conservation Strategy, of human activities that use or affect the marine environment."*

In 1978 the IUCN Commission on National Parks and Protected Areas developed a system of six categories of protected areas (marine and terrestrial) defined according to their objectives in order to set the base for a common language at international level (IUCN; 1994; Kelleher, 1999; Bishop *et al*., 2004). These categories are illustrated in Table 1.1.

Table 1.1 IUCN Protected Area Management Categories (IUCN, 1994)

Category No	Definition of IUCN Protected Area Management Categories
Category Ia	***Strict Nature Reserve***: protected area managed mainly for science. **Definition**: Area of land and/or sea possessing some outstanding or representative ecosystems, geological or physiological features and/or species, available primarily for scientific research and/or environmental monitoring.
Category Ib	***Wilderness Area*:** protected area managed mainly for wilderness protection. **Definition:** Large area of unmodified of slightly modified land, and/or sea, retaining its natural character and influence, without permanent or significant habitation, which is protected and managed so as to preserve its natural condition.
Category II-	***National Park***: protected area managed mainly for ecosystem protection and recreation. **Definition:** Natural area of land and/or sea, designated to (a) protect the ecological integrity of one or more ecosystems for present or future generations, (b) exclude exploitation or occupation inimical to the purposes of designation of the area and (c) provide a foundation for spiritual, scientific, educational, recreational and visitor opportunities, all of which must be environmentally and culturally compatible.
Category III	***Natural Monument*** : protected area managed mainly for conservation of specific natural features. **Definition:** Area containing one, or more**,** specific natural or natural/cultural features which is of outstanding or unique value because of its inherent rarity, representative or aesthetic qualities or cultural significance.
Category IV	***Habitat/Species Management Area***: protected area managed mainly for conservation through management intervention. **Definition:** Area of land and/or sea subject to active intervention for management purposes so as to ensure the maintenance of habitats and/or to meet the requirements of specific species.
Category V	***Protected Landscape/Seascape***: protected area managed mainly for landscape/seascape conservation and recreation. **Definition:** Area of land, with coast and sea as appropriate, where the interaction of people and nature over time has produced an area of distinct character, with significant aesthetic, ecological and/or cultural values, and often with high biological diversity. Safeguarding the integrity of this traditional interaction is vital to the protection, maintenance and evolution of such an area.
Category VI	***Managed Resource Protected Area*:** protected area managed mainly for the sustainable use of natural ecosystems. **Definition:** Area containing predominantly unmodified natural systems, managed to ensure long term protection and maintenance of biological biodiversity, while providing at the same time a sustainable flow of natural products and service to meet community needs.

In 1988 the 17th General Assembly of IUCN adopted resolutions on the primary objectives of MPAs and also supplied the first definition of the term "Marine Protected Area". IUCN defines a Protected Area as (Jones, 1994):

> *"An area of land and/or sea especially dedicated to the protection of biological diversity, and of natural and associated cultural resources, and managed through legal or other effective means."*

In this 1988 IUCN General Assembly the concept of establishing a system of MPAs was taken on and encouraged (Kelleher and Kenchington, 1992).

In 1992 the fourth IUCN World Congress on National Parks and Protected Areas was held in Caracas, Venezuela (Gubbay, 1995; NRC, 2001; Ray, 1999). One objective of the congress was to declare the protection of 20% of the global coastal zones by the year 2000. This objective should have been achieved by the establishment of Marine Protected Areas (Jones, 1994).

In 1992 the Convention on Biological Diversity (CBD) and also the United Nations Convention on the Law of the Sea (UNCLOS) compelled countries to safeguard the marine environment (Kelleher, 1999). The CBD was adopted by the United Nation Conference on the Environment and Development (UNCED). The CBD and in particular article 8 (*in situ* conservation) *a*, *b*, and *e* stressed the need for establishment of a system of MPAs as a tool to protect biodiversity (UNEP, 1992). Furthermore this conference adopted the so called "Agenda 21" whose 17th chapter called for the identification of world's most productive and high level biodiversity ecosystems by means of designation of MPAs (Gubbay, 1995; Kelleher *et al*., 1995).

In 1994 the IUCN Resolution 19.46 (World Conservation Union, IUCN, 1994; Jones 1994) states that a Marine Protected Area is defined as:

> "*Any area of intertidal or subtidal terrain, together with its overlying water and associated flora, fauna, historical and cultural features, which has been reserved by law or other effective means to protect part or all of the enclosed environment".*

Kelleher *et al*. (1995, Vol. I) added to the criteria identified by Salm and Clark (1984) three additional factors:

1. Naturalness;
2. Economic importance;
3. Practicability and feasibility.

All of these criteria establish the conservation value for a site and have been transformed by Jones (1994) and Agardy (1997) into the aims for management of MPAs.

In 1995 under the umbrella of the CBD, the Jakarta Mandate emphasized that the MPAs should: maintain the ecosystem functioning; encompass multiple use objectives; and consider the three levels of biodiversity (ecosystem, species and population or genetic) (Fontaubert *et al*., 1996).

1.4.1 Marine biodiversity in context

The biodiversity of planet Earth is the result of about 3500 million years of evolution. (Krattiger *et al*., 1994). The term "biodiversity" is quite recent and it has been widely utilised since 1992 when the Convention of Biological Diversity (CBD) at the Earth Summit conference which was held in Rio de Janeiro, Brazil. The term biodiversity is defined as (UNEP, 1992):

> "*The variability among living organisms from all sources including, terrestrial, marine, and other aquatic ecosystems and the ecological complexes of which they are part; this includes diversity within species (intra specific), between species (inter specific) and ecosystems.*"

"Species diversity" means essentially the number and variation of species that exists on the planet (Spellerberg, 1996). At present the precise number of species populating the Earth is still indefinite, but estimates range from 5 million to 100 million species

(Krattiger *et al*., 1994). UNEP (1995) asserted that only 13% of the existing species have been classified.

More specifically, "ecosystems diversity" refers essentially to three major groups: terrestrial, freshwater and marine (Salm and Clarck, 1984). In coastal areas there is a broad range of habitats with high biodiversity which provide food, shelter as well as nurseries to marine organisms.

Ecosystem diversity has largely been replaced by the habitats diversity. This is an easier concept to deal with, due to its well defined spatial boundaries (Gray, 1997). The generally accepted habitat definition has been given by CBD (UNEP, 1992) as: "*the place or type of site where an organism or population naturally occurs*". Conserving habitats allows preservation of genetic and biological diversity (Gray, 1997).

Although the marine environment embraces about 72% of the Earth's surface area and sustains over 90% of the global living biomass (GESAMP, 1997), the marine environment has lower biodiversity than the terrestrial realm. However the first seems to have a higher genetic diversity, particularly at phyletic taxonomic level, due to the marine origins of life in the sea (May, 1988). In fact some thirteen phyla are endemic of the sea (Grassle, 1991).

Conservation of marine ecosystems and their biodiversity is undoubtedly a major issue and the major threats to marine ecosystems and species are undoubtedly caused by anthropogenic activities. Ticco (1995) notes that there is not an established tradition aiming at protecting and managing marine areas. However this is not entirely true because there is a long history of resource conservation (Tomasevich, 1942), only the idea of marine reserves is relatively new. Management of ecosystems and marine species should be carried out in a sustainable way, thus preserving the delicate dynamics that links species with ecosystems (GESAMP, 1997).

1.4.2 Marine Protected Areas

The World Wide Fund for Nature (WWF/IUCN, 1998) reported that the IUCN identified more than 140 names used for Marine Protected Areas. Some of the common names are Marine Protected Areas, Marine Nature Reserves (MNRs), Biosphere Reserves, Marine Parks, World Heritage Sites, Natural Monuments, Fishery Reserves and Marine Sanctuaries (Salm and Clark, 1984; Allison *et al*., 1998). Those terms have been used to characterise different protection degrees and management objectives. However the generally preferred and used term is MPAs (Salm and Clark 1984). MPAs are fundamentally different from terrestrial protected areas (Agardy, 1999). An important factor underlying these differences is the fuzzy nature of boundaries in the fluid environment of the sea making it difficult to define boundary conditions to marine ecological processes and threats to those processes (Steele, 1998). Some authors point out that the boundaries of MPAs should be adaptable to the changes in spatial distribution of water masses composition and organisms. (e.g. Salm and Clark, 1984; Agardy 1994, 1997).

There are several approaches to conserve marine biodiversity and to ensure a sustainable use of coastal resources. The main approach used is Integrated Coastal Zone Management (ICZM) (Clark, 1992). The ICZM approach is a process which encompasses many tools and techniques, one of which is the establishment of MPAs in order to protect sensitive areas. MPAs are considered a necessary and integral part of wider ecosystem based on Coastal Zone Management policy.

MPAs can help achieve the three main objectives of marine resource conservation as defined in the World Conservation Strategy (IUCN, 1980):

- To maintain essential ecological processes and life support systems;
- To preserve genetic diversity;
- To ensure the sustainable utilization of species and ecosystems.

Regarding the list of objectives of an MPA, a vast literature has been produced in the last decades. Simplifying the aims of an MPA (Keller and Kenchington, 1992; Laffoley, 1995) could be referred essentially to:

- To guarantee protection to unique communities, habitat, ecosystems and ecological critical processes or representative;
- To protect rare and endemic species;
- To protect nursery areas;
- To preserve some marine areas within MPAs, in their natural state, not disturbed by human activities unless scientific or educational motivations;
- To maintain separate conflicting human activities;
- To safeguard historical sites;
- To protect natural and cultural MPAs characteristics, allowing only human activities which are compatible with those aims;
- To limit the areas for particular human uses considered compatible minimising the potential negative effects.

MPAs could encompass one or more of these aims. In general, one could say that small size MPAs tend to privilege a unique objective whereas large MPAs are often "multitasking" in terms of their objectives. The main objectives and the corresponding categories for the establishment of MPAs were reviewed by Jones (1994) and categorised in Table 1.2.

Table 1.2: List of objectives for the establishment of MPAs during the review by Jones (1994).

Categories	**Objectives**					
Scientific	Maintain genetic/ species diversity	Promote research	Education/ training areas	Conserve habitat and biota	Baseline monitoring areas	Protect rare/ important species
Economic	Promote/control tourism/recreation	Promote sustainable development	Recolonised exploited areas	Coastal protection	Alternative environmental economic arguments	
Cultural	Aesthetic value	Protect historical/ cultural sites.	Political reasons			
Ethical	Intrinsic absolute value					

Jones (1994) further combined some objectives which had similar terms. The definitive list of objectives is summarised in Table 1.3.

Table 1.3 List of objectives for the establishment of MPAs after the review by Jones (1994).

Categories	Objectives					
Scientific	Maintain genetic/ species diversity	Promote research	Education/ training areas	Conserve habitat and biota	Baseline monitoring areas	Protect rare/ important species
Economic	Promote sustainable development	Recolonised exploited areas	----------	----------	----------	
Cultural	Aesthetic value	Protect historical/ cultural sites.	----------			
Ethical	----------					

Regarding the scientific objective, Polunin (1983) states that protected areas would seem to be the most efficient tool for preserving genetic resources.

As shown (Tables 1.2 & 1.3), the concept of MPAs is generic in that they can be designated to protect wider interests.

The process of *designing* MPAs passes through four steps according to the National Research Council (2001). The first step is the evaluation of conservation needs at local and regional level; the second is the clear definition of the aims and objectives for the MPAs; the third is the physical and biological characterisation of the waters surrounding the marine area; the fourth is the site identification which should have the potential to be implemented.

1. *Conservation Needs*. The type of resources and the environmental characterisation of the habitat determine the local and regional conservation needs.
2. *Objectives and goals*. As stated above, these have to be fixed at the beginning of the designation process (Reeves, 2000).
3. *Biological and Oceanic Features*. In order to assess the appropriateness of potential sites, the collection and integration of information on threatened species and the oceanographic conditions of the area are needed. The latter should incorporate hydrographic features such as currents and fronts, recognition of upwelling zones, water quality and habitat maps.
4. *Site Identification*. The biological and oceanic information should be collated to achieve the objectives and define the size and location of the MPA.

As illustrated above, the MPA designing process should be based on a scientific methodology in the recognition and characterisation of marine habitat types and biological and physical processes (Stevens, 2002).

The IUCN has introduced in its guidelines for MPAs the term *representativeness* as a key criterion (IUCN, 1994). Given the fact that most MPAs are multi-tasking with respect to their objectives, the term "representativeness" is used to specify that MPAs should include core areas with a high biodiversity and productivity degree. The MPA should be representative of different marine habitat types. Representativeness encompasses also the concept of the preservation of the ecosystem functioning.

The size of a MPA should be defined according to its conservation objectives, quality of habitat types, protected species and biological communities' features (NRC, 2001). However, MPAs do have certain limitations due to the limited geographical extent of such areas. In fact the relative scale of MPAs often does not consider the species that enter the area only at certain times such as plankton, nekton, birds etc. The problem of the scale is crucial; the ecosystems should be seen within a spatial and temporal scale. Stevens (2002) recognises a hierarchy of spatial scales that identifies the marine environments (Table 1.4), highlighting that MPAs occur at scale lower than the regional one and in most case at local or site scale. Figure 1.1 shows the typical space and time scales of marine phenomena.

Table 1.4 Hierarchy of spatial scale for marine environments (Stevens, 2002).

Scale reference	Linear extent	Scale term	Name(s) of derived units	Typical components
Macroscale	1000s of km	Continental	Provinces	Geopolitical boundaries, oceanic basins, climate zones
Mesoscale	100s of km	Regional	Regions, bioregions, biophysical regions	Major discontinuities in physical, oceanographic and biological distributions
Microscale	10s of km	Local	Local units, biounits	Functional structural units with recognizable natural boundaries and internal homogeneity
Pica-scale	<10 km	Site	Sites	Individual physical and biological habitats (e.g. reefs, algal beds)

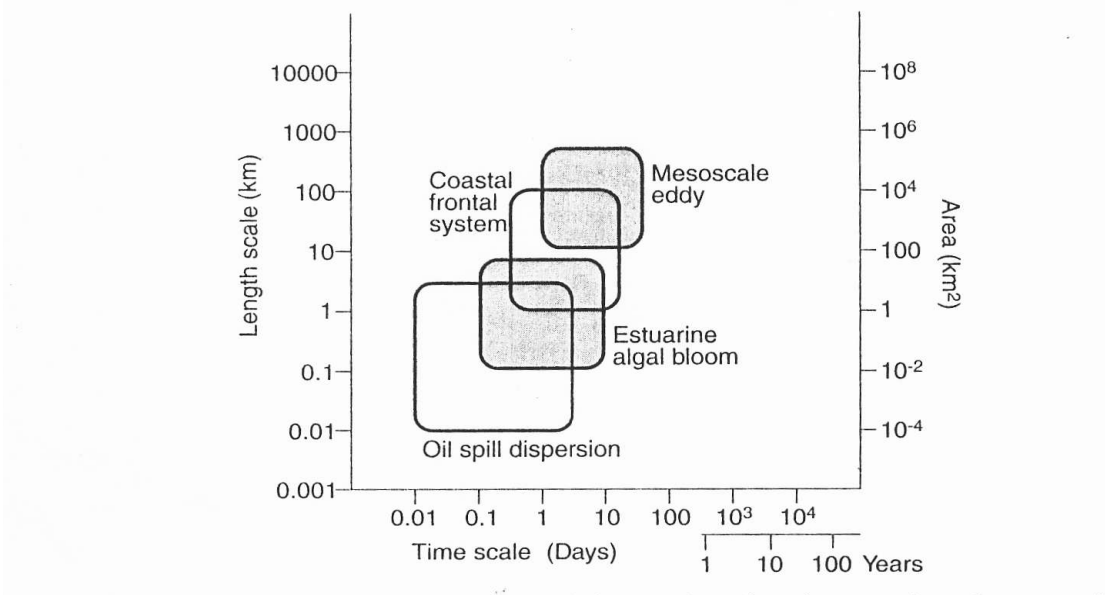

Fig.1.1 Space and time scale of various oceanic phenomena (from Robinson., 2005).

Regarding the *institutive process*, MPAs follow a methodological route which should overcome fixed stages, summarised by IUCN (Kelleher, 1999) as:

1. Definition of the *criteria* in order to identify areas where to establish MPAs;
2. *Zoning* process;
3. MPAs *Planning* and *Management*.

Regarding the criteria (used in the documented experiences) used to identify the areas to submit to protection regimes, the following are employed (Kelleher, 1999; Roberts *et al*., 2003):

- Biogeographical ;
- Ecological ;
- Naturalness;
- Economic Importance;
- Social Importance;
- Scientific Importance;
- National or international importance;
- Practicability;
- Repetition.

It is obvious that different typologies for MPAs exist, in relation to the different objectives which are ascribed to them (Baker, 2000).

The *zoning* process represents, together with management, the tool through which the institutive objectives could be met. Zoning is a means that allows designation of sites with a different degree of protection for each objective within a MPA; it depends on the legislative context and from the local realities involved (NRC, 2001) and should be tailored to the specific requirements of the specific areas (NOAA, 2003). Zoning is a spatial planning tool that aims to allow some activities which are linked to the socio-economic development of the resident communities, and separate - incompatible - activities, specifying that those are allowed only in certain areas; in this way zoning separate uses and user conflicts (Day, 2002). Usually MPAs present a core area of maximum protection plus buffer zones in which some, potentially impacting, human

activities are permitted (Reeves, 2000). In fact the main objectives of zoning reflect MPAs' objectives and aim usually to (Keller and Kenchington, 1992; Laffoley, 1995):

- Supply protection for critical marine habitats, ecosystems and biological processes;
- Protect specific zones within the MPA in their pristine state, avoiding any anthropogenic impact except for research;
- Preserve the naturalness of the MPA permitting a narrow spectrum of human activities;
- Avoiding disputes among human activities.

On the basis of the objectives pursued with the MPA institution and in accordance with the different body of legislation, there were developed, at global level, different procedures/approaches to the zoning process. However, on the basis of specific literature (Kelleher, 1999), applied methodologies refer to two main typologies:

- A mechanistic approach where a numerical weighted value is assigned to a potential site on the basis of a predetermined criteria;
- A "delphic" approach, where each aspect of the selection process takes into consideration the opinion of the interested and/or qualified people.

The first (mechanistic) typology is frequently encountered within the scientific literature, but is poorly utilised in practise because the delphic approach tends to produce more consistent results (Kelleher, 1999). Moreover, it should not be underestimated that the concept of a MPA, in its general definition, had changed profoundly and it had recognised the human presence as integral part of the environment. As noted by Agardy (2000), the human element should be never underestimated: the success of whichever MPA is strictly correlated to the clear identification of the user groups and stakeholders within the planning and management processes. Consequently the institutive process has changed profoundly and from a top-down route it has been transformed into a bottom-up process. This change demonstrates that the opinion of the local communities is now an integral part of the decision process. As highlighted by many authors, is not possible to institute and manage an MPA without the consensus and participation of the interested communities (Ramos, 1999).

Those considerations cannot be translated into a valid "recipe" for each real-world situation (Agardy, 1999). The guidelines for MPAs, written by the World Commission on Protected Areas (WCPA-IUCN) (Kelleher, 1999), which represent the synthesis of the experience conducted in different context, point out the aspects that should be taken into consideration. In this respect there are three main points which should always taken into account:

- Public interest, which should be pursued through the early involvement into the process;
- Equity. The community and users needs should be considered in an equable way;
- Guarantee the rights of the existent compatible uses.

So far we have seen that an MPA is a complex entity to design and to deal with and its implementation requires a multidisciplinary approach. In order to resolve these challanges, an objective *planning* is necessary (Ramos, 1999). The plan is a fundamental condition and it should state the management objectives and tools. The plan should be in line with the objectives of the area and should be revised periodically in order to be implemented (Reeves, 2000). Kelleher and Kenchington (1993) have proposed structuring MPAs according to two main models (also see Attwood *et al*., 1997; Salm *et al*., 2000). The first model sets the goal of controlling human activities in particular for small areas; the second model seeks the creation of a large MPA within different level of protection.

As highlighted above, there are many different approaches to MPA planning and management. Salm and Dobbin (1993) state that the approach chosen should be driven by the available resources as well as environmental, social, political and economic constraints.

Management of a MPA has changed into the crucial concept of adaptive management i.e. science and management should be placed in a so called "feedback loop" which will allow assessment of the management measures adopted Agardy (1994, 1997). Furthermore the key to the MPAs' adaptive management is the consultation of the local communities and their participation in the management process, thereby minimising

conflicts among groups. In this way the MPA will be accepted and legitimised by local communities (Kelleher and Kenchington, 1993; Beaumont, 1997).

Monitoring is a fundamental component of the MPA management. It is the tool through which it is possible to assess the state of the marine environment and detect changes and trends in marine ecosystems, habitats and communities (Kelleher and Bleakely, 1994). Monitoring allows periodical surveying of the MPA to evaluate whether the objectives are being met and to point out eventual enhancements. The National Research Council (2001) identifies, among other things, the key task of monitoring long-term trends of marine ecosystem features. In fact coastal systems are particularly fragile and subjected to anthropogenic impacts and changes in marine processes (Barale and Folving, 1996).

Research in MPAs is required to fill the major gaps in our understanding of marine ecosystems. MPAs give us an exceptional chance to investigate how the marine ecosystems work and how they vary. This process is essential to the implementation of the MPAs management. As many authors have highlighted (e.g. Agardy, 1994; 1997; Dayton *et al.*, 2000), MPAs are an ideal laboratory to translate science pragmatically into conservation. They allow study of the structure of marine ecosystems, to monitor their changes and to conduct investigations under almost pristine conditions. MPAs should represent the laboratory for experiencing different management approaches that could be used to supply guidelines on how to design and manage MPAs. As Agardy (1994) states, the role of MPAs is to work as "a buffer against unforeseen yet potentially disastrous management mistakes".

1.4.3 Marine Sanctuaries

As discussed in §1.4.2, also the term *sanctuary* falls within the wide term "Marine Protected Area" (Agardy, 1997; Salm and Clark 1984).

Marine Sanctuaries have been established to protect marine mammals (Scheffer *et al.*, 1984). One of the oldest, the Walrus Islands State Game in Alaska, was declared a

marine sanctuary in 1960 (Kenyon, 1960). In 1954 the "Seal Beach" on Kangaroo Island, South Australia, was established to preserve the Australian sea lions (*Neophoca cinerea*) and New Zealand fur seals (*Arctocephalus forsteri*) (Robinson and Dennis, 1988). These early attempts were focused on land protection, whereas contemporary sanctuaries try to preserve also the off shore habitat in which marine mammals live.

Many marine mammal populations have been hunted for centuries. In recent years, however, the major threats to marine mammal populations are essentially due to: bycatch (Perrin *et al*., 1994), decreasing prey abundance (Earle, 1996), chemical pollution (O'Shea, 1999), acoustic pollution (Richardson *et al*., 1995; Gordon and Moscrop, 1996), entanglement in fishing nets (Laist 1996; Laist *et al*. 1999), spoiled habitat by anthropogenic impact (Whitehead *et al*., 2000) and climatic changes (MacGarvin and Simmonds, 1996). In order to respond to these threats, the establishment of marine sanctuaries can be considered as the best approach to preserve marine mammals. However, protected areas have been declared more often for threatened species such as monk seals (*Monachus* spp.), manatees, whales, and river dolphins, whereas there are few protected areas for migratory cetaceans and none for pinnipeds (Reeves, 2000). So far, these attempts could be considered as a starting point for the conservation process of marine mammals, which should lead to an implemented management system (Agardy 1994).

Since the majority of MPAs have been established on coastal habitats, a marine mammal sanctuary in a pelagic environment poses new issues that should be tackled. In fact the term '*pelagic*' encompasses species, dynamics and ecosystems that are found in the water column and are not directly connected to the substrate as in shallower systems.

The spatial distribution of pelagic species is mainly shaped by meanders of water currents and by the interaction between physical and biological processes, which in turn support the growth and maintenance of planktonic communities. The latter processes occur at meso to macro spatial scales (Table 1.4) and at seasonally and decadal time scale. These processes determine trends of productivity that cause often a patchy distribution of the pelagic species. It could be asserted that physical processes steer the

time period and the scale of primary production and affect the spatial distribution of planktonic organisms or "plankton biogeography" (Hyrenbach *et al*., 2000). Kenney *et al*. (1996) and Forney (1999) showed that spatial distribution of cetaceans can shift due to changes in zooplankton concentration and other prey density or oceanographic features to exploit regions of higher productivity. It is therefore crucial to investigate and define the so-called persistent oceanographic features such as water currents and fronts which are more difficult to tackle due to their mobility and changeable nature (Hyrenbach *et al*., 2000). This consideration leads to the conclusion that to protect marine mammals, pelagic sanctuaries should have supple boundaries. These biogeographic boundaries should be identified by investigating the ocean attributes such as sea surface temperature (SST) and *chl*, and subsequently the distribution of marine mammals. The persistent oceanographic features could be identified by means of satellite remote sensors.

1.5 THE MEDITERRANEAN SEA

The Mediterranean Sea is located between Europe, Asia and Africa (about 46°N, 30°N, 6°W and 36° E) and covers a surface of about 2.5 million km^2 and a volume of 3.7 million km^3 with the only connection to the world ocean represented by the narrow Strait of Gibraltar. The Mediterranean comprises two major basins, the Western and the Eastern, which are separated by the Strait of Sicily. The Western Mediterranean extends for about 0.85 million km^2 and the Eastern Mediterranean for about 1.65 million km^2. These main basins have several smaller regional seas which show different topographies (Fig. 1.2) that determine the water circulation and water mass distribution (La Violette, 1995). The Mediterranean Sea is almost an enclosed basin, but is linked (1) to the Atlantic by the Strait of Gibraltar (15 km wide andwith an average depth of 290 m, and maximum depth of 950 m), (2) to the Sea of Marmara by the Dardanelles (between 450 m and 7.4 km wide and 55 m deep) and (3) to the Red Sea by the Suez Canal (120 m wide and 12m deep).

The Mediterranean region is characterised by a so-called "Mediterranean climate" with warm, dry summer seasons over the whole basin, with considerable rainfall in the north

and relatively dry in the south. The weather conditions are controlled by the interactions of the Atlantic Ocean, the Eurasian and the North African pressure system which produce, particularly during winter periods, high spatially weather variability. The atmospheric temperature increases from north to south and from west to east. Surface winds in the Mediterranean are generally from the north and west (Batisse and de Grissac, 1995).

The evaporation over the surface throughout the Mediterranean is a strong phenomenon which is not compensated by precipitation input, thus causing quite high salinity. The Atlantic waters (about 35,000 km^3 per annum) which enter the Mediterranean through the Gibraltar Strait balance the water evaporation loss.

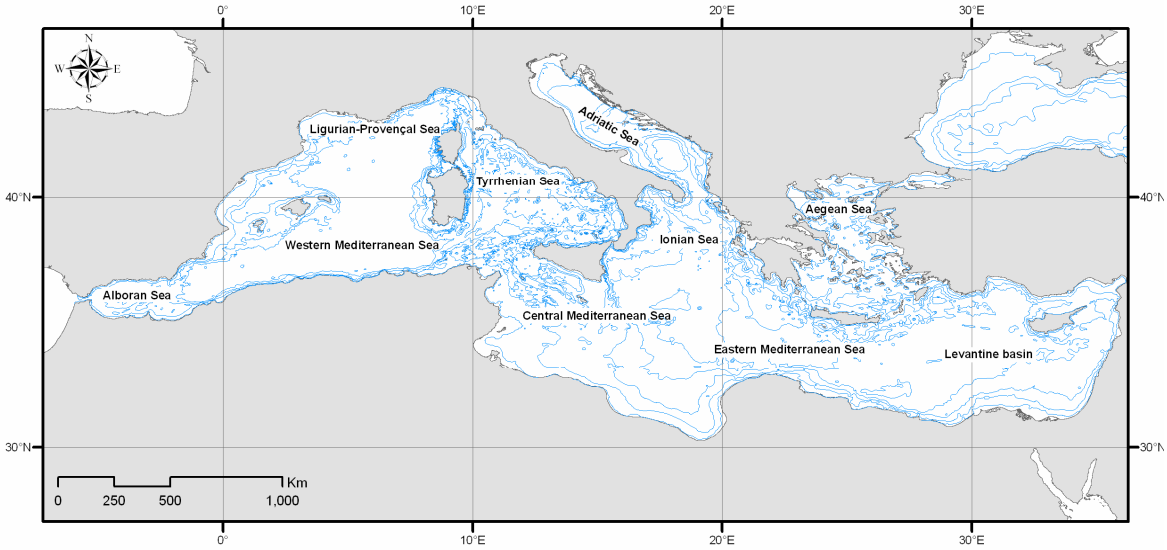

Fig. 1.2 Mediterranean Sea, highlighting the nomenclature of the main seas (USGS Map 1:250.000).

The Mediterranean Sea has in general very feeble tides (averages of 20-30 cm). Tides are, however, notable in the northern Adriatic Sea (1m) where they cause the "*Acqua alta*" (high waters) phenomenon. "*Acqua alta*" is the term used for the exceptional tide peaks (> 110 cm) that occur periodically in the northern Adriatic Sea. These peaks reach their maximum in the Venetian lagoon, where they cause partial flooding of Venice and Chioggia. This phenomenon occurs mainly between autumn and spring, when the astronomical tides are reinforced by the prevailing seasonal winds i.e. *Scirocco* (south-east) and *Bora* (north-east). The sea level rising increases the destructive action of the

swell towards the coastal defences and the sand bar which divides the Venice lagoon from the open sea (Ferla, 2003).

The surface current systems in the Mediterranean basin are strongly influenced by the surface water flow from the Atlantic into the Mediterranean (from the west to the east) which forms gyres. The salinity of Atlantic waters entering the Mediterranean is about 36 whereas in the western and eastern basins salinity is 38 and 39.5 respectively (Batisse and de Grissac, 1995). The other important current in the Mediterranean is the vertical convection which allows the balancing of salinity and recycling of nutrients. The Mediterranean Sea is a temperate oligotrophic (low primary production) basin (Sournia, 1973), with low nutrient concentrations throughout the water column and throughout the year. However some sub-basins are characterised by limited patches of high chlorophyll concentration which occur mainly during spring. The eastern basin shows a higher level of oligotrophy than the western basin.

The Atlantic surface waters entering the Mediterranean are poor in nutrients; the major input of nutrients comes from river and agricultural runoff (Miller, 1983). The continuous input of nutrients from land into coastal waters causes frequent eutrophication phenomena, especially in the Adriatic Sea due to industrial and agricultural runoff through the Po river. The Adriatic Sea is one of the most productive areas of the Mediterranean basin (Böhm *et al*., 2003). Estimates based on the ocean colour sensor observation retrieved by the Coastal Zone Color Scanner (CZCS) sensor conducted by Antoine *et al*. (1995) confirmed that the Adriatic Sea showed the highest phytoplankton biomass and primary production of all the Mediterranean sub-basins. Using CZCS data, Barale *et al*. (1986) showed a direct relationship between winter-spring phytoplankton spatial distribution within the northern Adriatic Sea and the River Po freshwater run off. Indeed the heterogeneity of phytoplankton pigments is ruled by the fluctuations caused by the river run off. Figure 1.3 shows an example of chlorophyll-like pigment concentration (*chl*) map retrieved by Moderate Resolution Imaging Spectroradiometer (MODIS) sensor within the Adriatic basin, showing the large plume caused by the River Po. The high input of nutrients caused by river runoff, can cause eutrophication, a term that derives from ancient greek *eutrophia* (eu=good, trophòs=food)**,** and describes an aquatic environment rich in nutrients (specifically nitrates and phosphates). This high input of nutrients due to anthropogenic or natural

sources causes a proliferation and excessive growth of the aquatic plant organisms and may lead to anoxia in the water column. The phytoplankton and algal growth can affect the oxygen balance since the oxidation (decomposition) of organic matter causes the water to become turbid, the oxygen to be depleted and some marine organisms to die due to anoxia (UNESCO, 1988). Eutrophication phenomena occur particularly in the summer season due to the stratification of the water column. Winter mixing processes allow the oxygen to reach the deep waters and nutrients to reach the surface layers allowing upwelling phenomena to occur (Cruzado, 1985), which compensates to an extent for deoxygenation.

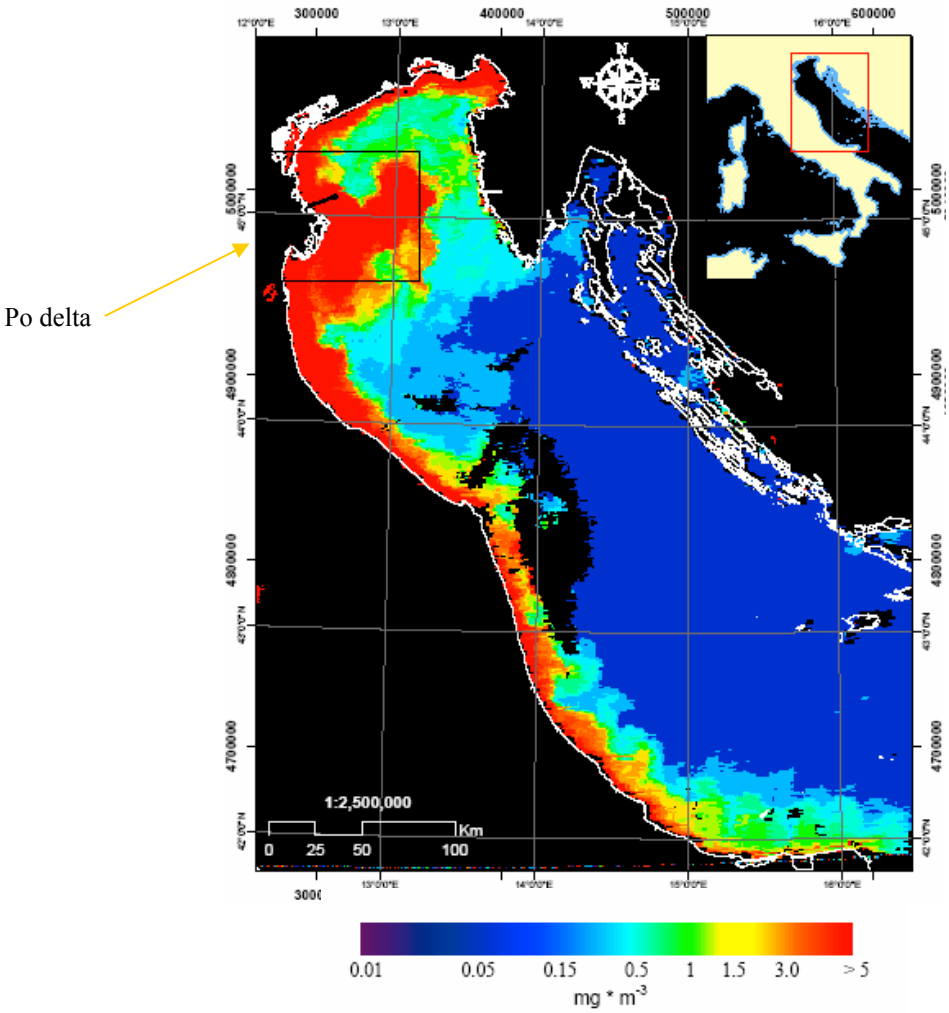

Fig. 1.3 Daily *chl* map (mg m^{-3}) retrieved from MODIS sensor of the Northern Adriatic basin (October 2005) with highlighted the Po delta and the river plume (in red).

The Mediterranean basin lies in the middle of a system of patchy tectonic plates that cause high volcanic and seismic activity. The geomorphology of Mediterranean coasts is consequently characterised mostly by mountainous landscapes, and rocky shores cover about 54% of the total shoreline. There are also alluvial plains for the major fluvial systems such as Ebro, Rhône, Po and Nile. These rivers cause a large sediment input into the Mediterranean sea as well as severe erosive processes (~15 ton/ha per year) (Batisse and de Grissac, 1995). It should be noted that although the Mediterranean continental shelf is quite contracted, the coastal marine areas which extend up to this shelf host high biodiversity ecosystems. Usually coastal areas are the most productive of the whole Mediterranean because they receive the nutrients derived by telluric shocks.

Regarding the marine habitats, seagrass meadows, rocky bottom and estuaries have a considerable ecological value. These habitats are vital not only for the ichtyofauna, but also for endangered Mediterranean species such as sea turtle (*Caretta caretta*), monk seal (*Monachus monachus*) and birds (Ramade, 1990).

Phanerogam species(seagrasses) in the Mediterranean build up prairies in shallow waters down to a depth of 40m. Seagrass meadows are significant for several species such as fish, crustaceans and sea turtles because they provide shelter, food, breeding and resting areas. The most important Mediterranean phanerogam species are the *Posidonia oceanica*, *Zostera marina* and *Cymodocea nodosa*. These species are considered endangered. *Posidonia oceanica* meadow represents the most important and typical Mediterranean habitat. Seagrass meadows, particularly of *Posidonia oceanica*, have a strategic role in protecting the coast from erosive processes, in stabilising sea bottom and shore by catching the sediments, decreasing current flow, and increasing water quality by emitting oxygen. The *Posidonia* meadows are the most productive ichtyofaunal habitats in the Mediterranean (Batisse and de Grissac, 1995). The most devastating activity on the seagrass beds seems to be the trawling fishery. Indeed, trawling affects the prairies because trawlers are dragged on the bottom causing physical degradation of the habitat by impacting fish and invertebrate assemblages and altering sediment type (Sánchez-Jerez *et al*., 1999).

As noted previously, another important Mediterranean ecosystem is the rocky habitat commonly referred to as hard bottoms. They represent a small fraction of the marine

environment compared to the spatial extent of the soft bottoms, but they represent a high scientific and economic value. The hard bottoms host a high biodiversity often characterised by sessile organisms with modular structure i.e. algae, sponges, cnidarians, bryozoans, tunicates. These biocoenotic assemblages are often dominated by algae, some of those are biogenic constructors. The hard bottom communities have a complexity which can sometimes be compared to that of coral reef (Bellan-Santini *et al*., 1994). Hard bottoms have a great economical value due both to fisheries, as they host an ichtyofauna of great commercial value, and to nautical and diving tourism. These ecosystems are quite delicate and are threatened mainly by pollution, fisheries and tourism, as well as rising sea temperature due to climate change (Bianchi and Morri, 2004).

Other important habitats to preserve are Mediterranean wetlands and lagoons, which also support high biodiversity and productivity. Estuaries also represent important habitats since there are almost 70 rivers which discharge into the Mediterranean.

Pollution is a major issue in the Mediterranean. Since the only flow of water from the east to the west (i.e. towards the Gibraltar Strait) is a deep water stream, most of the pollutants discharged into the Mediterranean will remain within the basin. The majority of pollutants are derived from land-based activities as well as sewage, industrial and agricultural runoff. Intense vessel traffic throughout the Mediterranean, particularly oil tankers, is also a major concern. The vessel traffic causes disturbance to the marine mammals and in particular to the cetacean populations (Stocker, 2002).

Although the Mediterranean Sea is characterised by an overall low primary production rate, it shows a high degree of biodiversity due essentially to its particular paleogeographic and ecological characteristics. Paleogeographic characteristics have caused the evolution of different biogeographic regions and the ecological characteristics encompass a wide range of climatic and oceanographic conditions (Bianchi e Morri, 2000). The Mediterranean species are almost Atlantic-Mediterranean species (about 62%) immigrated from the Atlantic Ocean. However, the Mediterranean basin hosts several endemic species (almost 20%) whilst the rest are circumtropical (13%) or Indo Pacific (5%) immigrated through the Suez Canal from the Red Sea. The species diversity decreases from the Western towards the Eastern basin, which hosts a

much lower number of species. Also the benthic and littoral populations follow the same east-west decline in species diversity, and decreasing in species diversity from north to south (Ketchum, 1983).

The percentage of endemic species is particularly elevated for sessile species such as ascidians (50.4%) (Pérès and Picard, 1964), sponges (42.4 %), hydroids (27.1 %) (Pérès and Picard, 1964), echinoderms (24.3%) (Tortonese, 1985), and is significant also for decapod crustaceans (13.2%) (Pérès and Picard, 1964) and fish (10.9%).

The main Mediterranean biogeographic regions are summarised in Table 1.5 (Batisse and de Grissac, 1995). These are mainly determined by the natural division created by the submarine ridge between the island of Sicily and the African coast (Tunisian coast) which divides two main sections of the Mediterranean Sea: the Western and the Eastern basin.

Table 1.5 Main Physical Characteristics of the Mediterranean Marine Region (Batisse and de Grissac, 1995).

Biogeographic Subdivision		
Location	**Area (km^2)**	**Maximum depth (m)**
1. Alboran Sea	69,000	1,375
2. Algerian Basin	700,000	2,000
3 Tyrrhenian Basin	247,000	3,000
4 Ionian Basin	938,000	5,092
5 Levantine Basin	667,000	3,000
6 Aegean Sea	214,000	3,543
7 Adriatic Sea	131,000	1,324
Total Mediterranean Sea	2,966,000	

1.6 PROTECTION OF MEDITERRANEAN MARINE AREAS

The Mediterranean Sea is universally recognised as a sea where the combination of extraordinary natural and cultural values coexist. However, the intense human pressure is increasingly threaten the above mentioned values. The biodiversity of the Mediterranean marine region has been almost neglected when compared with the terrestrial region, although the sea has a fundamental economic and cultural importance for the Mediterranean countries. The Mediterranean Sea covers only 0.82% of the

surface area and 0.32% of the volume of the world oceans, but roughly 8500 species are found in the Mediterranean, i.e. between 4% and 18% of the total global marine species (Bianchi and Morri, 2000). Mediterranean biodiversity has been depleted due to the pressure of anthropogenic impact and the actions taken to protect biodiversity are still insufficient. Most of the major Mediterranean marine habitats are in danger and MPAs have been recognised as effective tools to protect the marine environment. In the Mediterranean hundreds of MPAs have been declared during the recent decades to ensure protection of sites encompassing the most valuable marine habitats and species (Abdulla *et al*., 2008). However, so far protected areas cover a minimal surface in the Mediterranean region (Boudouresque, 1994). According to Abdulla *et al*. (2008), MPAs and managed areas in the Mediterranean cover approximately 4% of the Mediterranean Sea (Fig.1.4). Coastal MPAs amounts to only the 0.4% of the total surface of the Mediterranean Sea.

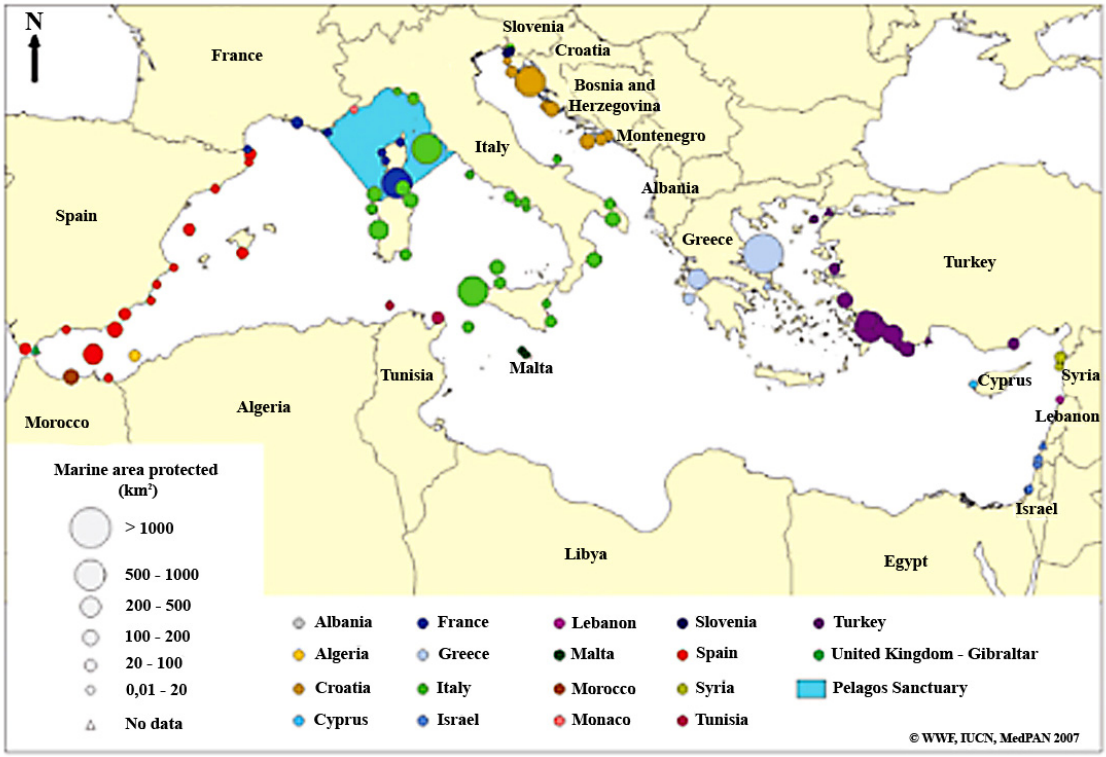

Fig.1.4 Distribution of Mediterranean MPAs. Relative size of each MPA is shown according to different class sizes. Different colours represent different countries (from Abdulla *et al*., 2008).

1.6.1 Marine Protected Areas in the Mediterranean Sea

In the Mediterranean 200 MPAs have been established so far, but evidence of their effectiveness is scarce (Fraschetti *et al*., 2005). In the Mediterranean region, the term MPA covers a variety of different situations, which differ in their ecological and hydrographical context as well as in their use. Furthermore, Mediterranean MPAs are subjected to different jurisdictional, management and enforcement measures. There are several different situations ranging from large, multi-tasking marine areas to sanctuaries that are almost closed to human activity. These differences reflect the options that were identified at the time of their designation, such as the management plan and zoning, and also the available resources (Francour *et al*., 2001). A common characteristic of many Mediterranean MPAs is their location in shallow rocky areas. Aesthetic values seem to be the strongest driving force in determining the establishment of Mediterranean MPAs. In fact the presence of high aesthetic value seascapes led to their being considered as natural monuments (Harmelin, 2000). Also Boero (ICRAM, 2002) highlights that among the reasons leading to the establishment of an MPA, the aesthetic feature is often given a primary role in the Mediterranean. However, the problem of using aesthetic criteria is the associated subjectivity. The Mediterranean MPAs are almost always formed by hard, rocky bottoms since these tend to host the more aesthetically valuable living beings, such as sessile benthic organisms.

A review conducted by Boudouresque (1996) on the Mediterranean MPAs (especially regarding EU countries) shows that experiences within the Mediterranean Sea are hardly comparable with the experiences conducted elsewhere in Europe. However, specificity does not rely only on political and administrative aspects expressed at local and government level. More relevant seems to be the strong and constant human presence in the Mediterranean basin and also the social and economic structure of the wealthiest countries which have influenced the marine environment through impacts on the coastal zone, conflicting uses of the same resources, etc. Boudouresque (1994) and Harmelin (2000) observed that, in the Mediterranean Sea, the majority of MPAs are not selected on criteria fixed beforehand such as those identified by the IUCN (e.g. ecological criteria and information), but rather on the basis of historical and political opportunities. In the majority of cases the processes of MPA designation and selection

were carried out without the support of a clear scientific methodology (Fraschetti *et al*., 2002). As Francour *et al*. (2001) stated, MPAs can be strategic to the conservation of marine habitats if their design were based on scientific criteria. This consideration defines a new decisive criterion: opportunity. The opportunity has, in effect, been a key criterion for establishing MPAs in some cases. Nonetheless the main objectives for the establishment of a Mediterranean MPA have essentially been the conservation of sensitive areas, threatened species and pristine habitats.

Given the fact that Mediterranean MPAs differ significantly in their physical and biological features (§1.6) which should drive the designing and management process, the poor knowledge regarding the MPAs efficacy is palpable (Fraschetti et al., 2002). One other element which characterises Mediterranean MPAs is their size. In general, there is a correspondence between targets and a MPA's size. Smaller MPAs generally have fewer objectives, whereas larger areas can protect a higher number of species and habitats and have multiple objectives (multiple-use MPAs) which may be unclear or incompatible (Harmelin 2000, Badalamenti *et al*. 2000, Francour *et al*., 2001). Large areas are difficult to control and manage. Multiple-use MPAs tend to target a balance between biodiversity protection and human use. Spain, France and Italy, due to the considerations outlined above and relative to the socio-economic structure of these countries, have small MPAs but with multiple objectives. The question is whether management measures at small scale can significantly reverse the degradation of Mediterranean ecosystems that has already occurred.

Bianchi and Morri (2000) illustrate that experiences in the Mediterranean seem to indicate that areas of less than one square nautical mile in surface should be enough to host the biodiversity typical of Mediterranean rocky coast, at least for some key groups of marine organisms (e.g. gorgonians, fish, etc.). So far, MPAs have worked as separate entities, without being interconnected by a functional network (Abdulla *et al*., 2008). Therefore it is opportune to establish systems of MPAs, tightly interconnected to each other under the umbrella of the same management measures, formed by numerous small neighbouring areas and well distributed geographically. This system can have an effect beyond the boundaries of the single MPAs by ensuring the exchange of larvae, migratory species and gene flow (Abdulla *et al*., 2008). Single and isolated protected areas would be insufficient to achieve the same effects (Francour *et al*., 2001). New

MPAs should be declared to ensure protection to valuable habitats within the different Mediterranean ecoregions in order to create a balanced network (Notarbartolo di Sciara, 2005). The aim of an ecological network of MPAs is to preserve biodiversity of the whole ecoregion (Rodrigues *et al*., 2004). A network of MPAs can succeed if each individual MPA meets its conservation objectives. A new holistic ecological approach has now been developed and designing the MPAs as parts of an interconnected network makes possible to go beyond the more traditional approach of MPAs designed as single and separated entities.
A recent definition of a network of MPAs is (IUCN/WCPA, 2007):

> "*A collection of individual marine protected areas operating cooperatively and synergistically, at various spatial scales, and with a range of protection levels, in order to fulfil ecological aims more effectively and comprehensively than individual sites could alone. The network will also display social and economic benefits, though the latter may only become fully developed over long time frames as ecosystems recover*."

The IUCN/WCPA- Marine Summit (IUCN/WCPA, 2007) called for the establishment and implementation of national and high seas MPAs network by 2012. Since 1976 Mediterranean countries and the European Community adopted the first Regional Seas Programme under the umbrella of UNEP to protect biodiversity and address the conservation issues with a regional approach (Barcelona Convention, 1976). Mediterranean countries are continuously collaborating under a legal framework in order to build up a network of MPAs.

Three main issues related to the development and success of Mediterranean MPAs as tools for conservation and management have been highlighted (Badalamenti *et al*. 2000, Garcia Charton *et al*. 2000, Pinnegar *et al*. 2000; Planes *et al.* 2000, Sanchez Lizaso *et al.* 2000):

i. MPAs are the right tool, for the conservation and management of marine ecosystems, but so far the unsystematic design, implementation, enforcement and evaluation has produced contrasting evidence about their effects on marine ecosystems encompassed and their success at meeting the stated objectives;

ii. There is a substantial lack of knowledge about the physical and biological processes as well as the biological communities; research on MPAs should be driven by empirical studies supported by theoretical bases;
iii. The interest in MPAs is constantly growing and also the willingness for the development of an interconnected network of MPAs.

1.6.2 Sanctuaries in the Mediterranean Sea

The only *Sanctuary* designated within the Mediterranean Sea is the *Pelagos* Sanctuary for Marine Mammals initially conceived as a tool to preserve cetaceans and monk seal *Monachus monachus*. However, monk seal has no longer been recorded within the *Pelagos* sanctuary area.

The International *Pelagos* Sanctuary for Mediterranean Cetaceans centred in the Ligurian Sea (north-western Mediterranean Sea) is an area for the conservation of marine mammals extending over 87,500 km^2 (equivalent to approximately 4% of the Mediterranean sea surface). Covering part of Tyrrhenian Sea and the Tuscan Archipelago, this sanctuary is composed of French, Italian and Monaguesque territorial seas extending 12 nautical miles and including the adjacent high sea areas (Fig. 1.5). *Pelagos* Sanctuary is, to date, the only MPA which represents the high-sea ecosystems in the Mediterranean. Most of the surface occupied by the sanctuary is on the high seas (Abdulla *et al*., 2008).

The area now covered by the *Pelagos* sanctuary was previously known for its high biodiversity and also the threats to its cetaceans and other pelagic species (e.g. drift nets, boat collisions, chemical, contaminant and acoustic pollution). It was thus decided that a conservation tool be designed to allow enactment of protective measures even on open seas, in a zone that (according to maritime law) is open to all countries for maritime traffic, navigation and exploitation of natural resources. It was therefore proposed that this area be designated as an international sanctuary thereby requesting all countries, once the Sanctuary was established through the appropriate international legal processes, to respect any conservation measure requested by its management authority.

The cetacean sanctuary was affirmed in the North western Mediterranean Sea in 1993 by the Italian, French and Monaco ministers (Gordon *et al*., 2000). This led to the Declaration of Intents for the conservation of cetaceans in the Corsican-Ligurian-Provençal basin. In 1995, to make possible the creation of a MPA on the high seas in the Mediterranean region, the Barcelona Convention Protocol for Specially Protected Areas and Biodiversity was amended. Given that the Mediterranean is a semi-closed sea, there are no Exclusive Economic Zones (EEZ; width of 200 nautical miles) the national authorities of the Mediterranean countries have jurisdiction only over 12 nautical miles offshore (Reeves, 2000). On November 25, 1999 the Republics of France and of Italy and the Principality of Monaco signed the agreement for the creation of a Mediterranean Cetacean Sanctuary (Notarbartolo di Sciara, 2008). The Sanctuary agreement specified:

(1) the protection of cetaceans against direct take and intentional disturbance;
(2) a veto of use of driftnets longer than 2.5 km (according to European Union, EU, regulations the usage of such fishing equipment was completely forbidden from 1 Jan. 2002);
(3) the regulation of new fishing techniques that may cause cetacean entanglement or hinder the abundance of their prey.

The Parties also agreed to regulate and eventually forbid high-speed motor boat racing and to regulate the nature of whale watching activities, recognising that an excessive number of boats, a noisy and violent approach in critical feeding habitat zones may induce the animals to alter their behaviour temporarily or permanently.

The Cetacean Sanctuary was ratified by Italy with Law n. 391 of 11th October 2001 and entered into force on February the 21th 2002. Furthermore the Sanctuary has been entered into the list of Specially Protected Areas of Mediterranean Interest (SPAMI) envisaged within the Protocol for Special Protected Areas and Biological Diversity of the Barcelona Convention. Under the auspices of the Barcelona Convention's Protocol, high sea areas identified as SPAMI should thus gain the needed legal protection as the Protocol requires all Parties adhering to the Convention (at the moment the 20 Mediterranean coastal states and the entire European Union) to respect the protection measures established within each individual SPAMI.

Beyond the *Pelagos* Sanctuary, the only other MPA dedicated to the protection of cetaceans in the Mediterranean is the Lošinj Dolphin Reserve in Croatia, established in 2006 (Abdulla et al., 2008, Fig. 1.5). Moreover, in order to protect the only Mediterranean pinniped species, two protected areas have been established to preserve the endangered Mediterranean Monk seal (*Monachus monachus*). These are the National Marine Park of the Northern Sporades in Greece, and Foça Specially Protected Area in Turkey.

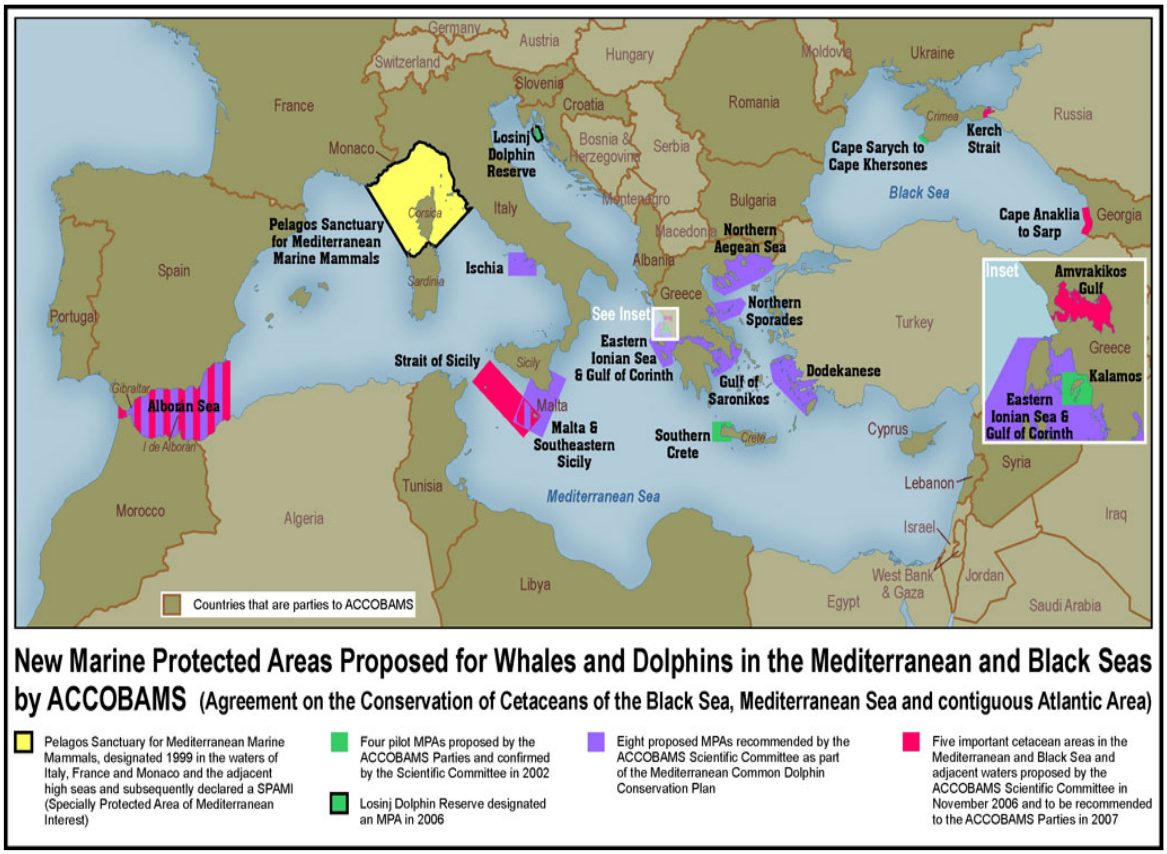

Fig. 1.5 Map of the existing and proposed MPAs for whales and dolphins in the Mediterranean and Black Seas by Agreement on the Conservation of Cetaceans of the Black Sea, Mediterranean Sea and contiguous Atlantic area (ACCOBAMS) (Abdulla *et al.*, 2008). In yellow is highlighted the Pelagos Sanctuary (Ligurian Sea), whereas in circled green the Lošinj Dolphin Reserve (Adriatic Sea).

1.7 OCEAN REMOTE SENSING

Although it is relatively simple to obtain a long time series of oceanographic measurements at specific locations, obtaining synoptic time series globally has been frustrated by the vastness of the oceans. In consequence, oceanography has historically suffered acutely from a lack of data, a problem which satellite techniques offer the only practical solution. Indeed, Earth Observation (EO) satellites enhance our ability to observe the oceans, remote sensing of the ocean from satellites allowing unique, quick, elevated, repeated global coverage of ocean surface features and the collection of information on a global basis. The applications of satellite data within oceanography are diverse and extensive, being useful to biological, chemical and physical oceanography. Such data acquisition cannot be achieved with traditional measurements from oceanographic vessels; instruments on ships and on buoys cannot cover whole oceans instantaneously (Fig. 1.6).

If the processes are relatively *time-invariant* and spatially homogeneous then measurements from ships may reveal clear patterns. But to study *time-varying* processes at ocean basin scales oceanographers are faced with severe challenges which may only be overcome with the use of EO satellites. In addition some type of measurements made by satellites cannot be made by conventional methods. RS offers a wide range of capabilities, complementing conventional *in situ* data collection techniques, for the synoptic and systematic evaluation of bio-geochemical and physical processes at the global, regional and local scale (Table 1.4). Indeed, the physical processes that occur within the ocean are observed across a wide range of spatial scales from small surface ripples to ocean basin fluctuations. The timescale is a key factor in monitoring the oceans. Most EO satellites revisit the same area in one day, allowing a daily coverage of a study area.

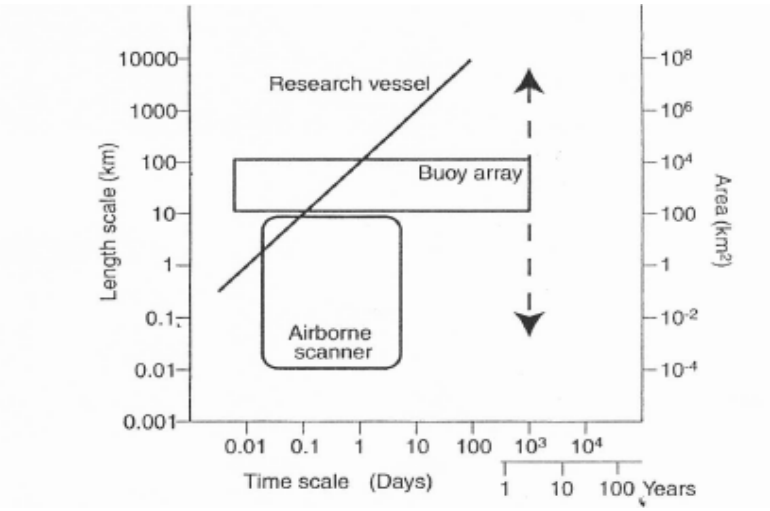

Fig. 1.6 Sampling scales from airborne remote sensing, a single research vessel and an array of buoys (from Robinson, 2004).

The major advantages of marine remote sensing are to be found in the long-term, large-scale monitoring of entire basins and particularly in terms of:

- Synoptic overview and the possibility of analysing a study area in a wider context (extended spatial coverage);
- Repetitive observations over long periods at global and regional scale with high spatial resolution (repetition capabilities);
- Possibility of accurate comparison of the temporal variations.

Having stated above the strategic and crucial role of satellite remote sensing in observing the marine ecosystems, the limitations of RS also have to be highlighted:

(i) EO satellites can observe only the surface layer of the oceans and are limited to a two-dimensional spatial view. This is a major limitation since the vertical structure of the ocean is of very great significance. However, whatever variability occurs at depth, it is the surface variables of temperature and velocity and of salinity and dissolved gases which control the exchange of energy and matter between the ocean and the atmosphere;

(ii) EO platforms are poor at resolving high frequency time variability at a given location due to discrete overpasses once or twice every day, or every several days. Any process occurring in less than a few days is not resolved by most sensors;
(iii) EO sensors operating in the visible and infra-red part of the spectrum are unable to penetrate the cloud which in some locations for much of the time obscures the sea-surface;
(iv) EO satellites only measure a limited subset of variables;
(vi) Remote sensing requires *in situ* observations for calibration of satellite sensors.

1.7.1 Oceanographic variables and processes measurable from space

The idea that the oceans could be observed from space was first proposed and developed in the mid-1960s. The "modern era" of oceanographic remote sensing was perhaps born in 1978 when three highly successful satellites were launched: the short-lived SEASAT satellite (with a wide array of sensors including an altimeter, a scatterometer, a scanning multichannel microwave radiometer and a *Synthetic Aperture Radar*, SAR), Nimbus-7 (with the *Coastal Zone Colour Scanner*, CZCS) and TIROS-N (carrying the *Very High Resolution Radiometer*, VHRR) (Pearce & Pattiaratchi, 1997). To a large extent, today's satellite measurements of the ocean derive from National Aeronautics and Space Administration's (NASA) 1978 SEASAT mission (Bernstein, 1982) and from NASA's NIMBUS-7 mission, also launched in 1978 and as of 1989.

Satellites used to monitor the oceans are mostly polar-orbiters, or rather orbit the earth at 800-1000 km over the poles with a revisit period of one to a few days, and generally have a high spatial resolution (small pixel size on the surface).

The range of oceanic variables measured from space is very wide including phytoplankton pigment concentration and suspended sediment, sea surface temperature, sea surface height, surface winds, ocean currents, and surface roughness.
There are four basic properties of the ocean which can be measured using the visible, infrared and microwave portions of the electromagnetic spectrum. These are:

• *ocean colour*, which is caused essentially by the presence and concentration of water constituents that cause the light to be absorbed or scattered. Ocean colour is used to measure the three optically influential substances: *chl*, suspended sediments and coloured dissolved organic matter (CDOM). Moreover, the term ocean colour includes the optical properties and those variables which describe the physical properties of the water column constituents, i.e. absorbance (a) and backscatter coefficients (b_b), beam attenuation coefficient (c) and the water colour are utilised to characterise optically the oceanic waters (Mobley, 1994). These variables are retrieved from the remote sensed data by calculating the capability of the water medium to absorb, to backscatter and attenuate the electromagnetic energy. These geophysical variables assists in the study of phytoplankton distribution, dispersion of river and outfall effluent plumes, upwelling regions and surface circulation patterns.
• *sea surface temperature*, which reveals surface circulation patterns including thermal fronts and upwelling zones.
• *sea surface elevation*, where microwave altimeters measure the distance between the satellite and the sea surface to study ocean circulation and tidal heights.
• *sea surface roughness*, showing surface waves and wind from backscatter caused by wind on the ocean surface and also information regarding natural slicks or anthropogenic spills.

Colour and temperature can be measured using passive techniques in which electromagnetic radiation emitted by (or reflected from) the water surface and the atmosphere is received at the satellite sensor.

The term *ocean colour* is used to denote the visible light spectrum as observed at the sea surface, it allows to discriminate between marine water types. Seawaters can be classified according to the kind of constituents determining their optical properties as "case 1" or "case 2" (Morel and Prieur, 1977). Case 1 waters are usually pelagic areas, and are optically dominated by biological components such as phytoplanktonic pigments (living phytoplankton cells, microscopic unicellular algae, in particular containing green chlorophyll like pigments). In Case 1 waters only phytoplankton pigments and associated substances should affect the $L_w(\lambda)$ spectrum (Morel, 1988). Case 2 waters contain Case 1 constituents plus multiple independent components such as materials introduced from outside the water column which also affect the optical

properties. Case 2 waters often occur in coastal zones with high coastal run off, where biological components are associated with suspended sediments, CDOM and other particulate or dissolved substances (Barale and Folving, 1996).

EO sensors designed to detect changes in the colour of the sea reveal patterns reflecting the concentration of phytoplankton and sediment carried within the surface layer. Nimbus-7 carried the first sensor for measuring ocean colour, the CZCS, which was designed in order to determine *chl* from space. This sensor operated successfully from 1978 to 1986, providing a long-term global data set. Using *in situ* measurements, scientists had been able to develop mathematical relationship between pigment and plankton chlorophyll (Gordon *et al.*, 1980). CZCS had a spatial resolution at nadir of 800 m and provided the first view of the distribution and the abundance of phytoplankton over the global oceans based on observations approaching synoptic sampling, and demonstrated the ability to monitor how these patterns change both in time and space. CZCS imagery had also allowed investigation of relatively small-scale features (1-10 km) like jet, eddies, current meanders and surface ring structures. These features changed completely the understanding of the ocean processes.

CZCS was replaced by the *Sea-viewing Wide Field-of-view Sensor* (SeaWiFS), launched by NASA in July 1997 and operational since September 1997, in order to provide quantitative data strategic to investigate the bio optical properties of the oceans and also their contribution to the global carbon cycle. Figure 1.7 shows the amplitude of space and time scale achieved for SeaWiFS that is a medium-resolution sensor with high sampling frequency.

The SeaWiFS mission aimed also to understand the functioning of the oceans. SeaWiFS imagery at a spatial resolution of 1.1 km gave scientists a high quality insight to biological processes occurring from local to global spatial scale (McClain *et al*., 2004) for more than 10 years.

The primary application of the SeaWiFS sensor has been the study of annual primary production and in particular the spatial and temporal distribution of phytoplankton blooms. These observations have highlighted, as Sverdrup (1953) hypothesised, the tight relation between biological processes such as productivity patterns and physical

processes via vertical water motion, mixing phenomena and current dynamics. Indeed, according to Siegel *et al*. (2004) SeaWiFS observations have highlighted how the oceanographic processes influenced ocean primary production and have shown also the global ocean at high temporal and spatial resolution. Moreover SeaWiFS provided a long data record on *chl* content and water leaving radiances ($L_w(\lambda)$) which are particularly important in biological and biogeochemical studies (Siegel *et al*., 2004).

Ocean colour data are thus extremely useful for the study of ocean productivity and global biochemistry. Knowledge of the seasonal cycle of phytoplankton occurring in the euphotic layer is crucial to understanding the ocean's contribution into the global carbon cycle. The seasonal cycle of phytoplankton stock variation is extremely difficult to map from research vessels, since data collected from ships are widely spaced (Fig. 1.6) and oceanographic features tend to change rapidly during sampling. By means of ocean colour sensor it first became possible to monitor synoptically the spatial and temporal distribution of the phytoplankton biomass. Seasonal comparisons of satellite observations made possible the correlation between production rates and *chl* developing models and algorithms. These algorithms have led to estimates of how much carbon is incorporated in organic matter, supplying biogeochemical transformation rate at large scale, and estimates of regional and total primary production rate (Miller, 2004). Traditional shipboard sampling techniques were inadequate to derive such estimates on a global scale. Understanding the distribution of phytoplankton biomass, which is the base of the marine food web, is critical both for marine ecology and fisheries science. Before the advent of the ocean colour sensors, De Vooys (1979) reported that there was a great uncertainty regarding the magnitude of oceanic production and the historical data sets did not permit reliable estimates of the large-scale temporal and spatial variability.

SST measurements derived from infra-red sensors have been available for more than three decades and have revealed a wealth of detail of ocean eddies/meanders, fronts, current systems, circulation patterns and upwelling zones which could not have been observed from surface vessels (Robinson, 1985, 2004). The measurement of SST patterns using EO sensors is valuable to the study of a wide range of dynamical processes that occur in the surface layers of the ocean. The temperature in the upper layer of the ocean is subject to radiative processes and both entering and outgoing

surface heat fluxes. SST distribution over a large scale therefore generally mirrors the subsurface thermal structure which is in turn linked with the ocean currents (Pearce & Pattiaratchi, 1997). SST patterns play a significant role with respect to the connections between physical, chemical and biological processes. Moreover, the ocean fronts represent boundaries between distinct water mass types across which the temperature and/or salinity show marked horizontal spatial gradients. Ocean fronts are extremely important to investigate primary productivity since in a frontal regime cooler, nutrient-rich water meets the warmer, less rich water. The location and seasonal variation of fronts have been systematically observed by means of satellite infra-red imagery over the last decade. NOAA-*Advanced Very High Resolution Radiometer* (AVHRR) also at a spatial resolution of 1.1 km (Fig. 1.8) imagery provided the first synoptic view of Gulf Stream eddies showing their formation, their life span and their fate (Brown and Evans, 1982; Brown e*t al*., 1985).

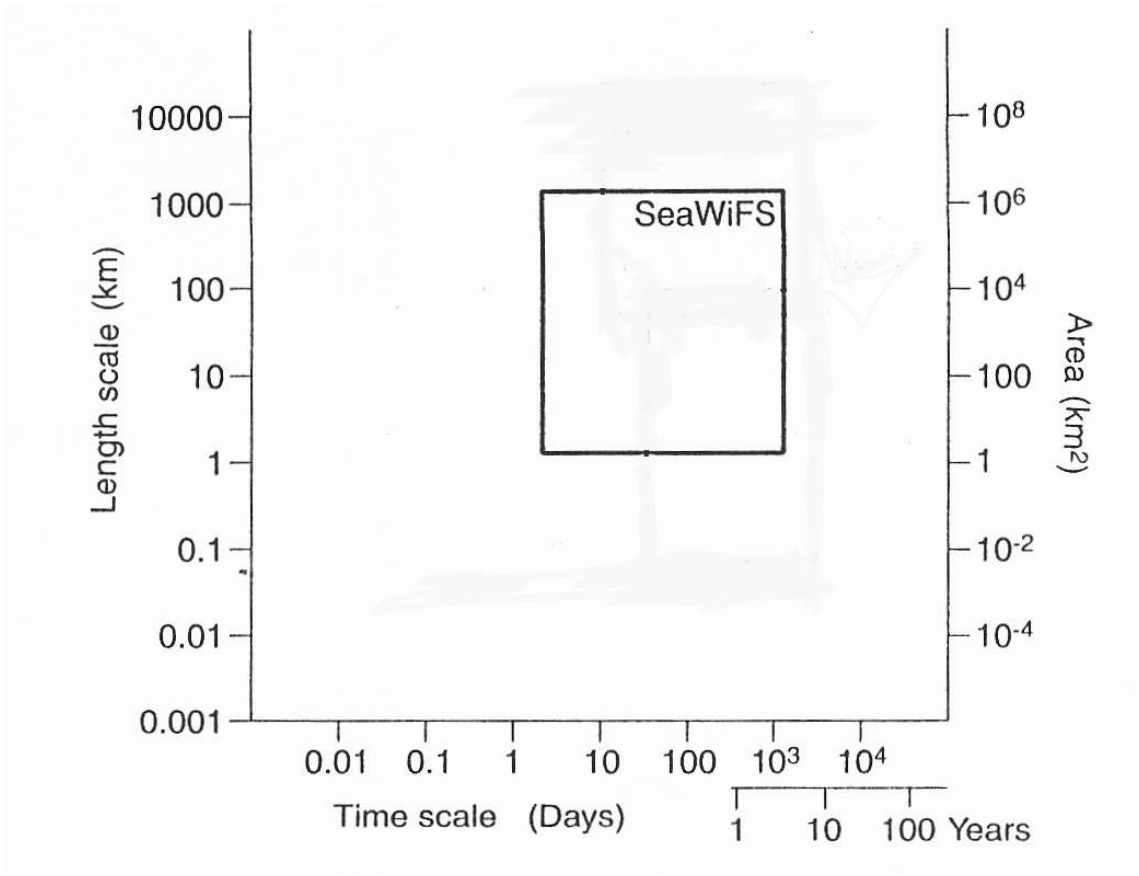

Fig. 1.7 Example of spatial and temporal characteristics of SeaWiFS sensor (Robinson, 2004).

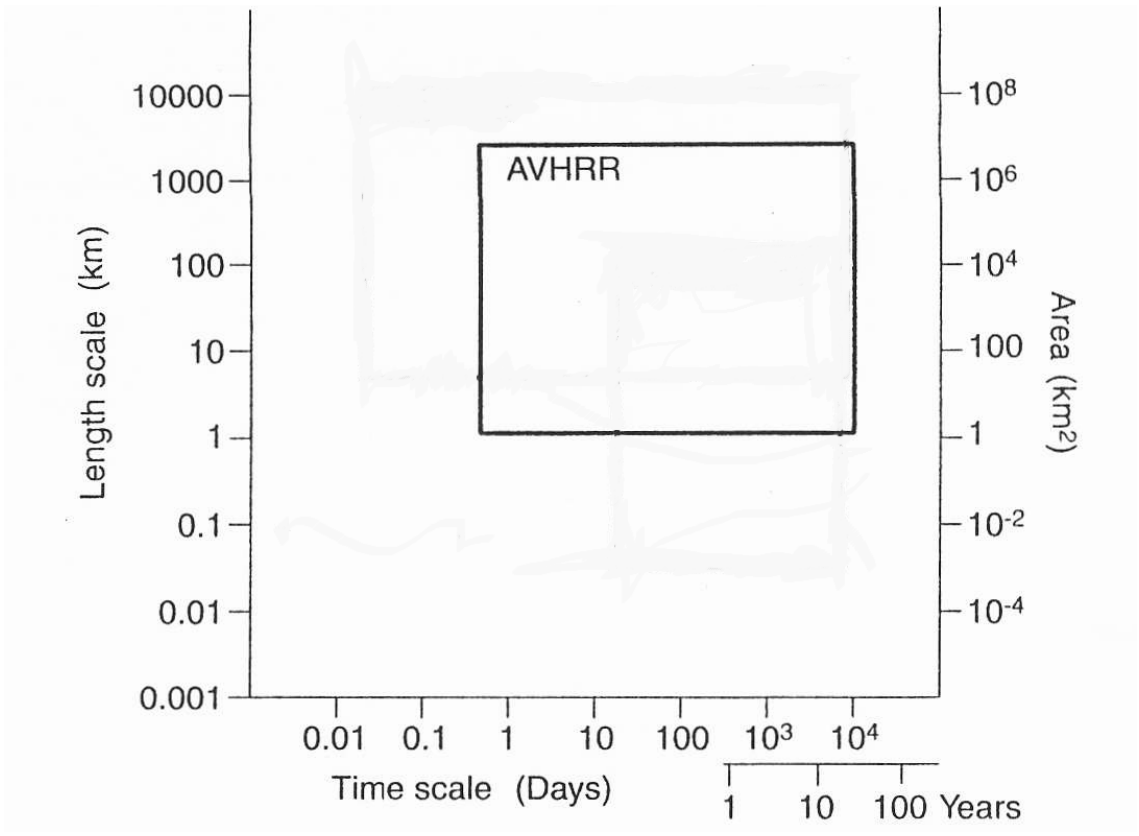

Fig. 1.8 Example of spatial and temporal characteristics of NOAA-AVHRR sensor (Robinson, 2004).

Table 1.6 shows the list of passive satellite platforms whose observations were used in the present thesis.

Table 1.6 List of satellite platforms used in the thesis (adapted from Schofield *et al*.2003).

Satellite/ Sensor	Nation/ Bands	Resolution (km)	Status
Orb-View SeaWiFS	USA 8	1.1	In orbit
ENVISAT MERIS	Europe 17	0.3-1.2	In orbit
NOAA AVHRR	USA 5	1.1	In orbit

During the last decades, the scientific community could have at their disposal observations retrieved by only a single satellite at a time. However this problem can now be partly overcome due to the increasing number of ocean colour and infrared satellites sensors in orbit. These now form a "constellation" of satellites which provide scientists with an exceptional amount of data. A particular area may thus be revisited by different sensors more than one time per day, leading to the possibility of monitoring changes in oceanic features at enhanced temporal scales. A further advantage lies in the different spectral and spatial resolution of the sensors. This capability is particularly useful in studying coastal waters where there is the need to monitor the biological phenomena at a small spatial scale and also to analyse the water optical signature, which can be determined with an enhanced degree of accuracy by means of an improved spectral-spatial resolution. The most recent passive sensor i.e. *Medium Resolution Imaging Spectrometer* (MERIS, European Space Agency) has a spatial resolution down to 300 m, permitting this new sensor to detect finer scale frontal features and plumes that occur in coastal zones (Table 1.6).

The new constellations of EO platforms have revolutionised the way of looking at the oceans, and have, to a large extent, replaced the earlier approach to observing the ocean by means of individual sensors. These might overcome the problems linked to the single measurements at a determined spatial and temporal scale.

1.7.2 Potential applications of satellite data to MPA monitoring

The coastal zone constitutes a particularly complex environment where the terrestrial and marine ecosystems interact. Remote sensing is considered to be strategic in the field of integrated coastal/marine environmental management (Barale and Folving, 1996). Its major contribution lies in the ability to extend observations beyond the domain of *in situ* sampling. Thereby RS in the marine environment has wide applications in littoral and shallow waters.

At present the major use of RS in coastal areas reported in literature relates to marine habitat mapping which enhances coastal planning and management (Salm *et al*., 2000). To date, RS and in particular airborne colour aerial photography have been widely used for mapping marine benthic communities in shallow coastal areas. Optical RS has been used in relatively shallow water for cartographic and bathymetric mapping.

Regarding the MPAs (coastal and pelagic) there is a need to control and monitor in a systematic way marine environmental conditions to achieve resources management based on specific information.

Traditional measurements collected at sea (from moored sensor arrays, by oceanographic campaigns or along shipping lanes) could not provide large-scale spatial coverage, but can provide only a discrete scientific description of marine ecosystems. As illustrated in §1.7, remote sensing represents a strategic supporting tool for MPAs due to its capability of comprehensively reading the marine environment through the observation and the integration of a conspicuous amount of data. RS has today an essential and unique role to provide effective monitoring of a specific area, i.e. continuous data collection and analysis.

The geophysical variables which could be taken into consideration as functional tools in monitoring and management the Marine Protected Areas are as follows:

(i) The *first class* (§1.7.1) of geophysical variables characterises the ecological state of the water and its constituents (e.g. plankton pigments, dissolved organic matter,

suspended inorganic sediments). The first class of variables could be retrieved by medium/low satellite sensors (spatial resolution of 300-1100 m) with the visible channels (Tassan, 1994). Direct use of these variables, or their interpretation, permits the investigation of phenomena such as water quality and phytoplankton blooms, primary productivity, bio-geochemical cycles, fluvial and coastal run off, sediment transport, water dynamics, exchanges between coastal zone and open sea, and climatic events (Barale, 1999). These variables represent the main indicators of coastal and pelagic waters. Consequently the measurement of ocean colour promises to become the major tool of environmental evaluation for the marine side of the coastal MPAs, the shelf/slope area, as well as for the high seas in general.

Moreover, studying the normalised water leaving radiances ($L_{wN}(\lambda)$) retrieved by hyperspectral optic remote sensed data, allows discrimination among different phytoplankton taxa and in the near future may permit photoautrophic organisms to be identified down to the *genus* (Millie *et al*., 1997; Schofield *et al*., 1999; Kirkpatrick *et al*. 2000).

The question of spatial and temporal resolution is particularly pertinent when observing MPAs. Moreover, it should be taken into consideration that spatial resolution is a key factor in deciding which sensor should be utilised to investigate biological oceanographic features within a MPA. Usually sensors at a spatial resolution of ~1 km are adequate in observing mesoscale regional processes (100s of km) whereas to investigate coastal local systems (micro scale processes, 10s of km) sensors such MODIS, MERIS and LANDSAT with a pixel size ranging from 300m to 30m are more appropriate. Figure 1.1 highlights the appropriate time and spatial scales for observations possible by means of satellite sensors.

(ii) The *second class* (§1.7.1) of geophysical variables includes SST which is an effective variable descriptive of a MPA. Thermal properties can be assessed by means of passive techniques sensitive to earth emissions in the thermal infrared or microwave part of the electromagnetic spectrum. Through the evaluation of thermal properties, one might derive important information of physical, dynamical or climatic nature. Indeed, the use of thermal sensors enables detection of fronts and upwelling, as well as location of surface slicks of certain kinds within the MPA waters. Usually thermal sensors have

a spatial resolution of ~1 km and are adequate in observing mesoscale regional processes (100s of km) occurring at basin scale and possibly affecting the MPA under investigation.

The design and management of MPAs is a developing field which encompasses both traditional approaches and newly available tools and techniques. Monitoring and management of MPAs needs, and gains advantage from, a higher degree of knowledge and information than ever before (Salm *et al*., 2000). MPAs have made explicit the necessity for both ecological studies at highly resolved spatial and temporal scales and an unprecedented level of understanding of coastal marine ecosystems. It could be asserted that the biology of marine ecosystems is poorly sampled at both spatial and temporal scales. Monthly sampling has been widespread, but at this scale is too coarse to elucidate for example the dynamics of phytoplankton blooms. Therefore it is essential to enhance by means of RS our capacity to describe accurately the biological marine dynamics which will allow us to enlarge our knowledge of the underlying processes. Such knowledge is the basis on which decisions concerning types and levels of use of marine resources are made. This knowledge will be reflected also in improved sampling design, which can be carried out at pertinent locations and times and will allow better understand of the variability of *in situ* measurements. Satellite remote sensors offer us the possibility of observing the biological features in a "non invasive" way (Schofield *et al*., 2003). Furthermore *in situ* campaigns, by their nature are labour intensive and expensive, particularly in marine environments. Satellite remote sensing is an alternative method which has demonstrated its effectiveness particularly for measurements of marine environmental variables and parameters. The use of RS has been steadily increasing in recent years, in terms of both the amount and range of applications as well as in the enhancement of methods and techniques (Robinson, 1985, 2004).

Remote sensed data could frame local data, or data collected *in situ* in a regional or basin perspective and compare them with historical data available, thus allowing an analysis of spatial and temporal variability of the MPA marine ecosystem. Investigating and integrating patterns of oceanographic features into MPA design might increase their efficacy. The design and management of a comprehensive monitoring programme should describe the state of the marine coastal ecosystems and the trends in its biology

and physics. As outlined in §1.7, the most up to date methodologies of marine environmental evaluation require an approach that integrates measurements. Remote sensors are essential to investigate dynamics occurring over regional and local scales and short time scales as part of such an approach. Indeed, typical environmental phenomena can affect entire marine regions over large spatial scales (from hundreds to thousands of km) and short time scales (from hours to days), and such processes are difficult to follow with *in situ* techniques. On the other hand, environmental variability reflects in sea surface features that show precise signatures, which can be best evaluated by orbital sensors (Barale, 1999). This capability qualifies RS as a powerful tool for investigating and observing oceanographic processes occurring on the sea surface and in proximity of the MPAs.

Having illustrated the potential of the passive sensors in monitoring coastal and pelagic areas, it is important to add that RS could be also helpful in protecting marine populations due to the open nature of marine systems and species. So far, MPAs have had insignificant influence on the protection of planktonic larvae and planktonic or pelagic adults. Understanding of the degree of dispersal patterns outside MPAs by means of remote sensors is essential to evaluate their effectiveness. In particular understanding of physical oceanographic processes and features such as currents, eddies and zones of mixing occurring onshore as well as fronts, could be strategic in the prediction of larval movement.

An MPA should take into consideration the dispersal of marine larvae (biological patterns) as well as oceanographic patterns (physical patterns) which are crucial processes to be considered while designing the objectives of any MPA (Carr & Reed, 1993; Roberts, 1997; Carr & Raimondi, 1999*a*; Planes *et al*., 2000). In particular marine biologists could profit from the contribution of enhanced understanding to investigate how coastal oceanographic dynamics cause connections between preserved marine populations (i.e. within protected areas) with unprotected populations outside (Carr, 2000).

Manca Zeichen *et al*. (2001), for example investigated the processes which determine coastal juvenile fish fauna settlement along a Mediterranean MPA, by means of integration and comparison among two different data sets such as *in situ* and retrieved

satellite SST skin. These authors showed the possible use of satellite data for predicting juveniles *Diplodus spp.* settlement in a coastal MPA.

There is a necessity for a strong interdisciplinary approach to the monitoring and management of coastal ecosystems. For MPAs to be effective, therefore, benthic ecologists, population geneticists, biological, chemical and physical oceanographers, need to work together to understand the linkages among biological and physical processes and marine communities. There is also the need for beginning integrated, multidisciplinary and monitoring programmes to define new, scientifically sound based for designing and planning of MPAs (Kelleher and Bleakely, 1994). To this purpose Boero *et al*. (1999) called for the adoption of a co-ordinated policy of protection of the marine ecosystems, which should allow a substantial network of MPAs to be built up that will work as sensors of environmental conditions.

Monitoring environmental conditions in MPAs by means of RS techniques will lead to a long-term data series and imagery archive, providing an ideal tool to evaluate at relatively low cost the impact of environmental changes. Moreover, *in situ* monitoring programmes of broad spatial scale and long duration, due to funding shortages, are often out of the reach of those charged with management of MPAs.

MPAs' design and efficacy can potentially be dramatically enhanced by better use of existing scientific methodologies. MPAs alone provide insufficient protection because they are not isolated from critical environmental changes. Marine communities located within MPAs are significantly subject to the highly variable oceanographic conditions of the water masses that continuously stream through them. Communities and ecosystems outside the MPAs should therefore be preserved, thus allowing the effectiveness of MPAs to be protected. Indeed currents have a strong influence on dispersal of both organisms and pollutants and thus have the potential for significant regional impact over local scale. The efficacy of MPAs in protecting marine populations is limited by large-scale oceanographic dynamics (e.g. hydrographic circulation patterns and episodic events) that ought to be tackled by conservation measures within and outside the protected areas (Allison *et al*., 1998); MPAs tend to preserve only marine communities within their boundaries. The most important reason that the biological

efficacy of MPAs is limited is that scales at which fundamental processes occur in marine systems are often much larger than the scales that reserves can embrace.

Another fundamental issue relevant to the design and consequent of effectiveness of MPAs is the occurrence of periodic climatic fluctuations that can bring ruin to marine populations within MPAs. The effects of the natural fluctuations on the MPAs should be investigated (Jones, 1994). Large-scale environmental events can change dominant hydrological patterns, water temperature and upwelling conditions, and subsequently modify the holopelagic and benthic communities. Since MPAs are usually intended to be permanent, their design must be effective under both extreme and moderate conditions (Allison *et al*., 1998). Therefore major efforts should be focused toward an improved understanding of fundamental oceanographic dynamics. Enhanced understanding of how large scale fluctuations have an effect on coastal ecosystems would also highlight how MPAs will respond to such effects. Forecasting those anomalies will ease the assessment of the efficacy of MPAs in the long term. It is critical that monitoring programs be designed to collect appropriate information in order to assess an MPA's effectiveness. Finally, long term monitoring of MPAs should be integrated with short term studies, this would produce a valuable insight to the bio-physical oceanography of the MPA.

Lourie and Vincent (2004) asserted that an improved knowledge, on a wide spatial framework, of linkages and magnitude of processes, is necessary to define conservation issues that guarantee the description and continued existence of species and habitats within marine ecosystems. Since scientific understanding of marine systems is rising rapidly also thanks in part to advances in remote sensing, such knowledge and techniques have important repercussions on planning of and for MPAs. Lourie and Vincent (2004) recommended investigating within biogeographic frameworks the processes that sustain species distributions to supply appropriate guidelines for current conservation.

1.7.3 Earth Observation Satellites for Mediterranean monitoring

Since 1998 the Mediterranean Sea was included in several environmental monitoring programmes such as the Global Monitoring for Environment and Security (GMES) and the Mediterranean ocean Forecasting System (MFS).

GMES, conceived by the European Space Agency (ESA), encompassed space, airborne and terrestrial sensors, aiming to achieve sustainable development and in particular look at global climate change and pollution. The scope of GMES and in particular one of its activities (Marine Environment and Security for the European Area; MERSEA) was to build up a European capability for the surveillance, monitoring and environmental predictions of physical, biogeochemical and ecosystem dynamics from global to regional scale (Zodiatis *et al*., 2003). In particular MERSEA (strand 1) aimed at coupling different satellite data archives with data collected *in situ* and environmental modelling (Johannessen *et al*., 2002). ESA is setting up the remote sensors to maintain a long term running GMES services (Liebig and Aschbacher, 2005).

Contemporaneous to the MERSEA project, the Mediterranean countries agreed to build up international activities to the observing, modelling and forecasting of Mediterranean Sea by means of long term operational oceanographic monitoring (Zodiatis *et al*., 2003). To this purpose, since 1999 the MFS has been developed including two major phases: Mediterranean Forecasting System Pilot Project (MFSPP), and Mediterranean Forecasting System Towards Environmental Predictions (MFSTEP) leading to the recently established Mediterranean Operational Oceanography Network (MOON), all within the framework of the European Global Ocean Observing System (EuroGOOS) activity. GOOS encompasses a network of remote platforms, *in situ* oceanographic systems, and a wide range of coastal and ocean predicting models, as well as an integrated data set coupling observing systems and models that supply updated oceanographic products to the user community (IOC, 1998). MFSPP aims to forecast the fluctuations of primary production at basin and local scale by means of progress and enhancement of the operational observation and prediction system in the Mediterranean Sea. This project incorporates a massive amount of information such as remote sensing

data, *in situ* observations collected by buoys and vessels, basin circulation and coastal oceanographic models and additionally ecosystem models (Pinardi *et al*., 2003).

MFSTEP, although basically the continuation of MFSPP, had as primary objectives the enhancement of the operational predicting and monitoring system in the Mediterranean region as well as the publicising of the strategic value and efficacy of the forecasting products to the end users (Pinardi and Coppini., 2010). The two phases of MFS started to supply the user community with predicted weekly data for SST, salinity, water currents, and sea level for the whole Mediterranean basin. This is being continued by MOON.

The continuous use of information collected by the outlined programmes could be crucial in understanding the key biological and physical processes which sustain the most valuable Mediterranean marine ecosystems that MPAs aim to protect.

CHAPTER 2

STUDY AREA SELECTION & METHODOLOGY

2.1 INTRODUCTION

This chapter illustrates the rationale for selecting the particular Mediterranean MPAs considered in this study, highlighting their characteristics in terms of physical and biological features. The MPAs were selected on the basis of their specific location within the Mediterranean basin. Since the majority of Mediterranean MPAs have been established on coastal habitats, the study sites identified were mainly coastal areas except the *Pelagos* International Sanctuary which lies in a pelagic area. The MPAs identified are mainly located in the Western Mediterranean Sea, which has as eastern border the line which links Cape Bon (Tunisia) with Cape Lilibeo (Sicily, Italy) (ICES, 2004), except the island of Malta, which lies within the Central Mediterranean Sea.
In this section the conclusive considerations of Lourie and Vincent (2004), stated in §1.7.2 i.e. to investigate the magnitude and the nature of the processes that sustain the habitats and species diversity in the Mediterranean MPAs, will be challenged expanded by highlighting not only the MPAs selected as test sites but also the oceanography of the sub-basin in which they are located.

Moreover, this chapter focuses on the methodological approach chosen to the monitoring of Mediterranean MPAs. In this context RS was selected as primary analysis tool in order to monitor the ecosystem functioning and to understand and define the main bio-physical processes that occur in the Mediterranean MPAs selected as test sites. The role of RS here is that of supplying a synoptic qualitative and quantitative assessment of the bio-physical variables which characterise the Mediterranean MPAs and mirror the oceanography of the basin in which they are located.

This investigation was carried out mainly by using data collected by the EO sensors. This section (§ 2.4) describes the satellite sensors selected in order to answer to the question about how can we improve our way of observing the Mediterranean MPAs in order to enhance the monitoring and consequently the protection regime. There will be

presented the characteristics of the passive sensors used and also examined the satellite imagery processing methodology in order to retrieve the geophysical parameters.

2.2 STUDY AREAS

2.2.1 Selection of study areas

In order to respond to the research question i.e. whether RS be successful in monitoring MPAs (§1.2.1) an analysis of the oceanographic regimes and dynamics of the Mediterranean basin was previously performed in order to select the MPAs to investigate. Since the general aim is to explore RS and applications to Mediterranean MPAs, it is crucial to verify if and how RS works for MPAs that are broadly representative of sites already designated MPAs or likely to become MPAs. There were selected a range of areas types that tests the approach presenting different features and attributes to highlight limits or opportunity.

The defined criteria for study area selection were the following:

1. The oceanographic regime and dynamics of the Mediterranean sub basins in which the MPAs are located;
2. The biological processes characterising the sub-basin i.e. the spatial and temporal scale of chlorophyll variability;
3. The presence of key habitat and protected species in the MPA i.e. for coastal MPAs *Posidonia oceanica* meadows, hard bottom biocoenoses, *Laminaria spp*. beds and for pelagic MPA the presence of cetaceans.

Two coastal MPAs were selected in sub basins characterised by intense cyclogenetic activities which cause marked algal blooms. The coastal Italian MPA was selected because it houses rocky bottoms biocoenoses with high species diversity. Hence, it has been designated *Long Term Ecological Research Network Site* (LTER) and for this reason *in situ* data sets were available. These data were particularly useful in testing the

accuracy of a high resolution ocean colour sensor. The second coastal MPA was selected because it is located in a sub-basin subject to the entrance of the Atlantic water into the Mediterranean Sea. Its sea beds are characterised by the brown algae *Laminaria rodriguezii*.

The third coastal MPA was chosen because it lies in an oligotrophic basin and shows low biodiversity with the exception of the *Posidonia oceanica* meadows. In particular it was selected to test the validity and the possible limitations of ocean colour data in identifying trends of the biological processes in MPAs showing very low chlorophyll concentrations.

The only high sea MPA is extremely interesting due to the presence of high pelagic species diversity i.e. in particular cetaceans. It was chosen because is the only pelagic MPA in the Mediterranean basin and it presents a recurrent phytoplankton bloom which show among the highest chlorophyll concentrations of the Mediterranean Sea. The study of this geophysical parameter enables to define its seasonal and interannual pattern.

The sub-basins selected were the Ligurian-Provençal Sea, the Alboran Sea and the Central Mediterranean Sea (Fig. 2.1).

The western basin includes the Ligurian-Provençal Sea and the Alboran Sea. The Ligurian-Provençal Sea basin hosts the Portofino MPA and the *Pelagos* International Sanctuary and has a pronounced offshore seasonal phytoplankton bloom (Barale *et al*., 2008). The Alboran Sea hosts the Al Hoceima National Park and was selected due to its oceanographic features such as the gyre system generated by the entrance of the Atlantic water into the Mediterranean basin. The last MPA selected lies within the Central Mediterranean Sea, notable for not only the oligotrophy of this sub-basin but also for the role of this eco-region in the water mass exchange between the western and eastern sub-basins across the Strait of Sicily (Sorgente *et al*., 2003).
As stated above, all the four areas selected are located in a particular basin showing different oceanographic features (Fig. 2.1).

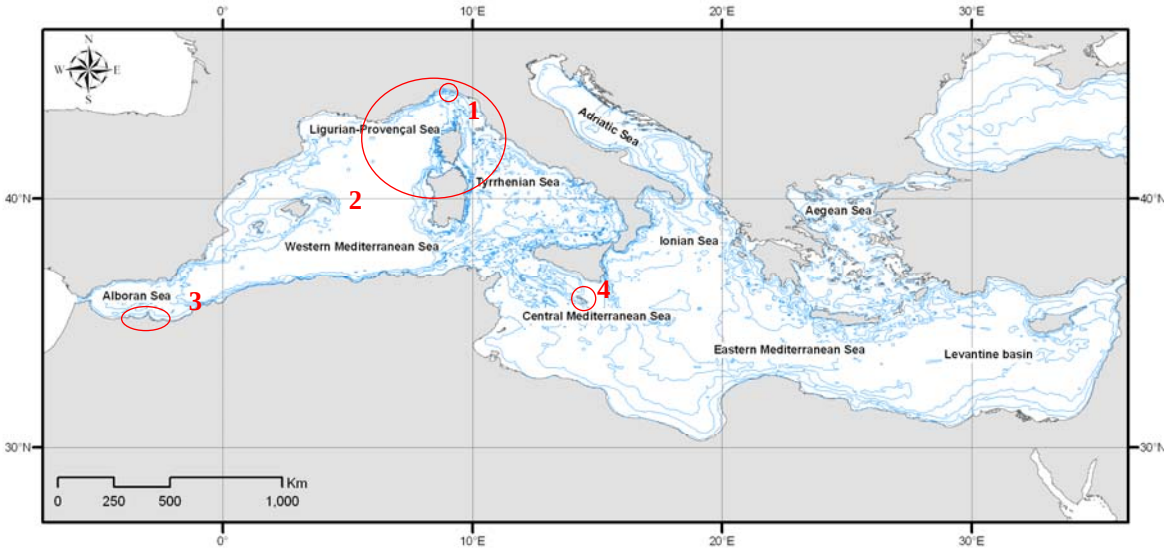

Fig. 2.1 Mediterranean Sea, highlighting the nomenclature of the main seas and the study sites selected. 1. Portofino MPA, 2. *Pelagos* International Sanctuary, 3. Al Hoceima National Park and 4. Malta island (USGS Map 1:250.000).

The Portofino MPA is encompassed within the Thyrrenian Sea which lies between Italy and the islands of Sardinia and Corsica and in particular within the northern section of the Tyrrhenian Sea (the Ligurian Sea).

The *Pelagos* Sanctuary lies in part within the Ligurian Sea, but it extends over the west within the so-called Ligurian-Provençal Sea. The latter is located on the western side of Sardinia and Corsica and is delimited on the eastern margin by the Corsica channel (between Corsica and the Elba island) that divides it from the Tyrrhenian Sea. It encompasses the Ligurian Sea and the Gulf of Lion and extends over a region of about 1.52×10^{11} km^2 (Astraldi *et al*., 1994). The Ligurian-Provençal Sea has two major rivers which flow into it, the Rhone in France and the Ebro in Spain. The continental shelf in this region is quite shallow with several submerged canyons, apart from the river deltas, particularly that of Ebro's river which stretches for about 100 km off shore (Batisse and de Grissac, 1995).

The Al Hoceima National Park lies within the Alboran Sea, located on the eastern section of the Gibraltar Strait, between the coasts of Spain and Morocco. This basin is subject to the Atlantic water flowing into the Mediterranean through the Gibraltar Strait.

The last area selected was the north western Maltese area of Rdum Majjesa and Ras Raheb. This is the only site selected which lies on the Central Mediterranean Sea. In particular the island of Malta is situated on a shallow shelf, the Malta-Ragusa rise, part of the submarine ridge which extends from Ragusa peninsula of Sicily southward to the African coast of Libya.

2.2.1.1 Portofino Marine Protected Area

The National Portofino MPA is located along the north-western Italian coast and is facing the Ligurian Sea. It covers 13 km of coast line and 346 ha of surface and is characterised by a very low population density. In 1935 a terrestrial part of the Portofino Promontory was declared protected area. The Portofino MPA was incorporated on the list of marine reserves in 1982 by the Italian Merchant Marine Ministry, through Law 979/82 (Law for the Protection of the Sea). The law 394/91 on Natural Protected Areas confirmed the designation, however the official establishment of an MPA surrounding the peninsula occurred in 1999 by ministerial decree.

Portofino MPA lies in the middle of one the most densely-populated coastal regions of the north-western Mediterranean, characterised by many activities such as shipbuilding industries, mariculture, fishing, nautical and underwater tourism (Tunesi and Diviacco, 1993; Salmona and Verardi 2001). The Portofino MPA encompasses a stretch coast of about 13 km facing the Ligurian Sea (Fig. 2.2a). This area is notable both for its environmental importance, in particular for its coastal and marine ecosystem, and also for its tourist economical value. In figure 2.2b is shown the MPA's zoning.

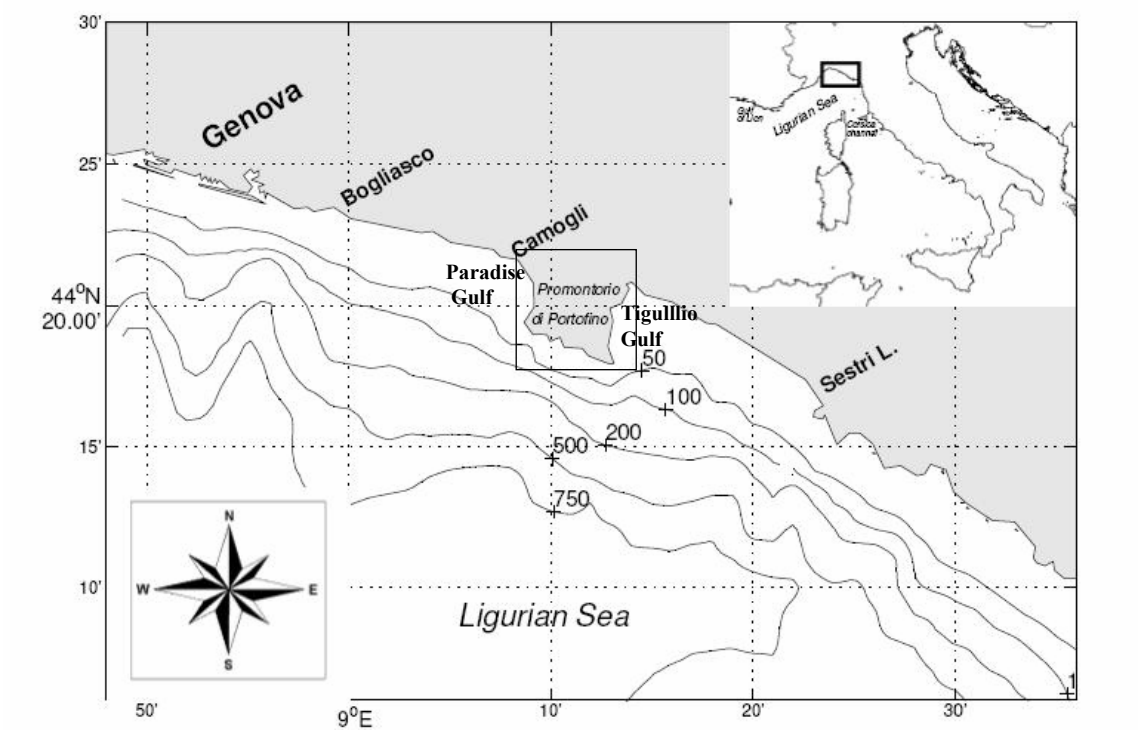

a)

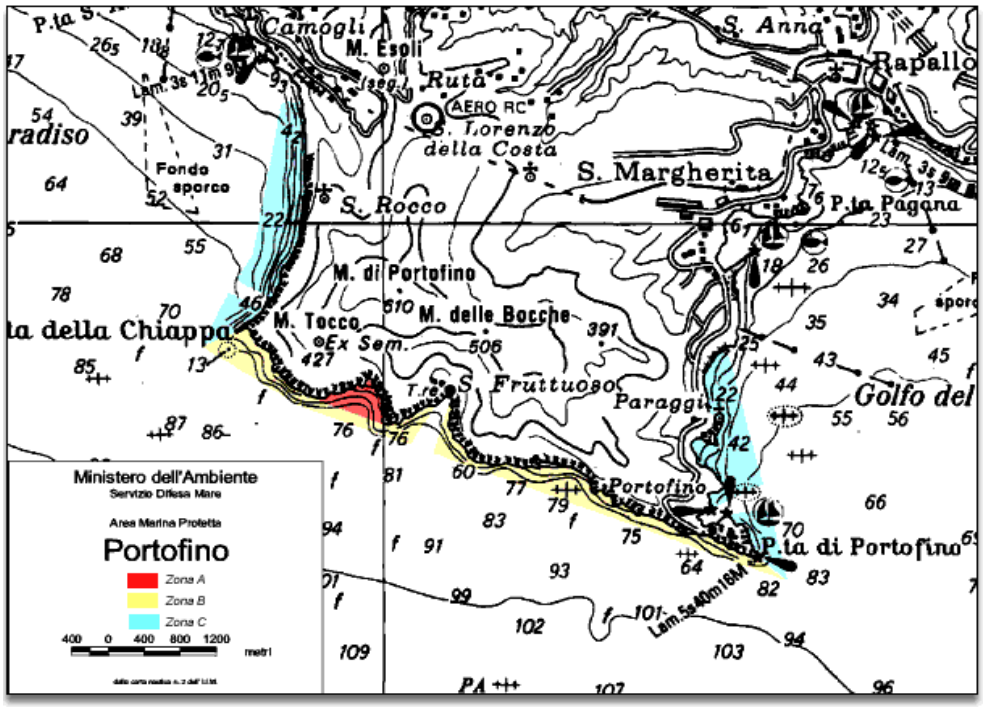

b)

Fig. 2.2 a) Portofino MPA highlighted in the rectangle encompassing the Portofino Promontory (Doglioli, 2004), b) Portofino MPA zoning (in red zone A, in yellow zone B and in light blue zone C) (courtesy of the Italian Environmental and Conservation Territory Ministry).

The Portofino Promontory is characterised by a hilly (maximum height 610 m) coastline which plunges abruptly into the sea (Fig. 2.3). This stretch of coast is characterised by a

narrow continental shelf with a very steep slope, deepening from 50 to 500 m in a few km. Along this coast, the abrupt headland of the Portofino Promontory extends into the sea for more than 4 kilometres, with a roughly rectangular shape. The southern side of this Promontory is characterised by submerged and very steep cliffs, while the western and eastern sides descend more gradually. The geomorphological features and the hydrodynamic conditions favour the development of a rich and very diverse environment (Cattaneo Vietti *et al*. 1982; Salmona and Verardi 2001). In particular the coast is characterised by small submarine caves and canyons. The submerged cliffs and ravines of the Portofino Promontory, generating different seabed habitats, host an abundant and diverse fauna and flora and consequently a high level of marine biodiversity. The rocky shore of the southern slope of the promontory associated with the particular oceanographic conditions has allowed the settlement of a typical Mediterranean habitat, a rich and diversified coral biocoenosis. This habitat is between 30 to 50 m in depth, and is dominated by horny corals, sponges, Madreporaria and Bryozoa. Portofino houses the red coral (*Coralllium rubrum*) which is particularly threatened because it is a species of commercial interest and was included in the Barcelona (1976) and Bern (1979) Conventions which aim to protect the biodiversity in the Mediterranean Sea.

The western and eastern slopes of the promontory are sandy and host sea grass (*Posidonia oceanica*) meadows (Salmona and Verardi, 2001). The eastern slopes are degrading more gradually and are particularly important for sea grass. This plant, as previously highlighted, has a great ecological value in the Mediterranean sea, since it consolidates the seabed, defends the shores from erosion, houses a rich fauna, and provides food and nursery areas.

In 2007 Portofino MPA was recognised as Long Term Ecological Research Network Site (LTER) in 2007 (Castellano *et al*., 2008). The Italian Portofino MPA can be considered as a pilot coastal area to acquire long-term observations of the ecosystem dynamic, which could help the MPA management body to improve the marine environmental quality and evaluate the efficacy of the management within the MPA's boundaries (Cattaneo-Vietti and Tunesi, 2007).

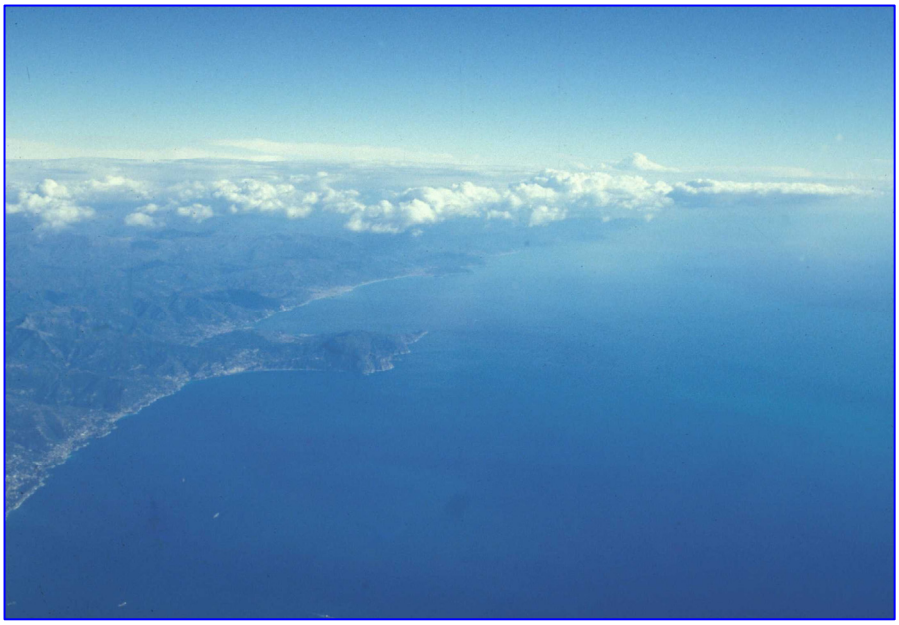

Fig. 2.3 Portofino Promontory and the neighbouring stretch of coast from an aerial view (courtesy of Dr. L. Tunesi).

2.2.1.2 *Pelagos* International Sanctuary

The *Pelagos* Sanctuary is defined to the west by a line extending from the tip of the Giens Peninsula on the western coast of France (43°01'70"N, 6°05'90"E), towards Cape Falcone in northwestern Sardinia (40°58'00"N, 8°12'00"E), and from Cape Ferro in north-eastern Sardinia (41°09'18"N, 009°31'18"E) towards Fosso Chiarone on the western coast of Italy (42°21'24"N, 11°31'00"E) (Fig. 2.4).

The motivations for the creation of this Mediterranean sanctuary (§1.6.2) are linked to information obtained from research activities conducted since the late 1980s. Observations indicated the presence of notable cetacean concentrations within this area coupled with a conspicuous variety of pelagic macrofauna populations such as tuna, swordfish, sunfish, shark and giant devilray, thus representing a high degree of marine diversity.

Fig. 2.4 *Pelagos* Sanctuary (highlighted in dark blue). The flags highlight the ground border points (courtesy of the Italian Environment and Territory Conservation Ministry).

Populations of striped dolphins (*Stenella coeruleoalba*), sperm whales (*Physeter macrocephalus*) and fin whales (*Balaenoptera physalus*) are abundant within the Sanctuary (Gordon *et al*., 2000; Clark, 2002). Also pelagic species such as Cuvier's beaked whale (*Ziphius cavirostris*), the long-finned pilot whale (*Globicefala melas*), Risso's dolphin (*Grampus griseus*), the common dolphin (*Delphinus delphis*), and the coastal bottlenose dolphin (*Tursiops truncatus*) occur frequently in the *Pelagos* Sanctuary (Notarbartolo di Sciara, 1994) (Table 2.1). The above mentioned species are endangered by floating nets which can cause entanglement, pollution, and also prey depletion due to overfishing (Aguilar, 2000; Gordon *et al*., 2000). According to Berube *et al*. (1998), the dolphin populations monitored within the *Pelagos* sanctuary can consist of several tens of thousands individuals, whereas whales (e.g. *Balaenoptera physalus*) can achieve one thousand individuals.

Table 2.1 Cetacean species presence in the Western Mediterranean Sea as reported in literature (adapted from Notarbartolo di Sciara , 2002).

Cetacean species found in the Sanctuary	**Data on population estimates and genetics**	**References**
Balaenoptera physalus Fin whale	Approximately 1000 individuals in the Sanctuary, of which 350 have been identified. Population estimate in the western Mediterranean is >3,500 individuals Mediterranean population is genetically isolated from Atlantic conspecifics	Berube *et al*., 1998. Forcada *et al*., 1995 ; 1996. Zanardelli *et al*., 1998.
Stenella coeruleoalba Striped dolphin	Approximately 25,000 individuals in the Sanctuary. Recent estimates 13,000 individuals. Mediterranean population (>126,000) is likely to be reproductively isolated from Atlantic conspecifics	Forcada and Hammond, 1998. Lauriano *et al*., 2009. Garcia-Martinez *et al*., 1999.
Physeter catodon Sperm whale	Present at low densities within the Sanctuary Population of Mediterranean sperm whales is isolated form the Atlantic population.	Pavan *et al*., 2000. Gordon *et al*., 2000.
Tursiops truncatus Bottlenose dolphin	Present in the Sanctuary throughout the continental shelf (but rare off Liguria). No population estimate exists for the Mediterranean sea	
Delphinus delphis Short-beaked common dolphin	Very rare, but present throughout the Sanctuary Population estimate in the south-western Alboran Sea is 15,000 individuals	Forcada, 1995.
Grampus griseus Risso's dolphin	300 photoidentified and currently resighted individuals in the Sanctuary	Airoldi *et al*., 1999.
Globicephala melas Pilot whale	Intermittently present in the Sanctuary's offshore waters.	
Ziphius cavirostris Cuvier's beaked whale	Present in the Sanctuary, and regularly sighted in specific locations (e.g., off Imperia).	

Oceanography of the Ligurian-Provençal Sea The Ligurian-Provençal basin (Fig. 2.5) is characterised by a significant volcanic activity still in action (Batisse and de Grissac, 1995). The sheer coasts were generated by the tectonic movements which had thrown up the Alps. The Ligurian-Provençal Sea is influenced by severe seasonal atmospheric conditions in winter, caused by cold-dry northerly-western winds such as the Mistral and Tramontana. These winds induce strong air-sea interaction processes that cause water evaporation and heat loss. Those processes induce the surface layer to

become dense enough to sink, producing the Deep Water Formation (DWF) particularly in the Gulf of Lion region (Gascard, 1978) (Fig. 2.5), and to generate a cyclonic gyre (Bunker, 1972).

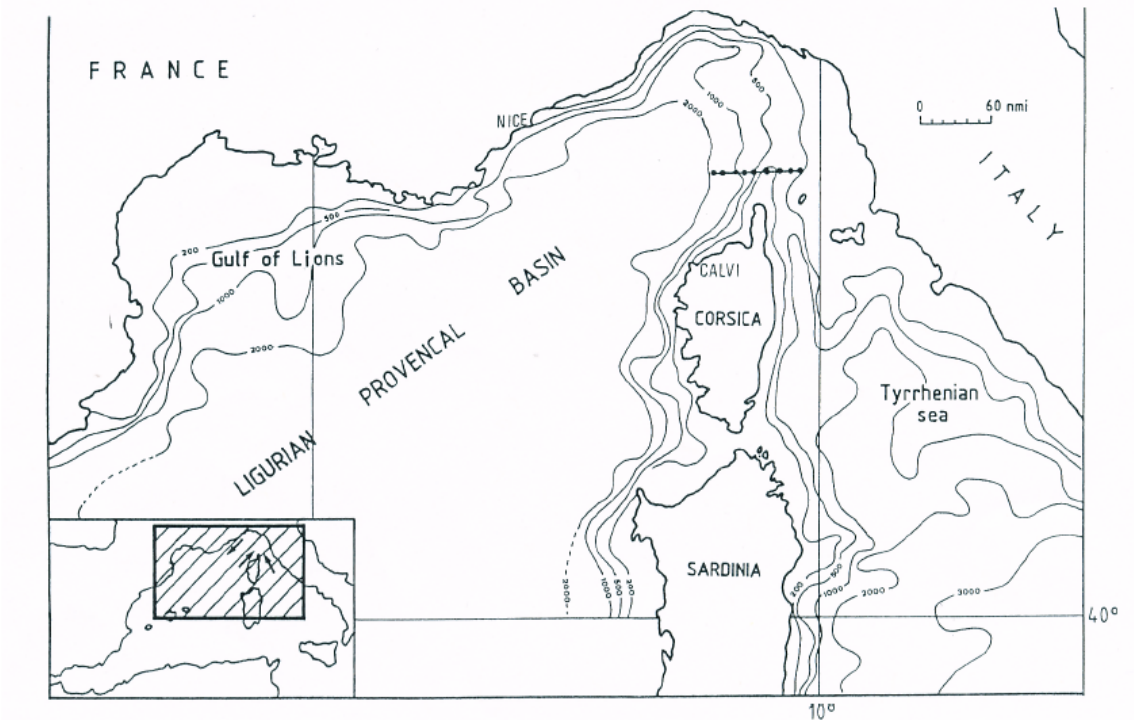

Fig. 2.5 The Ligurian-Provençal Sea (Astraldi *et al*., 1995).

General Circulation The general circulation within Ligurian-Provençal Sea follows a cyclonic gyre (Fig. 2.6), due to the presence of baric depressions which produce an intensification of the coastal currents towards the west. This vortex has an elliptic shape with the major axis oriented NE/SW (Astraldi and Gasparini, 1984; Manzella, 1983; Stocchino and Testoni, 1977; Papa, 1980). The gyre is always present throughout the year and shows a seasonal cycle; its extension and intensity are related to the seasonal variations of the atmospheric forcing (Esposito and Manzella, 1982). The Ligurian coastal circulation is part of the general cyclonic circulation of the Western Mediterranean Sea and the external limit of this current is similar to an Atlantic current with the internal part constituted by eastern waters (Molcard *et al*. 2002). This hydrodynamic feature involves the two main Mediterranean water masses i.e. the surface water of the Modified Atlantic Water (MAW) and the Levantine Intermediate Water (LIW) below. In the coastal area, water coming from both the western (West Corsica Current, WCC) and eastern (Tyrrhenian Current) sides of Corsica join together in the north of the island in the so-called Ligurian coastal current that flows westwards

alongshore roughly following the bathymetry as far as the Gulf of Lion and the Catalan Sea (Astraldi and Gasparini, 1986; Astraldi *et al*., 1994) (Fig. 2.6). In winter the flow in the Corsica channel increases whereas the flow on the western side of Corsica remains steady during the whole year (Astraldi and Gasparini, 1986; Buffoni *et al*., 1997).

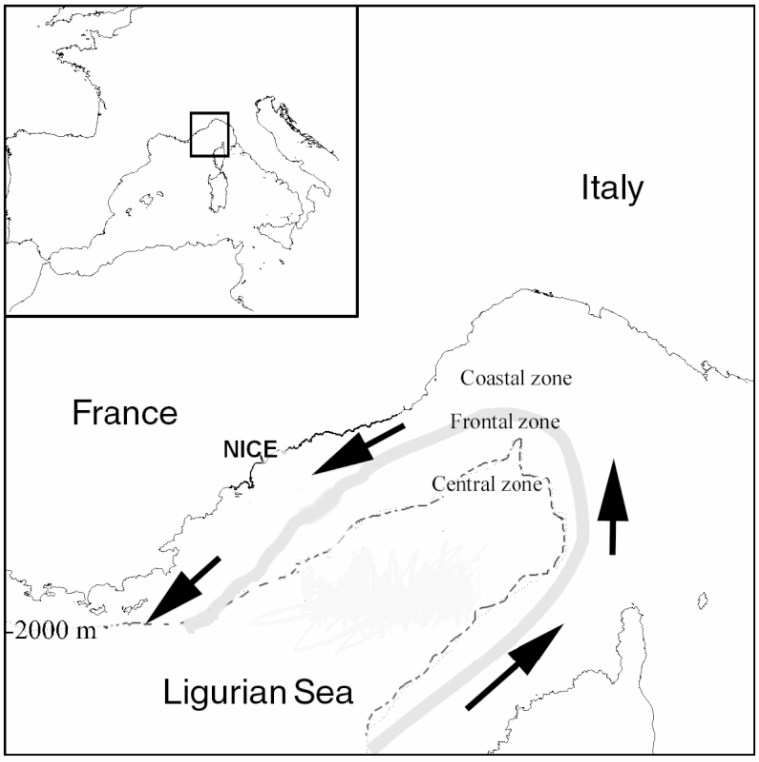

Fig. 2.6 Surficial currents circulation scheme within Ligurian-Provençal Sea (Tamburini *et al*., 2003).

The study of the hydrological data retrieved by several *in situ* campaigns has allowed a general framework of the movement of the water masses to be described. Studies have highlighted on a large scale the trend and the interaction of the main currents flowing within Ligurian Sea (Hela, 1963; De Maio *et al*., 1975; Stocchino and Testoni, 1977). The main current comes from east and pushes the surficial waters toward the west with a mean speed from 0.25 to 0.4 ms^{-1}. At depths of about 1000 m, this current maintains the same direction but has a much lower speed of around 0.05 ms^{-1}. A branch of this current, at the latitude of Hyères islands, runs toward the south then bends toward the east as far as the coast of Corsica island. Here, after following the coastal profile, it interacts with a Tyrrhenic current originating from S/SE which goes between Corsica island and Capraia island (Corsica channel), forming a new current which moves North (Fig. 2.6). In proximity to the coast, in particular on a line with Portofino Promontory, this current generates a coastal anticyclonic current directed towards the east (Dagnino,

1978). The resulting circulation along the Portofino MPA (Fig. 2.2) is in the general north-west direction, following the coast, with only short periods of reversal associated with northerly winds. The profiles of temperature and salinity within the Eastern Ligurian shelf show that the stratification starts in May and lasts until October. From November to April the thermocline is generally absent (Astraldi and Manzella, 1983; Astraldi and Gasparini, 1986).

The very narrow continental shelf, in combination with the Portofino Promontory, produces a tunnel effect of the north-west coastal current, which flows approximately along isobaths and follows the narrow shelf. This effect increases significantly the current dynamics of the area. Furthermore, the deep sea dynamics can interact with the coastal current. The water masses present in the area, besides being influenced by the presence of the coast, are modified by the open sea conditions (Doglioli *et al*., 2004). Moreover, the Paradiso Gulf (Fig. 2.2) time series of *in situ* measurements (SIAM database) has demonstrated the presence of an anticyclonic eddy with intensity ~10% of the incoming shelf current and with extension <15 km (Doglioli *et al*., 2004), associated with an eastward counter current in the lee of the cape. This eddy seems to persist in the winter period.

The coasts which surround the *Pelagos* Sanctuary are mostly rocky; only the eastern coasts of Corsica and Tuscany are plains with sandy beaches. Within the *Pelagos* Sanctuary there are some islands such as Corsica and the northern part of Sardinia (Fig. 2.5), Hyères Isles, Port-Cros, the Ligurian Isles, the Tuscan archipelago and the islands of the Bonifacio strait. The continental shelf is quite narrow along the rocky shores and widens along the plains of Tuscany and Corsica.

The bathymetry of the Corsican-Provençal basin ranges from depths of 2,500 m to 2,700 m. The rocky coasts have submarine canyons and caves which generate particular geomorphological as well as hydrological features. These geomorphological characteristics house a variety of habitats and biocenotic assemblages.

The hydrological features are generated by the physical processes occurring within the basin which form vertical front systems, thus allowing the nutrients to come up to the surface and underpin primary production. The cyclonic Ligurian current which, together

with the permanent front, is the prevailing current within the sanctuary favours the occurrence of high rates of primary production within the region encompassing Corso-Ligurian Basin and the Gulf of Lion (Jacques, 1990), thus allowing a rich pelagic biodiversity. Such productivity maintains high mesopelagic zooplankton biomass consisting mainly of *Meganyctiphanes norvegica*, the krill that is seasonally abundant and on which Mediterranean fin whales feed (Orsi Relini *et al.*, 1998).

2.2.1.3 Al Hoceima National Park

The National Park of Al Hoceima is a terrestrial park that faces the Alboran Sea and extends over approximately 40 km of coast; it lies nearby the town of Al Hoceima and is 150 km east of the Gibraltar Strait (Fig. 2.7). This coastal National Park (without the peripheral marine and terrestrial zone) extends from Pointe Boussekur to Cala Iris (Fig. 2.8) and covers a total surface of 308 km^2 (285 km^2 of terrestrial area and 23 km^2 of marine area). It encompasses a variety of habitats of a very high biological value. The dominant features within the National Park are the stretches of extremely wild rocky coast. The calcareous coastal massif of Bokkoya, which is the most notable geomorphological feature of this coast, juts out the sea forming cliffs of more than 600 m in height. These calcareous cliffs form steep overhangs interspersed with rock slides and small pebbles beaches.

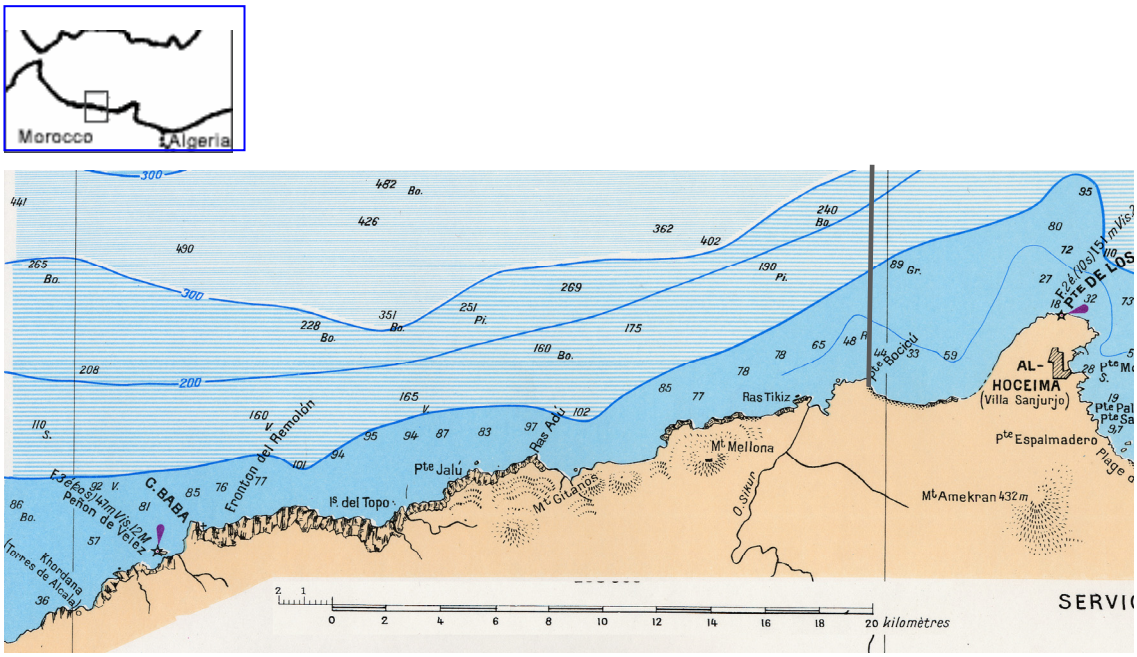

Fig. 2.7 Al Hoceima National Park (Morocco) (scale 1:203000) (French Navy Hydrographic Service, Paris, 1964). The western border (Pointe Boussekur) is shown on the right whereas the eastern border (Cala Iris) is off the map.

The marine species inhabiting the Al Hoceima National Park waters are influenced by the entering of the MAW into the Mediterranean Sea through the Gibraltar Strait and therefore have two origins. In particular the presence of marine flora as *Laminaria rodreguizii* characterises this area. The fish fauna shows a high biodiversity, this area hosting more than 100 species and being used for spawning and as a nursery area. The Park waters host also the red coral (*Corallium rubrum*) on the rocky substrates as well as the vulnerable giant bivalve species *Patella ferruginea*. The area also hosts sporadically the Mediterranean Monk Seal (*Monachus monachus*). Several authors have reported the presence of monk seal during recent decades between the area of coast extending from Al Hoceima to Cap des Trois Fourches (Avella & Gonzalez, 1984; Bayed & Beaubrun, 1987), despite Aguilar (1998) having stated that the monk seal population in this area may consist of few (approximately 10) individuals. At present there are not specimens resident in this area, however some specimens have been sighted along the Park's coast.

The other notable feature of the National Park is the rich avifauna with roughly 80 species, including osprey (*Pandion halieatus*), Audouins's gull (*Larus audouini*), white-eyed gull (*Larus cachinans*), Bonelli's eagle and golden eagle.

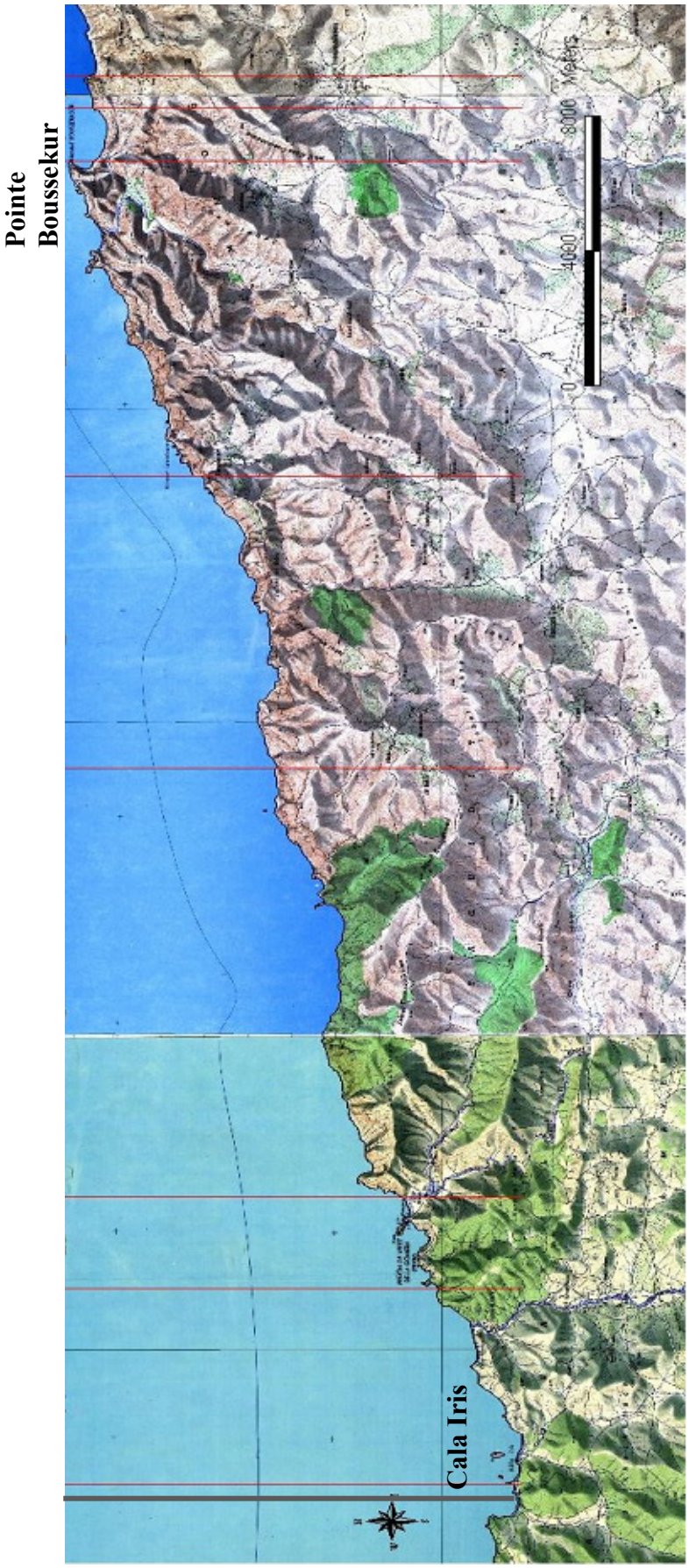

Fig. 2.8 Al Hoceima National Park (Morocco) (scale 1:50000, Conic Conform Lambert Projection of North Morocco) (Moroccan Military Geographic Institute, the map is a merging of three maps Al-Hoceima, 1970; Rouadi, 1970; Beniboufrah, 1968) (courtesy of the Park authority). The merged map shows the eastern (Cala Iris) and the western coastal borders (Pointe Boussekur) of the Park.

Oceanography of the Alboran Sea The Gibraltar Strait is the "highway" where the exchanges between the Atlantic oceanic waters and Mediterranean waters occur (Bayed, 1991). The mean depth of the Alboran basin is around 1500 m (Miller, 1983). The MAW, which is lighter than the Mediterranean water, flows in the surface and passes through the Gibraltar Strait which is 13 km wide and 300 m deep. The amount of the MAW water mass is estimated to be around 53.0 10^{12} m^3 per annum (Béthoux, 1980). Its salinity is about 36.15-36.18 psu, and the annual mean is about 36.6 psu (Lacombe *et al.,* 1981; Béthoux, 1980; Lacombe et Richez, 1982), whereas its SST ranges from 17°C in March to 21° in August (Lacombe et Richez, 1982). In contrast, the Mediterranean water flows from the western basin towards the Atlantic, following the bottom of the Gibraltar Strait. The amount of this water mass is of the same quantity as the Atlantic one, and is estimated around 50.5 10^{12} m^3 p.a. by Béthoux (1980). The salinity of this Mediterranean water is estimated to range from 37.9 to 38.4 psu (Béthoux, 1980) and its SST is around 13.3°C (Lacombe and Richez, 1982).

General Circulation The major surface current within the Mediterranean is the flow of water from Atlantic Ocean towards the east through the Gibraltar Strait. The density differences between western Mediterranean basin, Atlantic basin and eastern Mediterranean cause the transport of water through the Gibraltar and Sicilian Straits and contribute to the formation of an anticyclonic circulation of the surficial and intermediate water masses in the whole western basin (Lacombe and Tchernia, 1972; Millot, 1991, 1999). This system is one of the main circulation "engines" in the Mediterranean due to the fact that evaporation losses are higher than water gains due to precipitation, river run-off and exchanges with the Black Sea. In the western basin this fresh water debit (i.e. gain in salinity) leads to a transformation of the Atlantic water mass into a more saline and denser form and is also responsible for the upstream across the Gibraltar strait, which tends to restore the thermohalin balance of each basin (Ovchinnikov, 1974). The second "engine" responsible for the circulation and the water masses modification in the western Mediterranean Sea is the wind.

The east to west water flow system which exits the Mediterranean is not a surface stream, but an intermediate and deep water which overpass the Gibraltar Strait and re-emerges into the Atlantic (Batisse, de Grissac, 1995). Thus, the western Mediterranean

is characterised by at least four water masses of different origin and with specific behaviour.

The first one is the surface the MAW which occupies the upper 200-300 m in the Alboran Sea and which is formed in the Strait of Gibraltar. At medium depth flows the LIW between 400 and 700-800 m formed at the Strait of Sicily and underneath the Western Mediterranean Deep Water (WMDW) between 800 and 3000 m formed in winter in the North-western Mediterranean. At the bottom, over 3000 m has been observed the Bottom Water (BW) which is formed in the North-western Mediterranean (La Violette, 1994). Sometimes it is possible to add a fifth water mass, located between the LIW and the WMDW, the Winter Intermediate Water (WIW).

The seasonal temperature cycle is accentuated by the MAW (Sparnocchia *et al.,* 1994; MEDATLAS Consortium, 1997), which penetrates into the Mediterranean basin at the surface through the Gibraltar Strait. This circulation is due more to the difference in salinity between the Atlantic water and Mediterranean water (Tintoré *et al.,* 1988; Perkins and Pistek, 1990) than to the wind effect. The MAW layer is 200-300 m deep and circulates mainly along coastal zones from the west to the east then again towards the north in an anticyclonic gyre within the western Mediterranean basin (Fig. 2.9 and 2.10). After having crossed the Gibraltar Strait, the MAW forms two anticyclonic gyres within the Alboran Sea (Lanoix, 1974; Gascard et Richez, 1985) (Fig. 2.9). The western gyre is almost always present whereas the eastern is occasional (Millot, 1991) (Fig. 2.10). Satellite imagery shows that these two gyres swing over a period of some weeks (Heburn and La Violette, 1990).

On its passage, the MAW is subjected to evaporation and it mixes with the deeper water layers, which change its characteristics and increase its salinity and density. Within the Gibraltar strait its salinity is about 36.6 psu but this increases to 38.3 psu within the Sicilian strait (Lacombe et Richez, 1982), rising to 39.5 psu in the Eastern basin (Batisse, de Grissac, 1995).

Offshore from the National Park, general water circulation corresponds to the south branch of the anticyclonic gyre orientated west-east (Lacombe & Richez, 1982; Herburn & La Violette, 1990) (Fig. 2.9).

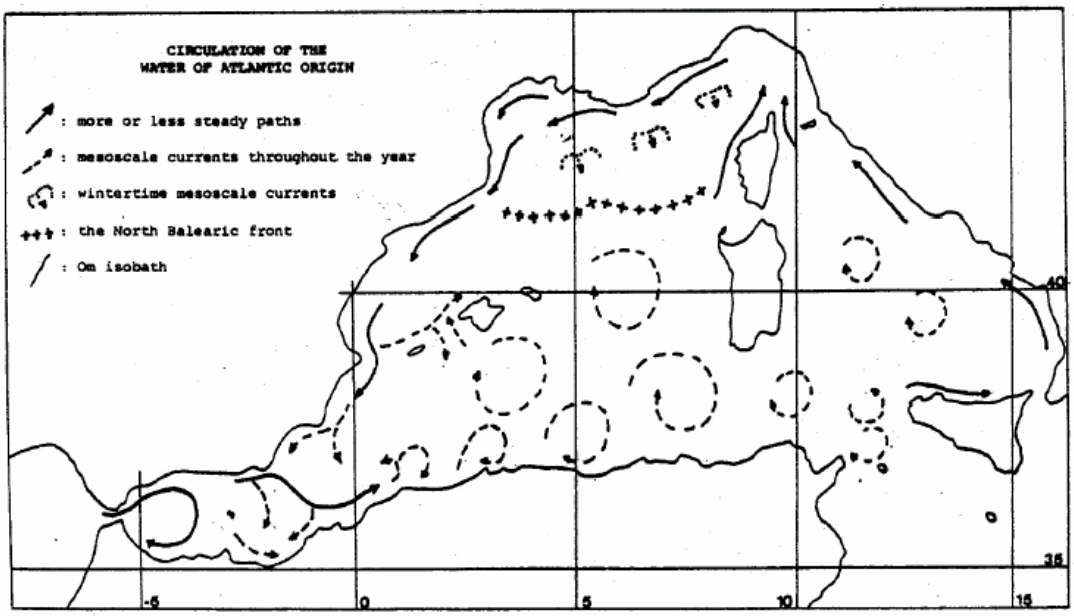

Fig. 2.9 MAW circulation (Millot, 1990)

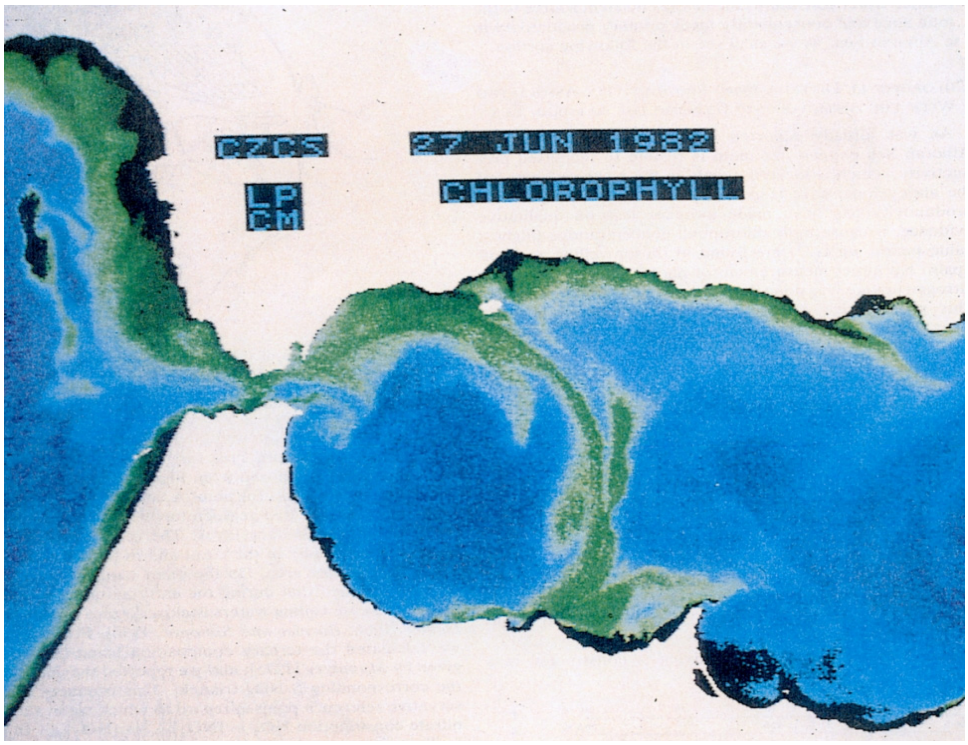

Fig. 2.10 Behaviour of the Atlantic Water entering the Gibraltar Strait, the satellite image (CZCS) highlights the chlorophyll –*a* rich waters (in green) (Jacques et Tréguer, 1986).

2.2.1.4 Rdum Majjesa and Ras ir-Raheb MPA (NW Malta)

The Maltese Archipelago is a group of small low islands located in the Central Mediterranean sea (Fig. 2.11) at a distance of about 96 km from Sicily and 296 km from the Tunisian coast. The archipelago is made up of three main inhabited islands (Malta, Gozo and Comino) together with several uninhabited islets (Mifsud *et al*., 2003). Generally the Maltese archipelago is characterised by a southwest to northeast inclination, with the north-eastern sides of the main islands gently sloping, and the western and southern coastlines essentially characterised by steep cliffs.

This MPA supports a representative selection of all major biotopes occurring around the Maltese islands. The study area is of high environmental, scientific, cultural and economic relevance. Moreover, the significance and importance of the marine environment within this region is complementary to its terrestrial counterpart since the adjacent coastal zones have a high scientific, cultural and economic value. This MPA extends along approximately 11 km of coast oriented from north to south on the north western shore of the island of Malta; its outer boundary follows the 50m depth contour (Fig. 2.11).

The coastline of Maltese Islands is shaped by the geological structure of limestone features. Upper coralline limestone formation and blue clay slopes dominate the north western coastline. The major characteristic feature of the study area is the *rdum*, a special kind of marine cliff related to a specific geological structure prone to mass movement. These feature form when marls of blue clay crop out at sea level and are overlaid with the massive strata of the Upper Coralline Limestone.

The study area is outstanding for the heterogeneity of its seabed geomorphology. The heterogeneous nature of the seabed supports a rich and diverse flora and fauna. Five main biotic assemblages characterise the area: (1) those on hard substrata characterised by photophilic algae (*Cystoseira spinosa*) and at greater depths communities of sciaphilous algae (*Dictyopteris poliploides, Cystoseira squarrosa*, *Sargassum vulgare* and *S. acinarium*), (2) *Posidonia oceanica* and *Cymodocea nodosa* meadows, (3) fine sands which support bivalve molluscs populations, (4) coarse sands, (5) stones and pebbles (CAMP, 2002). *Posidonia oceanica* extends as the dominant species over large

areas of the seabed and supports several demersal fish species as well as the protected bivalve *Pinna nobilis*. Seagrass meadows occur on sand as well as on bedrock, and extend along the whole area continuously. The *Posidonia* meadows support also cephalopods and demersal fishes (UNEP, MAP, RAC/SPA, 2003).

In the area there is a community of arbuscular rhodolites (calcified red algae) found elsewhere on the European and Atlantic coasts subjected to strong tidal currents; in the Mediterranean the association is commonly described as free living melobesia. The Loggerhead turtle *Caretta caretta* also occurs in the study area but does not breed within the study area borders.

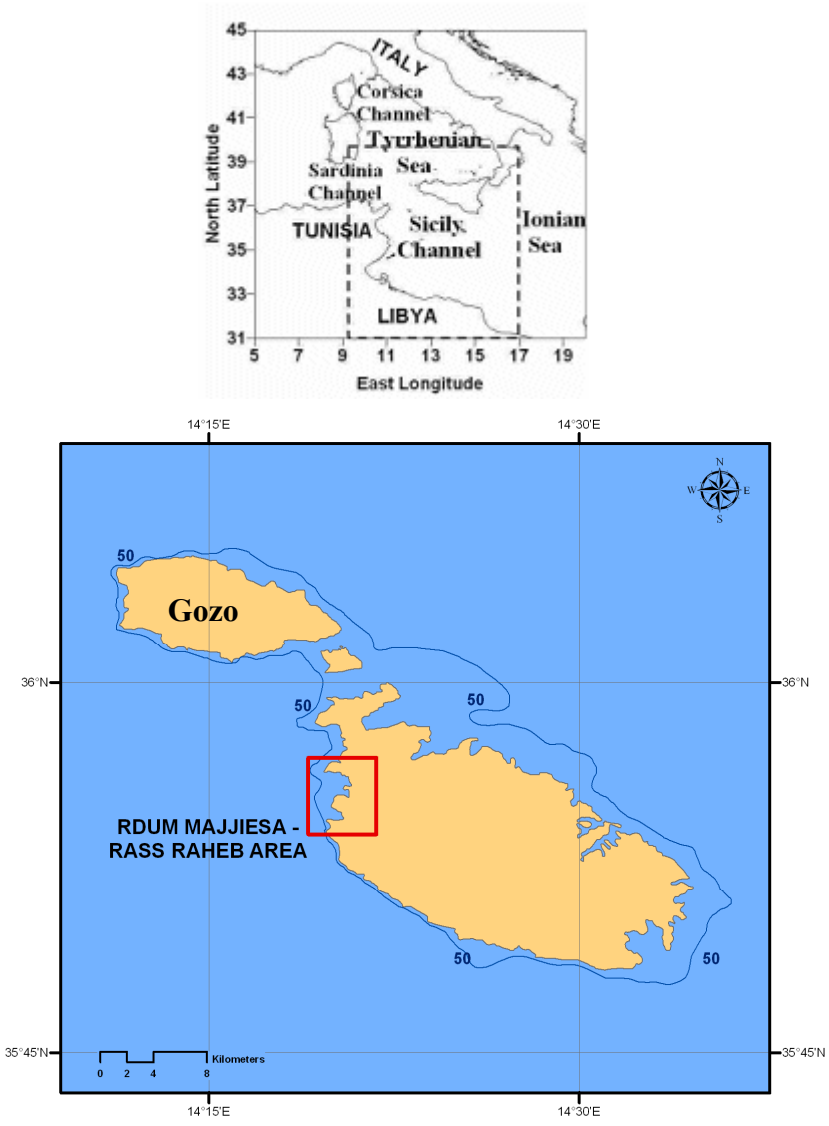

Fig. 2.11 The Maltese Archipelago with the Rdum Majjesa and Ras ir-Raheb MPA highlighted (NW Malta) and the 50 m depth contour (Geographic Projection, WGS84).

Oceanography of the Central Mediterranean Sea The Central Mediterranean area encompasses the Sicilian Channel and is a large and dynamically active area which links the eastern and the western Mediterranean sub-basins across the shallow sill at the Strait of Sicily (Fig. 2.12). This region plays an important role in the water mass exchange between the two sub-basins. The strait at the western end between Sicily and Tunisia (Sicilian Channel) is 150 km wide and is mostly shallow (200 m). However there are two narrow channels (sill systems) which are the main exchange route for the LIW between the eastern and western Mediterranean sub-basins. The first sill has a depth of 365 m whereas the second sill is deeper at around 430 m. Both sills are oriented toward north. The eastern end is over 500 km wide, encompassing the Malta channel on the north between Sicily and Malta and on the south the wide opening between Malta and Libya (Fig. 2.12) (Manzella, 1994).

There are mainly two-layer flows through the Strait of Sicily with the surficial fresher eastward flow of the MAW (in the upper 200 m) under which there is a deeper salty westward flow of LIW which crosses the Strait before entering the Tyrrhenian Sea (Sorgente *et al*., 2003). This LIW mass is formed as the result of the winter winds which causes the evaporation processes. The water masses thus sink after being becoming saltier and denser. MAW and LIW flows are characterised by a significant seasonal and interannual variability.

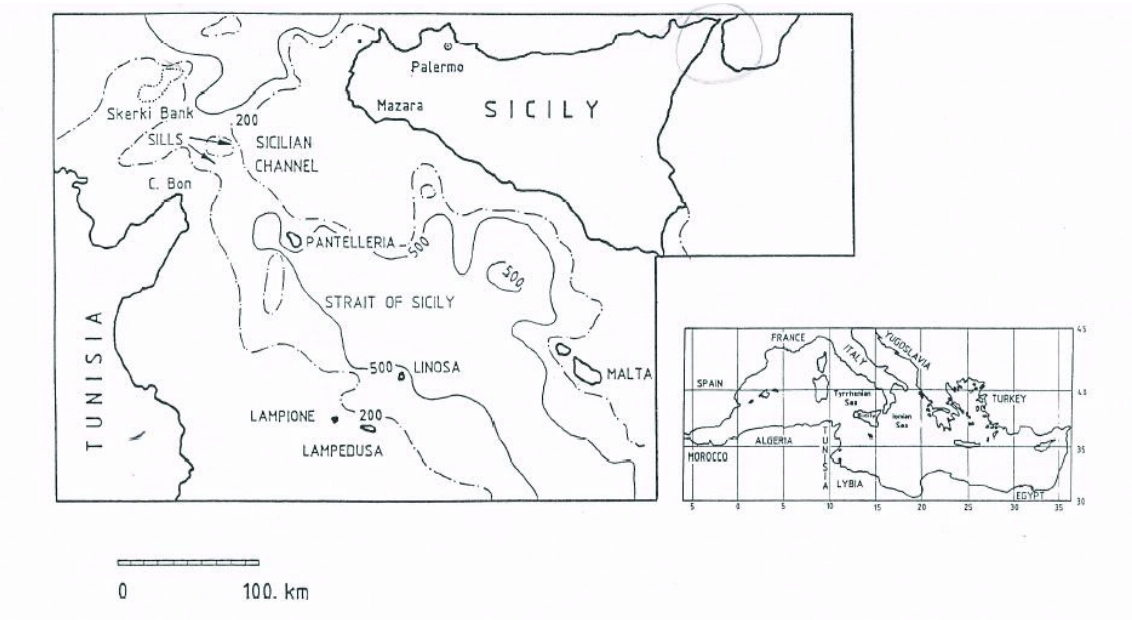

Fig. 2.12 The Strait of Sicily and the Mediterranean basin (Manzella, 1994).

General circulation The circulation in the area is mainly driven by the general flow in the Sicilian channel (Fig. 2.12). The MAW entering from the Atlantic through the Gibraltar Strait becomes saltier and warmer flowing along the African coast towards the east (Warn-Varnas *et al*., 1999). According to Morel (1972), the MAW shows a quite stable salinity, ranging from 37 psu (winter) to 37.5 psu (summer). There are three branches of the MAW, the first of which enters the Tyrrhenian Sea flowing along the northern Sicilian coast. The other two MAW branches flow towards the eastern basin through the Sicilian channel across the large gap between Sicily and Tunisia (Astraldi *et al*., 1999). The main flows occur along the Tunisian coast whereas the other flux flows along the southern Sicilian shelf forming the northern meandering Atlantic Ionian Stream (AIS) across the Malta channel. This current flows southeast-wards and turns back northward around Malta exhibiting small vortices (Drago *et al*., 2003).

The LIW, as stated above, is being formed in the north-eastern Levantine basin in winter due to the cooling and evaporation processes. The LIW, which flows in the opposite direction to the MAW, moves from the east and enters the Strait of Sicily through the quite large and deep passage between Sicily and Libya mainly at the Medina sill, located to the southeast of Malta (Manzella, 1994). LIW penetrates over the western basin across the Strait of Sicily and the Sicily channel at an intermediate depth. The LIW shows a salinity that does not vary seasonally (Morel, 1972; Manzella, 1994) and is persistently 38.74-38.75 psu (Warn-Varnas *et al*., 1999). When the LIW enters the Tyrrhenian Sea it mixes with the upper and lower waters, becoming saltier, and it then flows along the Italian coast (Sparnocchia *et al*., 1999). The LIW flux is not constant throughout the year but it is subject to seasonal variability, the winter flux being 2-3 times higher than that of summer (Manzella *et al*., 1988).

Between the surficial water (MAW) and intermediate water (LIW) there is a third and seasonally variable transitional layer flowing between these two water masses (Morel, 1972; Manzella *et al*., 1988; Sparnocchia *et al*., 1994). During winter, the surface water being colder, the density difference between MAW and LIW and thus the transition layer thickness is at minimum due to the mixing processes occurring in that season which cause a saltier surface water. On the other hand, during summer the water column is more stable due to the stratification and a well-defined thermocline forms, temperature steeply decreasing with depth. This causes the formation of a transition

layer with a maximum thickness due also to the lack of vertical mixing in this season (Manzella, 1994).

2.3 OVERVIEW AND COMPARISON OF STUDY AREAS

The Mediterranean MPAs were selected taking into consideration the different oceanographic regimes and dynamics of the Mediterranean sub-basins in which they are located. The Mediterranean sub-basins present different circulation pattern; the sub-basins with energetic circulation show higher chlorophyll concentrations. Seasonal chlorophyll cycle within each sub-basin have different timing and intensity in response to local physical events.

The marked features among the study sites lie essentially in the distinctive physical processes occurring which drive the biological processes and in particular the spatial and temporal scales of chlorophyll (*ch*l) variability which leads to the primary production variability. Indeed, c*hl* is a measure of the photosynthetic capacity and consequently represents an estimate of plant biomass (Miller, 2004).

Usually a basin it is defined oligotrophic if *chl* is lower than 0.1 mg m^{-3}, mesotrophic if *chl* ranges from 0.1 to 1.0 mg m^{-3} and eutrophic if *chl* is higher than 1.0 mg m^{-3} (Colella, 2006). Mediterranean is one of the most oligotrophic sea in the world due to the fact that nutrients are scarce (Batisse and Grissac, 1995); the Mediterranean *chl* levels usually range from 0.01 to 5 mg m^{-3}. Nevertheless, the Mediterranean Sea shows marked seasonal increases of surficial biomass and values higher than 5 mg m^{-3} may be recorded in upwelling areas or at the river deltas.

The western Mediterranean is characterised by small to medium scale physical processes (<10 km), these local regional forcing influence the biological response, consequent phytoplankton growth and the chlorophyll distribution (Arnone, 1994). The highest biological production within the Western Mediterranean is recorded along the coasts of the Ligurian-Provençal Sea and in the Alboran Sea. In the Ligurian- Provençal Sea the cyclonic current and wind (e.g. Mistral) events favour the formation of large

eddies (Morel and Andre, 1991). These cause vertical mixing processes which allow the deep water rich in nutrients to reach the surface and these upwelling processes trigger the biological production. Hence, as result of the enhancement of nutrients at the surface corresponds an enhanced chlorophyll concentration.

Alboran Sea shows energetic advective upwelling events and consequent horizontal and vertical nutrient fluxes that cause an increased chlorophyll concentration (Arnone, 1994). The Atlantic water enters the Mediterranean and causes the formation of an anticyclonic gyre and a flow of deep-intermediate water rich in nutrients towards the Atlantic which enhance the potential for primary production. In the sites surficial *chl* may achieve 5 mg m^{-3} during late winter-spring.

The lowest biological production has been recorded within the Eastern basin (Batisse and Grissac, 1995) and in a particular within the Ionian and Levantine basins. However, when MAW encounters the warmer Ionian Sea it produces the Maltese front, which, produces coastal upwelling along the southern coast of Sicily that could extend far offshore on the Malta platform (Drago *et al*., 2003).

Despite the fact that the MPAs selected house high biological diversity, it should be taken into account that the study sites follow the biodiversity gradient typical of the Mediterranean Sea, showing a decreasing diversity from the north towards the south and from the west towards the east (Batisse and Grissac, 1995).

Table 2.2 shows the key attributes of the sub-basins where the MPAs are located resuming how they compare and differ.

Table 2.2 Key features of the Mediterranean sub-basins and of the MPAs. The ranking for habitat and species diversity spans from 1 (minimum diversity) to 4 (maximum diversity).

MPA	Sub-basin	Cyclogenetic Activity	Upwelling events	Oligotrophic conditions	Habitat diversity	Species diversity
Portofino	Ligurian-Provençal	X			4	4
Pelagos Sancuary	Ligurian-Provençal	X	X		2	4
Al Hoceima	Alboran	X	X		3	2
Rdum Majjesa and Ras ir-Raheb	Central Meiterranean			X	1	2

2.4 SATELLITE DATA ACQUISITION

In order to detect the main biophysical parameters driving the MPAs considered, data retrieved by remote passive sensors were utilised. In particular were chosen optical sensors i.e. SeaWiFS (NASA), MERIS (ESA), and also the thermal sensor i.e. AVHRR (NOAA).

Satellite ocean colour data has been used to provide unique and important information on surface phytoplankton distribution (e.g. chlorophyll). Chlorophyll (C_{sat}) average concentration "seen" by remote sensors is correlated with phytoplankton biomass in the water column, the layer which contributes to the colour of ocean surface can reach a depth of 30 m or deeper for clear water.

SeaWiFS data were selected due to their easy availability at no cost and to their spatial resolution of 1.1 km which allows monitoring phytoplankton dynamics from regional down to local scale. This sensor is specifically designed to allow the retrieval of the *chl*, which represents the light-absorbing photosynthetic pigments.

SeaWiFS has a temporal resolution of 2 days (although a given target can be imaged daily, in different parts of the scan), a scan width of 58.3°, a scan coverage of 2,800 km, a nominal resolution of 1.13 km at nadir, and a tilt capability between –20° and +20°. The sensor detects 8 bands of the visible and near infrared parts of the electromagnetic spectrum (400-700 nm) (Appendix 1). The original data acquired from the Goddard Space Flight Centre (NASA) were Level 1A (L1A) data in High Resolution Picture

Transmission (HRPT) format, stored in Hierarchical Data Format (HDF). L1A products contain all the raw Level 0 data (raw radiance counts from all bands plus spacecraft and instrument telemetry) with calibration and navigation data appended (Feldman, 2003). These data were converted to Level 2 (L2) geophysical products, including *chl*, by means of the algorithms set available in the SeaWiFS Data Analysis System (SeaDAS) software package (Fu *et al*., 1998), with additional modifications as described in Melin *et al*. (2000) and in Sturm and Zibordi (2002). Despite the fact that in the Mediterranean Sea ocean colour data are affected by calibration problems, SeaWiFS data were analysed in order to investigate the regional hydrological characteristics which persist along the study areas considered.

The nominal accuracy of ocean colour data in surface chlorophyll retrieval (case 1 waters) by means of standard bio-optical algorithms (OC4v4 for SeaWiFS and Algal_1 for MERIS) is ~35% on average when compared to *in situ* observations (D'Ortenzio *et al*., 2002; Claustre *et al*., 2002, Bosc *et al*., 2004; Colella 2006;Volpe *et al*., 2007). The bias is particularly relevant in the Mediterranean within the lower range of chlorophyll values, due to the fact that the chlorophyll distribution in the water column in the Mediterranean Sea is different to other sites. This would affect the attenuation of the light field in the water column and the interaction of light with the main water constituents (Colella, 2006). In addition, the presence of aerosol which has an anthropogenic (industrial) and natural (due to suspended Saharan dust) origins requires particular algorithms for the atmospheric corrections applied to ocean colour imagery of the Mediterranean Sea (Claustre *et al*., 2002).

By using the standard SeaWiFS algorithm (OC4*v*4), the more oligotrophic study areas selected will be more affected by the above mentioned bias. However, it should be noted that this thesis focuses on the seasonal and annual chlorophyll patterns within the study areas rather than on the retrieval of the absolute chlorophyll values. SeaWiFS maps were therefore processed and analysed in order to monitor *chl* and to document its space and time variability.

The second ocean colour sensor used was the ESA MERIS sensor aboard of ENVISAT 2 satellite. The sensor detects 15 bands encompassing the visible and the near infrared parts of the electromagnetic spectrum (Appendix 1). This sensor has two spatial

resolutions which span from 1200 m for the ocean down to 300m for coastal and land applications. MERIS has a swath width (scan coverage) of 1,150 km and it covers the earth globally every 3 days although, as SeaWiFS, a given target can be imaged daily, in different parts of the scan.

MERIS data were acquired at processing level 2 (L2) *chl* product (concentration of *chl*-like pigment in mg m^{-3} of water). Using the data browser (ESA archive) the daily cloud free full and reduced resolution images were selected contextually to the sampling campaigns carried out *in situ* during year 2004. Level 2 encompasses two chlorophyll products obtained by the use of two different algorithms so-called algal_1 and algal_2 respectively. These calculate differently the concentration of chlorophyll in mg m^{-3} of water with respect to the different types of water considered i.e. Case 1 and Case 2 waters (§1.7.1).

Colella (2006) reported that chlorophyll values measured with MERIS Algal_1 algorithm are markedly higher than that estimated with SeaWiFS (OC4v4). The Remote Sensing reflectance (R_{RS}) measured by MERIS is lower than that measured by SeaWiFS due to the different atmospheric correction applied, thus Algal_1 overestimates *chl* respect to SeaWiFS estimates.

In order to measure geophysical parameters such as the SST skin and detect the thermal variability, SST skin maps retrieved by the thermal sensor NOAA-AVHRR were processed and analysed. The AVHRR scanner detects 5 bands sensing in the visible, near-infrared and thermal infrared portions of the electromagnetic spectrum (Appendix 1). The AVHRR sensor shows the same spatial resolution of SeaWiFS i.e. 1.1 km and it has a scan coverage of 2900 km. The accuracy of SST skin observations is 0.1-0.2 K (Robinson, 2004).

2.4.1 Use of satellite data

In order to address the general questions highlighted in §1.2.1 and in particular to describe by means of different remote sensors the bio-physical processes that influence the MPAs, RS data sources for each experimental chapter were selected as follows.

In chapter 3 and 4 there were used ocean colour data at medium spatial resolution for each of the MPAs selected. Only in chapter 5 were higher spatial resolution ocean colour data utilised in order to compare these with the data collected *in situ*. The SST skin maps used in all of the MPAs selected were retrieved, as stated in §2.4, by the AVHRR thermal sensor.

In chapter 3 the SeaWiFS weekly averaged *chl* maps relative to the year 2002 were processed and analysed for each of the study sites. The focus here was primarily on spatial variations. These analyses were performed in order to understand what bio-physical factors were characterised and how they influence the test sites, thus allowing a comparison among the study sites.

SST skin maps were used to highlight the biophysical processes occurring within the test sites. Weekly means were used to compare SST skin maps with the SeaWiFS *chl* maps.

In chapter 4 a temporal analysis in the *Pelagos* Sanctuary was conducted, processing and analysing the whole freely available SeaWiFS archive (1998-2004). The investigation focused on the spatial and temporal variability of *chl* fields as well as their seasonal and interannual variability, i.e. a primarily temporal focus.

In chapter 5 the use of optical remote sensed imagery was coupled with *in situ* measurements in order to investigate the short-term physical-chemical and biological processes occurring along the coastal zone. The problem tackled here was mainly methodological, i.e. assessing the reliability of optical satellite sensors for coastal zone monitoring. Thus there were analysed chlorophyll maps at higher resolution, and two different algorithms were tested. The satellite images requested were retrieved by the

MERIS sensor. MERIS data were chosen to monitor and analyse the biophysical parameters pattern such as *chl* at local scale, i.e. along the Portofino MPA. Two MERIS spatial resolutions corresponding to *in situ* sampling campaigns were requested (i.e.: MERIS Full Resolution at 300m and MERIS Reduced Resolution at 1100 m). MERIS images were first processed and geo-registered. Geo-registered algal_1 and algal_2 satellite *chl* (mg m^{-3}) products were finally analysed and correlated with the discrete chl-*a* data collected *in situ*.

Daily SST skin maps were analysed contextually to the surface temperature data collected *in situ*. Correlation between SST skin satellite data and *in situ* collected data was not performed due to the high (0.1-0.2 K) precision of the SST skin data retrieved by the AVHRR sensor and also to their reduced spatial resolution compared to that of MERIS sensor.

2.5 CONCLUSIONS

In this chapter the selected study sites were depicted and the rationale underneath their selection, i.e. their specific location within the Mediterranean basin, was emphasised. The oceanography of the biogeographic regions in which the MPAs are located was highlighted and a comparison among the study areas was supplied.

The passive sensors utilised in this study were described and their potential strengths and weaknesses i.e. accuracy of the satellite measurements highlighted. The satellite data processing and analysis carried out in each experimental chapter was outlined and the link between purposes and experimental approach described.

CHAPTER 3

PHYTOPLANKTON DYNAMICS IN THE MEDITERRANEAN MPAs: A SATELLITE REMOTE SENSING APPROACH

3.1 INTRODUCTION

This chapter considers how the geophysical parameters retrieved by Earth Observation (EO) satellites enable to supply a clear description of the biophysical processes occurring in the proximity of the MPAs. This analysis was carried out for each of the four MPAs illustrated in chapter 2.

The climatological *chl* monthly means retrieved by the historical ocean colour imagery (e.g. CZCS and SeaWiFS) shows that the Mediterranean basin is geographically subdivided into the western and the eastern basins. The western basin shows higher *chl* values (Morel and André, 1991) than the eastern which shows a uniform oligotrophic appearance (Antoine *et al*., 1995). Within the western basin localised mesotrophic patterns are notable in both the Ligurian-Provençal Sea where a sizeable offshore algal bloom is notable seasonally, and in the Alboran Sea, in particular within the gyre system generated by the entrance of the MAW into the Mediterranean sea.

The climatological *chl* monthly means show higher *chl* values during winter due to the enhanced vertical mixing which favours the upwelling of nutrients to the surface layer. During summer lower *chl* values are recorded due to stratification of the water column and to reduced runoff (Barale, 2003). The atmospheric Mediterranean circulation is dominated in winter by the trade winds regime whereas in summer the circulations is influenced by the African tropical circulation. These climatic conditions determine the wide thermal range of the sea surface between winter and summer (Buongiorno Nardelli *et al*., 2007). The analysis of satellite thermal data (SST skin) elucidates the circulation and its seasonal variability. The Mediterranean SST fronts are seasonal and follow the heating cycle of the basin (Phillipe and Harang, 1982). During winter the thermal gradients are representative of the integrated circulations whereas in the warm season

these mirror the dynamics of the upper layers. From a climatological point, the northern region is characterised by cylogenetic events which are atmospherically forced. On the other hand the southern region does not show any cyclogenetic activity except in the Alboran Sea gyre which is not caused by atmospheric forcing (Santoleri *et al*., 1994) but it is caused by the entrance of the MAW into the Mediterranean sea.

3.2 MATERIALS AND METHODS

As already illustrated in §2.4 the main biophysical parameters in this chapter were retrieved by means of optical and thermal sensors. In particular the chlorophyll images were retrieved by SeaWiFS and the thermal images by AVHRR.

AVHRR images were particularly useful in having the same spatial resolution of SeaWiFS (Appendix 1). In order to highlight the biophysical processes occurring within the study areas the same temporal scale was used for the ocean colour data, namely the weekly means.

3.2.1 Satellite data

SeaWiFS data were analysed in order to investigate the regional hydrological characteristics which persist along the study areas considered. In particular the analysis of the ocean colour imagery was performed to highlight the *chl* trends over space and time and in particular the seasonal evolution of phytoplankton biomass and its spatial structure within the areas considered.

The *chl* retrieved from satellite data by means of standard bio-optical algorithms, as stated in §2.4, display a bias of about 30% on the average when compared to *in situ* observations (D'Ortenzio *et al*., 2002; Claustre *et al*., 2002, Bosc *et al*., 2004; Volpe *et al*., 2007). In the present study the NASA standard algorithm (OC4V4) (O'Reilly, 1998, O'Reilly *et al*., 2000) was utilised. SeaWiFS images were acquired by the Laboratory for Satellite Oceanography at the National Oceanography Centre, Southampton (NOCS,

University of Southampton, UK) and supplied by the NASA SeaWiFS Project. The SeaWiFS sensor was chosen to retrieve *chl* within the study areas described in chapter 2. The whole SeaWiFS data archive (1997 to 2004) is freely accessible to the scientific community and it is downloadable through NASA ocean colour website (http://oceancolor.gsfc.nasa.gov/). The data used are the so called Local Area Coverage (LAC) data with the highest spatial resolution (1.1 km). The daily images relating to year 2002 were selected from the SeaWiFS archive. The L1A products containing the raw Level 0 data (raw radiance counts from all bands) plus calibration and navigation data (Feldman, 2003) were downloaded and converted into L2 products (*chl*) by means of the SeaDAS software package (Fu *et al*.,1998). The atmospheric correction algorithms based on the studies by Gordon and Wang (1994) and Siegel *et al*. (2000) were applied to the L1A products, which converted the radiance values into LwN(λ). A series of flags were later applied in order to mask land, clouds and invalid pixels. The L2 product (*chl* in mg m^{-3}) was retrieved, as outlined above, by applying the Ocean Chlorophyll 4 algorithm (OC4) proposed by O'Reilly *et al*. (1998) with revised numerical coefficients (OC4.v4) (SeaWiFS, 2000). This is an empirical algorithm which provides the chlorophyll *a* + phaeophytin *a*. It is used mostly for "Case 1" waters where only phytoplankton pigments and associated substances should affect the water leaving radiance spectrum. This algorithm has an underlying theoretical basis that stems originally from the work of Clark *et al.* (1970) and is based on a statistical regression between the observed chl-*a* and the maximum reflectance ratio ($R_{RS(\lambda 1)}/R_{RS(\lambda 2)}$) retrieved in two different bands (see below). R_{RS} is the remote-sensing reflectance (i.e. the water-leaving radiance divided by the irradiance incident on the sea surface). $R_{RS(\lambda 1)}$ is the highest value among R_{RS} (443), R_{RS} (490) and R_{RS} (510).

The SeaWiFs *OC4.v4* empirical algorithm is explained by the equation 3.1:

$$C = 10^{(a_0 + a_1\rho + a_2\rho^2 + a_3\rho^3 + a_4\rho^4)} \qquad \text{Equation (3.1)}$$

where

$$\rho = \log\left[\max\left(R_{rs}(443,490,510)\right) / R_{rs}(555)\right]$$

$a_{0\text{-}4}$=0.366,-3.067,1.93,0.649,–1.532.

In order to retrieve *chl* in mg m^{-3} of water from the images, the equation 3.2 was applied:

$$Chl(mg/m^3) = (e^{(0.035*DN)})/100 \qquad \text{Equation (3.2)}$$

Individual SeaWiFS images were later re-mapped on a rectangular projection (cylindrical equidistant) grid of 1834 elements and 2636 lines (i.e. 4834424 pixels), covering the Western Mediterranean basin, with a pixel resolution of 1.1 km. The images encompass the area between 46.05° N and –6.5° E (upper left), and 30°N and 20.5° E (lower right). Finally SeaWiFS images were averaged over weekly periods.
Figure 3.1 illustrates an example of SeaWiFS level 4 data (L4), or rather the weekly average *chl* product georeferenced available for 2002 cut on the central-western Mediterranean basin and highlighting the four study sites.

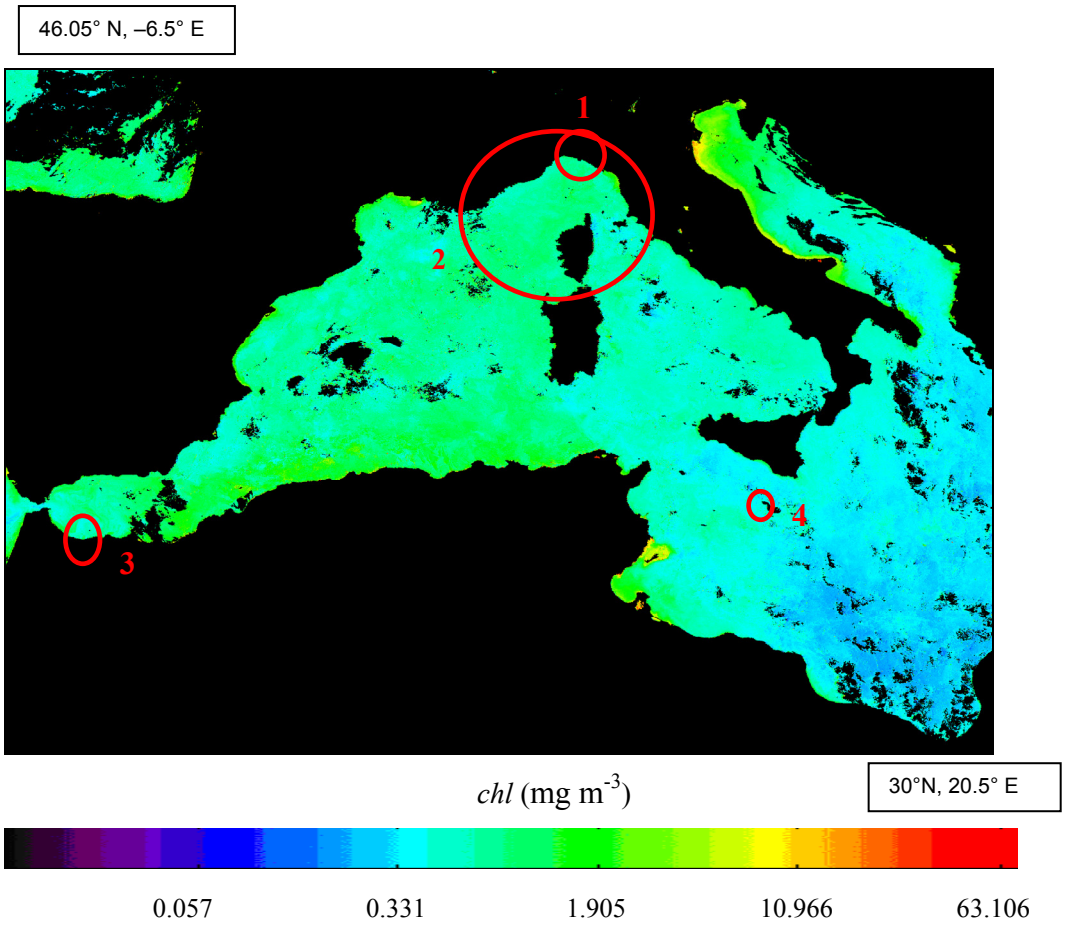

Fig. 3.1 Example of a weekly map (2002) of *chl* (mg m^{-3}) derived from SeaWiFS data according to the OC4v4 algorithm, Mediterranean basin (excluding Aegean Sea). Study areas are circled in red. 1. Portofino MPA; 2. International *Pelagos* Sanctuary; 3. Al Hoceima National Park; 4. Rdum Majjesa and Ras Raheb, Malta.

A small area covering the Portofino MPA was extracted from colour images and processed as shown above, in particular encompassing the area between 44.43°N and 8.86°E (upper left), and 43.97° N and 9.59°E (lower right).

Another area covering the *Pelagos* Sanctuary was extracted from SeaWiFS images, following the borders of the Sanctuary and encompassing a large part of the Ligurian Sea and in particular the area between 44.52°N and 6.09°E (upper left), and 40.78° N and 11.52°E (lower right). The images were analysed by means of ENVI, IDL (ITT Visual Solutions Inc.) and MATLAB software.

In order to characterise the waters along the Al Hoceima National Park from an oceanographic point of view, two sub areas from the original colour imagery were extracted. The first sub area highlights the Gibraltar Strait encompassing the Alboran Sea, in particular the area between 37.30 N and -5.87 E (upper left), and 34.47 N and -2.75 E (lower right). The second sub area focuses on the National Park waters encompassing the area between 35.60 N and 4.39 E (upper left), and 35.04 N and-3.84 E (lower right).

For the proposed Maltese MPA, a small area was extracted from SeaWiFS imagery. In particular encompassing the area between 36.01 N and 14.13 E (upper left), and 35.69 N and 14.66 E (lower right).

Mean values (σ) of chlorophyll concentration were calculated over weeks in order to derive the chlorophyll trend over the study year and identify the timing and magnitude of phytoplankton bloom peaks. Further information was obtained on the annual spatial distribution of chlorophyll by calculating the mean area occupied by a specific chlorophyll value within each study area. For each image the mean of the total extension (in km^2) covered by a particular *chl* was estimated. This procedure was extended to each image to obtain a *chl* distribution per km^2 for each week considered, producing histograms of the annual *chl* distribution (mg m^{-3}) per km^2 within the study areas.

Semi-quantitative analyses were performed by applying a threshold technique to the chlorophyll maps to discriminate clearer between a low (oligotrophic) and a high

(eutrophic, bloom) *chl* status within the study area. These analyses were performed in areas with high *chl* by dividing the chlorophyll spectrum observed during the considered year into two ranges (0.164-0.9 / 1.0-1.9 mg m^{-3} and 0.164-0.9 / 1.0-4.0 mg m^{-3}). The Mediterranean being an oligotrophic sea, *chl* values over 1.0 mg m^{-3} reported in the Ligurian Sea and in the Central Mediterranean Sea are considered to be a sign of an occurring bloom whereas the Alboran Sea shows higher maximum *chl* values achieving up to 4.0 mg m^{-3}. This cut-off was selected by considering the minimum and maximum *chl* values registered throughout the year within the study areas considered. The threshold technique allows conversion of data into values equal to 0 or 1; 0 corresponding to values falling out of the defined ranges and 1 corresponding to values falling within them.

In order to investigate the variation of *chl* over space, is possible to separate the areas with high *chl* from those with low *chl* by calculating the variation of *chl* per unit of distance, i.e. its gradient, being defined as the rate of change with respect to distance of a variable quantity (e.g. *chl*). Gradient is a vector that always points in the direction of maximum change, with a magnitude equal to the slope of the tangent to the curve at the point (Barozzi *et al*., 2002). The gradient vector field of a scalar function *f(x)* with respect to a vector variable $x = (x_1, ..., x_n)$ is denoted by ∇f where ∇ denotes the vector differential operator (Equation 3.3). By definition, the gradient is a vector field whose components are the partial derivatives of *f*:

$$\nabla f = \left(\frac{\partial f}{\partial x_1}, ..., \frac{\partial f}{\partial x_n} \right) \qquad \text{Equation (3.3)}$$

The analysis of the shift vector enabled identification of the regions where a high *chl* persisted, highlighting vectors with constant direction and intensity over time. This concept could be applied to find out the variation of *chl* on each single image between an area and its neighbouring ones, i.e. the spatial gradient (Barozzi *et al*., 2002). The analysis of the spatial gradient indicates the *chl* shift and its evolution over time, highlighting the areas where rapid changes in *chl* occur. It defines the transfer vector along the direction over which the major change in *chl* occurs. This analysis has been performed using the same rationale of the threshold analysis, but also considered areas

showing low *chl*. Calculating this entity for each range considered, the gradient vectors have been visualised graphically by means of contouring areas which displayed a particular *chl*. It should be noted that the spatial gradient derives from the differential calculus of the spatial distribution function along the two axes *x* and *y*. Therefore, when passing from a pixel with chlorophyll equal to 0, to another one showing a particular value of *chl*, the values are linked by a logarithmic function, thus producing an abrupt change of values moving from one point to the other.

Thermal images were collected from AVHRR (see Appendix 1) and were supplied by the *Deutsche Zentrum fur Lüft und Raumfahrt* (DLR, http://www.dlr.de), in particularly from the Earth Observation Data Service (EOWEB). The most important aspect of the SST maps is a reasonable cloud screening to ensure that only cloud free pixels are taken. Images are acquired as Multichannel Sea Surface Temperature Maps (MCSST) and all products are based on the brightness temperatures of AVHRR channels 4 and 5 (T4, T5) (McClain *et al*., 1985). SST is calculated by applying the "Split Window Technique" technique. This formula is based on the brightness temperatures mentioned above and corrects atmospheric attenuation mainly caused by water vapour in the atmosphere which normally leads to a significant drop in derived brightness temperature (Equation 3.4):

SST= A*T4+B*(T4-T5)+C*(T4-T5)*(SEC(sza)-1)+D*(SEC(sza)-1)+E Equation (3.4)

The coefficients A,B,C,D, and E are AVHRR- and day/night specific (Table 3.1). In addition, the sun zenith angle is needed for deriving the MCSST.

Table 3.1 AVHRR coefficients utilised for the equation 3.5.

Satellite	Time	A	B	C	D	E(K)	E(C)
NOAA-16	D	0.99932	2.30195	0.628966	0.0	0.0	-0.805742

Each pixel of an image has a brightness that can be represented digitally by a binary number called the digital number (DN). The number of brightness values within a digital image is determined by the number of bits available. The MCSST data are available into a 8-bit integer format (values from 0 to 255), grey value “0” is referred to

"LAND" whereas grey value "255" refers to "CLOUD" and "NO DATA". The pixel values (0-255) have no units and are direct conversions of the spectral brightness intensity. The SST range is from 0.125 to 31.75 (maximum temperature) °C, the lowest is referred to as "grey value 1" and the highest to "grey value 254". The radiometric resolution is therefore 0.125 °C. In order to obtain MCSST value in °C from grey values, following (Equation 3.5) must be applied on the imagery:

$$MCSST(C°) = DN * 0.125 \qquad \text{Equation (3.5)}$$

The MCSST data in sensor projection are remapped into a standard Mercator projection. The images were imported to ENVI and IDL for georeferencing, SST extraction and subsequent analyses.

Weekly means thematic maps, resulting from day-and night-time observations, were available from March until December 2002. Unfortunately the first two months of 2002 were missing due to technical problems with the NOAA-14 AVHRR which halted the data collection on October 2001 until the end of March 2002.
Figure 3.2 shows an example of AVHHR L4 data i.e. the weekly average SST skin product (2002) georeferenced cut on the central-western Mediterranean basin.

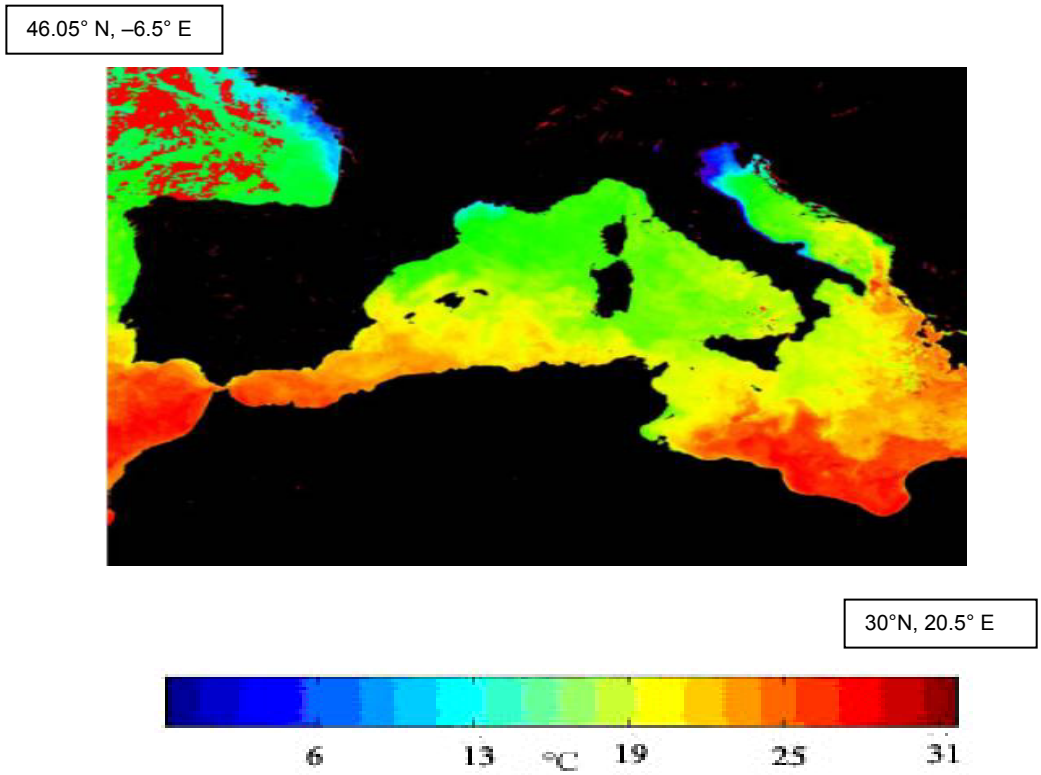

Fig. 3.2 Example of a SST skin map (2002) derived from AVHRR data, Mediterranean basin (excluding Aegean Sea).

3.2.2 Statistical Analysis

In order to verify the presence of phytoplankton blooms, statistical analyses were performed. Matrices of *chl* (mg m^{-3}) were prepared for import into the statistical software. The data preparation was carried out considering the whole *chl* maps set and extrapolating from the original matrix the study areas. Unfortunately cloud and land pixels were all set to a value of 0 by the algorithms above and were not discriminated by the statistical analysis performed. This problem was bypassed only for the *Pelagos* Sanctuary; being this a wide area, a sub marine area located on the North-Western zone of the Sanctuary between 44.07 N and 6.84 E (upper left), and 42.62° N and 9.30°E (lower right) was extracted. This sub area was chosen after the qualitative analysis conducted over the chlorophyll maps which clearly showed, during 2002, that the bloom appeared over the North-Western Area of the sanctuary. This pelagic area, due to the presence of high *chl* values during spring and autumn, was selected to test the efficacy of the statistical analysis performed and also avoided the effect of land which could bias the analyses for the presence of large number of values equal to 0.

Statistical analysis was performed by means of Principal Component Analysis (PCA) (Johnson and Wichern, 1982), Energy Distances (E-Distances) and Energy Statistic Test for Equal Distribution (E-statistic) (Szekely and Rizzo, 2004). The result of the E-Distances is a triangular matrix distance used for comparing clusters or samples. The E-distance between clusters was computed from the original pooled data, stacked in matrix x where each row was considered as a multivariate observation. The first row of the original data matrix was referred to the first week analysed, the next row to the second one and so on. The E-distance between two clusters Ci,Cj (e(Ci,Cj)) of size ni, nj proposed by Szekely and Rizzo (2004) is defined by equation 3.7:

$$e(C_i, C_j) = \left((n_i * n_j) \Big/ (n_i + n_j) \right) * \left[2M_{ij} - M_{ij} - M_{ij} \right] \qquad \text{Equation (3.7)}$$

where:

$$M_{ij} = 1/n_i * n_j \sum_{pi} \sum_{qi} \left\| X_{ip} - X_{jq} \right\| \qquad \text{Equation (3.8)}$$

$\|\cdot\|$ denotes Euclidean norm, and X_{ip} denotes the p-th observation in the i-th cluster.

Furthermore, the K-sample multivariate E-statistic for testing equal distributions was calculated between pairs of *chl* maps. This statistic was computed on the matrices generated (equations X,Y). In order to consider only significant comparisons and to minimise the pixel intercorrelation problem, the *p*-level was modified by using Bonferroni's correction (p*=p/k =0.05/52, being *k* the number of samples, in this case the number of weeks).

The *k*-sample E-statistic is defined by summing the pair wise e-distances over all k(k−1)/2 pairs of samples (Equation 3.9):

$$E = \sum e(C_i, C_j) \qquad \text{Equation (3.9)}$$

$$1 \le i < j \le k$$

In order to determine significance levels, a nonparametric bootstrap test (approximate permutation test) was performed. The statistical analyses were performed by means of RGUI free software (R Development Core Team, 2004).

3.3 RESULTS

In this section the results obtained by the analysis of the satellite data (§3.2.1) will be presented. Data will be shown divided for each study site. Regarding the Moroccan area, the analyses were conducted both for the Al Hoceima National Park and for the Alboran Sea where lies the area investigated. The *chl* maps and relative histograms are shown, plus the threshold analyses (performed only for areas with high *chl*), the spatial gradients analyses, the Principal Component Analyses (PCA) and lastly the SST skin maps.

3.3.1 Portofino Marine Protected Area

The Portofino study area is a coastal MPA placed along the north western Italian coast along the Ligurian-Provençal Sea (§ 2.2.1.1). Figure 3.3 shows the location of the Portofino MPA and the Portofino promontory surrounded by the gulfs of Paradise and Tigullio. Bathymetries along the coast are also indicated.

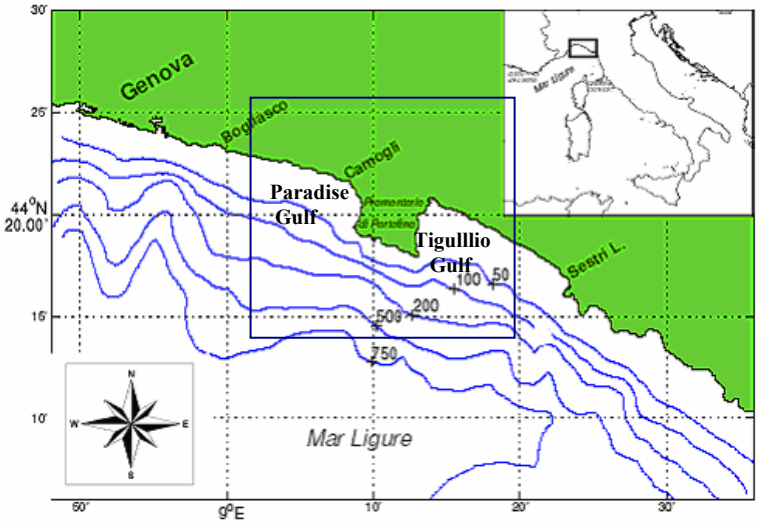

Fig. 3.3 Portofino MPA encompassing Paradise and Tigullio gulfs highlighted in the rectangle.

3.3.1.1 Ocean colour data

Appendix 2 shows the weekly trend of *chl* for the Portofino study area during year 2002 retrieved by SeaWiFS sensor. This area showed low values (0.3-0.5 mg m^{-3}) of *chl* throughout the whole year, although two notable phytoplankton bloom events took place. The first occurred between weeks 5 and 9, i.e. during February to early March (Fig. 3.4a and 3.4b) and encompassed the waters along and offshore the promontory (chlorophyll 1 to 1.5 mg m^{-3}).

The second bloom occurred between weeks 43 and 48 or namely during November (Fig. 3.4c and 3.4d), and developed along the Portofino Promontory achieving *chl* values around 1 mg m^{-3}.

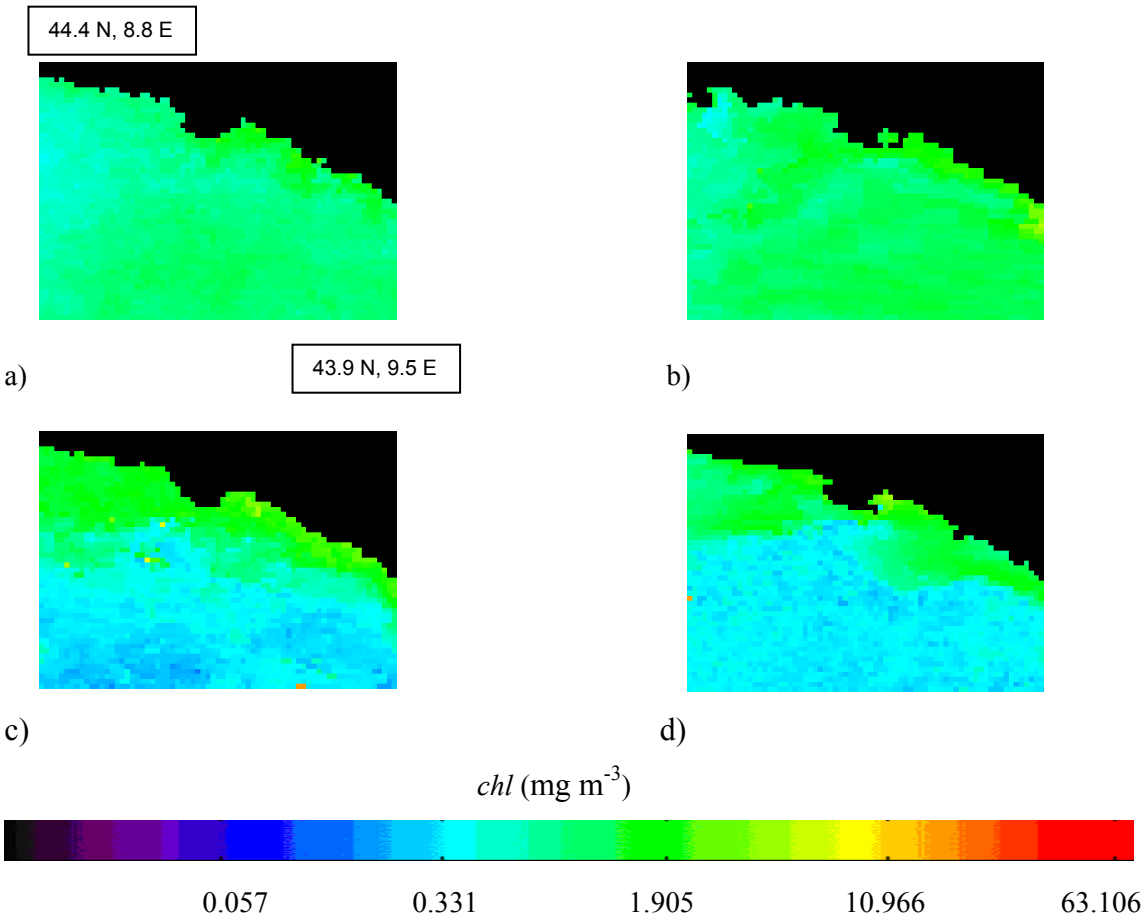

Fig. 3.4 Weekly maps of *chl* (mg m^{-3}) derived from SeaWiFS data, according to the OC4v4 algorithm, along Portofino MPA in 2002, weeks 5 (a), 9 (b), 43 (c), 48 (d) respectively.

Figure 3.5 shows the *chl* (mg m^{-3}) weekly mean calculated over the Portofino MPA area. During January 2002 *chl* values around 0.6 mg m^{-3} were evident, which culminated in the first bloom peak between weeks 5 and 9, attaining mean *chl* values

ranging from 0.8 to 0.95 mg m^{-3}. The bloom appeared to last roughly one month; *chl* values decreased abruptly to 0.4 mg m^{-3} at the end of March. During the summer months, lower *chl* values of around 0.20 mg m^{-3} were recorded. In October-November there was a clear visible increase of *chl*, achieving values of about 0.5 mg m^{-3}. Highest *chl* levels were recorded the last week of December 2002 (0.85 mg m^{-3}).

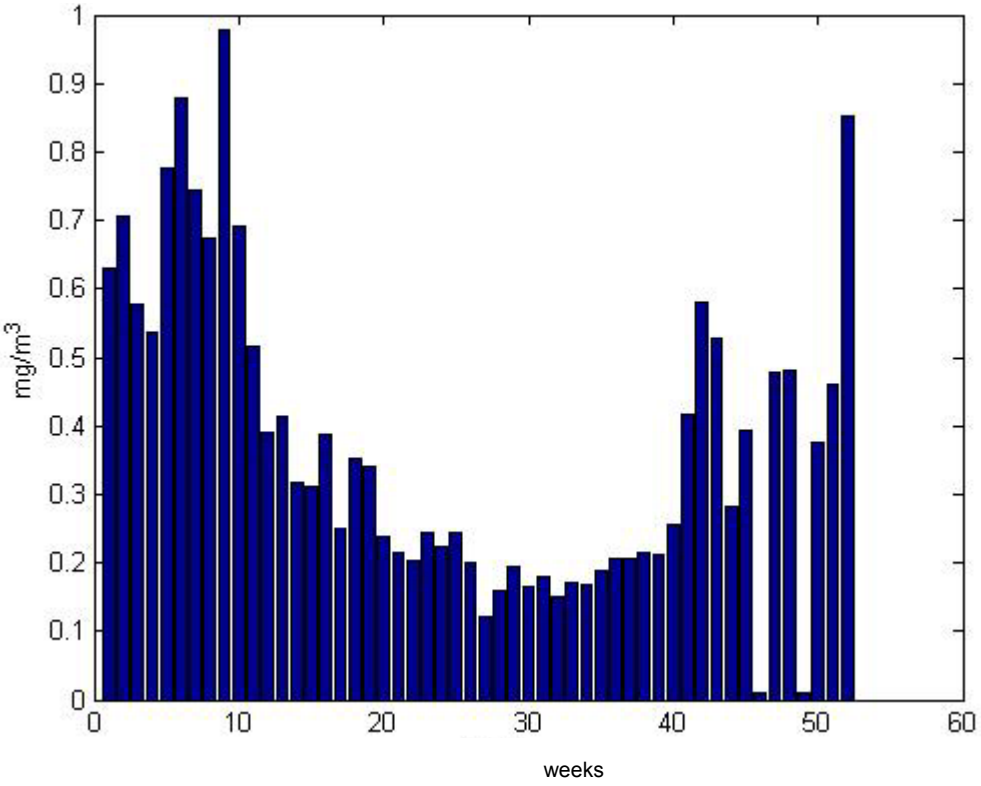

Fig. 3.5 Weekly averages of *chl* (mg m^{-3}) derived from SeaWiFS data averaged over the Portofino MPA during 2002.

Figure 3.6 shows the *chl* distribution plotted against the mean area extension covered weekly by a specific *chl* concentration. During the whole year the value of 0.3 mg m^{-3} covered an area of about 20 km^2 whereas value of 0.5 mg m^{-3} occupied areas of about 145 km^2, this last being the highest areas recorded. Spatial coverage of the highest *chl* values registered (around 1 mg m^{-3}) was of about 10 km^2.

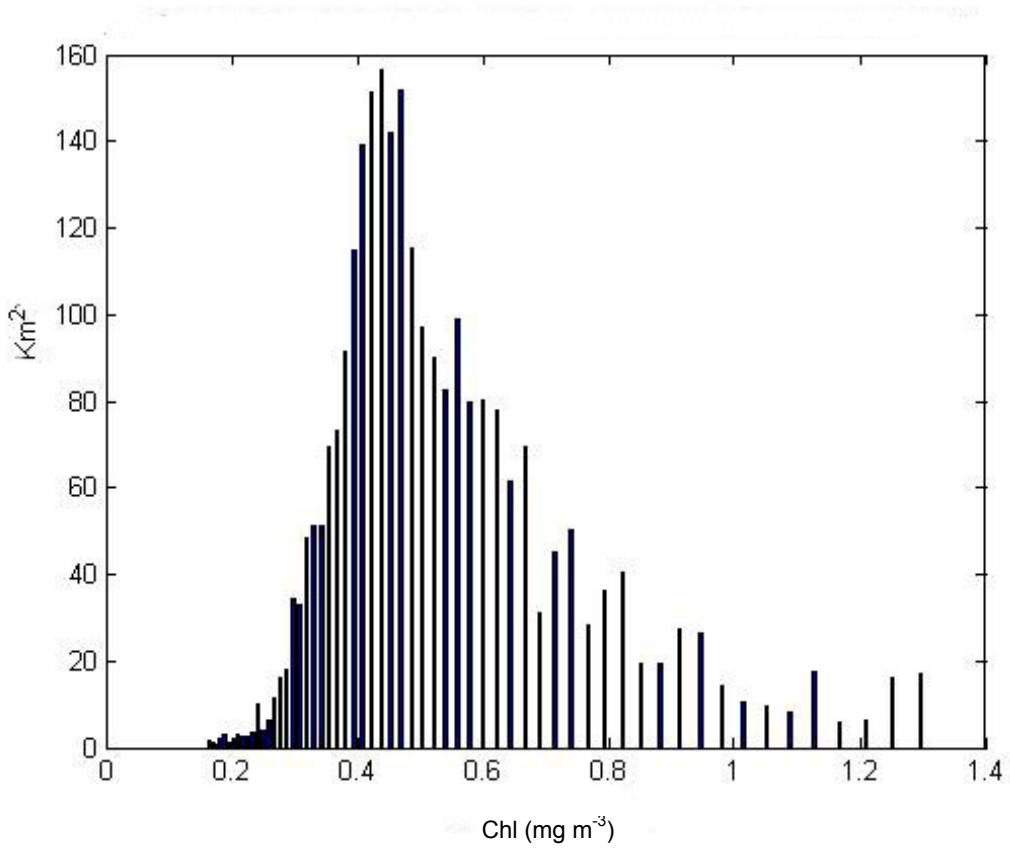

Fig. 3.6 Surface *chl* (mg m^{-3}) distribution per mean km^2 within the Portofino study area during 2002.

Spatial gradients estimated for the study area enabled spatial analysis of the phytoplankton blooms occurring. These analyses, calculated over the two *chl* ranges (§ 3.2.1) as 0.16 and 0.9 mg m^{-3} and 1.0-1.9 mg m^{-3} (Appendices 3 and 4), discriminated the areas with higher *chl* concentration and their shift throughout the year. *Chl* concentrations in the Portofino MPA were mainly within the range 0.16 and 0.9 mg m^{-3} (Appendix 3). *Chl* higher than 0.9 mg m^{-3} were recorded only in February, March and November (Appendix 4). Figure 3.7 shows the spatial gradients calculated within the two selected ranges for the same weeks on 2002. Patches of high *chl* content are first visible along the western side and along the eastern coast of the Promontory during week 4 (Fig. 3.7b). During week 5 the bloom spread covered Tigullio Gulf (Fig. 3.7d), and during week 6 the bloom surrounded the promontory towards Paradiso Gulf (Fig. 3.7f). During the first week of March (week 9) the bloom expanded over the waters offshore from the Portofino MPA (Fig. 3.7j). During March quite high *chl* values (0.5-0.8 mg m^{-3}) persisted along the Promontory and in particular within Tigullio Gulf (Appendix 3). During April the bloom disappeared and *chl* observed were around 0.3 mg m^{-3}.

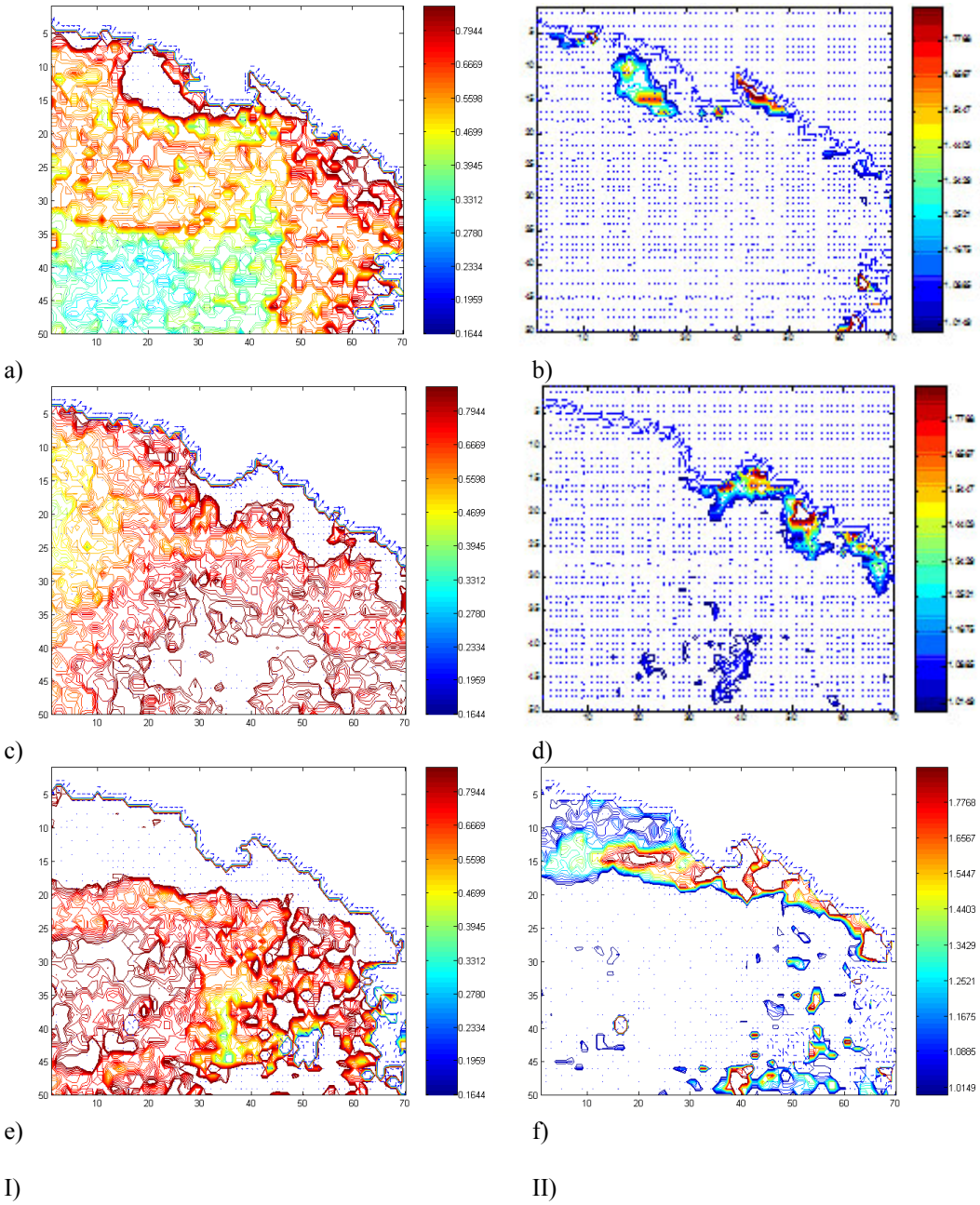

Fig. 3.7 Panel I: Spatial gradients of *chl* within the range of 0.16-0.9 mg m^{-3} and panel II within the range of 1.0-1.9 mg m^{-3} during weeks 4 (a-b), 5 (c-d) and 6 (e-f) (2002) along Portofino MPA.

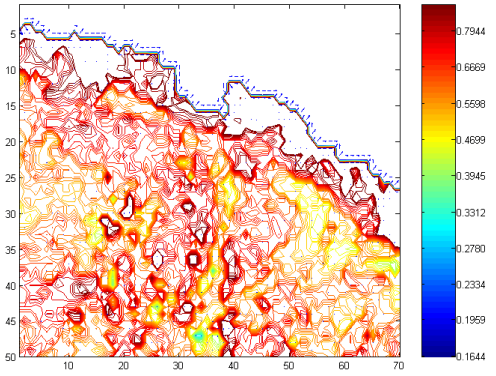

g)

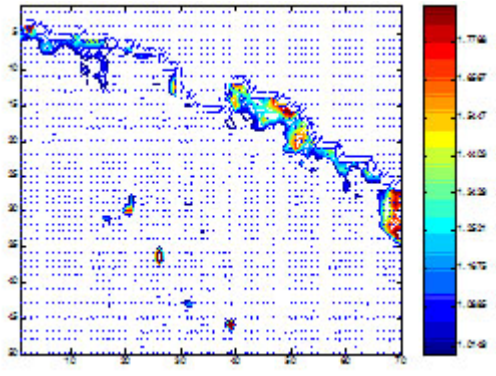

h)

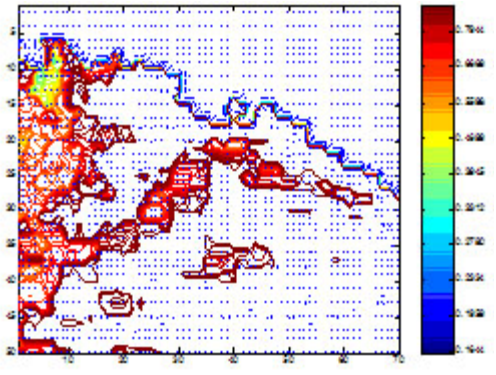

i)

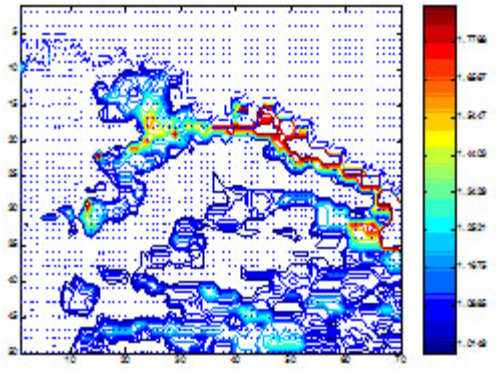

j)

I) II)

Fig. 3.7 Panel I: Spatial gradients of *chl* within the range of 0.16-0.9 mg m^{-3} and panel II within the range of 1.0-1.9 mg m^{-3} during weeks 8 (g-h) and 9 (i-j) (2002) along Portofino MPA (cont.).

Figure 3.8 shows the occurrence of the second phytoplankton bloom peak during the autumn when the higher values of *chl* (1 to 1.9 mg m^{-3}) were recorded along the Promontory. The area where *chl* first started to increase was along the western coast (Paradiso Gulf, Fig. 3.8a) during week 39. During October, in particular during week 43 the bloom expanded over the east (Fig. 3.8d). The high *chl* content patches in October were reduced compared to those recorded in February-March of the same year.

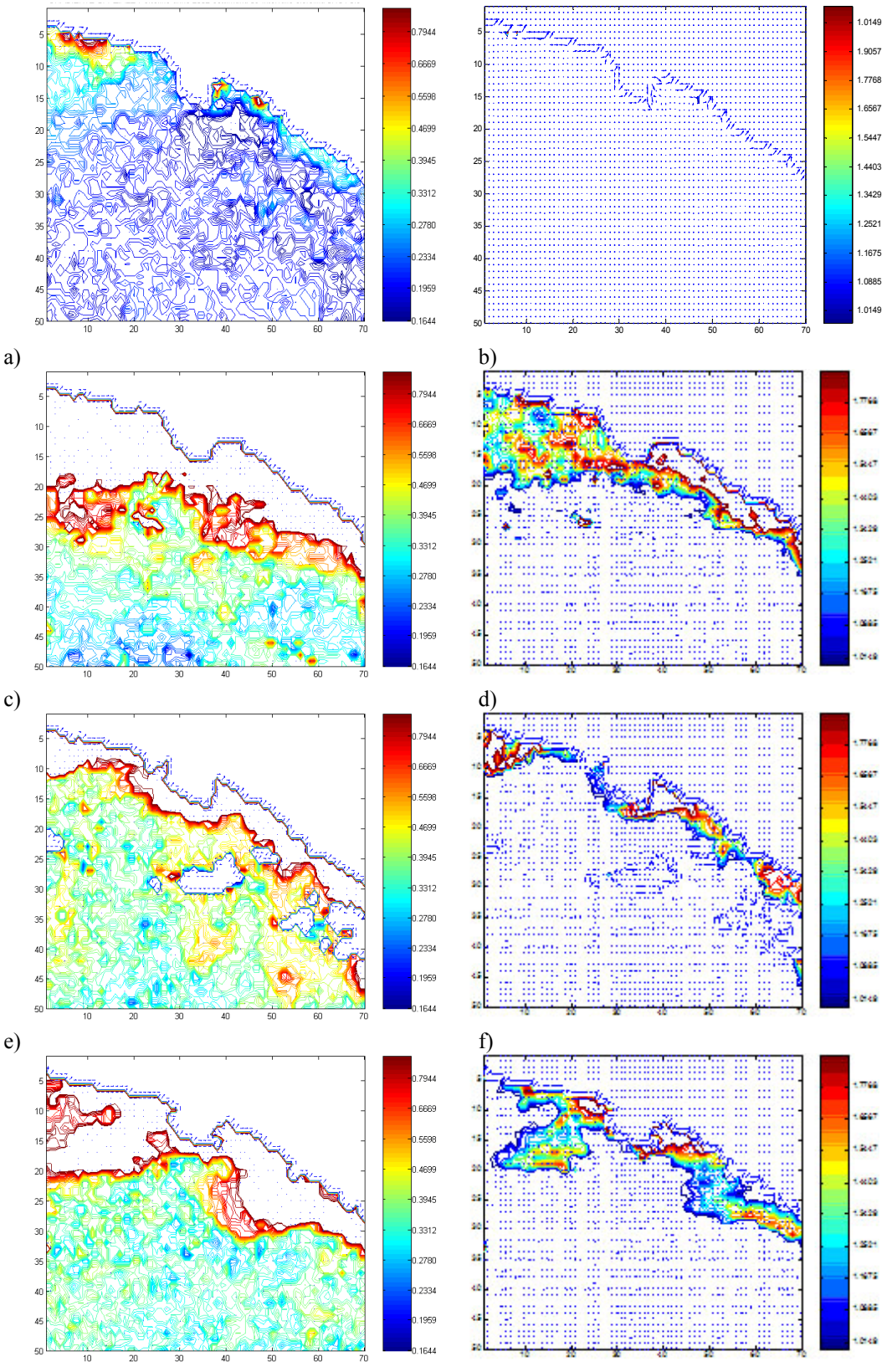

Fig. 3.8 Panel I: Spatial gradients of *chl* within the range of 0.16-0.9 mg m^{-3} and panel II within the range of 1.0-1.9 mg m^{-3} during weeks 39 (a-b), 43 (c-d), 47 (e-f) and 48 (g-h) (2002) along Portofino MPA.

PCA was performed on the X matrix containing the data for the whole 52 weeks and representing the *chl* maps. The plot of factor scores is shown in Figure 3.9. The weeks lying on the x axis are mainly dependent on the first factor. The ones located along the positive semi-axes are those showing a higher *chl* content (e.g. weeks 9 and 5) whereas those with lower *chl* concentration are placed along the negative semi-axes (e.g. 39 and 40). Since the position of week 52 was mainly dependent on the second factor, the first and the second components were plotted separately allowing to better interpret their meaning.

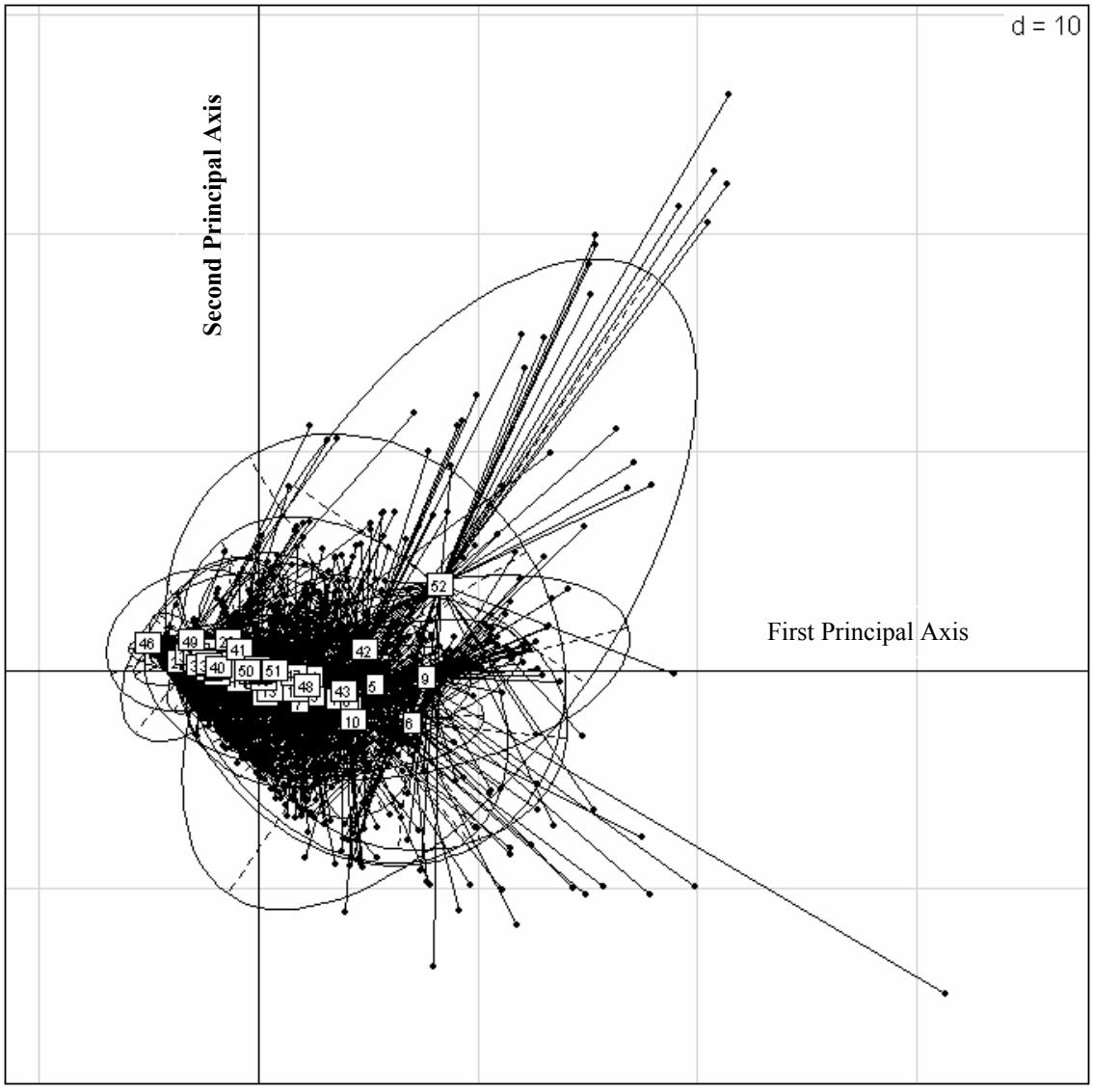

Fig. 3.9 A two dimensional plot of 52 weeks representing the *chl* maps based on Principal Component Analysis. Plot of the factor scores representing the first and the second principal components for Portofino study area during 2002. The factor scores were clustered by means of confidence ellipsoids per week; on the left are located the low scores whereas on the right the high scores .

Figure 3.10 shows the boxplot of the first component (factor scores) (PC1) derived by PCA, as shown on figure 3.8. PC1 described 24.2% of the total variability and expresses clearly the *chl* concentration. The presence of a clear seasonal trend of the *chl* concentration with higher mean values recorded in the winter-spring period and lower mean values recorded during the summer period was noted. The presence of the outliers was recorded during weeks 7, 15, 26, 46 and 49, these were due to almost 30% of cloud coverage on *chl* maps. These are not real outliers but artefacts of data, due to the fact that the cloud cover affect outcomes of statistical test, because the clouds have value 0.

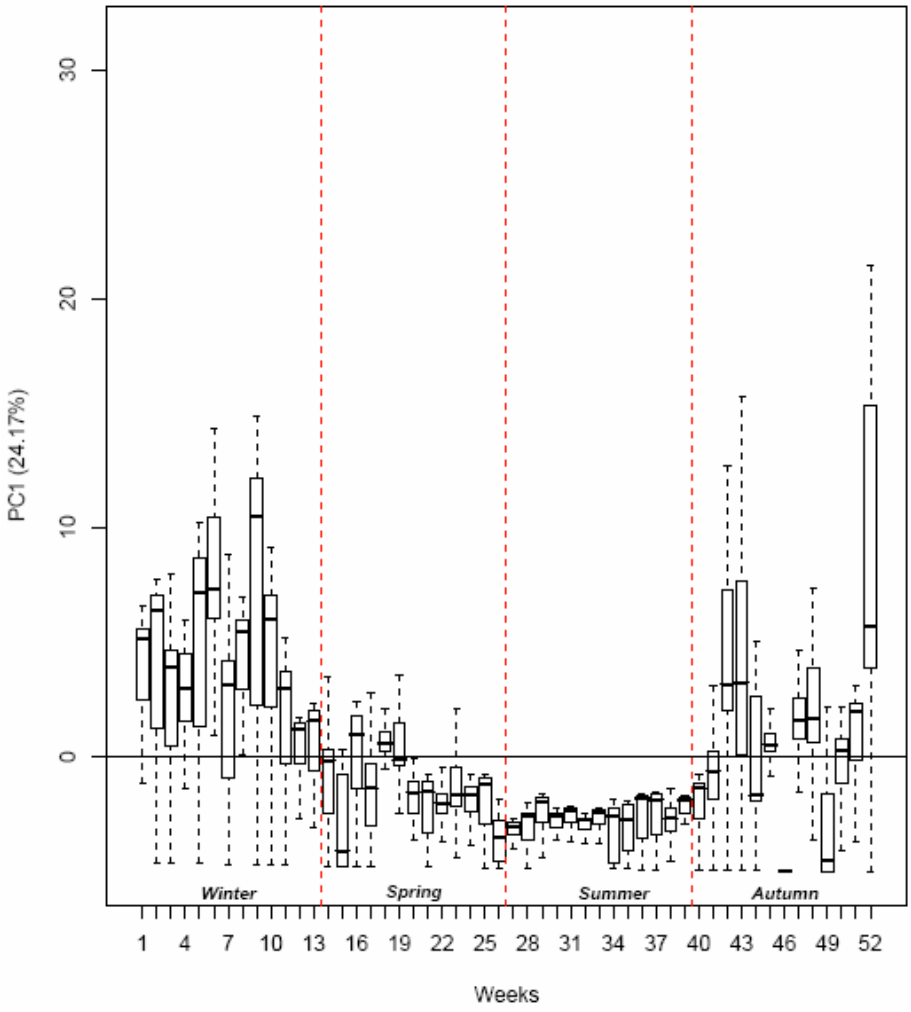

Fig. 3.10 Boxplot of the PC1 for Portofino study area during 2002. The boxes show the interquartile ranges (IQR) between the lower (25th percentiles) and the upper (75th percentiles) quartiles. The line in the boxes represent the median observation. The whiskers represent the 5th and the 95th percentiles.

As shown (Fig. 3.10), the spring phytoplankton bloom peak occurred between weeks 6 and 9. The second bloom was recorded between weeks 42 and 48 with lower *chl* mean values. During week 52 it was registered a *chl* peak. The second factor (PC2) derived by PCA (Fig. 3.9) described only 9.93% of the total variability (Fig. 3.11). This component does not show a clear trend due to the large presence of land on the images which is influential being land set at a value 0 such as the clouds.

In this site, the sum of the two signals due to cloud and land cover made the second component to be more difficult to interpret. The weight due to land, which occupies a large area in the matrix extrapolated, is remarkable and could obscure the variability caused by cloud coverage.

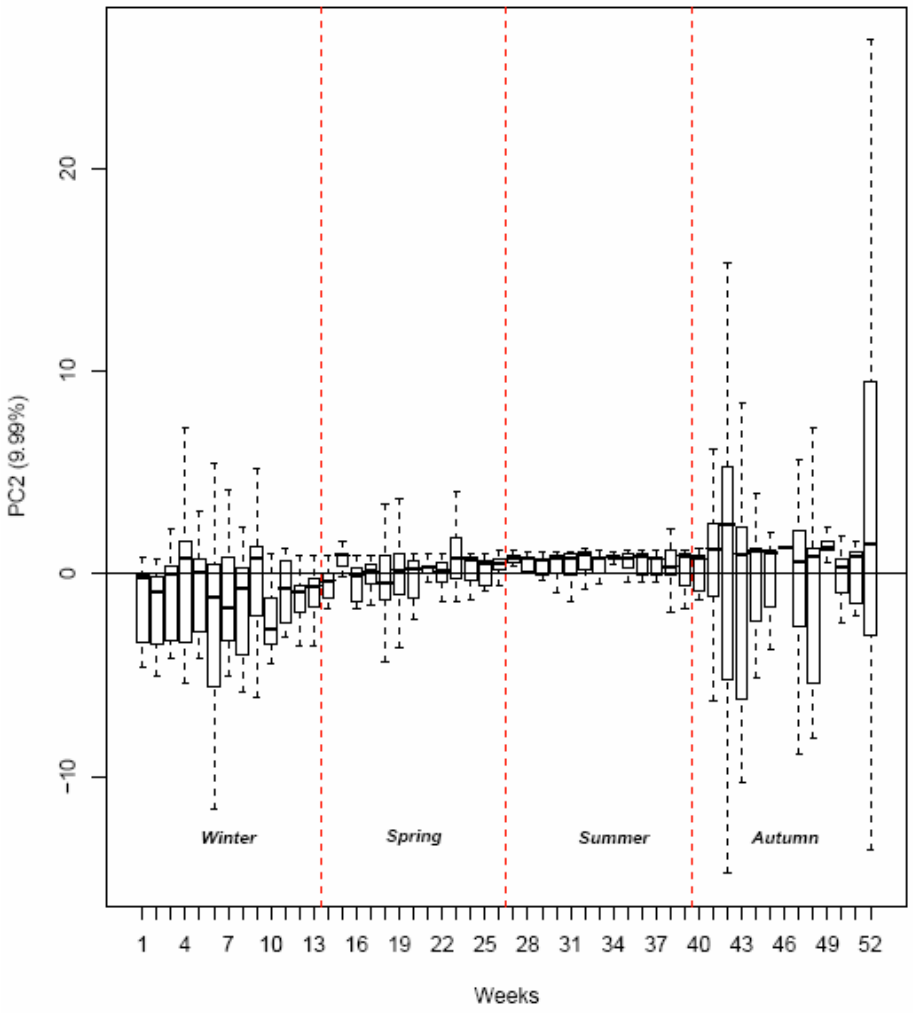

Fig. 3.11 Boxplot of the PC2 for Portofino study area during 2002. The boxes show the interquartile ranges (IQR) between the lower (25th percentiles) and the upper (75th percentiles) quartiles. The line in the boxes represent the median observation. The whiskers represent the 5th and the 95th percentiles.

The results of the k-sample E-statistic for testing equal distributions (§ 3.2.2) i.e. E-distances are presented in table 3.2. Distances calculated with relation to week W4 *vs.* W5, W8 *vs.* W9 and W9 *vs.* W10 were the highest recorded, excluding the W6 *vs*. W7 which was biased by the cloud coverage. This analysis thus highlighted a significant increase in the *chl* content during the winter period. From W10 the *chl* values started to decrease markedly, and only at the beginning of autumn (W 40 *vs*. W 41, W 41 *vs*. W 42) were significant distance values shown, implying a new increase in *chl*. High distances retrieved between W 45 *vs*. W 46, W 46 *vs*. W 47, and W 48 *vs*. W 49 were biased by cloud cover.

Table 3.2 E-Distances for the Portofino study area during 2002. Only the significant values modified by Bonferroni's correction at level $p<0.001$ are presented. The comparisons were made per following weeks.

Weeks	E-distances
W2 *vs.* W3	27.17
W4 *vs.* W5	64.30
W6 *vs.* W7	103.30
W7 *vs.* W8	32.50
W8 *vs.* W9	105.87
W9 *vs.* W10	74.40
W10 *vs.* W11	50.50
W11 *vs.* W12	33.50
W13 *vs.* W14	23.90
W14 *vs.* W15	37.10
W15 *vs.* W16	63.20
W16 *vs.* W17	31.80
W17 *vs.* W18	44.20
W19 *vs.* W20	44.00
W25 *vs.* W26	39.30
W28 *vs.* W29	9.37
W29 *vs.* W30	11.20
W31 *vs.* W32	5.85
W32 *vs.* W33	5.20
W38 *vs.* W39	9.40
W39 *vs.* W40	11.30
W40 *vs.* W41	16.90
W41 *vs.* W42	113.50
W43 *vs.* W44	57.60
W44 *vs.* W45	27.10
W45 *vs.* W46	222.60
W46 *vs.* W47	273.60
W48 *vs.* W49	133.80

3.3.1.2 Thermal IR data

Appendix 5 shows the trend of SST skin along the Portofino study area during 2002 retrieved by the AVHRR sensor. The SST skin during spring was between 14 and 20 °C. The coastal area showed colder SST. Warmer thermal fronts moving westwards at a temperature of about 20°C appeared on week 19. During May the area was wholly covered by waters achieving temperatures of about 22°C near the Promontory. In June SST started to increase rising to 25°C, but with colder SST (21-22°C) along the coast. SST skin remained constant over the summer period at around 25-26°C. In September the SST skin started to decrease down to 23°C across the whole area under consideration. In October SST skin was around 20°C (Fig. 3.12 a and b). During week 48 the cold coastal current (ca. 16°C) re-established (Fig. 3.12 c and d).

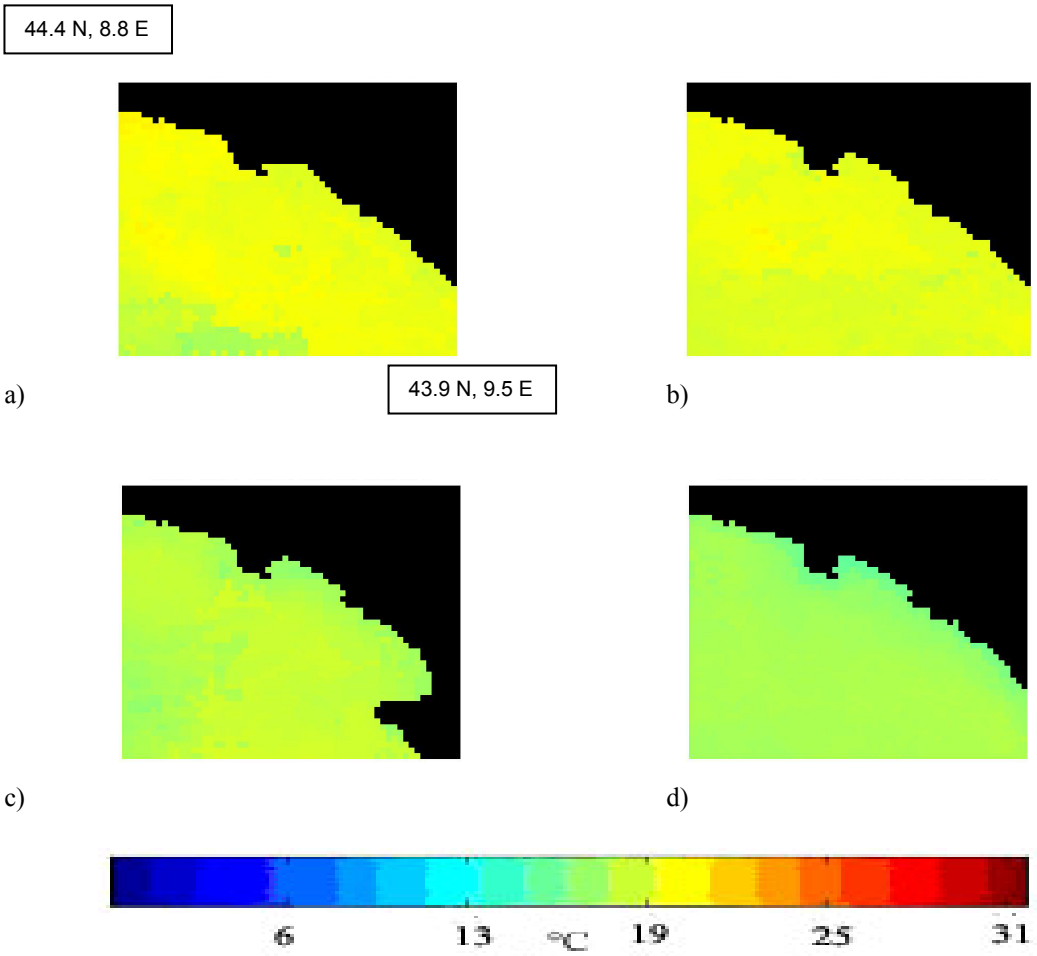

Fig. 3.12 Weekly maps of the SST skin derived from AVHRR along Portofino MPA: weeks 43 (a), 44 (b), 47 (c), 48 (d) respectively, during 2002.

3.3.2 *Pelagos* International Sanctuary

Figure 3.13 shows the International *Pelagos* Sanctuary within the Ligurian Sea and its ground border points. On the west of Corsica there is an abyssal plain 2500-2700 m deep whereas east of Corsica the area is characterised by a shallower (1600-1700 m) and uneven sea bottom.

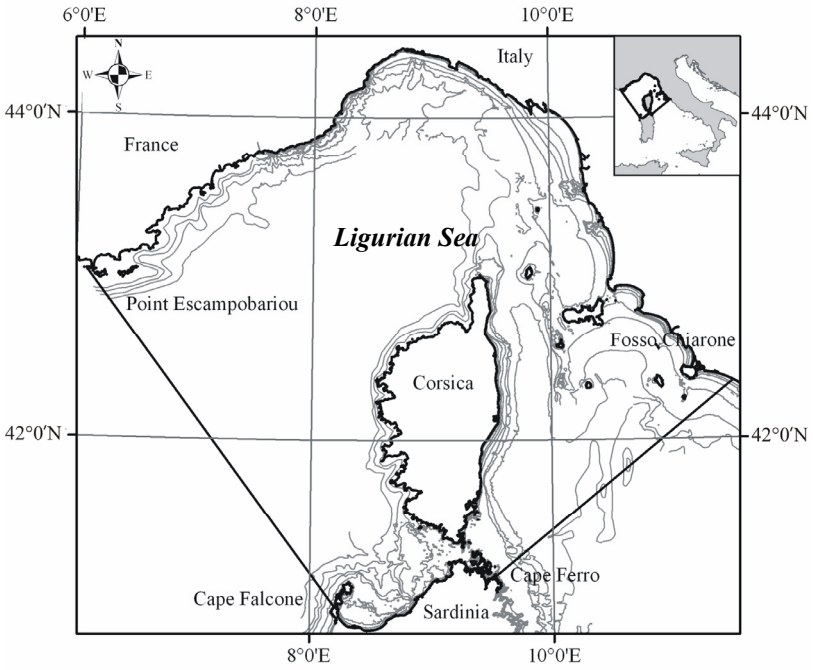

Fig. 3.13 The *Pelagos* International Sanctuary for Marine Mammals, with ground border points (Projection Universal Transverse Mercator, UTM 32, WGS84).

3.3.2.1 Ocean colour data

Analysis of the SeaWiFS images in this area *chl* showed a marked spatial and temporal dynamic with seasonal upwelling events prominent in the north-western zone particularly between weeks 5 and 12 with *chl* concentration over 1 mg m^{-3} (Fig. 3.14 a-f). This patch lasted till week 16 and started to shrink during week 17 (Fig. 3.14 h, i) when *chl* decreased, remaining recognisable until week 29. Between weeks 31 and 40 the whole study area showed a very low *chl* concentration. The beginning of a next upwelling event was observed during weeks 48, 51 and 52 (Fig. 3.14 j-l). Appendix 6 shows the *chl* weekly maps during 2002.

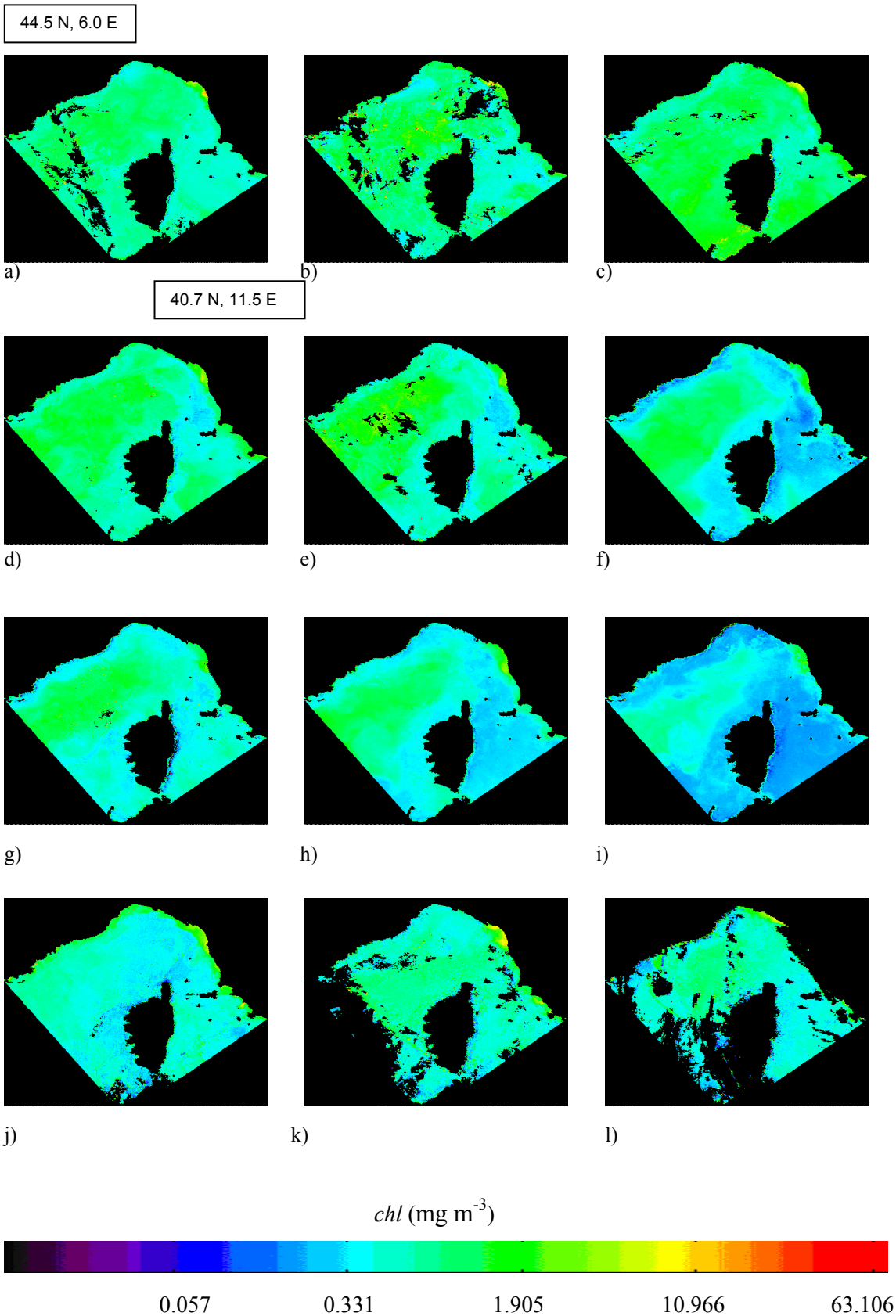

Fig. 3.14 Weekly maps of the *chl* (mg m^{-3}) derived from SeaWiFS data, according to the OC4v4 algorithm, within the *Pelagos* Sanctuary, 2002, weeks 5 (a), 6 (b), 9 (c), 10 (d), 11 (e), 12 (f), 13 (g), 16 (h), 17 (i), 48 (j), 51 (k) and 52 (l) respectively during 2002.

Figures 3.15 shows that mean weekly *chl* during 2002 within the Sanctuary area was highest (0.6-0.75 mg m^{-3}) between January and March with a peak at the end of February. Lower *chl* level were observed during summer months with *chl* values around 0.2 mg m^{-3}. From September *chl* started to increase again, reaching about 0.5 mg m^{-3} in December. However, it should be noted that during November and December the cloud coverage within the area of Sanctuary was quite high, so the calculated mean values are based on fewer weeks of observations than for other months.

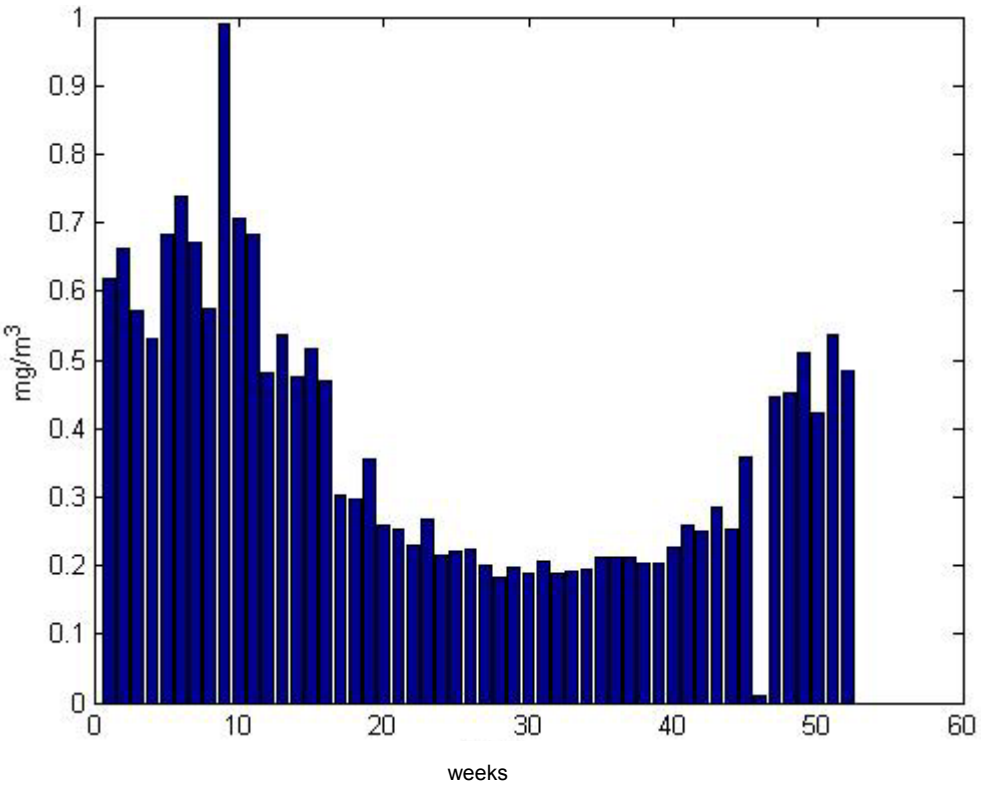

Fig. 3.15 Weekly averages of *chl* (mg m^{-3}) derived from SeaWiFS data averaged over the *Pelagos* Sanctuary during 2002.

Appendix 7 shows the results of the threshold technique applied to the *chl* interval 1-1.9 mg m^{-3}. This methodology enabled discrimination of *chl* pixels falling within the defined range (depicted in white). This analysis showed that a phytoplankton bloom event took place in the north-western zone during week 5 and expanded to its maximum extent during week 9, almost surrounding Corsica island (Fig. 3.16b). During weeks 10 and 11 (Fig. 3.16 c-d) the patch expanded, mainly in the north-western area and started to shrink during week 13, disappearing by week 17 (Fig. 3.16 e-f). The start of a

subsequent blooming event is recognisable during weeks 51 and 52 in the north-western area (Fig. 3.16h-i).

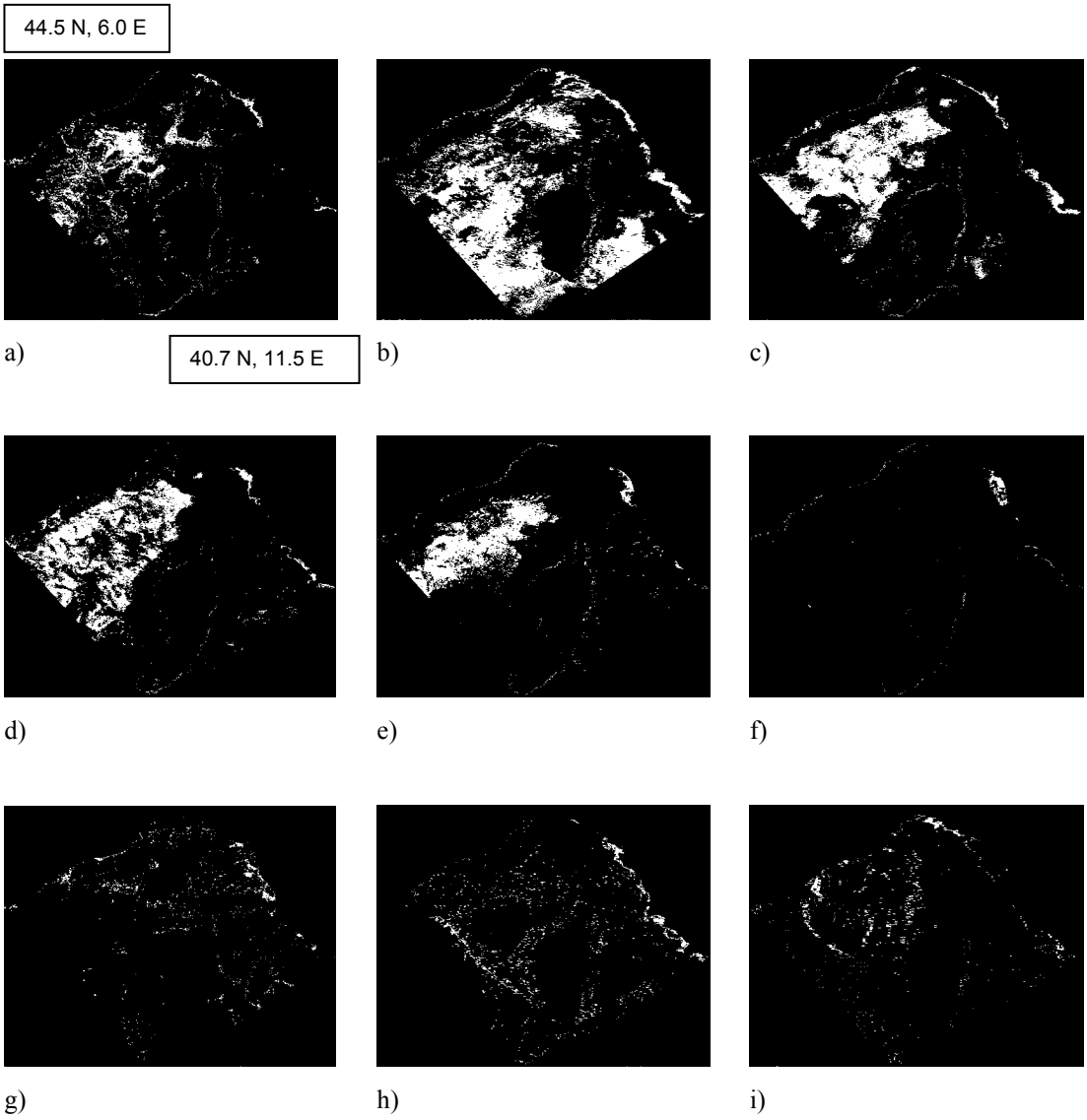

Fig. 3.16 Threshold analysis *chl* range between 1.0 and 1.9 mg m^{-3} (2002) within the *Pelagos* Sanctuary, weeks 5 (a), 9 (b), 10 (c), 11 (d), 13 (e), 17 (f), 49 (g), 51 (h) and 52 (i). White patterns show *chl* values falling within the defined intervals.

Figure 3.17 shows that the major area extension (ca. 5500 km^2) is noted for *chl* values around 0.5 mg m^{-3}, whereas higher *chl* values (0.8 and 1.0 mg m^{-3}) covered 1500 and 500 km^2 respectively. *Chl* levels within the *Pelagos* Sanctuary were mainly between 0.4 and 0.6 mg m^{-3}, which tended to cover the whole study area. However, the areas within the *Pelagos* sanctuary with highest *chl* values were mostly located in its north-western area.

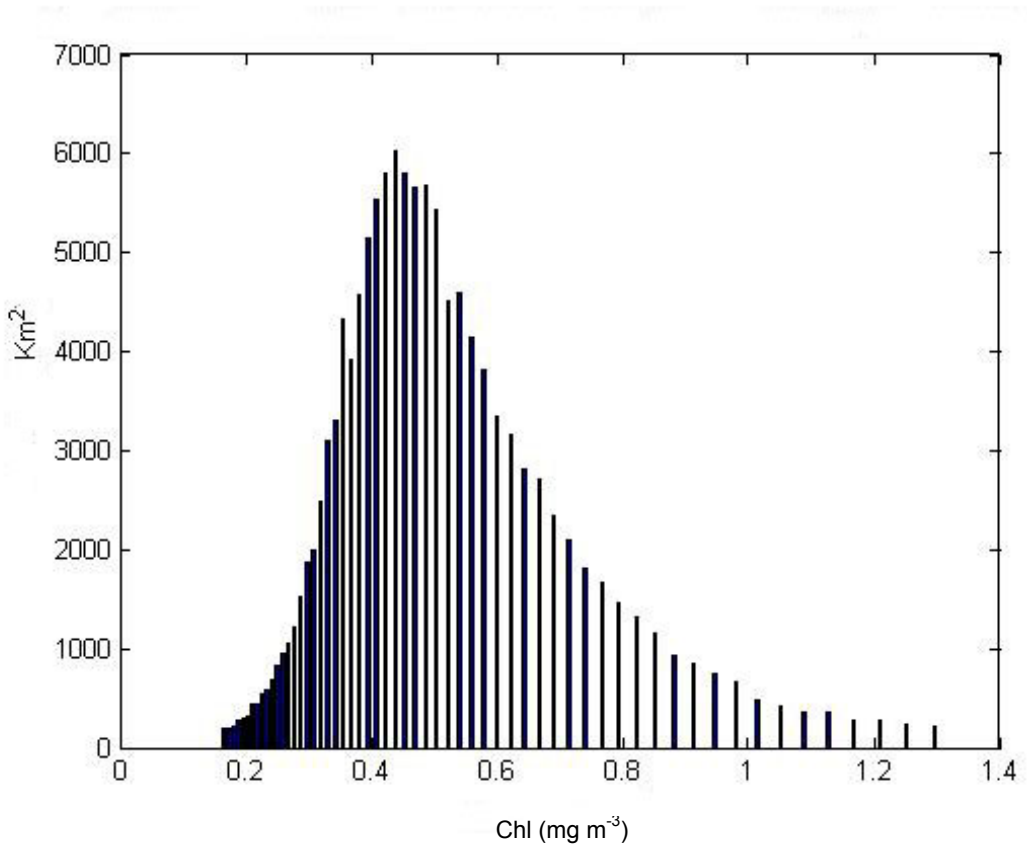

Fig. 3.17 Surface *chl* (mg m^{-3}) distribution per mean km^2 within the *Pelagos* Sanctuary during 2002.

Spatial gradients were particularly useful in discriminating exactly those areas richer in *chl* content within the *Pelagos* Sanctuary (Appendices 8 and 9). Figures 3.18a and 3.18b show the two *chl* intervals considered (0.16 and 0.9 mg m^{-3}, 0 and 1.9 mg m^{-3}) for week 10. It is clearly visible that an algal bloom occurred in the north-western area of the Sanctuary, reaching *chl* values of about 1.5 mg m^{-3}.

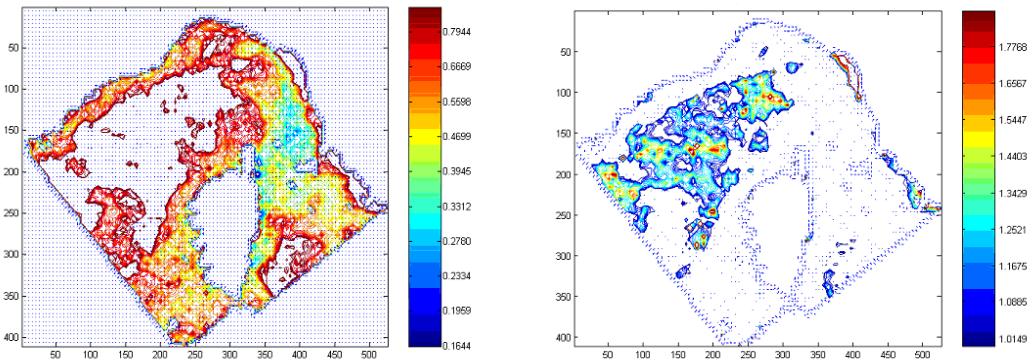

a) b)

Fig. 3.18 Panel *a*: Spatial gradients of *chl* within the range of 0.16-0.9 mg m^{-3} and panel *b* within the range of 1.0-1.9 mg m^{-3} during week 10 (2002) within the *Pelagos* Sanctuary.

In this study area PCA was applied only to the pelagic sub area shown within the rectangle in Figure 3.19a and zoomed in Figure 3.19b.

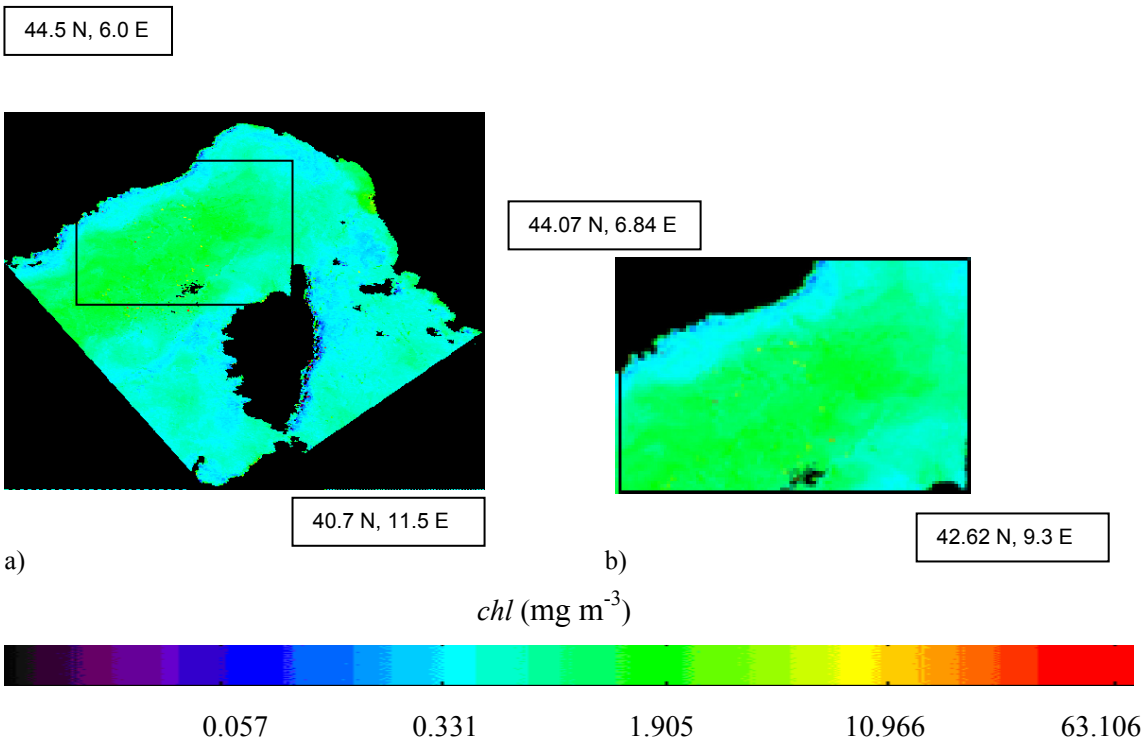

Fig. 3.19 a): SeaWiFS Level 2 *ch*l (mg m^{-3}) within the *Pelagos* Sanctuary and b) in the north-western sub area extracted within the *Pelagos* Sanctuary, 2002.

The plot of PCA factor scores is illustrated in Figure 3.20. The 50 weeks were placed along the first axis. Weeks 11, 6 and 10 showed the highest *chl* whereas lower values were recorded for week 39 and 44. Only week 14 was located on the y axis, implying its dependency on the second principal component.

Figure 3.21 shows the boxplot of the first component (factor scores). The first component described 23.6% of the total variability and expressed clearly the *chl* concentration. The presence of a clear seasonal trend of the *chl* concentration was notable, the first algal bloom occurring between weeks 5 and 11 with *chl* mean values ranging from 0.80 to 1.28 mg m^{-3}. Peak values of *chl* were reached in week 11. The second peak occurred between weeks 49 and 52. During the summer period low mean *chl* values were recorded, falling to within the interval 0.25 to 0.31 mg m^{-3}.

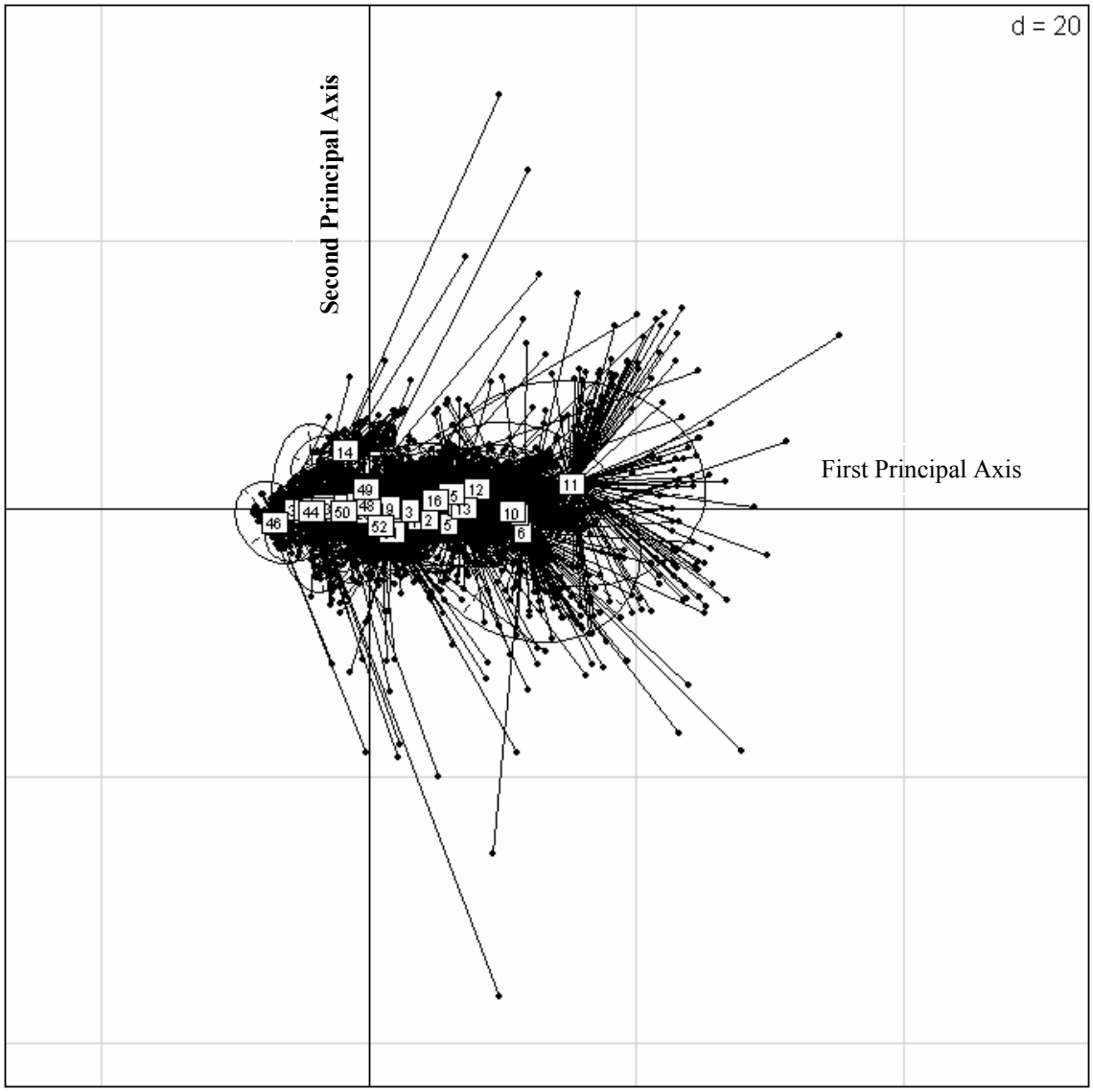

Fig. 3.20 A two dimensional plot of 52 weeks representing the *chl* maps based on PCA. Plot of the factor scores representing PC1 and PC2 for the north-western sub area within the *Pelagos* Sanctuary during 2002. The factor scores were clustered by means of confidence ellipsoids per week; on the left are located the low scores whereas on the right the high scores .

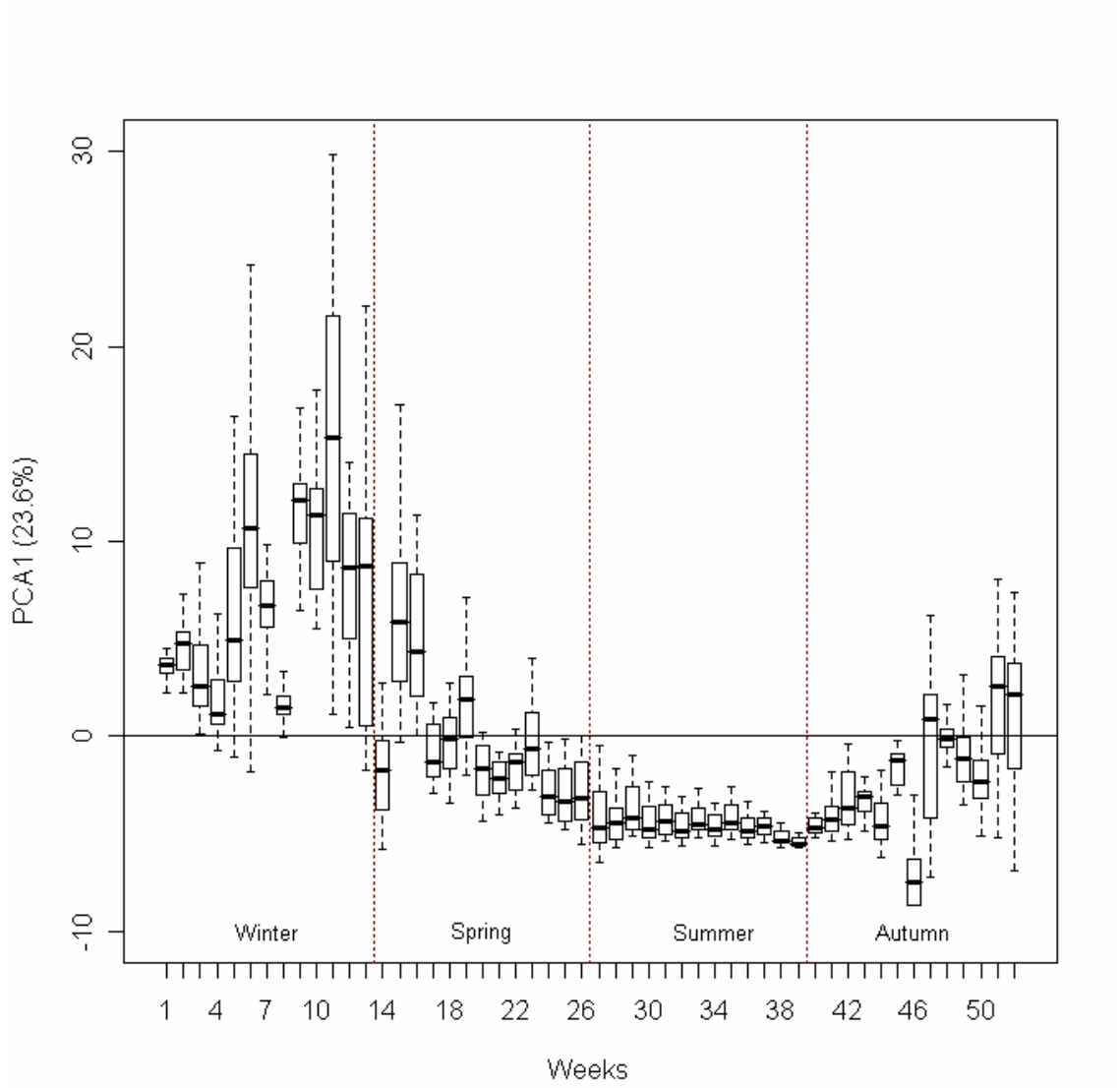

Fig. 3.21 Boxplot of the PC1, in the north-western sub area within the *Pelagos* Sanctuary during 2002. The boxes show the interquartile ranges (IQR) between the lower (25th percentiles) and the upper (75th percentiles) quartiles. The line in the boxes represent the median observation. The whiskers represent the 5th and the 95th percentiles.

On Figure 3.22 the PC2 describes only 3.3% of the total variability and seems to be influenced by the presence of a disturbed signal, probably due to the cloud coverage. The factor scores with high positive values were associated with presence of clouds along the east side of the *Pelagos* sanctuary area (e.g. weeks 13, 14 and 15), whereas those with low negative values (weeks 46, 51 and 52) were associated with clouds located along the west side of the Sanctuary. The images located around a value of 0 are associated with weeks with no cloud coverage (i.e. with a clear signal).

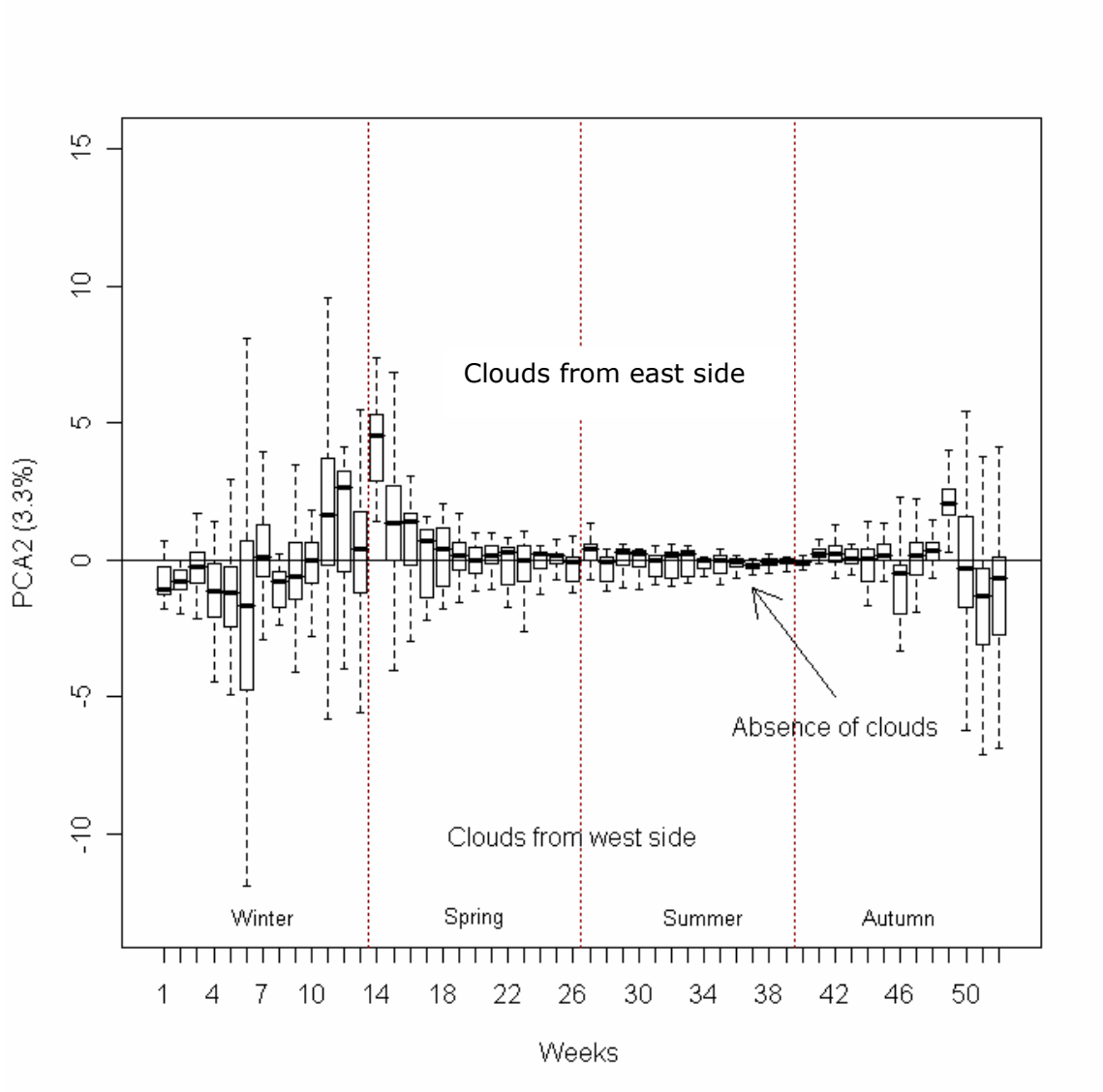

Fig. 3.22 Boxplot of the PC2 in the north-western sub area within the *Pelagos* Sanctuary during 2002. The boxes show the interquartile ranges (IQR) between the lower (25th percentiles) and the upper (75th percentiles) quartiles. The line in the boxes represent the median observation. The whiskers represent the 5th and the 95th percentiles.

Figure 3.23 shows the mean *chl* values calculated over the sub area selected (Fig. 3.19b). The highest *chl* values were recorded between weeks 9-11 and during week 51.

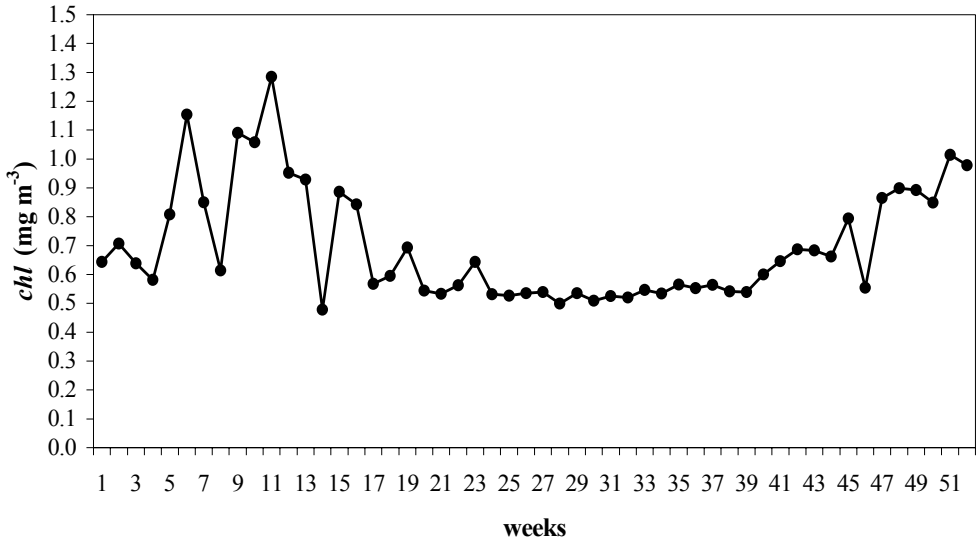

Fig. 3.23 Mean weekly *chl* (mg m^{-3}) in the north-western sub area within the *Pelagos* Sanctuary, during 2002.

Table 3.3 shows the K-sample multivariate E-distances. The first bloom started during week 4. E-distances retrieved in relation to W4 *vs*. W5, W5 *vs.* W6 and W6 *vs*. W7 were all significant. E-distance between W8 and W9 showed the highest value recorded. Distance between W16 and W17 illustrated a significant decrease of *chl* content. The *chl* concentration began to increase significantly again in autumn during W49, showing the higher distance between W48 and W49 and achieving its peak during W51. Significant distances displaying a decrease in *chl* content between W45 and W46, W46 and W47 and W49 and W50 were caused by bias due to cloud coverage.

Table 3.3 E-Distances for the *Pelagos* Sanctuary during 2002. Only the significant values modified by Bonferroni's correction at level $p<0.001$ are presented. The comparisons were made per following weeks.

Weeks	E-distances
W1 *vs*. W2	65.64
W2 *vs*. W3	89.74
W3 *vs*. W4	55.18
W4 *vs*. W5	306.9
W5 *vs*. W6	296.2
W6 *vs*. W7	301.4
W7 *vs*. W8	577.7
W8 *vs*. W9	1324.9
W10 *vs*. W11	250.3
W11 *vs*. W12	448.1
W13 *vs*. W14	851.1
W14 *vs*. W15	788.4
W16 *vs*. W17	564.7
W18 *vs*. W19	90.17
W19 *vs*. W20	278.3
W22 *vs*. W23	59.8
W23 *vs*. W24	181.2
W26 *vs*. W27	52.1
W37 *vs*. W38	38.7
W39 *vs*. W40	81.2
W41 *vs*. W42	23.8
W42 *vs*. W43	36.2
W43 *vs*. W44	26.9
W44 *vs*. W45	77.0
W45 *vs*. W46	329.7
W46 *vs*. W47	751.9
W47 *vs*. W48	677.3
W48 *vs*. W49	123.4
W49 *vs*. W50	80.0
W50 *vs*. W51	46.4
W51 *vs*. W52	285.7

3.3.2.2 Thermal IR data

Appendix 10 shows SST skin retrieved from AVHRR sensor within the *Pelagos* Sanctuary study area from April to December 2002. The SST skin during April was between 14 and 17 °C. At the end of April a warm cyclonic thermal front at a skin temperature of about 20°C was apparent (Fig. 3.24b). The north western area of the Sanctuary was the last to be affected by this warm cyclonic thermal front (Fig. 3.24c). During May the area was wholly characterised by warm waters reaching temperatures of about 21°C.

In late June and early July, SST started to rise up to 25°C and remained constant over the summer period at around 25-27°C (Appendix 10). In September SST skin started to cool down to 23°C over the whole area considered. In October SST was around 20-21°C. In November the colder front on the north western area of the Sanctuary at a SST skin around 17°C was noted to re-establish (Fig. 3.24d-f).

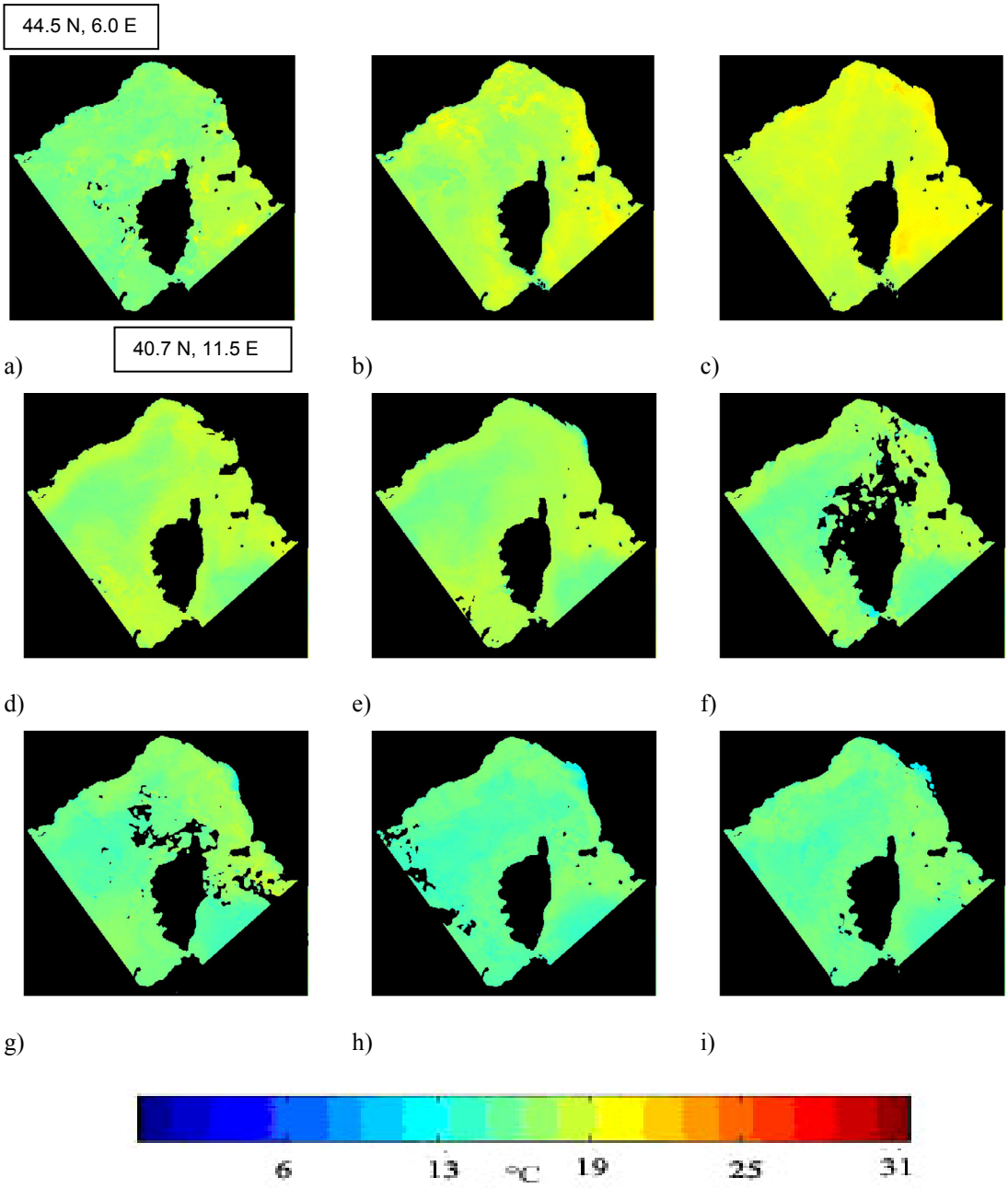

Fig. 3.24 Weekly maps of the SST skin derived from AVHRR within the *Pelagos* Sanctuary: weeks 19 (a), 20 (b), 21 (c), 47 (d), 48 (e), 49 (f), 50 (g), 51 (h) and 52 (i) respectively, during 2002.

3.3.3 Al Hoceima National Park

3.3.3.1 Ocean colour data

Figure 3.25 shows the Gibraltar Strait and Al Hoceima National Park facing the Alboran Sea. The image shown in figure 3.26 provides the detailed coastal line at a spatial scale of 1:50000 indicating the main locations along the coast and the National Park ground border points.

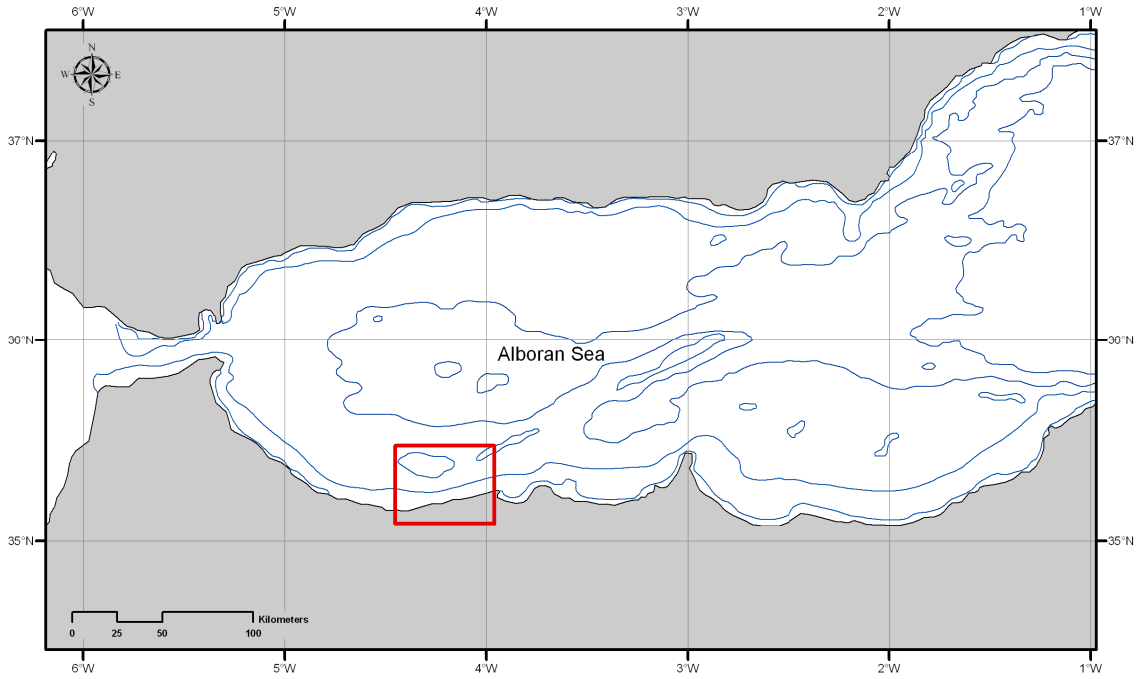

Fig. 3.25 Alboran Sea map, showing Gibraltar Strait and Al Hoceima National Park within the rectangle (Geographical projection, WGS 84).

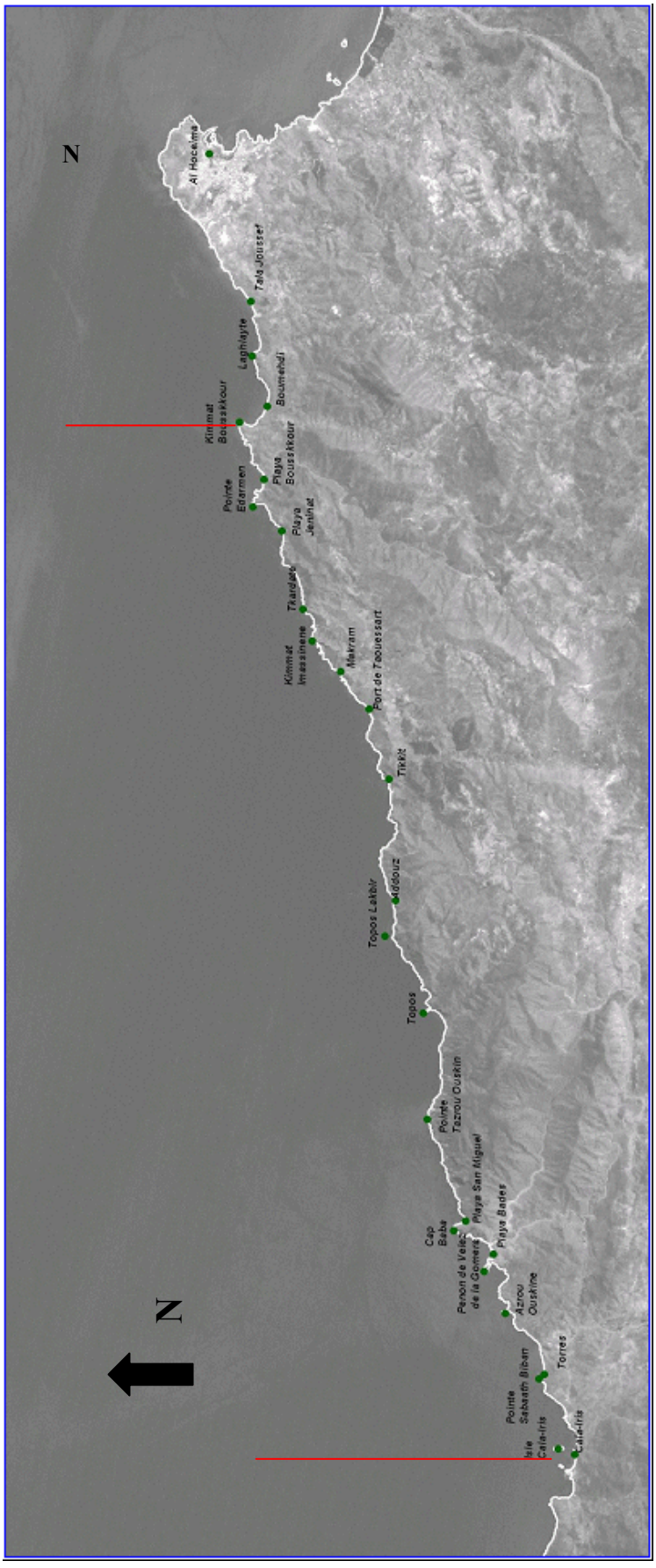

Fig. 3.26 Al Hoceima National Park (LANDSAT 7 ETM imagery, scale 1:50000, 30m resolution) highlighting the eastern and western borders.

Analysis of the SeaWiFS images in this area for *chl* in 2002 showed a marked spatial and temporal dynamic with seasonal bloom events particularly between weeks 5 and 12. Figure 3.27 shows *chl* within the Alboran Sea. As can be clearly seen, the winter period (weeks 3-8) shows high *chl* values (Fig. 3.27a-d). During week 10 (Fig. 3.27e) the MAW was notable with high *chl* content forming an anticyclonic gyre moving towards the east. The gyre is a particular well defined feature during spring (weeks 19-23; Fig. 3.27 g-i) but weakened during summer (Appendix 11). The gyre was again apparent throughout the autumn (weeks 37-49; Fig. 3.27 j-o).

Figure 3.28 shows *chl* levels along Al Hoceima National Park waters. During winter weeks and throughout spring, the anticyclonic gyre persisted along the Al Hoceima coast and transported *chl* rich waters (weeks 4 to 23; Fig. 3.28 a-i), whereas in summer the MAW engine diminished (Appendix 12). At the end of summer the gyre was again visible and affected the Al Hoceima National Park waters, particularly between weeks 37 and 48 (Fig. 3.28 j-n).

Appendices 11 and Appendix 12 show the *chl* maps within the Alboran Sea and Al Hoceima National Park waters respectively.

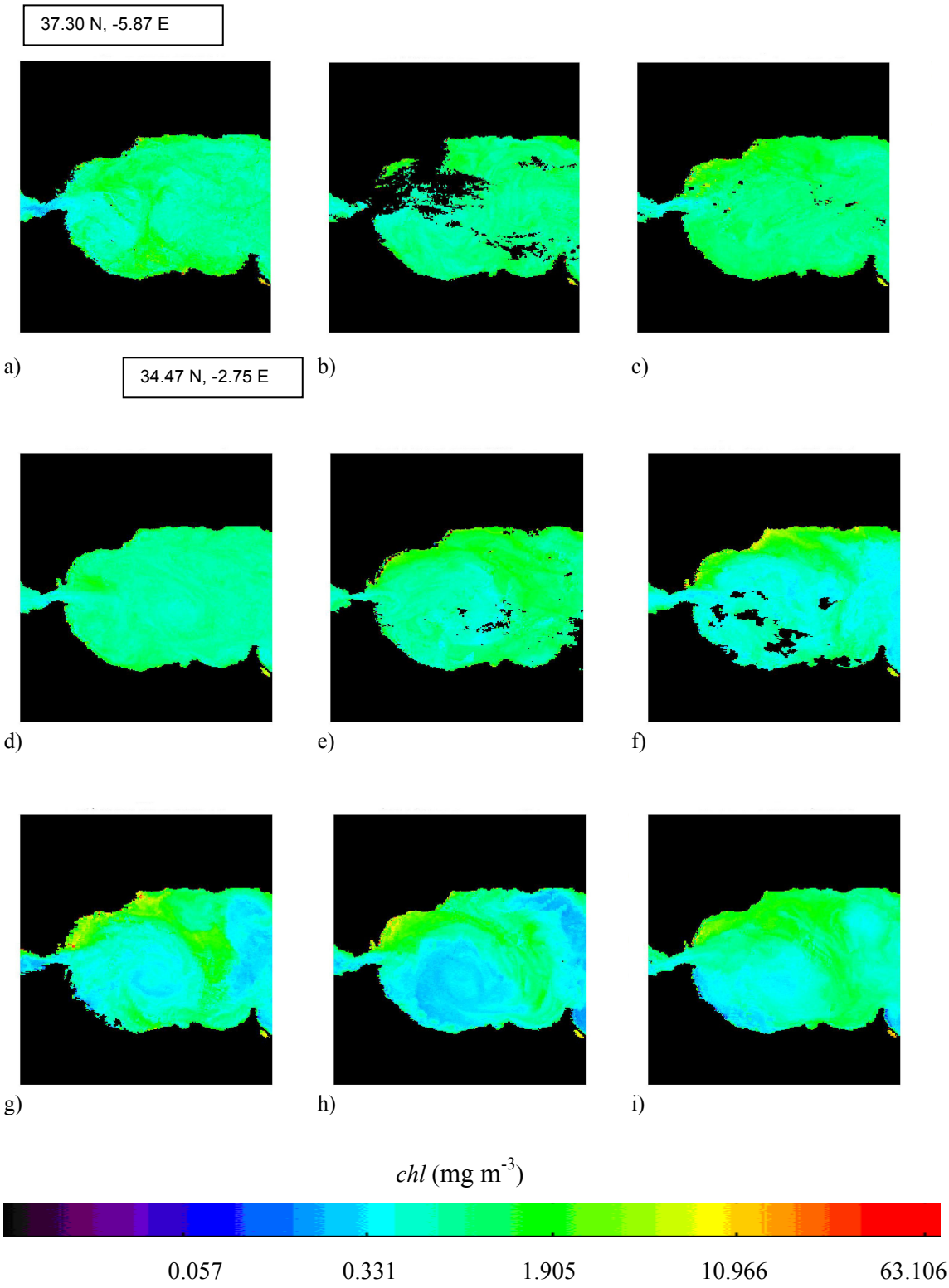

Fig. 3.27 Weekly maps of *chl* (mg m^{-3}) derived from SeaWiFS data, according to the OC4v4 algorithm, within Gibraltar Strait (Alboran Sea) during 2002: weeks 4 (a), 5 (b), 6 (c), 8 (d), 10 (e), 12 (f), 19 (g), 20 (h) and 23 (i), respectively.

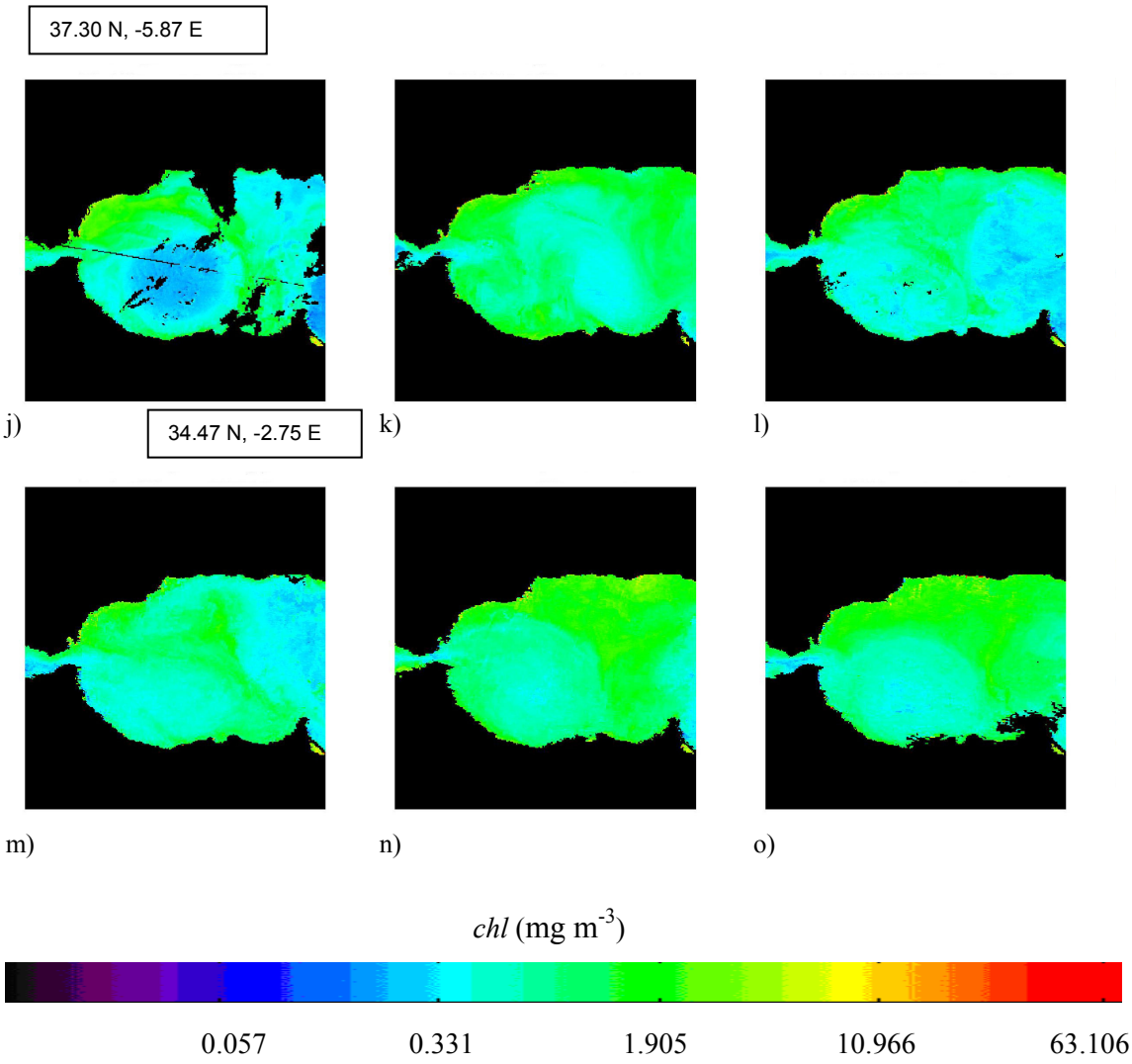

Fig. 3.27 (cont.) Weekly maps of *chl* (mg m^{-3}) derived from SeaWiFS data, according to the OC4v4 algorithm, within Gibraltar Strait (Alboran Sea) during 2002: weeks 37 (j), 41 (k), 43 (l), 45 (m), 48 (n) and 49 (o) respectively.

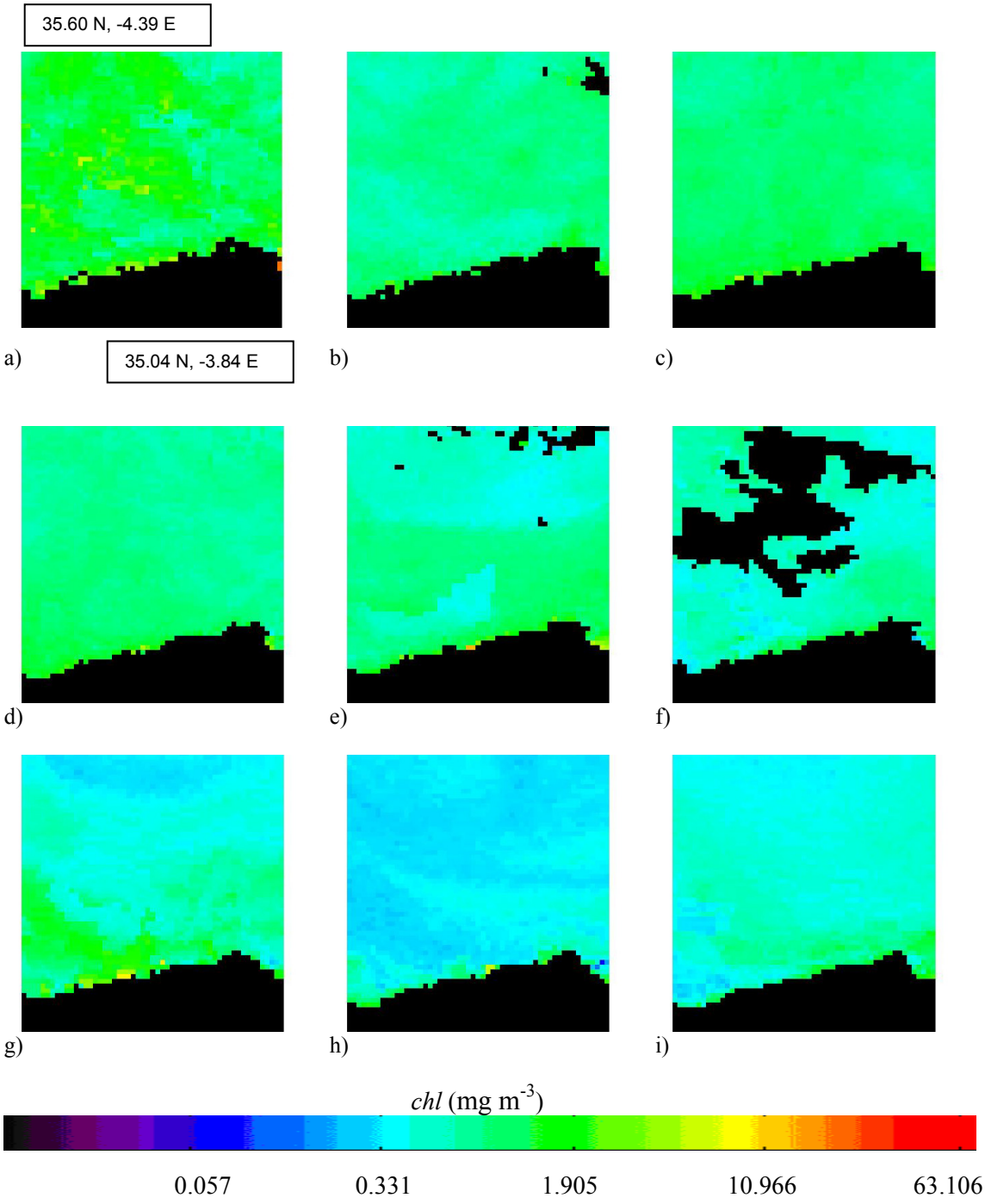

Fig. 3.28 Weekly maps of *chl* (mg m^{-3}) derived from SeaWiFS data, according to the OC4v4 algorithm, along the Al Hoceima National Park waters during 2002: weeks 4 (a), 5 (b), 6 (c), 8 (d), 10 (e), 12 (f), 19 (g), 20 (h) and 23 (i), respectively.

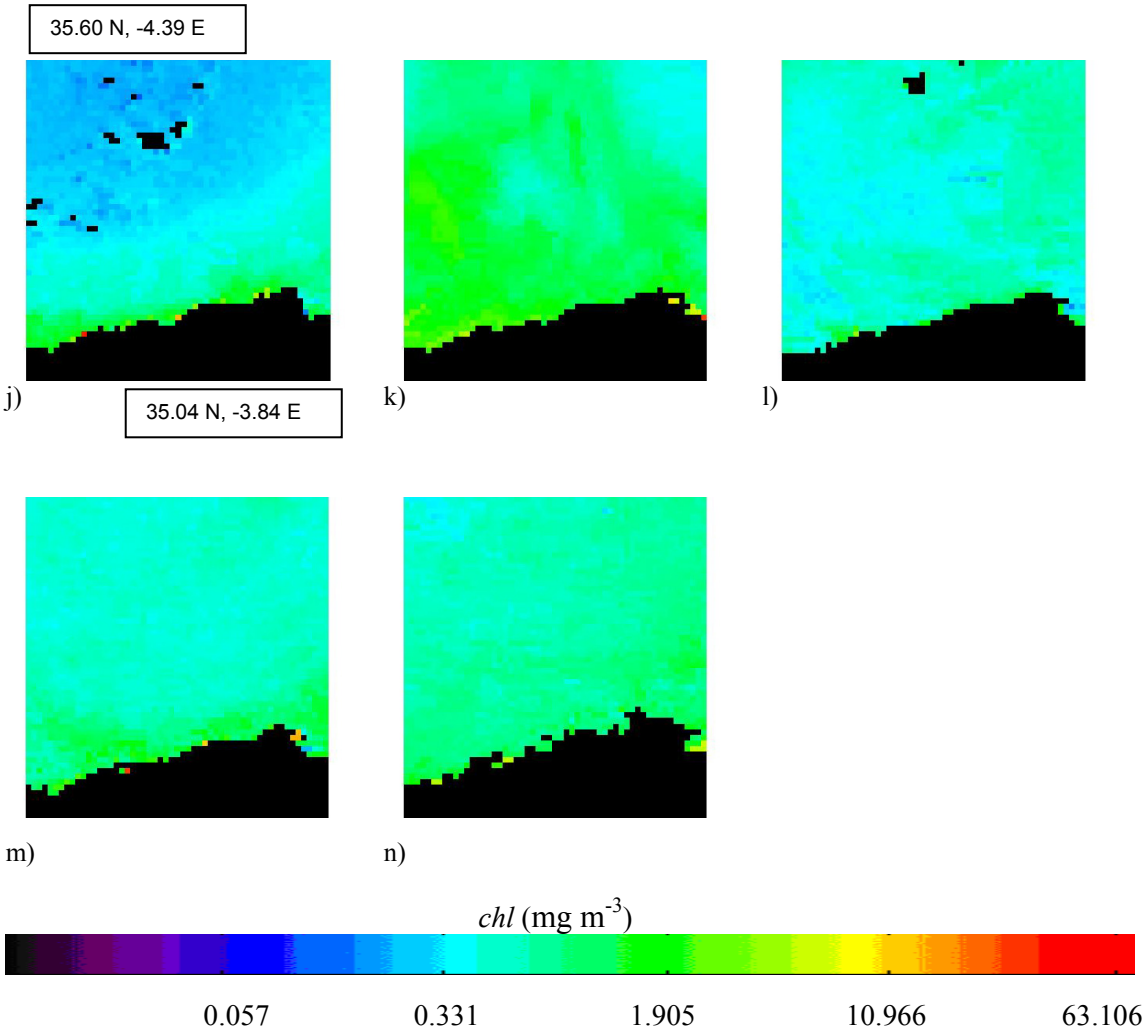

Fig. 3.28 (cont.) Weekly maps of *chl* (mg m^{-3}) derived from SeaWiFS data, according to the OC4v4 algorithm, along the Al Hoceima National Park waters during 2002: weeks 37 (j), 41 (k), 43 (l), 45 (m) and 48 (n) respectively.

Figure 3.29 shows the mean weekly *chl* trend during year 2002 within the Alboran Sea waters; the two clear peaks which were noted for the North-western Mediterranean Sea, are not visible. *Chl* is quite high throughout the year considered. However the highest *chl* values were recorded in early February with values around 0.85 mg m^{-3} and in November with concentrations up to 1.0 mg m^{-3}. High concentrations were recorded also in June (around 0.8 mg m^{-3}) whereas in July the lowest *chl* values were recorded (around 0.4 mg m^{-3}). From September *chl* started to increase again, reaching a peak comparable to the peak in October.

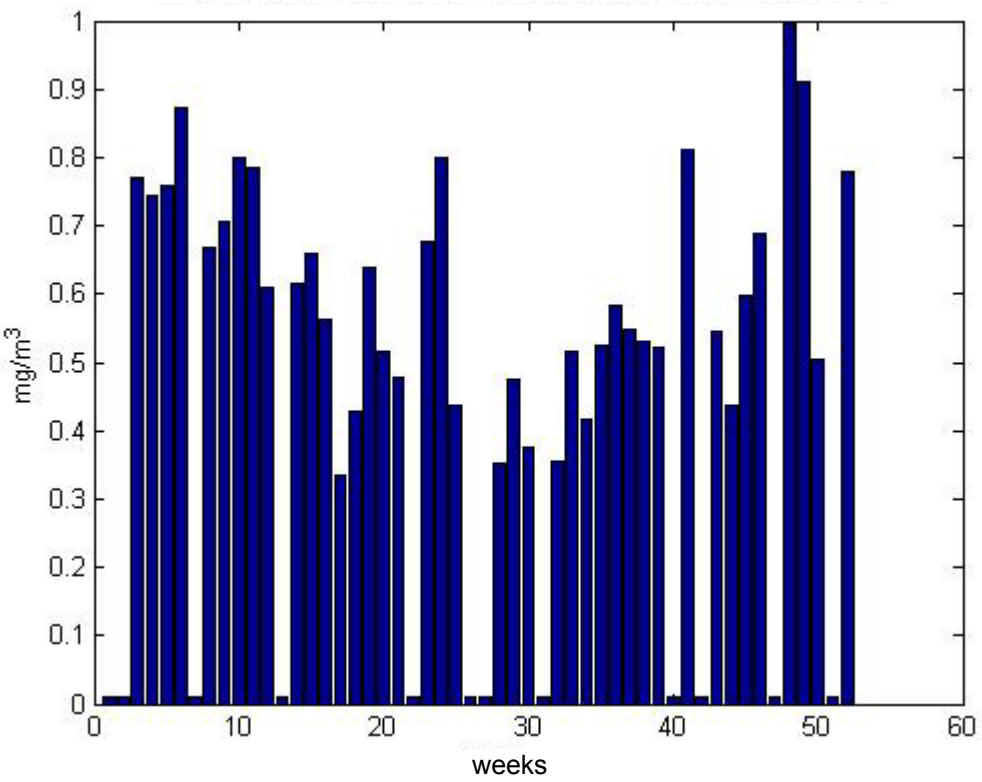

Fig. 3.29 Weekly averages of *chl* (mg m^{-3}) derived from SeaWiFS data averaged over the Alboran Sea during 2002.

Threshold analysis performed over the *chl* interval between 1.0 and 3.0 mg m^{-3} illustrated clearly that those waters rich in *chl* are transported by means of the Medium Atlantic Water (MAW) anticyclonic gyre (Appendix 13). Figure 3.30 a-c shows the gyre formation in particular between weeks 4 and 10, and figure 3.30 h shows the re-formation of the gyre during week 35. The gyre widened during week 41, affecting the region of the Al Hoceima National Park, and lasted until week 49 (Fig. 3.30 j-l). The widest extension of the gyre was observed during week 48 (Fig. 3.30 k).

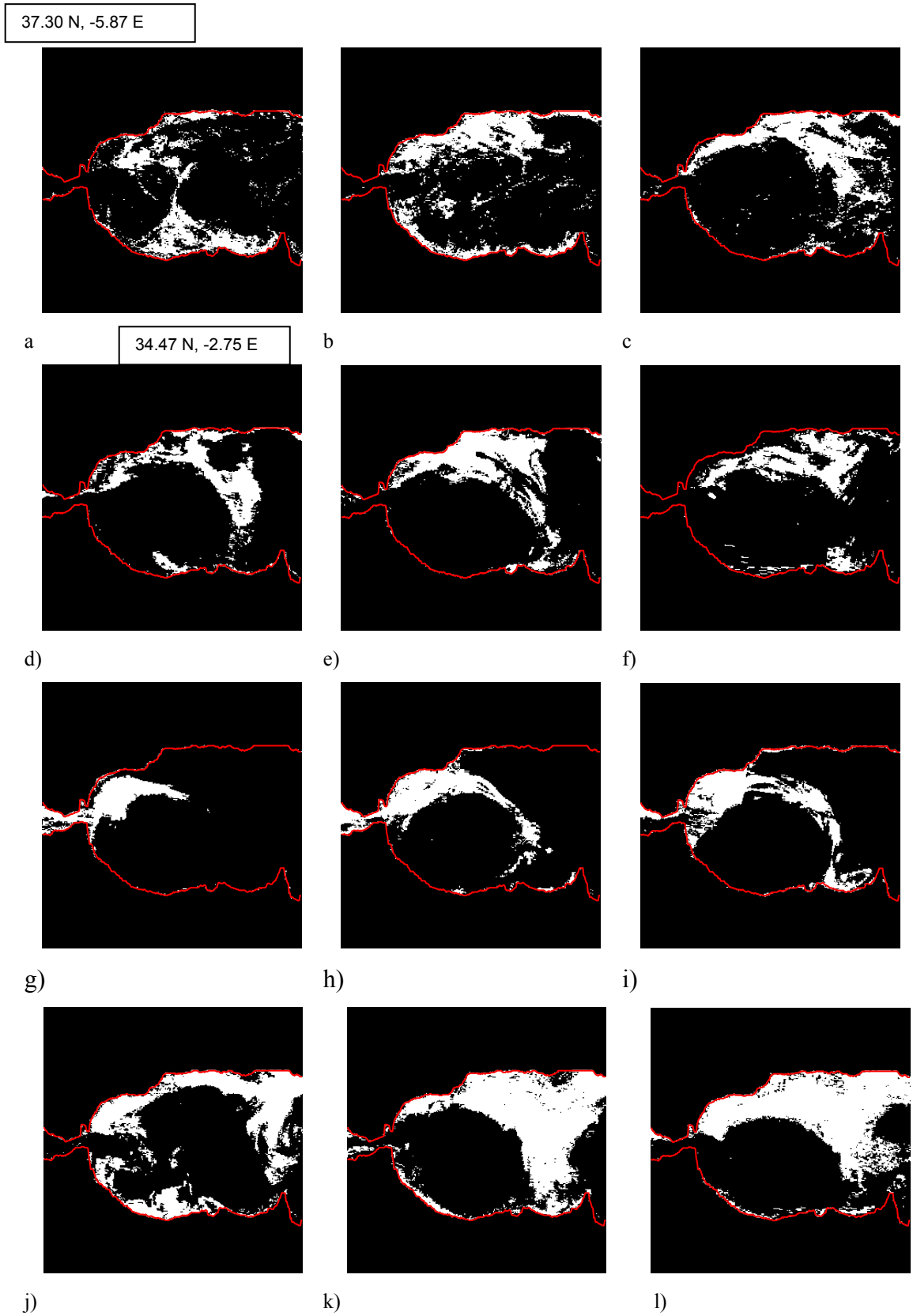

Fig. 3.30 Threshold analysis *chl* range between 1.0 and 3.0 mg m^{-3}, within the Gibraltar Strait (Alboran Sea) during 2002: weeks 4 (a), 6 (b), 10 (c), 19 (d), 23 (e), 24 (f), 34 (g), 35 (h), 36 (i), 41 (j), 48 (k) and 49 (l) respectively. White patterns show *chl* values falling within the defined intervals. Red lines show the coast line surrounding the Gibraltar Strait.

The distribution of *chl* concentration per mean km^2 (Fig. 3.31) shows a unimodal distribution associated with frontal and coastal waters (0.75 mg m^{-3}). The largest area extension recorded is 1700 km^2 covered by values *chl* of 0.75 mg m^{-3}. This analysis showed that during the year investigated *chl* concentrations between 0.6 and 0.8 mg m^{-3} tended to be predominant over the whole Alboran basin. It should be also noted that high values of *chl* such as 1.0, 1.5, 2.0 and 2.5 mg m^{-3} covered 700, 180, 100 and 50 km^2 respectively.

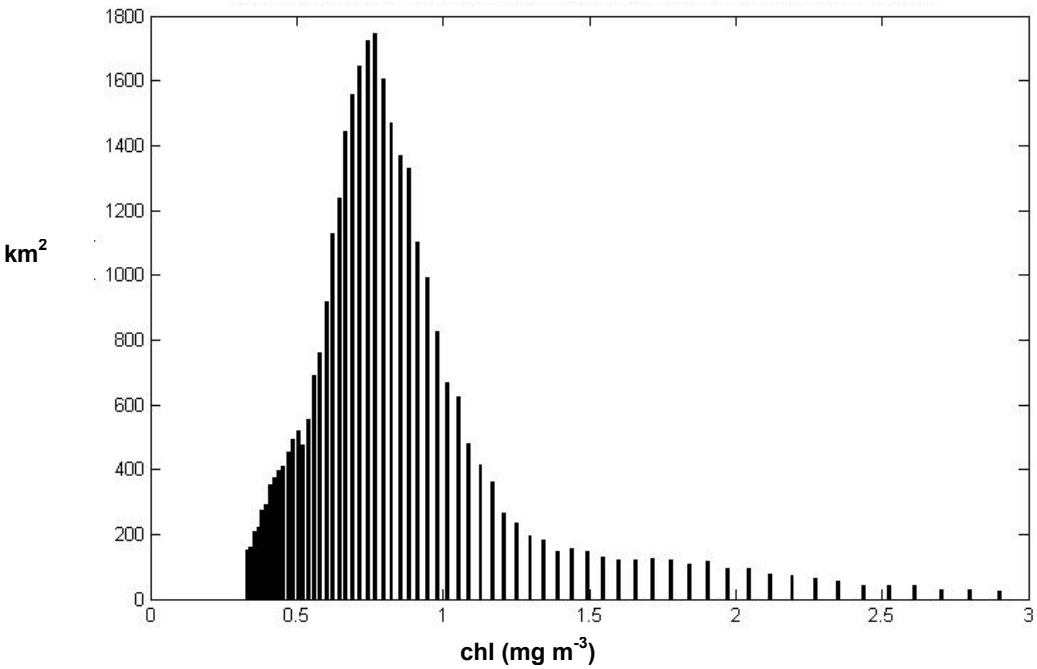

Fig. 3.31 Surface *chl* (mg m^{-3}) distribution per mean km^2 within the Alboran Sea (the whole basin) during 2002.

Spatial gradients were useful in discriminating the areas with the highest *chl* content within Alboran Sea (Appendices 14 and Appendix 15). Figure 3.32 a-d shows the two *chl* intervals considered (0.16 and 0.9 mg m^{-3}, 1.0 and 4.0 mg m^{-3}) for weeks 10 and 19. It is clearly notable that the MAW gyre transports the waters rich in *chl* content.

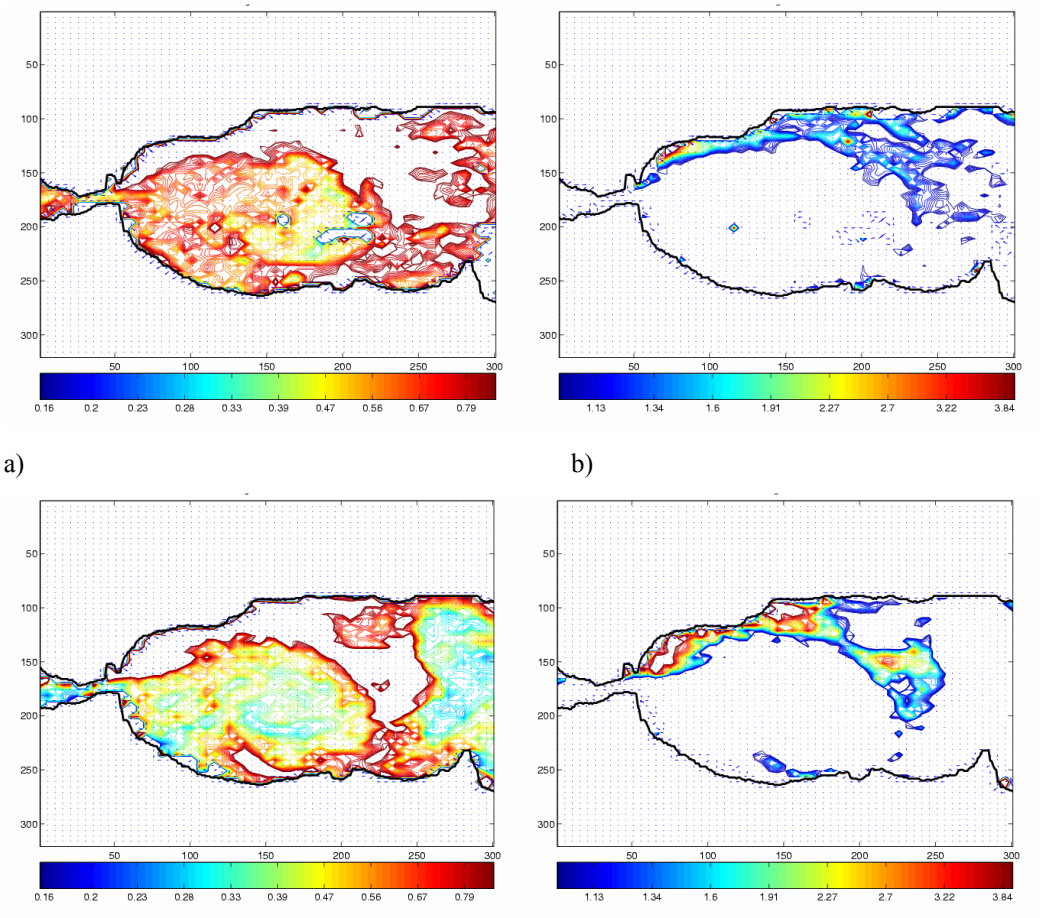

a) b)

c) d)

I) II)

Fig. 3.32 Spatial gradients of *chl* within the range of 0.16-0.9 mg m^{-3} (panel I) and within the range of 1.0-4.0 mg m^{-3} (panel II) during weeks 10 (a-b) and 19 (c-d) (2002) within the Alboran Sea.

During September the MAW was newly visible and expanded during November encompassing wide areas of the Spanish coast (Fig. 3.32 e-l).

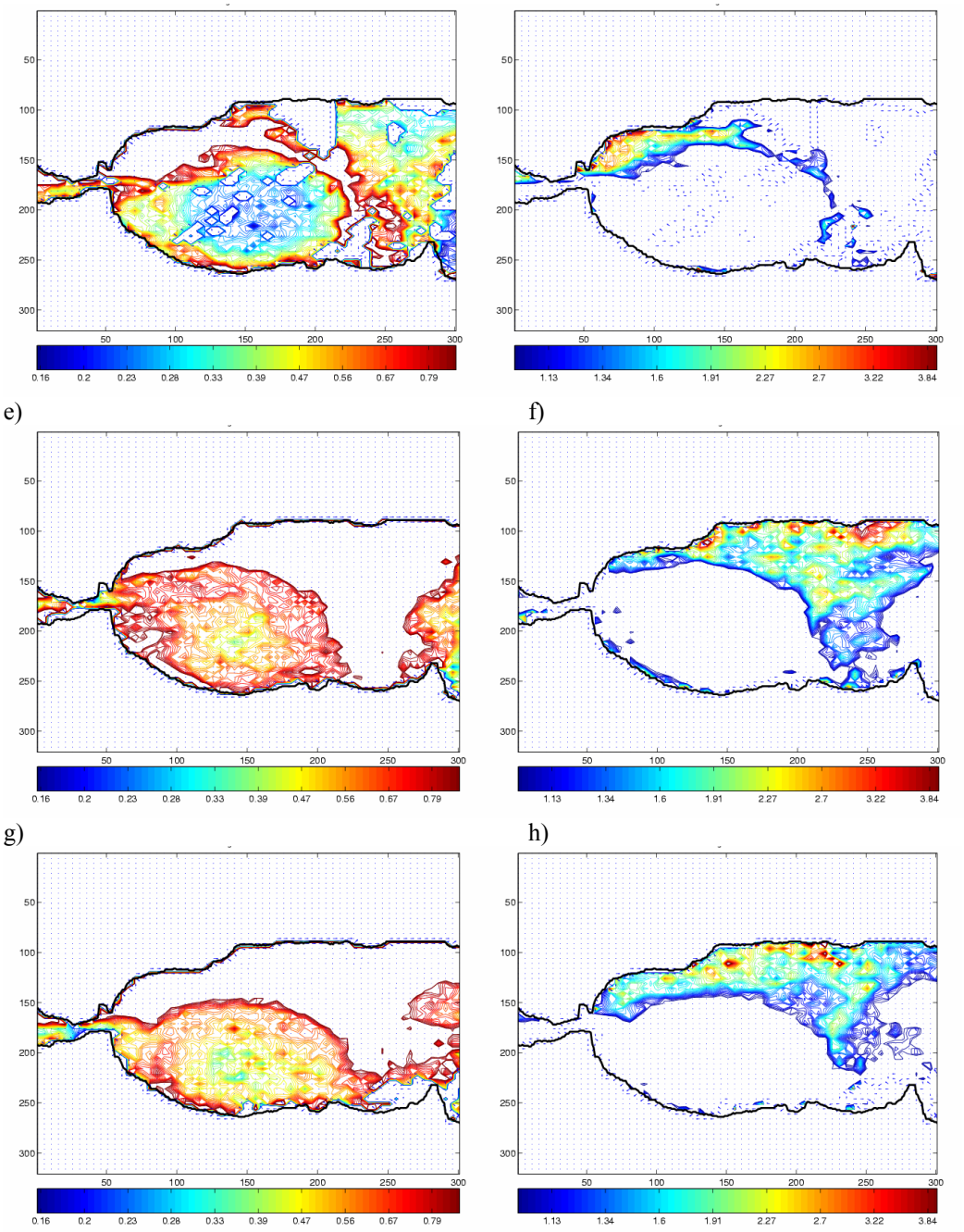

Fig. 3.32 (cont.) Spatial gradients of *chl* within the range of 0.16-0.9 mg m^{-3} (panel I) and within the range of 1.0-4.0 mg m^{-3} (panel II) during weeks 37 (e-f), 48 (g-h) and 49 (i-l) (2002) within the Alboran Sea.

The plot of factor scores resulting from the PCA performed on the X matrix (containing the data for the whole 52 weeks and representing the *chl* map) is shown in Figure 3.33. The weeks mainly dependent on the first factor and showing the highest *chl* were located on the positive x semi-axes and were weeks 49 and 48 respectively whereas the week showing the lowest *chl* was week 17.

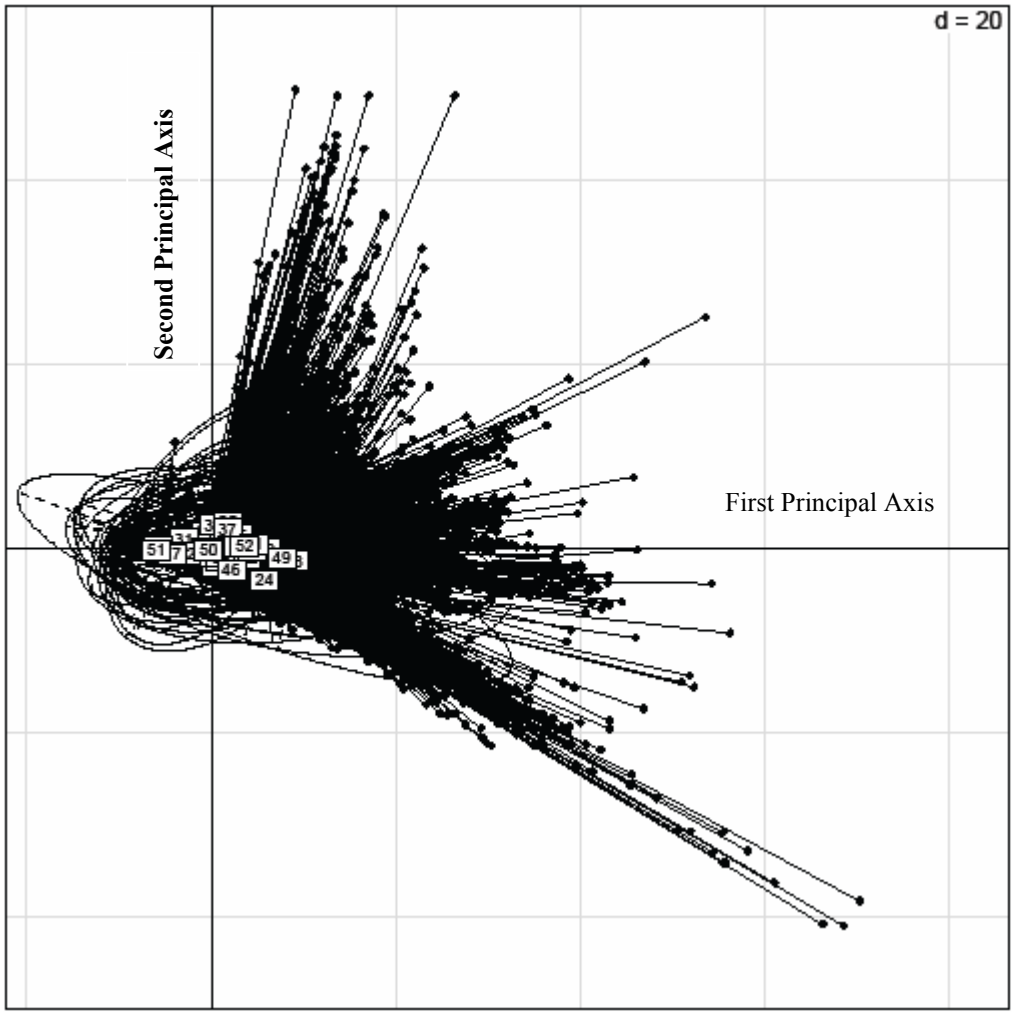

Fig. 3.33 A two dimensional plot of 52 weeks representing the *chl* maps based on PCA. Plot of the factor scores representing the PC1 and the PC2 for the Alboran Sea during 2002. The factor scores were clustered by means of confidence ellipsoids per week; on the left are located the low scores whereas on the right the high scores .

Since several images were placed on the negative X semi-axis on the plot of factor scores (Fig. 3.33), this caused the boxplots of the first component to fall partly on the negative Y semi-axis (Fig. 3.34), however the medians are always positive. The first component described 33.1% of the total variability and expressed the *chl* concentration.

As evident (Fig. 3.34) the trend of the *chl* concentration seem to follow an intermittently blooming pattern throughout the year, with similar values in spring and autumn. During the summer period, particularly in June and August, the medians were positive.

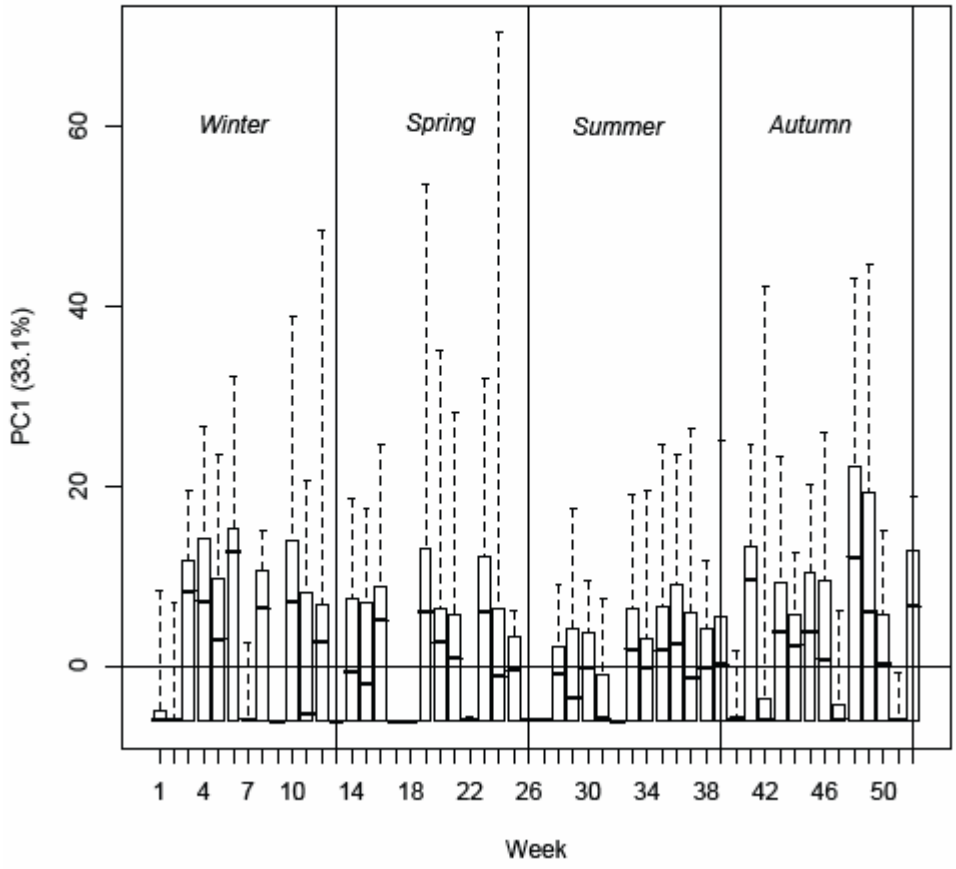

Fig. 3.34 Boxplot of the PC1 within the Alboran Sea during 2002. The boxes show the interquartile ranges (IQR) between the lower (25th percentiles) and the upper (75th percentiles) quartiles. The line in the boxes represent the median observation. The whiskers represent the 5th and the 95th percentiles.

The PC2 explained the 8.1% of the total variability (Fig. 3.35). As explained previously for Portofino MPA, the meaning of this component is not completely clear due to the land cover effect on the images. In this site, the sum of the two signals due to cloud and land cover made the second component to be more difficult to interpret. The weight due to land, which occupies a large area in the matrix extrapolated, is remarkable and could obscure the variability caused by cloud coverage.

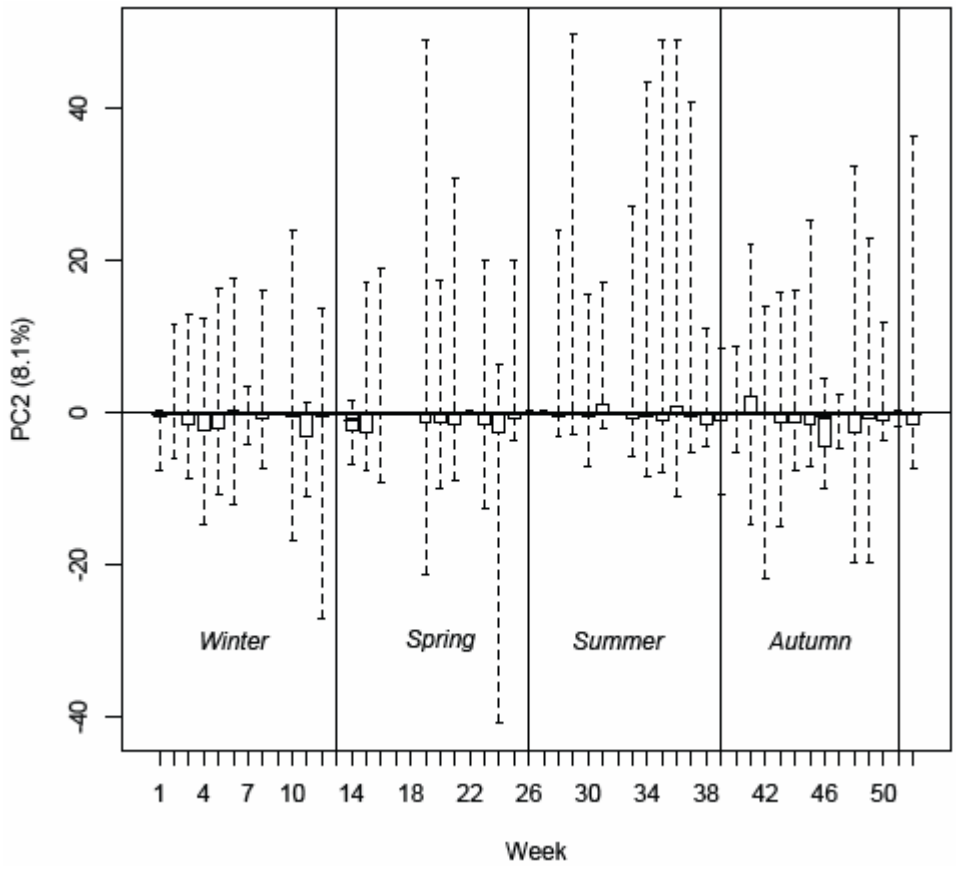

Fig. 3.35 Boxplot of the PC2 within the Alboran Sea during 2002. The boxes show the interquartile ranges (IQR) between the lower (25th percentiles) and the upper (75th percentiles) quartiles. The line in the boxes represent the median observation. The whiskers represent the 5th and the 95th percentiles.

Table 3.4 shows the K-sample multivariate E-distances. The E-distances retrieved in relation to W4 *vs*. W5 were the only significant whereas those calculated between the following pair of weeks (e.g. W4-W16) were corrupted by cloud coverage. The E-distance between weeks 16 and 17 shows an abrupt decrease of *chl* whereas E-distance between W17 and W18, W18 and W19, W19 and W20 were all significant showing a progressive increase in *chl*. The highest distance was recorded between W18 and W19. During summer, between weeks 24 and 25 there was a significant decrease in *chl* whereas E-distance between weeks 32 and 33 showed a significant increase of *chl* with a high distance recorded.

In autumn the *chl* fluctuated markedly, showing significant E-distance between weeks 43 and week 44, between weeks 44 and 45 and between weeks 49 and 50 and not corrupted by clouds. In cases where the clouds affect seriously the satellite imagery, the e-distance result biased, because the distance does not represent a real difference in *chl* between the two weeks considered.

Table 3.4 E-Distances for the Alboran Sea during 2002. Only the significant values modified by Bonferroni's correction at level $p<0.001$ are presented. The comparisons were made per following weeks.

Weeks	E-distances
W2 *vs*. W3	444.8
W4 *vs*. W5	64.1
W5 *vs*. W6	100.1
W6 *vs*. W7	680.2
W7 *vs*. W8	503.3
W8 *vs*. W9	600.4
W9 *vs*. W10	670.0
W10 *vs*. W11	116.8
W11 *vs*. W12	100.0
W12 *vs*. W13	521.5
W13 *vs*. W14	476.4
W15 *vs*. W16	72.5
W16 *vs*. W17	520.8
W17 *vs*. W18	0.0
W18 *vs*. W19	720.1
W19 *vs*. W20	70.2
W21 *vs*. W22	420.7
W22 *vs*. W23	629.1
W23 *vs*. W24	117.3
W24 *vs*. W25	243.3
W25 *vs*. W26	290.3
W27 *vs*. W28	320.2
W30 *vs*. W31	60.8
W31 *vs*. W32	190.8
W32 *vs*. W33	465.4
W37 *vs*. W38	63.3
W38 *vs*. W39	38.3
W39 *vs*. W40	297.5
W40 *vs*. W41	599.5
W41 *vs*. W42	347.7
W42 *vs*. W43	229.2
W43 *vs*. W44.	40.1
W44 *vs*. W45	61.7
W45 *vs*. W46	60.2
W46 *vs*. W47	237.6
W47 *vs*. W48	613.3
W49 *vs*. W50	254.6
W50 *vs*. W51	334.9
W51 *vs*. W52	281.7

The weekly mean *chl* concentration along Al Hoceima National Park (Fig. 3.36) showed that *chl* peaks occurred between January and February with mean values of 0.75-1.0 mg m^{-3}, and between October and December with mean values around 0.85 mg m^{-3}. During summer *chl* fluctuated around 0.4 mg m^{-3}.

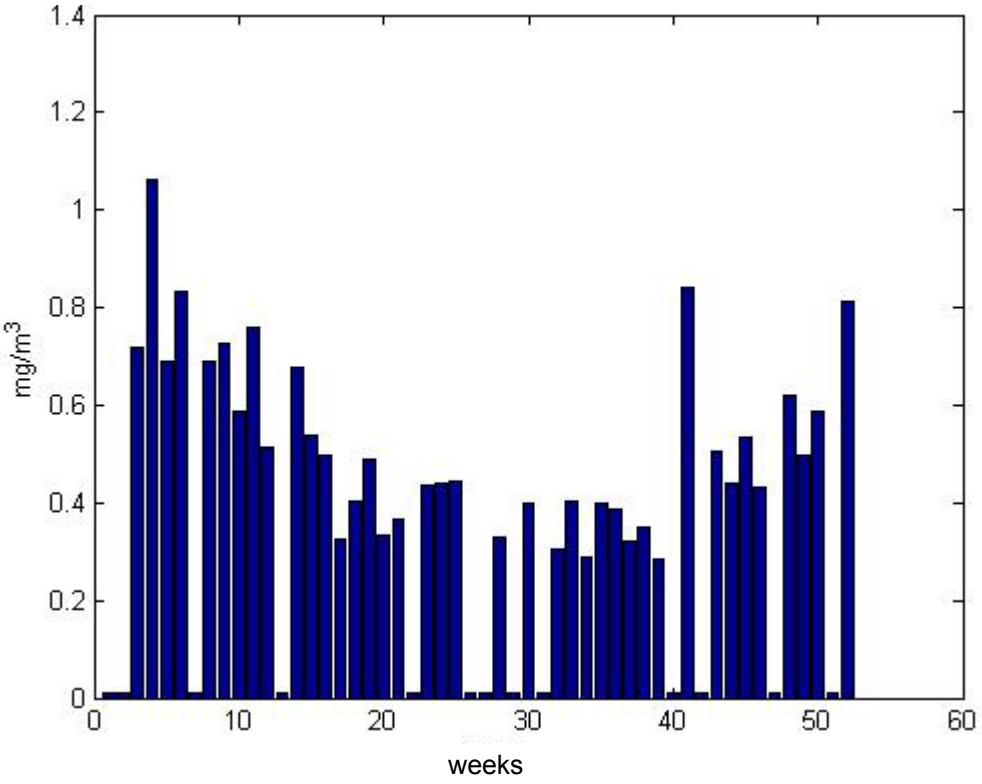

Fig. 3.36 Weekly averages of *chl* (mg m^{-3}) derived from SeaWiFS data averaged over the Al Hoceima National Park during 2002.

The distribution of *chl* per mean km^2 (Fig. 3.37) shows a bimodal distribution. The two main *ch*l peaks were 0.5 and 0.75 mg m^{-3} with a coverage of 70 km^2 and 190 km^2 respectively. Values of 1 mg m^{-3} covered 60 km^2. Higher *chl* values were negligible in terms of their area coverage. The chlorophyll distribution had one mode associated with the central oligotrophic waters (0.5 mg m^{-3}) and a second mode for coastal waters (0.75 mg m^{-3}; Fig. 3.37).

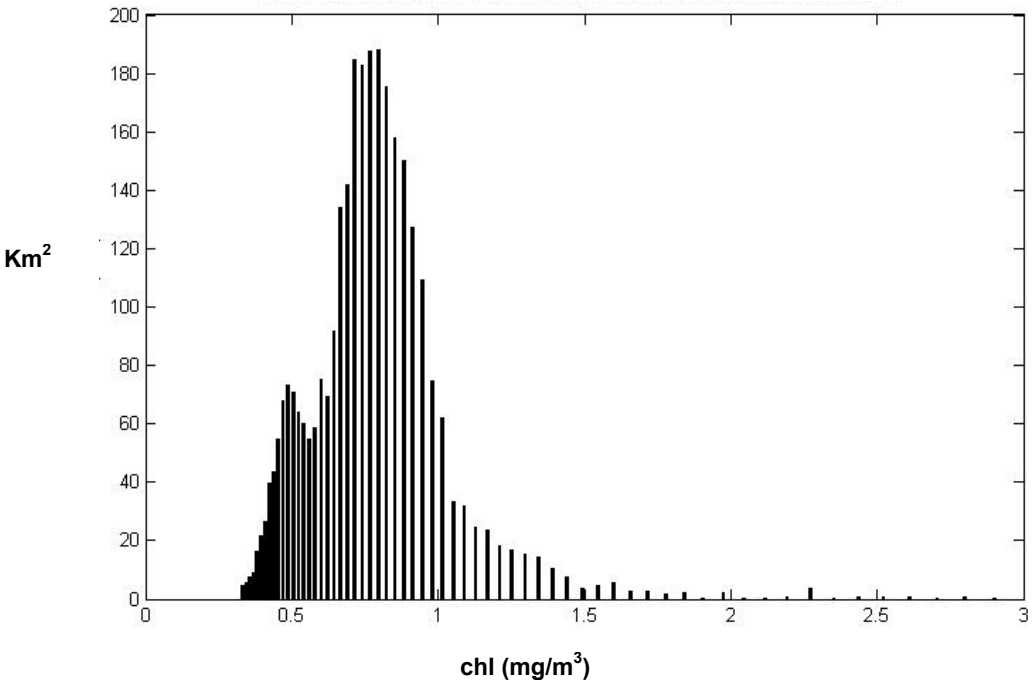

Figure 3.37 Surface *chl* (mg m^{-3}) distribution per mean km^2 along Al Hoceima National Park during 2002.

Appendix 16 shows the spatial gradient calculated considering the range of 0.16-0.9 and Appendix 17 the gradient calculated within the range of 1.0-3.0 mg m^{-3} along Al Hoceima National Park. The higher chlorophyll values were located along the coast, i.e. where the anticyclonic gyre persisted.

The patches with the highest *chl* and with the major extension were recorded during January (week 4;Fig. 3.38 a-b) and October (week 41; Fig. 3.38 e-f).

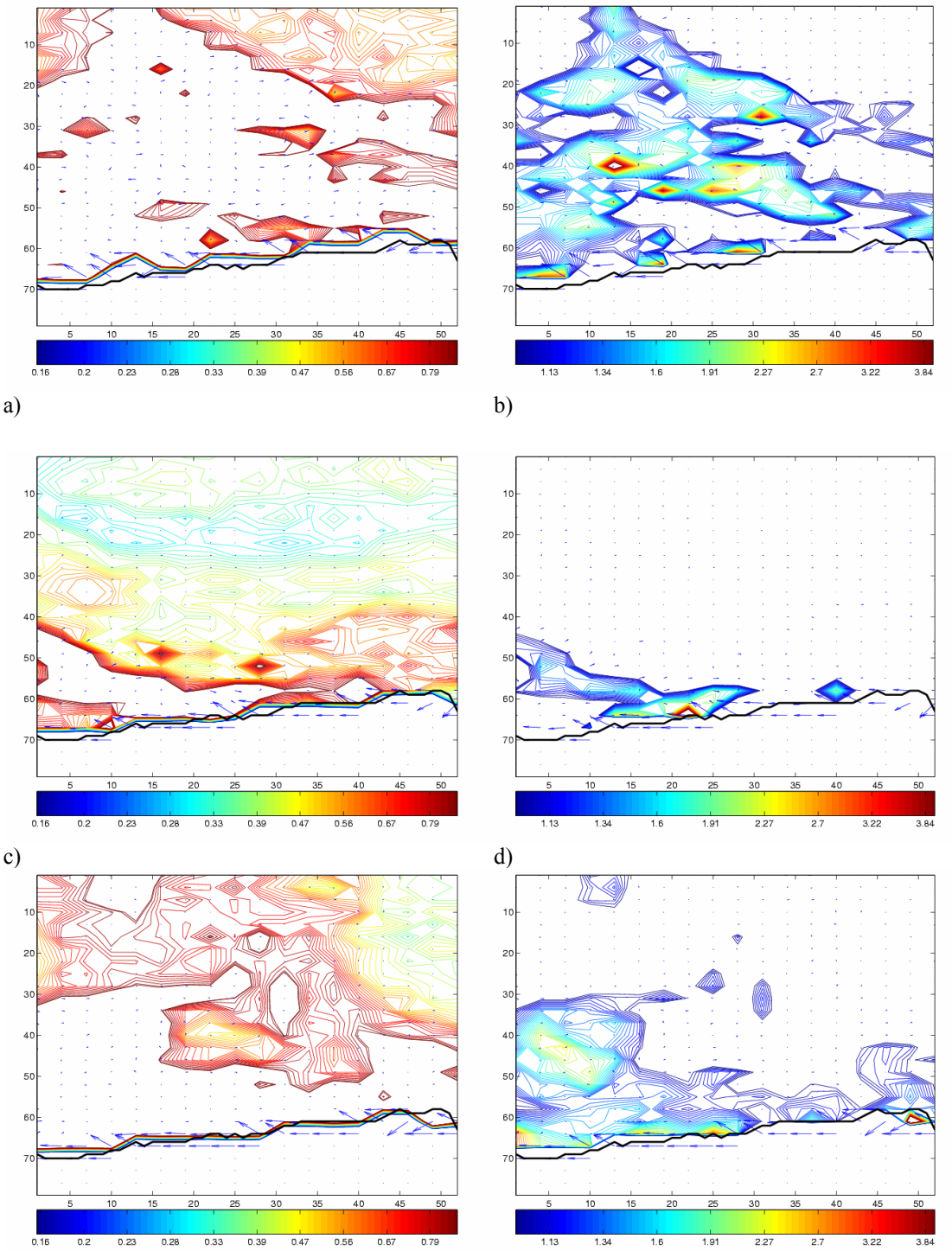

Fig. 3.38 Spatial gradients of *chl* within the range of 0.16-0.9 mg m^{-3} (panel I) and within the range of 1.0-3.0 mg m^{-3} (panel II) during weeks 4 (a-b), 19 (c-d) and 41 (e-f) (2002) along Al Hoceima National Park waters.

The plot of factor scores for Al Hoceima resulting from the PCA performed on the X matrix containing the data for the whole 52 weeks and representing the *chl* map, is shown in Figure 3.39. The weeks mainly dependent on the first factor and showing the highest *chl* were located on the positive x semi-axes and were 4, 41 and 52 respectively.

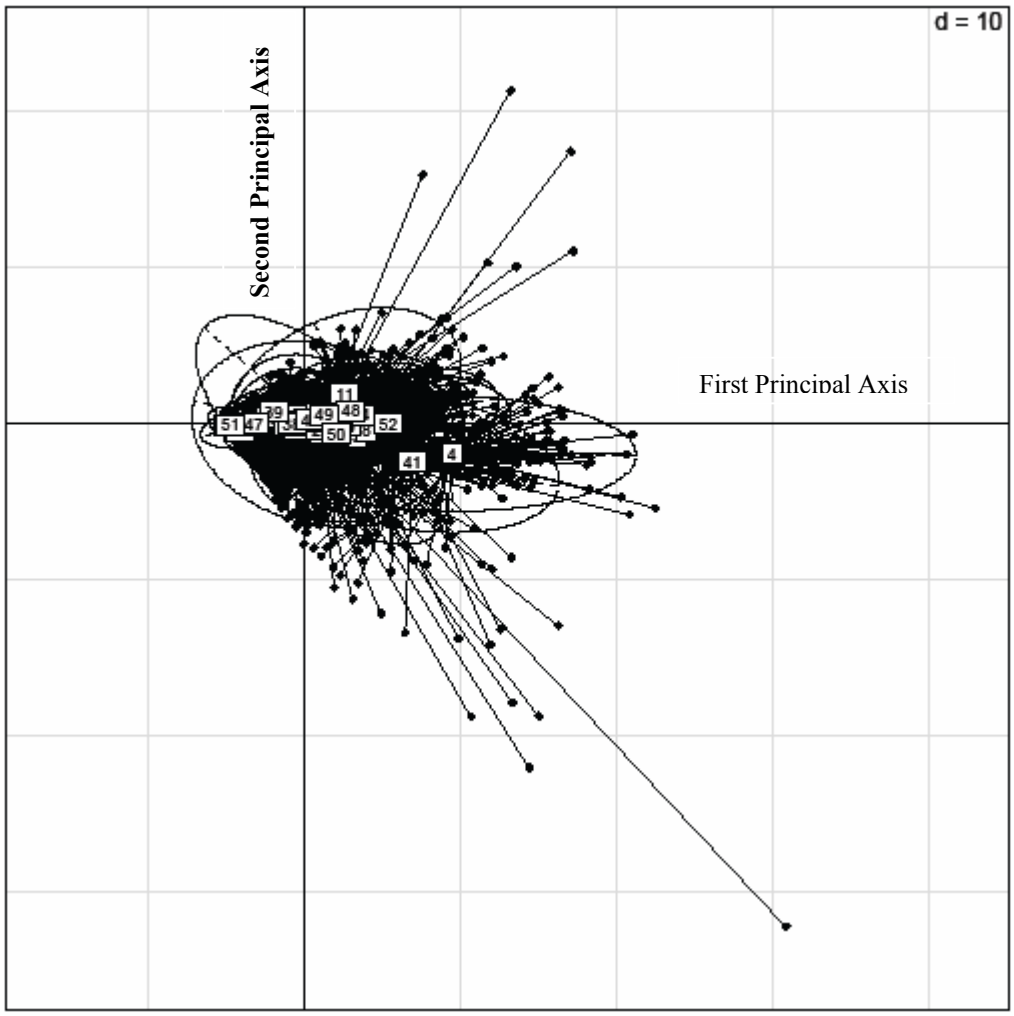

Fig. 3.39 A two dimensional plot of 52 weeks representing the *chl* maps based on PCA. Plot of the factor scores representing the PC1 and PC2 for Al Hoceima study area during 2002. The factor scores were clustered by means of confidence ellipsoids per week; on the left are located the low scores whereas on the right the high scores .

Figure 3.40 shows the boxplots of the PC1. The PC1 described 39.4% of the total variability and expressed the *chl* concentration.

The presence of a clear seasonal trend of the *chl* concentration here was again notable, the first algal bloom occurring between weeks 4 and 14. Other peaks occurred in autumn (weeks 41) and in winter (week 52). During late spring and summer period low but positive mean *chl* values were recorded.

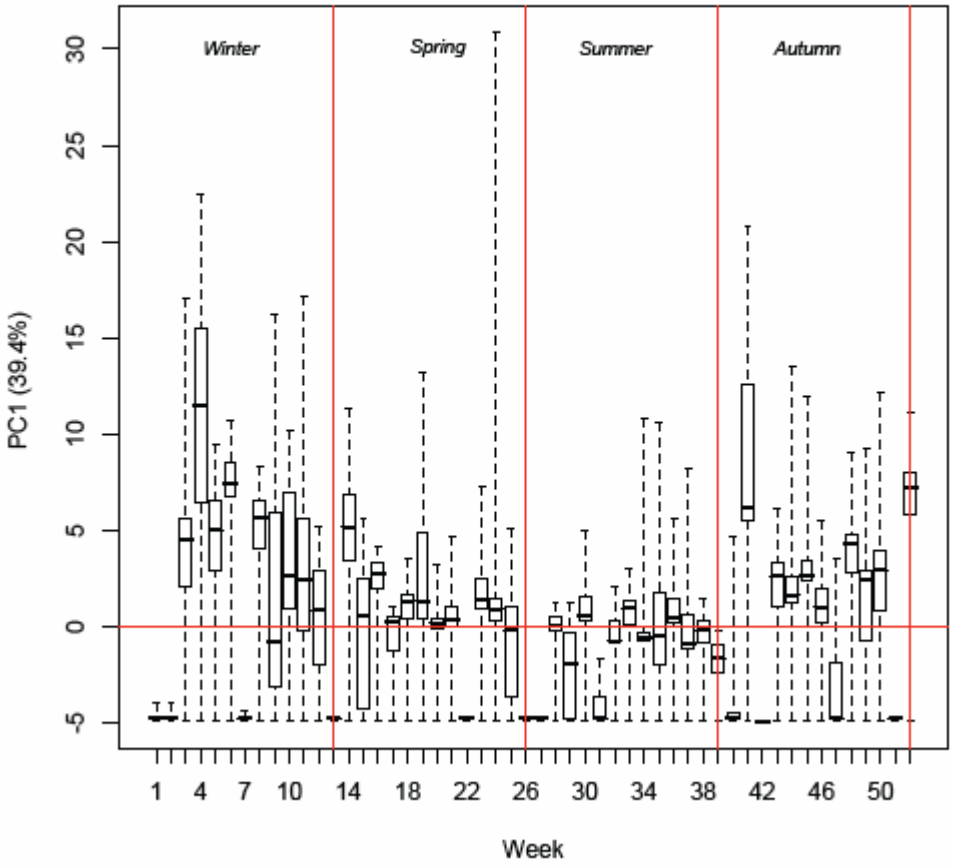

Fig. 3.40 Boxplot of the PC1 along Al Hoceima study area during 2002. The boxes show the interquartile ranges (IQR) between the lower (25th percentiles) and the upper (75th percentiles) quartiles. The line in the boxes represent the median observation. The whiskers represent the 5th and the 95th percentiles.

The PC2 explained about the 6.6% of the total variability (Fig. 3.41). As explained previously for the Alboran Sea, the meaning of this component is not completely clear due to the land cover effect on the images. The cloud and land cover signals made the second component to be more difficult to interpret. The weight due to land, which occupies a large area in the matrix extrapolated, is remarkable and could obscure the variability caused by cloud coverage.

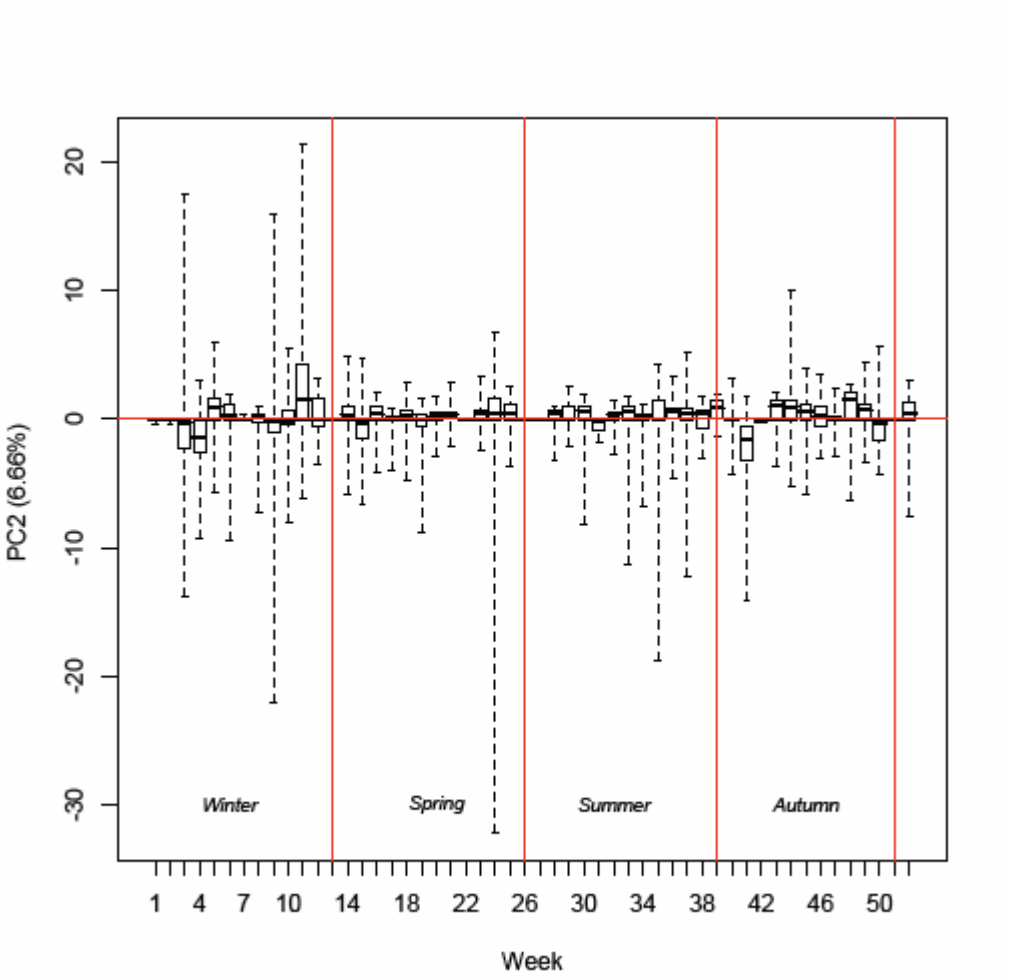

Fig. 3.41 Boxplot of the PC2 along Al Hoceima study area during 2002. The boxes show the interquartile ranges (IQR) between the lower (25th percentiles) and the upper (75th percentiles) quartiles. The line in the boxes represent the median observation. The whiskers represent the 5th and the 95th percentiles.

Table 3.5 shows the K-sample multivariate E-distances. The E-distances retrieved in relation to W4 *vs*. W5 and between W5 *vs*. W6 were the only significant whereas those calculated between the following pair of weeks (e.g. W6-W16) were corrupted by cloud coverage. The E-distance between weeks 16 and 17, W17 and W18, W18 and W19, W19 and W20 were all significant and showed a fluctuation of the *chl*. Also during summer, between weeks 32 and 35 a significant fluctuation of *chl* was observed; E-distance between weeks 36 and 37 showed a significant increase of *chl*.

In autumn the *chl* fluctuated showing significant E-distance between weeks 44 and week 45 and between weeks 45 and 46; the other distances were corrupted by clouds.

Table 3.5 E-Distances for the Al Hoceima study area during 2002. Only the significant values modified by Bonferroni's correction at level $p<0.001$ are presented. The comparisons were made per following weeks.

Weeks	E-distances
W2 *vs*. W3	181.3
W3 *vs*. W4	74.6
W4 *vs*. W5	95.9
W5 *vs*. W6	22.4
W6 *vs*. W7	283.1
W7 *vs*. W8	240.2
W8 *vs*. W9	1781.1
W10 *vs*. W11	1560.3
W11 *vs*. W12	26.3
W12 *vs*. W13	115.7
W13 *vs*. W14	210.9
W14 *vs*. W15	53.0
W15 *vs*. W16	26.5
W16 *vs*. W17	36.3
W17 *vs*. W18	11.2
W18 *vs*. W19	14.4
W19 *vs*. W20	26.1
W21 *vs*. W22	112.7
W22 *vs*. W23	146.3
W25 *vs*. W26	85.8
W27 *vs*. W28	113.4
W28 *vs*. W29	27.1
W29 *vs*. W30	35.7
W30 *vs*. W31	100.1
W31 *vs*. W32	70.4
W32 *vs*. W33	14.5
W33 *vs*. W34	20.9
W34 *vs*. W35	18.1
W35 *vs*. W36	13.7
W36 *vs*. W37	10.7
W38 *vs*. W39	18.3
W39 *vs*. W40	46.5
W40 *vs*. W41	250.6
W41 *vs*. W42	300.1
W42 *vs*. W43	169.7
.	.
W44 *vs*. W45	11.9
W45 *vs*. W46	16.9
W46 *vs*. W47	63.8
W47 *vs*. W48	129.2
W48 *vs*. W49	21.2
W49 *vs*. W50	16.9
W50 *vs*. W51	155.4
W51 *vs*. W52	281.7

3.3.3.2 Thermal IR data

The remotely sensed SST field in the Alboran Sea was investigated using AVHRR data. Appendices 18 and 19 show Sea Surface Temperature skin within Alboran Sea and along Al Hoceima National Park respectively from April to December 2002. Figure 3.42 shows SST skin within the Gibraltar Strait from week 19 to 23. During week 19 the gyre formed at a temperature of 16 °C (Fig. 3.42 a). The cold gyre persisted until week 23. During week 25 the Gibraltar Strait warmed up to 25 °C (Fig. 3.42 f). In August the anticyclonic thermal front at a skin temperature of about 21 °C was observed again, cooling to 19 °C in September and to16 °C between November an December (Fig. 3.42 j-l).

Figure 3.43 shows SST skin along Al Hoceima National park. The SST skin during week 19 was about 21 °C (Fig. 3.43 a). During week 20 a colder SST skin was observed along the coast at about 16 °C (Fig. 3.43 b). In June SST skin started to warm to 23 °C, but the colder stretch along the coast at 18 °C was still visible (Fig. 3.43 d-f). During July the area was wholly characterised by warm waters reaching temperatures of about 26-27°C apart from the coastal stretch which was at 21 °C (Fig. 3.43 g-h). During August the SST skin recorded were 28 °C offshore and 24 °C along the coast. September was the last month where the colder thermal front along the coast was visible (Fig. 3.43 i-j). During October and November the SST skin was about 23 and 18 °C respectively and the colder coastal front had disappeared (Fig. 3.43 k-l).

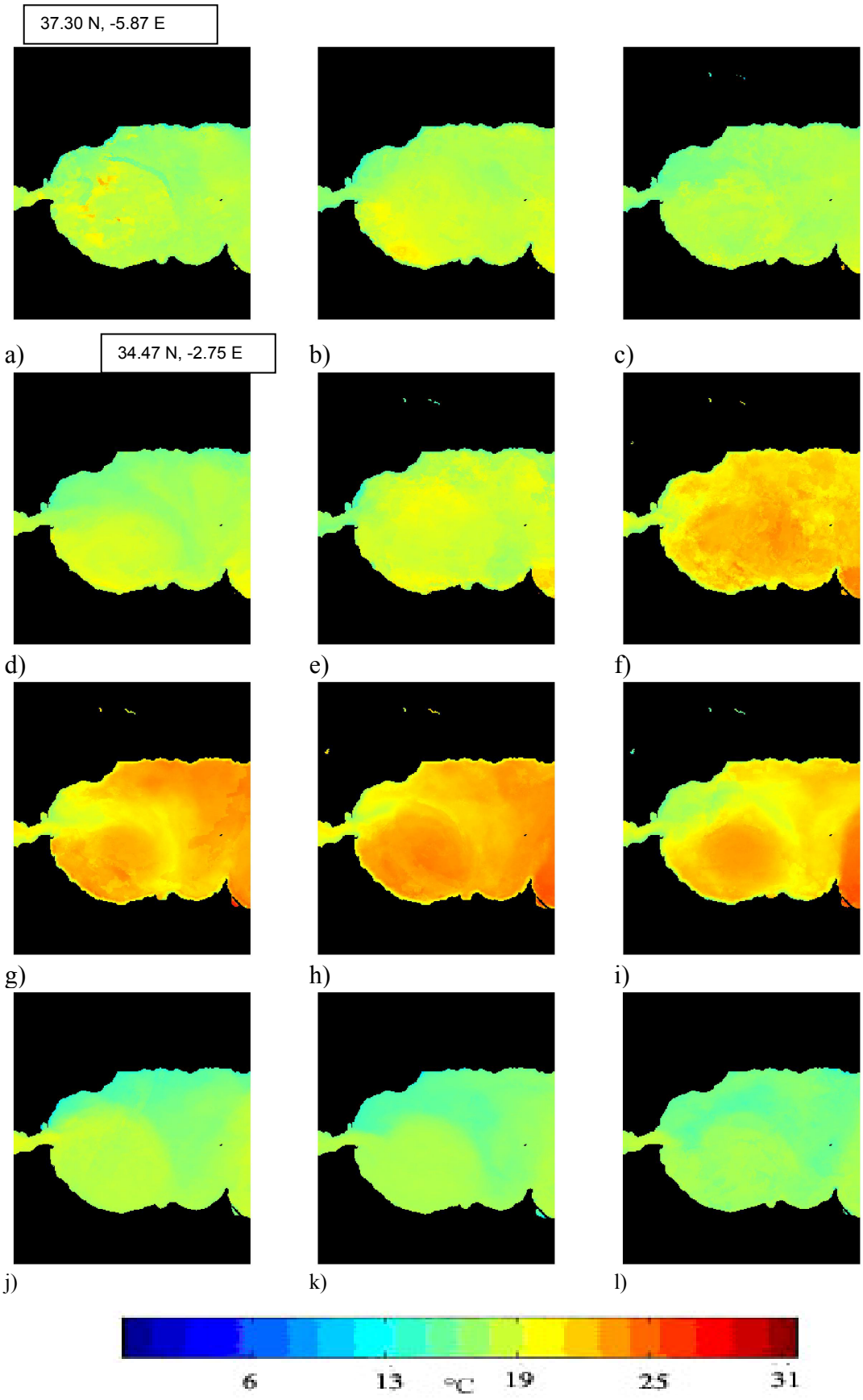

Fig. 3.42 Weekly maps of the SST skin derived from AVHRR within the Alboran Sea: weeks 19 (a), 20 (b), 21 (c), 23(d), 24 (e), 25 (f), 30 (g), 33 (h), 36 (i), 48 (j), 49 (k) and 50 (i) respectively, during 2002.

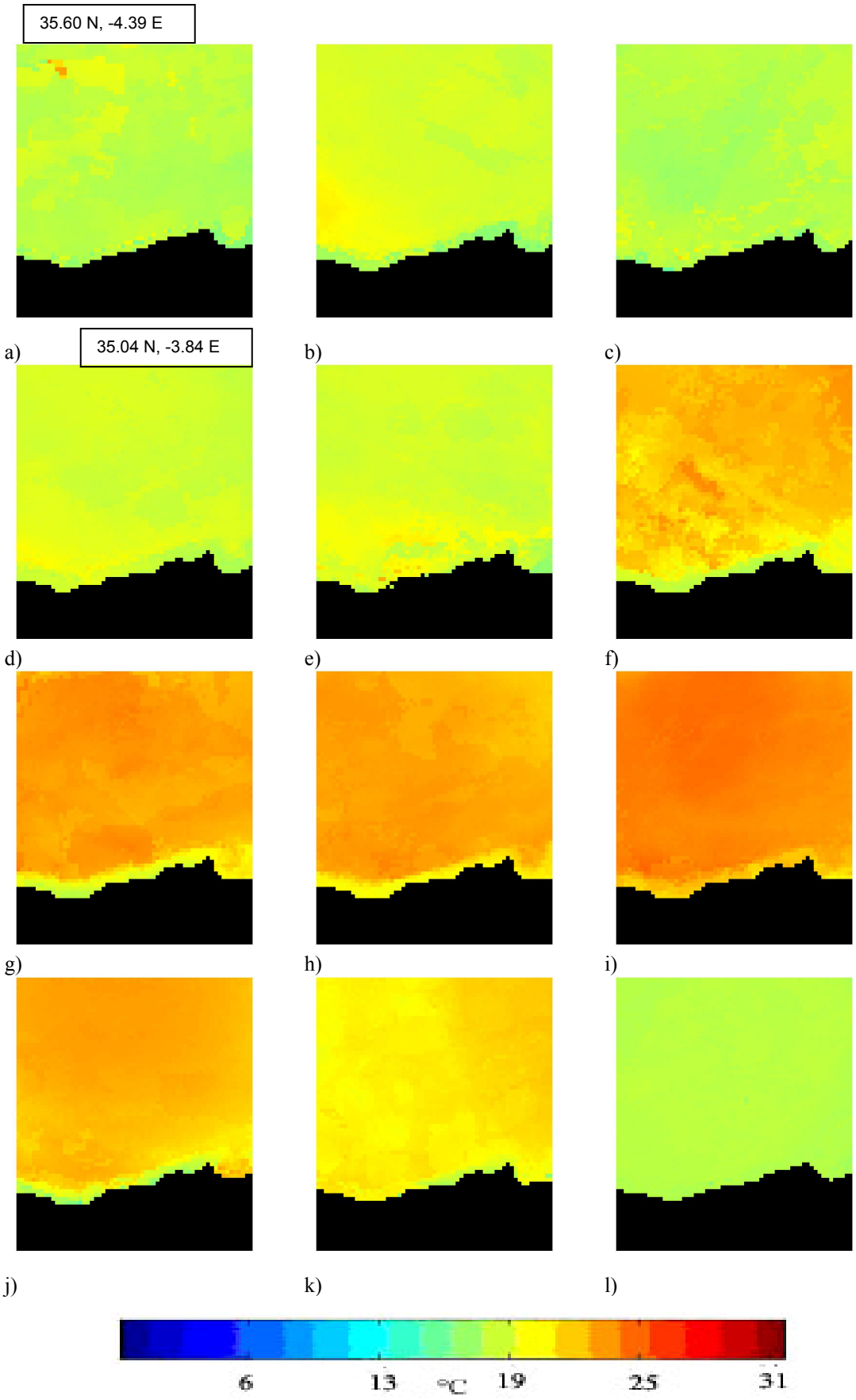

Fig. 3.43 Weekly maps of the SST skin derived from AVHRR along Al Hoceima National Park: weeks 19 (a), 20 (b), 21 (c), 23(d), 24 (e), 25 (f), 27 (g), 28 (h), 32 (i), 36 (j), 41 (k) and 48 (l) respectively, during 2002.

3.3.4 Rdum Majjesa and Ras Raheb MPA

The Rdum Majjesa and Ras Raheb MPA located on the North western of the Maltese island (Fig. 3.44).

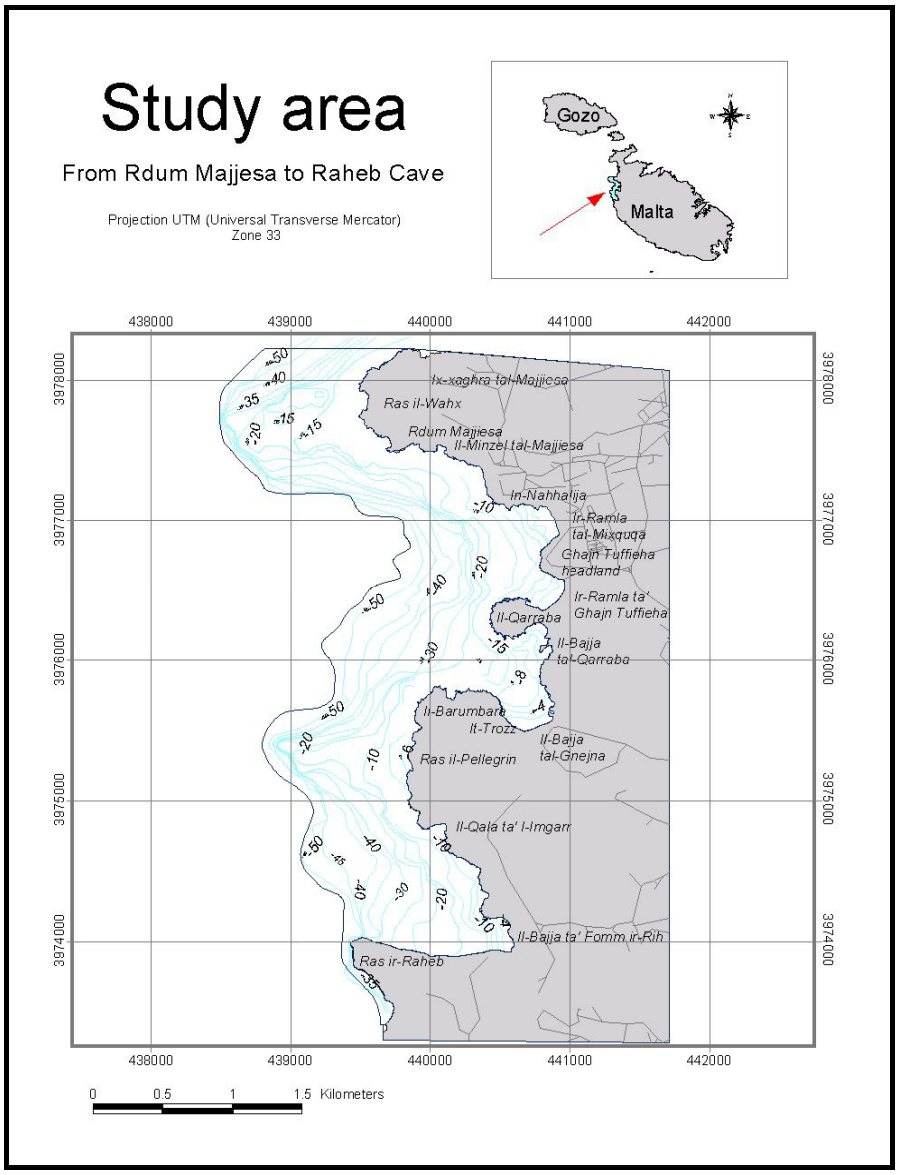

Fig. 3.44 Rdum Majjesa and Ras Raheb (NW Malta) MPA (Agnesi *et al*., 2003).

3.3.4.1 Ocean colour data

The Maltese MPA being relatively small area, the *chl* maps will take into consideration the whole island. Appendix 20 shows the weekly *chl* maps along the Maltese coast

during 2002. The images show that the highest *chl* concentrations during the first weeks (weeks 2-8; Fig. 3.45 b-e). and during weeks 50 and 52 along the north-western and eastern coast (Fig. 3.45 n-o). From the end of May the *chl* concentration started to decrease to 0.05 mg m^{-3}. In December high *chl* concentrations surrounding the island were recorded, with peaks along the north-western area of 1.0 mg m^{-3} (Fig. 3.45 n-o).

The weekly mean *chl* concentration along the Maltese coasts (Fig. 3.46) reached maximum values during the winter weeks, whereas the minimum values occurred during summer. The weekly mean *chl* concentration showed that the *chl* peaks occurred between January and February with mean values of 0.35-0.45 mg m^{-3}, and in December with mean *chl* values around 0.35 mg m^{-3}. During summer *chl* fluctuated around 0.15 mg m^{-3}.

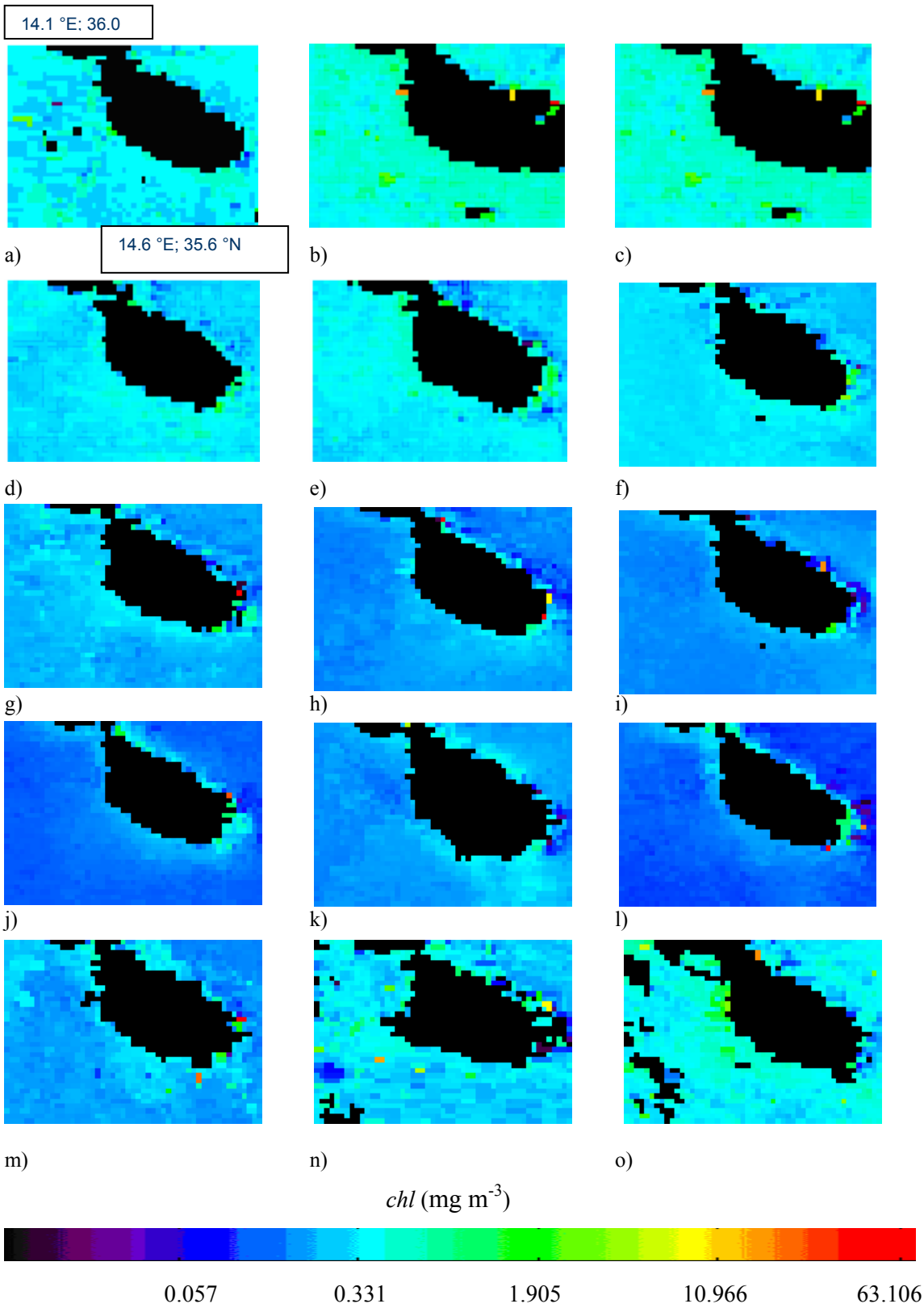

Fig. 3.45 Weekly maps of *chl* (mg m^{-3}) derived from SeaWiFS data, according to the OC4v4 algorithm, along the Maltese waters during 2002: weeks 1 (a), 2 (b), 4 (c), 7 (d), 8 (e), 11 (f), 12 (g), 16 (h), 18 (i), 24 (j), 28 (k) and 33 (l), 45 (m), 50 (n) and 52 (o).

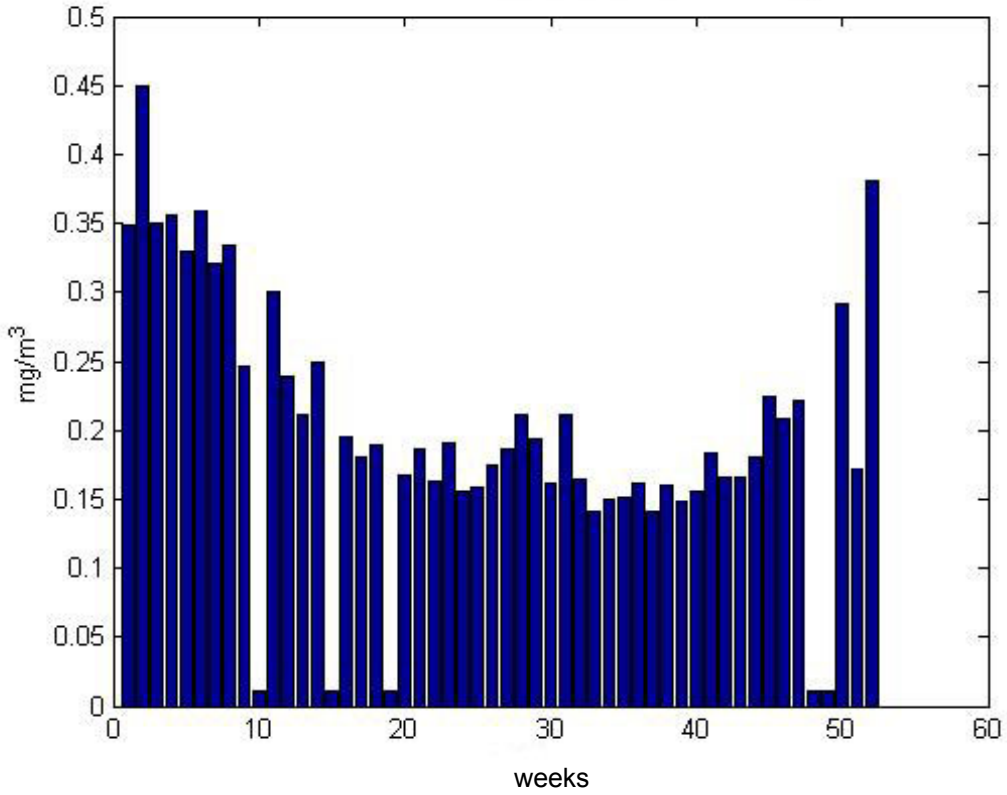

Fig. 3.46 Weekly averages of *chl* (mg m^{-3}) derived from SeaWiFS data averaged along the Maltese waters during 2002.

The distribution of *chl* per mean km^2 (Fig. 3.47) shows a unimodal distribution. The *chl* peak was about 0.35 mg m^{-3} with a coverage of 75 km^2. *Chl* values of 0.5 only covered 20 km^2 and higher *chl* values were negligible in terms of area coverage.

.

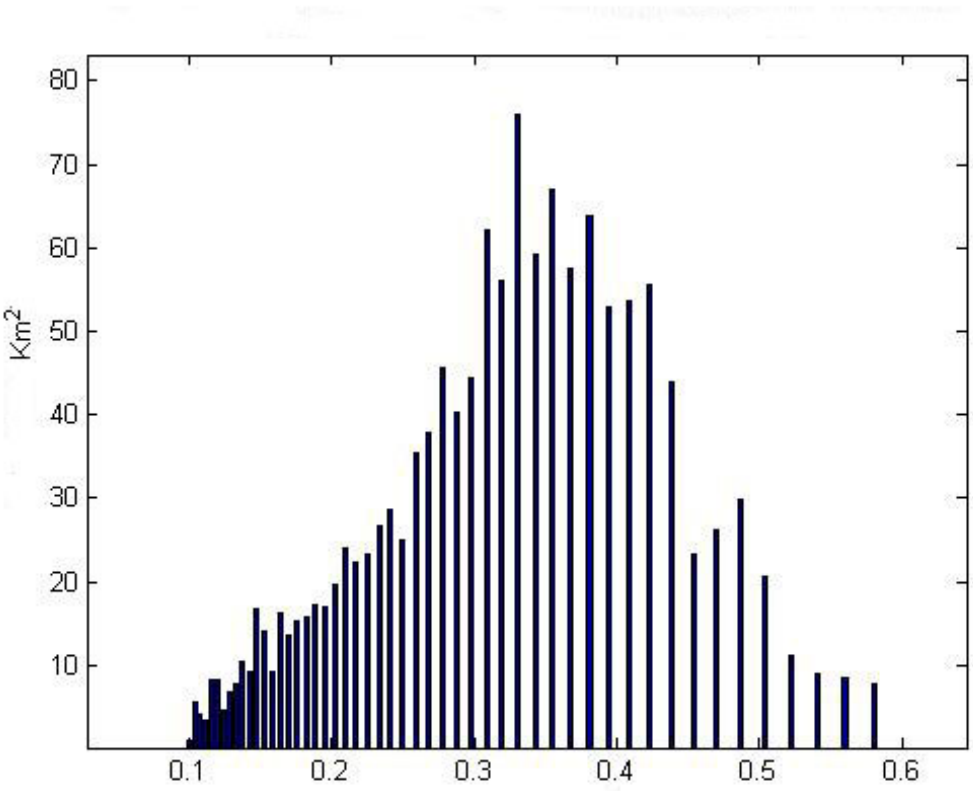

Fig. 3.47 Surface *chl* (mg m^{-3}) distributed per mean areas (km^2) along the Maltese coast during 2002.

The analysis of the spatial gradient within the *chl* range 0.1 to 0.9 mg m^{-3} (Appendix 21) showed that during week 2 the highest *chl* values were located along the western coast, and during week 5 the highest *chl* values were located along the north-western coast (Fig. 3.48 a-c).

Between weeks 9 and 17 (Appendix 21 and Fig. 3.48 d) the highest *chl* values were located along the southern region and between weeks 21 and 39 high *chl* patches were recorded along the east side of the island (Fig. 3.48 e and Appendix 21). During week 52 (Fig. 3.48 f) the patches with the highest *chl* (0.70 mg m^{-3}) were recorded again on the western side of the island.

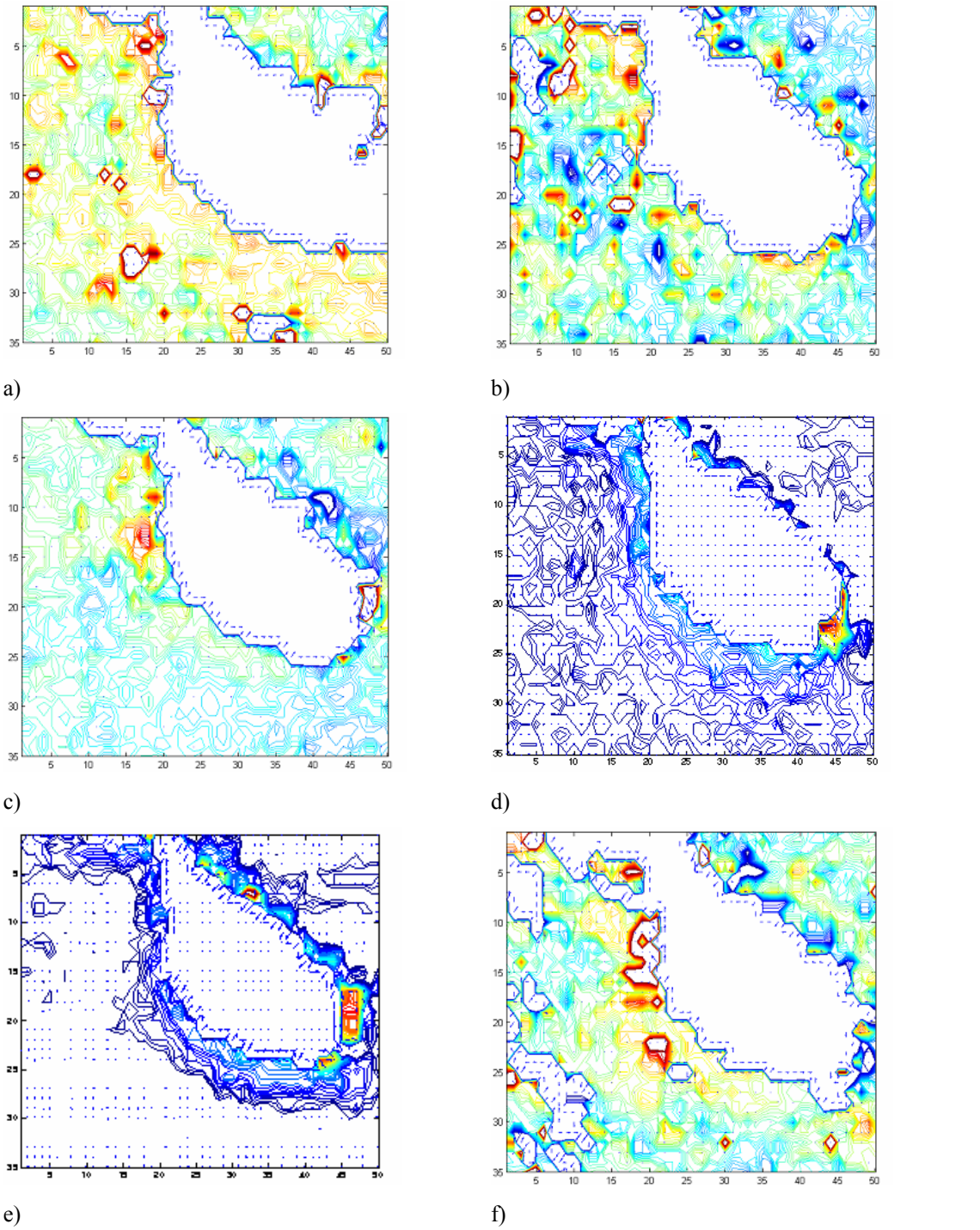

Fig. 3.48 Spatial gradients of *chl* within the range of 0.16-0.9 mg m^{-3} during weeks 2 (a), 4 (b), 5 (c), 17 (d), e (22) and 52 (f), along the Maltese waters during 2002.

The Plot of PCA factor scores is illustrated in Figure 3.49. The weeks mainly dependent on the first factor and showing the highest *chl* were located on the positive x semi-axes and were weeks 2, 52 and 50 respectively.

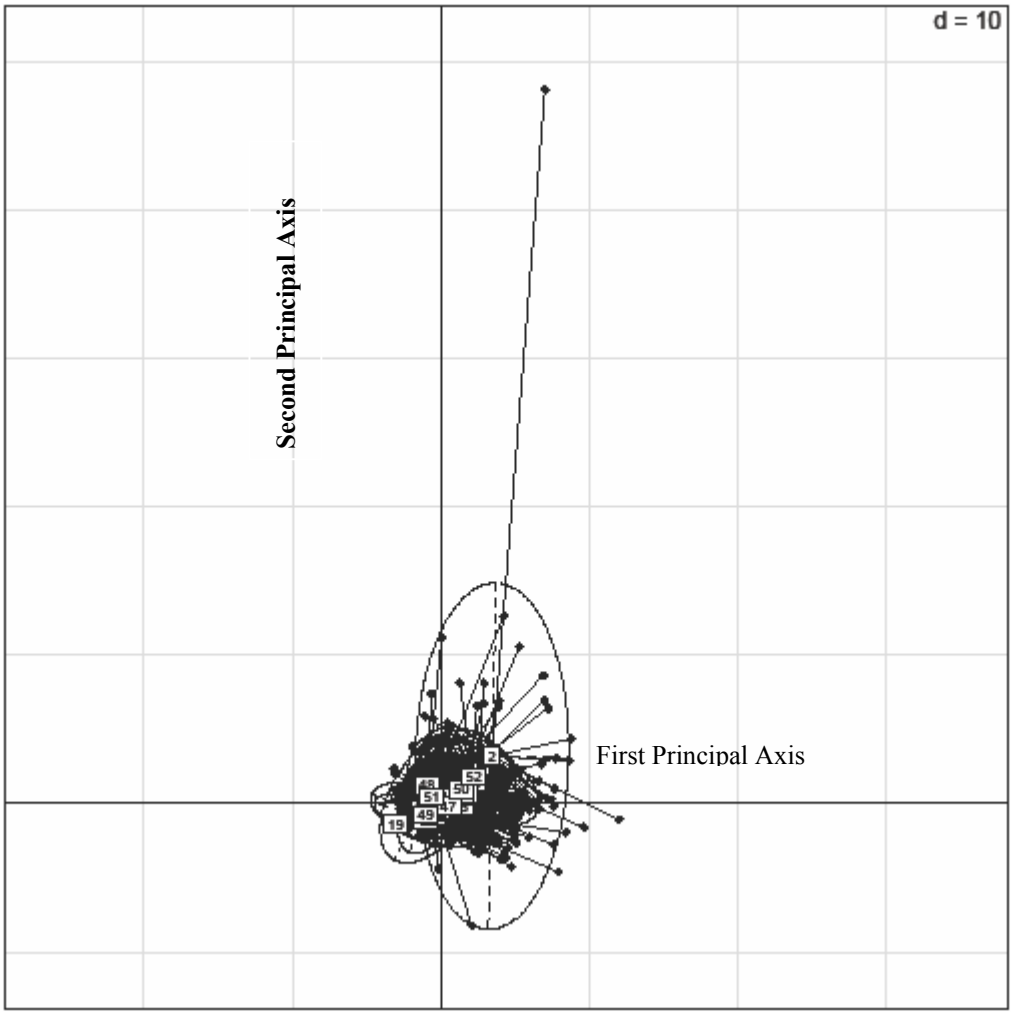

Fig. 3.49 A two dimensional plot of 52 weeks representing the *chl* maps based on PCA. Plot of the factor scores representing the PC1 and PC2 for the Maltese waters during 2002. The factor scores were clustered by means of confidence ellipsoids per week; on the left are located the low scores whereas on the right the high scores .

Figure 3.50 shows the boxplot of the PC1 (factor scores). The PC1 described 9.0% of the total variability and expressed *chl* concentration. The presence of a clear seasonal trend of the *chl* concentration was notable, the first algal bloom occurring between weeks 2 and 4. The second peak occurred during weeks 50 and 52. Minimum mean *chl* values were recorded in late spring and summer.

The PC2 explained about the 6% of the total variability (Fig. 3.51). The meaning of this component is not completely clear due to the land cover effect on the images. The cloud and land cover signals made the second component to be more difficult to interpret. The weight due to land, which occupies a large area in the matrix extrapolated, is remarkable and could obscure the variability caused by cloud coverage.

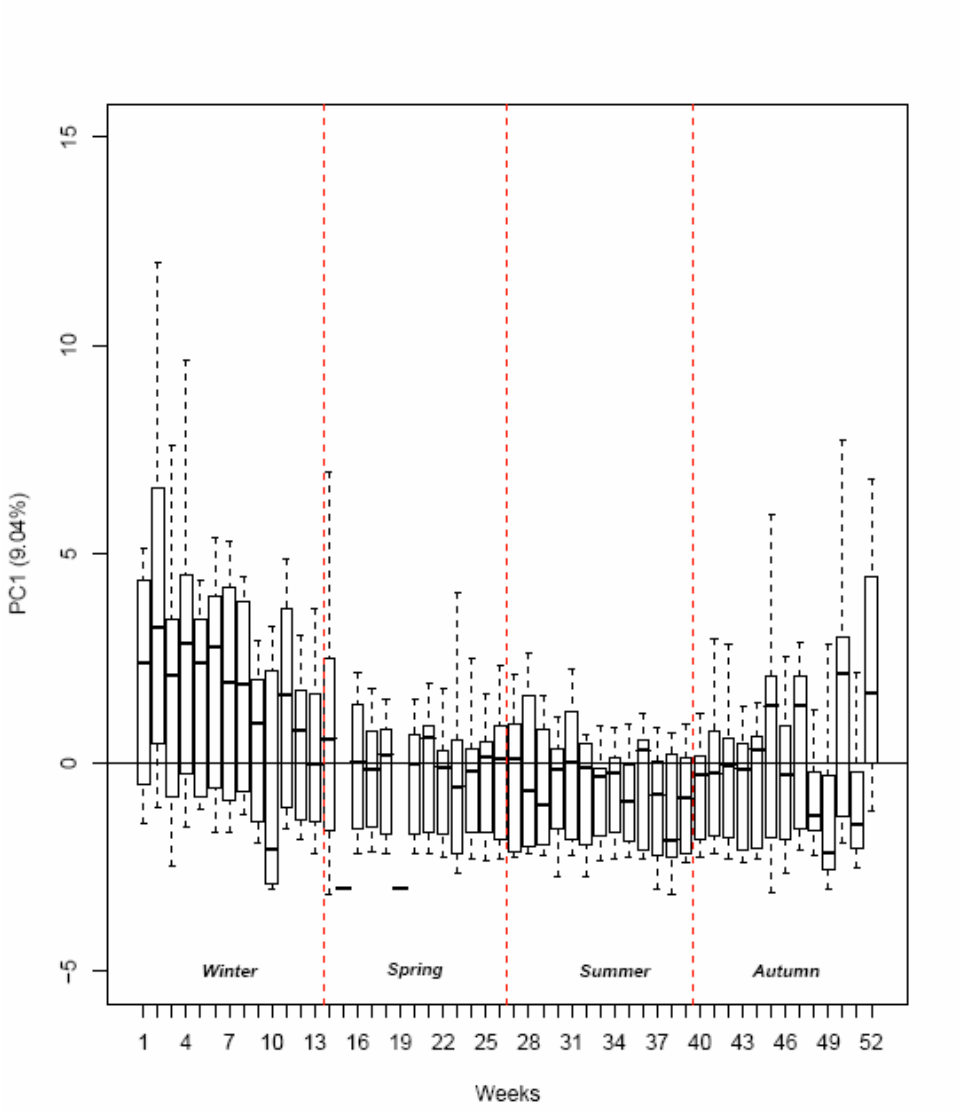

Fig. 3.50 Boxplot of the PC1 along the Maltese waters during 2002. The boxes show the interquartile ranges (IQR) between the lower (25th percentiles) and the upper (75th percentiles) quartiles. The line in the boxes represent the median observation. The whiskers represent the 5th and the 95th percentiles.

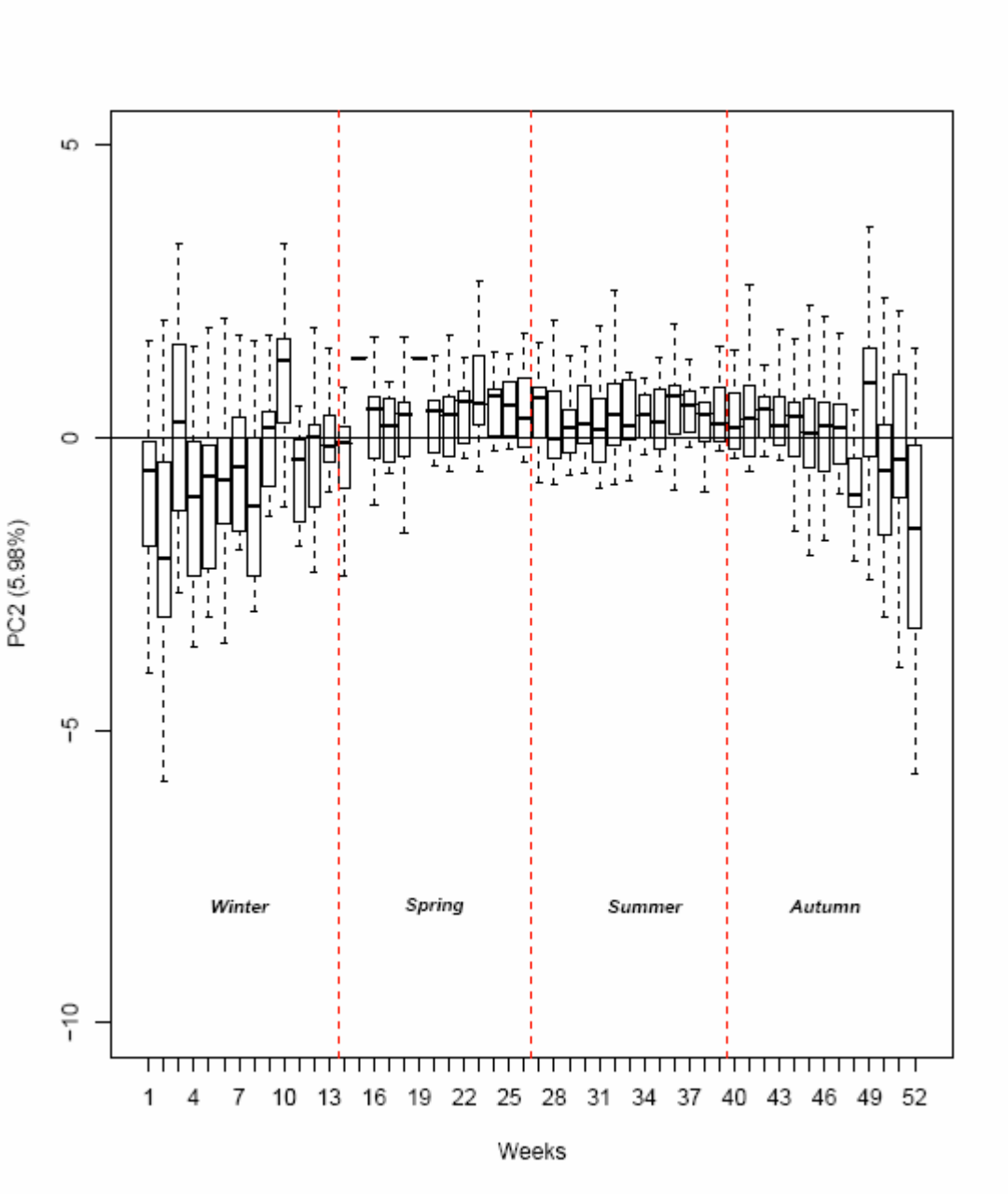

Fig. 3.51 Boxplot of the PC2 along the Maltese waters during 2002. The boxes show the interquartile ranges (IQR) between the lower (25th percentiles) and the upper (75th percentiles) quartiles. The line in the boxes represent the median observation. The whiskers represent the 5th and the 95th percentiles.

Table 3.6 shows the K-sample multivariate E-distances. Significant E-distances retrieved in relation to weeks 10, 15, 19, 48 and 49 were caused by bias due to the high cloud coverage. Due to the extremely low *chl* registered along Maltese waters, the E-distances do not discriminate between weeks showing *chl* differences equal to 0.10 mg m^{-3}.

The only significant distances were between week 50 and week 51 and between week 51 and week 52. These last distances illustrated a significant increase of *chl* during December, showing the highest distance recorded.

Table 3.6 E-Distances for the Maltese waters during 2002. Only the significant values modified by Bonferroni's correction at level $p<0.001$ are presented. The comparisons were made per following weeks.

Weeks	E-distances
W9 *vs*. W10	19.48
W10 *vs*. W11	30.33
W14 *vs*. W15	85.01
W15 *vs*. W16	74.19
W18 *vs*. W19	69.62
W19 *vs*. W20	68.44
W47 *vs*. W48	21.01
W49 *vs*. W50	33.67
W50 *vs*. W51	26.87
W51 *vs*. W52	43.89

3.3.4.2 Thermal IR data

Appendix 22 shows SST skin along Maltese waters. Figure 3.52 a-d shows the island of Malta surrounded by a cold vein in particular during late spring, summer and autumn with a SST difference of about 3°C. During the summer months SST recorded were extremely high reaching around 29°C in August. In winter SST was more homogeneous within the area considered (Fig. 3.52 g-i).

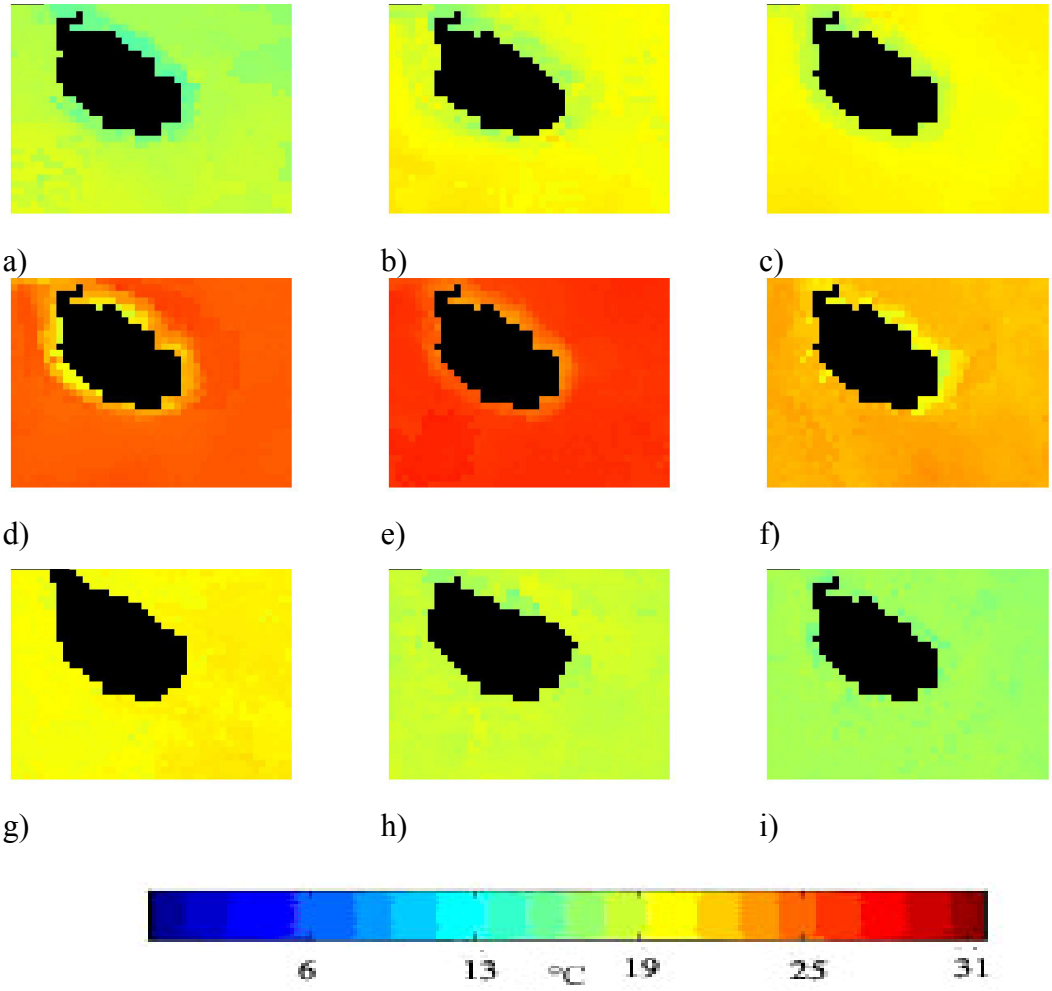

Fig. 3.52 Weekly maps of the SST skin derived from AVHRR along the Maltese waters during weeks 19 (a), 20 (b), 22 (c), 28(d), 34 (e), 43 (f), 48 (g), 50 (h) and 52 (i) respectively, during 2002.

3.4 DISCUSSION

From the analyses conducted it is possible to affirm that the time scale appropriate to monitor the time varying biophysical processes occurring within the Mediterranean basin may range from seven to ten days. The weekly averages utilised for this study were particularly useful to point out the trend of the biophysical variables and in particular of the chlorophyll content within the MPAs considered.
Moreover, the SST data enabled monitoring of the hydrological conditions which persist along the areas investigated. It should be emphasised, however, that the *chl* and SST assessment carried out using satellite ocean colour and thermal sensors are limited to the surface and do not account for subsurface chlorophyll and temperature distribution. However for this last geophysical parameter, as stated in §1.7.1, whatever variability occurs at depth SST skin distribution generally mirrors the subsurface thermal structure associated to the ocean currents.

Spatial resolution of the SeaWiFS and AVHRR imagery were appropriate while studying large areas such as *Pelagos* Sanctuary and Al Hoceima National Park. For smaller areas such as Portofino and Malta, the resolution of the sensors used did not enable precise visualisation of the oceanographic conditions which persisted along these MPAs. For those areas, sensors with higher spatial resolution should be used. In fact for MPAs covering from 5 to 15 km, satellite ocean colour data with a spatial resolution of 300m, as provided by MERIS, should be used. For larger MPAs (>15 km) medium resolution sensors are appropriate.

PCA allowed to convert a matrix of *n* rows and *m* columns i.e. the satellite image into a bivariate representation by using the first two principal components (PC1 and PC2). The original matrix contains mainly *chl* values along with lower number of observations belonging to clouds and land. From the position of the ellipsoids on the factorial plane and by its comparison with the original images, is possible to affirm that PC1 represented *chl*. When the ellipsoid lay on the positive semi-axes, this pointed out a week showing a higher *chl*. By looking at the ellipsoids, the weeks which had the highest x-axis absolute value, were those which showed that a bloom was occurring. It should, however, be considered the fact that within the PC1 along with *chl* there are also

the effect of clouds and land. These noises lowered the total variability explained by the PC1. However, most of the noise was encompassed within the PC2. From a series of ocean colour images, the added value of the PCA and of the box plots of the PC1, is the representation of the *chl* patterns throughout the year considered. This analysis was chosen because within a MPA is extremely important to detect not only the absolute values of *chl* but rather the *chl* patterns.

PCA worked extremely well in off shore areas with almost no land such as the sub-area within the *Pelagos* Sanctuary. Here, the meaning of both the principal components was clear. The PC1 expressed the variation on *chl* whereas the PC2 expressed clearly the cloud cover and the position of clouds on the images. The *Pelagos* case study was really important in demonstrating the value of the statistical approach used in order to extrapolate from the RS data the maximum information.
In the other coastal sites taken into consideration, PCA worked extremely well for the PC1 which expressed the variation on chlorophyll field. However, for the PC2, this was affected by the signals due to land and cloud cover, resulting in a variability not explainable univocally by one factor. The fact that land and clouds affect the PCA's second component in coastal MPAs, does not affect the information provided by RS i.e. *chl* patterns.

The E-distance test was applied on the images and not on the PC1. This test was performed in order to find a correspondence between the PCA and the satellite images. Results of PCA were confirmed by the E-distances test when considering the same images. Indeed, E-distance compared the matrices representing following weeks and calculated the Euclidean distance among them. When the distances between two images resulted high, this may mean that a bloom is occurring or that one of the two images is seriously affected by cloud cover. E-distance enabled calculation of the significance rate after performing the comparison among weeks. This test strengthened the results obtained by the PCA by quantifying the difference among weeks while bloom period occurred.

Figure 3.53 shows the main surficial currents in the Mediterranean Sea, which will lead the reader to the following discussion and to the understanding of the main bio-physical processes that occurred during 2002 along the Marine Protected Areas analysed.

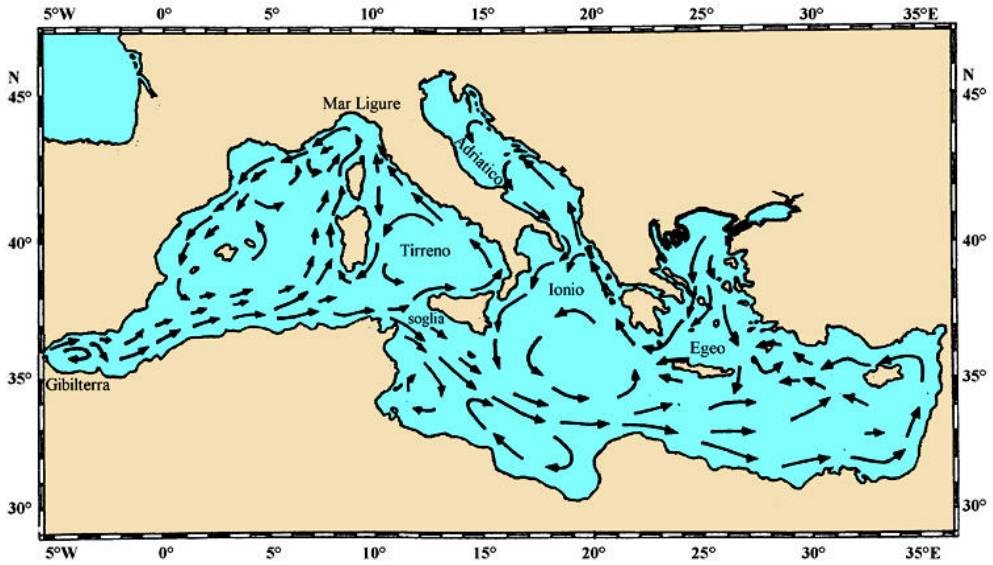

Fig. 3.53 Main superficial currents in the Mediterranean (Tait, 1985)

The outcomes and observations for each of the MPAs investigated will first be considered and discussed, and then a comparison made of these different MPAs

3.4.1 Portofino Marine Protected Area

The analysis of the chlorophyll maps has shown clearly a bimodal trend of phytoplankton within the Portofino MPA. The major peak occurred in early winter, whereas the second minor peak in early autumn. The seasonal cycle displayed a progressive increase in phytoplankton biomass from autumn to the end of the year. The highest *chl* were recorded in February whereas the lowest were observed in July. The Portofino waters were characterised by *chl* of about 0.4 mg m^{-3} which covered the widest spatial extension throughout the year considered. The *chl* recorded demonstrated that the waters surrounding this MPA are oligotrophic, in accordance with Castellano *et al*. (2008) who stated that these oligotrophic characteristics showed an interannual variability with a low biomass in the surficial layer, that decreased in the last years.

The analysis of spatial gradients identified that the *chl* fell mainly within the lowest range considered (0.16-0.9 mg m^{-3}) whereas during early winter *chl* fell within the highest range analysed (1.0-1.9 mg m^{-3}). The spatial gradient showed that generally the highest concentrations moved from the eastern side of the Portofino promontory

(Tigullio) towards the western side (Paradiso Gulf) i.e. following the Ligurian cyclonic north westward coastal current. However, the high *chl* values recorded during the end of January on the western side of the Promontory, could have been caused by the recirculation due to the anticyclonic eddy evidenced by Doglioli et al. (2004). As stated in §2.2.1.1, this anticyclonic eddy is associated with an eastern counter current in the lee of the Promontorio (cape). On the other hand, the highest *chl* values within the Tigullio gulf could also have been caused by the Entella river which has its estuary on the western MPA border (Tigullio Gulf). During November the largest patch falling within the highest *chl* range was recorded along the coast and in particular along Paradiso Gulf.

PCA enabled visualisation of the PC1 of the *chl* field. In particular, positive peaks indicated high *chl* values associated with algal blooms, whereas negative peaks indicate images contaminated by cloud cover. According to this interpretation, the onset of the blooming period is seen to occur in late winter, secondary peaks appeared in late autumn, following the constant, reduced levels of summer, in good agreement with what reported for the planktonic field of the Western Mediterranean by Margalef (1985).

PC2 did not provide further insight. The highest significant distance recorded by means of E-statistics was between the end of February and the beginning of March, thus confirming those periods as corresponding to the onset of the phytoplankton bloom. The onset of the second minor bloom occurred at the beginning of November, showing significantly higher distance than successive weeks not corrupted by clouds.
The SST values retrieved for Portofino were in accordance with those calculated by Santoleri *et al*. (1994) for the Ligurian-Provençal Sea. The analysis of SST skin showed a persistent cold coastal current along the Portofino Promontory during spring, which lasted until June. From July until the beginning of November the SST skin was almost homogenous within the MPA waters. At the end of November the cold current was again visible. At the beginning of October a cold thermal front moving westwards was observed. It is possible to note the inverse correspondence between SST and chlorophyll features along the coast during October through to November.
SST analysis conducted by Castellano *et al*. (2008) evidenced an increase of the mean SST along the water column in the last years in respect with the previous decade (1985-1995) and in particular an increase of the SST skin during spring and autumn which has caused a longer warm season. The study area is characterised by a remarkable

interannual variability, thermal anomalies were recorded during summer of 2003 and during autumn and spring of 2006-2007 with recorded SST skin higher than the average of the period, which were caused by atmospheric thermal anomalies (Castellano *et al*. 2008). Interannual variability recorded, according to Castellano *et al*. (2008), affects the phyto and zooplanktonic populations, modifying their response in particular during spring season.

3.4.2 *Pelagos* International Sanctuary

The year 2002 presented a major proliferation of algal biomass which started during winter months (in particular with a major chlorophyll peak in February), with lower *chl* levels during summer and a successive increase during autumnal months which reached its peak in December. The *chl* maps show a marked space-time heterogeneity, particularly prominent (on a seasonal scale) in the Sanctuary's north-western area. In this area, low *chl* values occurred in winter, followed by massive blooming in early spring. Accordingly with Longhurst (2006) the depth of winter mixing at the end of inter determines the pre bloom conditions. The patches of low *chl* are thought to be induced by the northerly wind pattern (*e.g.* the Mistral), which causes convection processes that lead to deep water formation (Millot, 1990) and remove the algae from the euphotic zone. The subsequent blooming occurring in spring, in contrast, is thought to be triggered by the increasing irradiance and the onset of stratification, which follows the relaxation of the wind pattern (*i.e.* of the vertical mixing that prevented the blooming in winter, but produced also a substantial nutrient increase in the euphotic zone). As shown on the *chl* maps in general the spring bloom takes place in March and continues through April. Once the stratification is established, evolution occurs toward a summer oligotrophic situation. An autumnal bloom, usually weaker than the spring bloom may occur when the wind stress increases and the surface irradiance decreases, thus causing the vertical nutrient flux to increase (Longhurst, 2006).
The above results confirmed that within the study area the typical phytoplankton seasonal dynamics follows a typical temperate seasonal cycle (Marty *et al*., 2002). This classical vernal cycle is described by Longhurst (2006) as Case 2 model and occurs also in the North Atlantic region.

Threshold analysis identified precisely the location of the bloom patch with high chlorophyll content on the north-western area of the Sanctuary and monitored its span. The north-western area of the Ligurian Sea could be considered one of the most productive area of the western Mediterranean.
The analysis of the spatial gradients identified the spatial trend of the north-western bloom patch and the cyclonic circulation that characterises the Ligurian Sea; this Sea has a seasonal cycle related to the seasonal variations of the atmospheric forcing (Esposito and Manzella, 1982, Millot 1999). In the coastal area, water coming from both western and eastern sides of Corsica island flows north joins in the so-called Ligurian coastal current, that flows along shore roughly following the bathymetry in the southwesterly direction (Astraldi and Gasparini, 1986, Millot, 1999). In winter the flow in the Corsica channel (between the islands of Elba and Corsica) increases, whereas the flow on the western side of Corsica remains steady during the whole year (Astraldi and Gasparini, 1986; Buffoni *et al*., 1997).

The PCA worked extremely well for the *Pelagos* Sanctuary in terms of insight to the oceanographic characteristics of the MPA. This outcome is due to the fact that a sub (pelagic) area was extracted from the Sanctuary's area, encompassing almost no land. PC1 expressed mainly the variation on chlorophyll field whereas PC2 expressed clearly the presence of clouds on the images. The onset of the blooming period for the year considered (2002) was in winter followed by repeated oscillation at the weekly scale. In this period the upward mixing of nutrients and the averaged irradiance within the mixed layer allowed a slight increase in the autotrophic biomass and its net growth (Margalef, 1985). During summer the PC1 trend showed almost no variability and minimum chlorophyll values persisted, this due to the stratification and to the well established thermocline which prevents the flux of nutrients towards the euphotic zone, thus limiting the development of autotrophic biomass in the surface layer (Morel and Andre, 1991; Bosc *et al*., 2004).
In autumn the change of the meteorological conditions and the consequent wind patterns cause vertical mixing of the water column to increase which stimulates the upper layer fertilisation and leads to an increase of *chl*. The oscillation of the statistical indicator during this season could be also due to the increasing occurrence of cloudy *chl* maps.

Having taken into consideration only the bloom area, PC2 was influenced by the cloud coverage on the chlorophyll maps. The PC2 boxplot enabled characterisation of the cloud displacement on the chlorophyll maps. The E-distances calculated revealed that the onset of the bloom occurred at the start of February with a significant increasing in chlorophyll content until the end February; at the end of March the start of a significant decrease of chlorophyll concentration was recorded.

During late autumn a significant increase in *chl* was evident, which led to a secondary *chl* peak in December. This pattern is closely comparable to that found by D'Ortenzio and Ribera d'Alcalà (2008) namely that in the North Western Mediterranean area (latitude> 41° N) the bloom timing follows a four phase pattern. An initial increase in winter (November-December) is followed by a slight decrease during the first months of the year and by the development of the *chl* annual maximum in early spring and a final decay in late spring/early summer. However, the second phase was not clearly revealed by the *chl* maps analysed in the present study, possibly due to the interannual variability which could modify the amplitude of the four phases. D'Ortenzio and Ribera d'Alcalà (2008) classified the North western area of the basin as "blooming area" which follows the North –Atlantic dynamics identified by Longhurst (2006), as mentioned above, as Case 2 model.

The analysis of SST skin identified an inverse correspondence between the phytoplankton distribution within the Sanctuary and the SST features. In the Ligurian-Provençal Sea the cyclonic gyre and the consequent upwelling causes lower temperatures off the *Pelagos* Sanctuary. The SST winter data were in accordance with those recorded for the Western Mediterranean by Flos (1985) and by Santoleri *et al*. (1994), which are determined by the severe meteorological conditions typical of the northern section of the Western Mediterranean. This cold cell in winter extends throughout the northern region (Santoleri *et al*., 1994). During spring this cold cell was still present. The north western sub area showed, particularly during late spring and autumn the coldest SST skin recorded due to the more rapid cooling occurring during autumn in the northern region. During summer the cold patch disappeared and the Sanctuary showed an homogenous SST skin.

3.4.3 Al Hoceima National Park

The *chl* maps focused on the Alboran Sea helped to analyse the trend of the seasonal cycle along the Al Hoceima waters. The distribution of phytoplankton biomass in the Alboran Sea is ruled primarily by the inflow of the MAW into the Mediterranean Sea with the formation of one or two well-defined cyclonic gyres (Bosc *et al*., 2004). The year investigated did show only one cyclonic gyre i.e. the western gyre. The phytoplankton bloom appeared in early winter and covered - almost homogeneously - the whole area, whereas in early spring the waters rich in biomass are transported by the anticyclonic gyre. The phytoplankton (*chl*) maxima were observed in the northern part of the anticyclonic Alboran Sea gyre i.e. along the Spanish coast during spring and early autumn. In this area the nutrients are transported into the photic zone and consequently the upwelling takes place (Minas *et al*., 1991) . Unlike the other areas considered above, here the two phytoplankton maxima showed the same level of chlorophyll content. D'Ortenzio and Ribera d'Alcalà (2008) defined the region along the Spanish coast as a "blooming area" i.e. where intense bloom occurs in early spring.
The central region of the Alboran Sea, namely where the western anticyclonic gyre occurs, it was classified by D'Ortenzio and Ribera d'Alcalà (2008) an "intermittently blooming area", meaning that the bloom event is subjected to a pronounced interannual variability of the phytoplankton dynamics (Bosc *et al*., 2004). Historical ocean colour data (Morel and André, 1991; Marty *et al*., 2002; Bosc *et al*., 2004) showed in this region years with peaks of phytoplankton biomass followed by years showing oligotrophic conditions.
The western anticyclonic gyre, moving in south-western direction hits the coasts of Al Hoceima National Park, transporting phytoplankton biomass along Al Hoceima waters. In this area the biomass maxima were centred in early winter an in early autumn because the strong mixing associated with the Alboran gyre provides continuous resupply of nutrients throughout the year Arnone (1994). During summer the weakening of the gyre causes a minimum of phytoplankton biomass (around 0.4 mgm^{-3}) however significantly higher than in other regions (Bosc *et al*., 2004): nevertheless the gyre is still recognisable. This mixing eliminates the nutrient limited conditions that occur in the other areas considered. In fact the physical mixing of Atlantic and Mediterranean waters contribute to the enhanced *chl* in the Alboran gyre frontal system.

The threshold analysis identified that the maximum extent of the bloom, showing the highest *chl*, occurred in late autumn.
The histograms of *chl* showed a bimodal pattern, although the Alboran Sea showed two modes less pronounced, which highlighted the higher average *chl* concentration in the frontal and coastal region; the lowest *chl* levels were recorded within the central oligotrophic gyre subregion. This pattern is in accordance to what was found for the same region by Arnone (1994) through analysis of CZCS imagery.

Spatial gradients highlighted that the anticyclonic gyre transporting waters extremely rich in phytoplankton biomass flows mainly along the Spanish coasts and that Al Hoceima National Park is hit by the gyre only in early winter and early autumn. However, waters along the coasts of Al Hoceima also showed high phytoplankton values during the other periods. It is notable that the distribution of *chl* per mean km^2 had the same highest peak as that calculated over the whole Alboran Sea. The waters surrounding Al Hoceima National Park thus showed an extremely high mean *chl*, taking into consideration the general oligotrophy of the Mediterranean basin and also with respect to the other areas analysed above.

PCA confirmed the Alboran Sea as an intermittently blooming area in accordance with the description by D'Ortenzio and Ribera d'Alcalà (2008). The high *chl* values recorded in summer are particularly notable. PCA confirmed that Al Hoceima was affected by the bloom which spread over several months brought by the anticyclonic gyre only during winter-early spring and during autumn. During the other months, the MAW entering the Mediterranean, forming the gyre and inducing the phytoplankton bloom did not hit the Al Hoceima coasts.
Temperature data have been shown to be a good indicator of the circulation in the Alboran Sea due to the strong thermal contrast between the water masses through the whole year investigated. In the Alboran Sea the most distinct thermal feature is the circulation around the anticyclonic gyre; the curvature of the SST contours indicates the Medium Atlantic Water inflow, particularly in winter. The Alboran gyre was not visible in spring due to the possible vertical homogeneity of the SST which does not show any circulation feature. In summer (July-September) the Alboran gyre was always visible, in accordance to that found by Santoleri *et al*. (1994). The period of maximum SST skin was recorded during August in accordance with Bosc *et al*.(2004).

The analysis of SST skin identified within the Alboran Sea an inverse correspondence between the SST features and the phytoplankton blooms following the gyre, particularly in late spring, early autumn and at the end of the year. During most of 2002 Al Hoceima waters were characterised by a cold coastal vein flowing south east. The inverse correspondence between SST and *chl* was visible particularly in winter when the SST showed similar values over the area investigated displaying the highest phytoplankton biomass. During the rest of the year the coolest waters were flowing along the coast where the highest *chl* levels were mainly located.

3.4.4 Rdum Majjesa and Ras Raheb MPA

D'Ortenzio and Ribera d'Alcalà (2008) defined two main trophic regimes for the Mediterranean basin. The first, located between 35° and 40° N, is similar to that of North Atlantic, whereas south of this limit the trophic regime is considered tropical or sub-tropical, showing a strong oligotrophy and a weak seasonal variability. The Maltese area, being located on the Central Mediterranean basin, lies on the southern limit of the first régime. However, the Maltese area, seemed to be more influenced by a oligotrophic rather than a North Atlantic (D'Ortenzio & Ribera d'Alcalà, 2008) régime.

The *chl* maps showed a bimodal pattern with peaks in spring and autumn. During 2002, the mean chlorophyll concentration showed a sinusoidal trend. The major proliferation of algal biomass started during early winter months whereas low biomass values were recorded during late spring-summer due to the occurring strong stratification. For the investigated area the main *chl* peak occurred during the winter months. The data analysed so far highlighted that, within the region surrounding the Island of Malta, chlorophyll content was very low during the whole year considered. As reported by Bricaud *et al*. (2002) SeaWiFS overestimates *chl* when compared with *in situ* chlorophyll data, particularly in the oligotrophic areas of the Mediterranean basin. Along Maltese coast the mean *chl* maxima (0.35 mg m^{-3}) covering the major area extension showed lower *chl* content than Portofino (§3.3.4.1 and §3.3.1.1) and *Pelagos* Sanctuary (§3.3.4.1 and §3.3.2.1), and almost the half the *chl* content of Al Hoceima (§3.3.4.1 and §3.3.3.1). The maximum *chl* retrieved are in accordance with Bosc *et al*.

(2004) whereas the minimum values in this study resulted higher i.e. 0.15 mg m^{-3} than that i.e. 0.03 mg m^{-3} calculated by the authors. However it should be noted that the above authors found a large interannual variation of *chl* in this area. These fluctuations in *chl* could be determined by the enhanced seawater temperature which causes a higher stratification of the water column and consequently a lower phytoplankton biomass level (Bosc *et al*. 2004). Limitations due to clear water, namely the possibility that the remote sensing reflectance (R_{RS}) measured from satellite could have been affected by the shallow sea bed and biased *chl* estimates, did not occur. Indeed particularly on the western Maltese coast the continental shelf is narrow and the bathymetry of 50 m runs very closely to the shore (§ 2.2.1.4 and Fig. 2.11).

The analysis of spatial gradients helped to identify preliminarily the hydrological features occurring along the study area during the year considered. The Maltese island presents an obstacle to the general surface water exchange between the western and eastern Mediterranean basins. The flow is predominantly set to the south-east in favour of the gradient flow from the western to the eastern Mediterranean basins (Fig. 2.1; Drago, 1994). During the year investigated, the island of Malta was not influenced by the chlorophyll-rich filament structure extending southeast of Sicily usually in spring as reported by Bosc *et al*. (2004).

It could be inferred that the high *chl* patches in the study area occurred during winter months mainly along the western coast, migrating towards the south-east during spring, following the south-eastern surficial current. During 2002 the highest phytoplankton biomass was along the western side of the Island of Malta and in particular along Rdum Majjesa and Ras Raheb MPA. According to Drago (1994) MAW to the west of Malta results in southeast surface current to the south of Malta, thus supplying water to the Malta channel in a south-easterly direction.

The PCA worked quite well for the Maltese area the PC1 expressed mainly the variation on chlorophyll the field. The onset of the blooming period for the year considered was found to be during winter. During late spring and summer the PC1 trend shows almost no variability and minimum chlorophyll values.

Due to the inclusion of large terrestrial areas within the matrix, the PC2 outcomes were not completely clear. In fact the signal filtering due to the disturbance of the cloud coverage did not came out properly due to the presence of land stretches which displayed, after having applied the algorithm, the same value of the clouds (i.e. zero).

Temperature data showed that during spring and early summer Malta was surrounded by a cold vein. In winter the SST appeared homogenous. SST skin data did not supply clear indications about the circulations around Malta island. The summer upwelling south of Sicily recorded by Santoleri *et al*. (1994) could be responsible of the cooler waters which contoured the Maltese eastern coast throughout the year considered.

3.4.5 Comparison of the study sites

In the Mediterranean Sea the phytoplankton growth cycle is identified by two predominant phytoplankton bloom periods occurring in spring and autumn. As already explained by Arnone (1994) the typical cycle starts in January or February when chlorophyll growth is light limited. Winter mixing supplies the nutrients to the surface layers and the bloom is only limited by the light intensity. As solar irradiation intensity increases in spring, the *chl* increases and the spring bloom takes place in March. However, the areas considered above presented high *chl* values usually in January, February and March with peaks occurring earlier in February or later in March.

After the bloom the *chl* decreases due to nutrient depletion, but the light availability remains high throughout summer. The *chl* reaches its minimum at the end of summer (August-September). In early autumn the mixing processes due to the enhanced winds resupply nutrients to the surface waters. These nutrients, together with the still high light intensity, cause the autumn bloom to take place. This bloom has its peak in November and declines in winter (December) due to a decrease in the intensity of available light. The biological cycle repeats in January (Arnone, 1994).

The pattern explained above recurs in the whole the Western Mediterranean. However, the specific months during which the transitions occur may differ, due to localised

processes in each of the test site considered. Both Portofino MPA and the *Pelagos* Sanctuary, located within the Ligurian-Provençal Sea, showed higher *chl* values in January, February and March, with peak blooming occurring in March. On the other hand the Alboran Sea and Al Hoceima showed blooms achieving peak biomass in February. For the *Pelagos* Sanctuary and Al Hoceima, the phytoplankton bloom continued in April and May. The Ligurian-Provençal Sea and the Alboran Sea retained relatively high *chl* values even in summer. Particularly Alboran Sea is impacted throughout the year by the incoming Atlantic water. Al Hoceima National Park waters showed high *chl* content throughout the year considered.

The island of Malta showed a bloom peak occurring in early winter (January-February), and in late March sign of oligotrophic conditions (i.e. low *chl* levels) were already visible. This oligotrophic state prevailed through the whole summer until September. In November the bloom took up again and a second minor peak was observed. However, it should be taken into consideration that the *chl* values along the island throughout the year considered were the lowest recorded if compared to the other MPAs analysed in this study.

The north-western basin (Ligurian Sea), particularly in winter, is strongly affected by the cyclogenic activity which is relatively intense. The analysis of the SST trend showed that this activity is persistent and appears as a cold current along the Ligurian coasts and, in particular, along the Portofino coasts during winter and spring. Moreover the severe meteorological conditions such as the continental dry winter winds, typical of the northern section of the western Mediterranean, induce evaporation processes and the formation of the denser waters (La Violette, 1994). In the Ligurian- Provençal Sea the cyclonic gyre and the consequent upwelling was visible as a cold cell partially covering the *Pelagos* Sanctuary. In summer the atmospheric forcing is minimal, so that the upper layer was stable and the SST homogeneous throughout the Sanctuary.

The other area affected by cyclogenic activity (caused by the MAW inflow into the Mediterranean) is Al Hoceima National Park. This gyre produces a cold current along the Al Hoceima coasts, particularly in autumn and winter.

The island of Malta differs from the other areas studied due to the lack of cyclogenic activity and to the fact that the southern region is less atmospherically forced (Santoleri *et al*., 1994). The SST analysed differed also in the fact that the cool current around the island was visible in spring and summer whereas in winter the SST appeared homogenous. Being the cool surficial current caused mainly by winds, it is possible to hypothesise that more intense winds occurring during late spring and summer rather than in winter. However, this phenomenon could also have been caused by erratic events.

3.4.6 Applications and implications

This chapter showed how RS can provide a usable meaningful insight to the oceanography of an MPA. The satellite passive sensors used have a synoptic coverage capable of encompassing the time and the spatial scale of the biological process such as the phytoplankton bloom phenomenon. As stated in §3.4, the spatial resolution of the ocean colour and thermal sensors utilised were particularly appropriate to investigate high-sea area such as *Pelagos* Sanctuary and wide coastal area (>15 km) such as Al Hoceima National Park, whereas for smaller areas such as Portofino and the Maltese MPA the spatial resolution of 1.1 km was too coarse. Nonetheless, ocean colour and thermal sensors used, delivered useful information in identifying the main oceanographic processes occurring along Portofino MPA and the island of Malta. However, in order to investigate Portofino and the Maltese MPA at a finer spatial detail, further studies should encompass the use of higher resolution ocean colour sensors. Moreover in areas such as Maltese MPA, which is located in one of the most oligotrophic basin of the Mediterranean Sea, the *chl* retrieved by using the global oceans algorithm OC4v4 were overestimated (Bricaud *et al*., 2002) particularly in the lower concentration ranges (< 0.4 mg m^{-3}) possibly due to the input into the seawater of the saharian dust brought by the so called “red rains” (Bosc *et al*., 2004). In order to overcome this limitation in these areas, regional bio-optical algorithms should be used (D’Ortenzio *et al*., 2002).

The alternatives to data derived from SeaWiFS are those derived by MERIS sensor (§2.4) which has a spatial resolution of 300m. In chapter 5 there will be shown an example of the use of MERIS in coastal monitoring of the Portofino MPA.
The AVHRR sensor worked properly in defining the seawater skin temperature and its trends along the study sites, however also its spatial resolution is coarse for the small study sites cited above. Nonetheless, this sensor is important in order to identify thermal anomalies within the MPAs.

The statistical approach used in this chapter was extremely useful and meaningful because it enables analysing quantitative differences among the satellite images. PCA enables representation of a multidimensional phenomenon in one dimension, i.e. considering only one variable at the time represented as the first or the second factor component. PCA is the most commonly utilised statistical technique in the analysis of RS imagery because it is particularly appropriate in comparing the images.
The fact that land and clouds affect the PC2 in coastal MPAs has no implications for using EO satellites as a tool in monitoring of MPAs located in coastal regions. Indeed the PC1 represents always the geophysical variable under investigation. Moreover, the use of E-distance strengthened the PCA results by performing comparisons between the satellite images or matrices and calculating the significant variations of the geophysical parameter under investigation, i.e. chlorophyll concentration. The E-statistic identified clearly the phytoplankton bloom onset or its decay, thus it should be considered a strategic statistics technique to monitor trends and anomalies of the geophysical parameters occurring in the MPAs.

3.5 CONCLUSIONS

Mediterranean Sea is an extremely complex and fragile basin which has been subjected for several decades to increasing anthropogenic influences. The aim of the MPAs is that of preserving the ecosystems and their biodiversity. This chapter has demonstrated the validity and the remarkable value of the RS observations to monitor and manage Mediterranean MPAs. Thanks to the series of ocean colour and thermal data provided by the SeaWiFS and AVHRR sensors, the seasonal variations of phytoplankton biomass

and SST skin were analysed over various MPAs located in different regions of the Mediterranean basin. Monitoring phytoplankton biomass and thermal trend of seawater is the first step required to characterise the biogeochemical seasonal cycle of the basin where a MPA is located. The monitoring process is crucial in order to detect possible modifications in the biogeochemical balance of the basin. These modifications, might be caused by environmental changes and thus provoking an evolution of the ecosystems.
In this chapter it was performed a short-term analysis whereas in chapter 4 is presented a long-term analysis of the algal biomass within a high-sea MPA.

In this chapter, the seasonal cycle of phytoplankton revealed generally a maximum in winter or spring and a minimum in summer, with differences at regional level due to the occurrence of the autumn bloom. From the analyses conducted so far, the most conspicuous features were the earlier onset of the spring phytoplankton bloom and the quasi-absence of the autumn bloom with respect to analyses of CZCS ocean colour data (Morel and André, 1991). The algal biomass estimates presented might be overestimates in particular in the lowest ranges of *chl*. This is due to the inaccurate atmospheric corrections applied to the standard SeaWiFS algorithm (OC4v4) in use for the world ocean and also to the particular bio-optical properties of the Mediterranean Sea (i.e. desert dust and high presence of CDOM) (Moulin *et al*., 2001). In order to retrieve refined estimates of *chl* along the Mediterranean MPAs, regional bio-optical algorithms should be used.

This chapter has demonstrated the possibility of characterising a MPA by depicting the system functioning, only by using EO satellites and almost at no cost, thus enabling identification of the main occurring biophysical processes.

CHAPTER 4

PHYTOPLANKTON DYNAMICS IN THE *PELAGOS* SANCTUARY (LIGURIAN-PROVENÇAL SEA)

4.1 INTRODUCTION

The geographic and climatic conditions of the north-western Mediterranean Sea are characterised by strong air-sea interactions that trigger convection processes that can mix the entire water column (over 2000 m). In particular, the north-western Mediterranean lies in a cyclonic centre where there is a combination of the lower Atlantic pressure with the polar fronts entering the Mediterranean Sea (Flos, 1985). The Mistral-Tramontana (northern winds) cold wind system is responsible of increasing the salinity and thus density of surface waters causing strong evaporation and cooling, thereby stimulating convection processes, in particular in the Gulf of Lions region, which produce the Western Mediterranean Deep Water (WMDW) formation (Gascard, 1978). This feature explains why the north-western Mediterranean Sea is nutritionally richer than the rest of the basin. The vertical mixing fertilises the photic zone, bringing nutrients from deeper layers to the surface and playing a vital role in the biological cycles of this entire near-coastal region (Astraldi *et al*., 1986, 1994). This mixing causes the seasonal onset of algal bloom in this region which could cover the entire north-western basin. The systematic fertilization of surface waters supports a large biomass of primary (and secondary) producers, as well as a highly developed food web, which includes a sizeable standing population of fin whales, *Balaenoptera physalus*, and various other marine mammals (Forcada *et al*., 1996). Extensive algal bloom episodes recur every year in the region, but show both a notable shift in their peak and different *chl* levels from year to year. Morel & André (1991), Arnone (1994) and Barale (2003) identified in the north-western basin a sequence of winter low *chl* levels (the so called Gulf of Lions “blue hole”) and notable spring blooms.

This chapter is focusing to observe and quantify the spatial and temporal pattern of chlorophyll distribution within the *Pelagos* Sanctuary (Fig. 3.11) due to the seasonal recurrence of marked phytoplankton bloom in this area (Barale, 2008). In particular this chapter deals with the problem of assessing *chl* as marker of algal biomass and its

seasonal and interannual patterns. This evaluation can be only achieved at large spatial scale by means of EO sensors in the visible spectral range. The development of ocean colour techniques can be used for characterising and monitoring the status and the trends of marine ecosystems.

Historically algal blooms patterns have been investigated in Mediterranean Sea by using ocean colour data collected by the CZCS in the 1980s. This approach has allowed identification of the algal bloom "hotspots" as well as assessing more general facets of algal biomass in the western basin (Morel and André, 1991). More recently, the use of historical time series of ocean colour data provide valuable information on phytoplankton blooms and dynamics over a range of spatial scales (from a few km to regional scale) and time scales (from days to years) that would not be available by any other means. In the present study, the long-term features of the *chl* fields in the north-western Mediterranean region and, in particular, the *Pelagos* International Sanctuary were investigated by means of ocean colour data time series, collected by orbital remote sensing. Seven years (1998-2004) of SeaWiFS data were analysed in order to monitor the concentration of *chl* and to document its variability in space and time (McClain *et al*., 2004). Mean *chl* images were generated for consecutive 10-day periods, to ensure (*quasi*-) continuous coverage of the area of interest. The primary aim was to supply a graphical representation of the historical series of *chl* maps in two dimensions in order to investigate the *chl* trend and its temporal fluctuations. Secondly this work aimed to enforce strengthen qualitative considerations deriving from a visual analysis of *chl* maps with quantitative methodological tools (statistical inference). Considering *chl* as a phytoplankton biomass index, the surface patterns appearing in the SeaWiFS imagery were used to trace the seasonal sequence of events that supports the extraordinary ecology of the *Pelagos* Sanctuary. Such data on phytoplankton dynamics, retrieved synoptically from satellite data, are of the outmost importance in order to understand the baseline of all ecological relationships within the *Pelagos* Sanctuary, thus contributing to potentially better management of this unique MPA.

4.2 METHODS

4.2.1 Remotely Sensed Data & Processing

The SeaWiFS data set, used to monitor the evolution of the *chl* field in the region of interest, was collected with high spatial resolution (e.g. 1.1 km) – *i.e.* in Local Area Coverage (LAC) mode – during the period from 1998 to 2004. The original top-of-the-atmosphere un-calibrated images acquired from the Goddard Space Flight Centre (NASA) were Level 1A (L1A) data collected by HRPT receiving stations covering the European region and stored in HDF. These data were converted to L2 geophysical products, including *chl*, by means of the algorithms set available in SeaDAS software package (Fu *et al*.,1998), with additional modifications as described by Melin *et al*. (2000) and Sturm and Zibordi (2002). During the conversion process, the L1A data first undergo the atmospheric correction scheme used for the valid water pixels (Bulgarelli and Mélin, 2000; Sturm and Zibordi, 2002) and are then converted from top-of-the-atmosphere radiances to LwN(λ). Finally, the computation of *chl* was carried out using the band-ratio empirical algorithm OC4v4, described by O'Reilly *et al.* (1998, 2000), with revised numerical coefficients as reported by Mélin *et al.* (2000) (Equation 4.1)

$$chl = 10\exp\left(0.2974 - 2.2429r + 0.8358r^2 - 0.0077r^3\right) - 0.0929 \qquad \text{Equation (4.1)}$$

where:

$$r = \log_{10}\left[\frac{\rho(\lambda_1)}{\rho(\lambda_2)}\right]$$

ρ is the reflectance at the wavelengths $\lambda_1 = 490nm$ and $\lambda_2 = 555nm$.

It should be noted that this algorithm (Equation 4.1), where *chl* is inversely correlated to the ratio between the normalised water-leaving radiances or reflectances in the blue and the green part of the electromagnetic spectrum, showed lower performances at regional than at global scale (Gregg and Casey, 2004). This outcome is particularly true for the Mediterranean Sea (D'Ortenzio *et al*., 2002), due mostly, as already highlighted (§2.4.), to above-atmospheric correction problems arising from suspended Saharan dust

(Claustre *et al*., 2002) and to the presence of coccolithophores (phytoplankton species) which affect the *chl* retrieval due to the high reflectance of the coccoliths (plates of calcium carbonate). Since the scope of the work here was that of assessing the *chl* field patterns, the standard algorithm (Equation 4.1) was used and intrinsic limitations noted.

The *chl* images were co-registered and projected using the functionality of SeaDAS (Fu *et al*., 1998). To this end, all single images were re-mapped on a rectangular projection (cylindrical equidistant) grid covering the Mediterranean basin (with the upper left and lower right corner pixels in the grid at 46.0°N 6.5°E and 30.0°N 36.5°E respectively), reducing the original resolution (at nadir) from 1.2 km to 2 km. In order to address the short scale of variability, the chlorophyll images were averaged on a 10-day period basis. Composite (10-day period) mean fields were derived from the re-mapped images by simple time averaging. A sub-scene, bounded by 44.54°N 5.80°E (upper left) and 40.80°N 11.52°E (lower right), was then extracted from each *chl* composite image, and masked with a polygon reproducing the boundaries of the *Pelagos* Santuary (*i.e.* straight lines connecting Point Escampobariou, on the coast of France, to Cape Falcone, in Sardinia, Italy, and Fosso Chiarone, in Tuscany, Italy, to Cape Ferro, again in Sardinia, Italy, as shown in Fig. 3.11). The series of masked 10-day period composite maps of the *chl* field is shown in Fig. 4.1, panels (a) to (g), where each image is identified by year and start-end Julian dates of the 10-day period. The colour bar is the same for all the 10-day period composite maps and represents the *chl* values expressed in mg m^{-3}.

4.2.2 Statistical Analysis

In order to characterize the algal blooms appearing in the 10-day period composite maps, a statistical analysis was performed on the 252 masked *chl* sub-scenes, comprising 213 rows and 238 columns, and covering the whole area of the *Pelagos* Sanctuary. A second mask was created in order to discriminate between cloud and land pixels, which were all set to a value of 0 by the algorithm (Equation 4.1). The statistical analysis was performed by means of PCA (Johnson and Wichern, 1982) applied over the whole dataset in order to represent the *chl* trend in two dimensions during time. The *chl* maps were represented graphically by means of a boxplot carried out on the PC1. E-Distances and E-Statistic Test for Equal Distribution (Szekely and Rizzo, 2004) were

applied on satellite data to verify the existence of statistically significant differences between pairs of *chl* maps.

The result of the E-Distances test is a triangular matrix distance used here for comparing the *chl* maps. This analysis was conducted in order to verify differences within the *chl* distribution. The comparisons were carried out between images referred to the same 10-day period over the 7 years considered and between particular 10-day periods within the same year.

The E-distance between clusters was computed from the original pooled data, stacked in matrix X, where each row was considered as a multivariate observation. The first 213 rows of the original data matrix were referred to the first 10-day period analysed, the next 213 rows to the second one and so on. Thus, the dimension of the original matrix was 53676 rows (213 rows x 252 10-day period) and 238 columns (Equations 3.7, 3.8 and 3.9).

In order to consider only significant comparisons, *i.e.* those for which the value of E is significantly high, the *p*-level was modified using Bonferroni's correction (e.g. $p^*=p/k=0.05/252$). The test was implemented by non-parametric bootstrap (approximate permutation test) with *m* replicates.

The study of the PC1 analysed per each year considered did not determine the seasonality of the main study parameter, e.g. *chl*, nor its likely decreasing or increasing within the period considered (1998-2004). To this end, factor scores calculated on the first principal component were analysed by means of historical series techniques (Bee Dagum, 2002). The historical series analysed was decomposed in its components such as trend, seasonality or cycle and residuals based on an additive model.
The statistical analyses were performed by means of RGUI free software (R Development Core Team, 2004).

4.3 RESULTS

4.3.1 Surface features

The *chl* maps in Figure 4.1 show a marked space-time heterogeneity, particularly prominent (on a seasonal scale) in the Sanctuary's north-west. In this area, as shown in Figure 4.1, low *chl* values occur in winter (in particular between December and January), followed by a marked bloom in spring (March). As shown by the sequence of panels of Figure 4.1, in general the spring bloom takes place in March (from the Julian days 060-069) and continues through April (to the Julian days 111-120). Summer months show lower *chl* values (Julian days 152-244).

The most notable spring phytoplankton bloom occurred in 1999.At the end of March the bloom almost completely covered the western area of the Sanctuary (Fig. 4.1b). In contrast, spring 1998 showed the minimum bloom extent (Fig. 4.1a).

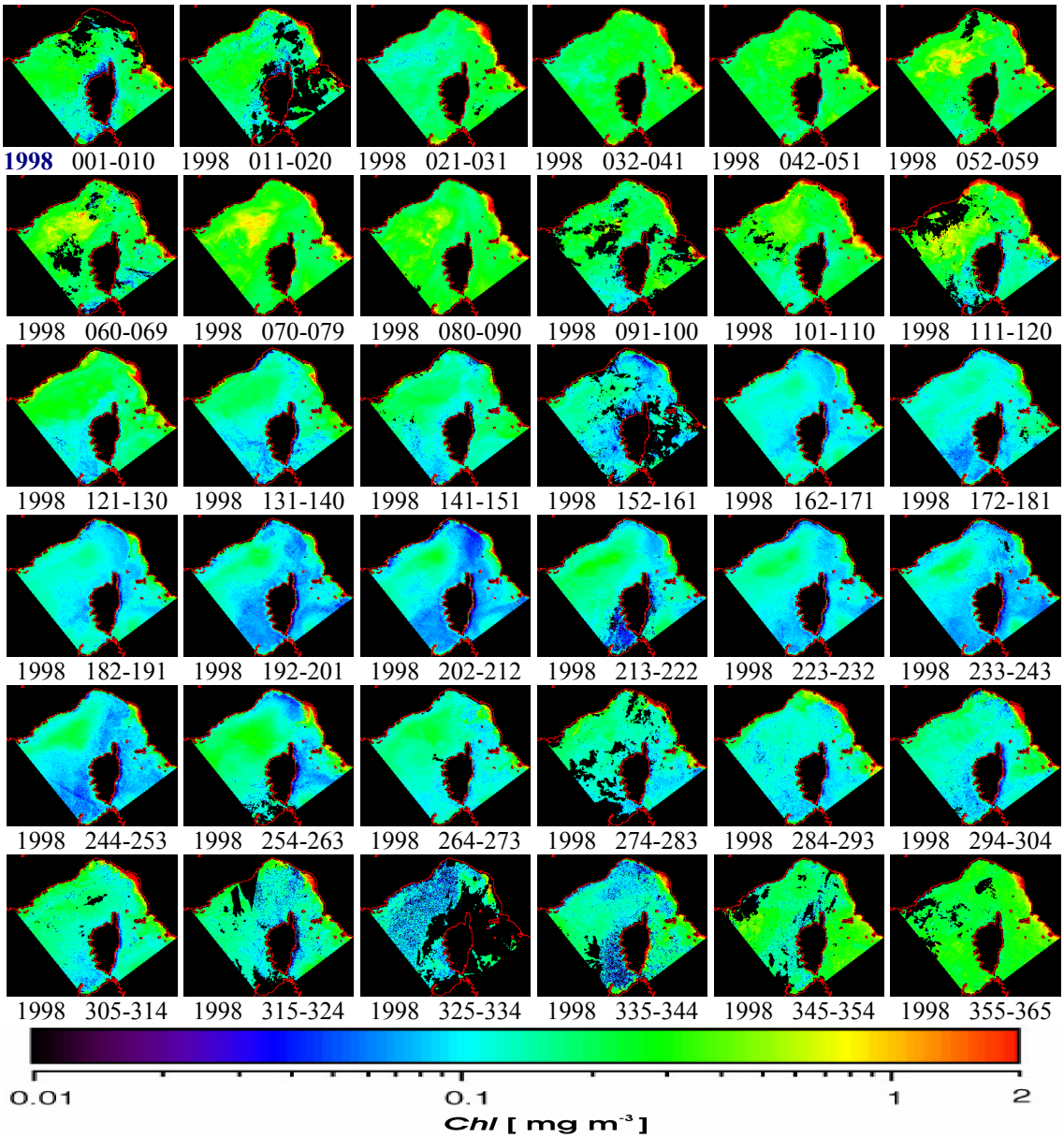

Fig. 4.1 (a) SeaWiFS-derived *chl* [mg m^{-3}] within the *Pelagos* Sanctuary (1998). Numbers indicate Julian day.

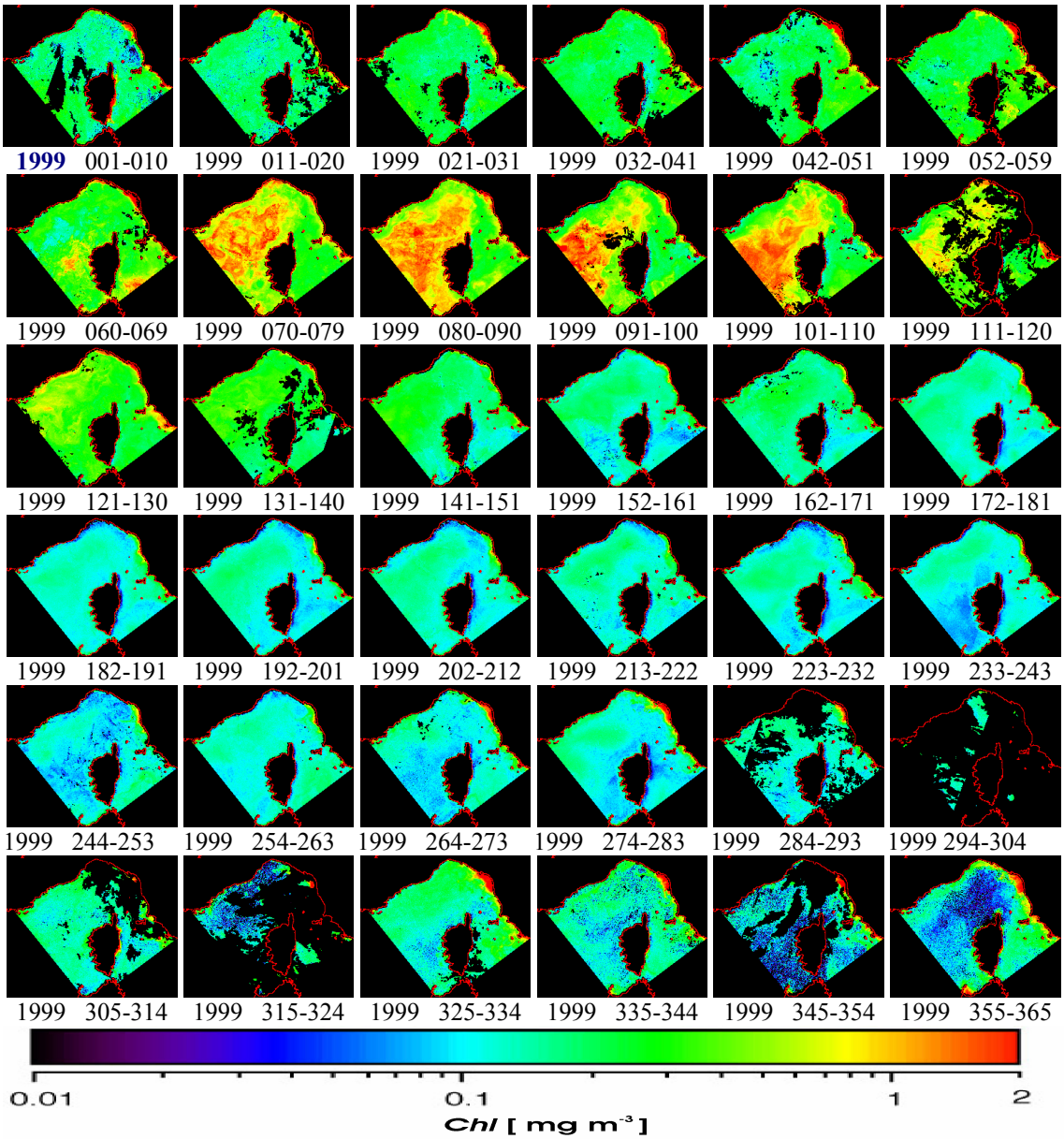

Fig. 4.1 (b) SeaWiFS-derived *chl* [mg m^{-3}] within the *Pelagos* Sanctuary (1999). Numbers indicate Julian day.

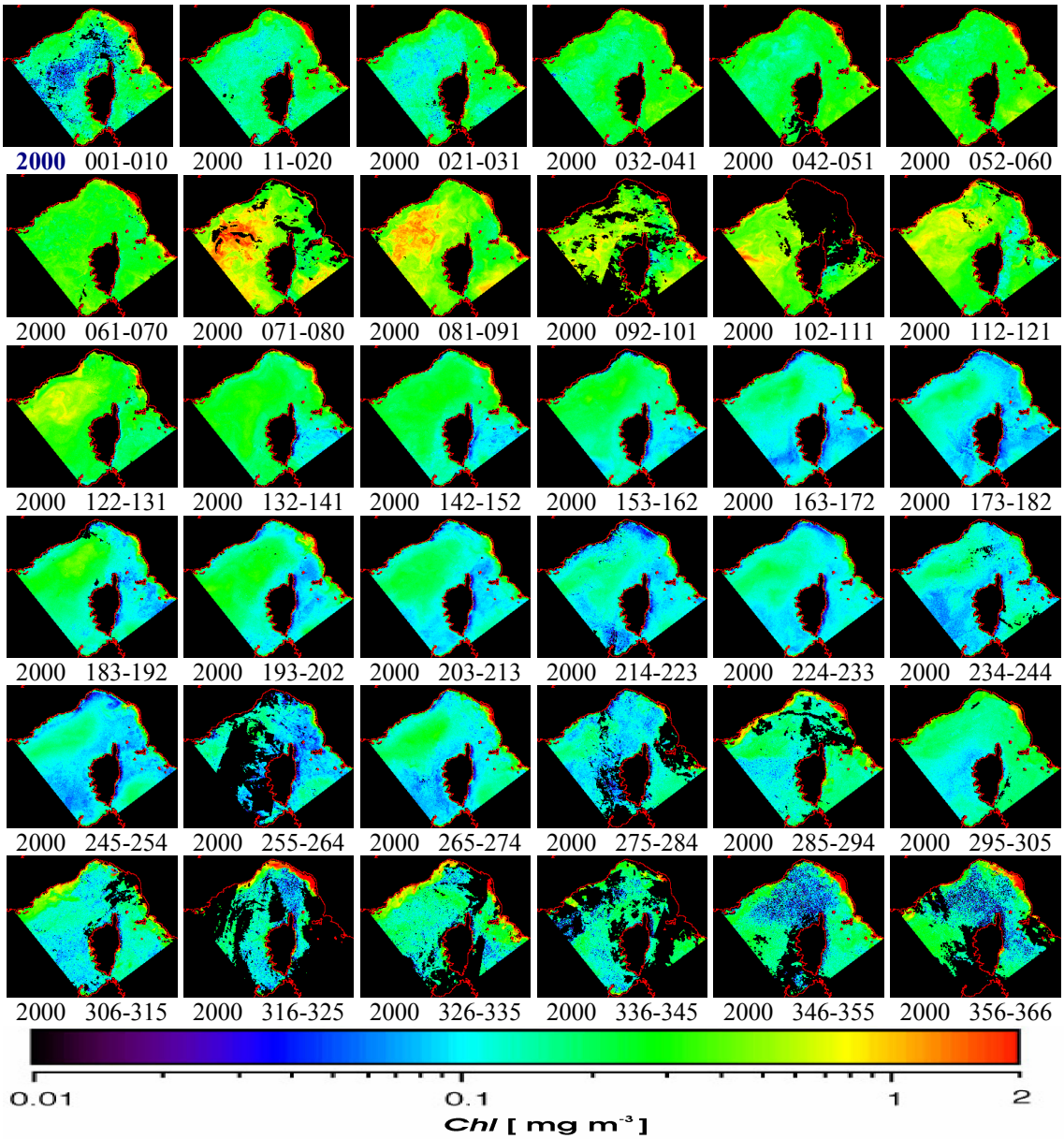

Fig. 4.1 (c) SeaWiFS-derived *chl* [mg m^{-3}] within the *Pelagos* Sanctuary (2000). Numbers indicate Julian day.

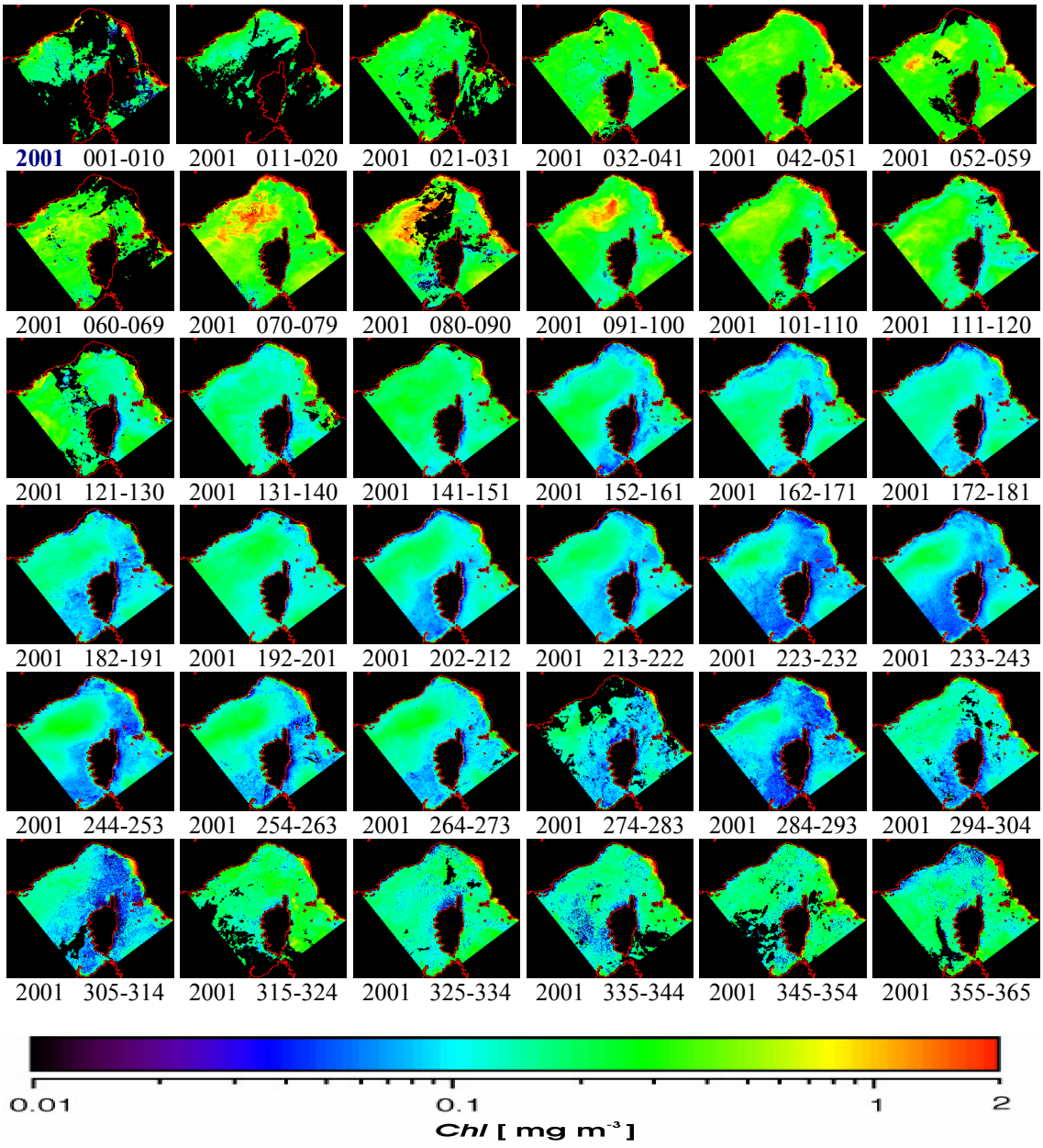

Fig. 4.1 (d) SeaWiFS-derived *chl* [mg m^{-3}] within the *Pelagos* Sanctuary (2001). Numbers indicate Julian day.

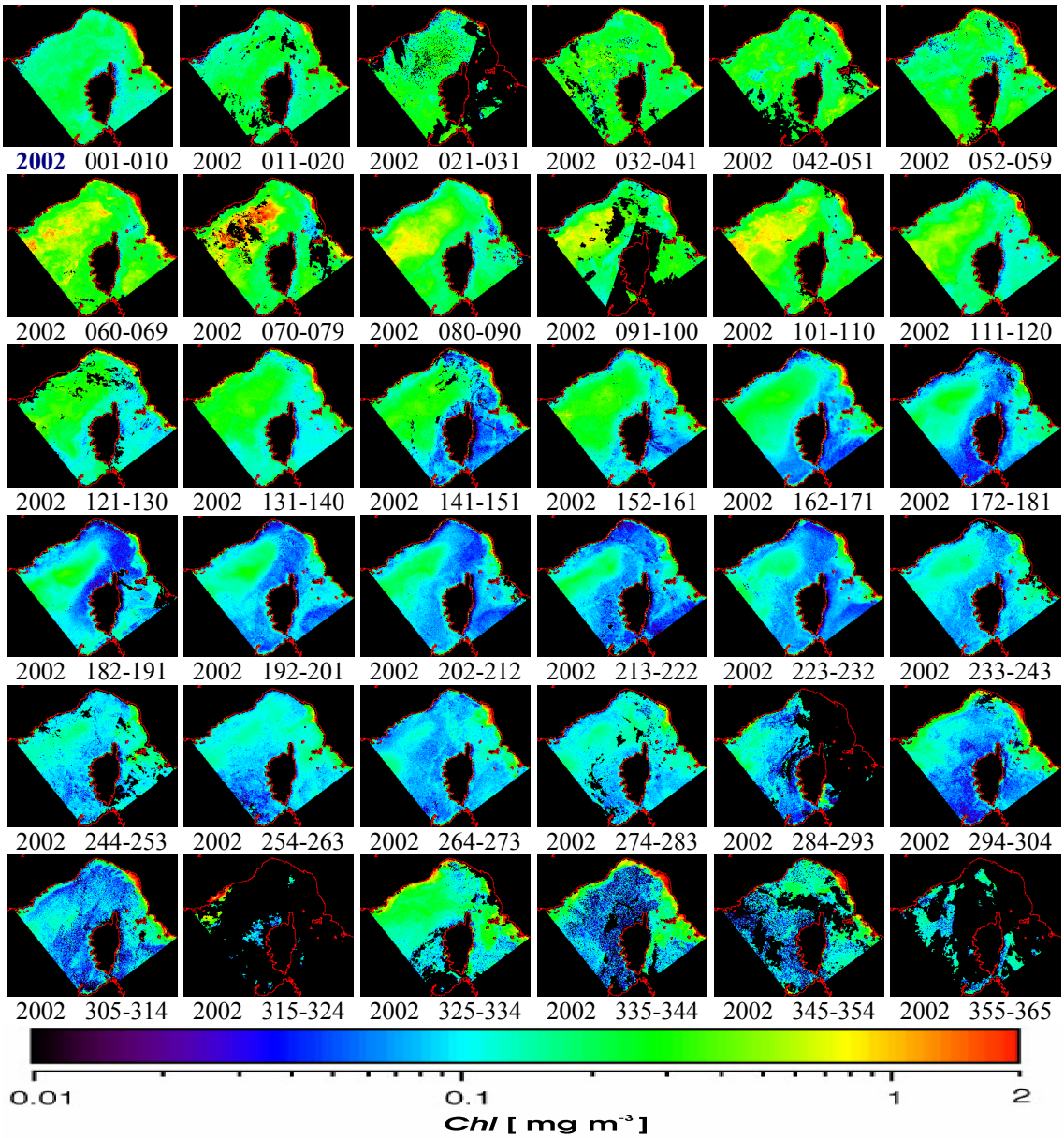

Fig. 4.1 (e) SeaWiFS-derived *chl* [mg m^{-3}] within the *Pelagos* Sanctuary (2002). Numbers indicate Julian day.

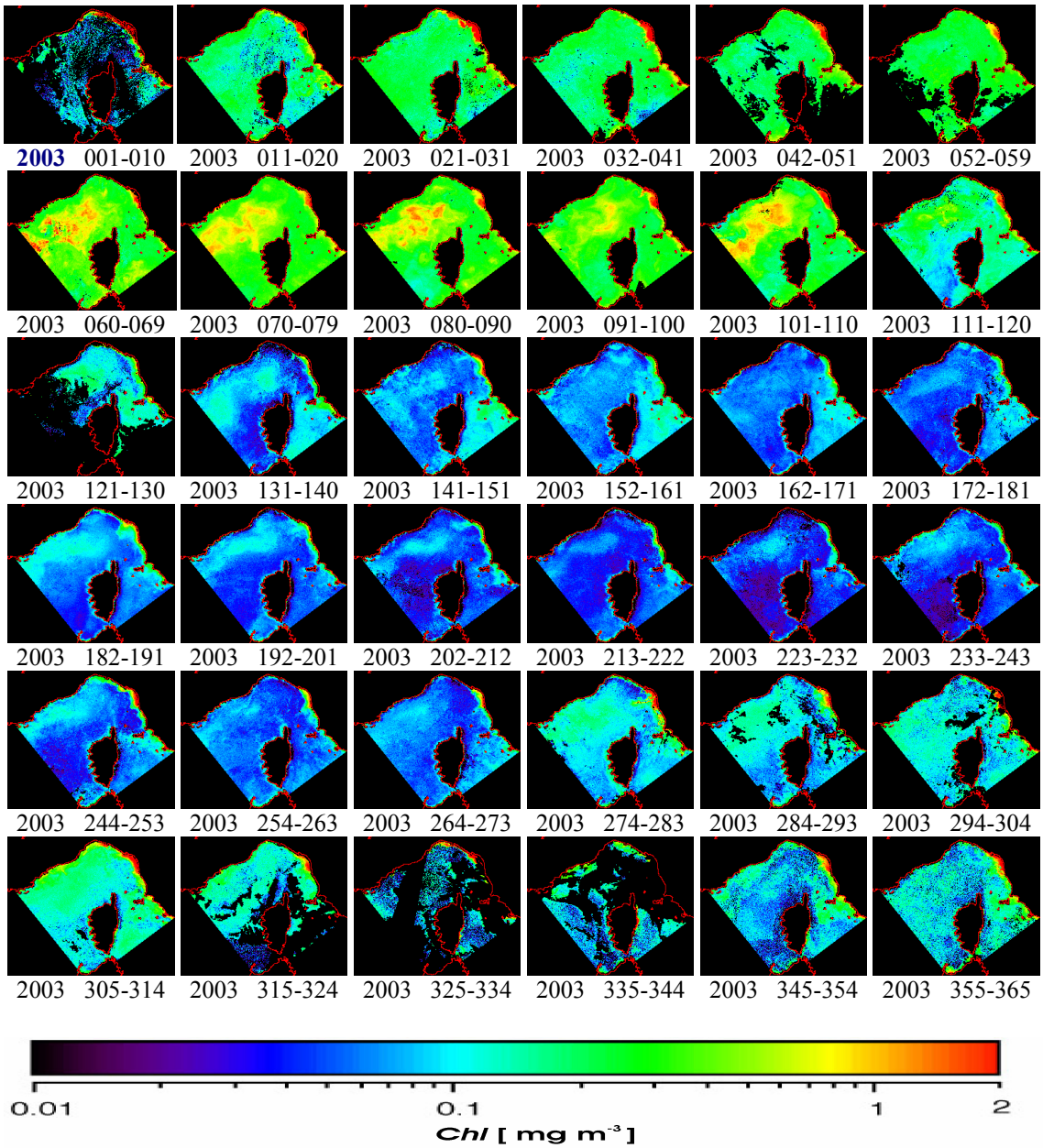

Fig. 4.1 (f) SeaWiFS-derived *chl* [mg m^{-3}] within the *Pelagos* Sanctuary (2003). Numbers indicate Julian day.

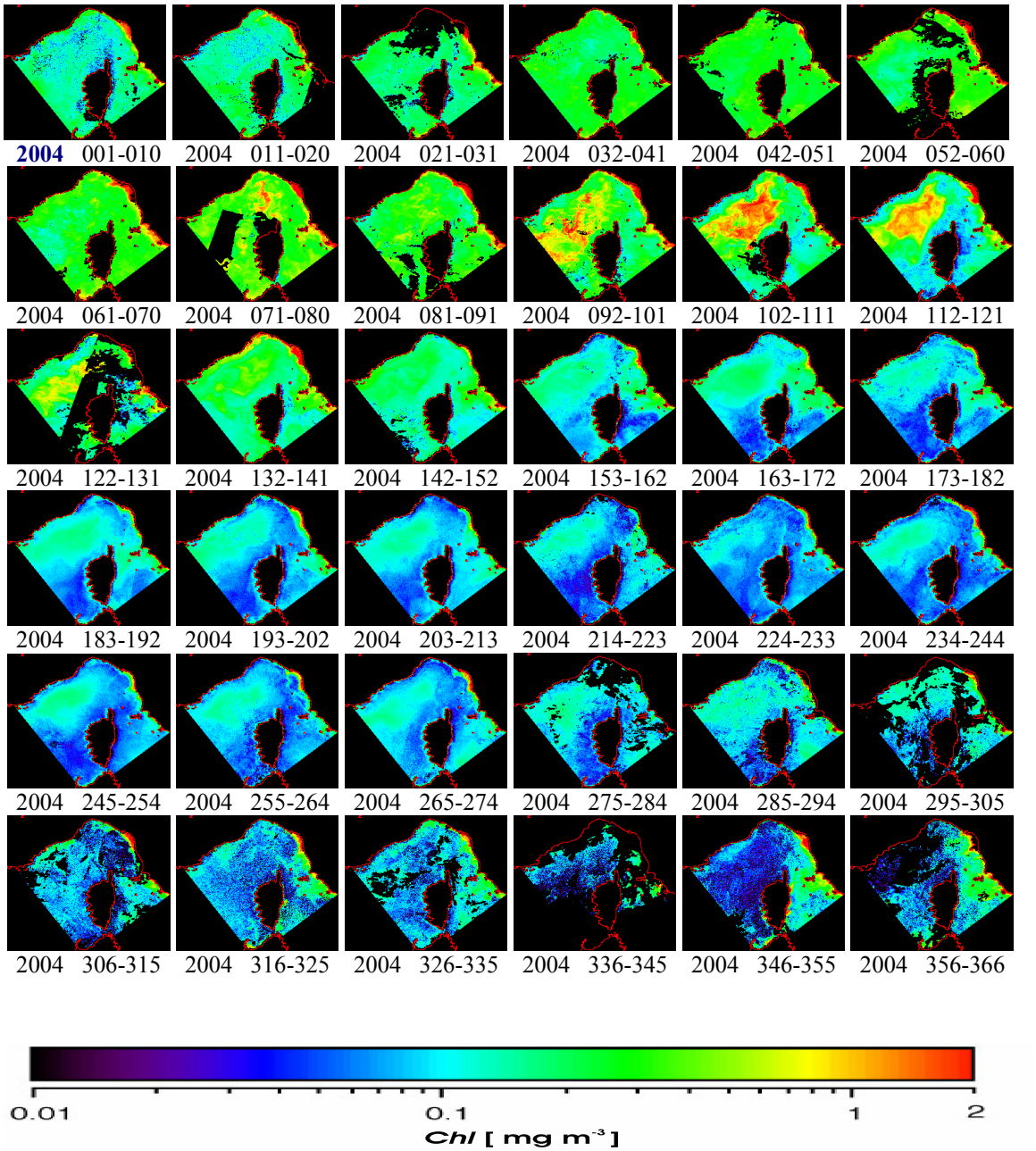

Fig. 4.1 (g): SeaWiFS-derived *chl* [mg m^{-3}] within the *Pelagos* Sanctuary (2004). Numbers indicate Julian day.

PCA was performed on the X matrix containing the data of the 36x7=252 10-day period. Since the images included also land areas, the signal was not completely clean and the first component was biased by factors unrelated to the *chl* field. The PC1 resulting from this analysis is represented by means of a box-plot in Figure 4.2. This component describes 33% of the total variability and expresses mainly variations in the *chl* field. In particular, positive peaks indicate high *chl* values, associated with algal blooms, whereas negative peaks indicate images contaminated by cloud coverage. According to this interpretation, the onset of the bloom period is seen to vary from winter to spring, *i.e.* from 10-day period 3-4 (as in 1998, 2001, 2002, 2003 and 2004) to 6-7 (as in 1999, 2000). Interestingly, an early onset is followed by repeated oscillations, at the monthly scale, of the statistical indicators (see *e.g.* 1998 and 2002), as if repeated blooms would come one after the other throughout spring. Conversely, a late onset is followed by a single massive bloom (see e.g. 1999 and 2000), lasting for the entire spring season.

Following the winter-to-spring period, the statistical indicators show a period of reduced or absent variability in all years. This pattern corresponds to the summer *chl* minimum, occurring in a period when stratification prevents the replenishing of nutrient levels in the euphotic zone.

Starting from 10-day period 26-27, when the stratification is broken up by the changing meteorological conditions of early autumn, the statistical indicators show again a series of successive oscillations at the monthly scale. This pattern is possibly linked to a general increase in *chl* values which culminate in November, stimulated by the upper layer fertilization due to (intermittent) vertical mixing that is linked to the wind patterns of this season. Noise introduced in the data set by the increasing occurrence of cloudy images explains the oscillations observed in November.

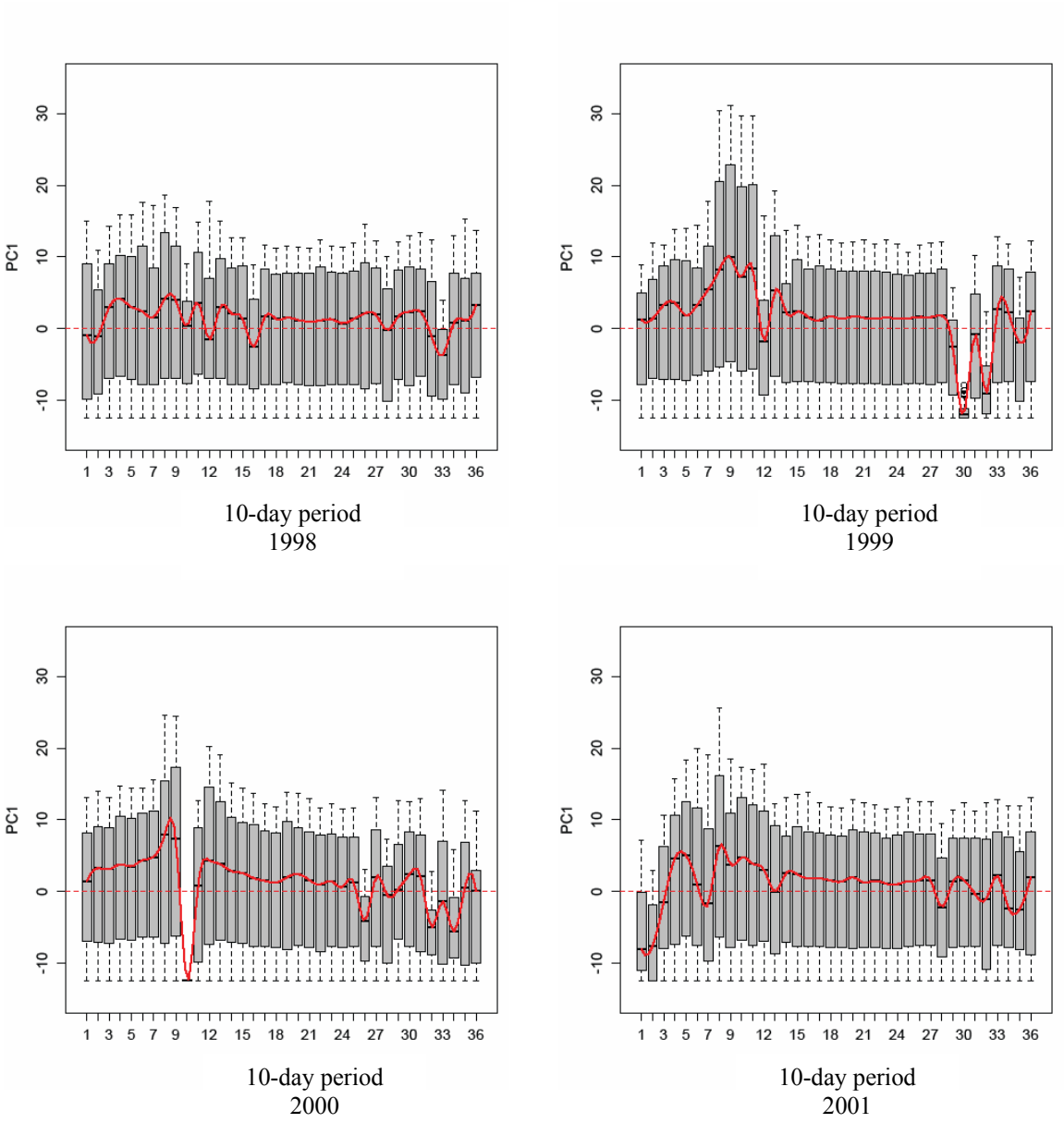

Fig. 4.2 Box-plots of the PC1 relative to the seven years period from 1998 to 2001. The red line indicates the interpolated curve computed over the medians.

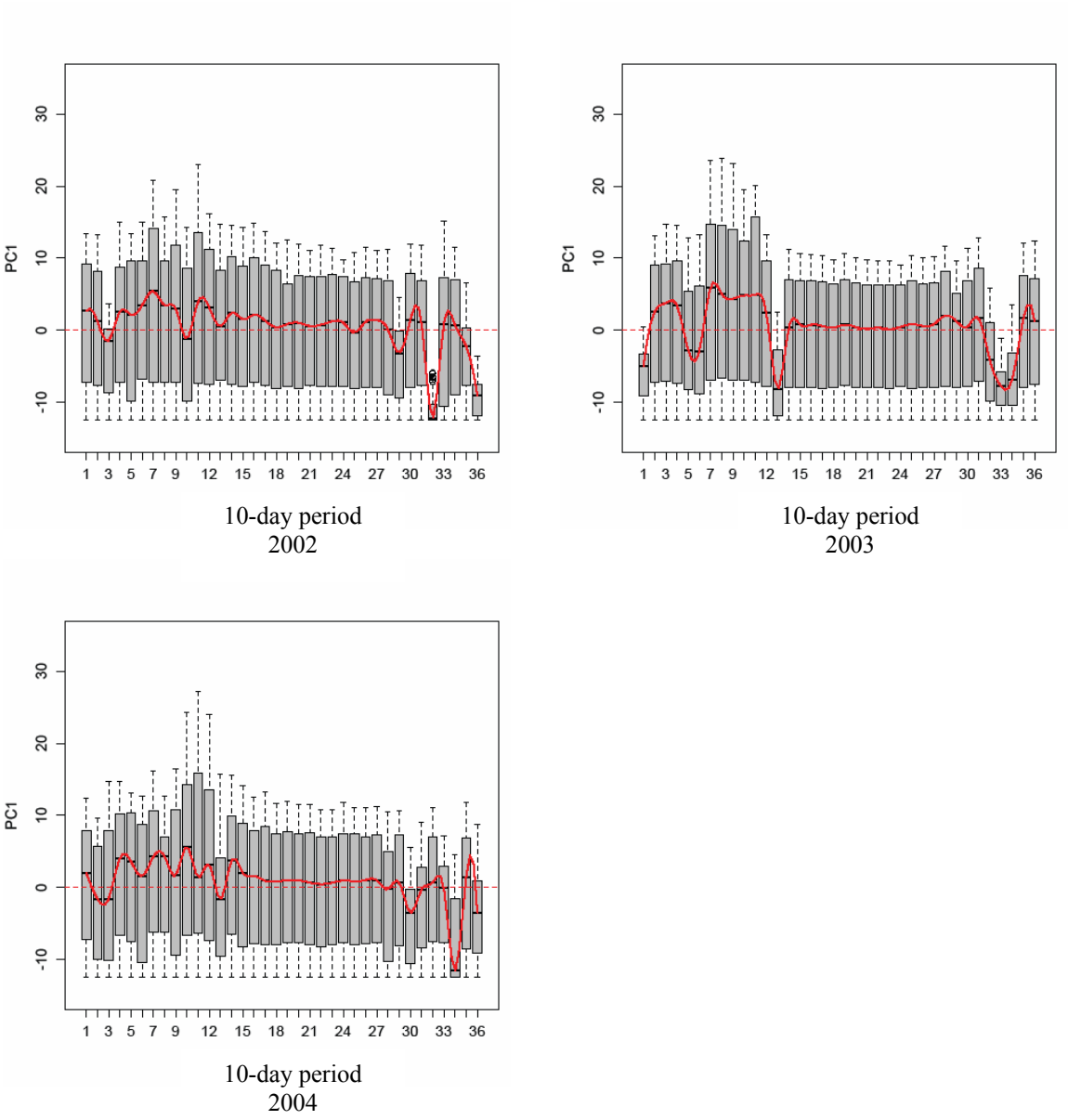

Fig. 4.2 (cont.) Box-plots of the PC1 relative to the seven years period from 2002 to 2004. The red line indicates the interpolated curve computed over the medians).

The results of the *k*-sample multivariate E-statistic for testing equal distributions are shown in Tables 4.1 and 4.2. Table 4.1 shows the comparisons between images referred to the same 10-day period in the seven years considered. The *chl* levels registered during spring (*e.g.* Julian days 070-079) and autumn (*e.g.* Julian days 294-304) of 1999 were significantly higher than in all other years. The comparison of spring data (*e.g.* Julian days 070-079) suggests that the *chl* behaviour can be considered homogeneous, namely the E-distances resulted not significant, over this period, in particular for the years 2001-2002.

Table 4.2 provides examples of comparisons carried out for successive images of a given season, in the same year, *i.e.* the 10-day period of spring (*e.g.* from Julian days 060-069 to 101-110) and the 10-day period of autumn (*e.g.* from 294-304 to 355-365), within 1999 and 2004. During 1999, the E values show a significant increase from Julian days 060-069 to 070-079. Following this rise, the levels were maintained constantly high during the following three 10-day periods. Conversely, rather erratic fluctuations appear after the abrupt change from Julian days 294-304 to 305-314. These fluctuations are due to the high cloud coverage on the imagery analysed (Fig. 4.1b). However it is interesting to note that the significant level recorded from Julian dates 335-344 to 345-354 is due to winter low *chl* levels also referred to as the Gulf of Lions "blue hole ".

During 2004, the E-values showed a significant increase in *chl* levels from Julian days 061-070 to 092-101. The significant value recorded from Julian days 295-305 to 306-315 shows an abrupt decrease in *chl* levels suggesting the anticipated (in November) formation of the "blue hole".

Table 4.1 E-Distance calculated on the PC1 calculated in correspondence of 10-day period 070-079 and 294-304 within years 1998-2004 (n.s.=not significant).

Comparison	E-statistic	p
1998 *vs.* 1999 070_079	113.1	<2.2e-16
1998 *vs.* 2000 070_079	213.2	<2.2e-16
1998 *vs.* 2001 070_079	32.7	<2.2e-16
1998 *vs.* 2002 070_079	20.08	n.s.
1998 *vs.* 2003 070_079	66.04	<2.2e-16
1998 *vs.* 2004 070_079	15.2	n.s.
1999 *vs.* 2000 070_079	60.9	<2.2e-16
1999 *vs.* 2001 070_079	216.9	<2.2e-16
1999 *vs.* 2002 070_079	184.9	<2.2e-16
1999 *vs.* 2003 070_079	289.9	<2.2e-16
1999 *vs.* 2004 070_079	153.2	<2.2e-16
2000 *vs.* 2001 070_079	113.8	<2.2e-16
2000 *vs.* 2002 070_079	92.5	<2.2e-16
2000 *vs.* 2003 070_079	158.4	<2.2e-16
2000 *vs.* 2004 070_079	213.2	<2.2e-16
2001 *vs.* 2002 070_079	7.7	n.s.
2001 *vs.* 2003 070_079	14.9	n.s.
2001 *vs.* 2004 070_079	19.4	n.s.
2002 *vs.* 2003 070_079	21.3	n.s.
2002 *vs.* 2004 070_079	14.2	n.s.
2003 *vs.* 2004 070_079	47.1	<2.2e-16
1998 *vs.* 1999 294_304	650.8	<2.2e-16
1998 *vs.* 2000 294_304	5.6	n.s.
1998 *vs.* 2001 294_304	6.77	n.s.
1998 *vs.* 2002 294_304	5.2	n.s.
1998 *vs.* 2003 294_304	22.5	n.s.
1998 *vs.* 2004 294_304	142.5	<2.2e-16
1999 *vs.* 2000 294_304	646.2	<2.2e-16
1999 *vs.* 2001 294_304	609.9	<2.2e-16
1999 *vs.* 2002 294_304	609.4	<2.2e-16
1999 *vs.* 2003 294_304	522.4	<2.2e-16
1999 *vs.* 2004 294_304	273.9	<2.2e-16
2000 *vs.* 2001 294_304	8.6	n.s.
2000 *vs.* 2002 294_304	5.07	n.s.
2000 *vs.* 2003 294_304	21.5	n.s.
2000 *vs.* 2004 294_304	143.9	<2.2e-16
2001 *vs.* 2002 294_304	5.08	n.s.
2001 *vs.* 2003 294_304	14.1	n.s.
2001 *vs.* 2004 294_304	125.5	<2.2e-16
2002 *vs.* 2003 294_304	15.5	n.s.
2002 *vs.* 2004 294_304	125.3	<2.2e-16
2003 *vs.* 2004 294_304	95.4	<2.2e-16

Table 4.2 E-Distances calculated on the PC1 calculated in correspondence of 10-day period from 060-069 to 101-110 and from 294-304 to 355-365 during 1999 and 2004 (n.s.=not significant).

Comparison	E-statistic	p
1999 060_069 *vs*. 070_069	106.7	<2.2e-16
1999 070_079 *vs*. 080_090	14.3	n.s.
1999 080_090 *vs*. 091_100	15.6	n.s.
1999 091_100 *vs*. 101_110	18.7	n.s.
1999 294_304 *vs*. 305_314	419.5	<2.2e-16
1999 305_314 *vs*. 315_324	188.7	<2.2e-16
1999 315_324 *vs*. 325_334	351.3	<2.2e-16
1999 325_334 *vs*. 335_344	15.6	n.s.
1999 335_344 *vs*. 345_354	111.3	<2.2e-16
1999 345_354 *vs*. 355_365	112.7	<2.2e-16
2004 061_070 *vs*. 071_080	44.9	<2.2e-16
2004 071_080 *vs*. 081_091	68.8	<2.2e-16
2004 081_091 *vs*. 092_101	54.7	<2.2e-16
2004 092_101 *vs*. 102_111	22.03	n.s.
2004 295_305 *vs*. 306_315	79.9	<2.2e-16
2004 306_315 *vs*. 316_325	22.7	n.s.
2004 316_325 *vs*. 326_335	26.3	<2.2e-16
2004 326_335 *vs*. 336_345	240.3	<2.2e-16
2004 336_345 *vs*. 346_355	303.3	<2.2e-16
2004 346_355 *vs*. 356_366	67.8	<2.2e-16

The historical time series is shown in Figure 4.3; scores of the PC1 are depicted on the upper panel. The seasonal cycle demonstrates that the phytoplankton bloom peaks occur between March and April. It should be also noted there is an increasing of *chl* in late autumn (November). The trend, calculated on the scores of the first principal component, shows a sensitive decrease in the *chl* content within the time period considered (1998-2004). In particular, the trend shows a maximum *chl* peak during 1999 and a successive decrease in *chl* values during the following years with a minimum registered in 2003. The year 2004 shows a slight increase in *chl* concentrations. In the lower panel of Figure 4.3 are shown the residuals calculated between the observed data and the model which did not result dependent on time and oscillated mostly around 0.

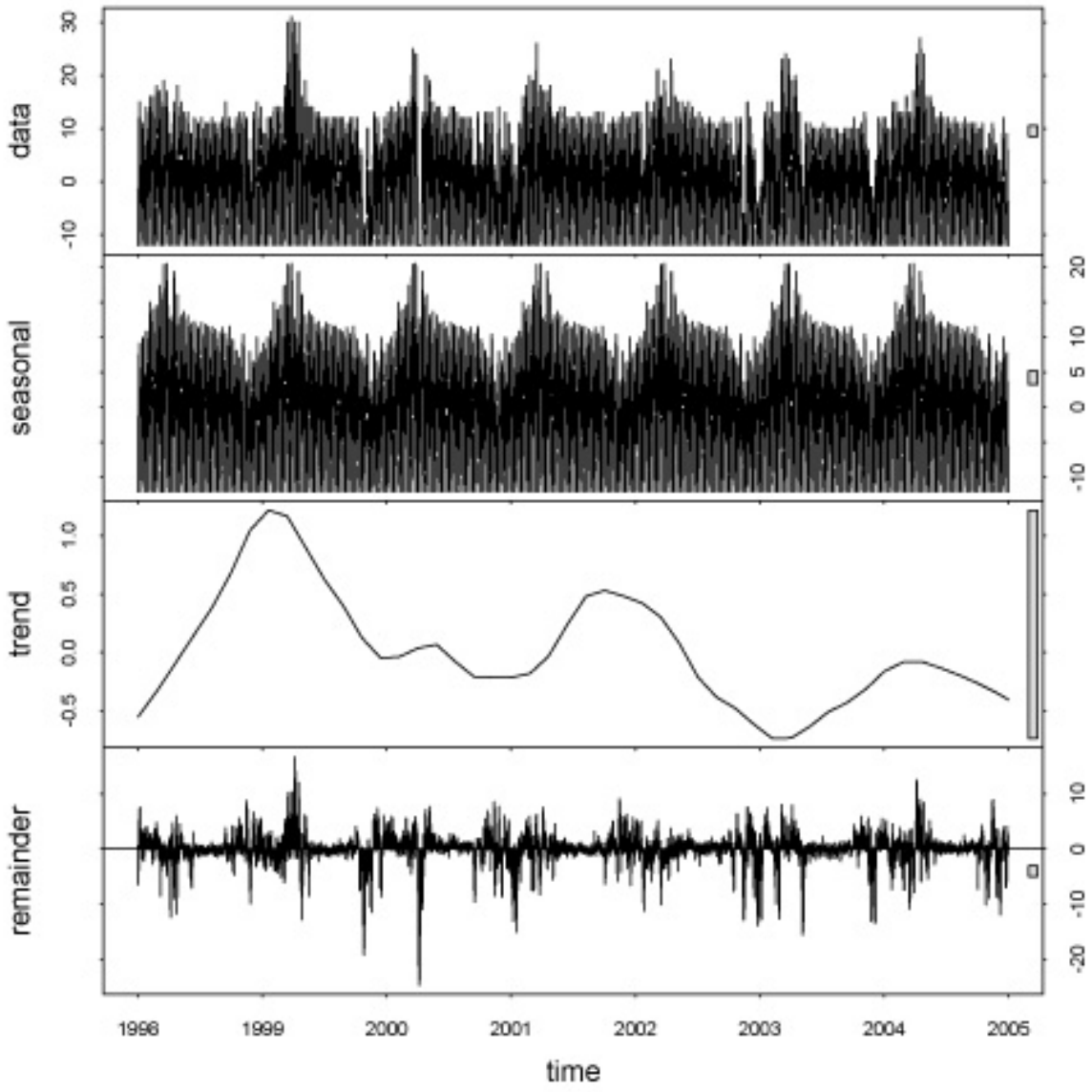

Fig. 4.3 Decomposition of additive time series calculated on the PC1 from 1998 to 2004. Each bar represents a 10-day period. Upper panel: observed data. Lower panel: residuals.

4.4 DISCUSSION

In this chapter the general aim stated in the introduction, namely the observation of the phytoplankton blooms patterns within the *Pelagos* Sanctuary, was achieved by quantifying its spatial and temporal recurrence and by assessing the seasonal and interannual variability of *chl*. Ocean colour data have been used in order to monitor the status and the trends of the system.

A statistical approach to the analysis of the remotely sensed *chl* field has been proposed and applied. The results of this statistical analysis allowed visualisation of the *chl* trend, within the entire area of interest, over a multi-annual period. Further, the analysis highlighted clear, recurrent, seasonal variations of *chl*, with the presence of a major peak in spring. Low *chl* values appeared in winter and were followed by sizeable algal blooms in March and April caused by the high nutrient concentrations and solar irradiance respectively. The bloom patch continued to be visible throughout summer and autumn. However during summer the *chl* is reduced due to the high stratification and the consequent lack of nutrient supply from deep layers and from coastal run off thus suggesting that the waters are nutrient depleted. The low *chl* values are also the result of the primary producers using up all of the nutrients made available by the antecedent wind-driven vertical mixing, combined with grazing by secondary producers. The growing biomass of these secondary producers, in turn, renders the north-western Mediterranean basin a preferred summer feeding ground for large marine mammals, such as the fin whale *Balaenoptera physalus* (Barale *et al.*, 2002).

As stated above, the patches of low *chl* are thought to be induced by the wind pattern prevailing in the north-west (*e.g.* the Mistral), causing convection processes that lead to deep water formation (Millot, 1990) and thus removing the phytoplankton from the euphotic zone. The subsequent blooming, in contrast, is thought to be triggered by the onset of stratification, which follows the relaxation of the wind pattern (*i.e.* cessation of the vertical mixing that prevented the blooming in winter, but also that produced a substantial increase of nutrients in the euphotic zone).

Secondary peaks appeared in late autumn (November), following the constant, reduced *chl* levels of summer, in good agreement with what reported for the planktonic field of the Western Mediterranean by Margalef (1985) and Arnone (1994). Those secondary peaks are due to the enhanced nutrients from autumnal mixing.

The decrease of *chl* observed from 1999 to 2003 and the consequent decrease of the algal bloom intensity highlighted by the historical series analysis are in agreement with the decrease of *ch*l average value found by Barale *et al*. (2008) in the whole Mediterranean basin. In temperate seas such as Mediterranean, the phytoplankton biomass is primarily subjected to nutrient availability (Cruzado, 1985). The decrease of *chl* could have been caused by the reduced vertical mixing which fertilises the surface waters with nutrients from the deeper layers; a more stratified water column limits the nutrient flux to the photic level and consequently the development of primary producers. Vidal *et al*. (2007) recorded in the NW Mediterranean during March-April 2005, low surface dissolved inorganic nutrient concentrations which increased to maximum with depth. In particular surface nitrates were around 4–6 µM whereas around 10 µM at depth, surface phosphates were around 0.4 µM and at depth below 0.1 µM.

The spring bloom of 1998 was the least pronounced and the shortest recorded in the *Pelagos* Sanctuary for the 7 years considered. This could be explained according to Barale *et al*. (2008) to the lack of deep convection in the Gulf of Lion occurred in 1997.

The more stratified water column recorded between 2000 and 2003, could have been due to the changes in the mean temperature of the Mediterranean Sea (Béthoux *et al*., 1998), increasing roughly 0.03 °C per year between 1985 and 2005 (Buongiorno Nardelli *et al*., 2007). In particular, annual average SST skin in 2003 was roughly 0.5 °C higher than other years from 1985 to 2005 (Buongiorno Nardelli *et al*., 2007).

Analysis of climatological data collected by the CZCS (1978-1985) (Barale *et al*., 2008) demonstrated that the relaxation of wind patterns and the consequent water column stratification ,due to the colder SST, used to occur later so that the spring bloom had its peak in April (1978-1985) rather than in March (1998-2004). Thus it can be hypothesised that the above mentioned increase of SST skin has caused between 1998

and 2004 an anticipation of the regional spring bloom (from April to March) within the Sanctuary area due to the earlier relaxation of the prevailing wind field (e.g. Mistral wind). The high SST skin recorded during 2003 could also explain the remarkable reduction in *chl* concentration and in bloom magnitude.

4.5 CONCLUSIONS

The analysis of the *chl* fields performed by means of ocean colour sensor in the *Pelagos* Sanctuary has allowed observation of the seasonal and interannual dynamics of the system at appreciably high temporal and spatial resolution.

The ocean colour imagery analysis performed, provided information at sufficiently high resolution to understand the seasonal and interannual phytoplankton dynamics which is of the outmost importance to underpin an effective management of the *Pelagos* Sanctuary**.**

Future developments of the present approach should foresee the integration of zooplankton biomass and cetaceans distribution data, collected concurrently to the satellite imagery within the *Pelagos* Sanctuary, so as to provide further essential biological data. The above mentioned information will potentially lead to the improved understanding of the baseline of the main ecological relationships within the *Pelagos* Sanctuary contributing for an effective management of the cetacean populations inhabiting this unique open water MPA.

CHAPTER 5

INTEGRATED ANALYSIS OF MARINE ENVIRONMENTAL VARIABLES WITHIN THE PORTOFINO MPA BY MEANS OF *IN SITU* DATA ACQUISITION SYSTEMS AND REMOTE SENSING.

5.1 INTRODUCTION

The coastal marine environment is a complex system and its management requires adequate information. In fact the MPA management body needs information useful to improve the marine environmental quality and to evaluate the efficacy of the management within the MPA's boundaries (Cattaneo-Vietti and Tunesi, 2007).
This study considers therefore different methodologies that could be integrated to lead to an increase in the use of satellite sensors to the continuous monitoring of coastal areas. The focus was the monitoring of physical and biological phenomena in a high value coastal marine protected area; the Portofino MPA (Ligurian Sea) was used as test site.

This chapter supplies an analysis relative to field data collected on 2004 in the Portofino MPA.

As already shown (chapter 3) satellite images have been used to characterise the bio-physical features occurring in the Portofino MPA by using optical and thermal imagery. The optical images used were at low spatial resolution. These *chl* maps, weekly averaged, were particularly useful in order to characterise the trend of phytoplankton bloom in the Portofino MPA. In this study, by contrast, daily optical images at both coarse and fine spatial resolutions were selected. Moreover two ocean colour algorithms for the two different water types (e.g. case 1 and case 2; Morel and Prieur, 1977; Morel, 1988) were tested on the study sites.
Critical assessment of the informative content of the remote sensed data utilised is also presented.

The study area encompasses the waters of the Portofino Promontory and the neighbouring stretch of coast (Tigullio Gulf on the eastern side and Paradise Gulf on the western side; Fig. 5.1a and b). This test site has been selected due to the recognition of the Portofino MPA as Long Term Ecological Research Network Site (LTER) in 2007 (Castellano *et al*., 2008). This *status* presents an opportunity to collect data to help to detect and understand environmental changes due to pollution, climate change and biodiversity loss. This area, as already highlighted in Chapter 2, is particularly important both for its environment (i.e. coastal and marine ecosystem) and also for its economical value as a tourist destination. From an oceanographic perspective the Portofino MPA lies within the Ligurian Sea, which is dominated by a well defined cyclonic gyre, with a seasonal cycle related to the seasonal variations of the atmospheric forcing (Esposito and Manzella, 1982). The resulting circulation in the coastal area of interest (Fig. 5.1b) is in the general north-westward direction, following the coast, with only a short period of reversal that is associated with northerly winds (Astraldi and Manzella, 1983; Astraldi and Gasparini, 1986).

5.2 EXPERIMENTAL DESIGN

The following sections will highlight the materials and methods used for the *in situ* sampling campaigns and satellite data processing. In particular the reliability of remote sensing imagery will be assessed by tackling the issue algorithm selection problem. An evaluation of MERIS products along with critical analysis of the algorithms supplied were performed; both MERIS algorithms (algal_1 and algal_2; Morel and Antoine, 2000; Doerffer and Schiller, 2007) were tested over the study area.
Detailed of statistical analyses performed area are also provided.

5.2.1 *In situ* sampling

In 2004 two hydrographic cruises were carried out across the Portofino coastal area (Fig. 5.1a), on 17 June and 17 November by the Department for the Study of the Territory and its Resources (DIP.TE.RIS) of the University of Genoa (Prof. P. Povero) and by CNR- ISMAR (Dr. G.P. Gasparini), La Spezia, Italy. Six transects perpendicular to the coast (approximately 35 stations) covered an area of about 50 km^2 from a depth of 5m to 100m. The whole water column was investigated using a calibrated multiparametric probe (Idronaut Ocean Seven 301). The parameters measured were sea temperature, salinity, dissolved oxygen, pH, and chlorophyll (*chl*)-*a* concentration. *In situ* data were later interpolated in order to create SST at 0 m and *chl -a* maps. The data acquired by the hydrographic cruises (Fig. 5.1b, Appendix 23), were employed to validate the measurements obtained by satellite.

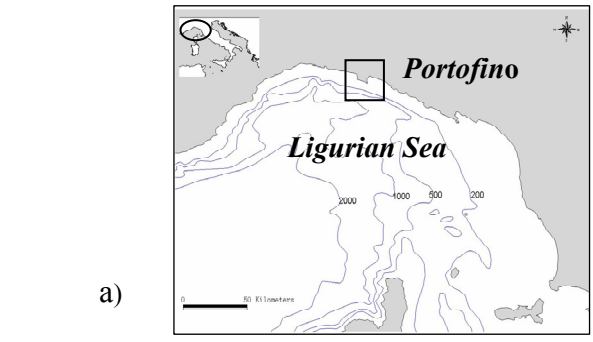

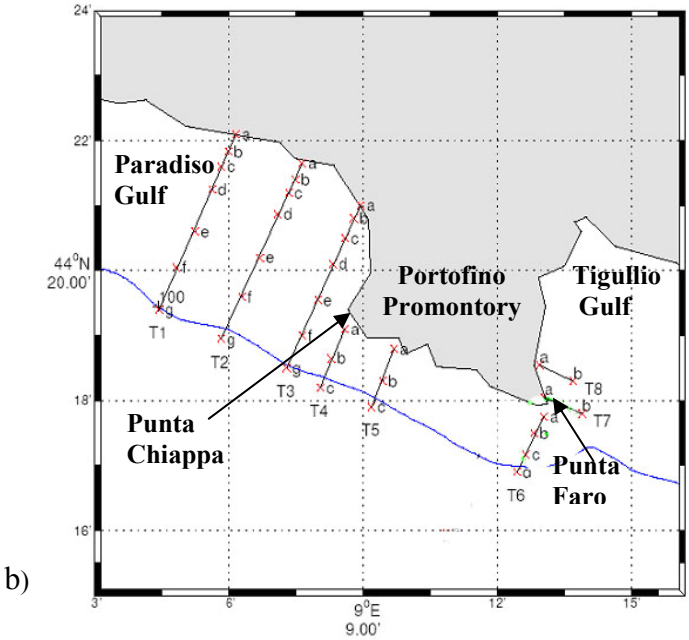

Fig.5.1 a) The study area in the Ligurian Sea; b) The Portofino Promontory and the sampling stations (a, b, c, d, e, f and g) on the transects (T) performed by the hydrographic cruises in November 2004. Blue line shows the bathymetry at 100 m.

5.2.2 Remotely sensed data and processing

EO data collected from ESA were chosen to monitor and analyse the biophysical parameters pattern such as SST skin and *chl* at regional (Ligurian Sea) and local scale (Portofino MPA). The satellite images were retrieved by the optical (MERIS) sensor present aboard the ENVISAT 2 satellite (Appendix 1). Satellite images were chosen utilising the ESA archive EOLI SA, the full ENVISAT sensor data archive (2002-present). SST skin data utilised were retrieved by the NOAA-AVHRR thermal sensor at a spatial resolution of 1.1 km (Appendix 1); images were downloaded from the German RS data archive (http://eoweb.dlr.de:8080/data-service). Two SST skin maps were retrieved for June and November 2004 at the same time the campaigns carried out *in situ*. The algorithm used for retrieving SST skin is based on the brightness temperatures of AVHRR channels 4 and 5 (T4, T5) (McClain *et al*., 1985).

Regarding the optical sensor, the two MERIS spatial resolutions corresponding to *in situ* sampling campaigns were requested (i.e. MERIS Full Resolution, MER_FR at 300m and MERIS Reduced Resolution, MER_RR at 1100 m). The data were acquired at L2 *chl* (in mg m^{-3} of water). Using the data browser the daily cloud free full and reduced resolution images were selected contextually to the campaigns carried out *in situ* during 2004 (Figs. 5.2-5.5).

L2 encompasses two chlorophyll products obtained by the use of two different algorithms, i.e. “algal_1” and “algal_2”. These algorithms calculate differently the concentration of chlorophyll in mg m^{-3} of water with respect to the different types of water considered. Algal_1 was developed for offshore waters (case 1 water; Morel, 1988), where only phytoplankton pigments and associated substances affect the water leaving radiance spectrum. The algal_1 algorithm is based on a semi-analytical model using a two colour band ratio ($R_{(445)}/R_{(555)}$) for *chl* <2 mg m^{-3} (Morel and Antoine, 2000).
The MERIS algorithm for the evaluation of the algal pigment in Case 1 waters uses the variation of the ratio (Equations 5.1 and 5.1a):

$$\rho_{i,j} = R(\lambda i)/R(\lambda j) \qquad \text{Equation (5.1)}$$

$$\rho_{443,555} = \left[\frac{b_b(443)}{a(443)} \Big/ \frac{b_b(555)}{a(555)} \right]^{-1} \qquad \text{Equation (5.1a)}$$

where

R = reflectance

i and j = wavelengths

b_b= backscattering

a=absorbance

These variations are inverted in order to build up the algorithm in a polynomial form as follows (Equation 5.2):

$$\log_{10}[Pigment - index] = \sum_{x=0}^{n} A_i \left(\log_{10} \rho_{i,j}\right)^x \qquad \text{Equation (5.2)}$$

where A= constant

the wavelengths to be considered are the following:

λ_i are $\lambda_2 = 443$ nm, $\lambda_3 = 490$ nm e $\lambda_4 = 510$ nm respectively (i.e. wavelengths within the blue, blue-green part of the electromagnetic spectrum);

λ_j is $\lambda_5 = 560$ nm (i.e. wavelength within the green part of the electromagnetic spectrum).

In contrast, algal_2 has been developed for coastal waters (case 2 water), with multiple independent components, i.e. phytoplankton pigments, total suspended matter and CDOM. Algal_2 is based on an artificial neural network (aNN) inversion procedure which relates directional water leaving radiance reflectance (R_{rs}) with the Inherent Optical Properties (IOPs) such as absorption (a) and scattering coefficients (b_b) or concentrations of different constituents present in coastal waters (Doerffer *et al*., 2002; Schiller and Doerffer, 2005; Doerffer and Schiller, 2007).

Portofino MPA waters could be considered as case I water due to the narrow continental shelf and as case 2 water due to the Entella river run off within Tigullio Gulf (Fig. 5.1b). For this reason, both MERIS algorithms should be considered while analysing Portofino MPA waters.

C*hl* estimated by algal_1 and algal_2 algorithms were both tested over the chl-*a* values retrieved *in situ* along the transects within the Portofino MPA.

Both daily AVHRR and MERIS imagery were analysed, geo-registered and projected using the functionality of ENVI (ITT Visual Solutions Systems Inc.) and BEAM (Brockmann Consult) software respectively. Images were re-mapped on a geographical projection (ellipsoid WGS-84). Two sub areas were extracted: the first covering the North-Western Mediterranean basin and in particular the Ligurian Sea (45°19'11" N, 7°40'05" E (upper left) and 42°15’33” N, 11°13’21” E (lower right) (Figs. 5.2, 5.3a, 5.4 and 5.5) and the second smaller area encompassing Portofino MPA and the neighbouring stretch of coast (44°49'34" N, 8°33'24" E (upper left) and 43°50'20" N, 9°44'29" E (lower right)) (Fig. 5.3b).

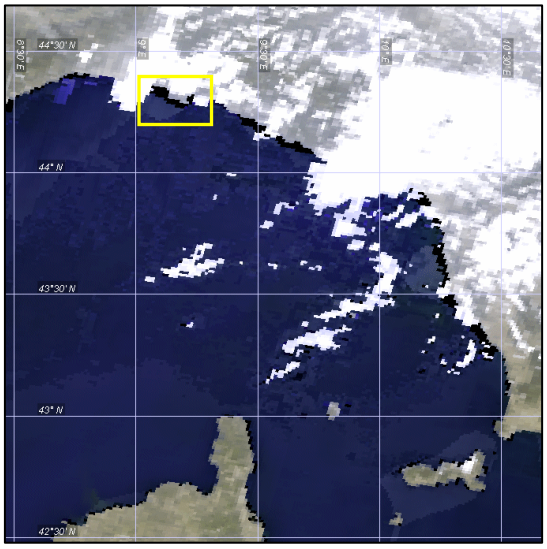

Fig. 5.2 Ligurian Sea MERIS RR 17/06/2004 level_1 RGB.

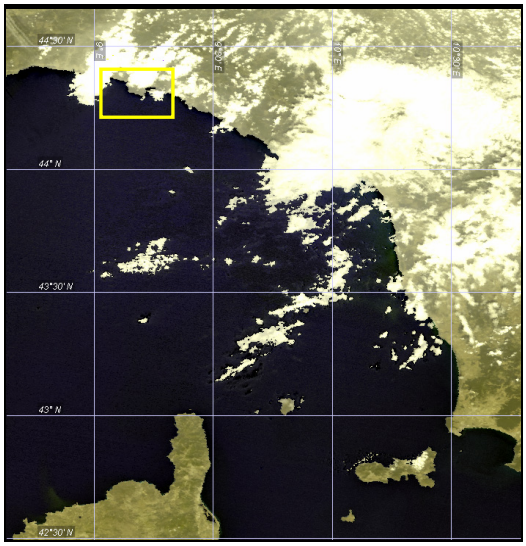

Fig. 5.3a Ligurian Sea MERIS FR 17/06/2004 level_1 RGB.

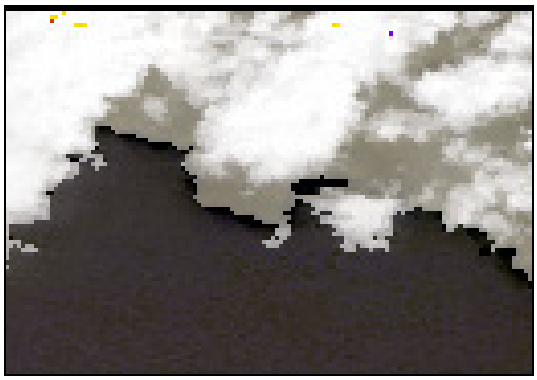

Fig. 5.3b Portofino area MERIS FR 17/06/2004 level 1_RGB.

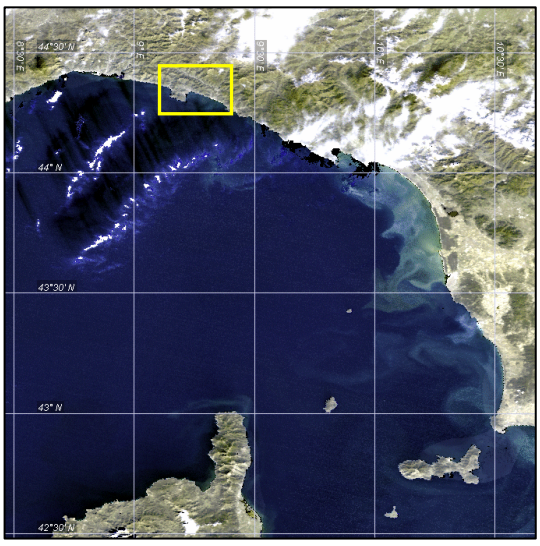

Fig. 5.4 MERIS FR 16/11/2004 Level 1_RGB.

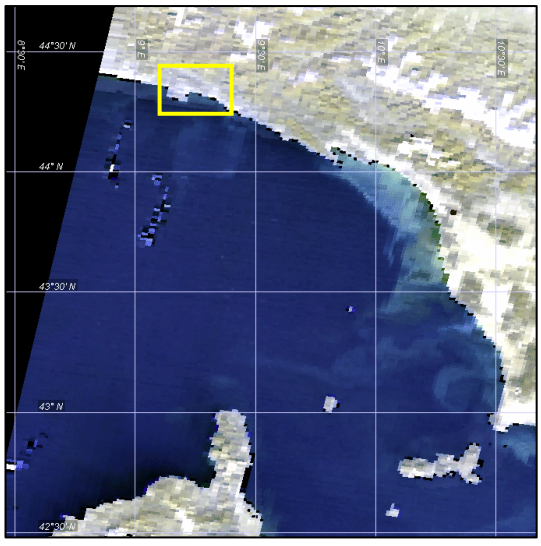

Fig.5.5 MERIS RR 17/11/2004 Level 1_RGB.

5.2.3 Statistical Analysis

Correlation between SST skin satellite data and data collected *in situ* was not performed due to the high accuracy (0.1-0.2 K) (Robinson, 2004) attained by the AVHRR sensor, further elaborations were not necessary. Geo-registered algal_1 and algal_2 *chl* (mg m^{-3}) products coming from MER_FR and MER_RR were extracted from the images, exported into text format and later imported into RGUI statistical free software (R Development Core Team, 2004). Match-up analysis based on comparison of *in situ* discrete *chl*-a measurements with MERIS derived *chl*, an interval of 0.002 degrees of latitude and longitude (~210 m) was chosen due to the reduced distance among the sampling stations, allowing consideration of a square of pixels surrounding the discrete *in situ* sampling station without overlapping to the next one. The comparison for MER_FR and *in situ chl*-a was performed by analysing all the sampling stations, whereas the relationship with MER_RR and *chl*-a was calculated analysing a reduced number of sampling stations due to the reduced spatial resolution of the former.

Relationships with *in situ* chlorophyll (averaged between 0 and 1m) and *chl* estimated by algal_1 and algal_2 algorithms were quantified using linear regression analysis; the former *in situ* averages showed high coefficient of variations (>10 %) thus indicating that these data were not homogenous.
Given that Portofino surficial waters oligotrophic, *chl* extrapolated from the algal_2 algorithm greater than 3 mg m^{-3} were not considered due to a sensor bias. The statistical significance (*p* value) of the most highly correlated variable was then determined as predictor of the best performing algorithm. If both algorithms would produce a significant *p* value (>0.05), one of the two can be selected on the basis of the determination coefficient (R^2).

5.3 RESULTS

In the following sections, the results obtained by the analysis of the satellite images and *in situ* data for 2004 is presented, focusing on Portofino MPA and in particular on the choice of the best performing algorithm.

The images chosen were MER_RR on the 17th June and MER_RR on the 17th November 2004. The analysis was performed on the MER_RR images. However, these matrices being at a broad scale, it was decided also to compare also the MER_FR image relative to the 17th June 2004 and 16th November 2004. This last comparison using data for consecutive day could be considered as being not a rigorous approach, however the MERIS_FR observations were missing for the 17th November 2004. This approach could be justified from the fact that it is possible to hypothesise that a day shift did not provoke such a remarkable change of *chl* but rather a change in its spatial distribution.

5.3.1 June 2004 observations

Figure 5.6a and b show the cloud free SST skin maps collected by the AVHRR sensor for 18/06/2004. Within the north western part of the Ligurian Sea a cold front (SST range from 18.5 to 20.0°C) was evident. In Portofino MPA (Fig. 5.6b) Paradise Gulf showed SST values between 22.0 and 22.5°C whereas Tigullio Gulf waters were warmer (from 22.5 to 23.8°C).

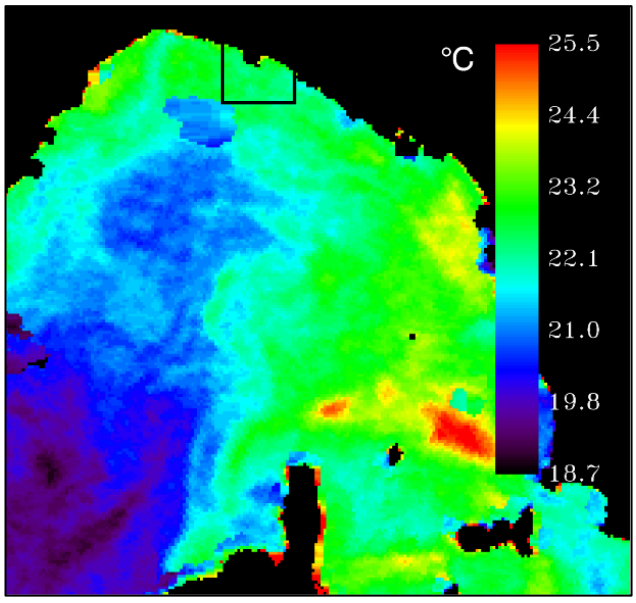

Fig. 5.6a AVHRR SST skin map on the 18/06/2004.

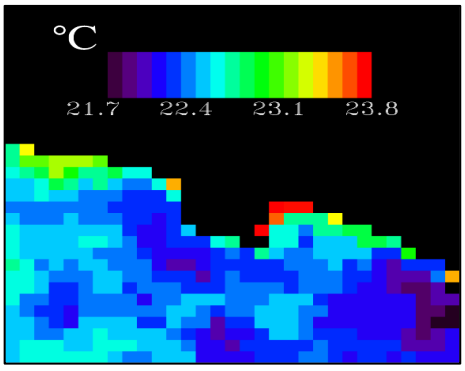

Fig. 5.6b Portofino area AVHRR SST skin map on the 18/06/2004.

Figure 5.7 shows the surface temperature map by *in situ* measurements on the 17th June 2004, a day before the satellite image. The peculiar thermal structure shown is an interpolation of the surficial waters and it does not provide any detail of the vertical structure of the subsurface temperatures.

A relatively cold vein was evident in the south-eastern border (T<21°C), while the warmest region was the Paradise Gulf (T around 22 °C). The comparison with satellite SST confirms that the Paradiso Gulf is a warm region. However the warmest region was the Tigullio Gulf; the SST map indicates lower temperature in front of Portofino promontory. The cold signature appeared to have a greater extension and more elongated westward, suggesting a possible westward current advection of the vein present in Figure 5.6b, the day after.

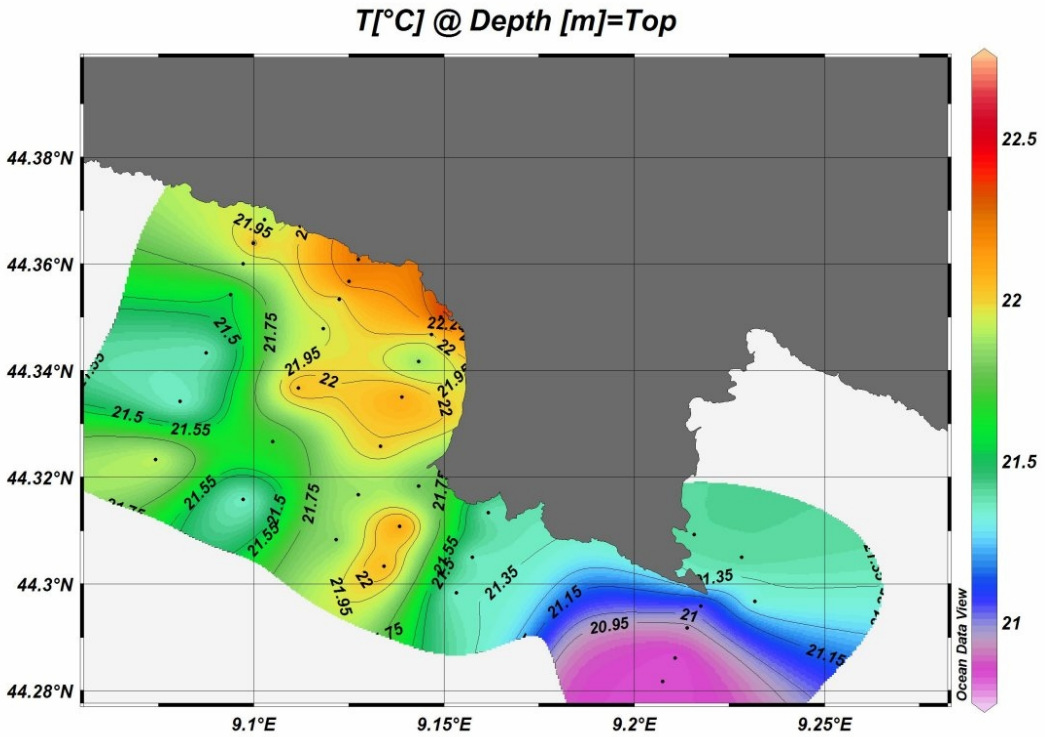

Fig. 5.7 SST skin map retrieved from *in situ* data on the 17/06/2004 (courtesy of Prof. P. Povero and Dr.G. P Gasparini).

Figure 5.8 shows the *chl* (mg m^{-3}) calculated with the algal_1 algorithm of the MERIS_FR imagery on 17 June 2004, highlighting the Ligurian Sea (Fig. 5.8a) and the smaller Portofino MPA (Fig. 5.8b). Clouds are displayed in white, whereas black zones are invalid pixels. The Ligurian Sea area showed patches with high chlorophyll concentration in proximity to the Arno river mouth, reaching values higher than 1.5 mg m^{-3}. The other patches with relatively high chlorophyll values (0.20-0.25 mg m^{-3}) were

located on the north-eastern part of the Ligurian Sea. The Portofino MPA showed relatively high chlorophyll (0.16-0.35 mg m^{-3}) concentrations offshore the western area (Paradise Gulf). The eastern area (Tigullio Gulf) was covered by clouds, but showed lower chlorophyll values offshore, ranging from 0.03 to 0.2 mg m^{-3}.

Figure 5.9 shows the same area as figure 5.8, but with *chl* calculated by means of the algal_2 algorithm. *Chl* on the north-western part of the Ligurian Sea showed higher values between 0.2 and 0.6 mg m^{-3} whereas near to the Arno river mouth the values were comparable with the one retrieved with the algal_1 algorithm (>1.5 mg m^{-3}; Fig. 5.9a).

Portofino MPA (Fig. 5.9b) showed *chl* from 0.05 to 0.24 mg m^{-3} offshore from the western area (Paradise Gulf) whereas for the eastern area (Tigullio Gulf) cloud free values ranged from 0.13 to 0.40 mg m^{-3}. The areas coloured in red show biased chlorophyll values (> 5 mg m^{-3}) due to algorithm errors (Fig. 5.9b). These biases are common across the coast where high concentration of CDOM and suspended sediment could provoke a saturation of the water leaving signal.
Correlation between the *chl* data retrieved from algal_2 (Fig. 5.9b) and the interpolated *in situ* SST map (Fig. 5.7) showed an inverse correspondence. The highest *chl* values were recorded offshore the promontory where lower SST were recorded.

Figure 5.10 shows the interpolated *in situ* map of the surface *chl* registered on the 17th June 2004. While a large part of the investigated area showed an almost negligible chlorophyll concentration, significant values were evident along stations of the westernmost transect. More specifically, figure 5.8b (algal_1 algorithm) indicates higher *chl* concentrations moving eastward the Portofino promontory. Figure 5.9b suggests a different phytoplankton displacement, however the lower concentration seems to be displaced equally (in front of Portofino promontory) to the *in situ* measurements.

Figure 5.11 shows the mean (σ), and the standard deviation (SD) of chl-*a* concentration calculated between 0 and 1 m for each *in situ* station on 17th June 2004.

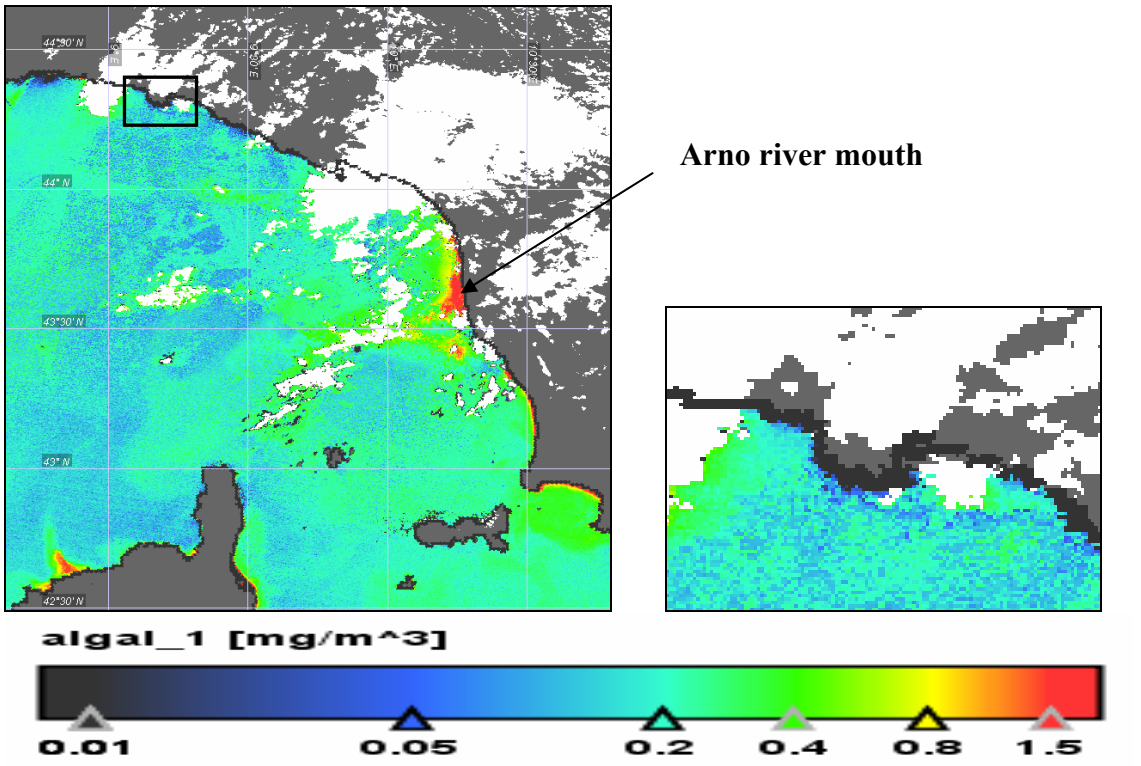

Fig. 5.8 a) Algal_1 Ligurian Sea MERIS_FR 17/06/2004. Fig. 5.8 b) Algal_1 Portofino area MERIS_FR 17/06/2004.

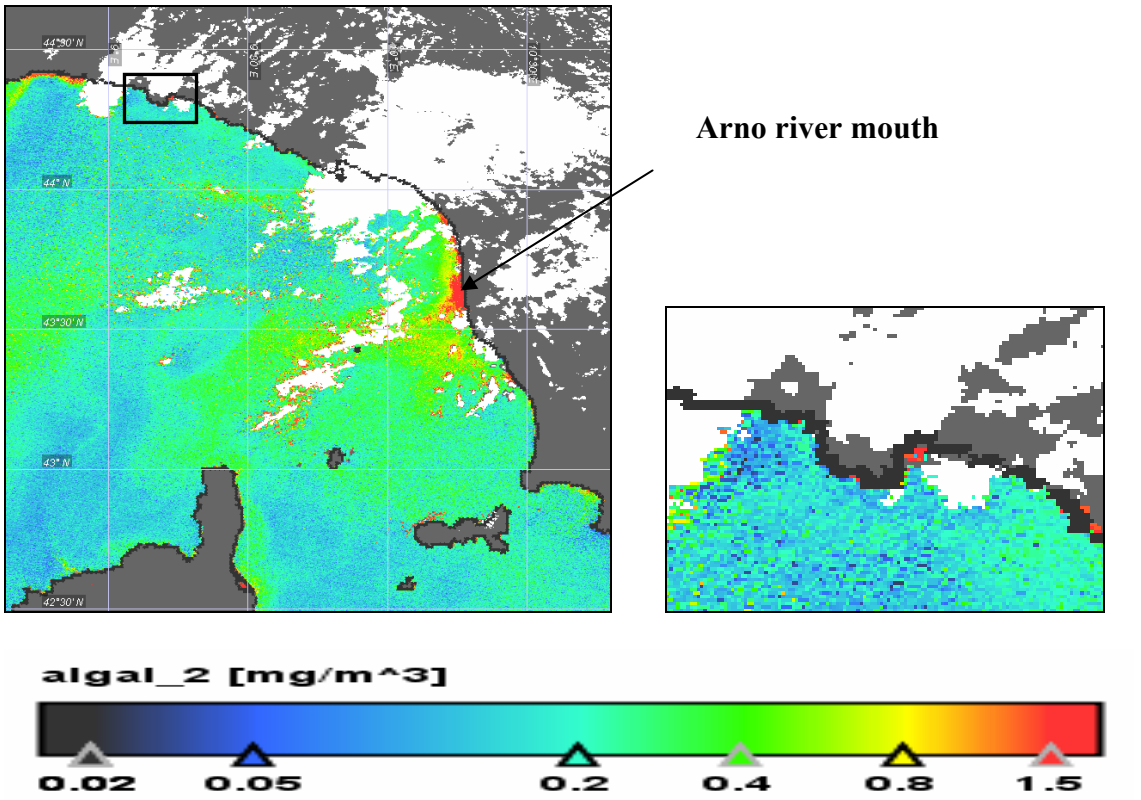

Fig. 5.9 a) Algal_2 Ligurian Sea MERIS_FR 17/06/2004. Fig. 5.9 b) Algal_2 Portofino area MERIS_FR 17/06/2004.

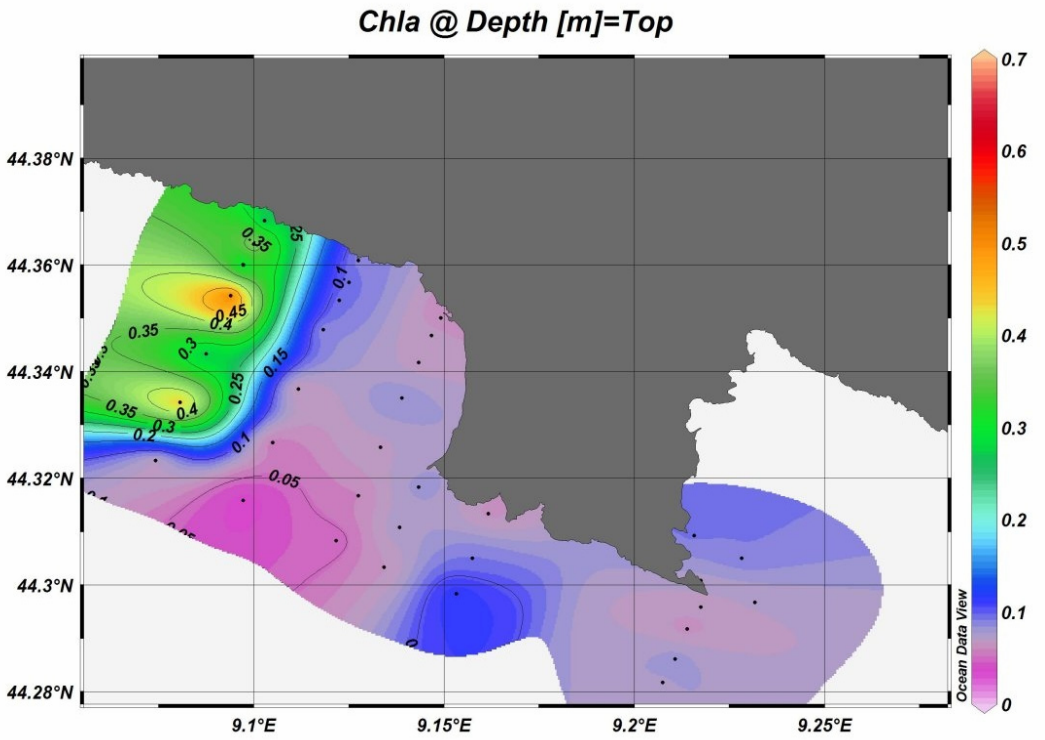

Fig. 5.10 Surface chl -*a* concentration interpolated within the study area on the 17/06/2004 (courtesy of Prof. P. Povero and Dr.G. P Gasparini).

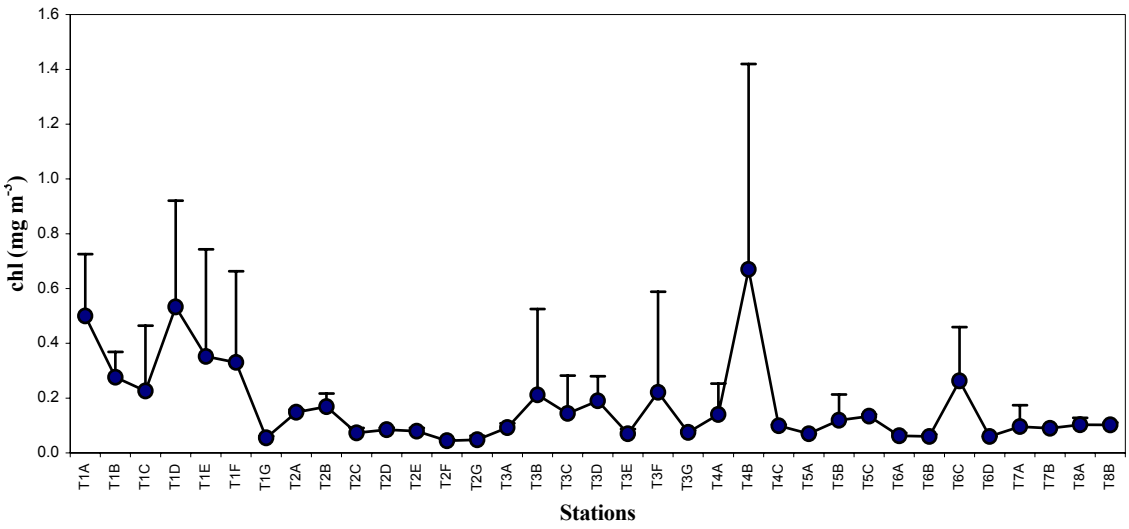

Fig. 5.11 Mean (σ) and standard deviation (DS) of chl *a* (mg m^{-3}) calculated along *in situ* sampling stations (Appendix 23) between 0 and 1 m on 17th June 2004. N=number of records.

Figure 5.12 shows the spatial distribution of the chlorophyll content across Portofino Promontory collected *in situ* (Fig. 5.1b) (averaged between 0 and 1m) on the 17th June 2004. Symbol sizes represent the first (Q1=25th percentile), the second (Q2=median=50th percentile), the third (Q3=75th percentile) quartiles and the minimum and maximum values of *in situ* (Fig. 5.12) data set. The highest values were recorded in the western side of the Promontory (Paradiso Gulf), with a maximum value recorded of 0.67 mg m^{-3}. On the eastern side (Tigulli Gulf) were registered lower values of 0.1 mg m^{-3}.

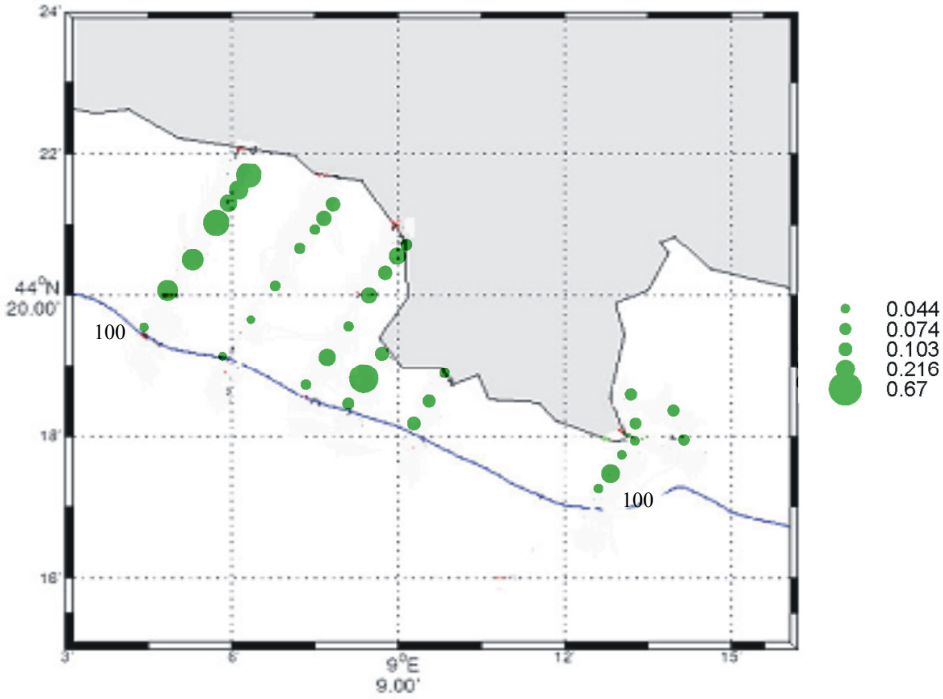

Fig. 5.12 Spatial distribution of mean chl *a* values (mg m^{-3}) (0-1 m) collected on 17th June 2004 in each sampling station (a, b, c, d, e, f and g) on the transects (T) in November 2004. Blue line shows the bathymetry at 100 m. (Fig. 5.1b).

Figure 5.13 shows the linear regression calculated by the comparison between the *chl* values calculated by means of the algal_1 and algal_2 algorithms respectively on the 17th June 2004. The algal_ 1 algorithm showed a lower estimate of *chl* than algal_2. The linear regression model for algal_1 vs algal_2 derived *chl* was statistically significant showing R2=0.58 (p <0.001). The result of an ANOVA test on the linear regression was F(1,33)=45.17.

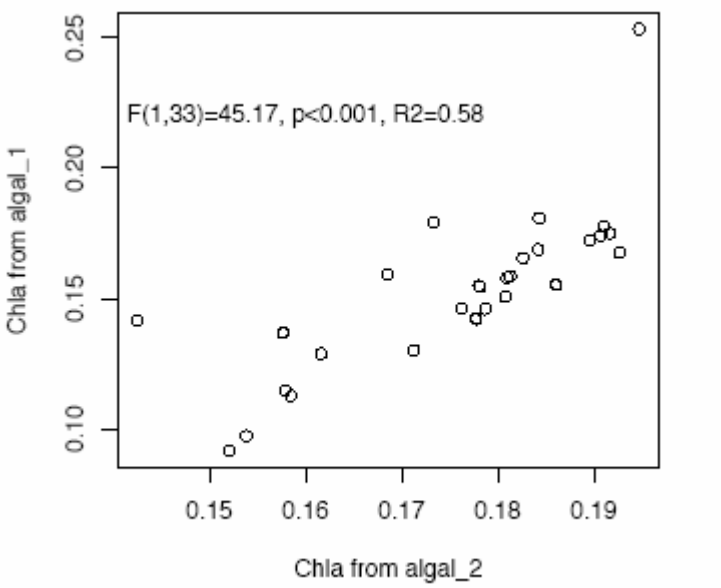

Fig. 5.13 Linear regression performed over algal_2 and algal_1 *chl* derived for the 17th June 2004.

A linear regression calculated for *in situ* chl *a* with algal_1 on 17th June 2004 was not statistically significant (p>0.05) showing R^2 = 0.01. The result of an ANOVA test on linear regression was F(1,33) = 0.43 (Fig. 5.14).

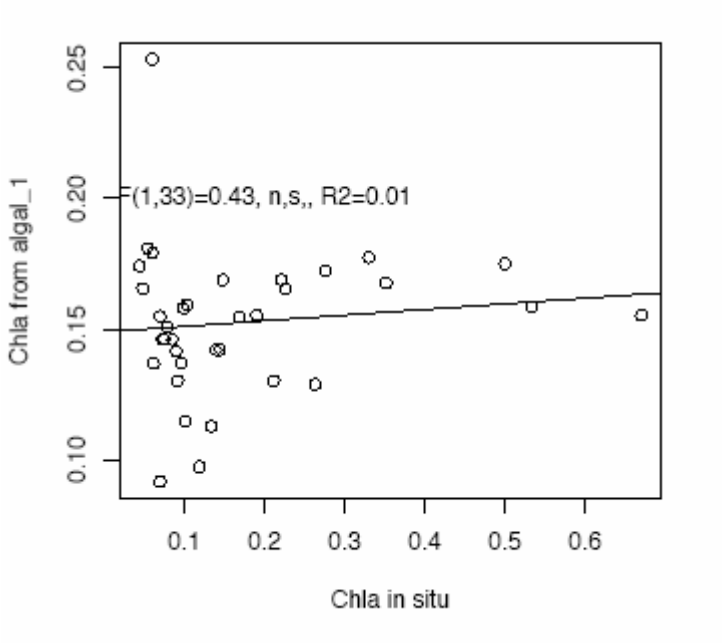

Fig. 5.14 Linear regression performed over chl-*a* collected *in situ* (0-1 m) and algal_1 derived *chl* data for 17th June 2004.

The inter-correlations between in situ *chl-a* and algal_2 for the same date gave significant linear relationship (p = 0.03; R2 = 0.12). The regression statistics gave a slope of 0.03 and an intercept of 0.17. The result of an ANOVA test on linear regression was F(1,33) = 4.86. (Fig. 5.15).

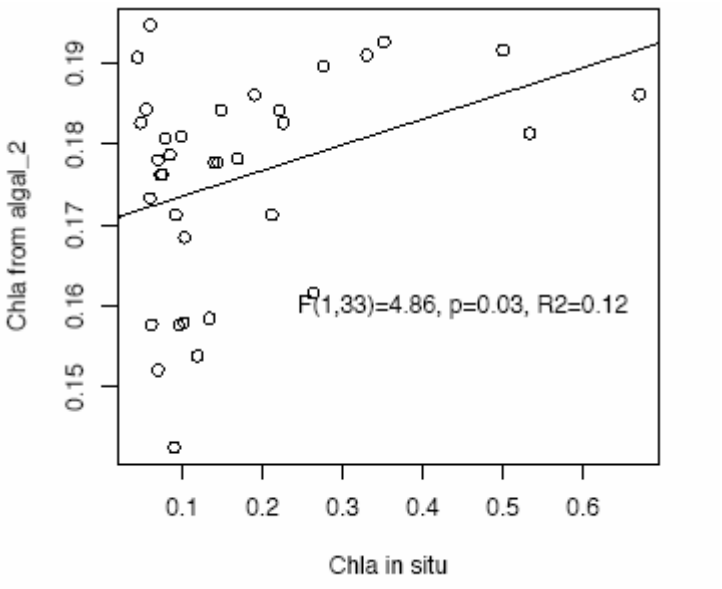

Fig. 5.15 Linear regression performed over chl-*a* collected *in situ* (0-1 m) and algal_2 derived *chl* data for the 17th June 2004.

The above analyses highlighted that algal_1 underestimated *chl* relative to the algal_2 algorithm.

5.3.2 November 2004 observations

The AVHRR SST skin map for the 17th November 2004 (Fig. 5.16) showed that the cold front was located on the north western area of the Ligurian Sea with SST ranging between 16 and 17°C (Fig. 5.16a). In contrast Portofino MPA was surrounded by warmer waters of about 18°C. Tigullio Gulf showed near shore SST values of around 18.2 °C and offshore around 18.7°C whereas Paradiso Gulf showed values between 17.6 and 18.2 °C (Fig. 5.16b).

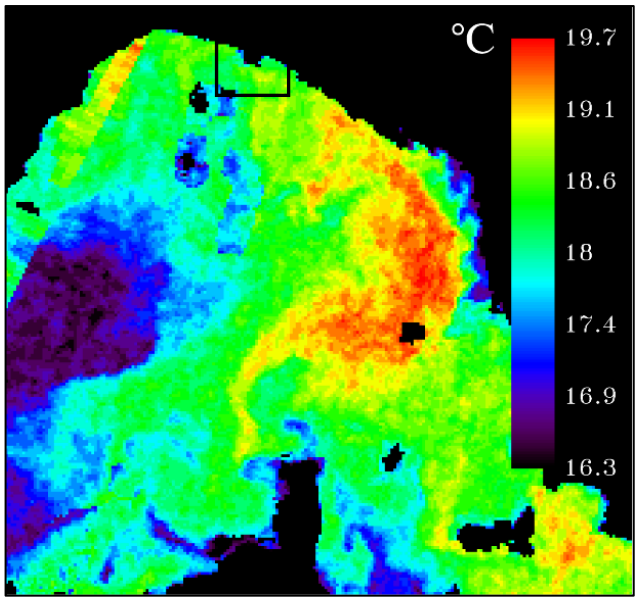

Fig. 5.16 a) AVHRR SST skin on the 17/11/2004.

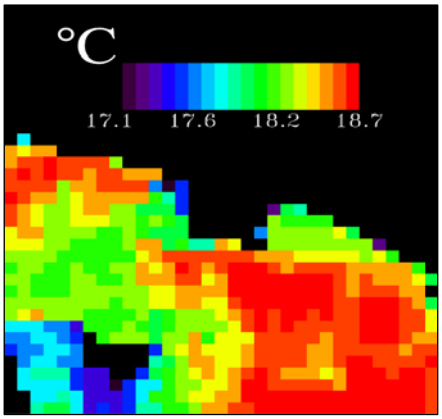

Fig. 5.16 b) Portofino area AVHRR SST skin on the 17/11/2004.

Figure 5.17 shows the surface temperature measured *in situ*. Warmer water is far from the coast, also if the range between the coastal and offshore surficial temperature is very low (0.1-0.2 C). Comparison of *in situ* temperature that shown on the AVHRR map shows correspondingly warmer water far from the coast, although specific details cannot easily compared due to different resolution.

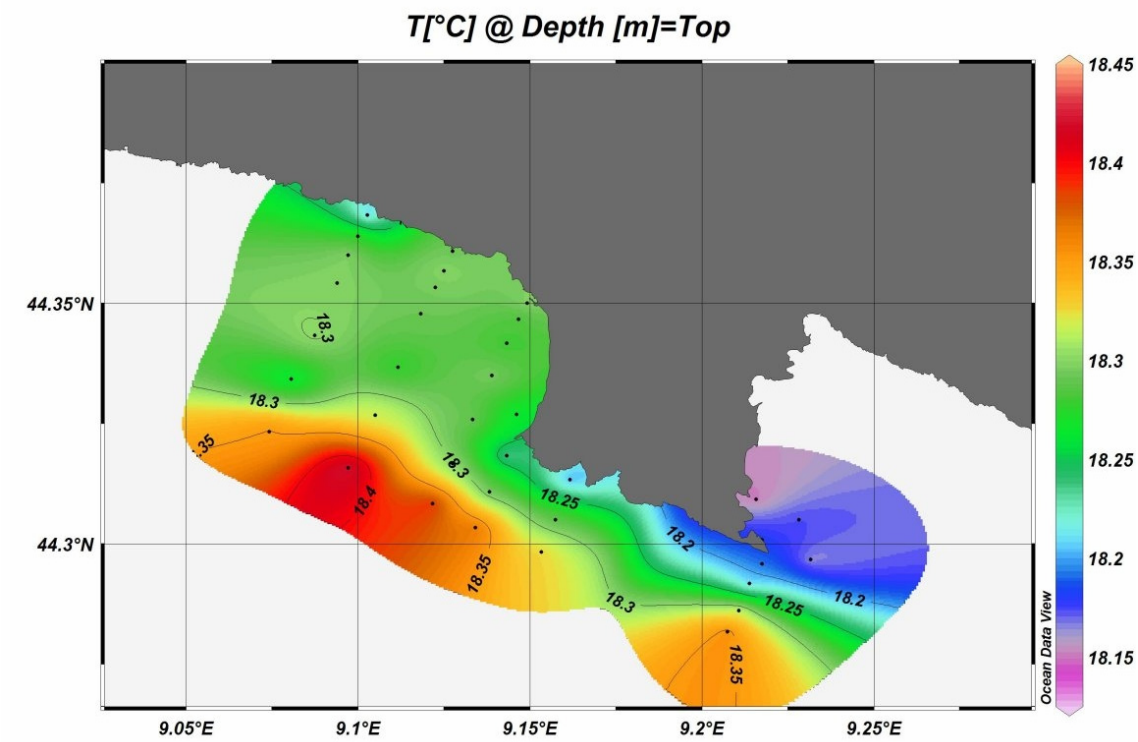

Fig. 5.17 SST skin map retrieved from *in situ* data on the 17/11/2004 (courtesy of Prof. P. Povero and Dr.G. P Gasparini).

Figure 5.18a and 5.19a show the *chl* maps calculated by means of algal_1 algorithm on the 16th MER_FR and 17th November 2004 MER_RR images respectively. *Chl* on the FR image of the16th November 2004 across Paradiso Gulf ranged between 0.35 and 0.55 mg m^{-3}, whereas across Tigullio Gulf *chl* was between 0.65 and 0.85 mg m^{-3} (Fig. 5.18b). In the Arno river mouth *chl* values of 5.0 mg m^{-3} were attained, whereas the north-western part of the Ligurian Sea achieved values between 0.15 and 0.35 mg m^{-3} (Fig. 5.18a).

Figure 5.19 shows the *chl* calculated by the algal_1 algorithm for the 17th November 2004 (RR) imagery. The Ligurian Sea showed the bloom onset with scattered phytoplankton patches (Fig. 5.19a).

The highest *chl* values were recorded in Paradise gulf (between 0.80 and 1.3 mg m^{-3}) and Tigullio gulf (between 0.95 and 1.7 mg m^{-3}) (Fig. 5.19b). Offshore from Tigullio Gulf the *chl* values lowered to 0.65-0.95 mg m^{-3} (Fig.5.19b). Regarding the north-western part of the Ligurian Sea, the *chl* values increased up to the range of 0.27-0.35 mg m^{-3}. This phenomenon could be caused by the autumnal algal bloom peak (Fig. 5.19a). The marine waters in front of the Arno mouth attained *chl* around 5 mg m^{-3}.

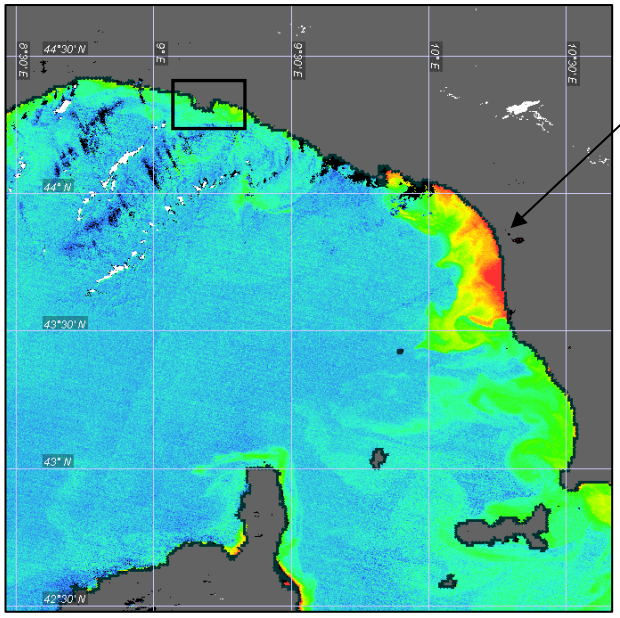

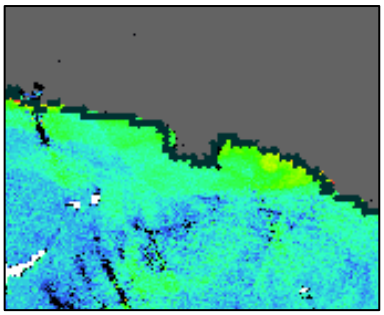

Fig.5.18 a) MERIS FR 16/11/2004.

Fig. 5.18 b) Portofino area MERIS FR 16/11/2004.

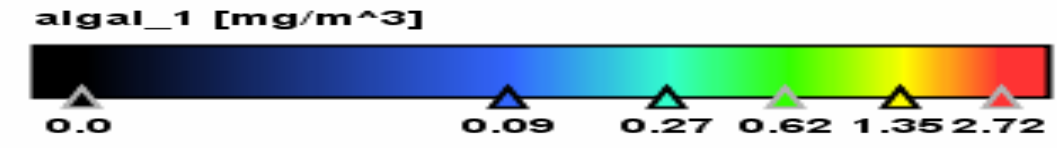

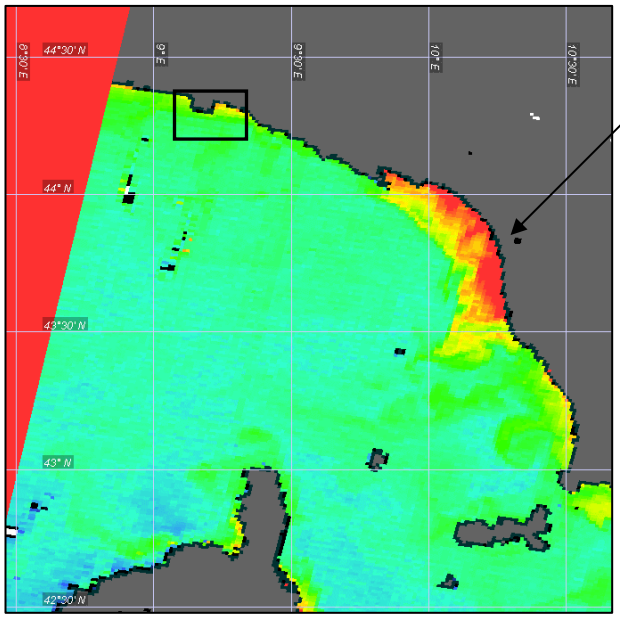

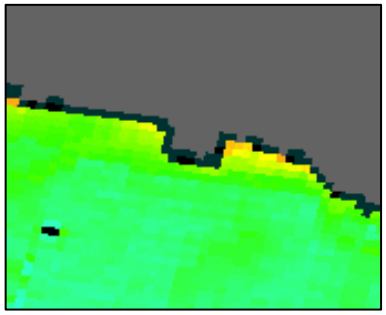

Fig. 5.19 a) MERIS RR 17/11/2004.

Fig. 5.19 b) Portofino area MERIS RR 17/11/2004.

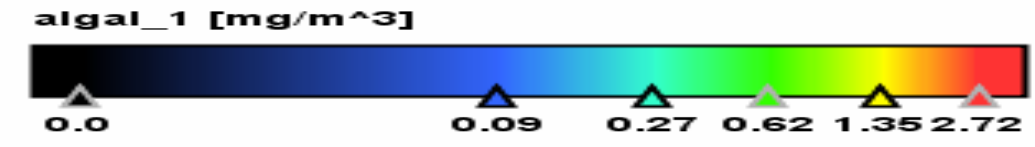

It is possible to note the inverse correspondence between satellite SST features (Fig. 5.16b) and satellite *chl* features (Fig. 5.19b) across the coast in the Portofino region images particularly within Tigullio Gulf meaning that higher *chl* are found with lower SST values.

The interpolated map of the surface *chl -a* retrieved *in situ* (Fig. 5.20) gives evidence of higher values, especially in the Paradiso Gulf (0.40-0.45 mg m^{-3}). The high spatial variability of *in situ chl* levels, however, makes comparison with satellite data difficult. Both distributions seems to align in terms of the higher coastal concentrations of *chl*.

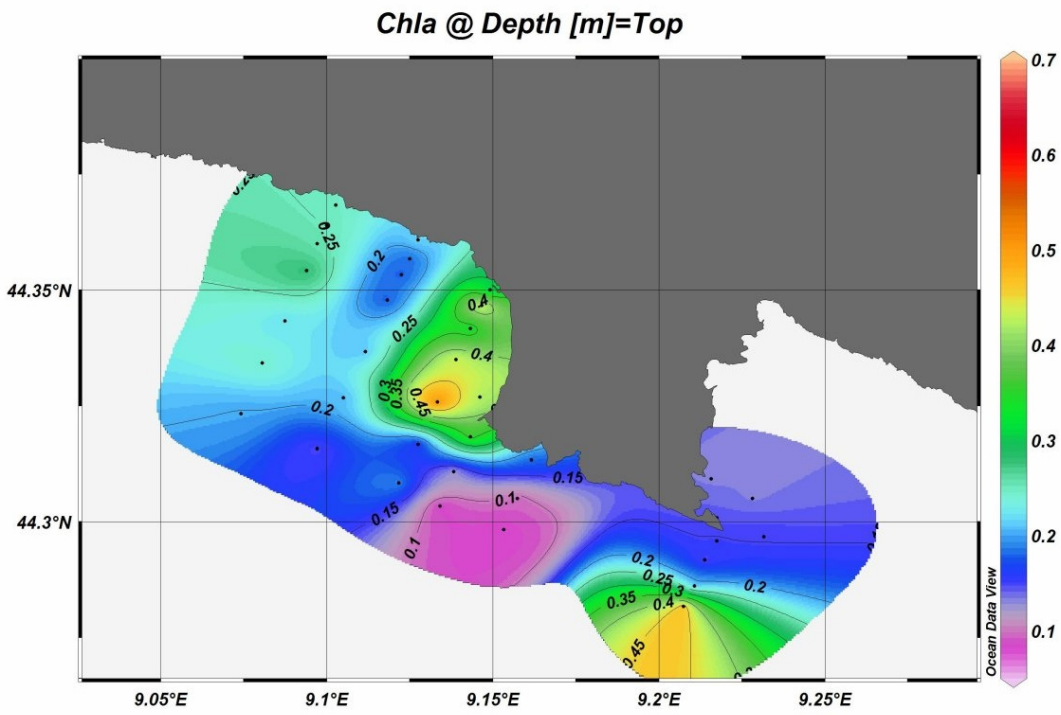

Fig. 5.20 Surface chl *-a* concentration interpolated from *in situ* surveys within the study area on the 17/11/2004 (courtesy of Prof. P. Povero and Dr.G. P Gasparini).

Figure 5.21 shows the mean (σ) and standard deviation (SD) of the chl-*a* concentrations calculated between 0 and -1 m for each sampling station on the 17/11/2004.

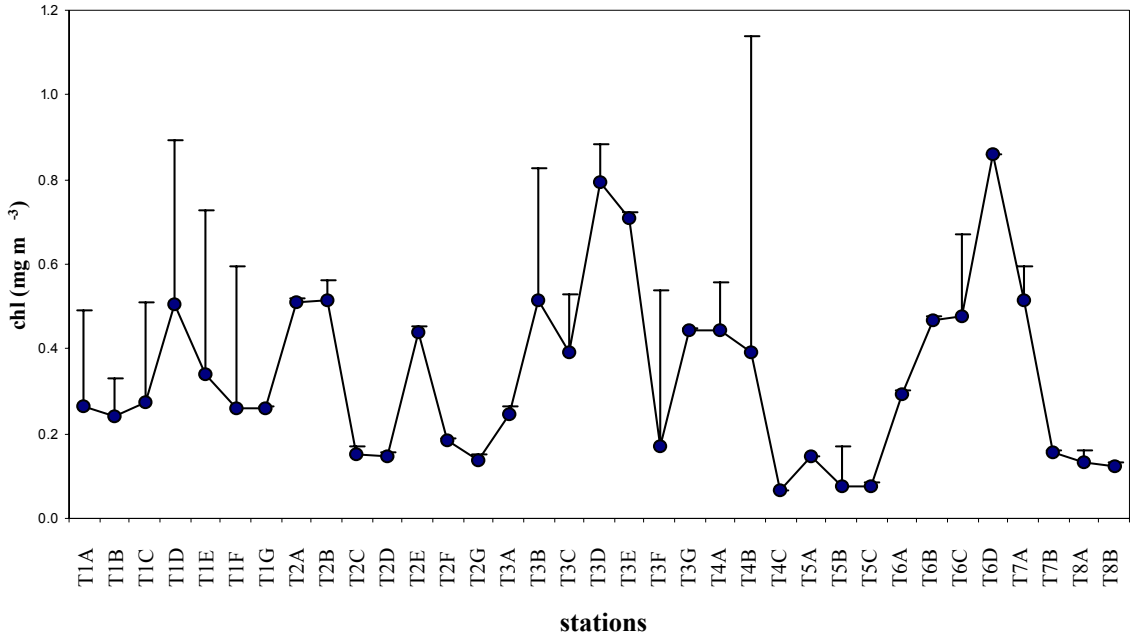

Fig. 5.21 Mean (σ) and standard deviation (DS) of *chl a (*mg m^{-3}) concentrations *in situ* sampling stations (Appendix 23) between 0 and 1m on 17th November 2004.

In tables 5.1 and 5.2 the stations used for the comparison between the *in situ* chl-*a* and MERIS algal_1 and algal_2 data for the 16th and 17th November respectively are presented. The few points considered for the 17th November are due to the reduced spatial resolution of the available image.

Table 5.1 Sampling stations (a, b, c, d, e, f and g; Fig. 5.1b) considered for statistical analysis between *in situ* chl -*a* (Appendix 23) on 17th November 2004 at 0m and satellite *chl* estimates retrieved by algal_1 and algal_2 MER_FR image on 16th November 2004. (T=transect).

MER_FR 16/11/2004	a	b	c	d	e	f	g
T1	X	X	X	X	X	X	X
T2	X	X	X	X	X	X	X
T3	X	X	X	X	X	X	X
T4	X	X	X				
T5	X	X	X				
T6	X	X	X	X			
T7	X	X					
T8	X	X					

Table 5.2 Sampling stations (a, b, c, d, e, f and g; Fig. 5.1b) considered for statistical analysis between *in situ* chl -*a* (Appendix 23) on 17th November 2004 at 0m and satellite *chl* estimates retrieved by algal_1 and algal_2 MER_RR image on 17th November 2004.

MER_RR 17/11/2004	a	b	c	d	e	f	g
T1					X		X
T2							
T3						X	X
T4							
T5			X				
T6		X		X			
T7							
T8							

Figure 5.22 shows the linear regression calculated by the comparison between the algal_1 algorithm applied to MERIS data (MER_RR) collected on the 17th November 2004 and the *in situ* data collected on the same date averaged between 0 and -1 m (Fig. 5.21). The regression statistics show a slope of 0.26 and an intercept of 0.74. The ANOVA test on linear regression was F(1,5)=4.40. The model shows R^2=0.46, but it did not achieve statistical significance (p=0.08).

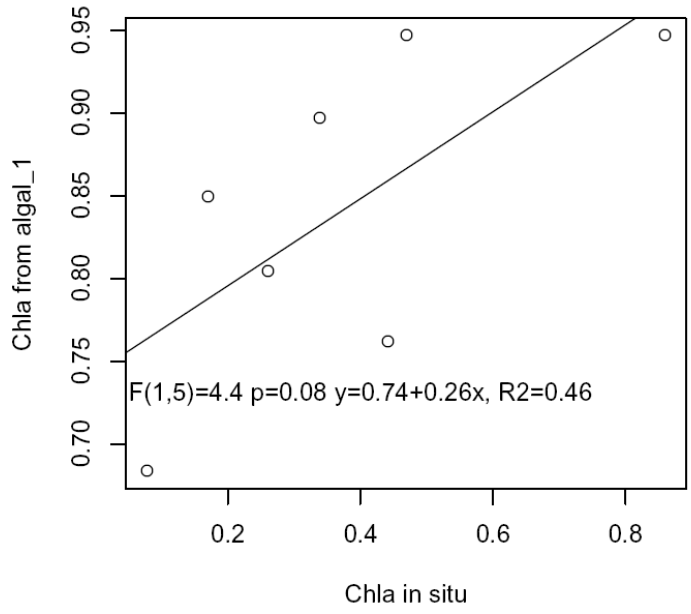

Fig. 5.22 Linear regression performed over chl -*a* collected *in situ* (0-1 m) on the 17th November 2004 and algal_1 *chl* collected for the 17th November 2004.

Figure 5.23 illustrates the linear regression calculated over the *in situ* data collected on the 17th November 2004 and the algal_2 algorithm applied on the matrix extrapolated from MERIS_RR collected on the same date were not significant, showing a R^2=0.27 (p=0.24). The ANOVA on regression was F(1,5)=1.82, not significant.

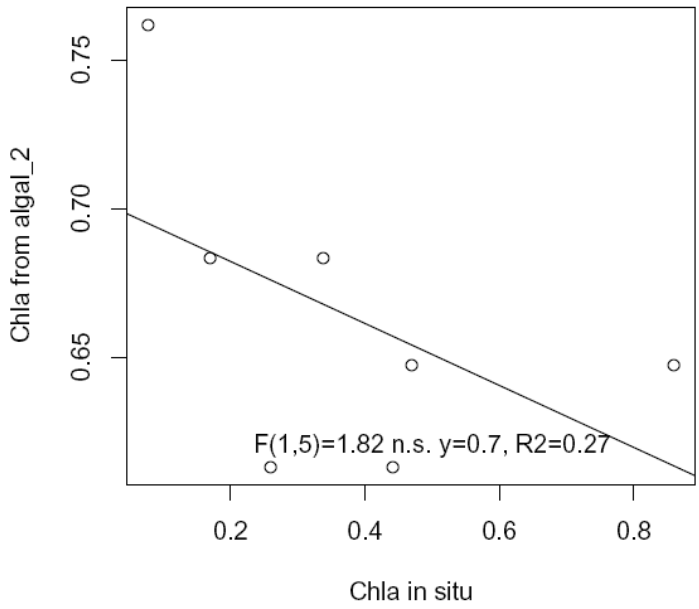

Fig. 5.23 Linear regression performed over chl -*a* collected *in situ* (0-1 m) on the 17th November 2004 and algal_2 *chl* collected on the 17th November 2004.

Figure 5.24 shows the linear regression calculated by the comparison between the algal_1 algorithm applied on MERIS data (MER_FR) collected on the 16th November 2004 and the *in situ* data of the 17th November 2004 averaged between 0 and 1 m (Fig. 5.21). The regression statistics report a slope of 0.32 and an intercept of 0.83. The ANOVA on regression was F(1,33)=6.79. The model was significant (p=0.01; R^2=0.17).

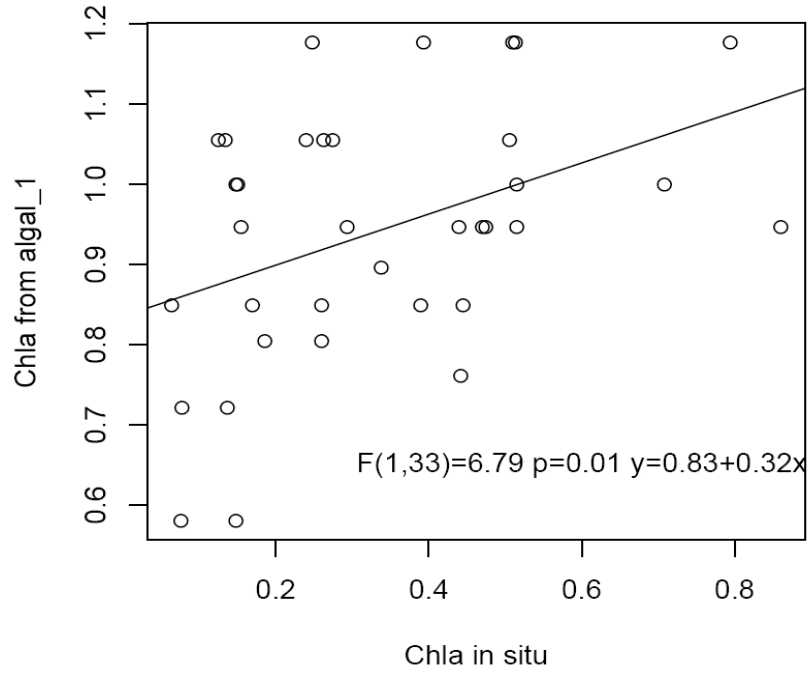

Fig. 5.24 Linear regression performed over chl -*a* collected *in situ* (0-1 m) on the 17th November 2004 and algal_1 *chl* on the 16th November 2004.

Figure 5.25 illustrates the linear regression estimated by the comparison between *in situ* (0-1 m) and the algal_2 algorithm applied on MERIS image (MER_FR) collected on the 16th November 2004. The ANOVA on regression was F(1,33)=0.96. In this case the linear model was not statistically significant (p>0.05).

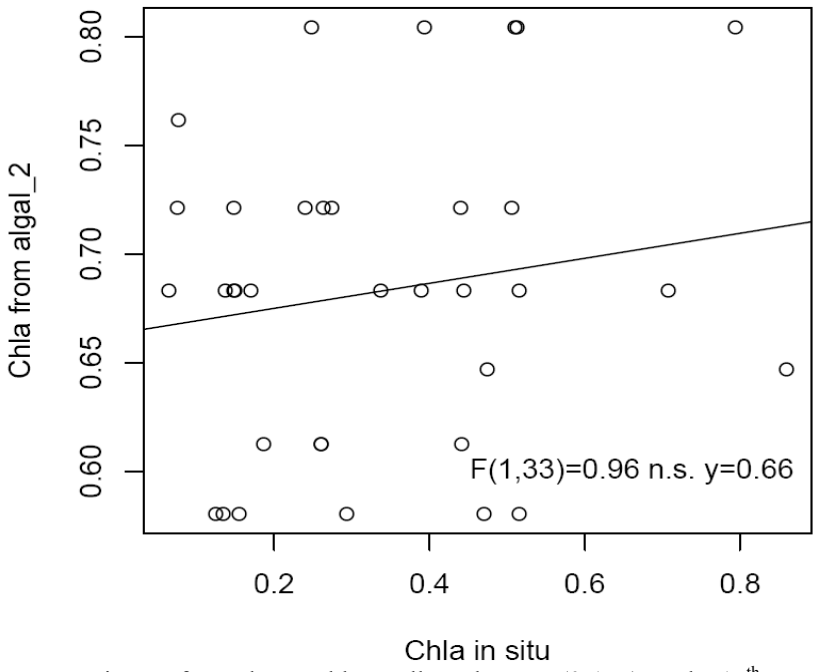

Fig. 5.25 Linear regression performed over chl -*a* collected *in situ* (0-1 m) on the 17th November 2004 and algal_2 *chl* for the 16th November 2004.

5.4 DISCUSSION

This analysis conducted on data sets coming from *in situ* and remote-sensing data it is suitable to evaluate the reliability of satellite sensors for coastal zone monitoring and to better understand the short-term environmental dynamics on the coastal area centred on Portofino MPA.

Only the chl *in situ* data collected between 0 and 1m were utilised in order to be compared to the satellite derived *chl*. These data were extremely useful in order to validate the MERIS algorithms in the Portofino MPA waters. The data presented considered two satellite daily images relatively to summer and autumn. This study demonstrated the value of medium spatial resolution ocean colour sensors in characterising the water type of an MPA.

Statistical comparisons performed could be considered audacious, however *in situ* samplings were carried out in a extremely narrow area. Being the transects of the *in situ* samplings located very close to the shore (until the bathymetry of 100m), it was almost impossible establishing which sub areas of the Portofino MPA were case 1 or case 2 waters and which of these areas were better modelled by MERIS agal_1 or algal_2 algorithms.

AVHRR sensor supplied accurate SST skin data at good resolution, whilst the estimate of satellite derived *chl* by means of the above algorithms was subject to a range of problems.

5.4.1. June 2004 observations

AVHRR SST skin map collected on the 18 June 2004 agreed partially with the *in situ* sampling campaign carried out on the 17 June 2004. *In situ* campaigns pointed out a substantial difference between water masses located on the western area (Paradiso Gulf) of the Portofino Promontory and those exposed to the open sea. According to Locritani *et al*. (2008), the western area of the Portofino Promontory (Paradiso Gulf) is less

affected by the Ligurian cyclonic circulation, whereas the area between Punta Faro a Punta Chiappa (Fig. 5.1b) is interested by the cyclonic current. Hydrologic characterisation of the water masses showed higher SST values on the north-western area of the Portofino Promontory (Paradiso Gulf) with respect to the lower values recorded on the south-east of the Promontory (between Punta Faro a Punta Chiappa). This difference was not clearly recorded by the AVHRR image analysed. This could be explained by the fact that there is a day shift with respect to the *in situ* sampling campaign. However, the highest SST values were recorded within Tigullio Gulf. Unfortunately, these data could have not been compared with the *in situ* data due to the lacking of *in situ* sampling stations within the Tigullio Gulf.

The analysis of the MERIS image for the 17th June 2004 highlighted that algal_1 underestimated the *chl* giving also a different spatial patterns relative to the results obtained using the algal_2 algorithm. Although the available *in situ* data covered a very reduced area, mainly across the coast, it was possible to find a good agreement with *chl* derived from satellite observations.
Given that the sampling stations few, it would have made no sense removing data points (i.e. outliers) in order to get a better fit of the linear regressions for *in situ vs.* satellite derived *chl*. Also removing the outliers, linear regression would have not changed significantly.

Linear regression analyses conducted over *in situ* data (0-1 m) on the 17th June and algal_2 was significant thus evidencing a better fit of this algorithm with this *in situ* data, in particular showing similar *chl* located offshore the Portofino Promontory.

The fact that Algal_2 seemed to estimate better *chl* depends on the weakening of the general circulation occurring in summer. June is usually a calm period where stratification of the water column starts to occur (Jacques, 1994). In this period it is possible to assume that algal_2 waters are predominant in the study area and that the currents weakening do not introduce offshore waters in the Portofino MPA. Indeed also the Entella river run off (on the eastern side of the Portofino Promontory) it is not counterbalanced by the cyclonic gyre and it is possibly causing an increase of terrigenous and littoral zone CDOM and suspended sediment. The anthropogenic inputs

by river run off are also enhanced by the increasing of the population due to summer tourism.

5.4.2 November 2004 observations

For this period two chlorophyll satellite maps were considered: one coincident with the *in situ* campaign and the other retrieved one day in advance.

The MERIS image collected on the 17th November showed on the western area of the Ligurian Sea the start of the autumnal phytoplankton bloom. High satellite derived *chl* values recorded in both days analysed in proximity of the Arno river could be due not only to the phytoplankton occurrence, but also to the anthropogenic inputs by river run off. These high values could be caused by the high levels of nutrients present in the river waters that provoked a high concentration of CDOM and suspended sediment.

Both algorithms on the 17th November 2004 showed higher *chl* than those collected *in situ*. These observations could be explained by the autumnal algal bloom visible offshore from the Portofino promontory, which caused an increasing coastal *chl*. This bloom was overestimated by algal_1 algorithm, whereas the algal_2 located correctly the highest values within the western portion of the Promontory Paradiso Gulf. Neither of the linear regression analyses conducted over *in situ* data (0-1 m) on the 17th November with algal_1 (p = 0.08) and algal_2 (n.s.) images collected on the same date were statistically significant. Moreover, the linear regression between *in situ* chl and algal_2 algorithm was negative. The model showed that R^2 was higher for the algal_1 algorithm, thus indicating a linear dependency with *in situ* chl -*a* and a better fit of this algorithm with the *in situ* measurements. However, it should be taken into account that the number of points considered for the above linear regression were few due to the reduced spatial resolution of the image analysed (MER_RR), for algal_2 data two further observations onshore were biased. Also for this reason, algal_2 observations did not show a linear relationship with *in situ* chlorophyll data.

The algal_1 observations retrieved the 16th November showed values comparable with those collected *in situ* the day after, particularly within Paradiso Gulf, whereas algal_2 overestimated *chl* across both gulfs. Results demonstrated that there was little evidence of day to day *chl* shifts so this approach should be considered valid. This was further on confirmed by the inter-comparison between *in situ* chlorophyll and algal_1 for 16 November 2004 which gave significant results.

In the days considered, the mesoscale (100s of km) dynamic structures within the Ligurian basin, showed by the *chl* maps, were similar to the microscale (10s of km) features in the Portofino area. Moreover, the fact that, in November, case algal_1 performed better than algal_2 algorithm could be explained by the presence across the study area of almost offshore waters due to the narrow continental shelf which characterises this stretch of coast. The Ligurian cyclonic current in this period of the year seem to introduce pelagic waters across Portofino Promontory. Indeed, the gyre is always present throughout the year, however, it shows a seasonal cycle being its extension and intensity related to the seasonal variations of the atmospheric forcing (Esposito and Manzella, 1982). It is possible to hypothesise that in autumn the cyclonic current is stronger. Further more, it should be also considered that during autumn the stratification is broken up by the changing of meteorological conditions of early autumn when the currents are stronger due to the northern winds. In fact *Grecale* (NE) and *Maestrale* (NW) winds are dominant in this period, leading to sea storms and water remixing (Morri *et al*., 1986). The stratification weakening was also confirmed by the *in situ* depth profiles of the water temperature at the sampling stations which ranged from 16 to 18 °C.

The inverse correlation found between satellite derived *chl* and satellite SST features showed that phytoplankton biomass and growth generally decline as the surface waters warm up. Phytoplankton biomass inversely responds to surface temperature and stratification (Behrenfeld *et al*, 2006).

The inverse correlation between SST and *chl* could be likely indicative of the presence of upwelling onshore, where colder subsurface water comes to the surface with nutrients that foster phytoplankton growth. This upwelling could be due to the Ligurian cyclonic

gyre with a resulting coastal circulation in the north-western direction across the Ligurian coasts (Doglioli, *et al.*, 2004).

5.5 CONCLUSIONS

The present study is a preliminary test to approach different methodologies which could lead to an increase in the use of satellite sensors to the continuous monitoring of coastal protected areas. In fact the use of remote sensed imagery in addition to the instruments already used in the study area, was particularly useful in order to obtain more information on the main biological and physical phenomena which persist within the Portofino MPA.

The study conducted within the Portofino MPA has highlighted the need of an integrated monitoring and analysis system of the main environmental variables so as to understand the processes which take place across the coastal zone, often characterized by high variability and deeply influenced by large scale phenomena.

Portofino MPA is characterised by a strong interannual variability with strong thermal anomalies recorded particularly in summer and by an increasing of the mean sea temperature over the entire water column registered during the last years. These phenomena have caused an increasing of SST during spring and autumn with an extension of the hot season (Castellano *et al*., 2008). SST skin maps retrieved by thermal sensor (AVHRR) are therefore particularly useful to monitor these regional scale phenomena and also to identify thermal anomalies. Moreover, for the dates analysed, SST skin observations showed an inverse relationship with satellite derived *chl*, thus indicating that SST data may strongly contribute to monitoring and further predicting phytoplankton bloom in the Portofino MPA.

In this study both MERIS_RR and MERIS_FR imagery retrieved by MERIS sensor were utilised. Reduced resolution (RR) at 1.1 km is particularly useful in characterising the Ligurian basin at a regional scale. However the spatial full resolution at 300 m (FR) resulted the most useful at local scale in order to investigate the study area with a finer

detail and to compare *in situ* sampling campaigns to satellite imagery. This is explainable with the small spatial extension of the study area considered. The two algorithms products supplied (algal_1 and algal_2) were particularly useful in order to study the typology of waters in the Portofino MPA.

Portofino test site responded differently to the two algorithms utilised. As it is highlighted in § 5.3 the stretch of coast responded in a non univocal mode to the use of algal_1 and algal_2 algorithms. The waters surrounding Portofino Promontory seem to be influenced by the regional oceanographic conditions which establish seasonally.

The above analyses have demonstrated that the outcomes of assessment are variable, *chl* derived from MERIS sensor is subject to various problems. The relationship between satellite data and *in situ* observations was not always reliable and consistent. "Sea truthing" infers that the *in situ* measurements supply better reliability than RS observations although with obvious problems of temporal and spatial coverage. This was partially true for Portofino MPA. First because the *in situ* maps shown, were interpolated maps and the outcomes of *chl* spatial distribution are subject to the interpolation model used. Secondly because some sub-areas of the Portofino MPA were not sampled (i.e. Tigullio Gulf). Conversely, MERIS sensor is an invaluable tool capable of synoptically encapsulating at fine spatial scale the oceanographic processes occurring locally in the MPAs waters and regionally with the Ligurian basin. However, the MERIS algorithms were not working always properly for the coastal area of interest, being these algorithms so far tested within the Mediterranean basin mainly offshore the Mediterranean French coast (Antoine *et al*., 2008). It should also be taken into account that the atmospheric correction algorithms applied to MERIS observations for the Mediterranean Sea are being implemented nowadays. These will be taking into consideration the particular atmospheric condition of the Mediterranean Sea such as the Saharan dust which affect the retrieval of the water leaving radiance signal (L_w) by the sensor particularly in oligotrophic waters. In fact as stated by Marullo *et al*. (2004) the MERIS algorithms error is not correlated with the measured *chl*. MERIS algorithms tend to overestimate *chl* mainly due to the particular optical components of the Mediterranean Sea which can alter its colour causing an absorption in the blue and an enhanced backscattering in the green part of the electromagnetic spectrum.

The results obtained so far offered a clue for further investigations which should be conducted in the study site throughout the year. Although *chl* derived from MERIS was subject to the problems highlighted above, MERIS images allowed to confirm that the Portofino MPA waters are oligotrophic, with low *chl* and consequently low phytoplankton biomass in the surface layer. According to Castellano *et al*. (2008), during the last years there was a decreasing trend of the chlorophyll content across the Portofino Promontory which could have a remarkable effect on the zooplanktonic populations.

The *in situ* measurements were particularly important in order to classify the Portofino waters. As already highlighted in §1.7, RS supplies information about the sea surface but much less about the water column characteristics. Therefore, it is crucial that the new *in situ* sampling campaigns be carried out seasonally and over long term in order to characterise the MPA waters also during winter and spring. Moreover, *in situ* measurements should be made with particular attention at surficial waters such that observations can be correlated to the RS observations in order to enhance the validation of the MERIS algorithms for Portofino MPA. More transects should be added to the sampling design of *in situ* campaign carried out in 2004. In particular it should be inserted at least three transects within the Tigullio Gulf where they were lacking. These transects should be perpendicular to the coast, located near the Entella river, with at least four sampling stations. This sampling design will allow to study at finer detail the influence of Entella river on the MPA water characteristics. It should be investigated the typology of the waters flowing within the two gulfs of the Portofino Promontory. Indeed, the waters in the south-western (Paradiso gulf) Portofino area may fall within case 1 waters, whereas waters in the eastern side, influenced by the Entella river which flows into Tigullio Gulf, may belong to case 2 waters. The area covered by the transects should be increased up to 75 km^2 from a depth of 5m to 100m. The above recommendations as to how *in situ* samplings should be designed, will contribute to an enhanced monitoring of the Portofino MPA.

The experience acquired so far, could lead to hypothesise that in the next years the coupling of data collected *in situ* by means of profilers and those supplied by satellites could allow to conceive a national system to the monitoring of the dynamics of the main environmental variables in the coastal Italian MPAs.

CHAPTER 6

DISCUSSION

6.1 REMOTE SENSING APPLICATIONS TO MARINE PROTECTED AREAS

This thesis has focused on the applications of satellite data to the monitoring and future management of vulnerable ecosystems and that are rich in biodiversity. MPAs should preserve ecosystem attributes such as health, vigour and resilience. However, these attributes are difficult to quantify. Management should be ecosystem-based and the ecosystem integrity should be maintained. This aim can be achieved by the development of a suite of ecological indicators whose properties can be both quantifiable and measurable rapidly at scales compatible with the processes under study. Satellite RS is a highly appropriate tool to detect the above mentioned ecological indicators. The benefits of RS lie in the synoptic, and repeatable quantitative datasets which encompass global, regional and local scales (Richardson and LeDrew, 2006). Last but not least, RS meets the requirements of repeated frequency and cost-effectiveness, at least for the scientific community.

The aims of this study i.e. whether we can better observe MPAs in order to enhance their management and protection regime and whether RS can be successful in monitoring and management MPAs, were mostly achieved. In this thesis a new approach to the use of RS as a monitoring tool for MPAs was developed. RS, to date has been mainly used to monitor synoptically the open oceans. However, MPAs could benefit enormously from the analysis of satellite imagery, including MPAs in both coastal and open seas areas. So far, interdisciplinary studies carried out in MPAs have mostly foreseen the use of biological and chemical techniques to study the biodiversity in a MPA to the identification and mapping of the benthic biocoenoses. However, those studies rarely included the study of the dynamics of the ecosystem as a whole. The biodiversity richness present in a MPA is constantly sustained by the dynamics of the bio-physical processes which persist within the basin where the MPA is located. In order to identify the bio-physical processes and characterise the MPA within the framework of a biological oceanographic perspective, RS proved to be a key tool, in

particular, in serving the process of monitoring. The monitoring process conducted by means of different approaches permits biogeographic characterisation of the MPAs investigated and formulation of suggestions for their management.

Temporal and spatial dynamics are extremely important for remote sensing when applied to MPAs, due to the inverse relationship between the spatial and temporal resolution that can be achieved using RS techniques. The problem of scale becomes crucial when observing the physical and biological phenomena of marine ecosystems; the spatial and temporal scales of the sensors utilised should, ideally, match those of the phenomena investigated (Robinson, 2004).

In this thesis the above problem has been considered in particular by examining whether the spatial and time scales of the phenomena under investigation were sampled adequately by the remote sensors used. Coastal water algal bloom occurring in a MPA, for example, have a variability in time ranging from 6 hours to 2 days and a time span from 1 to 3months. The spatial extent of an phytoplankton bloom could cover an area ranging from 200 to 1000 km (Robinson, 2004). Satellite sensors are capable of observing oceanographic processes from the basin scale (100s km) down to the microscale (10s km). Medium-resolution sensors with spatial resolution of 1 km and sampled every day are adequate for the mesoscale and microscale ranges (Robinson, 2004). The medium-resolution satellite sensors used have a synoptic coverage capable of encompassing the time and spatial scale of the biological process of interest such as a phytoplankton bloom, and to follow its growth and decay. However, medium-resolution sensors do not adequately resolve properly the pica-scale (<10 km), the short term events, or processes operating at hourly time scale such as those occurring in coastal areas; higher spatial and temporal resolution than that requested for the open ocean are required (IOCCG, 2000).

According to Brown *et al*. (2005), the coastal environment presents some shortcomings for the use of ocean colour data due to the low frequency of these data, which could be inadequate for monitoring this highly variable environment and its the bio-optical complexity in coastal waters. The retrieval of geophysical parameters in coastal waters could be extremely complex and tortuous due to the fact that coastal waters are so-called Case 2 waters (i.e. optically-complex) which are influenced by phytoplankton,

yellow substances and suspended particulate material other than phytoplankton, all of which vary independently from each other. With the advent of the ocean colour sensors at higher spectral resolution in the visible, algorithms for Case 2 waters have been improved in the recent years (IOCCG, 2000) due to the application of new mathematical and statistical procedures (Doerffer *et al*., 2002) and also to the improved atmospheric corrections. These developments have led to new products derived from ocean colour data such as concentrations of yellow substances and suspended sediments. The refinement of Case-2 algorithms has widened the applications of ocean-colour data to the coastal zone monitoring and management. However, the development of Case-2 water algorithms that work in specific eco-regions is still unresolved (IOCCG, 2000).

Physical-biological phenomena occurring along relatively small coastal MPAs could not be adequately sampled from sensors with a spatial resolution of 1 km. However, medium-resolution satellite observations offer, at present, the unique and robust mean to obtain a synoptic and spatially detailed overview of the MPAs.

This thesis has proposed a novel application of satellite passive sensors to the investigation of the MPA's functioning. The innovative application of satellite products lies in the partitioning of the main basin into ecological sub-basins (provinces) where the MPAs are located, thus encapsulating the MPA in a basin perspective. The concept of ecological provinces was developed by Longhurst (2007) and has proved extremely useful in the context of MPAs. According to Devred *et al*. (2007) remote sensing is now being used to map the boundaries of the ecological provinces. Ecosystem-based management cannot disregard the definition and the extent of the ecological provinces. The successful use of RS in monitoring the sub-basin where the MPA is located, or namely the biogeochemical province context, should lead to the substantial integration of RS techniques into the management of MPAs , thereby enhancing their protection regime.

Ocean colour and thermal infrared products (i.e. chlorophyll and SST skin maps) reveal a wealth of information about phytoplankton distribution and thermal variations of surface waters in MPAs. These can be used for advancement of knowledge on the bio-physical phenomena occurring in a MPA. These bio-physical processes are key

environmental indicators and confirm the ability of EO sensors to address also the local scale, giving an accurate insight to the MPA functioning.

The satellite sensors that have been chosen in this thesis were medium-resolution sensors with almost daily sampling depending on cloud coverage. Clouds seriously affect the electromagnetic radiation received by the passive sensors causing loss of coverage.

In the present thesis there were selected and analysed the key geophysical parameters retrieved by passive satellite sensors, i.e. the concentration of chlorophyll-like pigments (*chl*) and the sea surface temperature (SST skin). The additional benefit of RS was that *chl* and SST skin maps were obtainable at the same spatial resolution (1.1 Km).
The distribution of *chl* is one of the most fundamental properties of the ocean ecosystem; *chl* has been designated by the United Nations Framework Convention on Climate Change (UNFCCC) an "essential climate variable" (GCOS, 2004). The autotrophic biomass and the consequent detection of phytoplankton blooms are crucial ecosystem indicators.

Ocean colour data provide the only window into the pelagic and coastal ecosystems on a synoptic scale, improving the understanding and the predictions of the state of the MPAs. In this thesis the use of ocean colour products has been proposed for new coastal and pelagic applications.

RS can also detect thermal fronts and upwelling regions. The retrieval of ecological indicators (e.g. initiation, timing, amplitude and duration of spring bloom, thermal fronts and variability) by means of remote sensing that quantify some relevant characteristic of the MPA make possible to detect ecosystem change in response to perturbations. The combined use of SST and *chl* permits the detection of dynamic features and gives insight into MPA oceanographic dynamics.

Satellite observations offer spatially detailed images which span many years thus allowing the detection of spatial trends in biological phenomena continuously, typically over 10 years for ocean colour sensors and almost 30 years for thermal sensors. These

archival remote sensing data are invaluable in providing, by means of time series, the seasonal and interannual dynamics and thus the history of a MPA under investigation.

In contrast, the *in situ* sampling campaigns could never supply a synoptic and spatially detailed view of a marine ecosystem under investigation at the spatial scale of even small MPAs. However, *in situ* measurements are complementary to the detailed study of the temporal evolution of the processes investigated, in particular in coastal areas. But, it should be taken into account that the collection of sea-water samples always adds uncertainties to the *in situ* observations. *In situ* sampling is usually considered as the "truth" and is particularly important in validating the ocean colour algorithms tested on a MPA and also to obtain more accurate estimates of the chlorophyll concentrations. The value of satellite imagery in monitoring MPAs is that of offering a synoptic view or namely the ability to sample the entire area in an instant and spatially detailed information on geophysical parameters without the need for collecting any sea-water sample.

RS is particularly useful for the construction of ecological indicators due to the rapidity of coverage, resolution, repeat frequency, cost-effectiveness and also the ability to retrieve quantitative information on fundamental ecosystem properties in standard units. Nonetheless, the shortcomings of satellite observations should also be considered. The disadvantages of RS include the lack of remote sensors tailored specifically for costal zones. Moreover, as stated in §1.7, RS techniques cannot sample along the water column: satellite data cannot supply information about conditions at and below the thermocline and ocean colour sensors, by means of visible wavelengths, cannot penetrate beyond a few tens of metres. These limitations do not restrict the applicability of RS observations to an MPA, but imply that *in situ* samplings should be regularly carried out and considered in combination with RS observations. *In situ* platforms enable sampling of the entire water column supplying information on its vertical variability, but, the information is discrete, being derived from small sea-water volume analyses.

Satellites sample the entire area in an instant and the surface measurements reflect sub-surface processes. The surface controls the exchanges between the atmosphere and the oceans, and RS is considered to be the best sampling depth to study the interaction

processes (Robinson, 2004). The study of the dynamics of the water surface is crucial for the MPAs due to its repercussions for the water column in general and in particular at higher trophic levels i.e. though the food web. In the near future, ocean colour - by means of the identification of phytoplankton functional types - will be able to supply information on marine biodiversity.

Earth observations satellite have a crucial role to play in exploring the dynamical and bio-geochemical features, in mapping the ecosystems and their movement over time and will become of increasing importance in the future years for the rational management of the MPAs.

6.1.1 Remote sensing applications to the Mediterranean MPAs

In Mediterranean Sea, despite the efforts to create a network of MPAs (Notarbartolo di Sciara, 2005), MPAs have always been considered as separate entities and studied often in the context of the biology and ecology without being included in a basin perspective and without considering their ecosystem dynamics.

The specific aims of the experimental chapters and in particular the description of, by means of passive remote sensors, the oceanographic features occurring in the coastal and pelagic Mediterranean MPAs required an analysis of the spatial and temporal variability of the phenomena investigated.

The thesis was developed in three experimental chapters which aimed at describing, by means of the use of different remote sensors, the bio-physical processes occurring in Mediterranean MPAs selected due to their location within peculiar sub-basins. In order to fulfil this aim, three different approaches have been applied:

1. Use of RS techniques to understand the bio-physical dynamics which characterise the Mediterranean MPAs and to highlight the differences between the study sites selected;

2. Use of archive RS datasets to study and analyse the spatial and temporal variability of a bio-physical variable within the unique high-seas MPA;
3. Setting up a multidisciplinary monitoring system by matching remotely sensed observations with those measured at sea in a relatively small coastal MPA.

In chapter 3 the first methodological approach was applied. This study focused on the analysis of the chlorophyll concentration (*chl*) by means of medium-resolution optical sensors to determine the dynamics of phytoplankton bloom occurring across the study areas. The use of statistical analyses, applied on ocean colour data to estimate space and temporal variability of *chl*, helped to quantify robustly the seasonality and the dynamics of the phytoplankton bloom i.e. the initiation, the peak timing, the amplitude, and the duration.

The investigation also focused also on one of the most important physical properties that is directly or indirectly crucial to aquatic ecosystem processes i.e. sea surface temperature. SST skin variability and its trend were detected in the MPAs by means of satellite thermal sensor. Sea temperature is an important factor controlling the physiological functioning and health of many aquatic organisms.

Since the biophysical processes are highly dynamic in space and time, the spatial scales used in this chapter were (1) the mesoscale (100s of km), to identify the bio-physical regions and the major discontinuities in biological and physical distributions, and (2) the microscale (10s of km), to characterise locally the MPAs as local bio-units (Stevens, 2002). Since the main biological process studied was the occurrence of phytoplankton blooms, a weekly time scale was employed. Medium-resolution sensors used proved to be extremely efficient for tracking mesoscale oceanographic features, allowing continuous measurement, by means of ocean colour sensors, of *chl* as an index of phytoplankton biomass. The time period and the spatial scale of phytoplankton bloom depend on the physical processes which influence the bloom phenomena by supplying nutrients from the deep water, i.e. processes that were investigated by means of a thermal sensor by analysing the SST skin dynamics and evolution. RS can map upwelling in such way that a phytoplankton bloom can be predicted, being SST and *chl* often inversely correlated. In particular, the MPAs located within the Ligurian-Provençal Sea were characterised by a seasonal, well developed phytoplankton bloom.

The MPA located within the Alboran Sea showed an intermittent bloom throughout the year which followed the entrance of the MAW into the Mediterranean Sea. The MPA located within the Central Mediterranean Sea was characterised by a high oligotrophy throughout the year considered, with almost no notable seasonal bloom.

By means of the above analyses it was possible to characterise in detail the dynamics and trends of the biophysical processes occurring in the sub-basins in which the MPAs were located and to depict the system functioning.

The new approach applied in chapter 3, thanks to the use of satellite observations, supplied a synoptic and repeated view, and has consequently permitted the assessment and the identification of the oceanographic conditions of the MPAs investigated. Chapter 3 demonstrated that RS techniques were successful in analysing and defining the persistent oceanographic features and bio-geographic boundaries which are extremely difficult to tackle only by means of *in situ* sampling techniques due to their variable nature and limited spatial and temporal extent of coverage by *in situ* sampling. It should be taken into account that medium spatial resolution sensors were not tailored for coastal zone investigation and thus are not appropriate to investigate in detail physical processes occurring on scale of hours (e.g. winds and river discharge) in relatively small MPAs. However, bio-optical processes occur on longer time scales than the physical forcing and thus were adequately detected. Nonetheless, the major shortcoming was the spatial resolution.

The approach involving i.e. the use of archive RS data in order to study and analyse the time variability of a bio-physical variable within a high-sea MPA was developed in Chapter 4. The repeated frequency of satellite data collection made it possible to construct time series and to quantify objectively the seasonal, annual and interannual dynamics of the geophysical parameter i.e. *chl* and the ecological indicators such as onset, timing, amplitude and duration of the phytoplankton bloom.

Long time series of satellite observations are essential to analyse phytoplankton biomass dynamics at regional scale because they allow interannual comparisons. The main ecological indicators which characterise the bloom phenomenon may vary among the years and should carefully taken into account because they indicate an ecosystem's

variation. Interannual fluctuations in dynamics of phytoplankton blooms and anomalies for timing of *chl* maxima account for perturbations and long-tem changes which have significant impact on the higher trophic levels i.e. on the zooplankton populations.

Chapter 4 highlighted long-term variations, i.e. the seasonal and interannual patterns of *chl* content and fields, and the consequent spatial and temporal pattern of phytoplankton bloom within a high-sea MPA. This analysis of long-term trends in marine biological processes was crucial to understanding the dynamics of the phytoplankton biomass, its timing and biogeographical shift. Understanding the phytoplankton dynamics and associated natural fluctuations is crucial due to its effects on the whole food web, causing primarily a fluctuation in the displacement of zooplankton populations and secondarily an effect on the cetaceans which feed on them. This MPA encompass pelagic and neritic regions, representing areas suitable for foraging needs of the cetacean species found in the Western Mediterranean sea (Notarbartolo di Sciara *et al*., 2008).

Chapter 4 has demonstrated the remarkable value of ocean colour observations which could help to understand the mechanisms behind the variations of biological resources in terms of their abundance and distributions, particularly, in an MPA where the pelagic species are sustained by phytoplankton communities which in turn are supported and maintained by the interactions between physical and biological processes. The study of the spatial and temporal biological processes was tackled spatially by looking at mesoscale and temporally by considering the 10-day period as the basal time unit.

The third methodological approach i.e. the setting up of a multidisciplinary system which combines satellite observations with data collected at sea integrates ocean colour products at finer spatial resolution and SST skin observations with *in situ* measurements collected in a relatively small coastal MPA.

In chapter 3 this relatively small MPA was studied by analysing data retrieved by coarse resolution remote sensors. In chapter 5 the same area was investigated by means of a finer spatial resolution ocean colour sensor. The higher spatial resolution of the sensor used supplied a better insight to the biological phenomena occurring at local scale. This sensor and, in particular, the ocean colour products retrieved by the two algorithms

supplied were tested and validated with measurements collected *in situ*. The outcomes of these tests revealed that the algorithms performed differently depending on season, due essentially to the seasonal modification of the general circulation in the MPA investigated, *chl* being tightly coupled with the physical dynamics of the system.

6.2 IMPLICATIONS FOR THE MEDITERRANEAN MPAs

The analyses of the satellite data made possible the identification of the trends of biophysical processes and led to understanding the functioning of the Mediterranean MPAs by looking at the basins in which they were located. The dynamical trend of the sub-basin affects on the MPAs' ecosystems.

The recognition of upwelling zones, phytoplankton blooms and thermal fronts are crucial for the management of the Mediterranean MPAs. The hydrographic characterisation of the MPAs considered is extremely important to protect the critical ecological processes which support their unique and vulnerable habitats, communities and the ecosystems present within the analysed Mediterranean MPAs. As stated by Stevens (2002), the designing process for MPAs should be based on the recognition and characterisation of biological and physical processes and of marine habitat types. It should be added that, since the Mediterranean MPAs in the above preliminary phase of design usually lack the study and characterisation of biological and physical processes, these aspects become crucial in the monitoring and management phases.

RS techniques have allowed assessment of the bio-physical oceanographic features of the sub-basins in which the Mediterranean MPAs were located. These features should be investigated at adequate and appropriate spatial and temporal scales. Thus, in the monitoring process the problem of scale should be carefully taken into account. The added value of Earth Observation (EO) sensors is the possibility of looking synoptically at the MPAs within a well-resolved spatial and temporal scale.

The new methodological and statistical approach developed in chapter 4 should support the implementation of environmental policies, and is crucial to define and investigate

the effect of environmental conditions change on this particular high-sea MPA (*Pelagos* Sancuary). The definition of the biological features should drive future monitoring and management of this MPA. The management plan of this area, as stated by Notarbartolo di Sciara *et al*. (2008), should encompass the understanding of the physical and biological processes along with the information on the distribution of cetaceans. The use of the historical series of RS observations is crucial to highlight the interannual changes in primary production and water mass distributions, and how the physical and biological interactions shape the ecosystem structure, zooplankton fauna and cetacean distribution. Mesoscale processes influence the biological activity by affecting the spatial and temporal variability of phytoplankton biomass (Morel and André, 1991; Lévy *et al*., 1998), thereby modulating the spatial distribution of zooplankton organisms and consequently the spatial distribution of cetaceans present in the area (Cotté *et al*., 2009). Ocean colour remote sensing identified the biological oceanographic features which are key indicators to be correlated with data on biological population i.e. cetacean distribution.

Surveys conducted on this, the *Pelagos* Sancuary MPA (Forcada *et al*., 1996; Notarbartolo di Sciara *et al*., 2003; Littaye *et al*., 2004; Panigada *et al*., 2005) confirmed that the major presence of fin whales was recorded in the region of the Ligurian frontal system found in the Western Mediterranean, namely in areas where the phytoplankton bloom patch was recorded during the preceding spring season. The fin whale habitat use is linked to the cycle and patchiness of krill in association with environmental conditions (Cotté *et al*., 2009).

Moreover, the use of ocean colour high resolution satellite sensor provided a better and more meaningful insight to the oceanography of a relatively small MPA whereas the medium resolution sensor and traditional *in situ* measurements were strategic for the continuous monitoring of coastal MPAs. The future enhancement and refinement of the bio-optical algorithms for coastal zone along with the regionally optimised algorithm for atmospheric correction, tested on the Mediterranean waters, will supply more precise and usable information on the biological processes occurring in this MPA.

The integration of these methodologies resulted in a useful and meaningful means to reach the setting up of a multidisciplinary and integrated system for monitoring and

further management of this MPA. Furthermore, this interdisciplinary approach could provide crucial information on the main environmental features. This will permit the management body to assess the efficacy of the management process within the MPA's boundaries. However, usually *in situ* data are snapshots of a given situation at a given period, and to avoid it the sampling strategies should be with consideration of the oceanographic features under investigation. Sampling effort should cover the whole MPA waters namely supply a fine scale coverage with high sampling intensity.

The experience acquired so far, could lead to a hypothesis that in the coming years the coupling of data collected *in situ* by means of profilers and those supplied by satellites will permit conception of a Mediterranean system to monitor the dynamics of the main environmental variables in the coastal Mediterranean MPAs.

Other implications are related to the fulfilment of the MPA's objectives. The main objectives of an Italian MPA (European Union Directives 92/43/EEC and 79/409/EEC), that can be taken as example for the Mediterranean area, are (among others) the preservation of natural equilibrium, biological and ecological values, maintenance of biodiversity at all levels avoiding external impacts, and the use of the MPAs as control areas for the study of environmental changes. The present thesis has demonstrated that RS is one of the most promising tools to fulfil these objectives, particularly due to its ability in improving the regulatory monitoring. Only RS is capable of supplying a synoptic and repeated view of the ecosystem identifying the so called "natural equilibrium" and natural fluctuations or those caused by the environmental changes. Mediterranean MPAs can be seen as field laboratories for the enactment of innovative management models, which offer the opportunity of coupling the traditional sampling methodologies with the RS techniques to work towards safeguarding marine habitats and species. Satellite RS is a tool that could help to foster ecosystem-based management.

6.3 RECOMMENDATIONS

In order to assist the Mediterranean MPAs in meeting their objectives, the serious gap in knowledge about the physical and biological oceanographic processes should be filled by extensive use of RS monitoring techniques which permit (at much lower cost than *in situ* sampling), a meaningful insight to the oceanography of a Mediterranean MPA. It could be argued that designing, setting up and sending satellites is a costly operation. However, it should be added to this that satellite data for ocean monitoring are often available at no cost if used for scientific purposes.

Empirical *in situ* studies on marine organisms should follow a sampling methodology designed by taking into account the spatial and temporal variability of the main geophysical parameters retrieved by RS techniques. This approach should permit a better use of the resources available and consequently an enhancement of the management process and MPA's efficacy.

The above process should drive not only the monitoring and management process but also the process of designing MPAs, particularly the physical and biological characterisation of the waters surrounding the marine areas stated by the National Research Council (2001). Indeed, designing process passes through four steps already listed (§1.4.1). The RS has a significant and substantial role to play at stage 3 i.e. the assessment of the oceanographic features. RS data, as shown in the present thesis, should be exploited in order to detect upwelling zones, thermal fronts and currents, thus leading to the detailed characterisation of the MPA under investigation. In this process the observations retrieved by passive sensors (ocean colour and SST) should be coupled with those collected by active sensors (i.e. winds). This should be supported by a well defined systematic methodology based on scientific criteria (Stevens, 2002). The constellation of passive and active sensors, available at present, enables observation of several geophysical variables and processes at the time, and monitoring of an MPA with different spatial and temporal scales.

Moreover RS has a role to play also at stage 4, i.e. site identification. Indeed, the oceanographic information collected may also be utilised in defining the location and size of a MPA.

The extensive use of RS techniques in relatively small MPAs is crucial in the foreseen establishment of a MPAs network according to Francour *et al*. (2001), formed by numerous small neighbouring areas tightly interconnected. As, for example, the Portofino MPA and the *Pelagos* Sancuary are both located within the Ligurian-Provençal Sea and thus interconnected, they should be considered as a single system which objectives encompass the conservation of the cetacean populations and the safeguarding of the hard bottoms biocoenoses.

MPAs should be conceived taking into account the issue of spatial and temporal scale, Mediterranean MPAs often occurring at microscale (10s of km) or picoscale (<10 km), or at the scale of individual, discrete physical and biological habitats. RS techniques allow the regional scale (mesoscale) to be considered by placing the MPA in a broader context, i.e. in a basin context, by monitoring the species that enter the area only at certain times such as phytoplankton populations. The bio-physical information should be considered when defining the zoning process of an MPA. As stated in §1.4.2, zoning is the means through which the institutive objectives could be met. The zoning, on the basis of the oceanographic information retrieved by means of RS techniques, should be modified routinely on a spatial and temporal basis, taking into account the seasonal displacement of phytoplankton and zooplankton populations which drive the entire food web. The idea of temporal zoning should be developed and refined on the basis of the seasonality of the bio-physical dynamics as well as on the basis of the biology of the populations under protection.

This process could be applied to the north-western area of the *Pelagos* Sanctuary by promoting the establishment of a strict reserve zone during summer when the cetaceans feed, where and when navigation and professional fishing activities should be forbidden. For coastal MPAs it is more difficult to point out zones with a different degree of protection only on the basis of observations collected by the medium-resolution sensors, due to the generally small size of coastal MPAs. However, hyperspectral sensors, a term reserved for sensors with spectral resolution of few

nanometers with high-frequency observations, will be available soon with the launch of the geostationary ocean colour sensors. This will improve the pixel resolution contributing to improved applications in coastal MPAs.

MPAs should be seen and used as field laboratories where the scientific, innovative monitoring techniques illustrated in this thesis should be tested and management models refined. Contemporary techniques should be used in order to safeguard marine habitats and species and consequently modulate the human activities within MPAs. Not least, RS techniques should use MPAs as control areas in order to detect environmental changes.

RS techniques represent a strategic tool for the setting up of a network of Mediterranean MPAs which, as stated by Boero *et al*. (1999) and Agardy (2002), should be achieved and work as a sensor of environmental conditions. The interdisciplinary approach to the monitoring of MPAs illustrated in chapter 5, should become the rule, as stated by Kelleher and Bleakely (1994) for the designing and planning of MPAs. The large-scale oceanographic dynamics should be continuously monitored because they could limit an MPA's efficacy in protecting marine populations. As stated by Allison *et al*. (1998), large-scale environmental events can change the dominant oceanographic patterns and consequently modify and perhaps jeopardise the holopelagic and benthic communities and their spatial distribution. The increasing understanding of oceanographic processes and large scale fluctuations and their effects on coastal ecosystems should lead to an enhancement of the effectiveness of MPA design.

The long-term studies, such as those conducted in chapter 4, should be coupled with short term studies. Improved knowledge of the magnitude of processes is necessary (Lourie and Vincent, 2004) to guarantee the existence of species and habitats within the MPAs and their biogeographic distribution.

6.4 SUGGESTIONS FOR FUTURE WORK

The study conducted is a first attempt to characterise the Mediterranean MPAs by means of RS techniques. In all of these discussions by far the greater part of the text concerned *chl* as crucial ecological index of phytoplankton biomass. In the future, the estimates of chlorophyll should be retrieved by means of the use of regional bio-optical algorithms specific for the area of interest, decreasing the uncertainty of satellite derived *chl*.

The results obtained in this thesis need to be coupled with data on the spatial and temporal distribution of the key marine species and habitats which characterise each of the MPAs considered. In particular, phytoplankton functional types occurring in the MPAs should be investigated and identified. To this purpose, the higher spatial and spectral resolution of the new generation of ocean colour sensors is now making it possible to move towards the identification of phytoplankton types by the study of the distinct spectral signatures (Nair *et al.*, 2008).

Long-term studies should be conceived in order to study the effect of changes in SST on the phytoplankton species of a given region as well as the locations of phytoplankton concentrations (Mann and Laziers, 2008). Moreover, studies on the main zooplankton communities, in particular the northern krill *Meganyctiphanes norvegica* euphausiid typical of the Western Mediterranean, and their spatial and temporal displacement should be carried out and coupled with satellite data.

The analytical and statistical methods utilised in the present thesis should become routine analyses and the standard for the study of other Mediterranean MPAs. The present methodology should be applied to other Mediterranean MPAs coupled with *in situ* data coming from monitoring campaigns for calibration and validation of RS observations. This approach will lead to an enhanced reliability and efficiency of the proposed methodology.

The MPAs investigation requires an interdisciplinary approach due to the constant interplay between physics and biology. Much remains to be done to understand how

physical processes influence and modify the biological communities within the MPAs. Marine organisms respond to physical phenomena at a wide range of scales; future studies should focus on the physical-biological interactions within the MPAs and should take into account more than one spatial and temporal scale. These studies will make it possible to identify more effective management schemes.

These are only a few of the challenges facing the marine scientists working on MPAs in the near future.

APPENDIX 1
SATELLITE SENSORS TECHNICAL CHARACTERISTICS

OPTICAL SENSORS

SeaWiFS: Radiometric parameters

Channels	Band Centre (nm)	Band Width (nm)	Spatial Resolution (m)	Colour	Primary Use
1	412	20	1100	Violet	Dissolved Organic Matter (absorbance within violet)
2	443	20	1100	Blue	Chlorophyll (absorbance within blue)
3	490	20	1100	Blue/Green	Chlorophyll (absorbance within blue-green)
4	510	20	1100	Green	Chlorophyll (absorbance within green)
5	555	20	1100	Green /Yellow	Chlorophyll (backscattering within green)
6	670	20	1100	Red	Atmospheric Correction
7	765	40	1100	Near Infra-Red	Atmospheric Correction, aereosol radiance
8	865	40	1100	Near Infra-Red	Atmospheric Correction, aereosol radiance

APPENDIX 1
SATELLITE SENSORS TECHNICAL CHARACTERISTICS

MERIS: Radiometric parameters

Channels	Band Centre (nm)	Band Width (nm)	Spatial Resolution (m)	Colour	Primary Use
1	412.5	10	300-1200	Violet	Dissolved Organic Matter turbidity.
2	442.5	10	300-1200	Blue	Chlorophyll, maximum absorbance
3	490	10	300-1200	Blue/Green	Chlorophyll other pigments
4	510	10	300-1200	Green	Turbidity, suspended sediments, red tides
5	560	10	300-1200	Green /Yellow	Chlorophyll reference, suspended sediments
6	620	10	300-1200		Suspended Sediments
7	665	10	300-1200	Red	Chlorophyll Absorbance
8	681.25	7.5	300-1200		Chlorophyll Fluorescence
9	705	10	300-1200		Atmospheric Correction
10	753.75	7.5	300-1200	Near Infra-Red	O_2 Absorbance reference
11	760	2.5	300-1200	Near Infra-Red	O_2 Absorbance
12	775	15	300-1200	Near Infra-Red	Aerosol, Vegetation
13	865	20	300-1200	Near Infra-Red	Aerosol correction on the oceans
14	890	10	300-1200	Near Infra-Red	Water vapour absorbance reference
15	900	10	300-1200	Near Infra-Red	Water vapour absorbance, Vegetation

APPENDIX 1
SATELLITE SENSORS TECHNICAL CHARACTERISTICS

THERMAL SENSOR

AVHRR: Radiometric parameters

Channels	Wavelength (µm) NOAA 16	Spatial Resolution (m)	Primary Use
1	0.58-0.68	1100	Daytime cloud and surface mapping
2	0.725-1.10	1100	Land-water boundaries
3A	1.58-1.64	1100	Snow and ice detection
3B	3.55-3.93	1100	Night cloud mapping, sea surface temperature
4	10.30-11.30	1100	Night cloud mapping, sea surface temperature
5	11.50-12.50	1100	Sea surface temperature

APPENDIX 2 (a) Portofino MPA
Chlorophyll (*chl*) maps (SeaWiFS data year 2002)

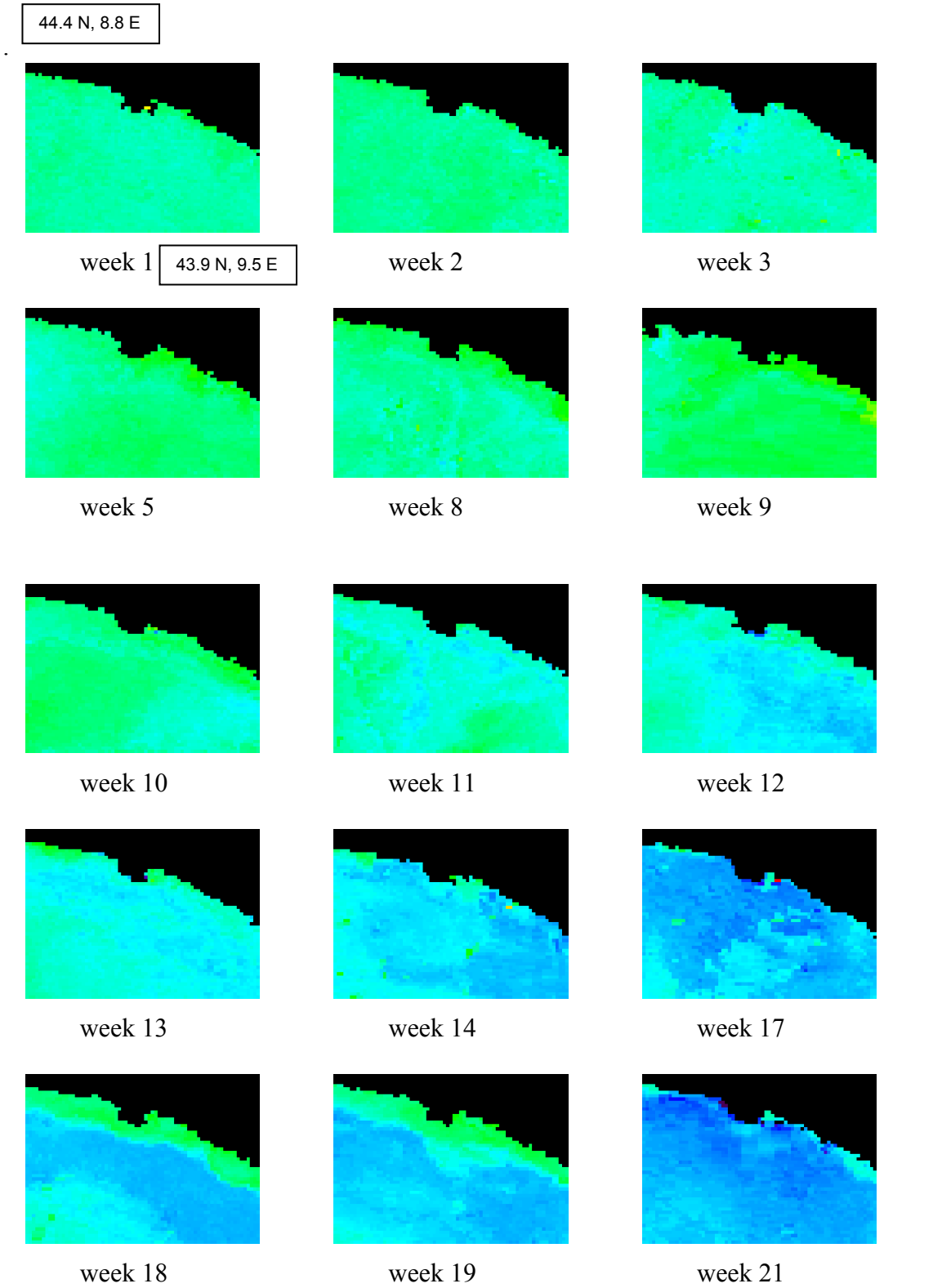

APPENDIX 2 (b) Portofino MPA
chl maps (SeaWiFS data year 2002)

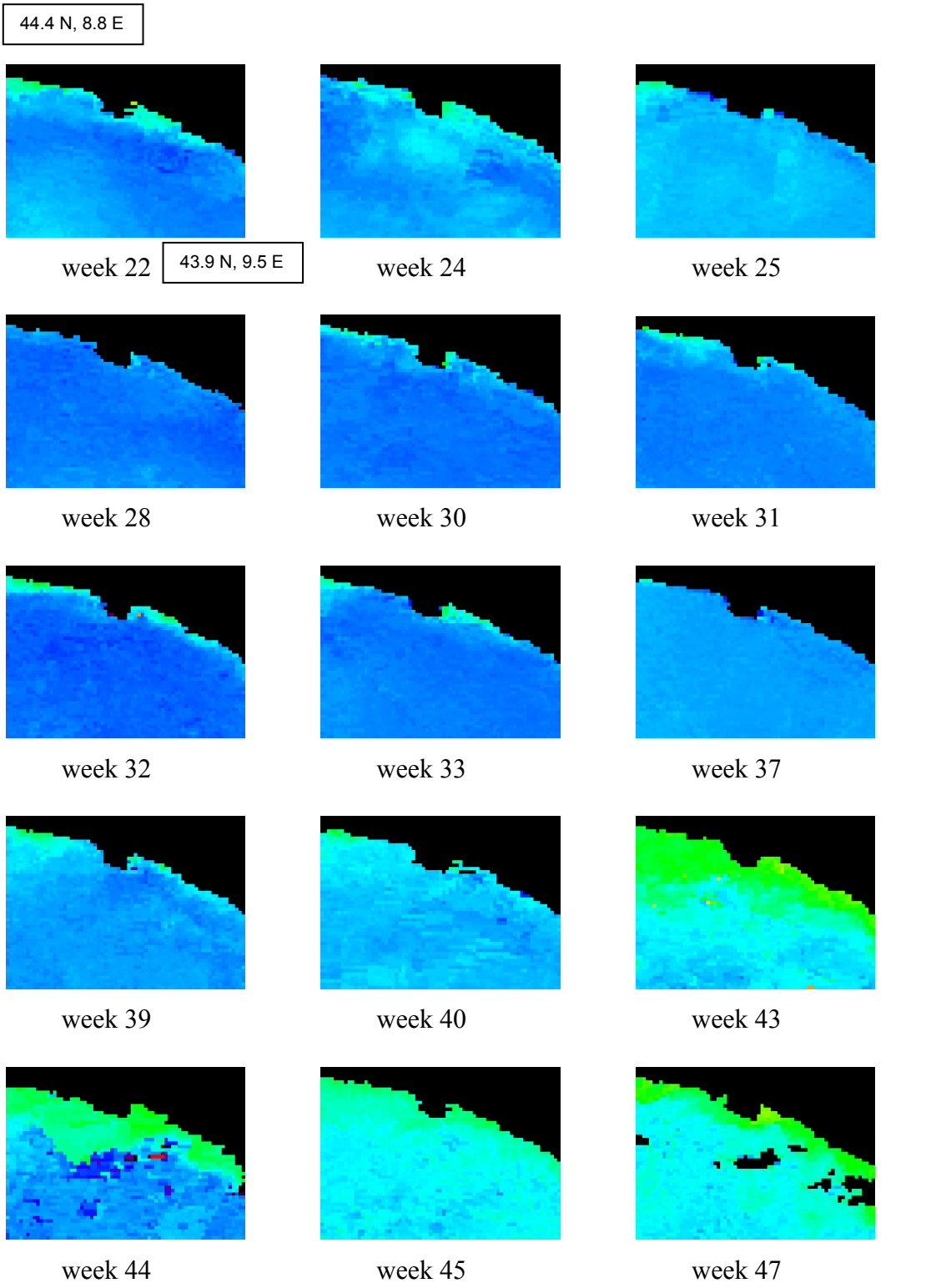

APPENDIX 2 (c) Portofino MPA
chl maps (SeaWiFS data year 2002)

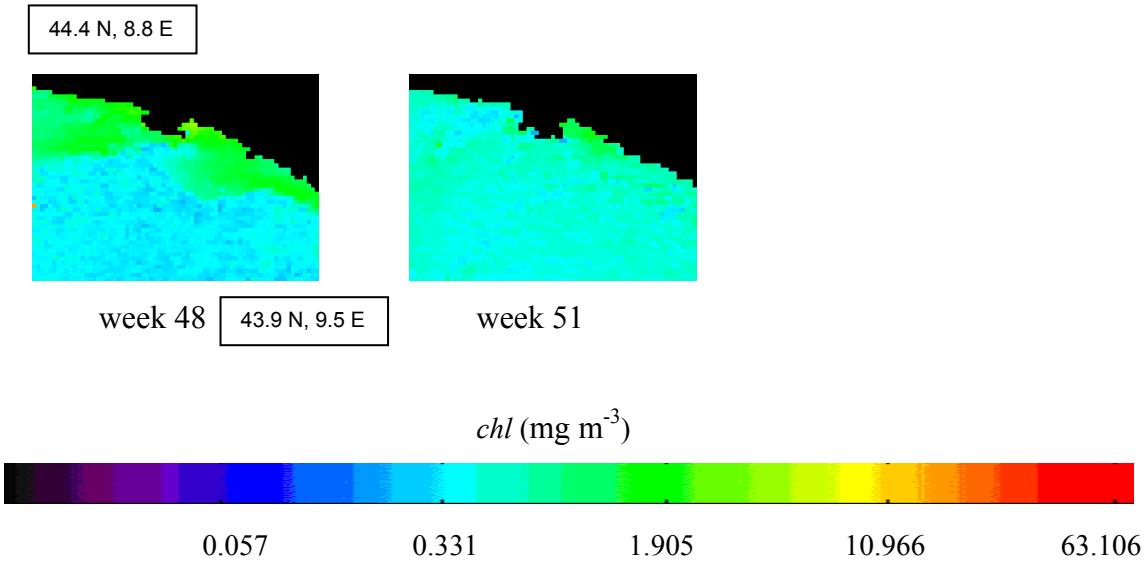

APPENDIX 3 (a) Portofino MPA
Spatial Gradient (*chl* range 0.164-0.9 mg m^{-3})

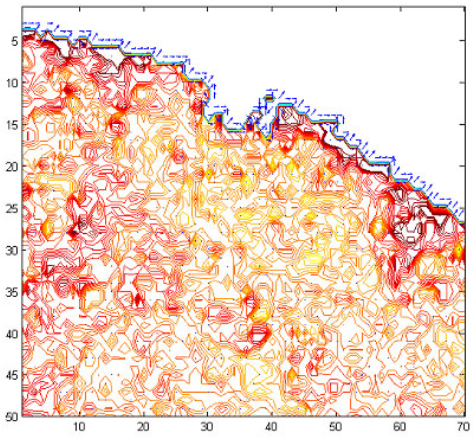

week 1

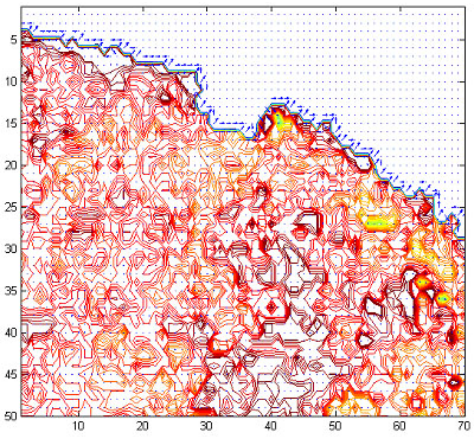

week 2

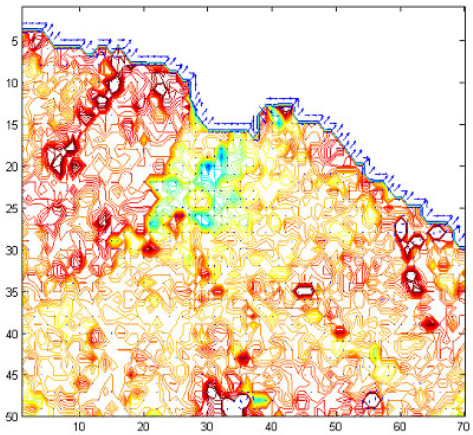

week 3

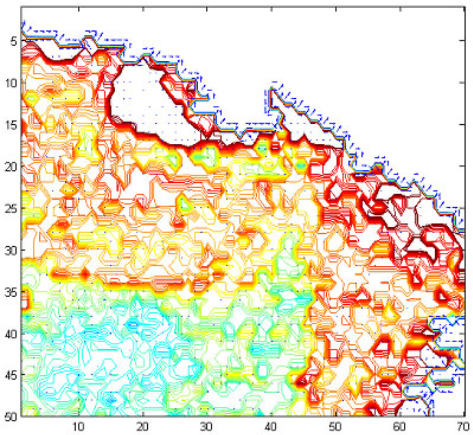

week 4

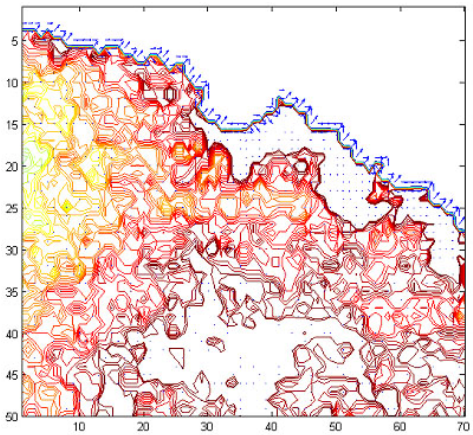

week 5

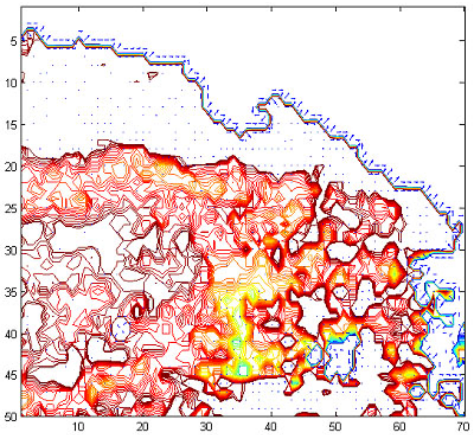

week 6

chl (mg m^{-3})

0.16 0.19 0.23 0.27 0.33 0.39 0.46 0.55 0.66 0.79

APPENDIX 3 (b) Portofino MPA
Spatial Gradient (*chl* range 0.164-0.9 mg m^{-3})

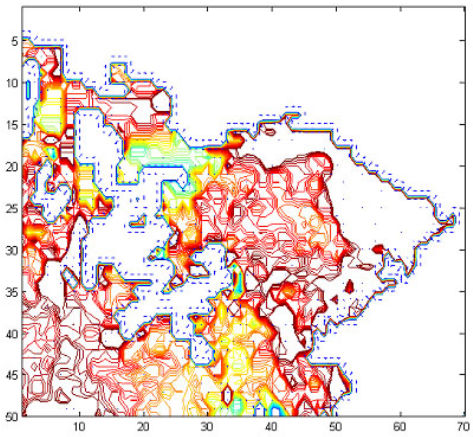

week 7

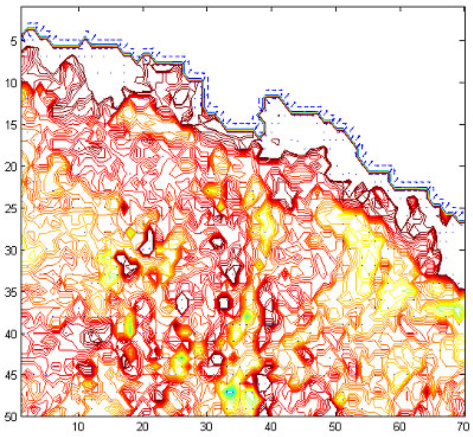

week 8

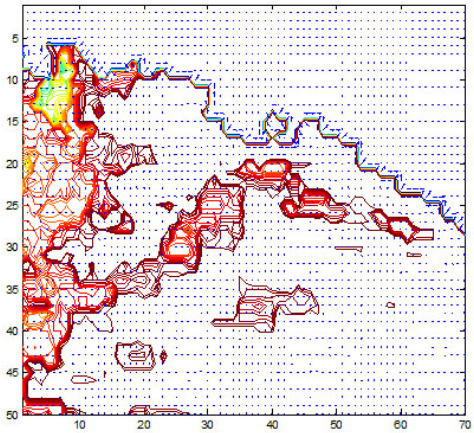

week 9

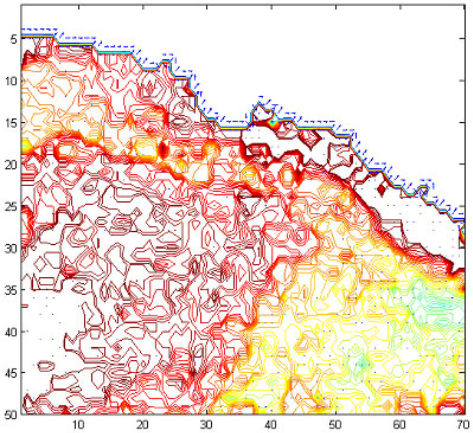

week 10

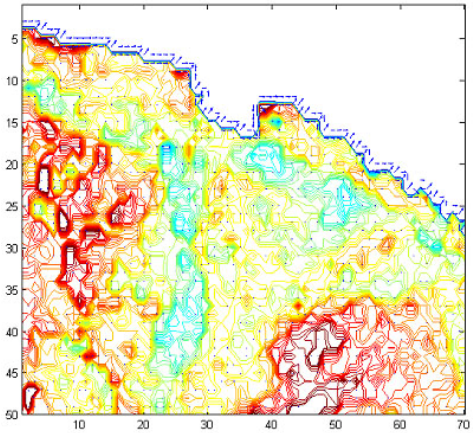

week 11

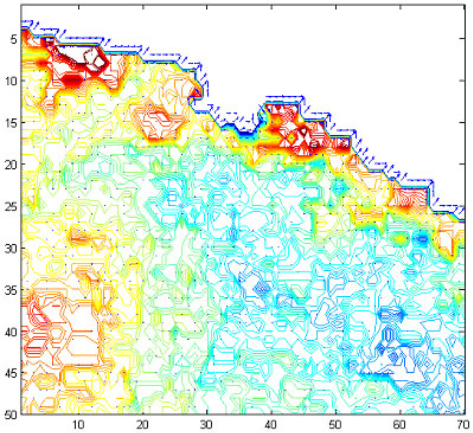

week 12

chl (mg m^{-3})

0.16 0.19 0.23 0.27 0.33 0.39 0.46 0.55 0.66 0.79

APPENDIX 3 (c) Portofino MPA
Spatial Gradient (*chl* range 0.164-0.9 mg m^{-3})

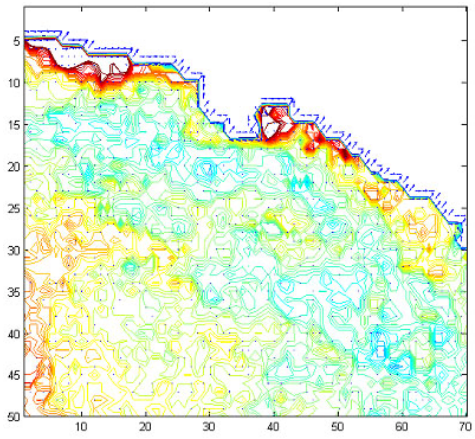

week 13

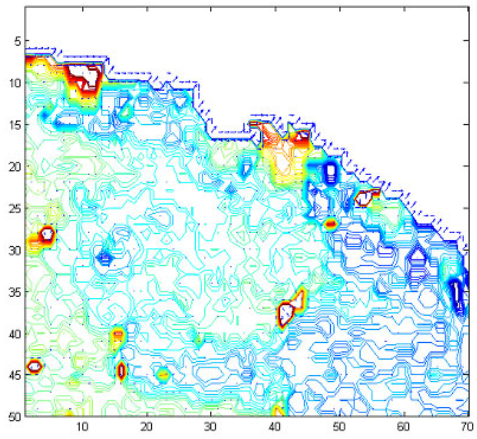

week 14

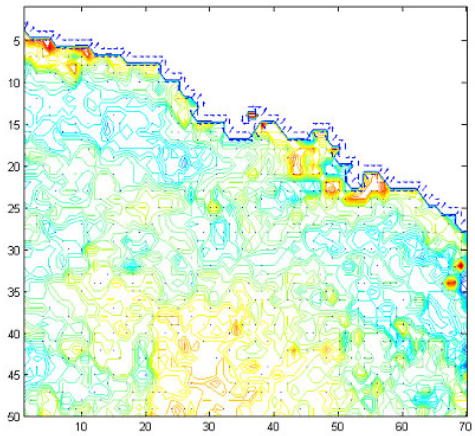

week 16

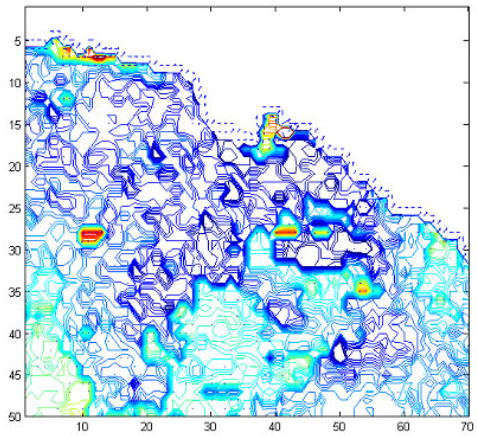

week 17

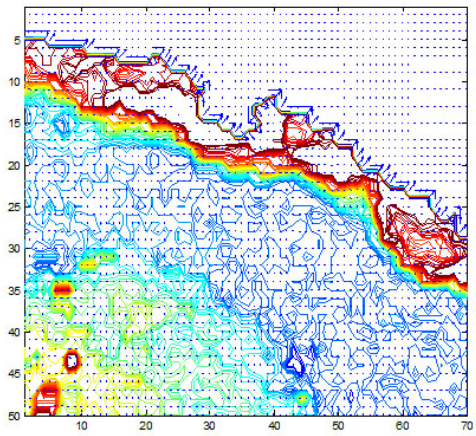

week 18

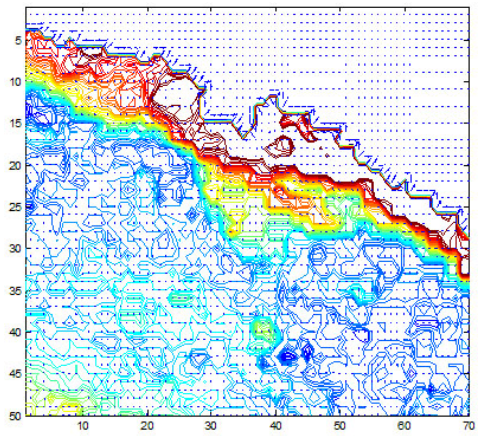

week 19

chl (mg m^{-3})

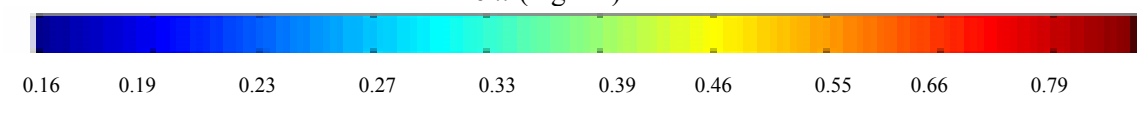

APPENDIX 3 (d) Portofino MPA
Spatial Gradient (*chl* range 0.164-0.9 mg m^{-3})

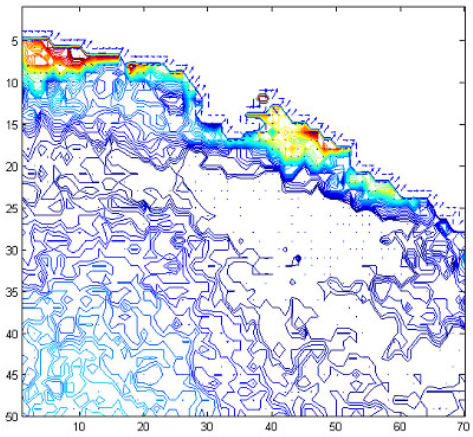

week 22

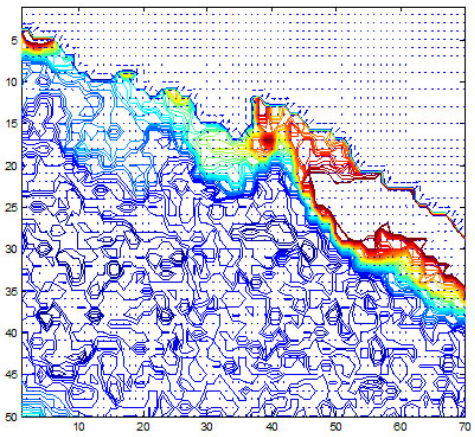

week 23

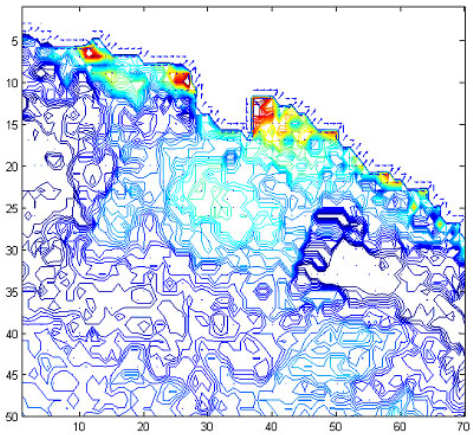

week 24

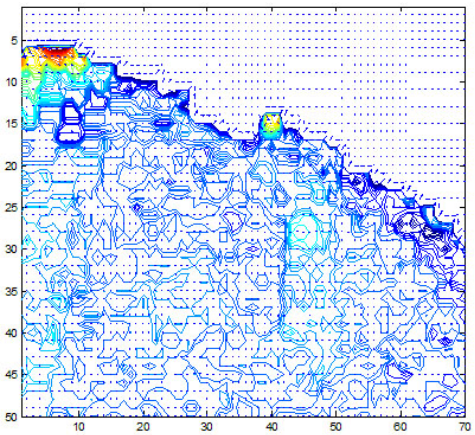

week 25

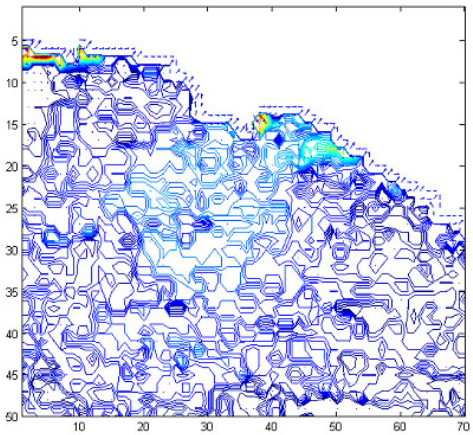

week 29

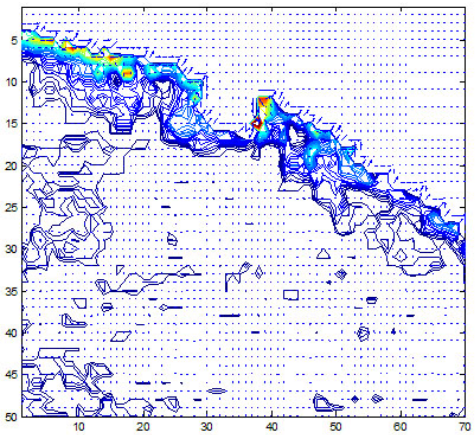

week 30

chl (mg m^{-3})

0.16 0.19 0.23 0.27 0.33 0.39 0.46 0.55 0.66 0.79

APPENDIX 3 (e) Portofino MPA
Spatial Gradient (*chl* range 0.164-0.9 mg m^{-3})

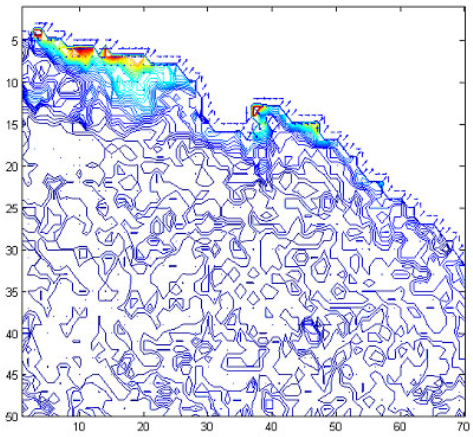

week 31

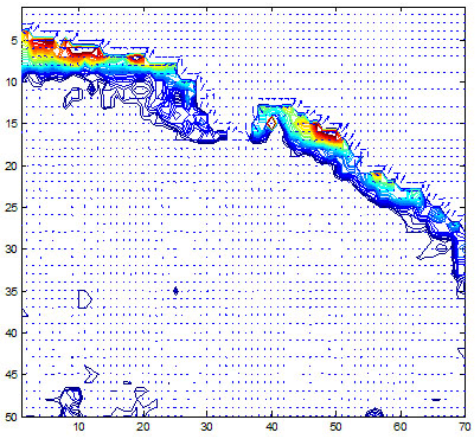

week 32

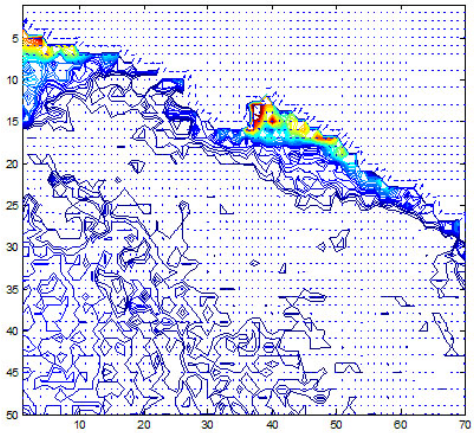

week 33

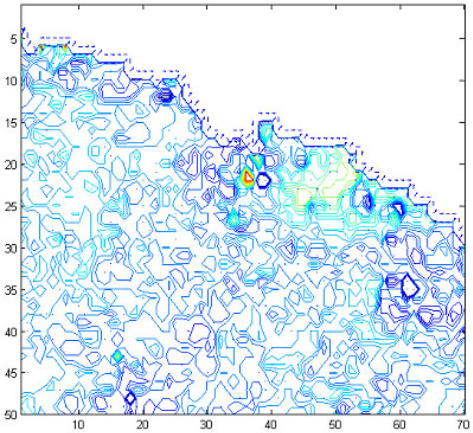

week 36

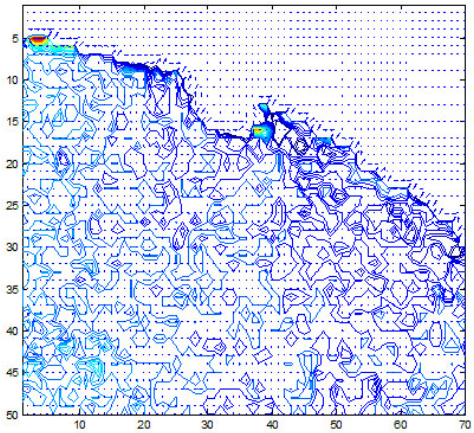

week 37

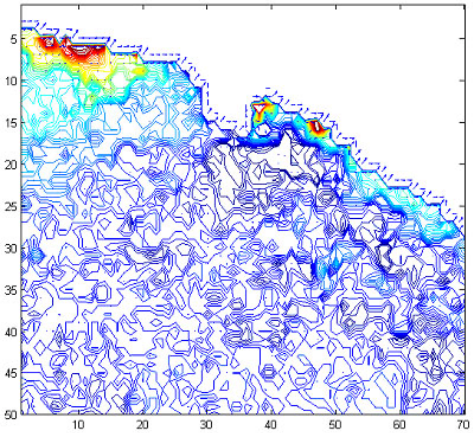

week 39

chl (mg m^{-3})

0.16 0.19 0.23 0.27 0.33 0.39 0.46 0.55 0.66 0.79

APPENDIX 3 (f) Portofino MPA
Spatial Gradient (*chl* range 0.164-0.9 mg m^{-3})

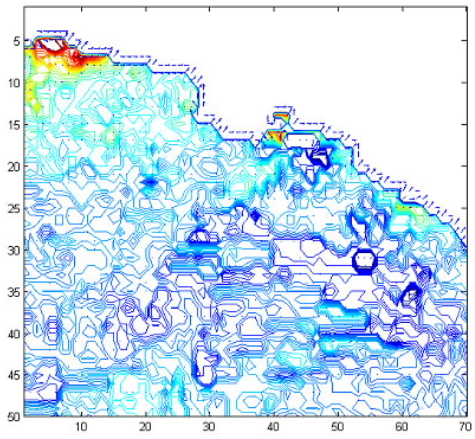

week 40

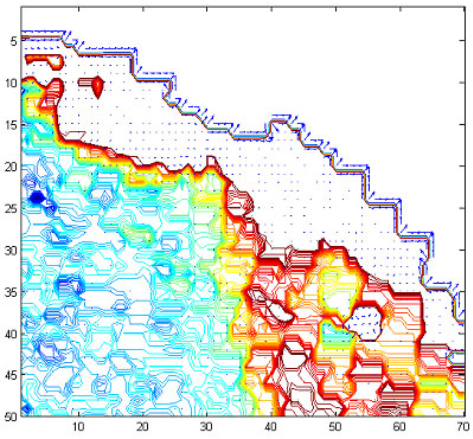

week 42

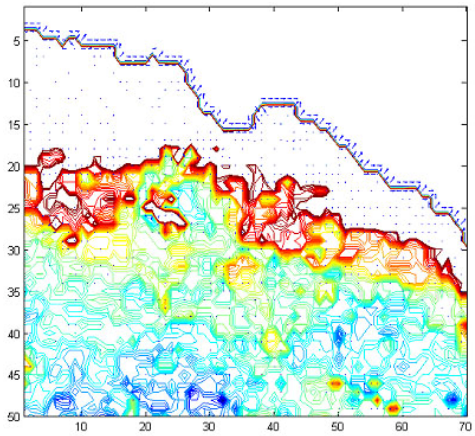

week 43

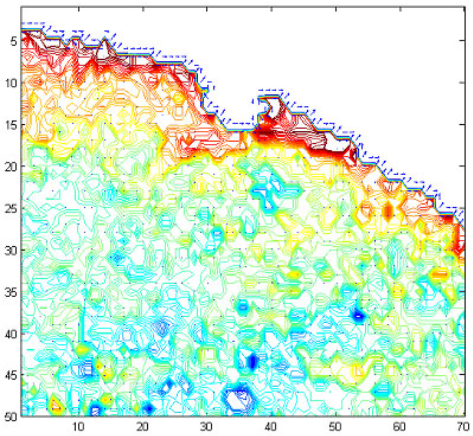

week 45

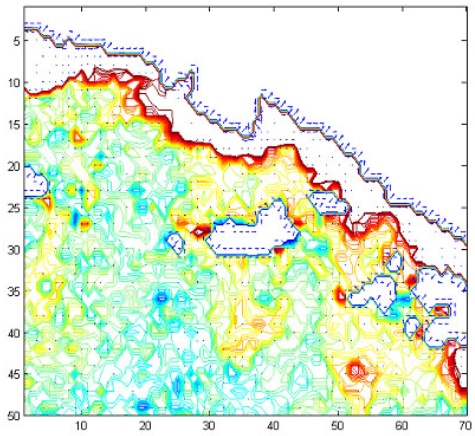

week 47

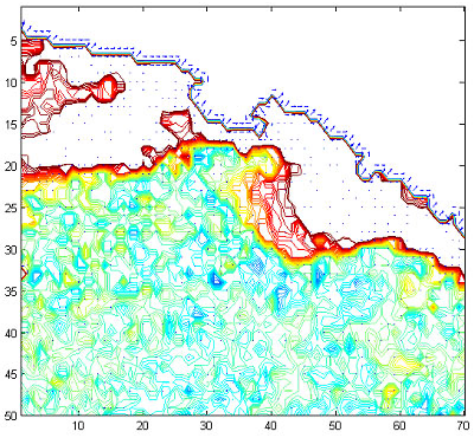

week 48

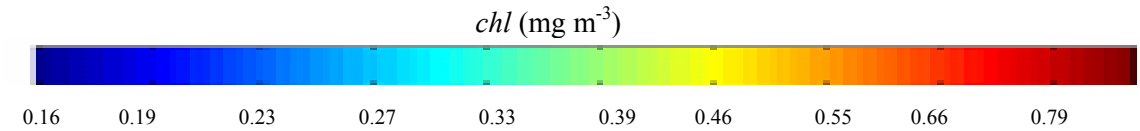

APPENDIX 3 (g) Portofino MPA
Spatial Gradient (*chl* range 0.164-0.9 mg m^{-3})

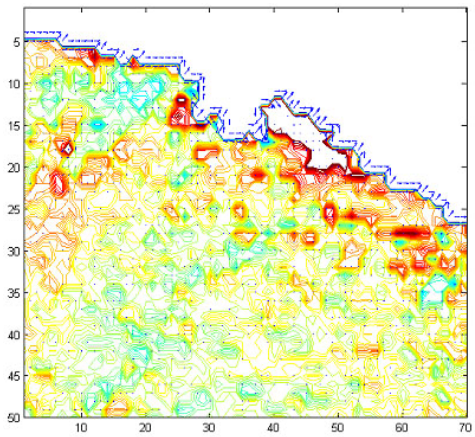

week 51

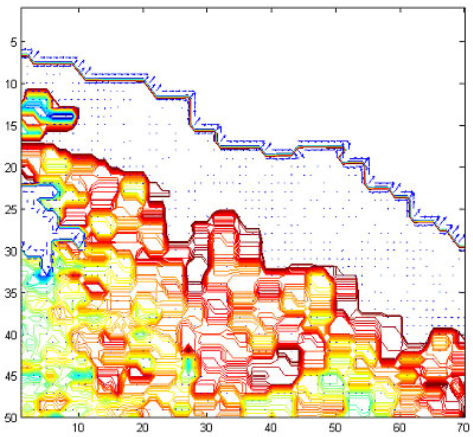

week 52

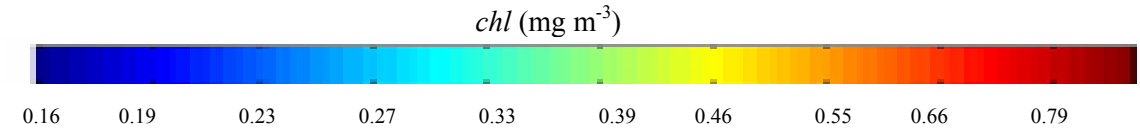

APPENDIX 4 (a) Portofino MPA
Spatial Gradient (chlorophyll range 1.0-1.9 mg m^{-3})

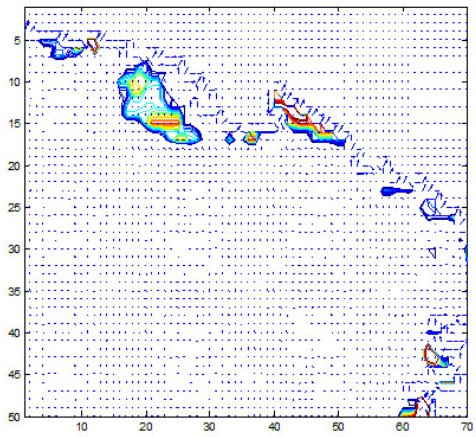

week 4

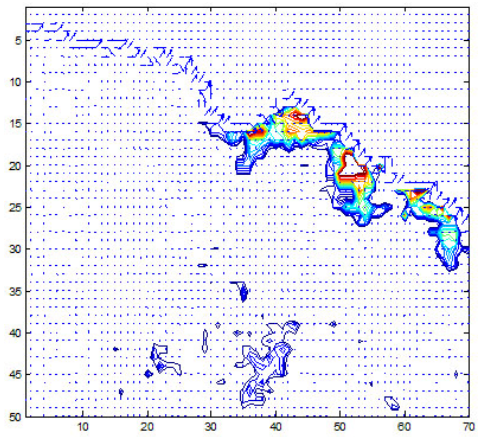

week 5

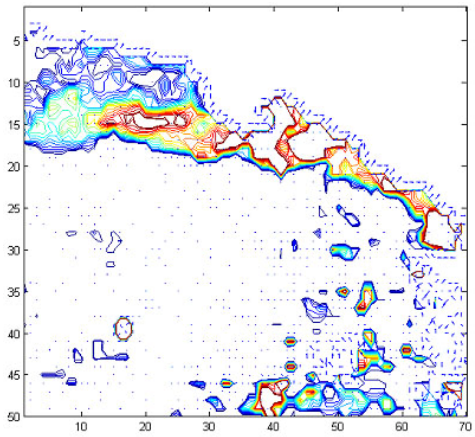

week 6

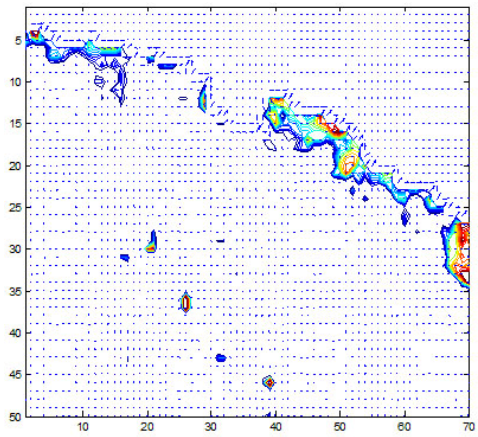

week 8

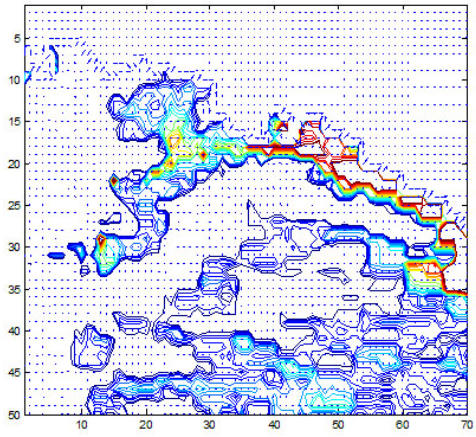

week 9

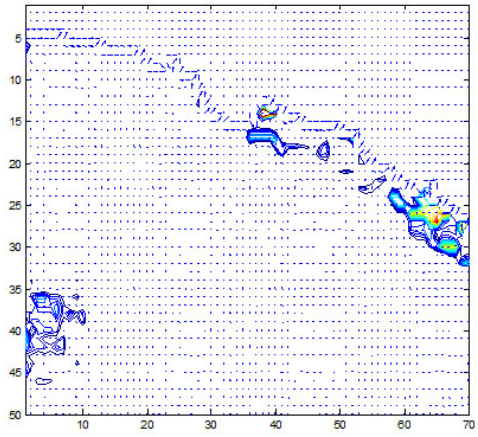

week 10

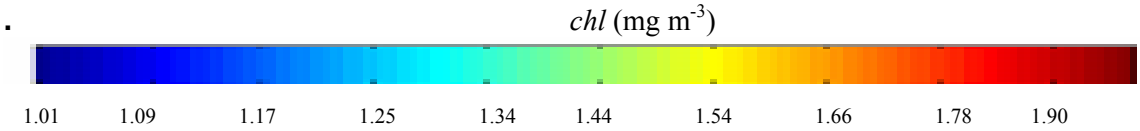

APPENDIX 4 (b) Portofino MPA
Spatial Gradient (chlorophyll range 1.0-1.9 mg m^{-3})

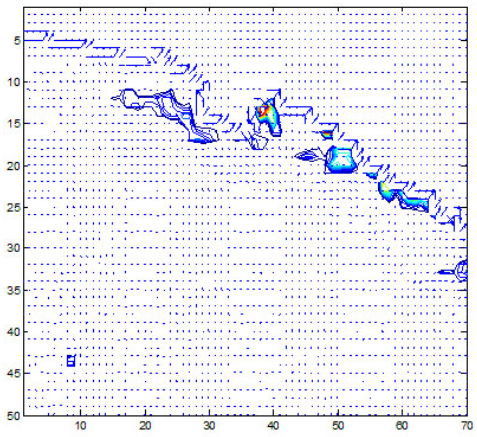

week 18

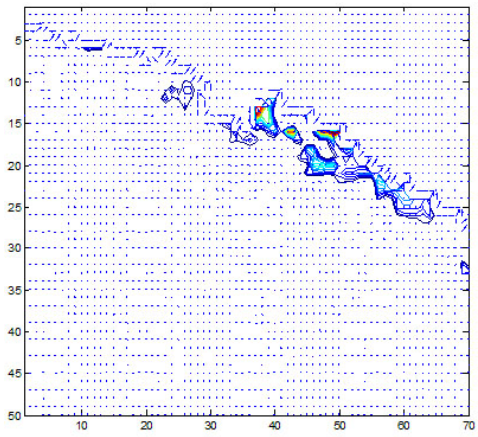

week 19

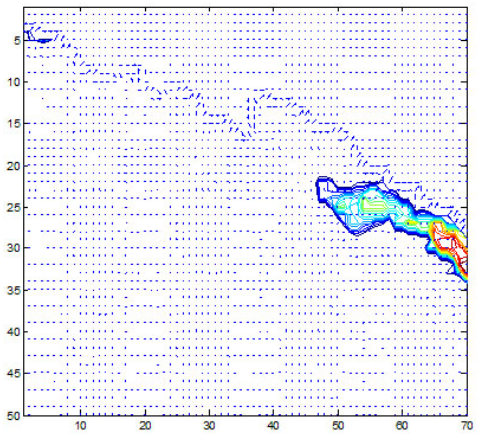

week 23

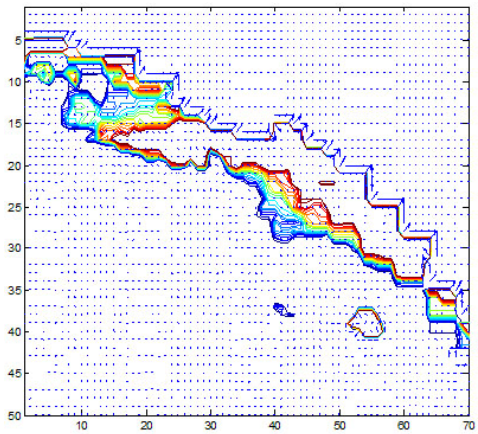

week 42

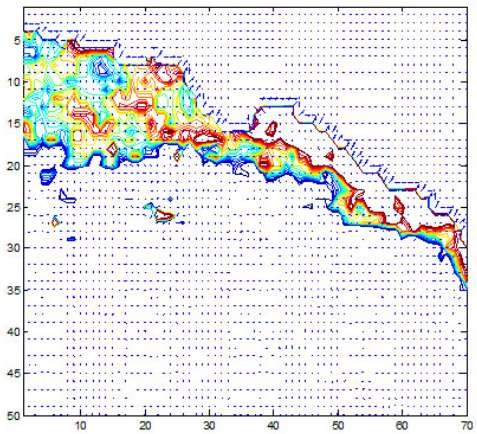

week 43

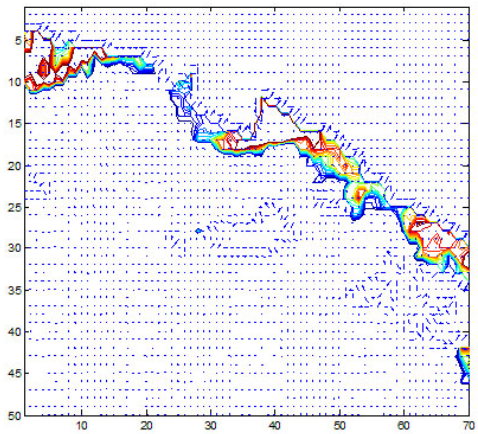

week 47

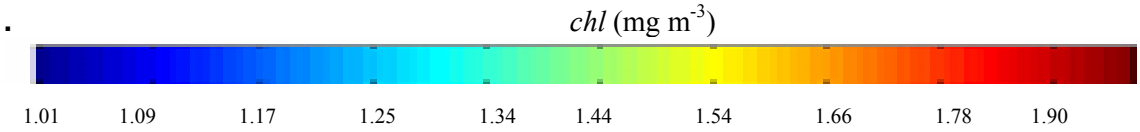

APPENDIX 4 (c) Portofino MPA
Spatial Gradient (chlorophyll range 1.0-1.9 mg m^{-3})

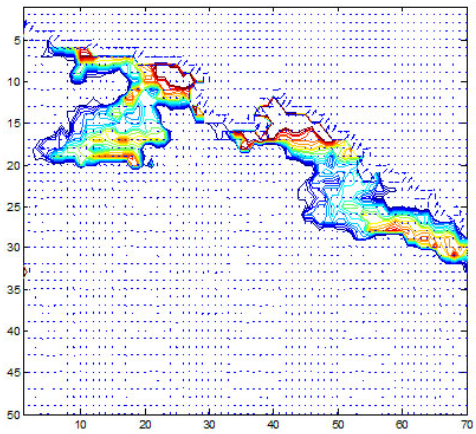

week 48

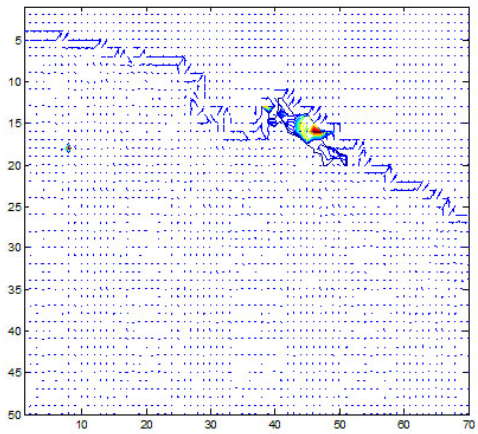

week 51

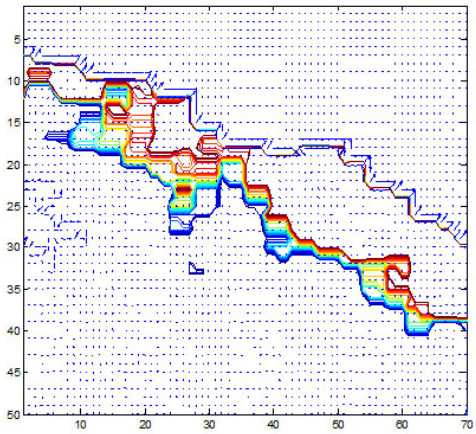

week 52

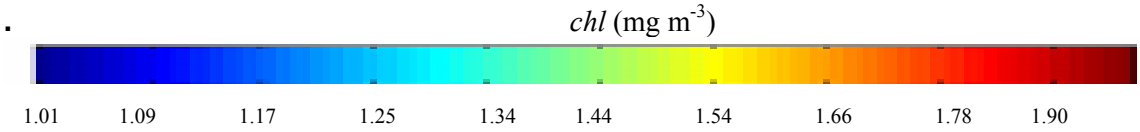

APPENDIX 5 (a) Portofino MPA
Sea Surface Temperature skin (SST skin) maps
(AVHRR data April-December 2002)

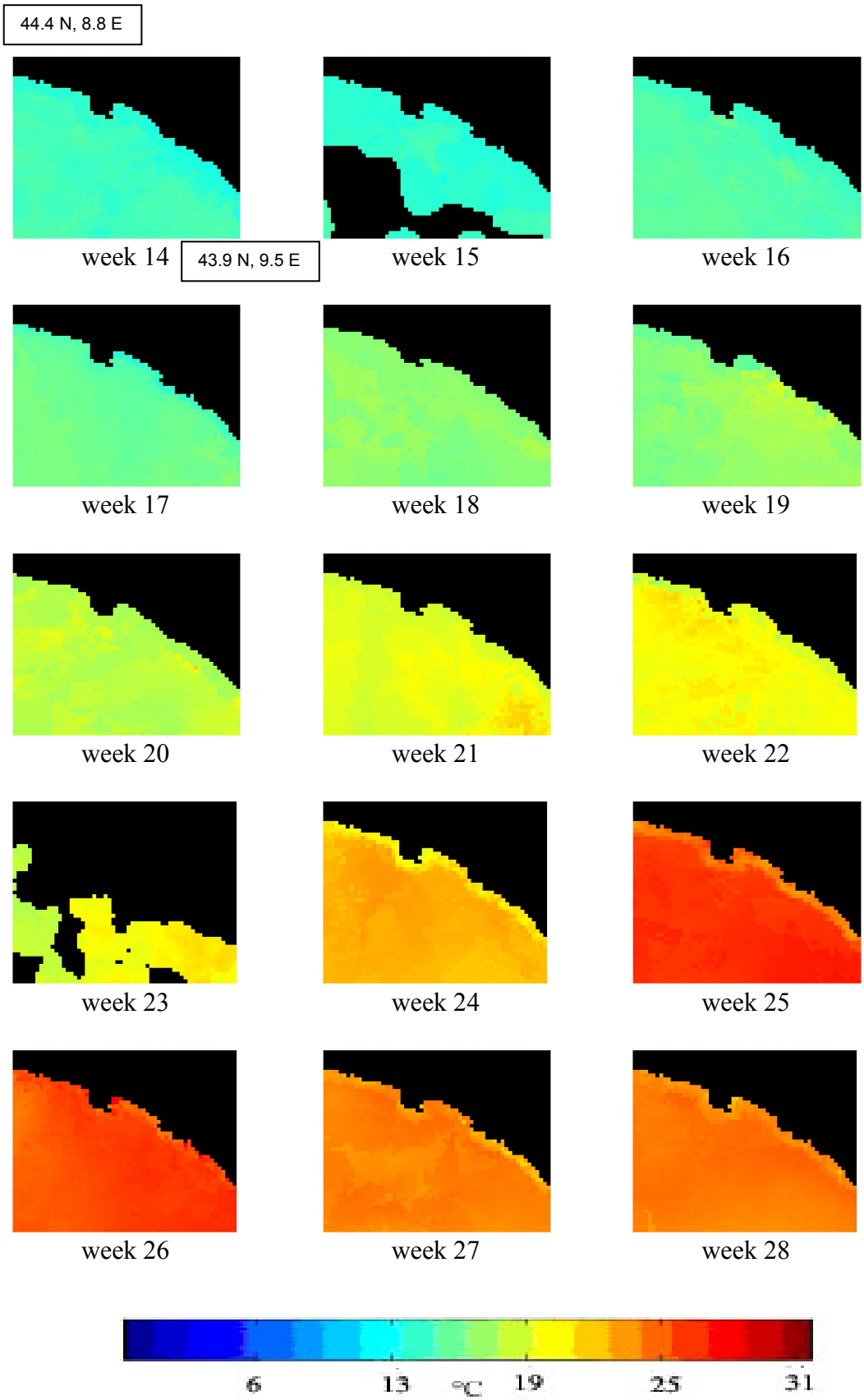

APPENDIX 5 (b) Portofino MPA
Sea Surface Temperature skin (SST skin) maps
(AVHRR data April-December 2002)

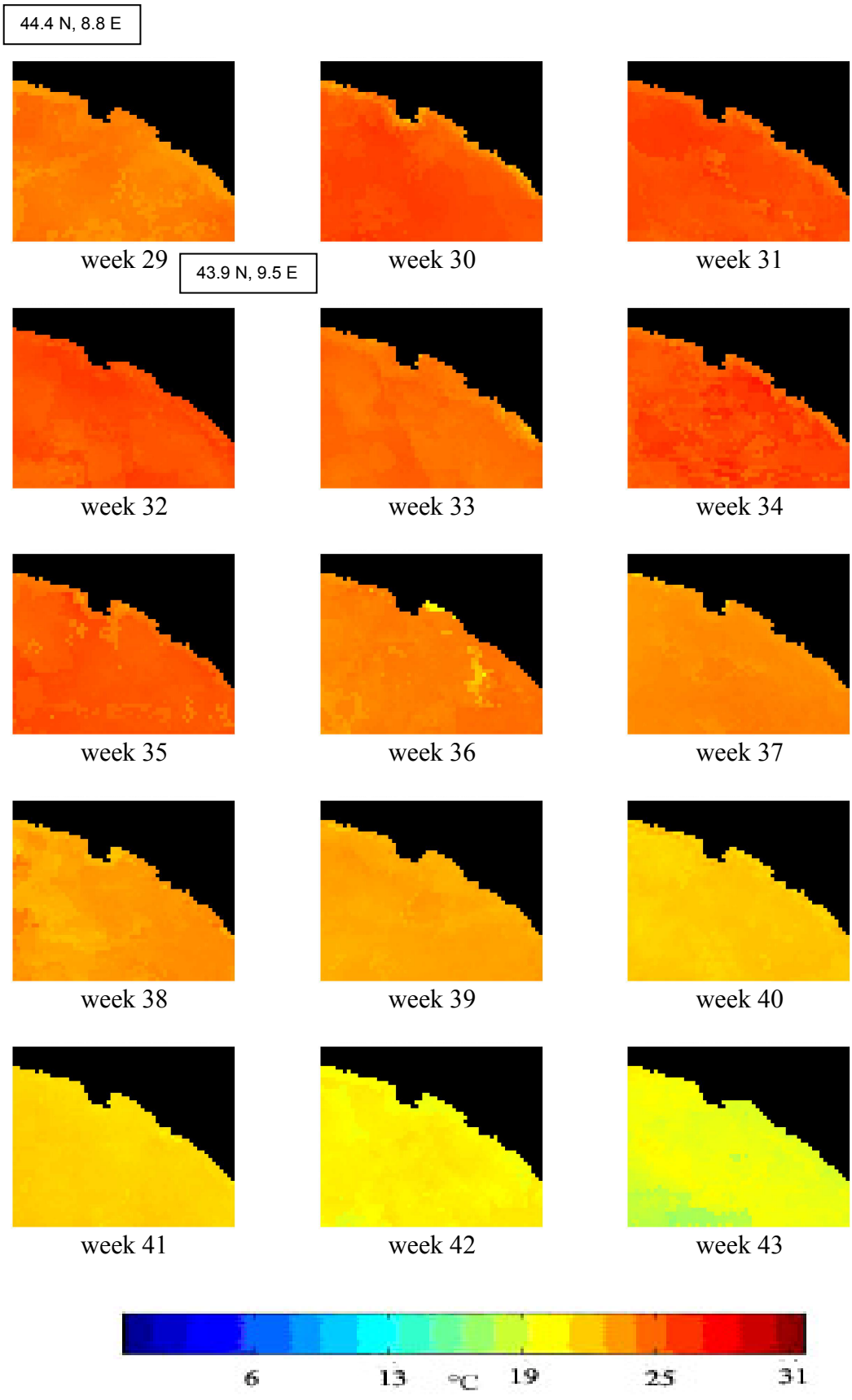

APPENDIX 5 (c) Portofino MPA
Sea Surface Temperature skin (SST skin) maps
(AVHRR data April-December 2002)

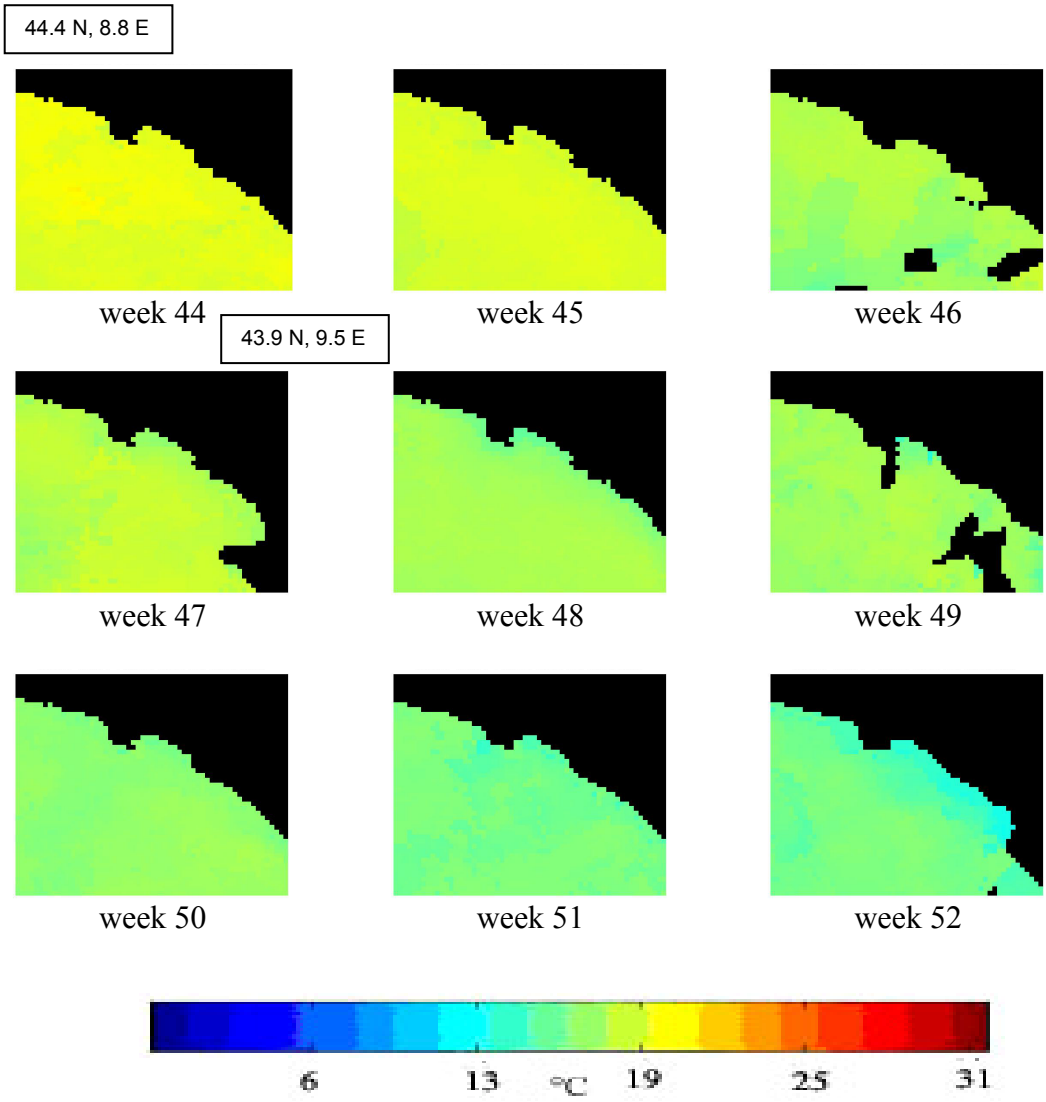

APPENDIX 6 (a) *Pelagos* Sanctuary
Chlorophyll (*chl*) maps (SeaWiFS data year 2002)

44.5 N, 6.0 E

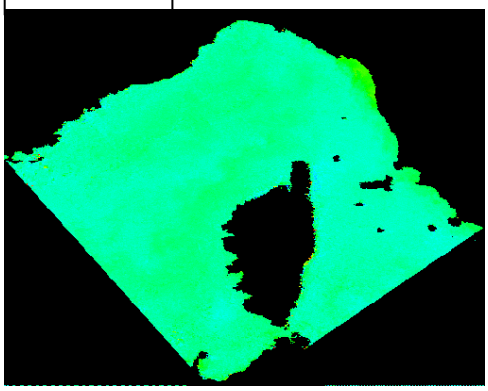

week 1

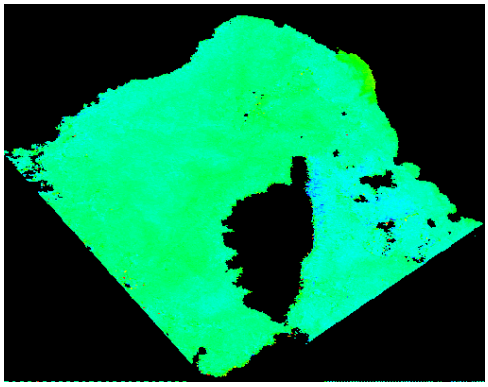

week 2

40.7 N, 11.5 E

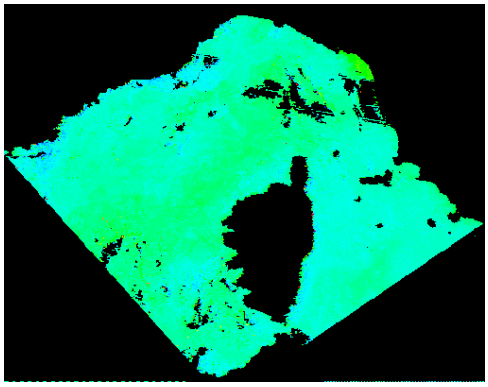

week 3

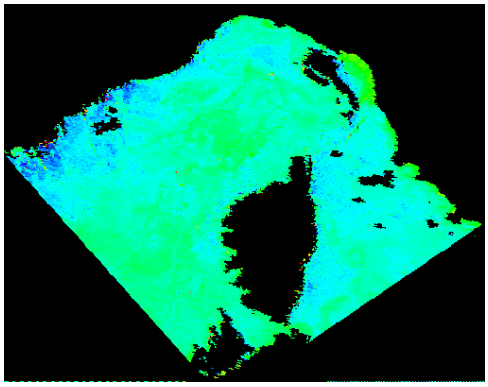

week 4

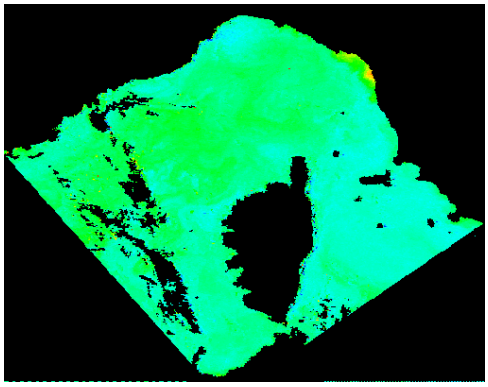

week 5

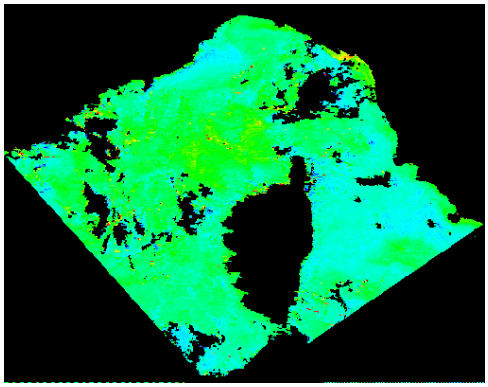

week 6

chl (mg m^{-3})

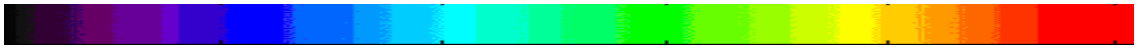

0.057 0.331 1.905 10.966 63.106

APPENDIX 6 (b) *Pelagos* Sanctuary
Chlorophyll (*chl*) maps (SeaWiFS data year 2002)

44.5 N, 6.0 E

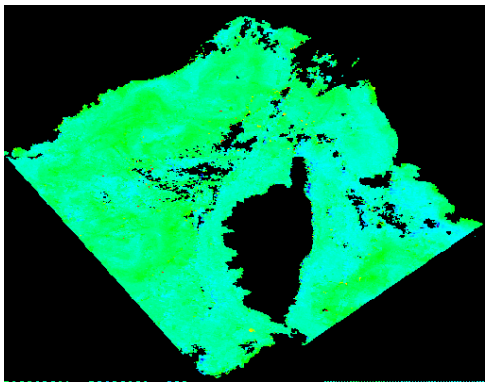

week 7

40.7 N, 11.5 E

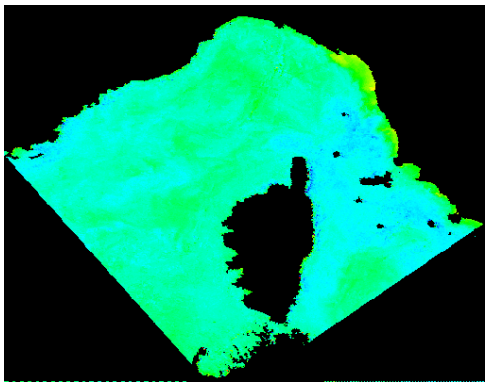

week 8

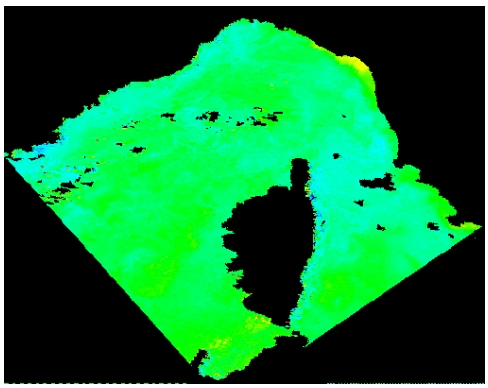

week 9

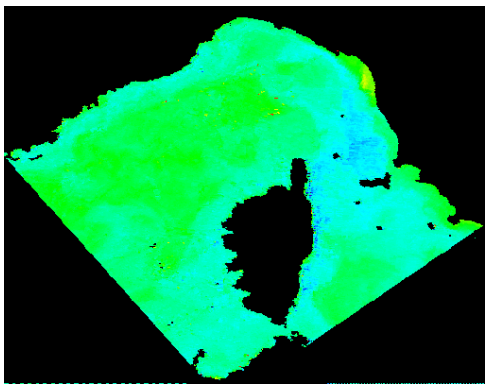

week 10

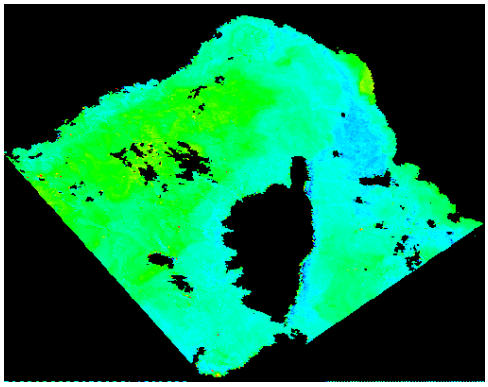

week 11

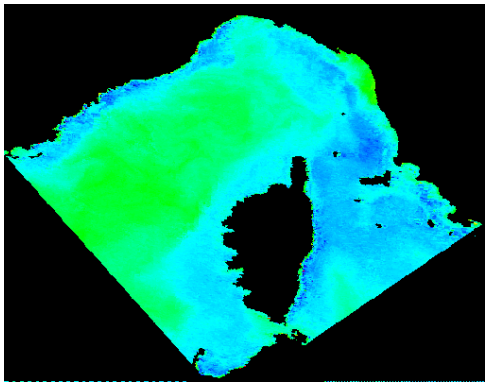

week 12

chl (mg m^{-3})

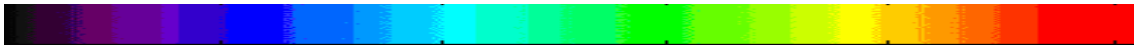

0.057 0.331 1.905 10.966 63.106

APPENDIX 6 (c) *Pelagos* Sanctuary
Chlorophyll (*chl*) maps (SeaWiFS data year 2002)

44.5 N, 6.0 E

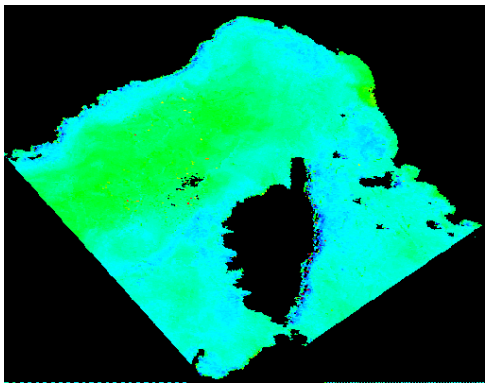

week 13

40.7 N, 11.5 E

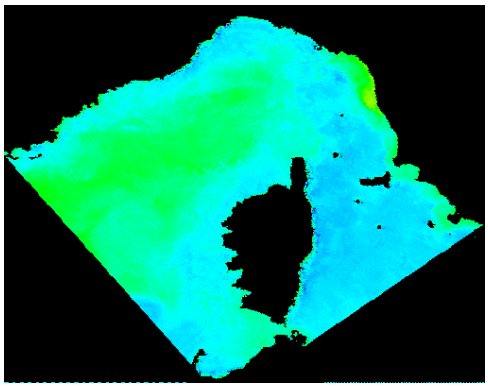

week 16

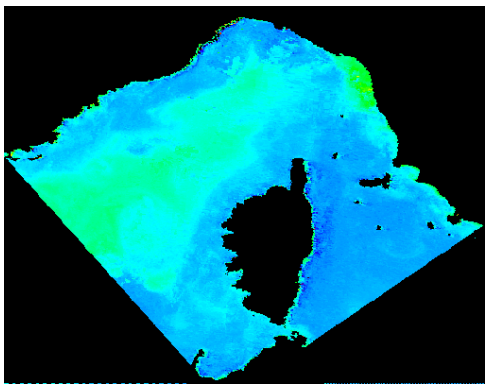

week 17

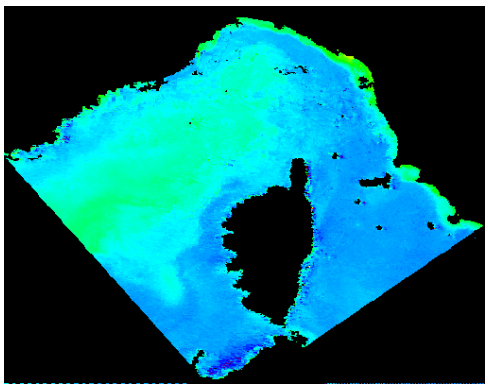

week 18

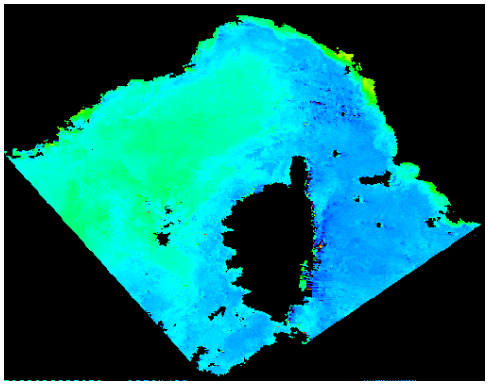

week 19

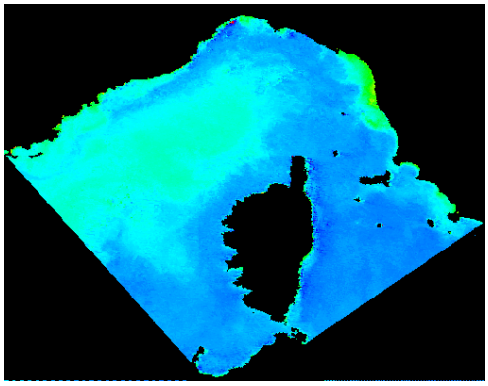

week 20

chl (mg m^{-3})

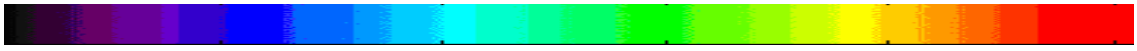

0.057 0.331 1.905 10.966 63.106

APPENDIX 6 (d) *Pelagos* Sanctuary
Chlorophyll (*chl*) maps (SeaWiFS data year 2002)

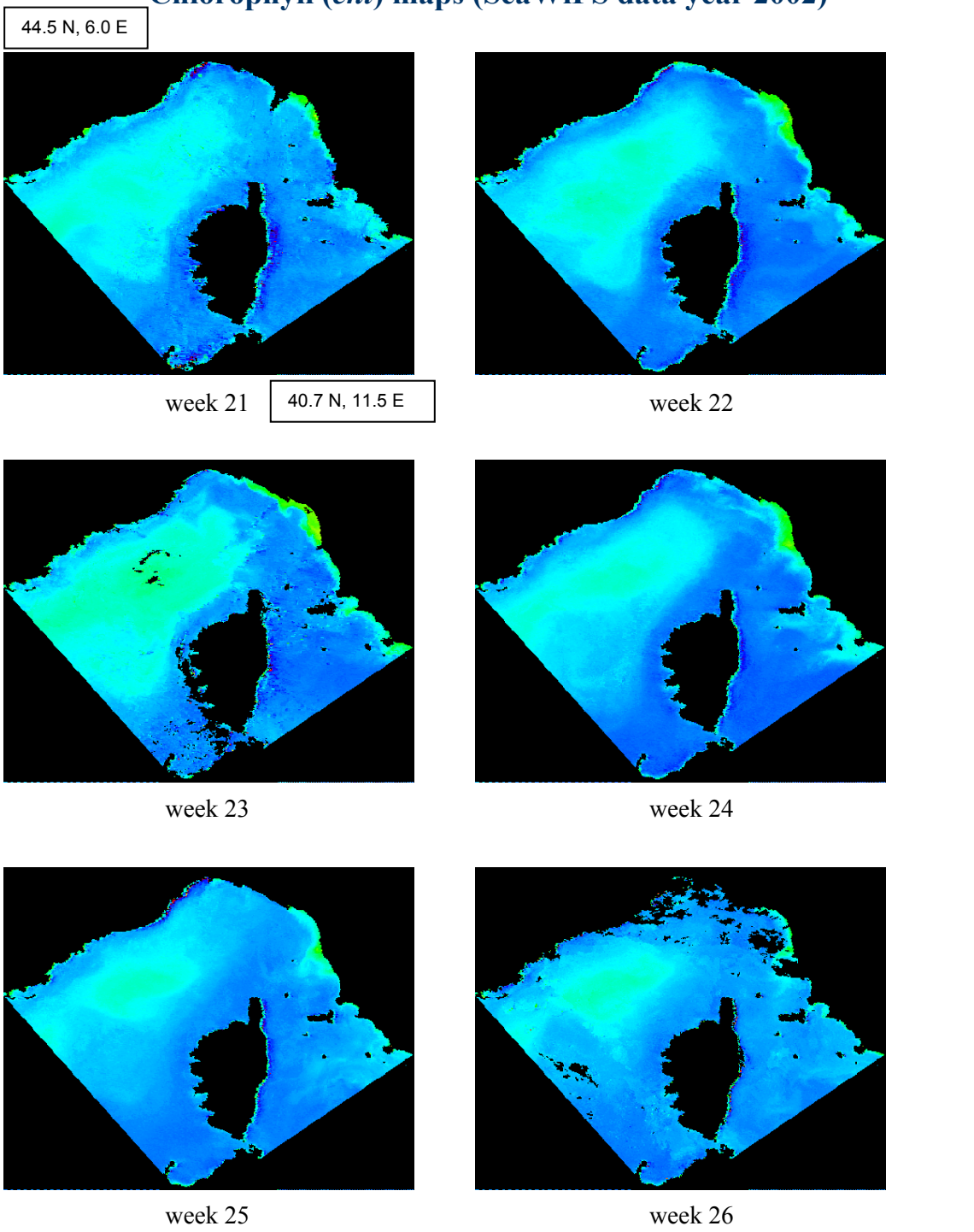

APPENDIX 6 (e) *Pelagos* Sanctuary
Chlorophyll (*chl*) maps (SeaWiFS data year 2002)

44.5 N, 6.0 E

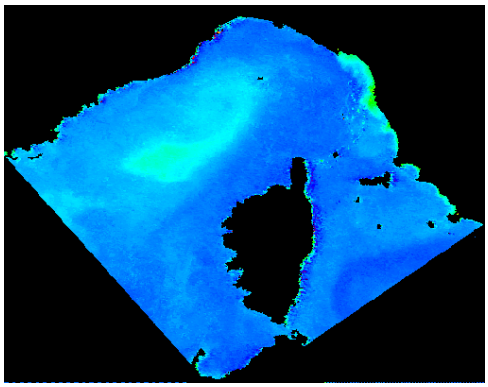

week 28

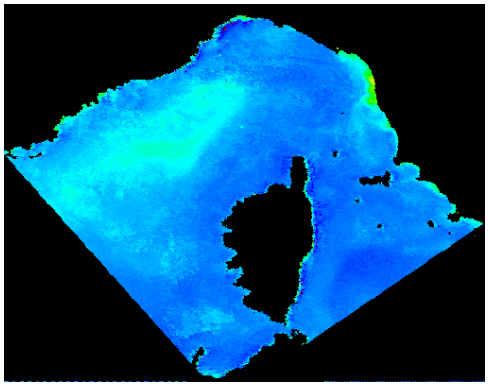

week 29

40.7 N, 11.5 E

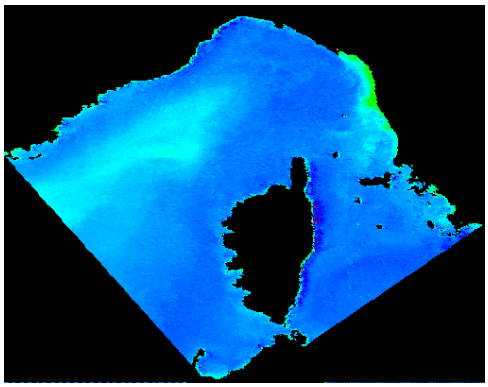

week 30

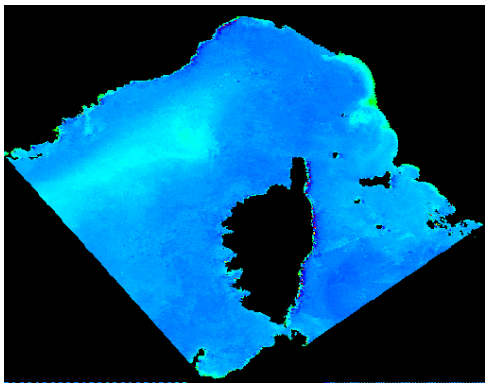

week 31

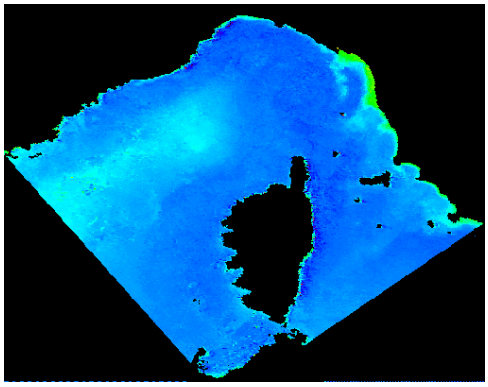

week 32

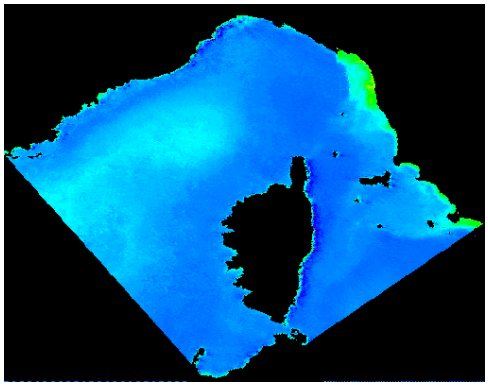

week 33

chl (mg m^{-3})

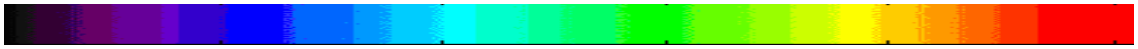

0.057 0.331 1.905 10.966 63.106

APPENDIX 6 (f) *Pelagos* Sanctuary
Chlorophyll (*chl*) maps (SeaWiFS data year 2002)

44.5 N, 6.0 E

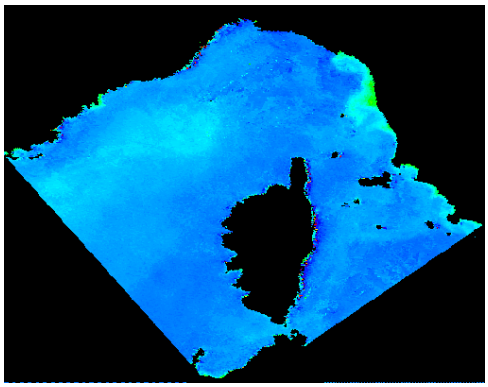

week 34

40.7 N, 11.5 E

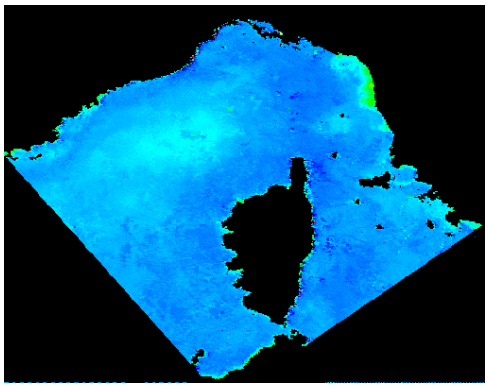

week 35

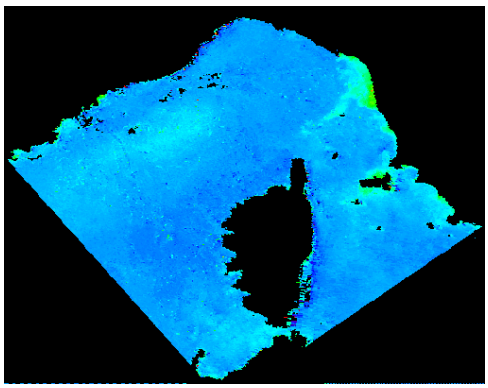

week 36

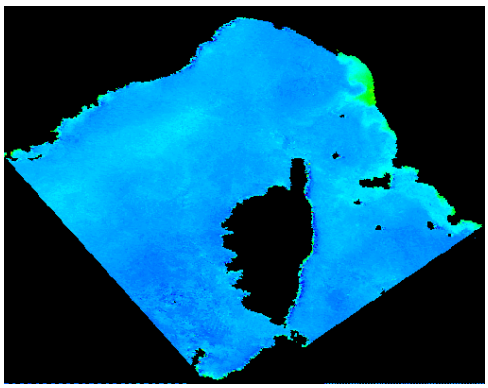

week 37

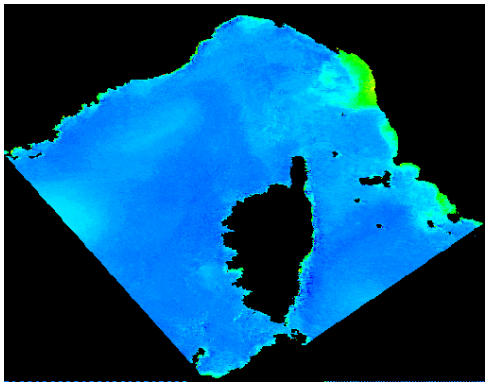

week 39

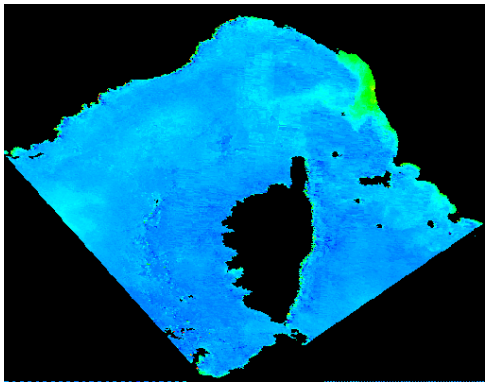

week 40

chl (mg m^{-3})

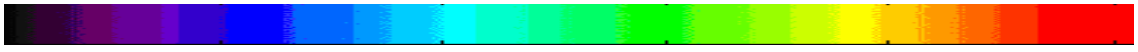

0.057 0.331 1.905 10.966 63.106

APPENDIX 6 (g) *Pelagos* Sanctuary
Chlorophyll (*chl*) maps (SeaWiFS data year 2002)

44.5 N, 6.0 E

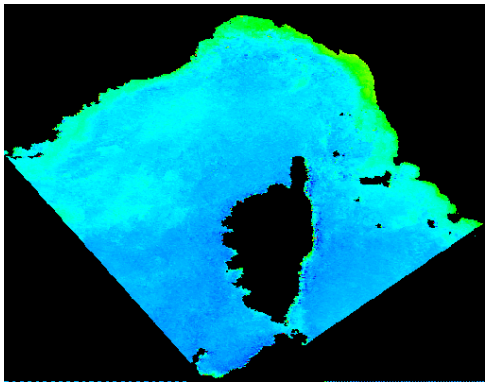

week 43

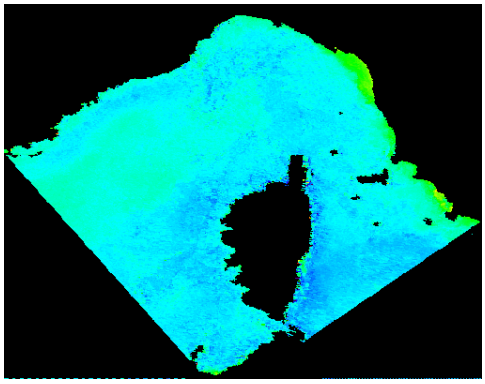

week 45

40.7 N, 11.5 E

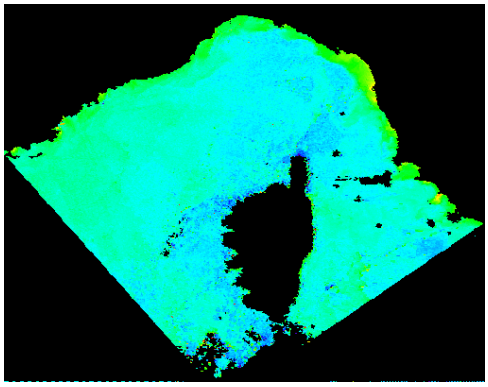

week 48

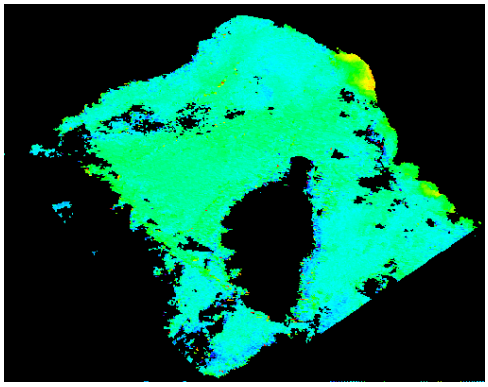

week 51

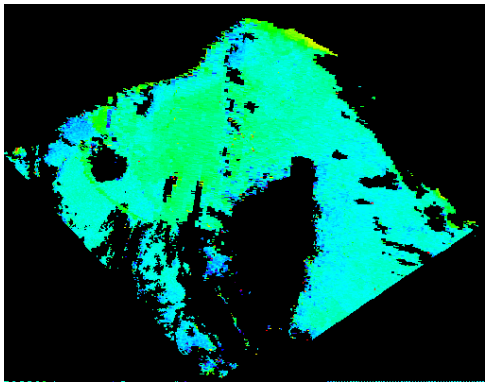

week 52

chl (mg m^{-3})

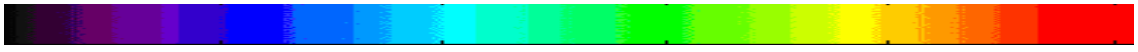

0.057 0.331 1.905 10.966 63.106

APPENDIX 7 (a) *Pelagos* Sanctuary
Threshold *chl* range 1.0-1.9 mg m^{-3} (SeaWiFS data year 2002)

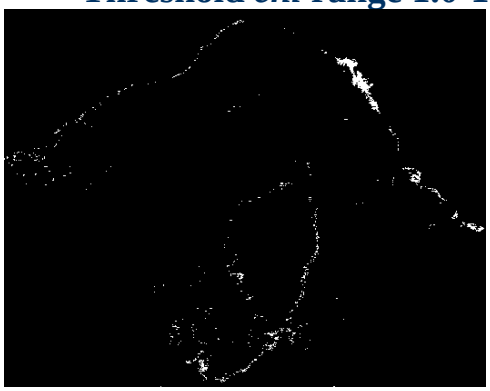

week 1

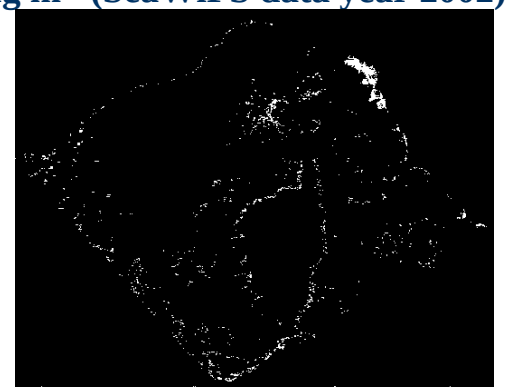

week 2

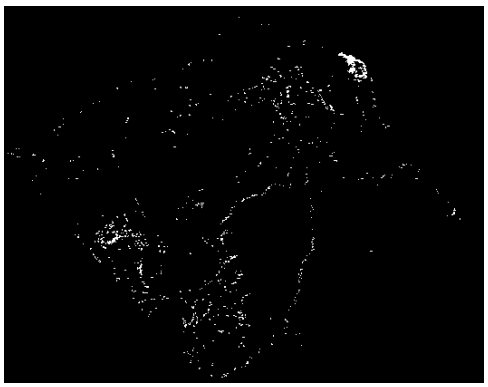

week 3

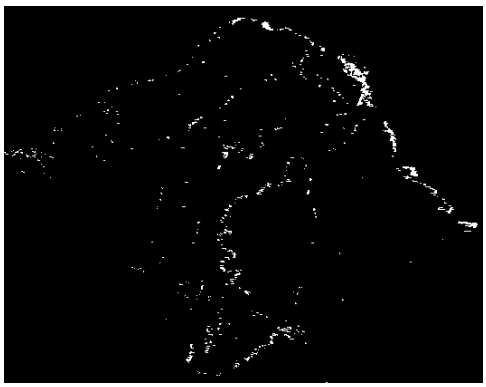

week 4

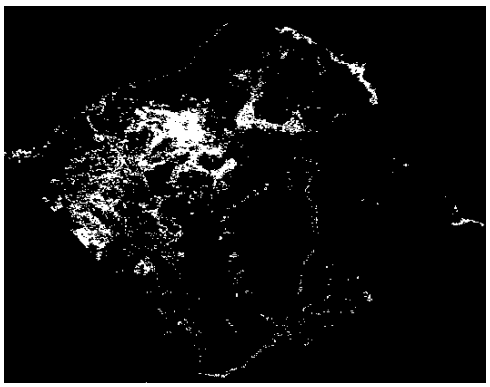

week 5

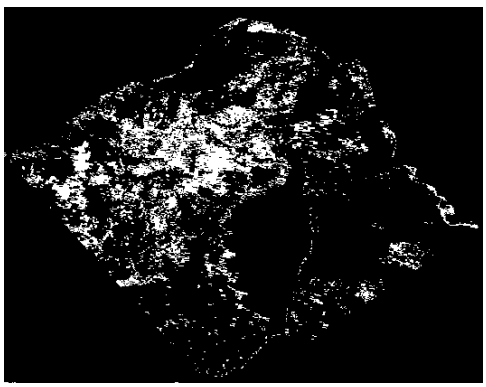

week 6

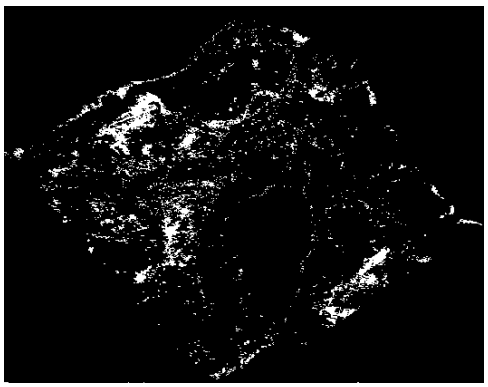

week 7

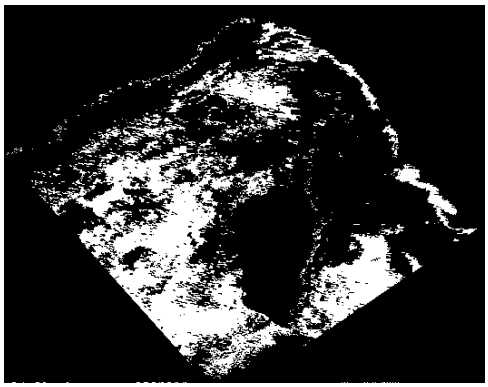

week 9

APPENDIX 7 (b) *Pelagos* Sanctuary
Threshold *chl* range 1.0-1.9 mg m^{-3} (SeaWiFS data year 2002)

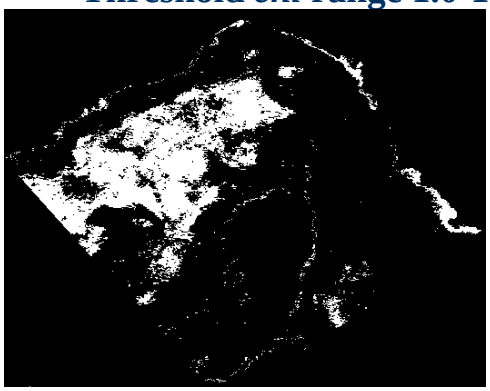

week 10

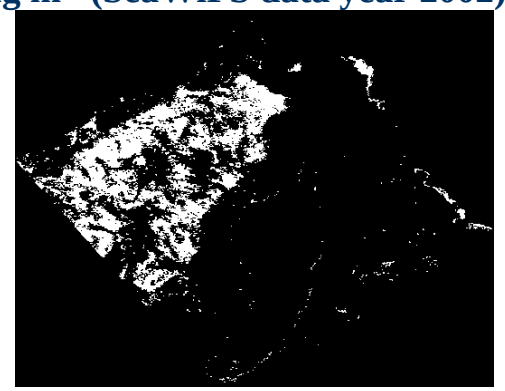

week 11

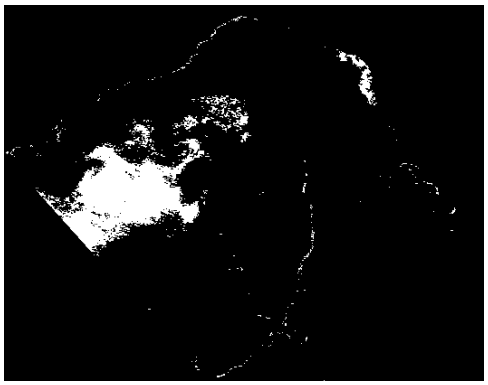

week 12

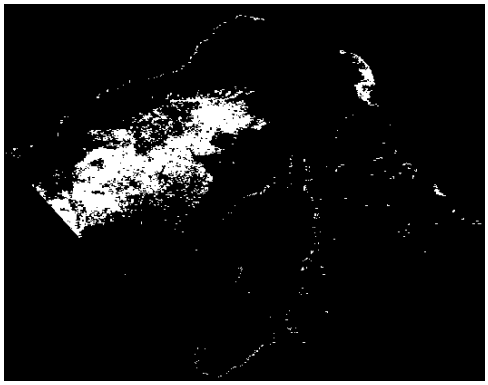

week 13

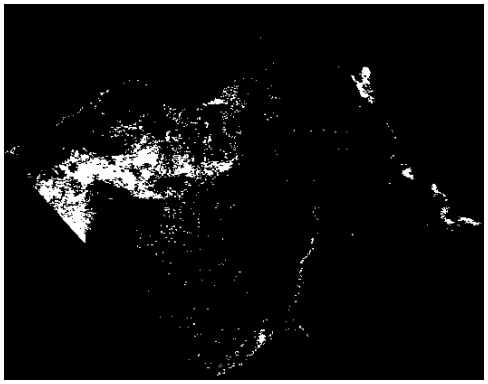

week 15

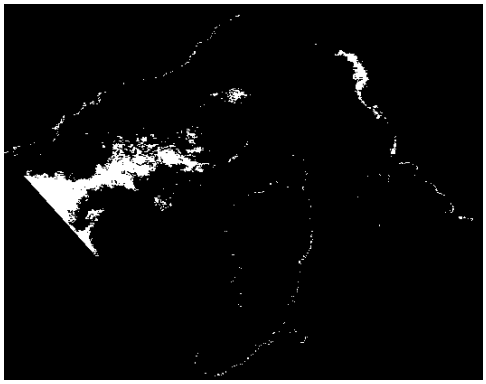

week 16

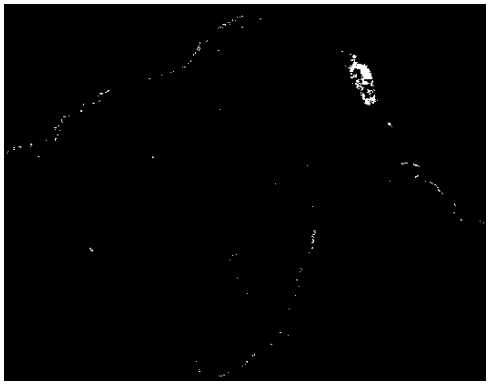

week 17

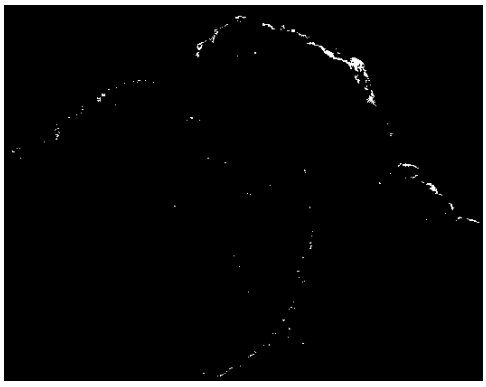

week 18

APPENDIX 7 (c) *Pelagos* Sanctuary
Threshold *chl* range 1.0-1.9 mg/m^3 (SeaWiFS data year 2002)

week 19

week 20

week 21

week 22

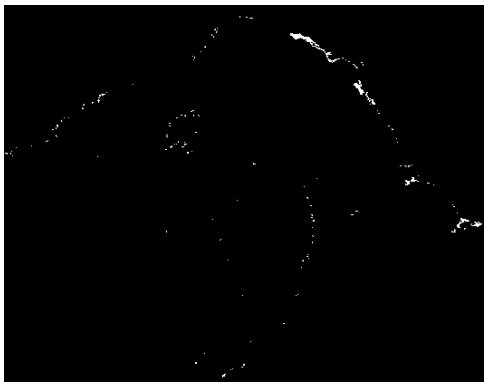

week 23

week 24

week 27

week 33

APPENDIX 7 (d) *Pelagos* Sanctuary
Threshold *chl* range 1.0-1.9 mg m^{-3} (SeaWiFS data year 2002)

week 39

week 41

week 43

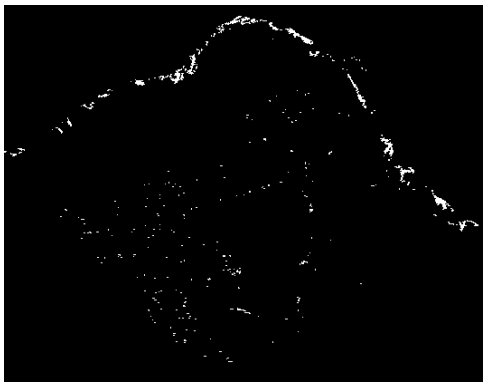

week 47

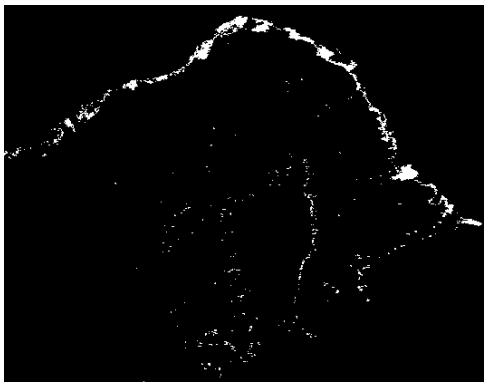

week 48

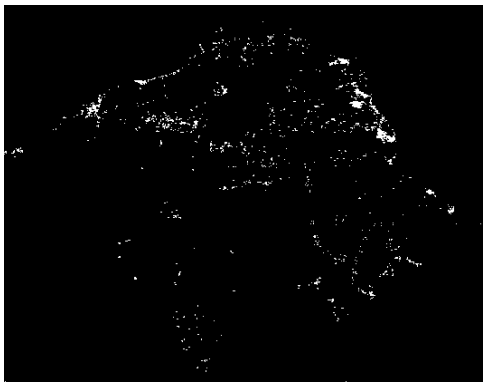

week 49

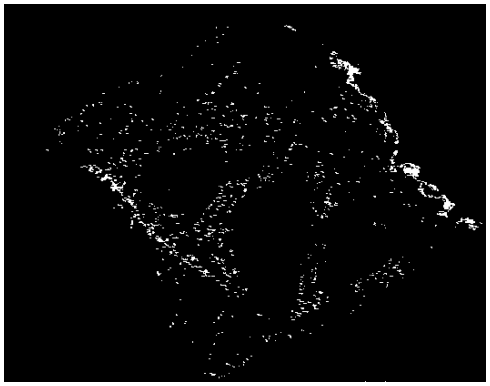

week 51

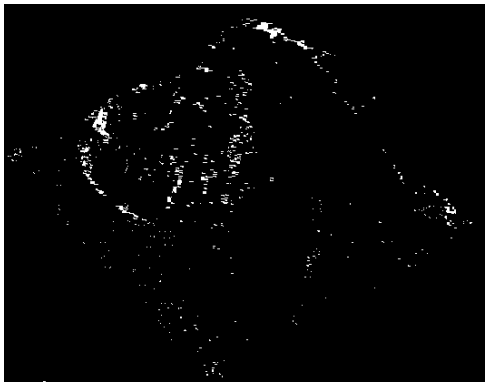

week 52

APPENDIX 8 (a) *Pelagos* Sanctuary
Spatial Gradient (*chl* range 0.164-0.9 mg m^{-3})

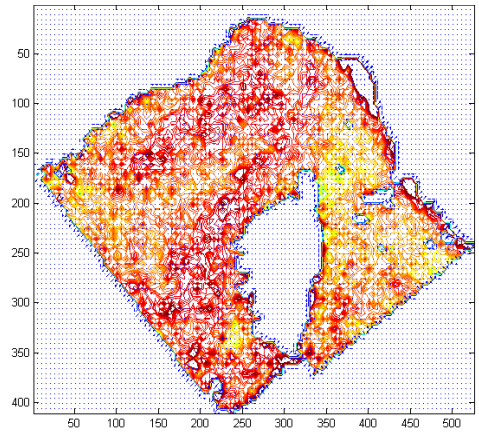

week 1

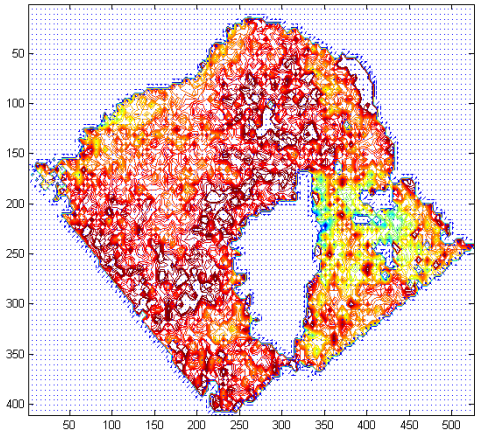

week 2

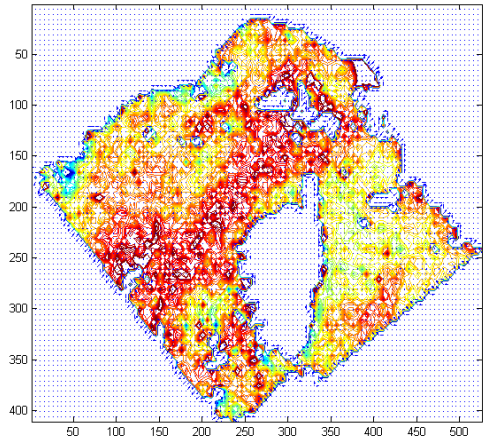

week 3

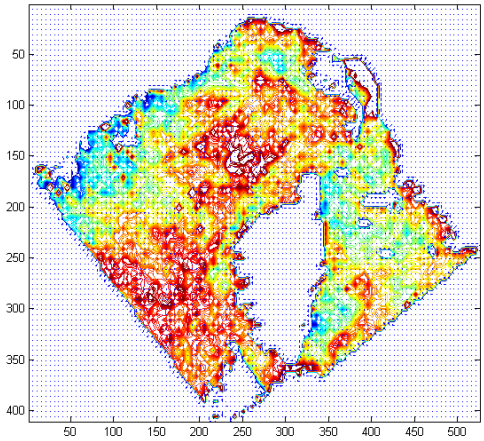

week 4

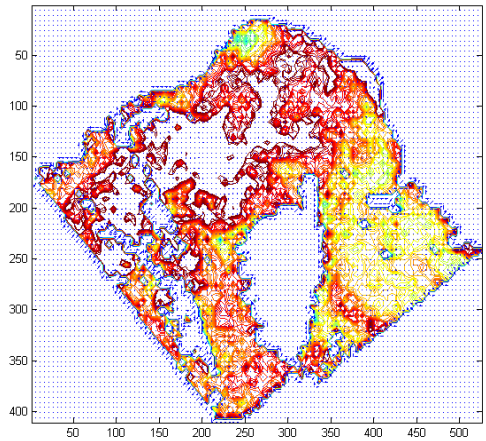

week 5

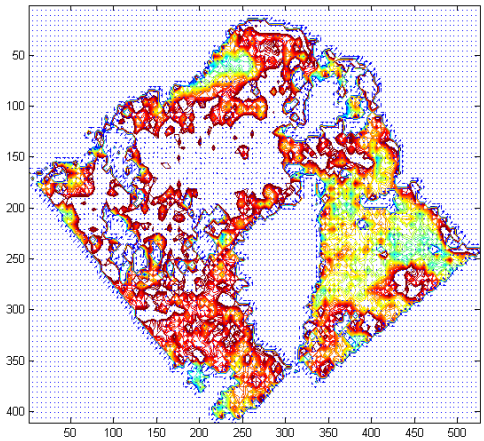

week 6

chl (mg m^{-3})

0.16 0.19 0.23 0.27 0.33 0.39 0.46 0.55 0.66 0.79

APPENDIX 8 (b) *Pelagos* Sanctuary
Spatial Gradient (*chl* range 0.164-0.9 mg m^{-3})

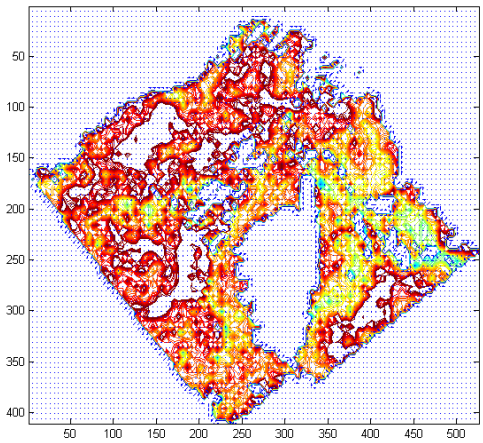

week 7

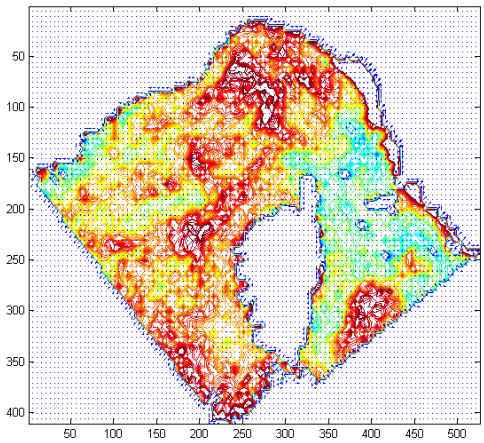

week 8

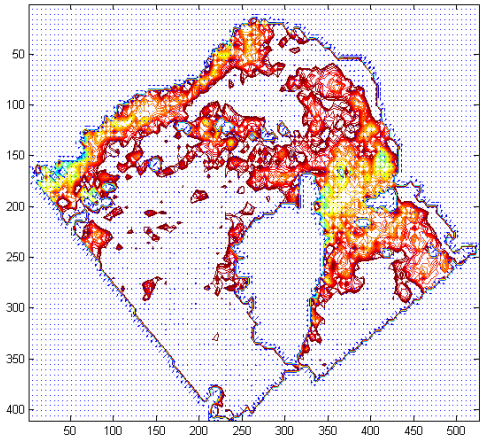

week 9

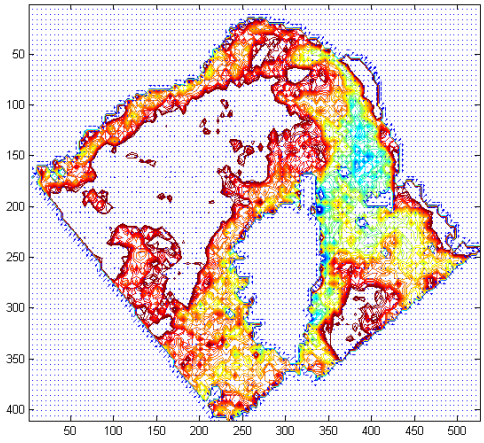

week 10

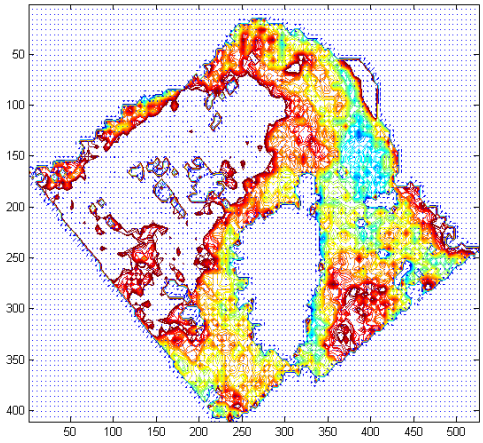

week 11

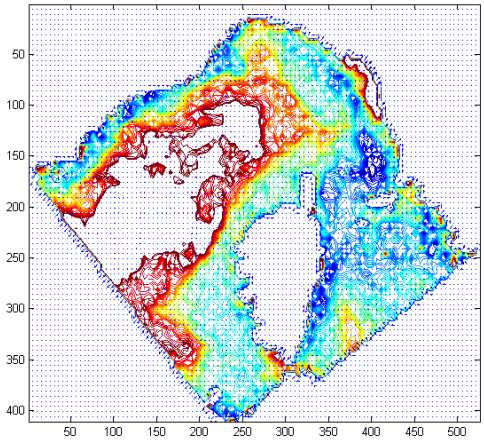

week 13

chl (mg m^{-3})

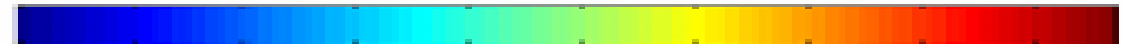

0.16 0.19 0.23 0.27 0.33 0.39 0.46 0.55 0.66 0.79

APPENDIX 8 (c) *Pelagos* Sanctuary
Spatial Gradient (*chl* range 0.164-0.9 mg m^{-3})

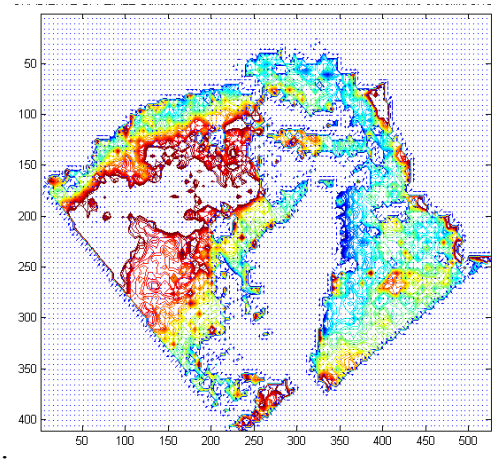

week 15

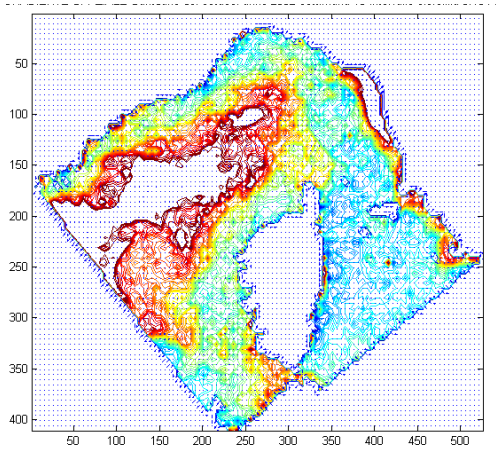

week 16

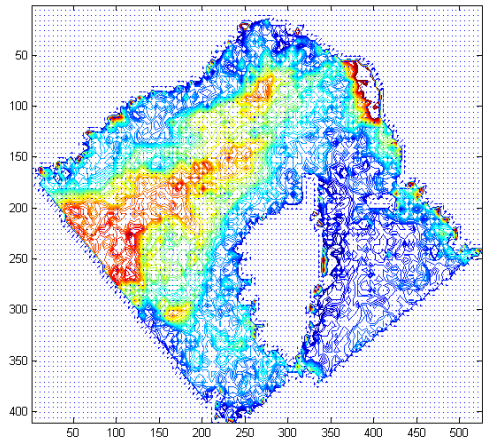

week 17

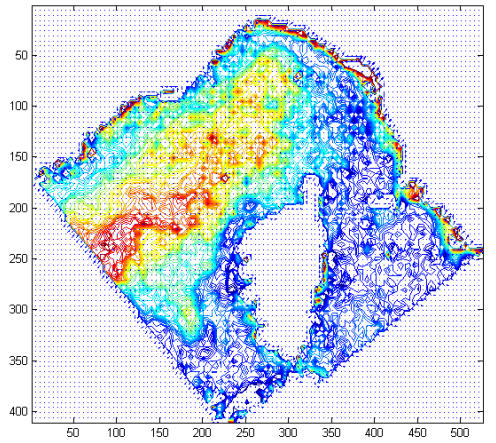

week 18

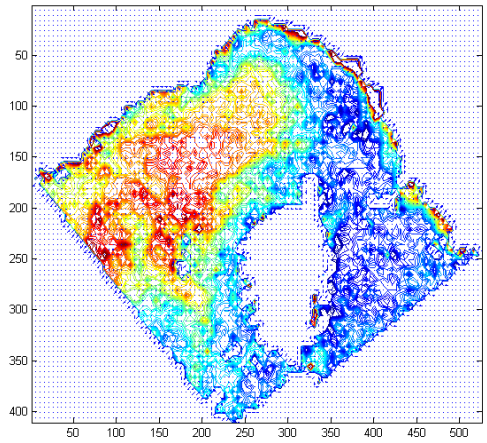

week 19

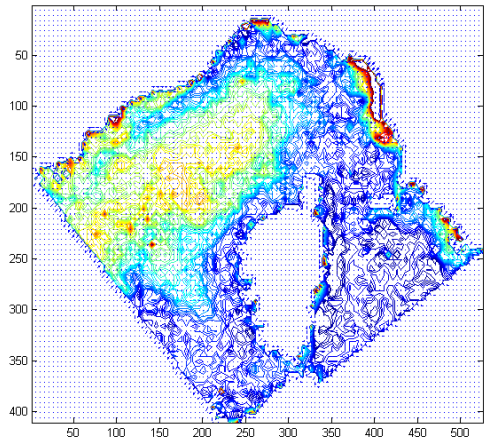

week 20

chl (mg m^{-3})

0.16 0.19 0.23 0.27 0.33 0.39 0.46 0.55 0.66 0.79

APPENDIX 8 (d) *Pelagos* Sanctuary
Spatial Gradient (*chl* range 0.164-0.9 mg m^{-3})

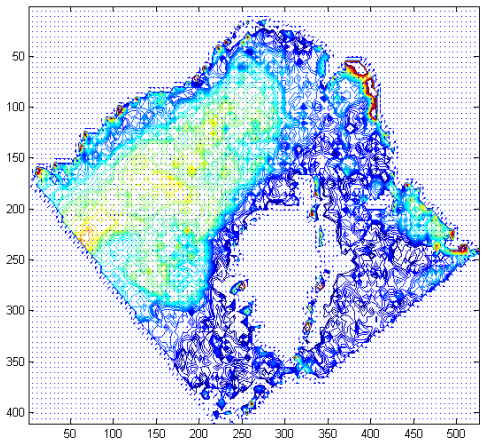

week 21

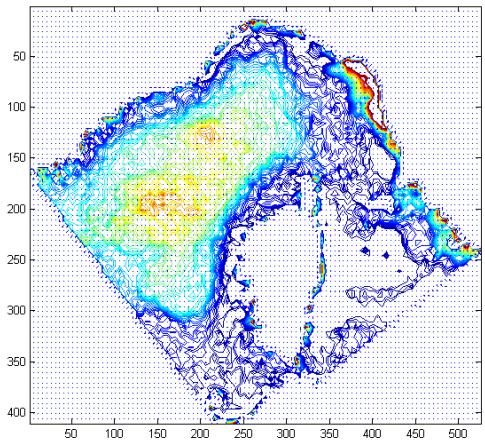

week 22

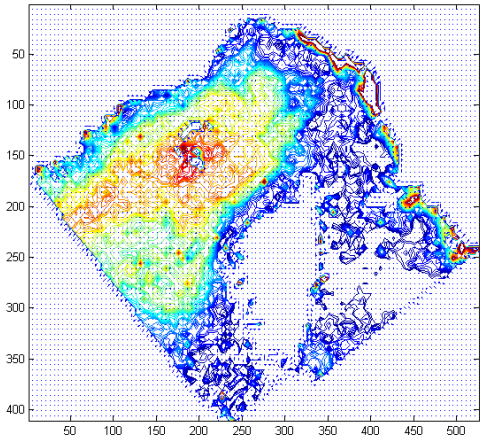

week 23

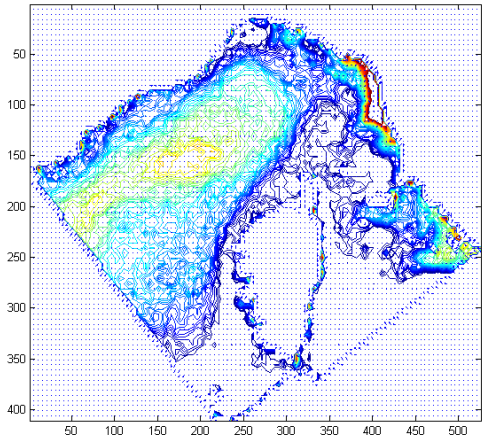

week 24

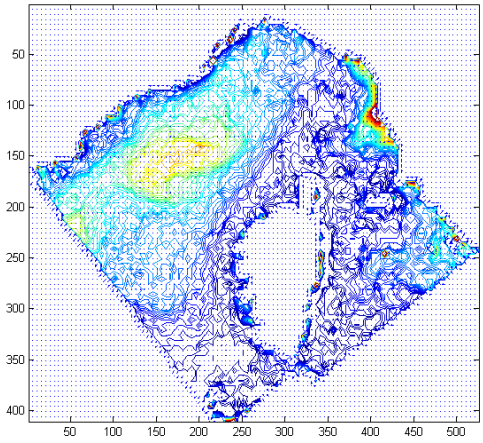

week 25

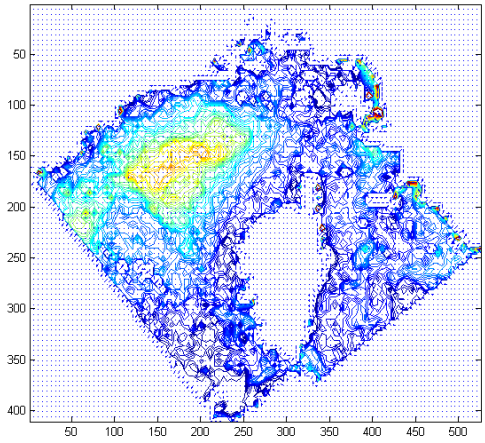

week 26

chl (mg m^{-3})

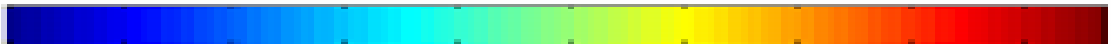

0.16 0.19 0.23 0.27 0.33 0.39 0.46 0.55 0.66 0.79

APPENDIX 8 (e) *Pelagos* Sanctuary
Spatial Gradient (*chl* range 0.164-0.9 mg m^{-3})

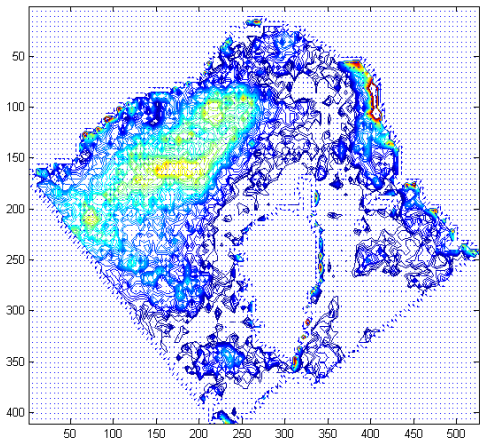

week 29

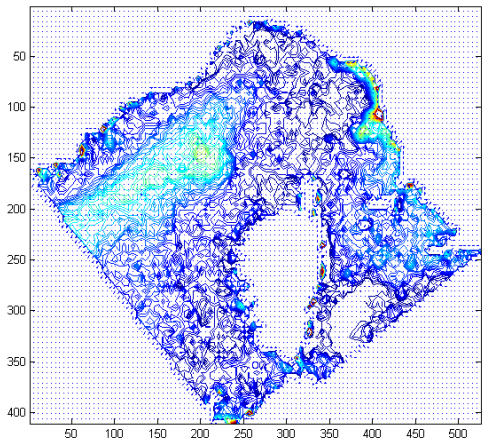

week 31

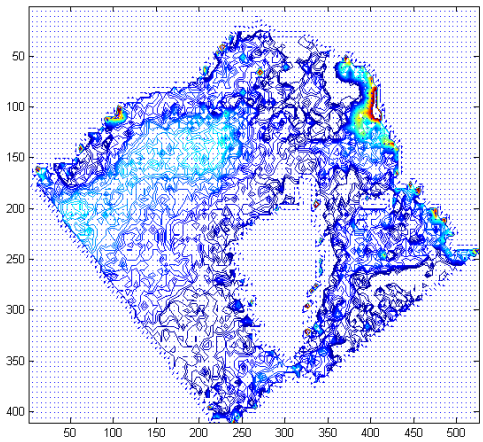

week 34

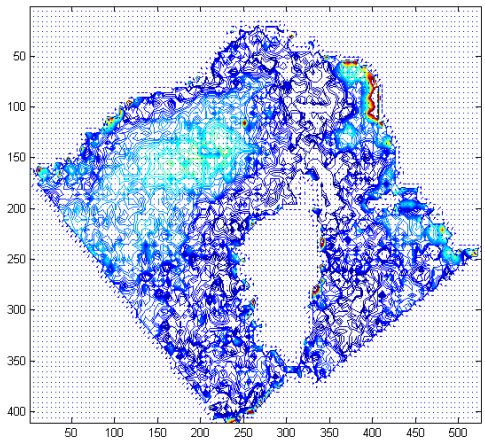

week 36

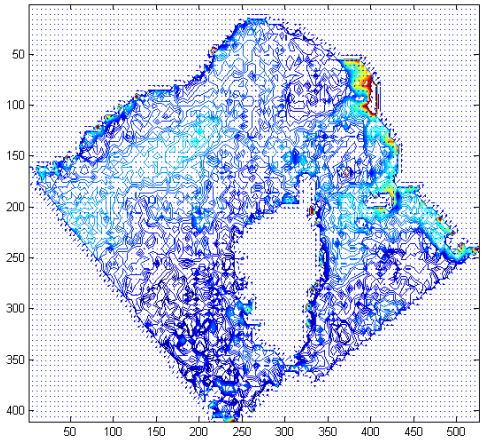

week 37

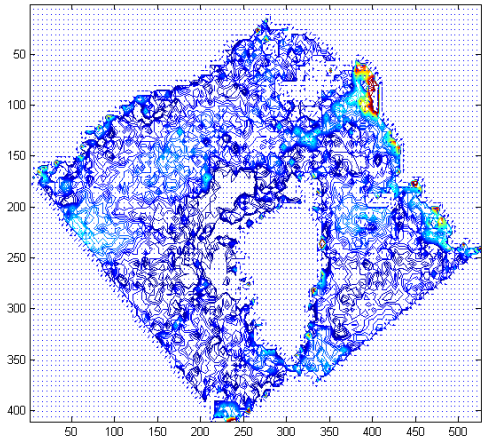

week 38

chl (mg m^{-3})

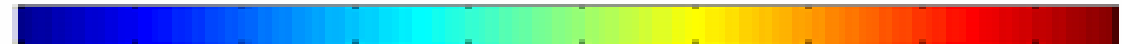

0.16 0.19 0.23 0.27 0.33 0.39 0.46 0.55 0.66 0.79

APPENDIX 8 (f) *Pelagos* Sanctuary
Spatial Gradient (*chl* range 0.164-0.9 mg m^{-3})

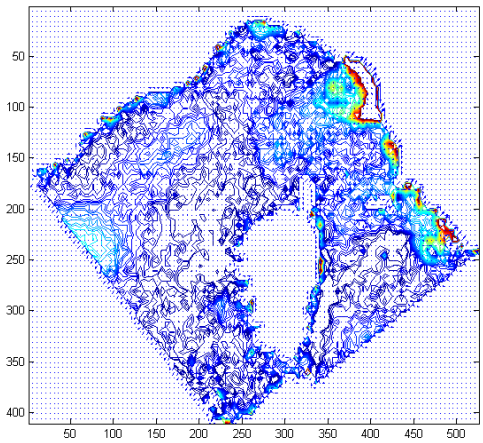

week 39

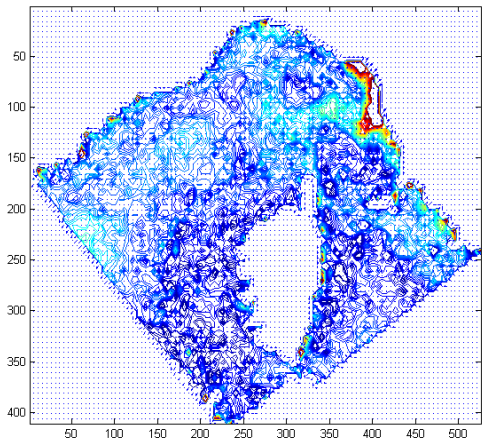

week 40

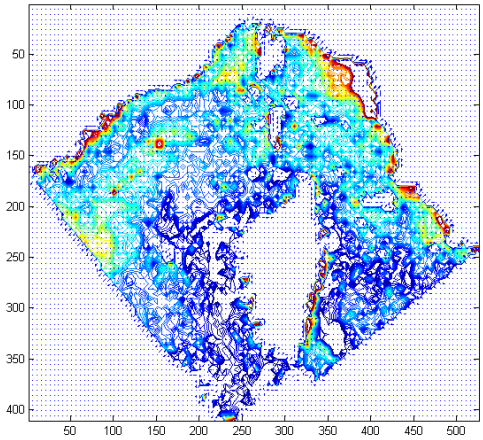

week 41

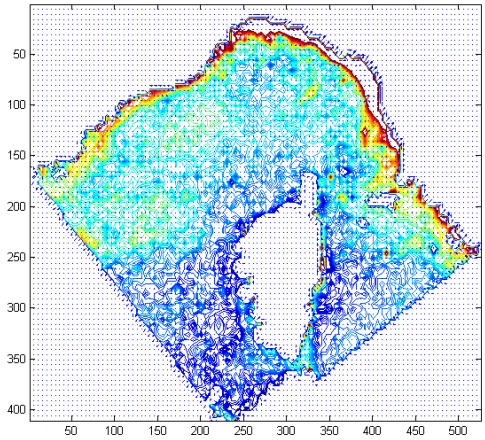

week 43

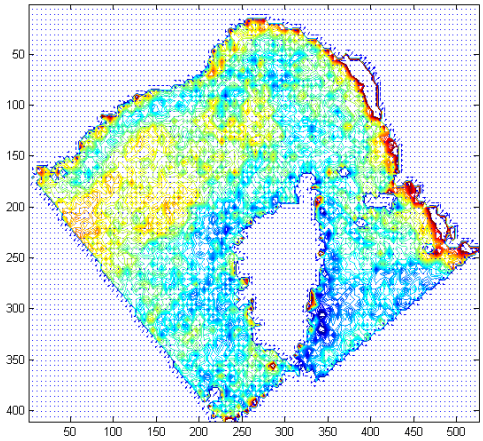

week 45

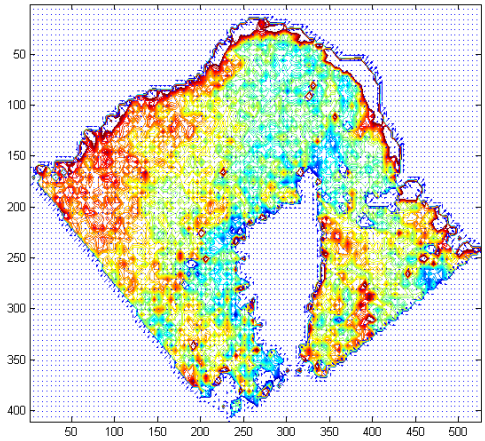

week 48

chl (mg m^{-3})

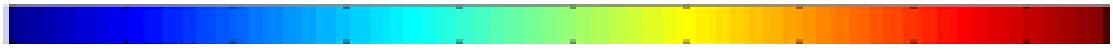

0.16 0.19 0.23 0.27 0.33 0.39 0.46 0.55 0.66 0.79

APPENDIX 8 (g) *Pelagos* Sanctuary
Spatial Gradient (*chl* range 0.164-0.9 mg m^{-3})

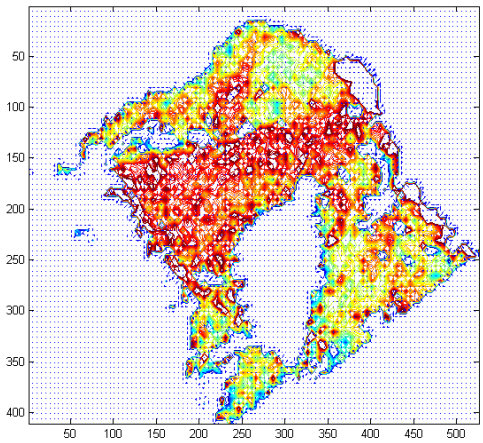

week 50

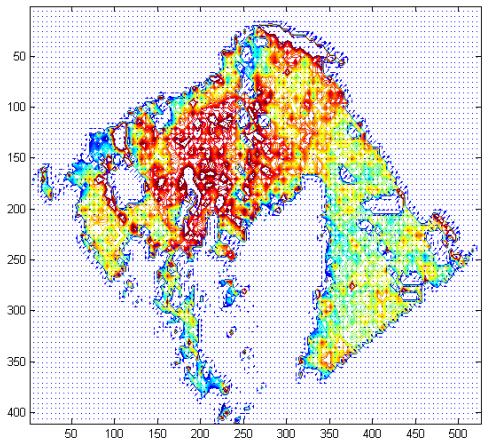

week 52

chl (mg m^{-3})

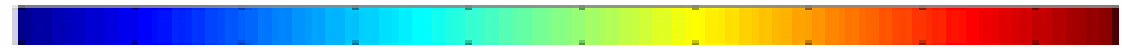

0.16 0.19 0.23 0.27 0.33 0.39 0.46 0.55 0.66 0.79

APPENDIX 9 (a) *Pelagos* Sanctuary
Spatial Gradient (*chl* range 1.0-1.9 mg m^{-3})

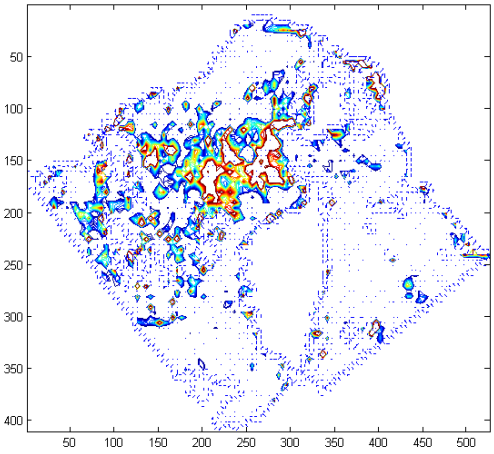

week 6

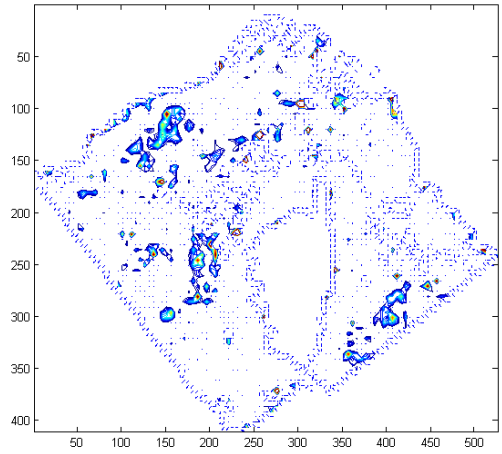

week 7

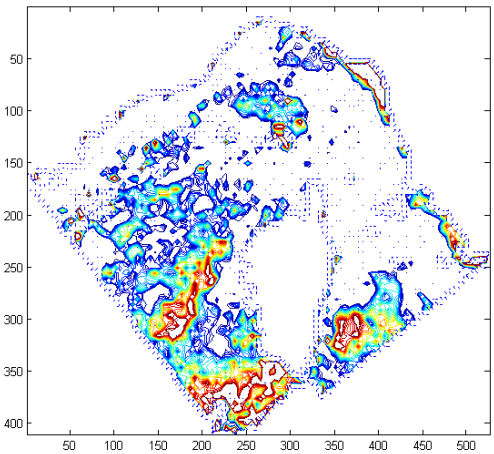

week 9

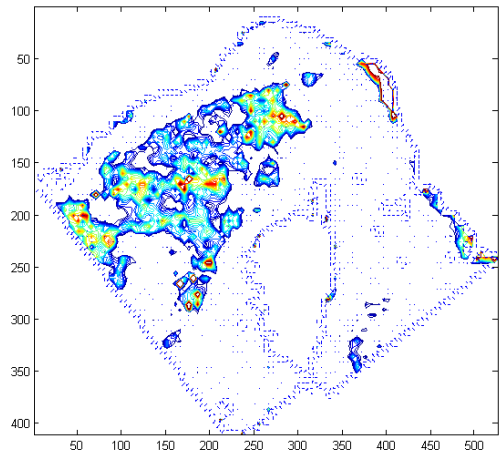

week 10

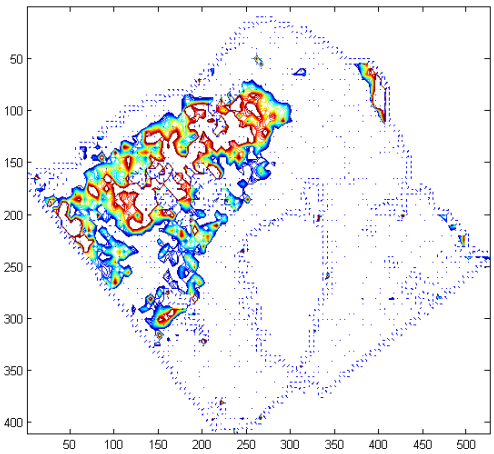

week 11

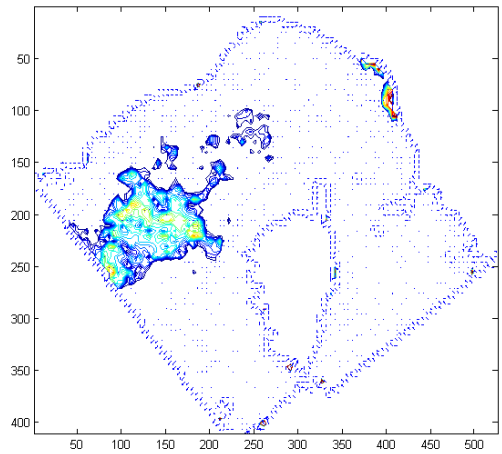

week 12

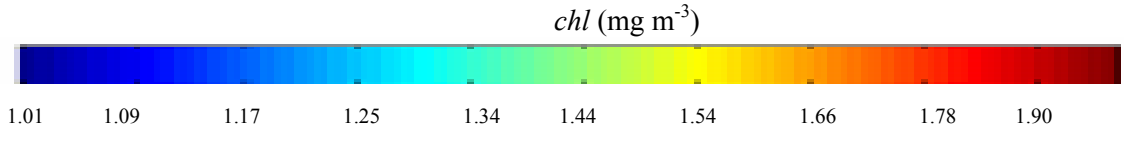

APPENDIX 9 (b) *Pelagos* Sanctuary
Spatial Gradient (*chl* range 1.0-1.9 mg m^{-3})

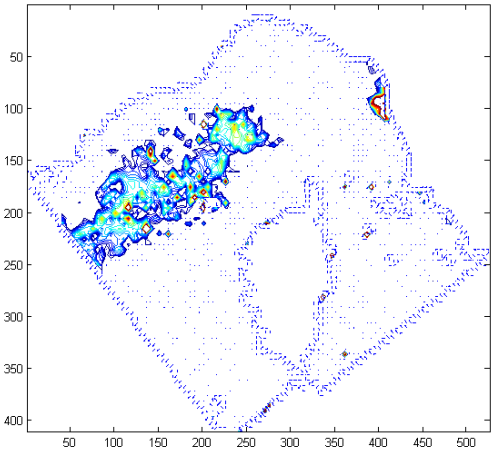

week 13

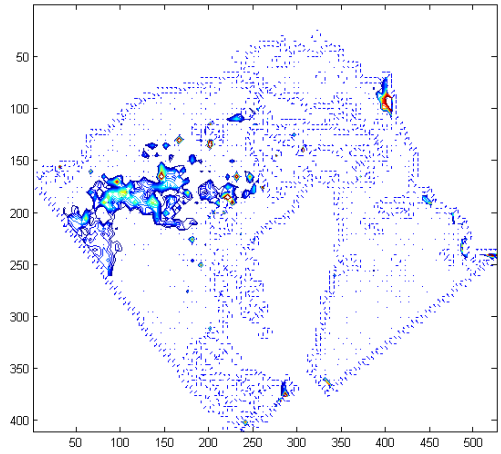

week 15

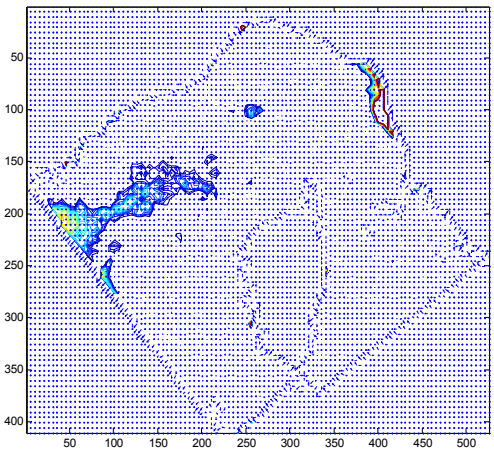

week 16

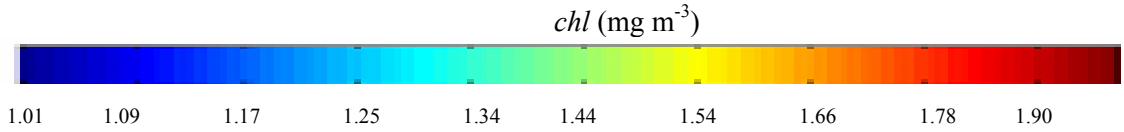

APPENDIX 10 (a) *Pelagos* Sanctuary MPA
Sea Surface Temperature skin (SST skin) maps
(AVHRR data April-December 2002)

44.5 N, 6.0 E

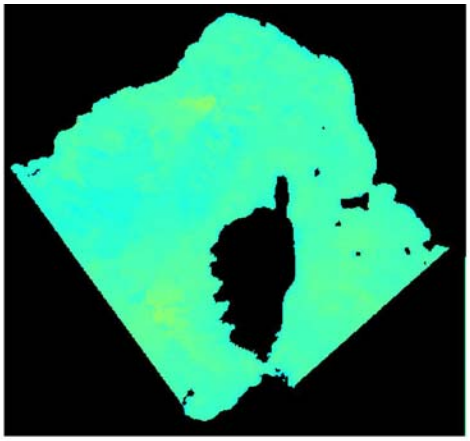

week 14

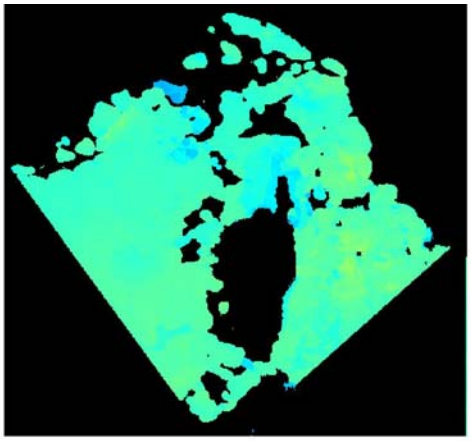

week 15

40.7 N, 11.5 E

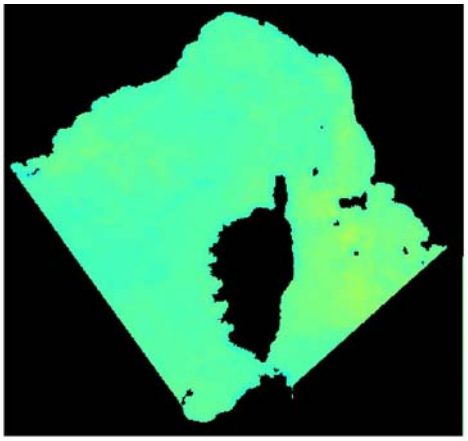

week 16

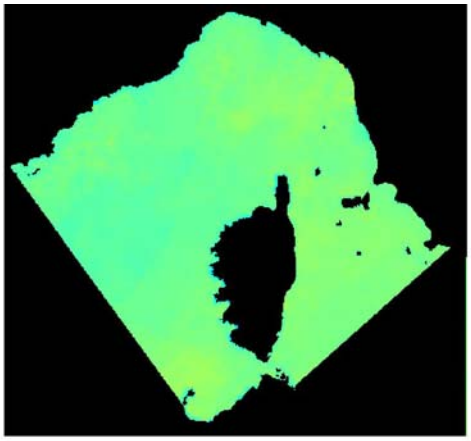

week 17

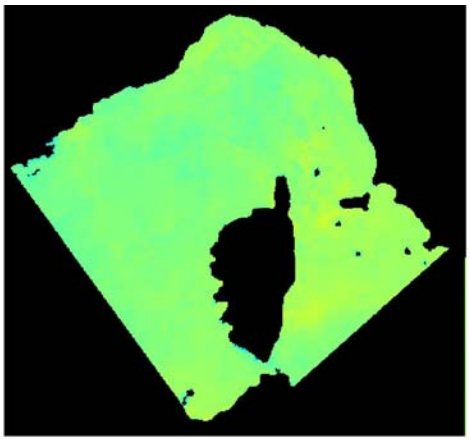

week 18

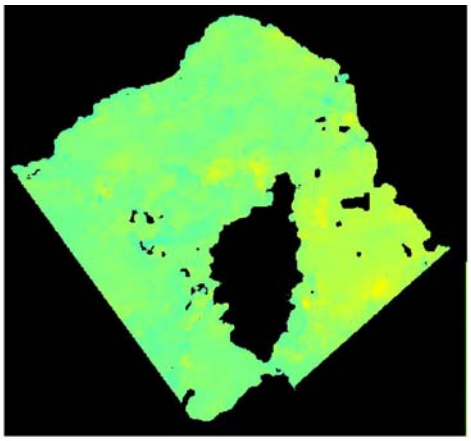

week 19

APPENDIX 10 (b) *Pelagos* Sanctuary MPA
Sea Surface Temperature skin (SST skin) maps
(AVHRR data April-December 2002)

44.5 N, 6.0 E

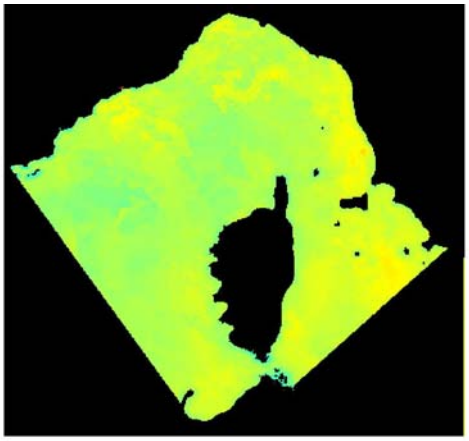

week 20

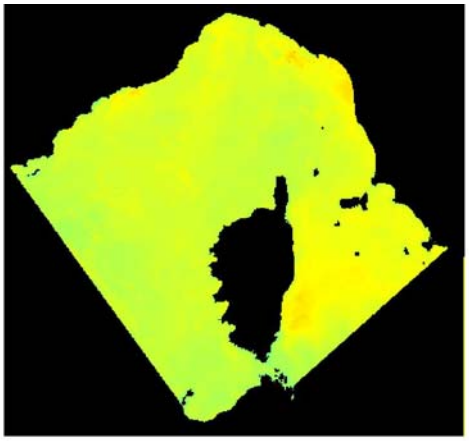

week 21

40.7 N, 11.5 E

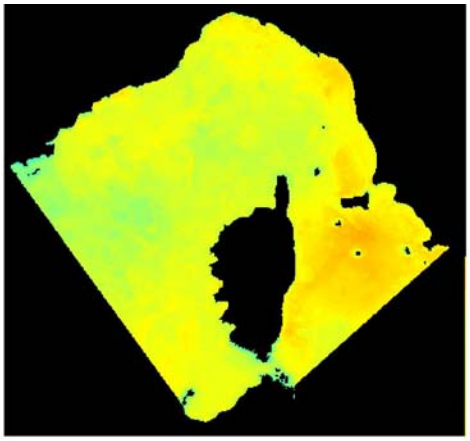

week 22

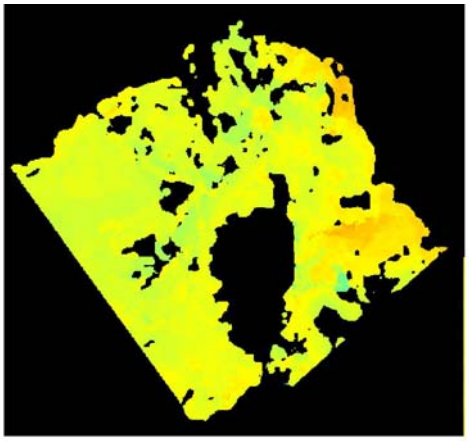

week 23

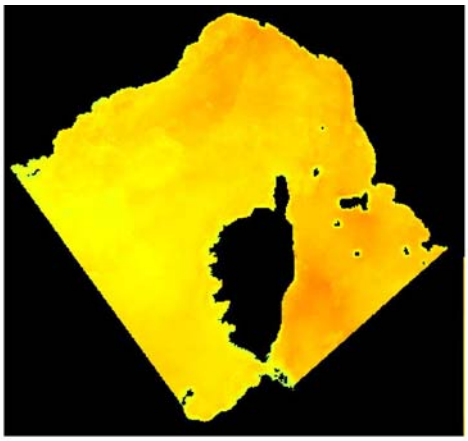

week 24

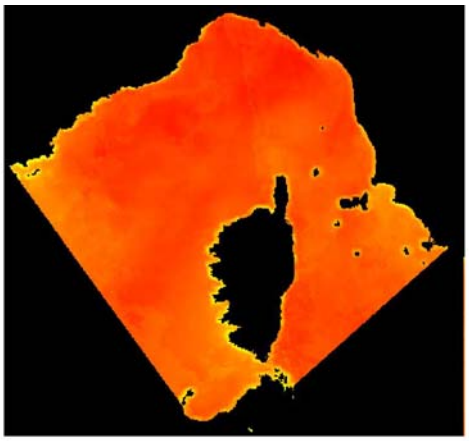

week 25

APPENDIX 10 (c) *Pelagos* Sanctuary MPA
Sea Surface Temperature skin (SST skin) maps
(AVHRR data April-December 2002)

44.5 N, 6.0 E

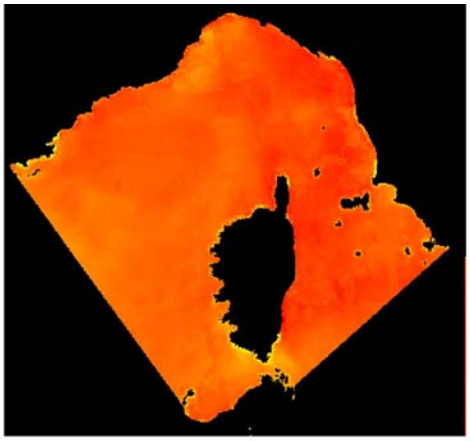

week 26

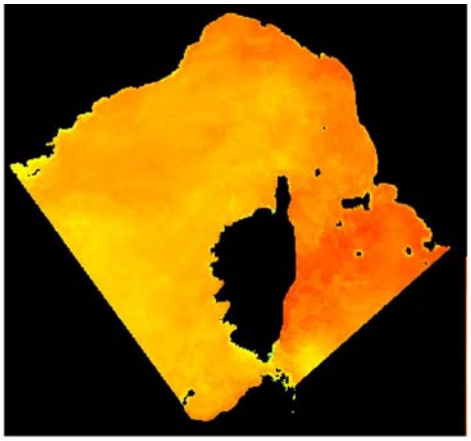

week 27

40.7 N, 11.5 E

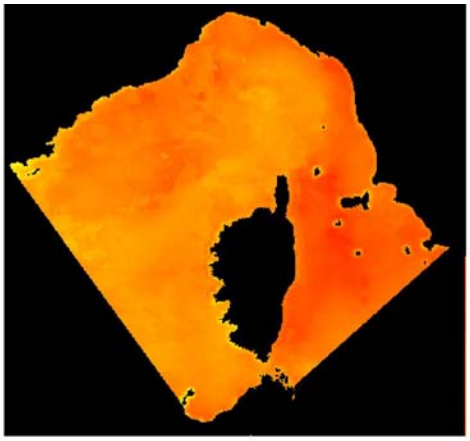

week 28

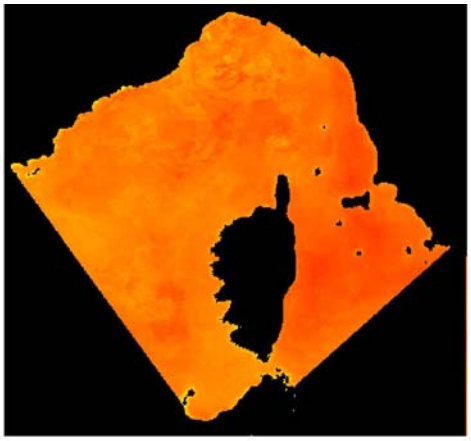

week 29

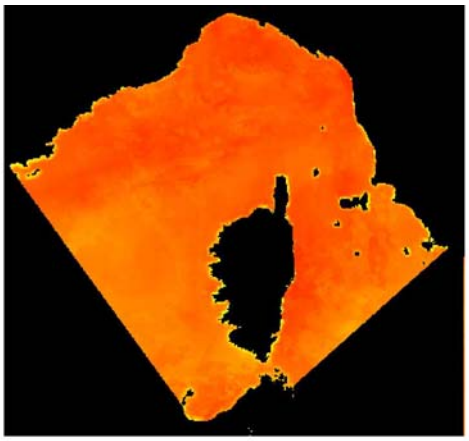

week 30

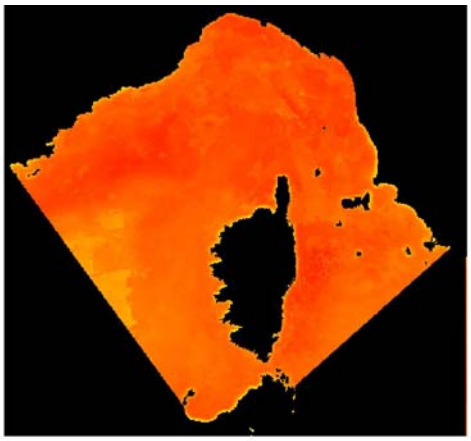

week 31

APPENDIX 10 (d) *Pelagos* Sanctuary MPA
Sea Surface Temperature skin (SST skin) maps
(AVHRR data April-December 2002)

44.5 N, 6.0 E

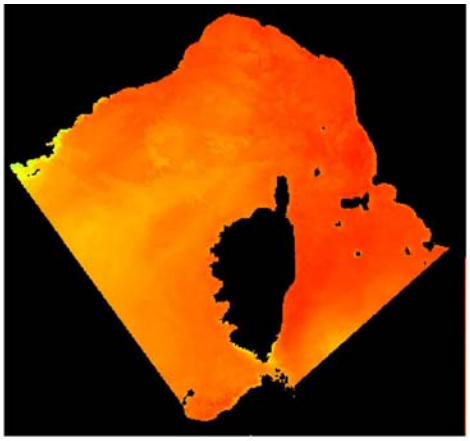

week 32

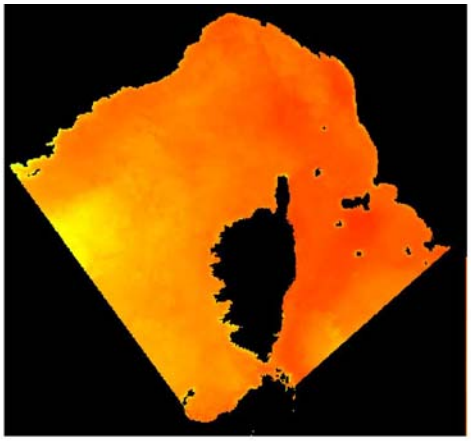

week 33

40.7 N, 11.5 E

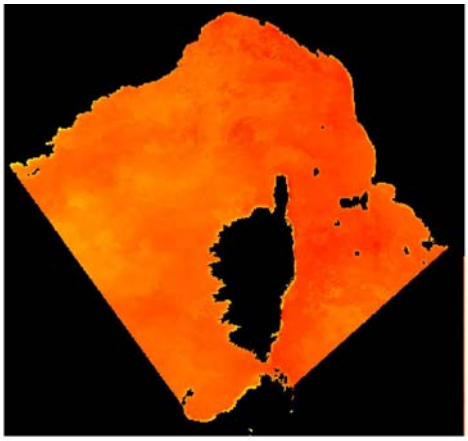

week 34

week 35

week 36

week 37

APPENDIX 10 (e) *Pelagos* Sanctuary MPA
Sea Surface Temperature skin (SST skin) maps
(AVHRR data April-December 2002)

44.5 N, 6.0 E

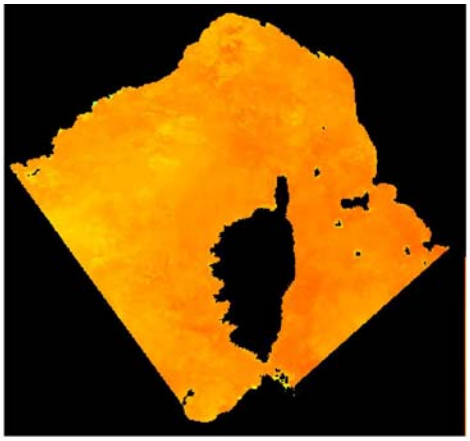

week 38

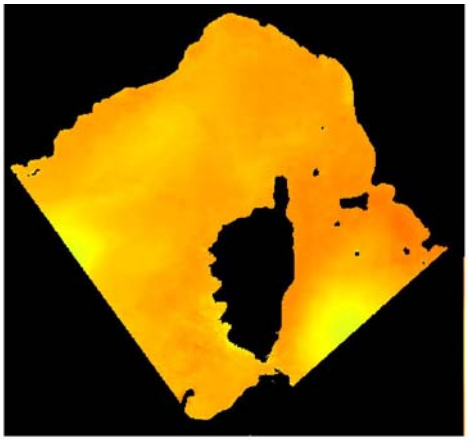

week 39

40.7 N, 11.5 E

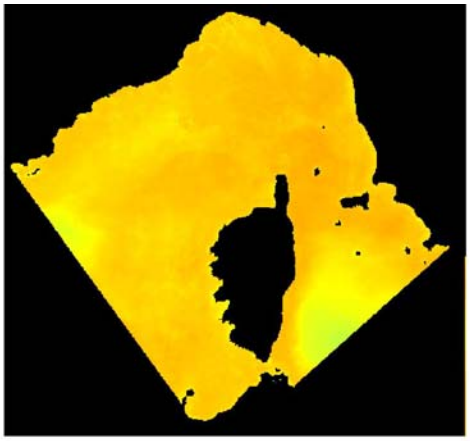

week 40

week 41

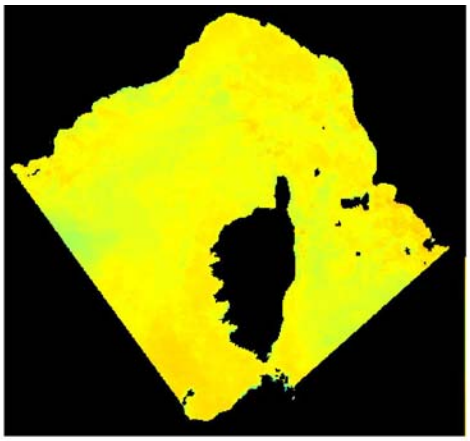

week 42

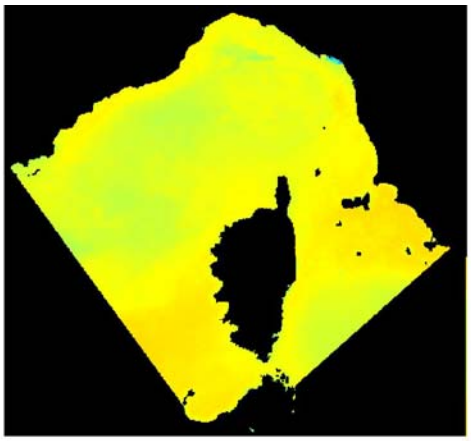

week 43

APPENDIX 10 (f) *Pelagos* Sanctuary MPA
Sea Surface Temperature skin (SST skin) maps
(AVHRR data April-December 2002)

44.5 N, 6.0 E

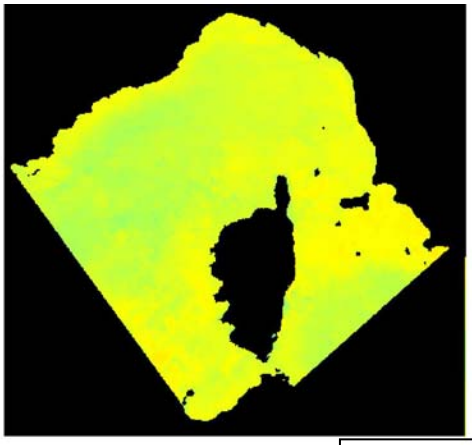

week 44

40.7 N, 11.5 E

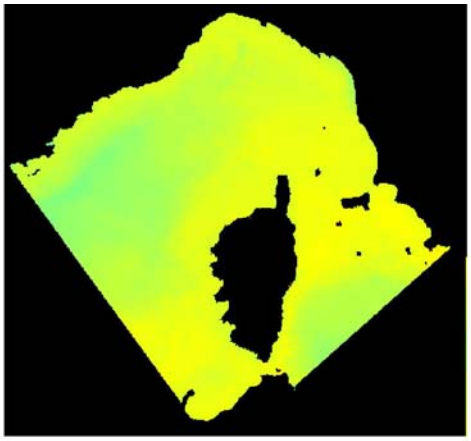

week 45

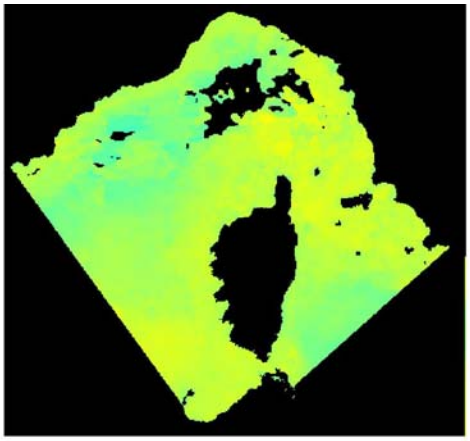

week 46

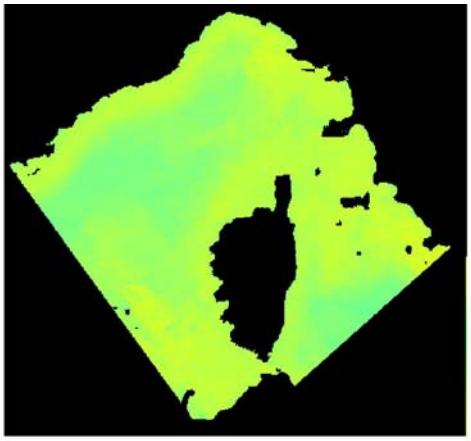

week 47

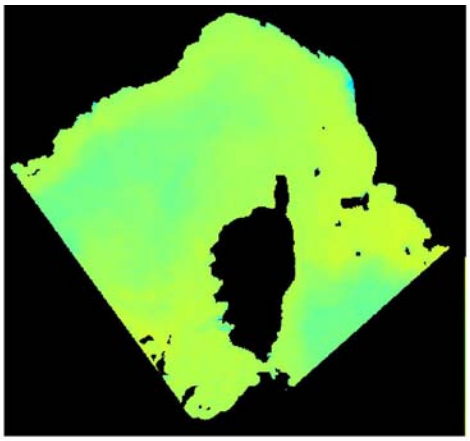

week 48

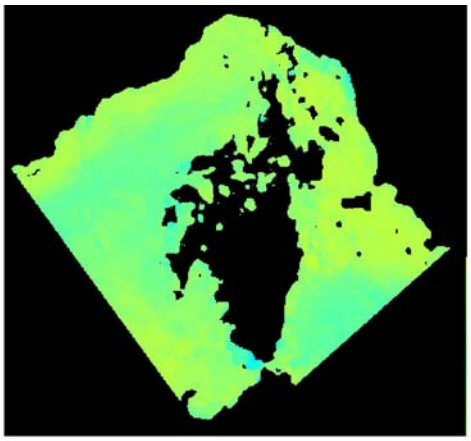

week 49

APPENDIX 10 (g) *Pelagos* Sanctuary MPA
Sea Surface Temperature skin (SST skin) maps
(AVHRR data April-December 2002)

44.5 N, 6.0 E

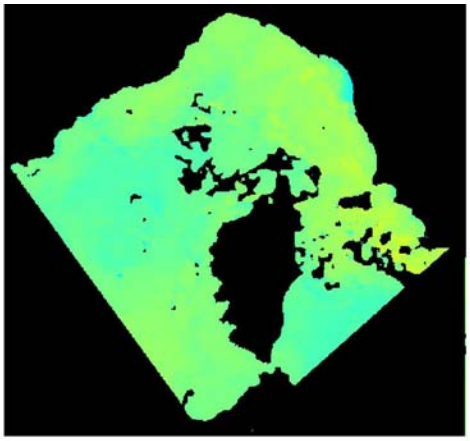

week 50

40.7 N, 11.5 E

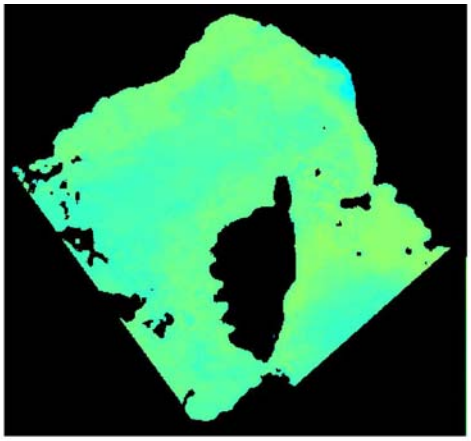

week 51

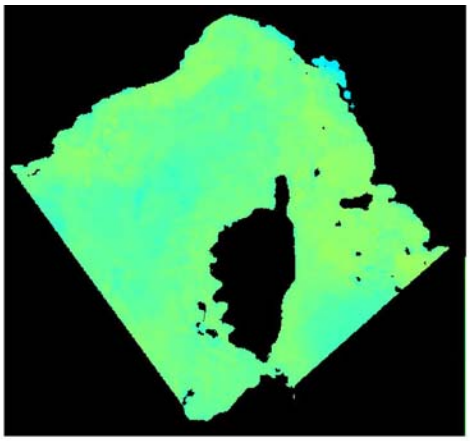

week 52

APPENDIX 11 (a) Alboran Sea
Chlorophyll (*chl*) maps (SeaWiFS data year 2002)

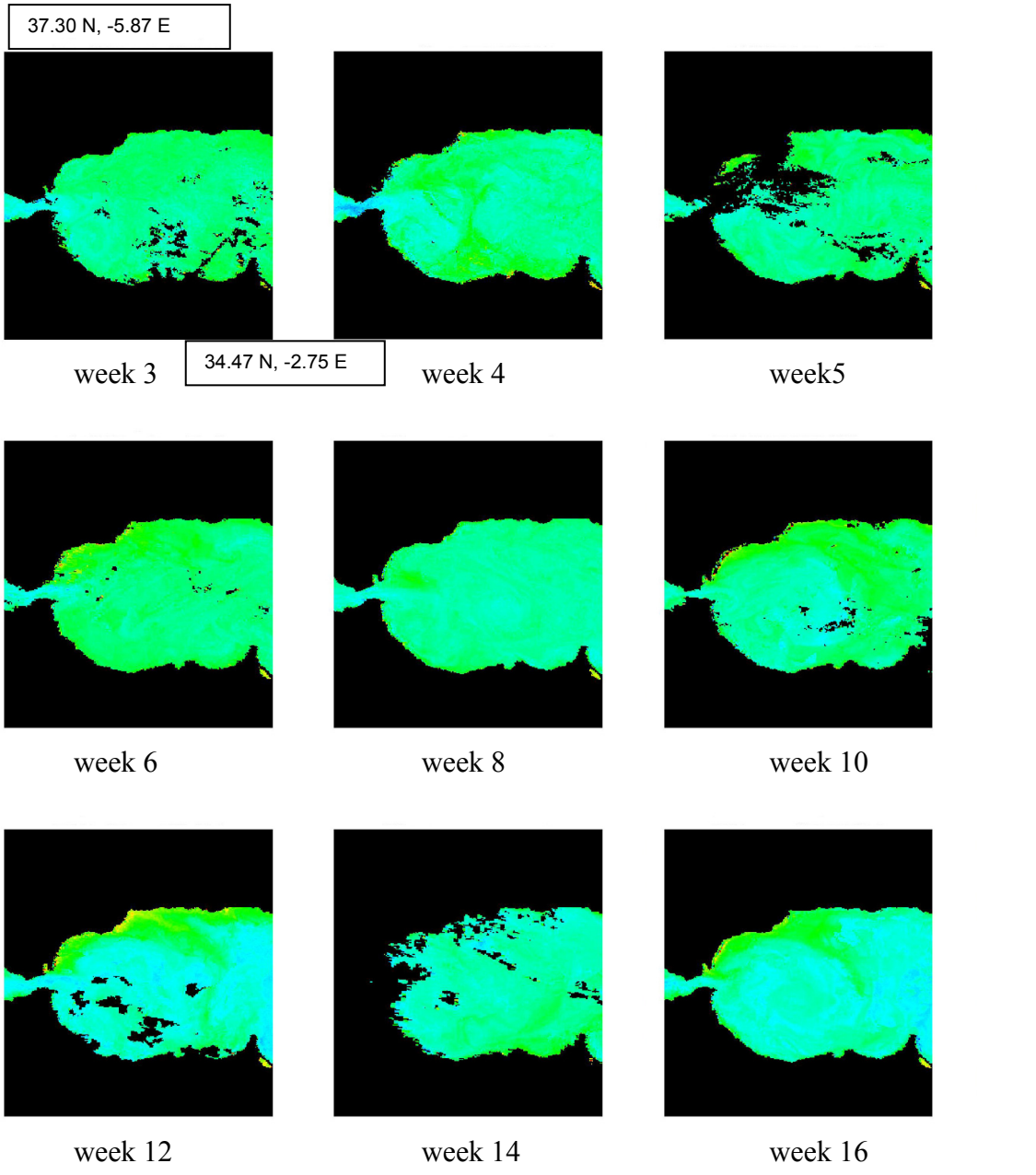

APPENDIX 11 (b) Alboran Sea
Chlorophyll (*chl*) (SeaWiFS data year 2002)

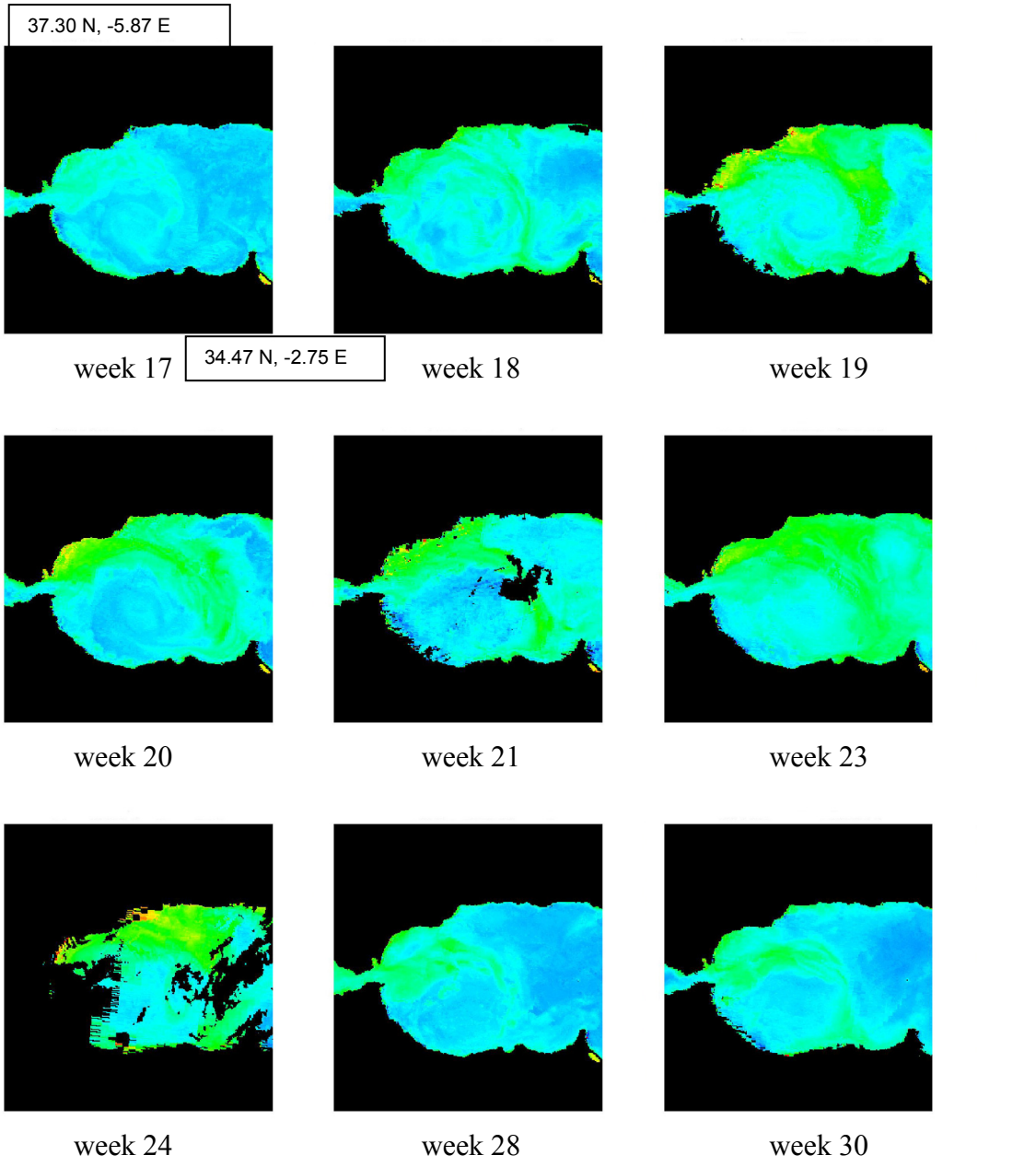

APPENDIX 11 (c) Alboran Sea
Chlorophyll (*chl*) (SeaWiFS data year 2002)

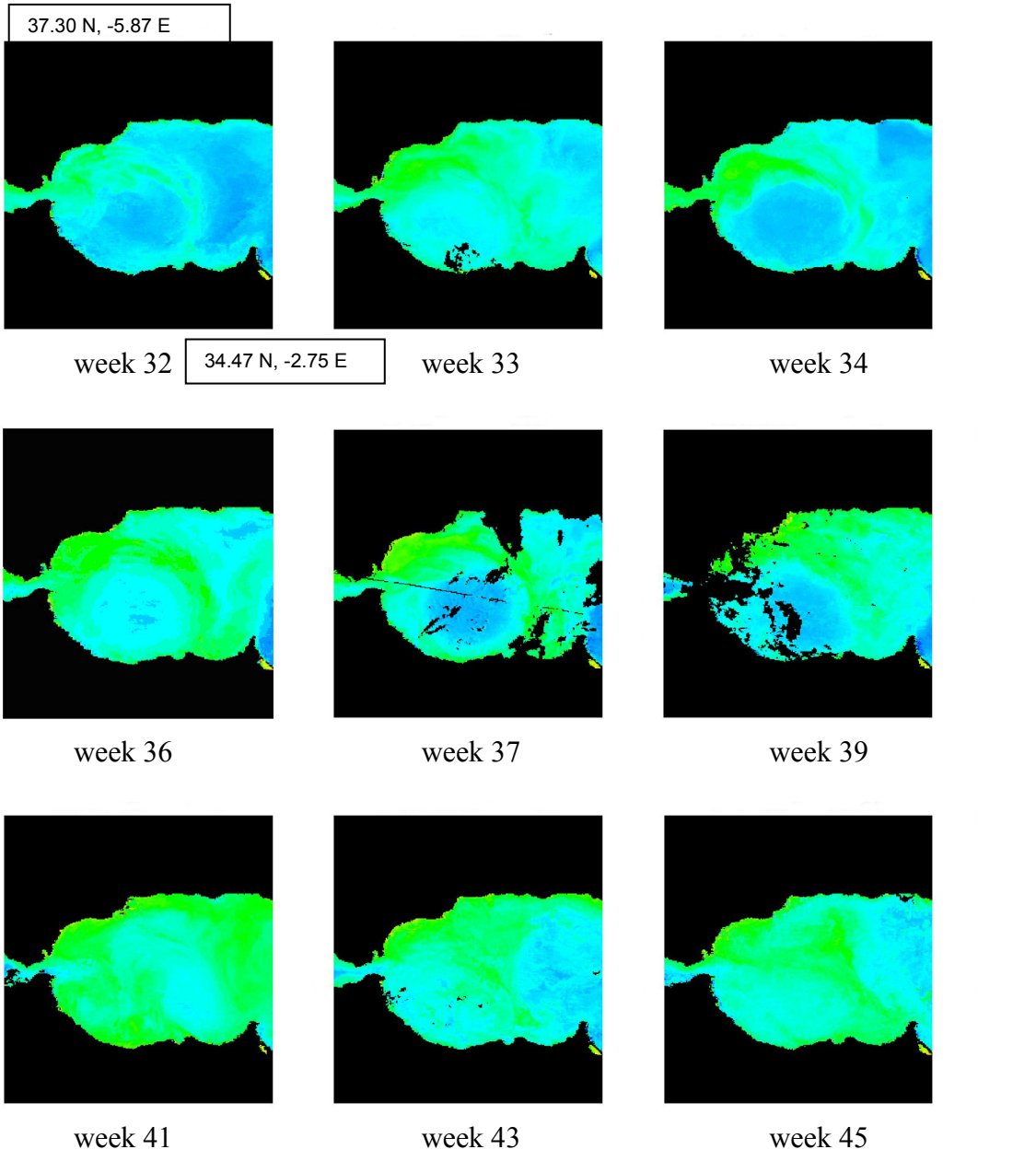

APPENDIX 11 (d) Alboran Sea
Chlorophyll (*chl*) (SeaWiFS data year 2002)

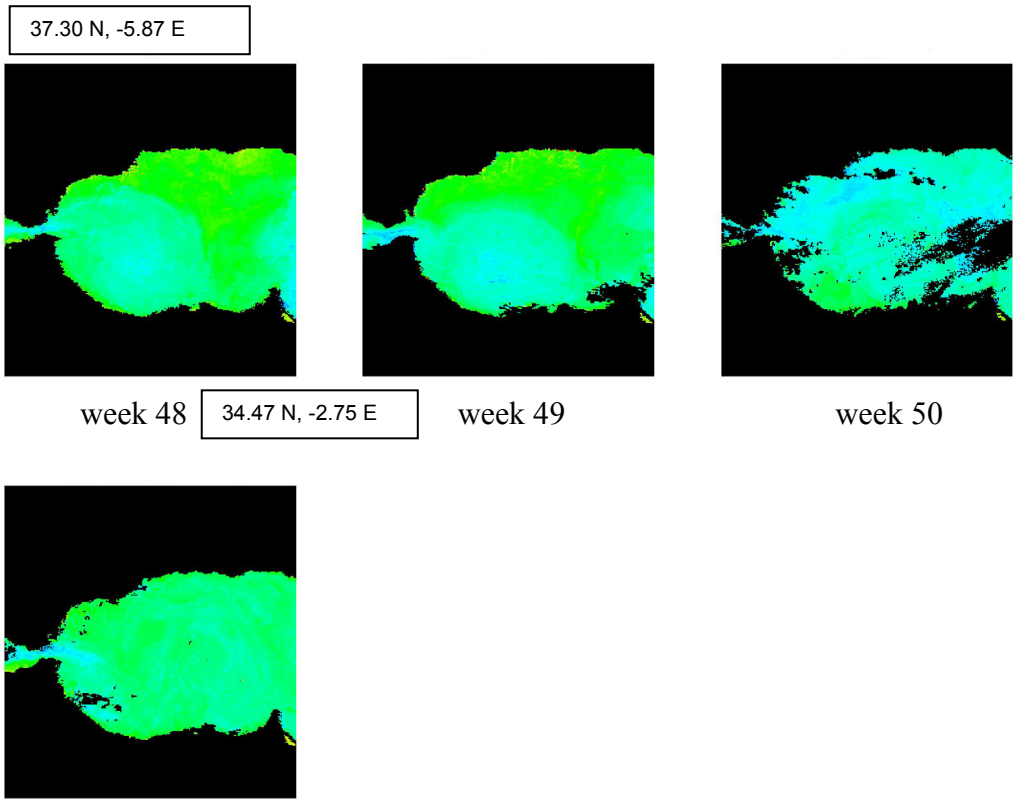

APPENDIX 12 (a) Al Hoceima National Park
Chlorophyll (*chl*) (SeaWiFS data year 2002)

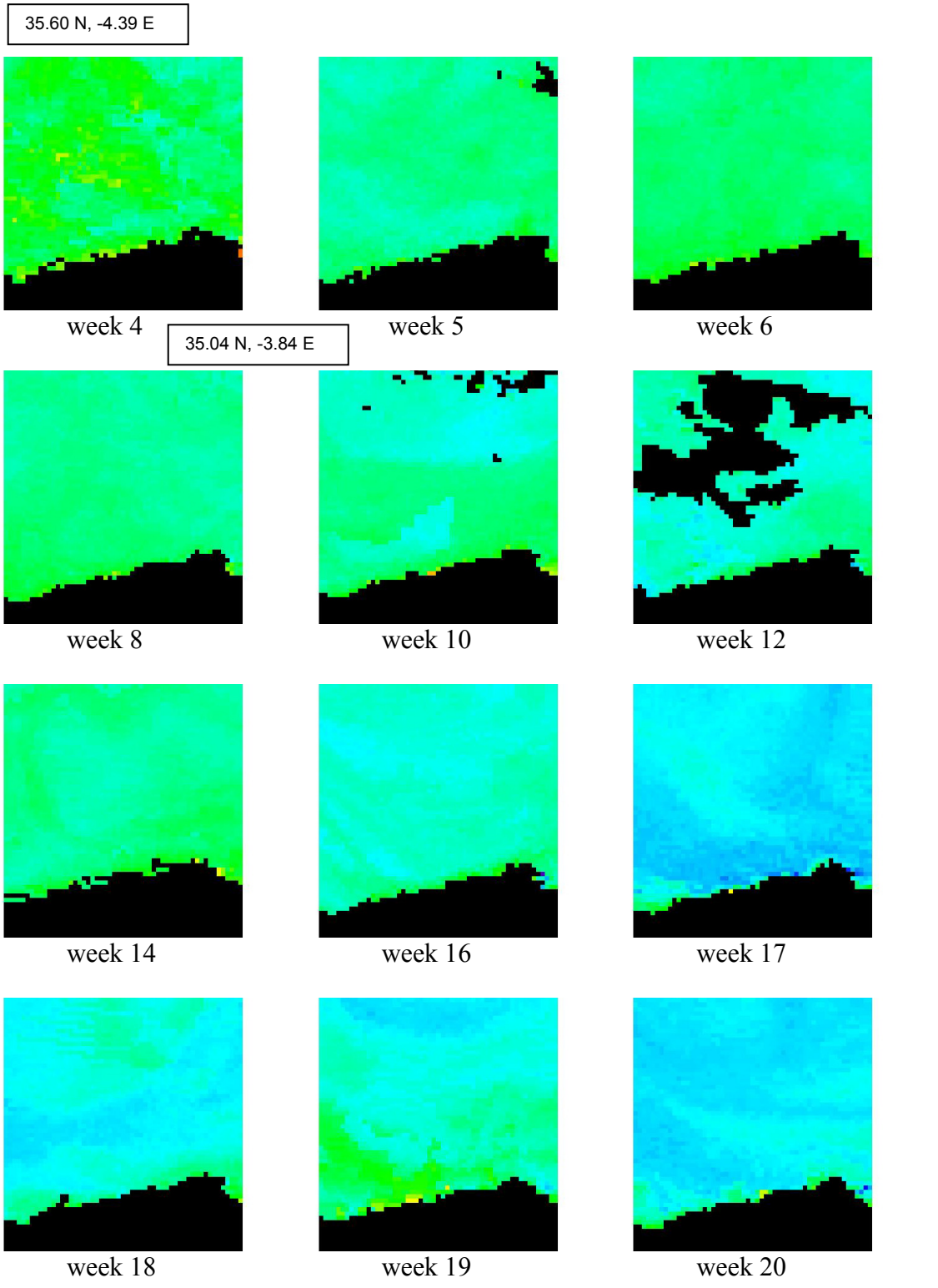

APPENDIX 12 (b) Al Hoceima National Park
Chlorophyll (*chl*) (SeaWiFS data year 2002)

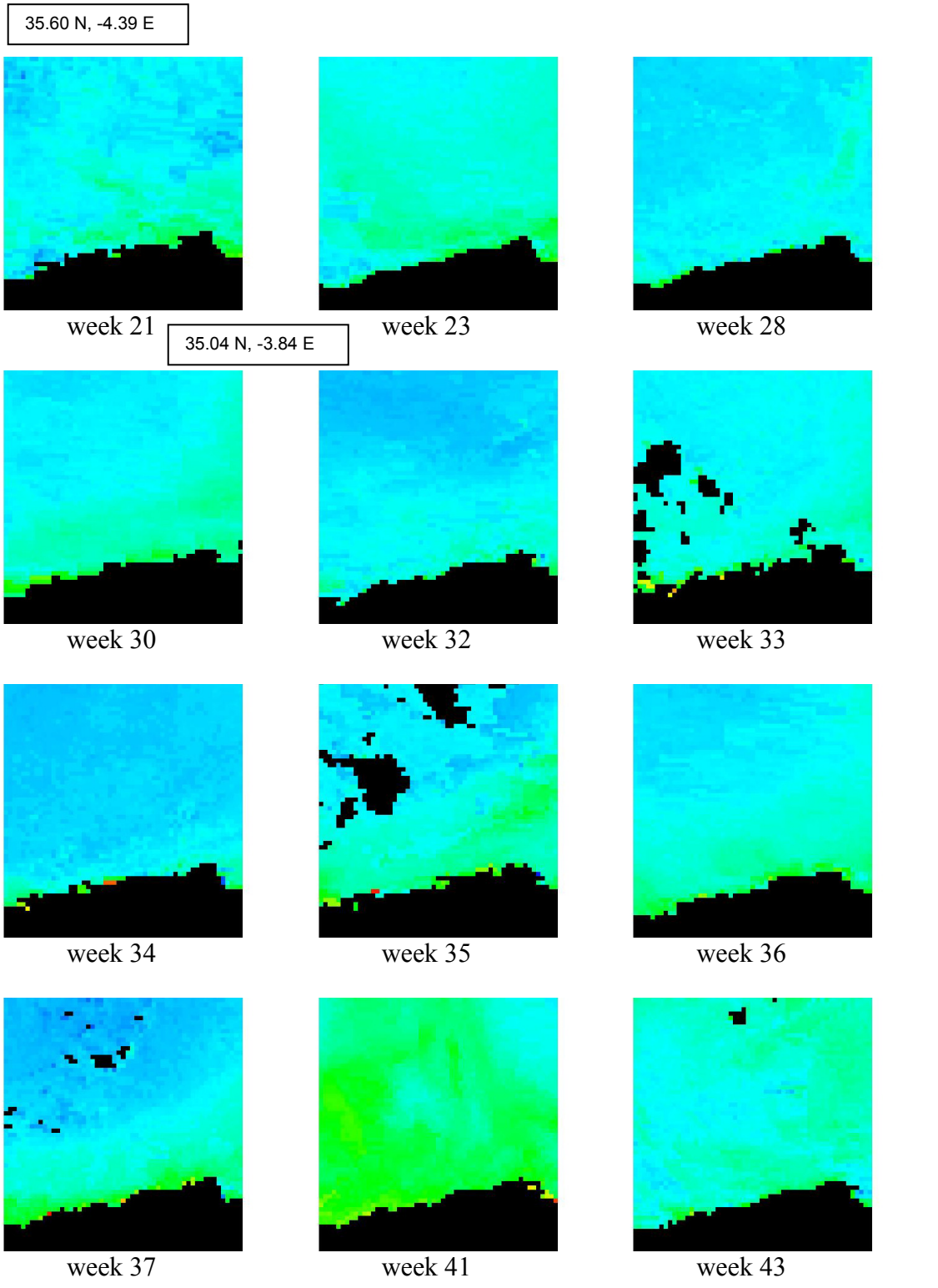

APPENDIX 12 (c) Al Hoceima National Park
Chlorophyll (*chl*) (SeaWiFS data year 2002)

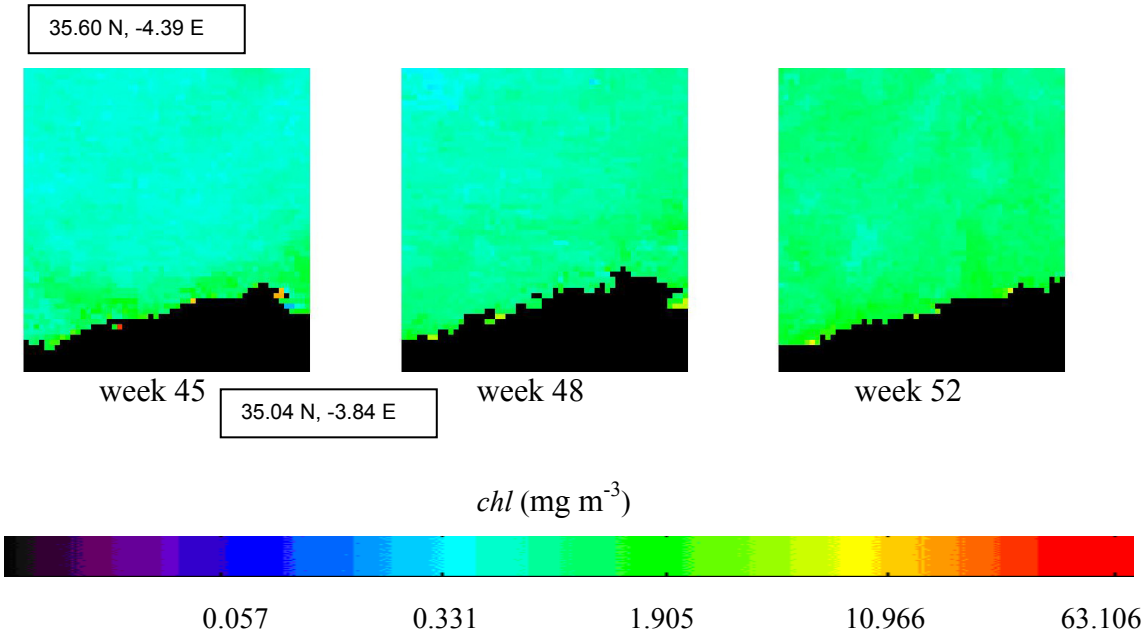

APPENDIX 13 (a) Gibraltar Strait
Threshold *chl* range 1.0-3.0 mg/m^3 (SeaWiFS data year 2002)

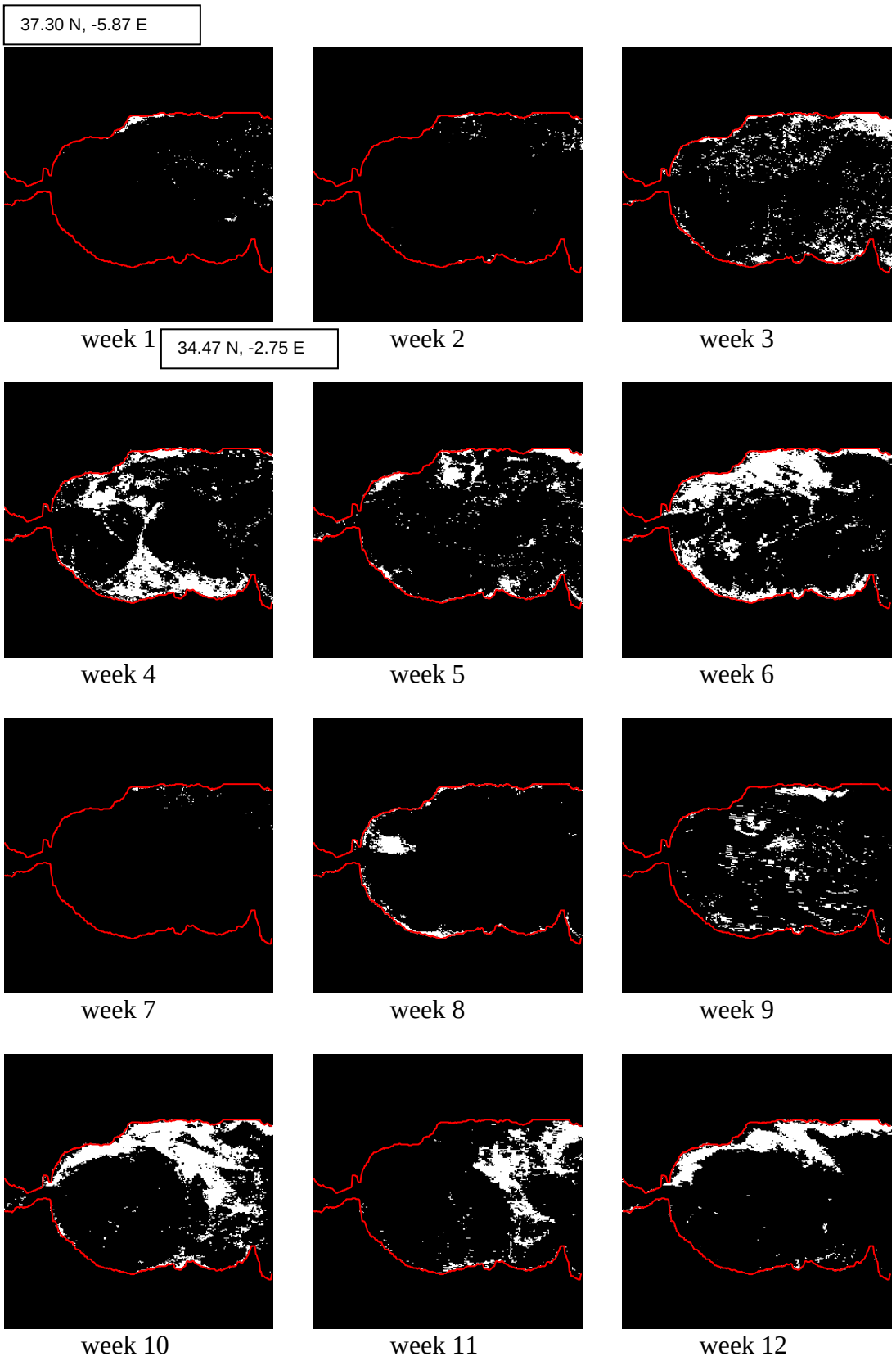

APPENDIX 13 (b) Gibraltar Strait
Threshold *chl* range 1.0-3.0 mg/m^3 (SeaWiFS data year 2002)

37.30 N, -5.87 E

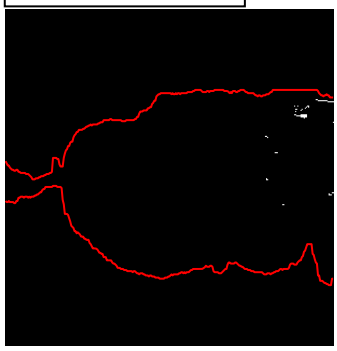

week 13

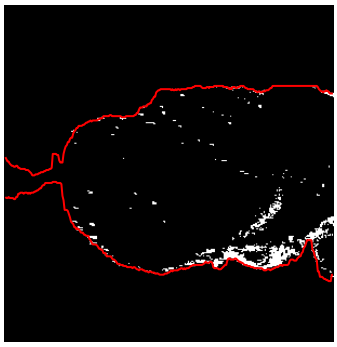

week 14

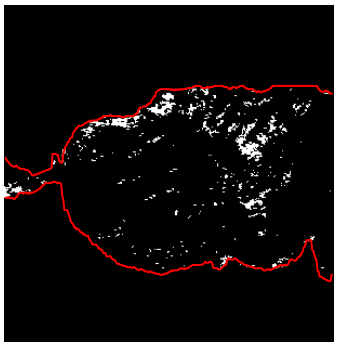

week 15

34.47 N, -2.75 E

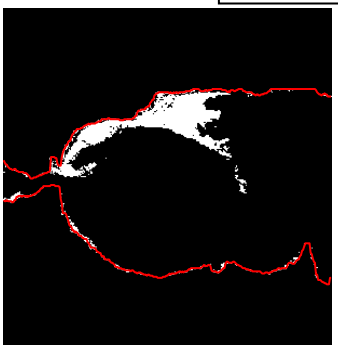

week 16

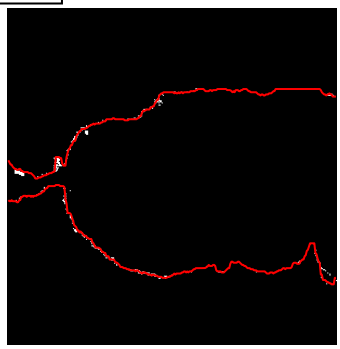

week 17

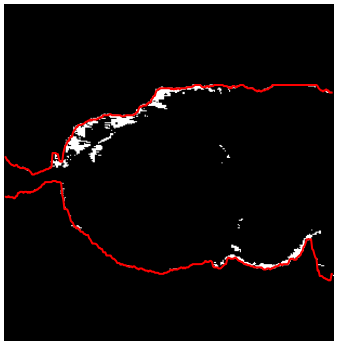

week 18

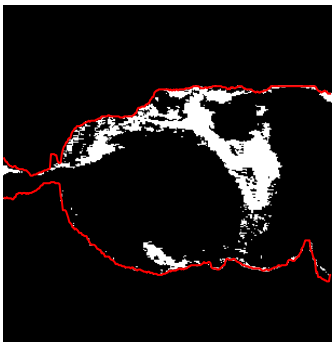

week 19

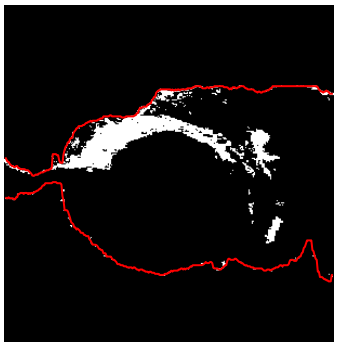

week 20

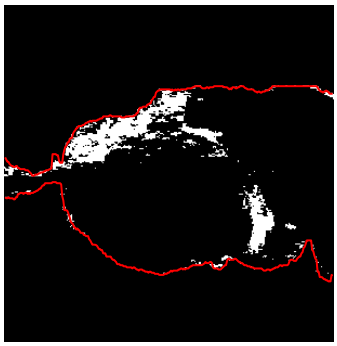

week 21

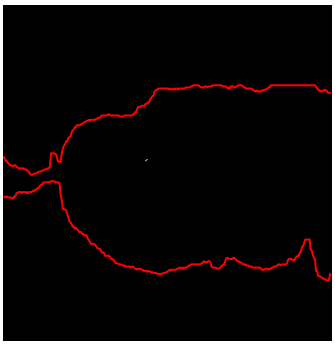

week 22

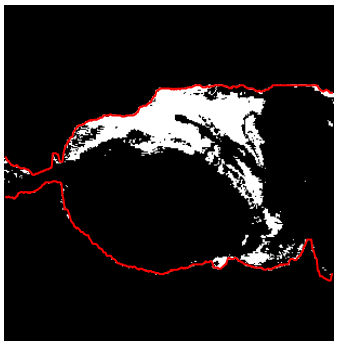

week 23

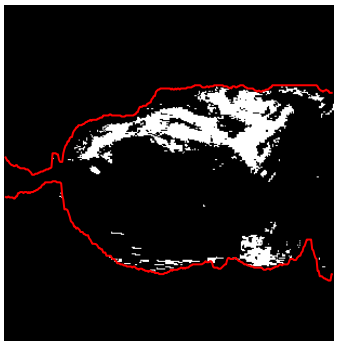

week 24

APPENDIX 13 (c) Gibraltar Strait
Threshold *chl* range 1.0-3.0 mg/m^3 (SeaWiFS data year 2002)

37.30 N, -5.87 E

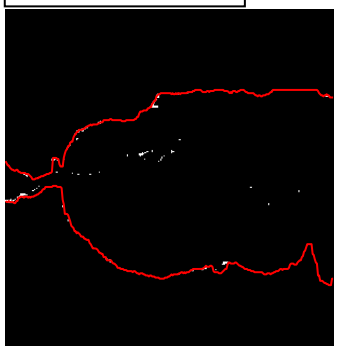

week 25

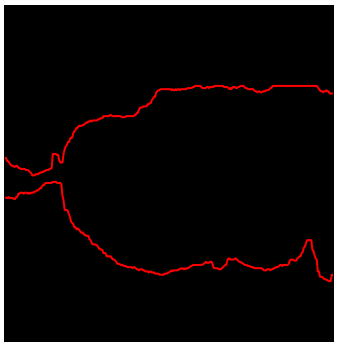

week 26

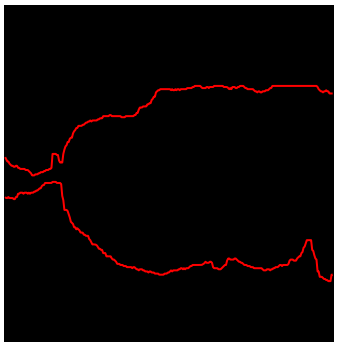

week 27

34.47 N, -2.75 E

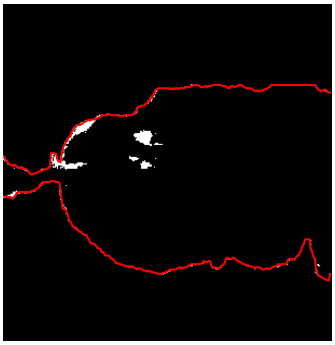

week 28

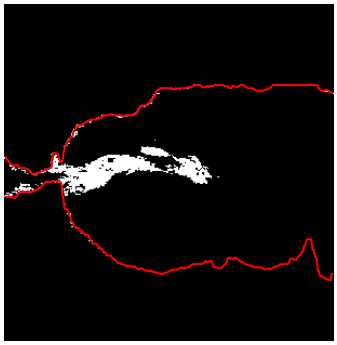

week 29

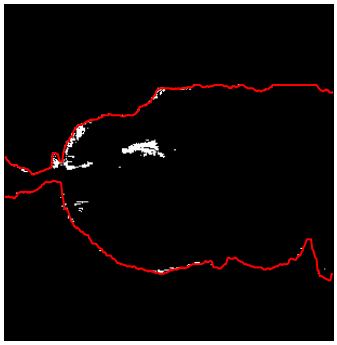

week 30

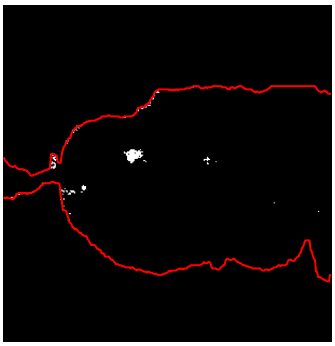

week 31

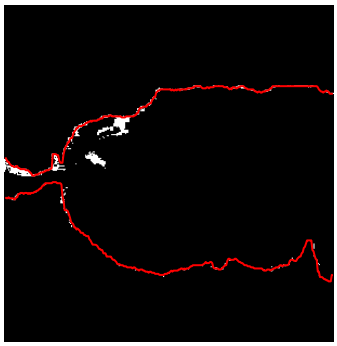

week 32

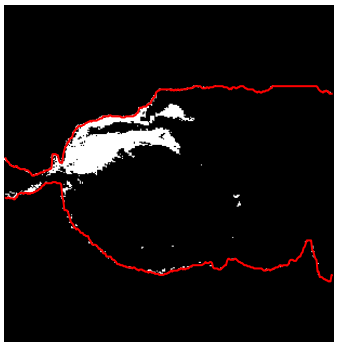

week 33

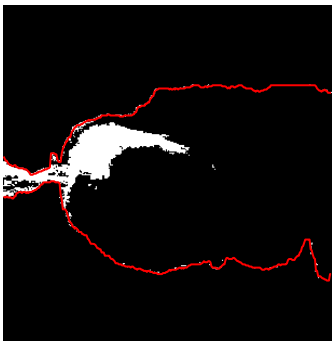

week 34

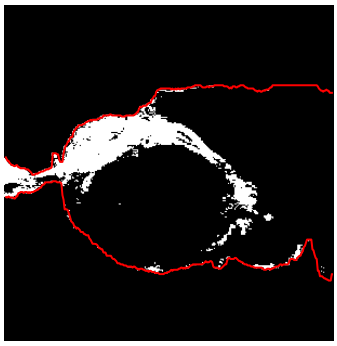

week 35

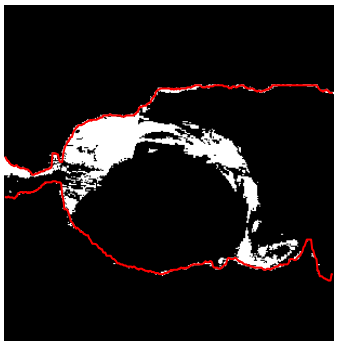

week 36

APPENDIX 13 (d) Gibraltar Strait
Threshold *chl* range 1.0-3.0 mg/m^3 (SeaWiFS data year 2002)

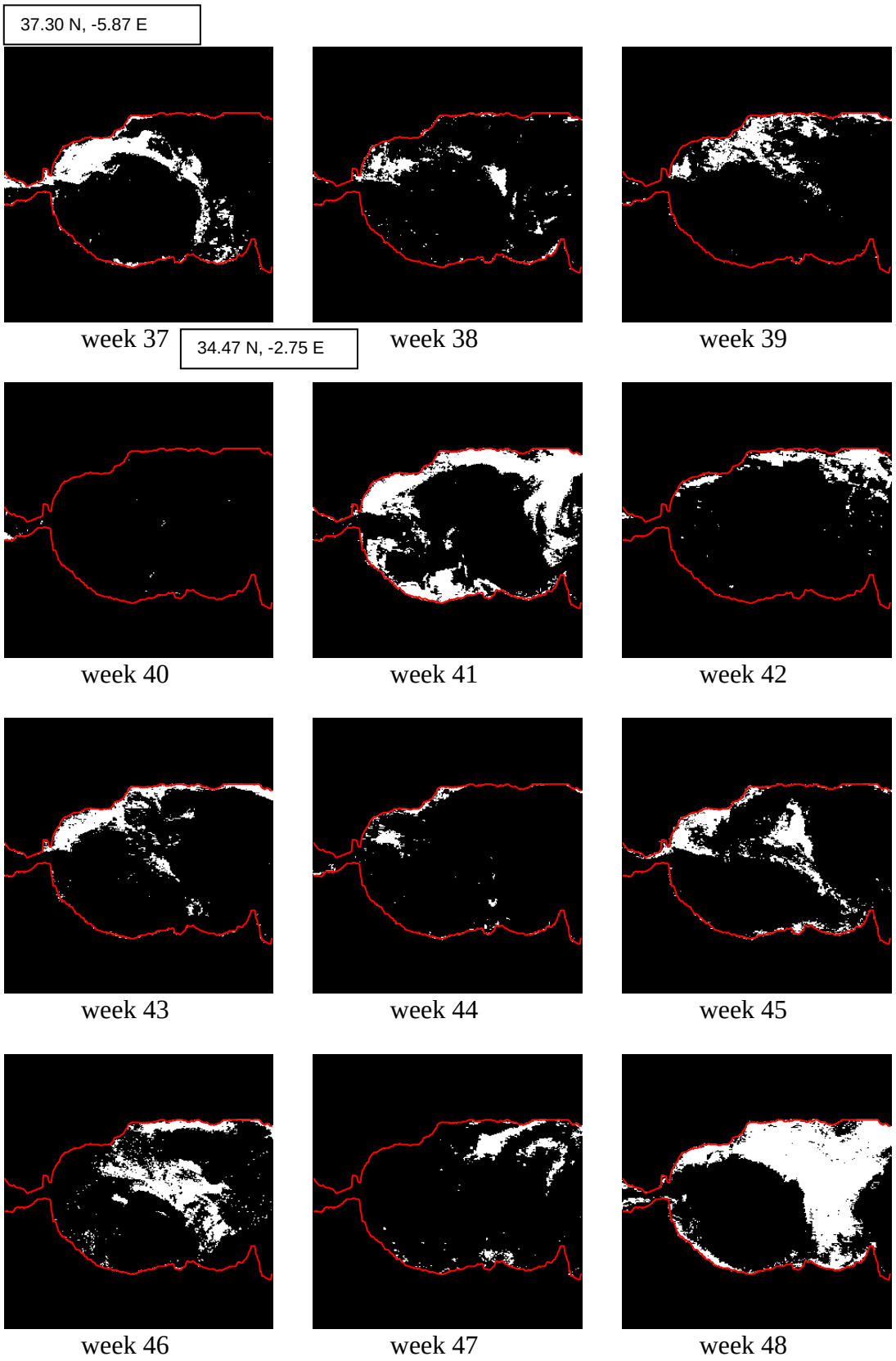

APPENDIX 13 (e) Gibraltar Strait
Threshold *chl* range 1.0-3.0 mg/m^3 (SeaWiFS data year 2002)

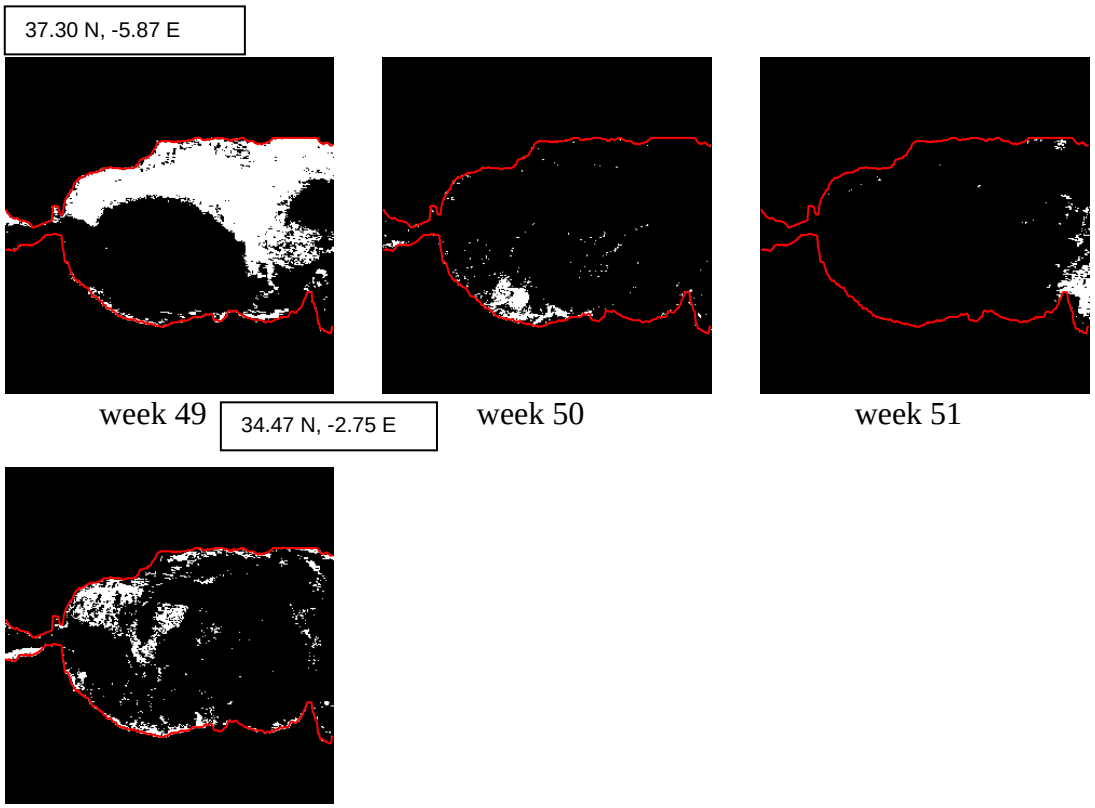

week 49 week 50 week 51

week 52

APPENDIX 14 (a) Gibraltar Strait
Spatial Gradient (*chl* range 0.16-0.9 mg m^{-3})

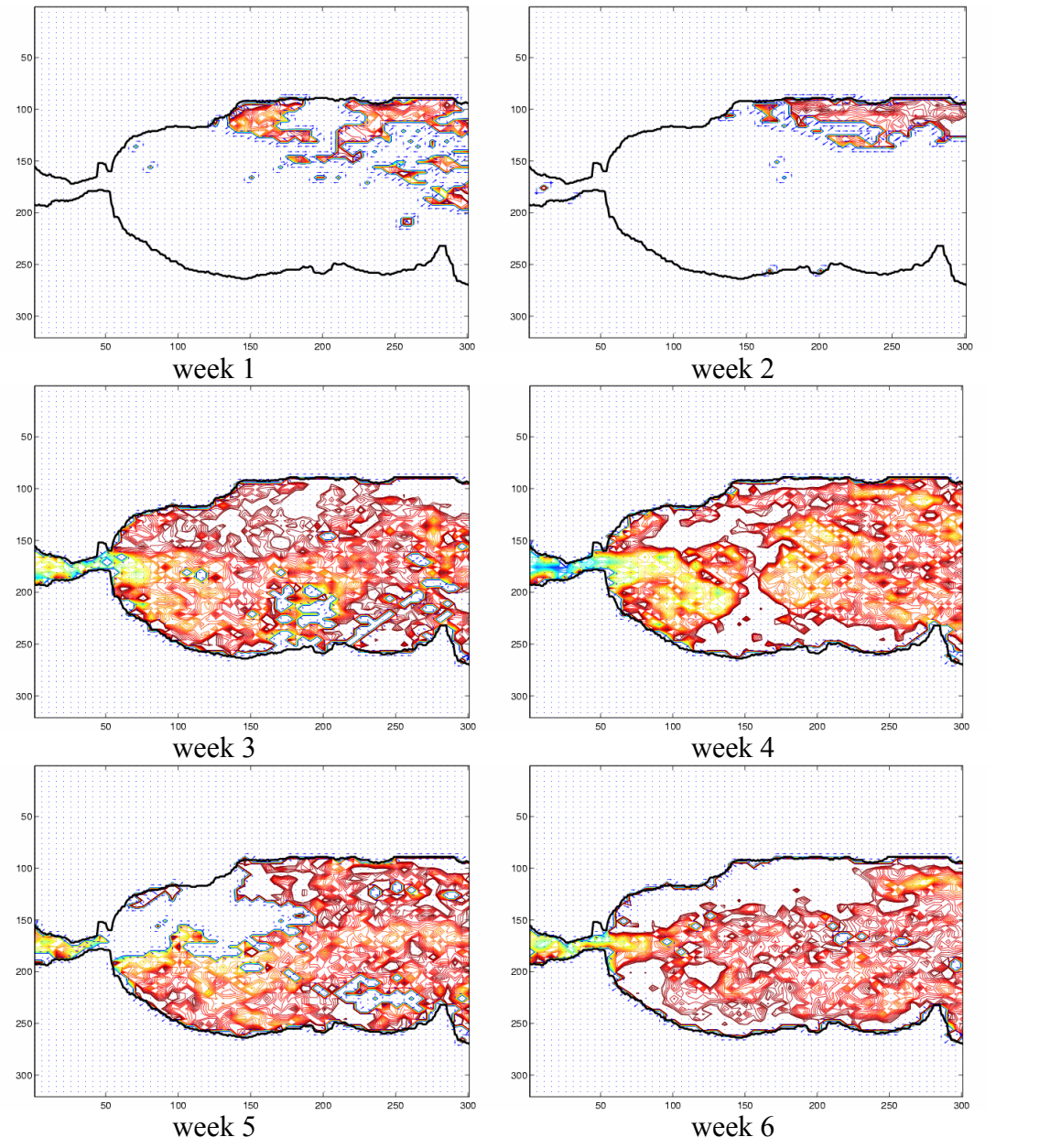

APPENDIX 14 (b) Gibraltar Strait
Spatial Gradient (*chl* range 0.16-0.9 mg m^{-3})

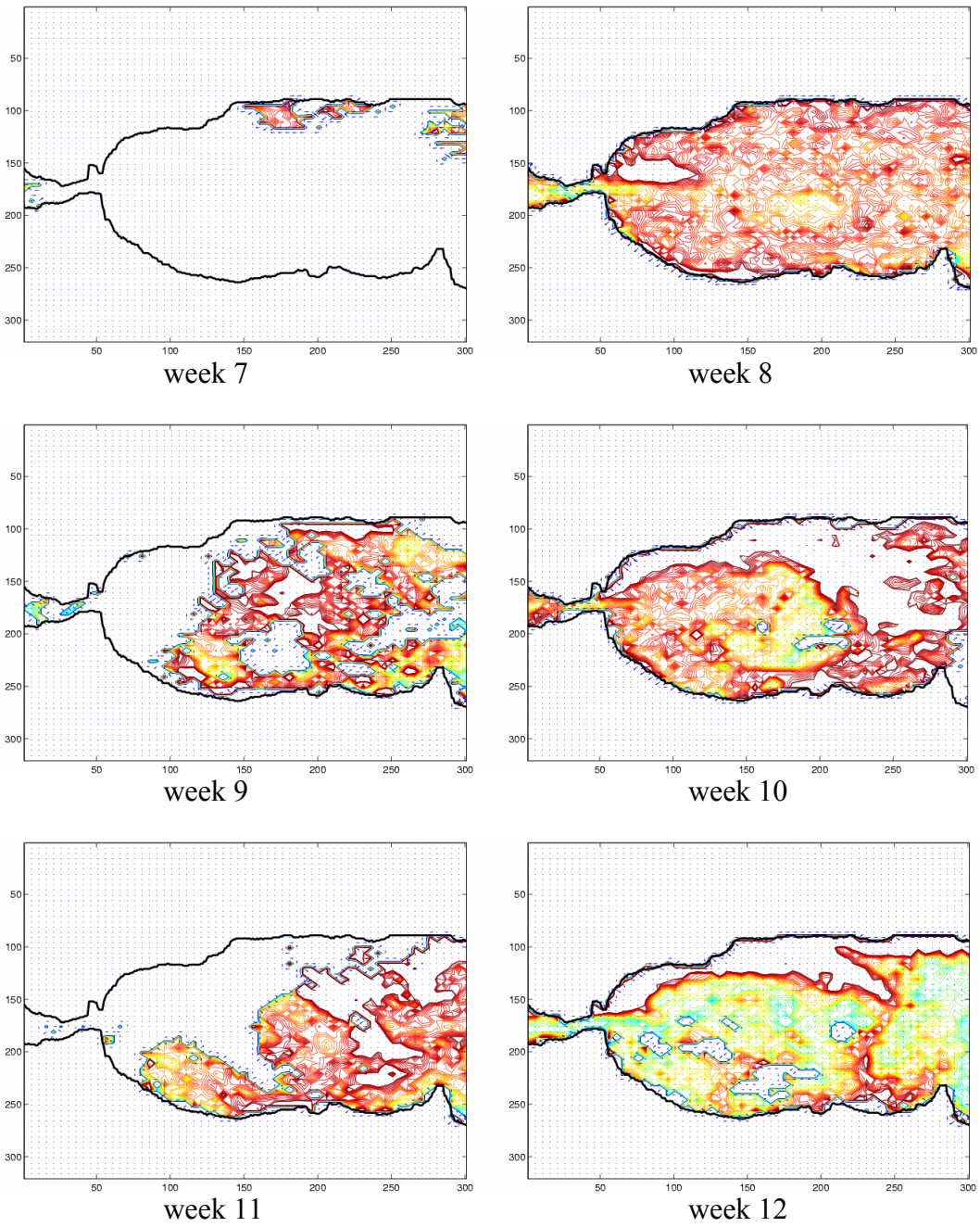

APPENDIX 14 (c) Gibraltar Strait
Spatial Gradient (*chl* range 0.16-0.9 mg m^{-3})

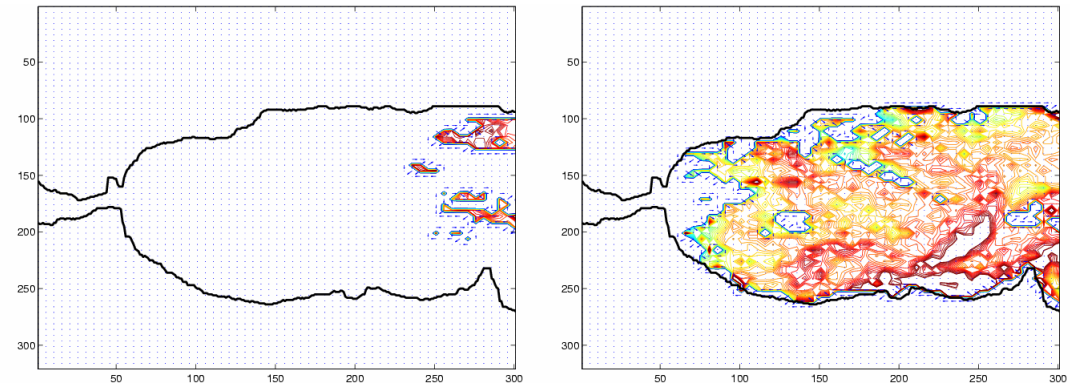

week 13 week 14

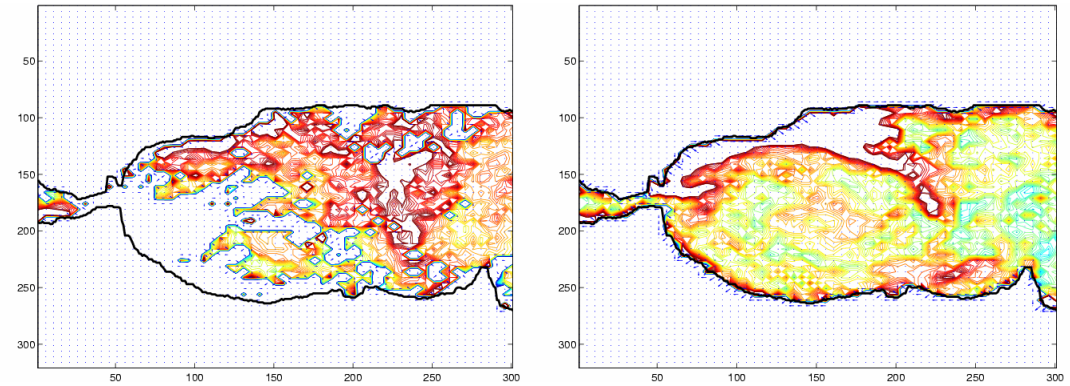

week 15 week 16

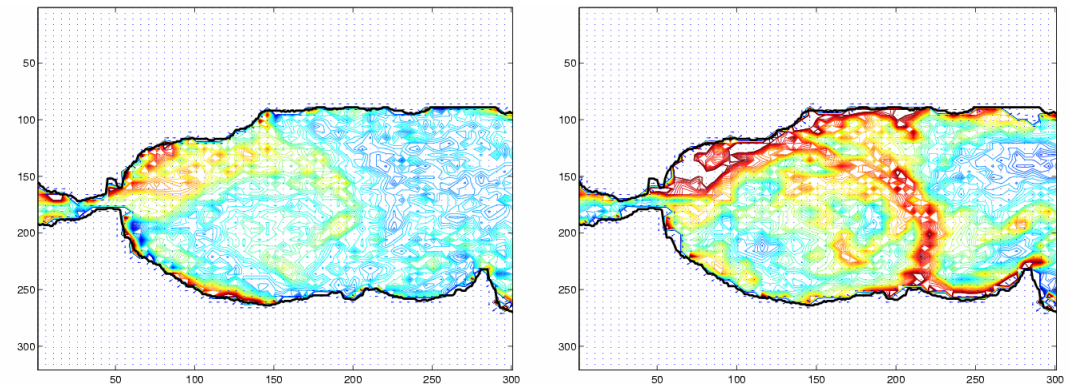

week 17 week 18

chl (mg m^{-3})

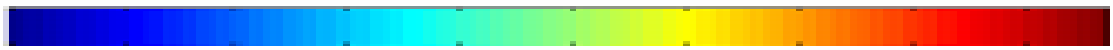

0.16 0.19 0.23 0.27 0.33 0.39 0.46 0.55 0.66 0.79

APPENDIX 14 (d) Gibraltar Strait
Spatial Gradient (*chl* range 0.16-0.9 mg m^{-3})

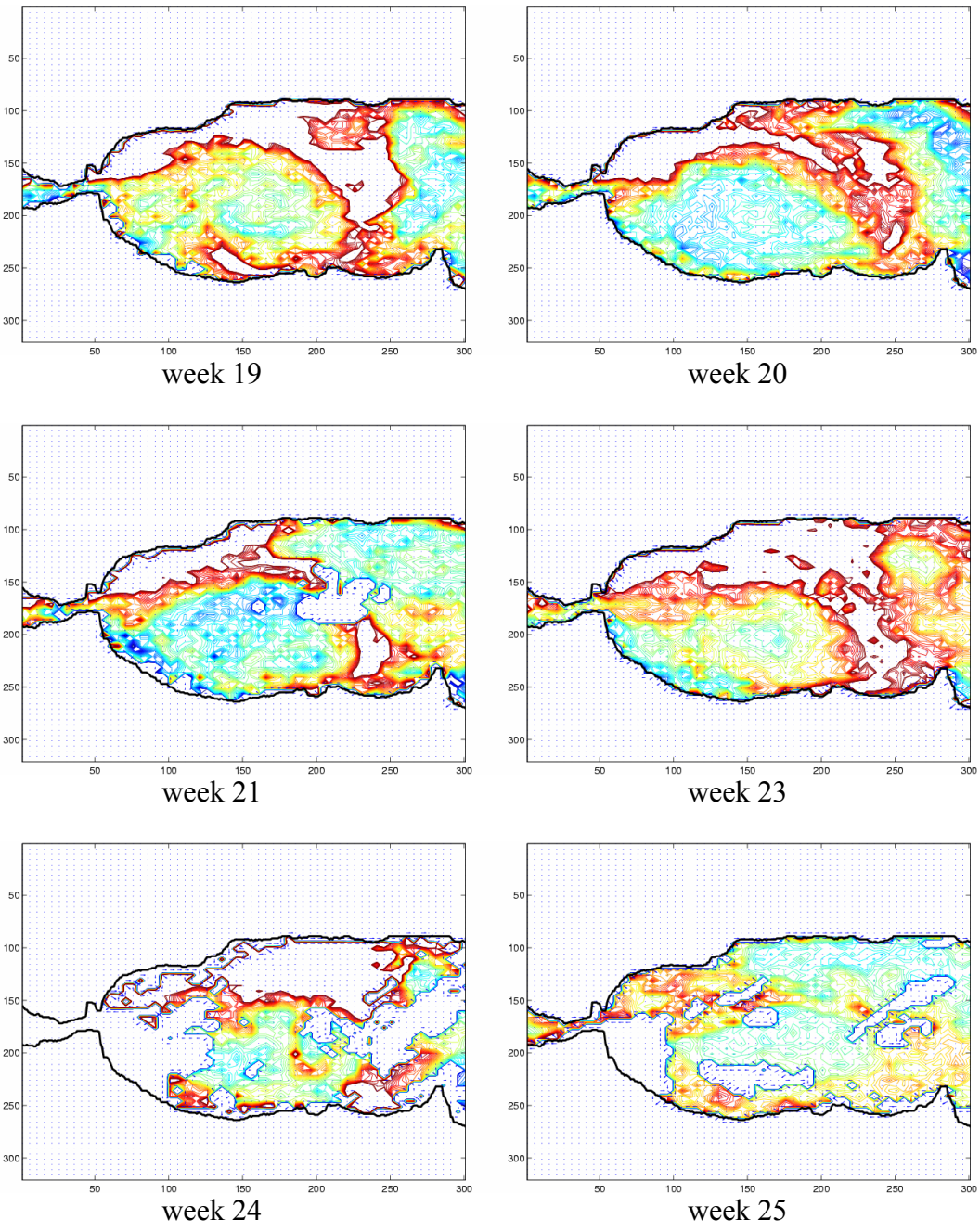

APPENDIX 14 (e) Gibraltar Strait
Spatial Gradient (*chl* range 0.16-0.9 mg m^{-3})

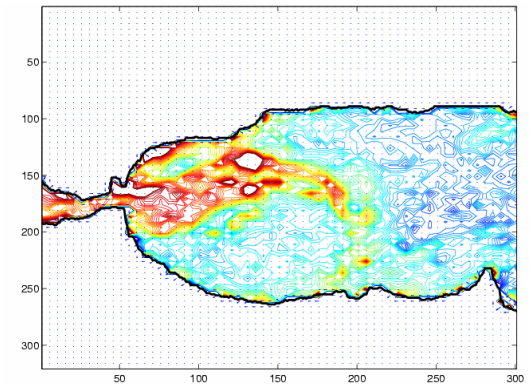

week 28

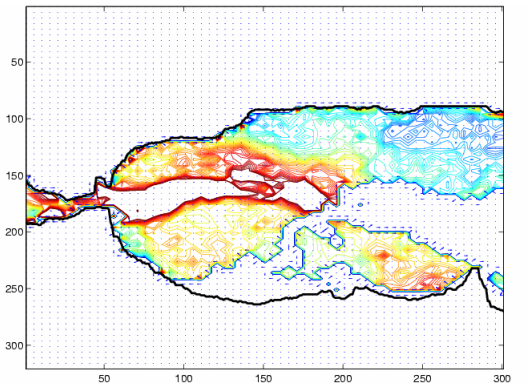

week 29

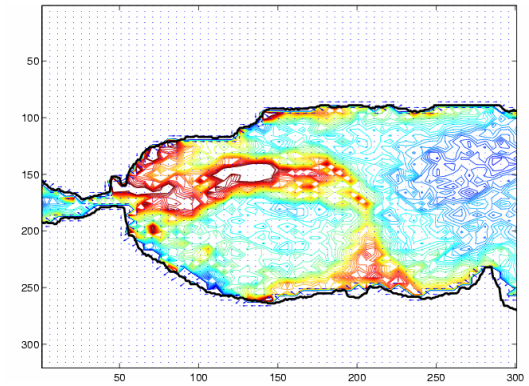

week 30

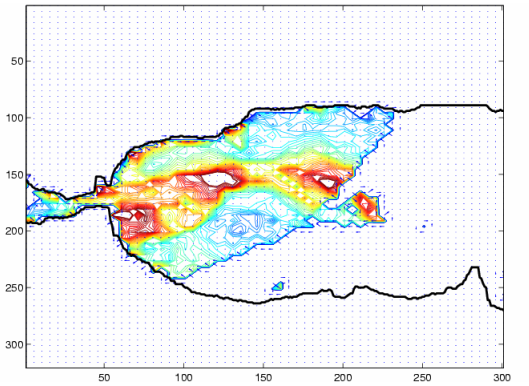

week 31

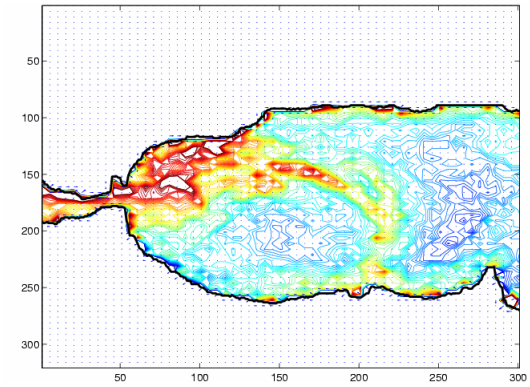

week 32

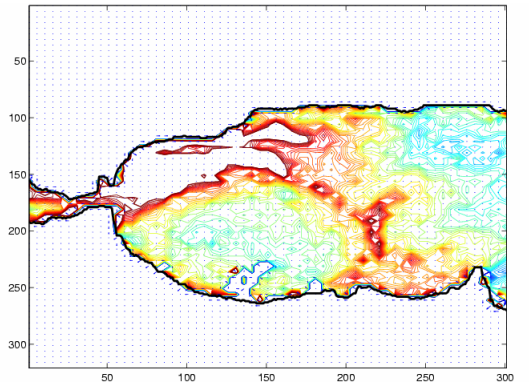

week 33

chl (mg m^{-3})

0.16 0.19 0.23 0.27 0.33 0.39 0.46 0.55 0.66 0.79

APPENDIX 14 (f) Gibraltar Strait
Spatial Gradient (*chl* range 0.16-0.9 mg m^{-3})

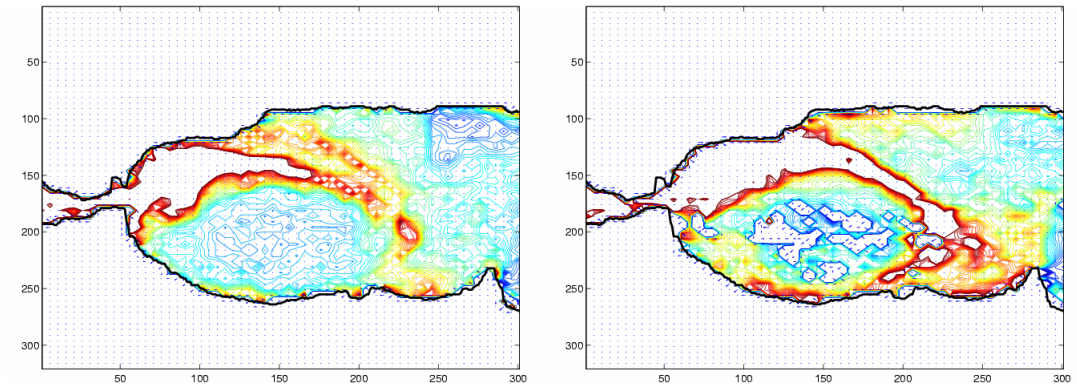

week 34 week 35

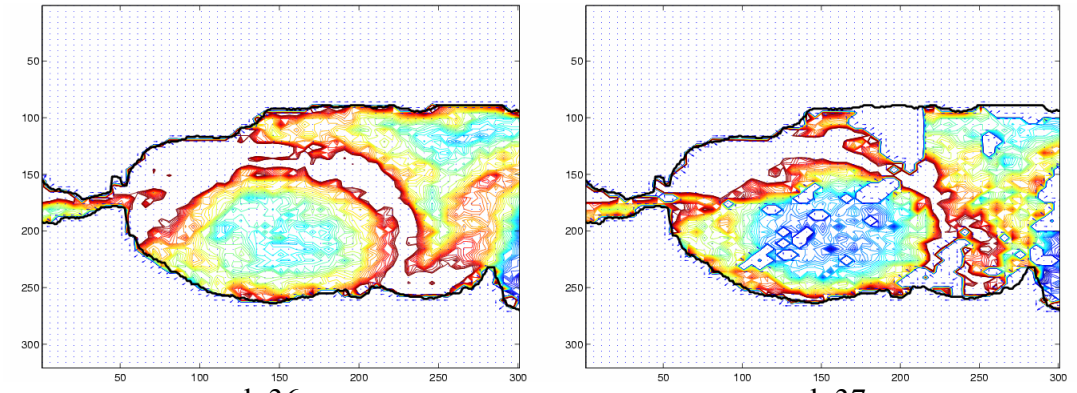

week 36 week 37

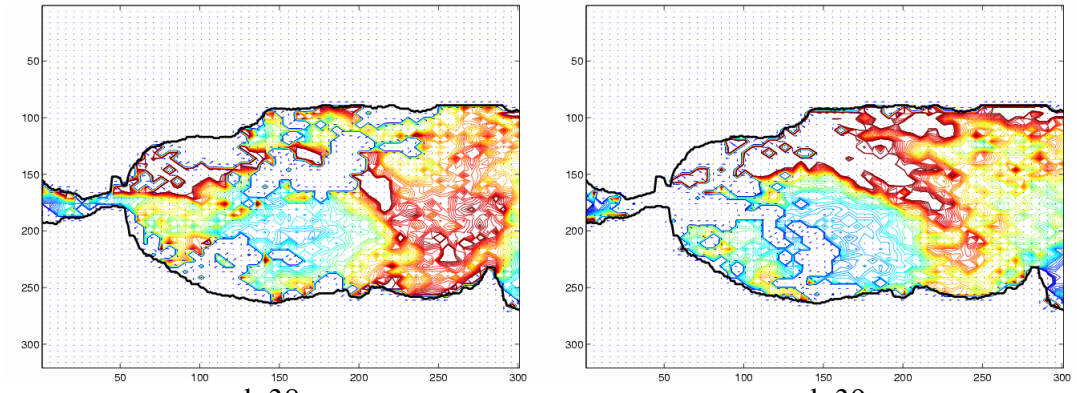

week 38 week 39

chl (mg m^{-3})

0.16 0.19 0.23 0.27 0.33 0.39 0.46 0.55 0.66 0.79

APPENDIX 14 (g) Gibraltar Strait
Spatial Gradient (*chl* range 0.16-0.9 mg m^{-3})

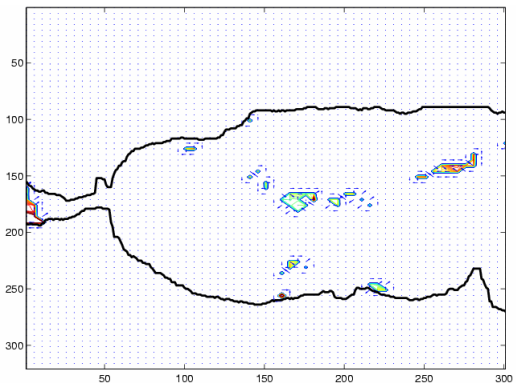

week 40

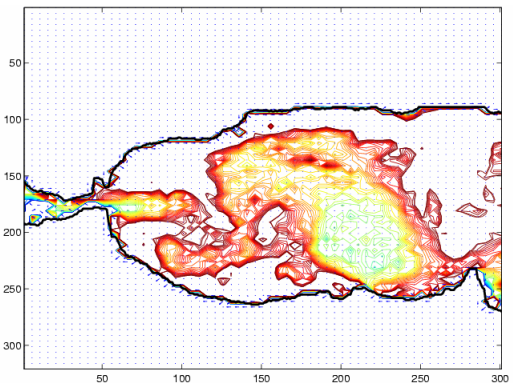

week 41

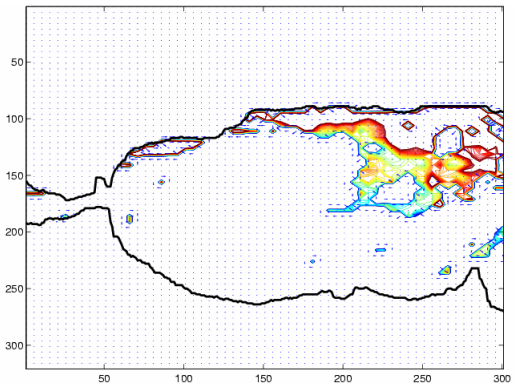

week 42

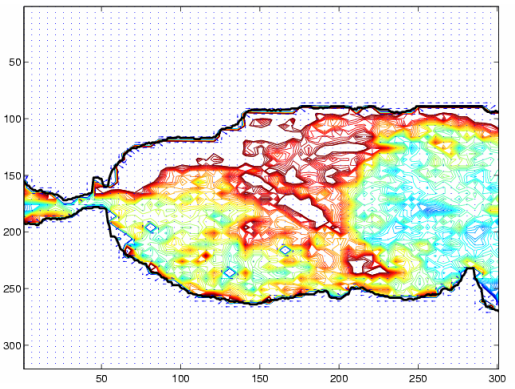

week 43

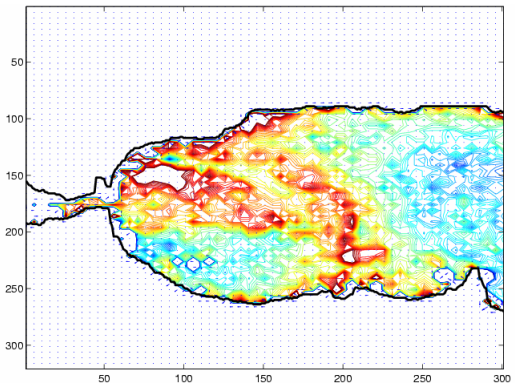

week 44

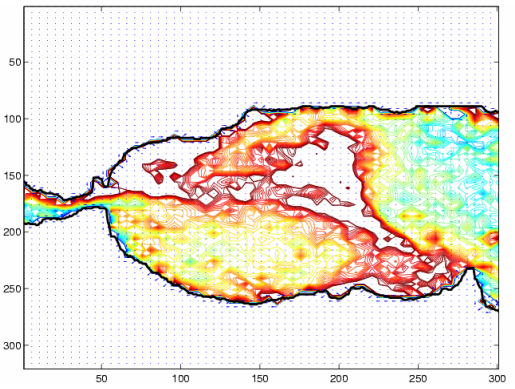

week 45

chl (mg m^{-3})

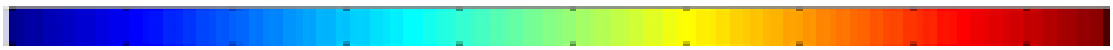

0.16 0.19 0.23 0.27 0.33 0.39 0.46 0.55 0.66 0.79

APPENDIX 14 (h) Gibraltar Strait
Spatial Gradient (*chl* range 0.16-0.9 mg m^{-3})

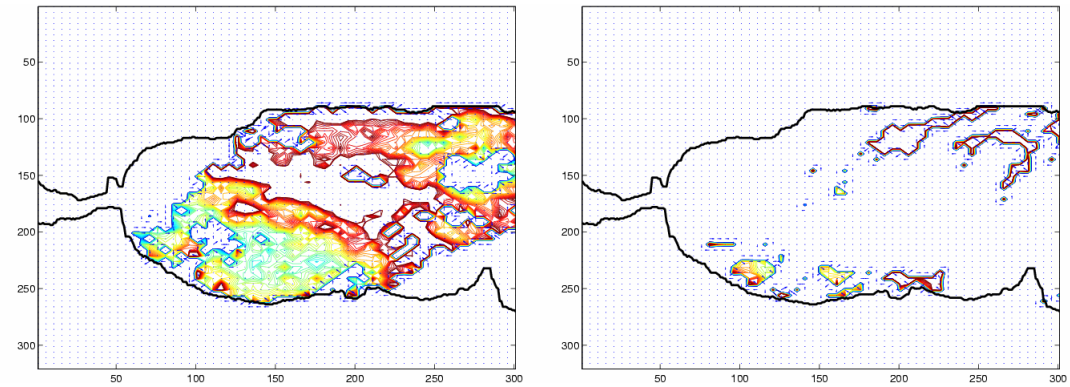

week 46 week 47

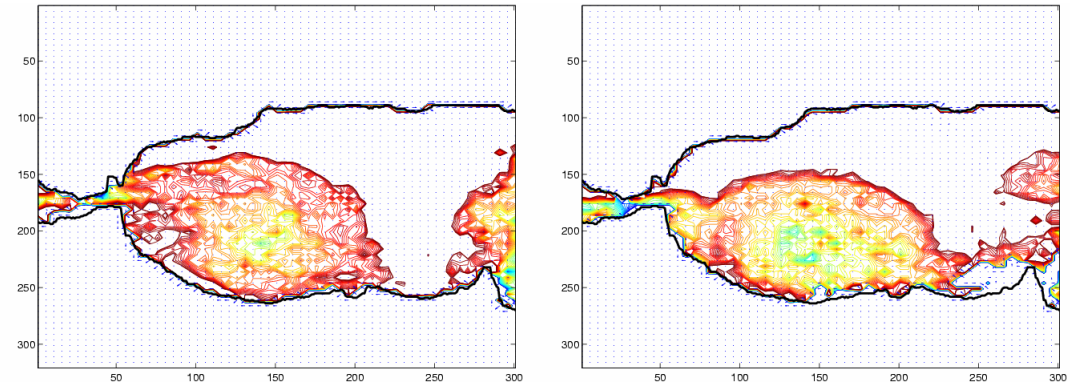

week 48 week 49

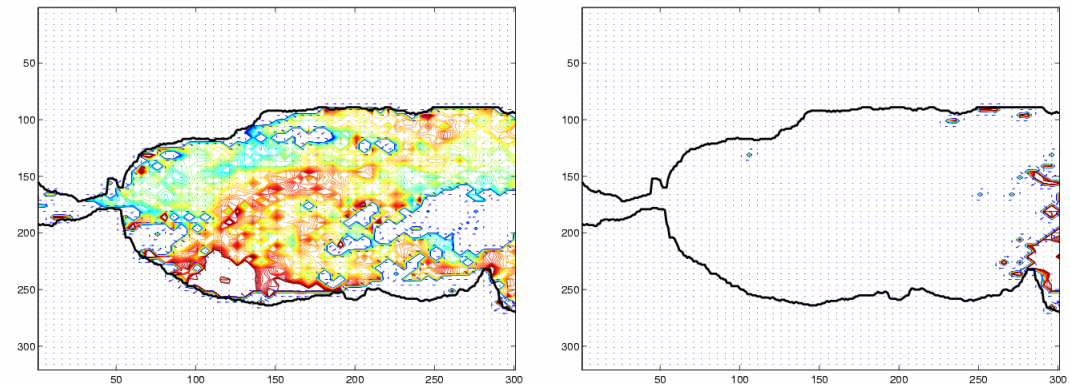

week 50 week 51

chl (mg m^{-3})

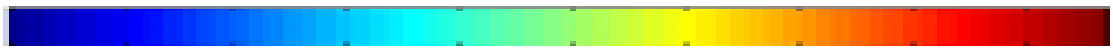

0.16 0.19 0.23 0.27 0.33 0.39 0.46 0.55 0.66 0.79

APPENDIX 14 (k) Gibraltar Strait
Spatial Gradient (*chl* range 0.16-0.9 mg m^{-3})

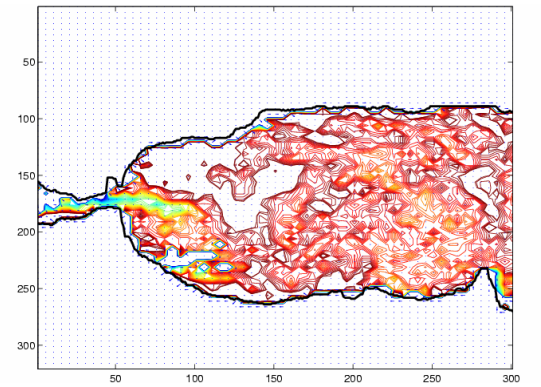

week 52

APPENDIX 15 (a) Alboran Sea
Spatial Gradient (*chl* range 1.0-1.9 mg m^{-3})

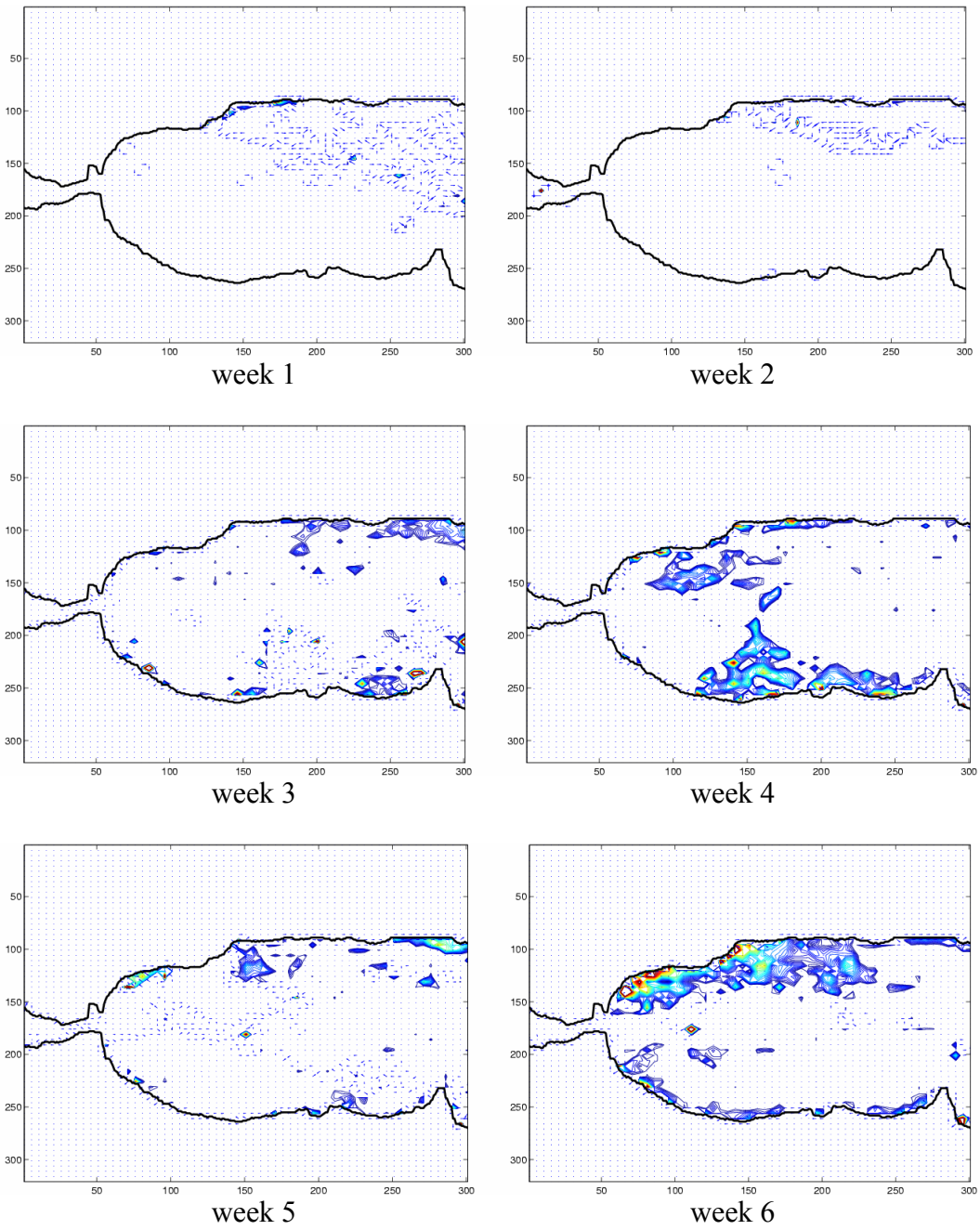

APPENDIX 15 (b) Alboran Sea
Spatial Gradient (*chl* range 1.0-1.9 mg m^{-3})

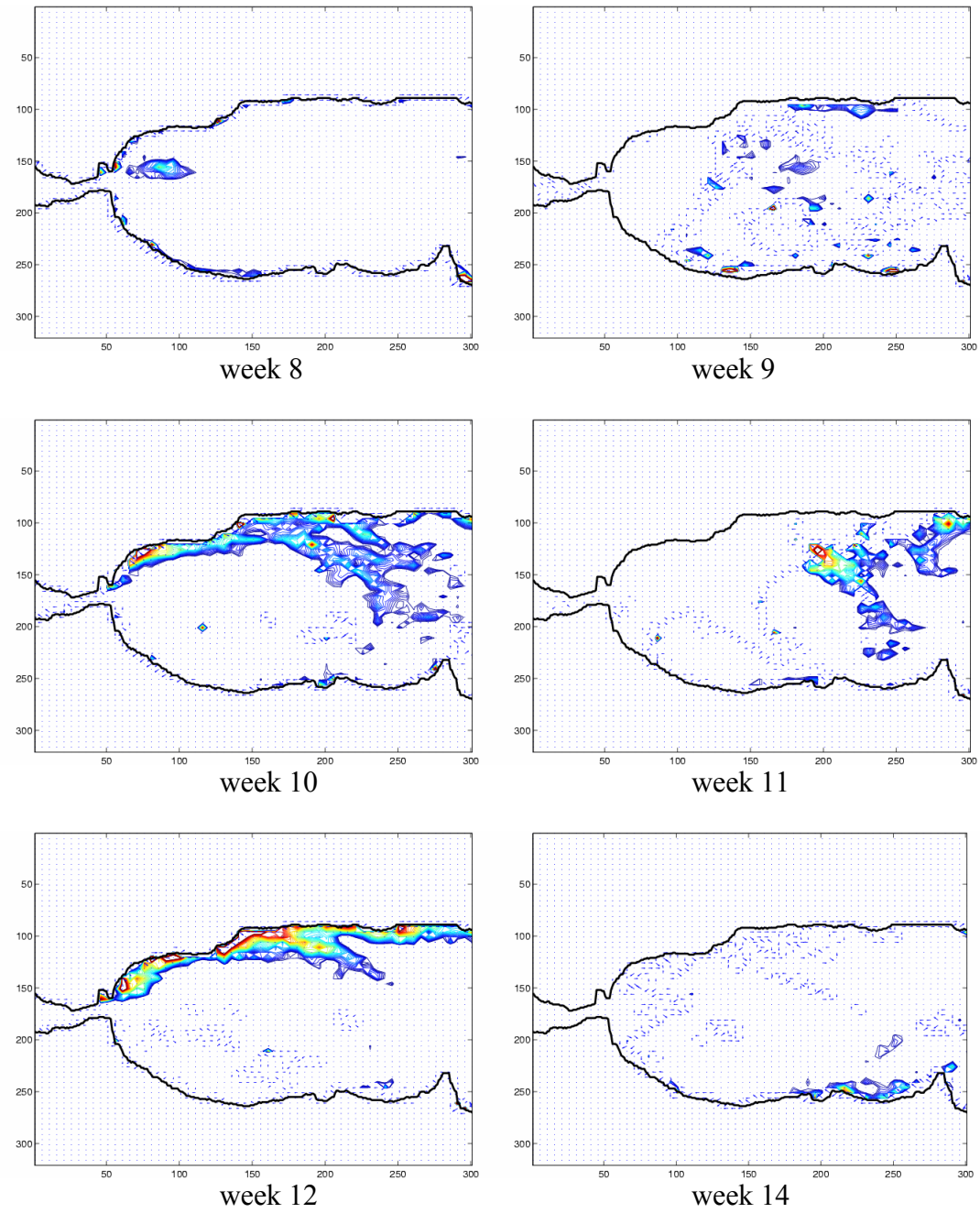

APPENDIX 15 (c) Alboran Sea
Spatial Gradient (*chl* range 1.0-1.9 mg m^{-3})

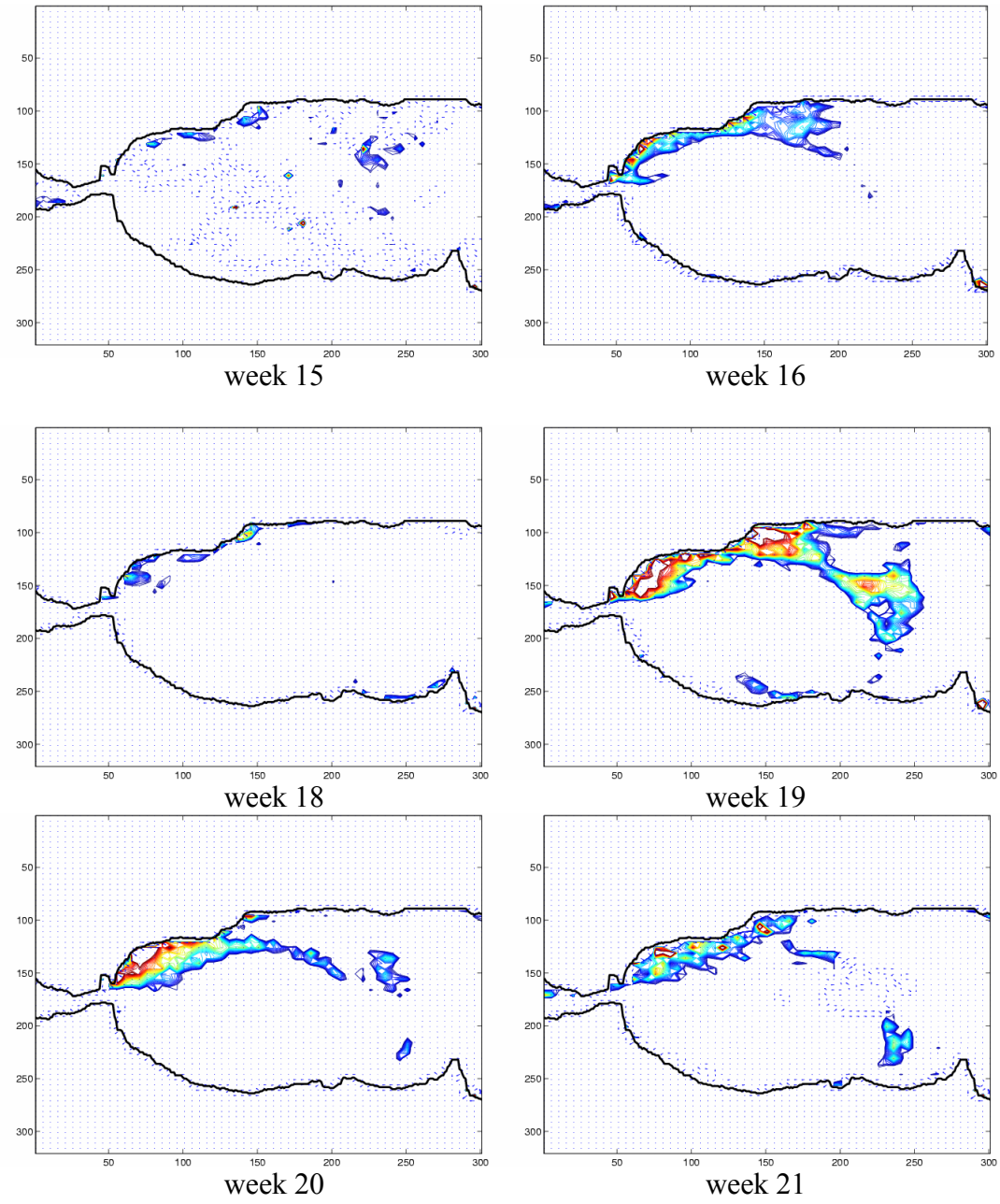

APPENDIX 15 (d) Alboran Sea
Spatial Gradient (*chl* range 1.0-1.9 mg m^{-3})

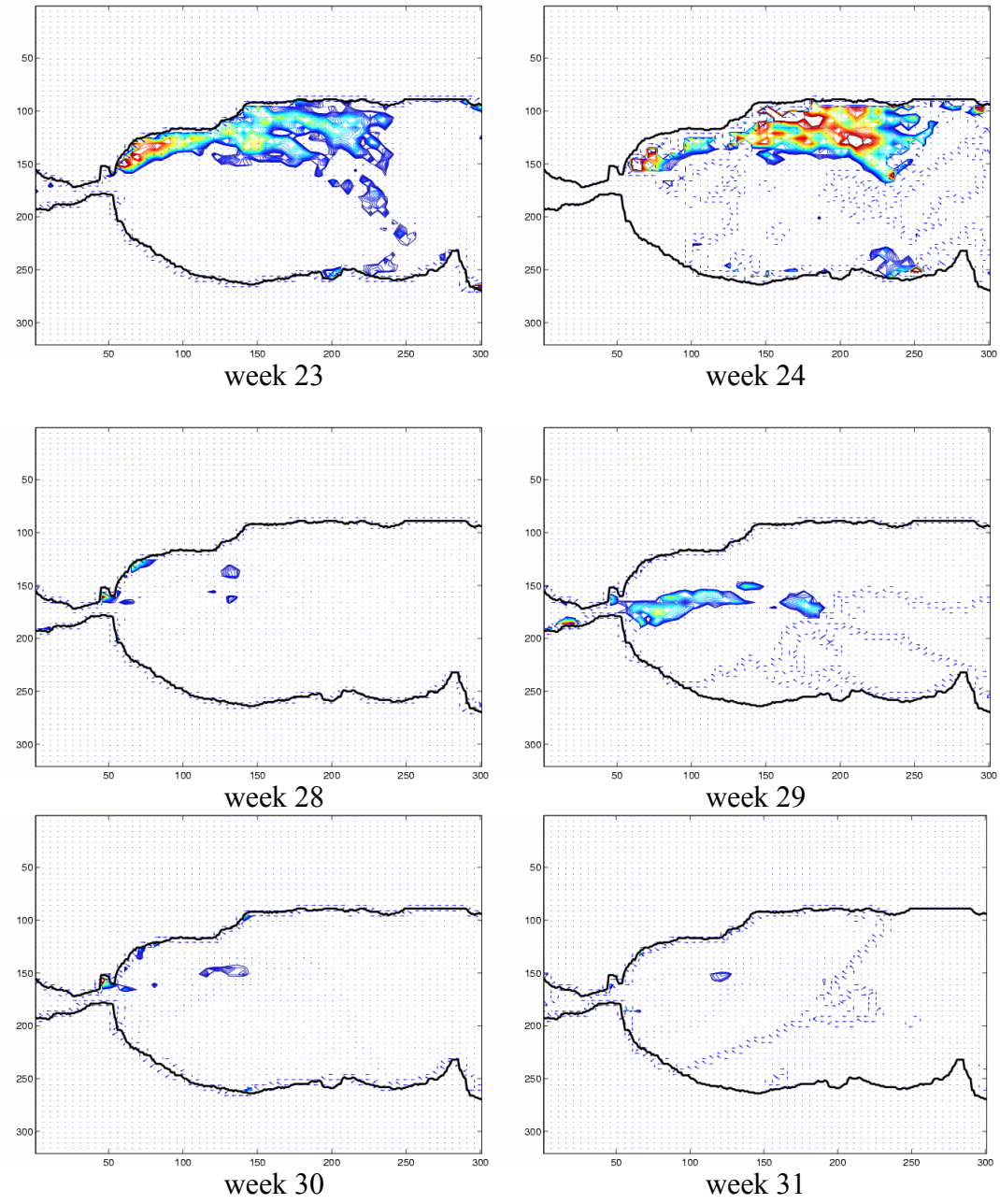

APPENDIX 15 (e) Alboran Sea
Spatial Gradient (*chl* range 1.0-1.9 mg m^{-3})

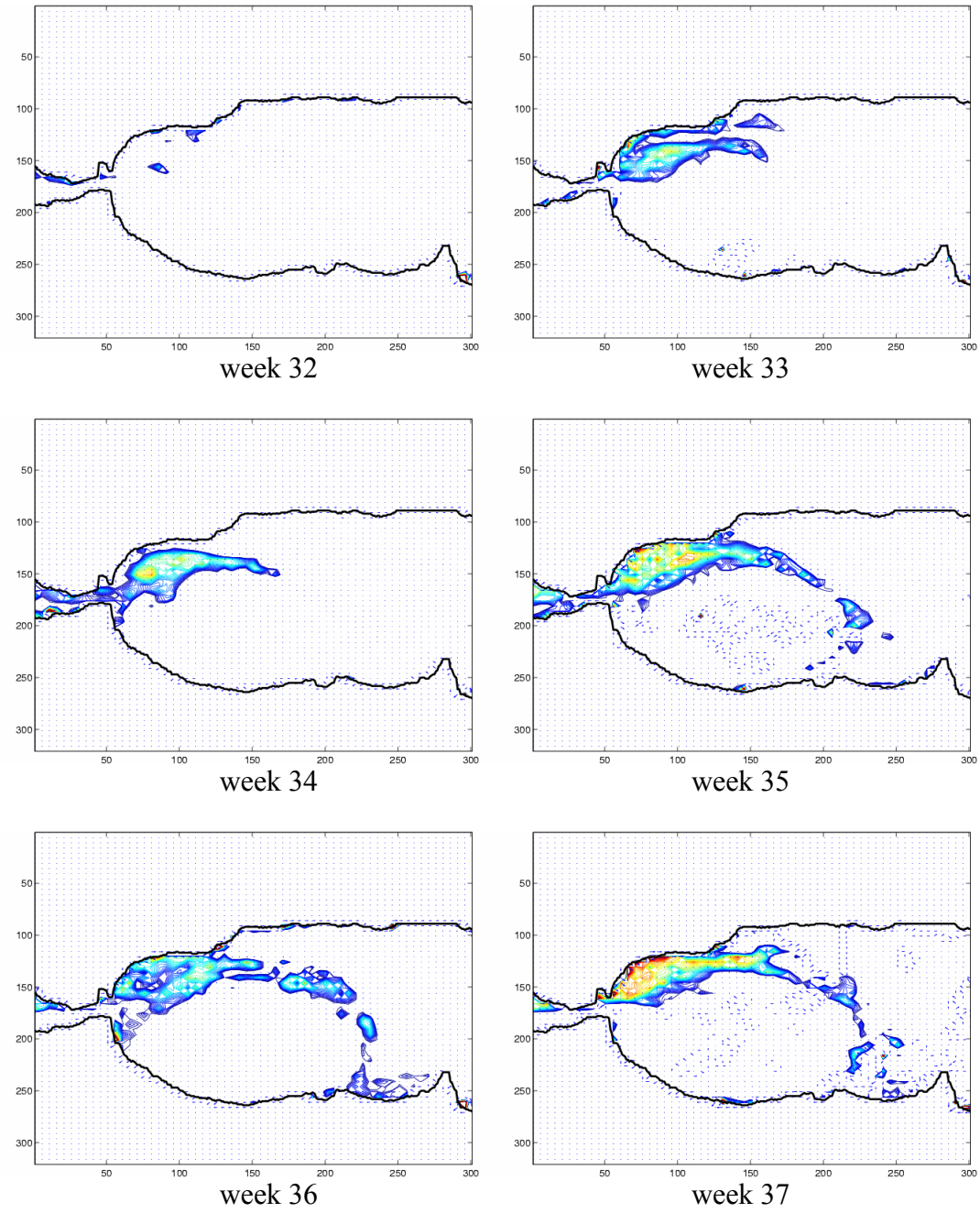

APPENDIX 15 (f) Alboran Sea
Spatial Gradient (*chl* range 1.0-1.9 mg m^{-3})

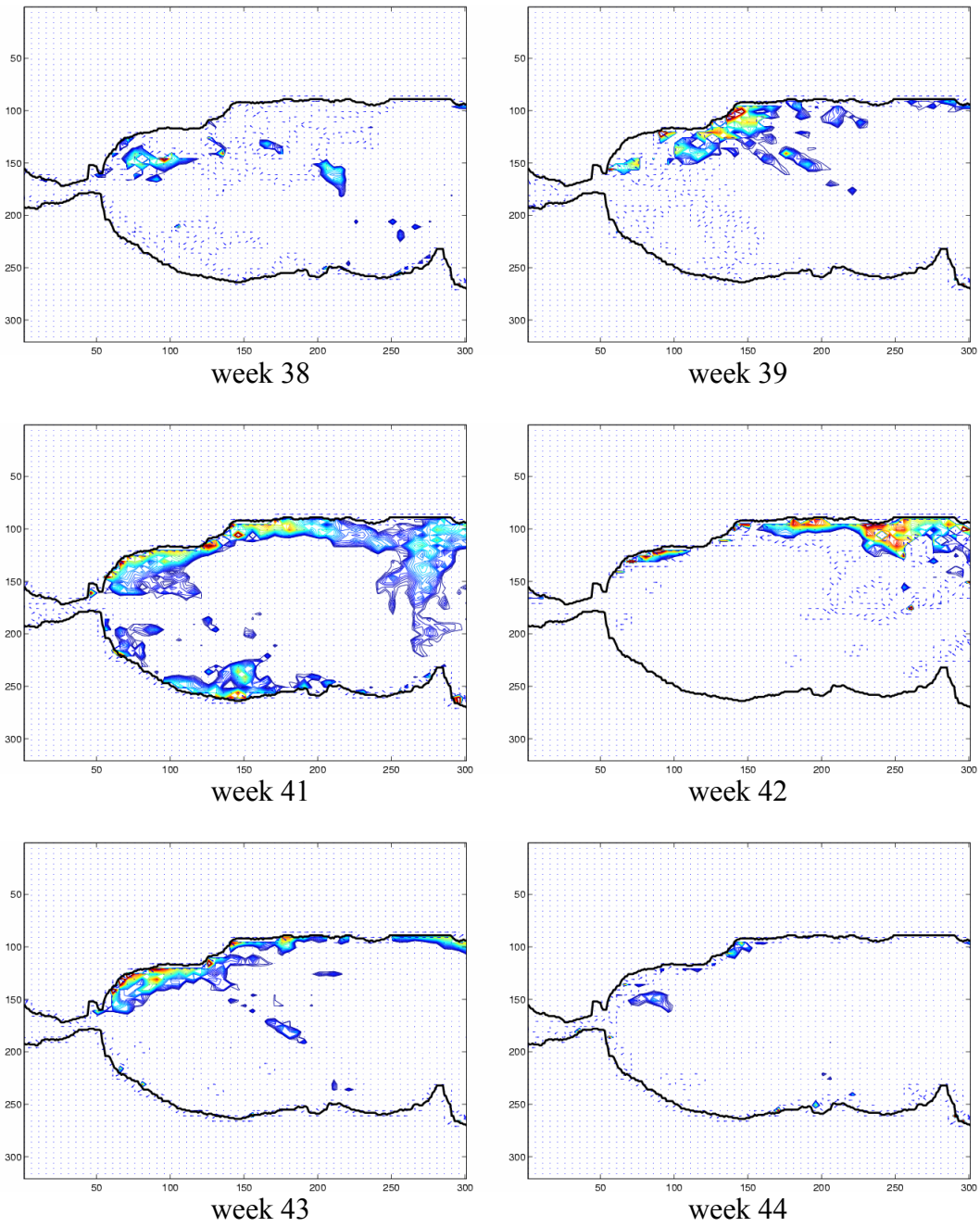

APPENDIX 15 (g) Alboran Sea
Spatial Gradient (*chl* range 1.0-1.9 mg m^{-3})

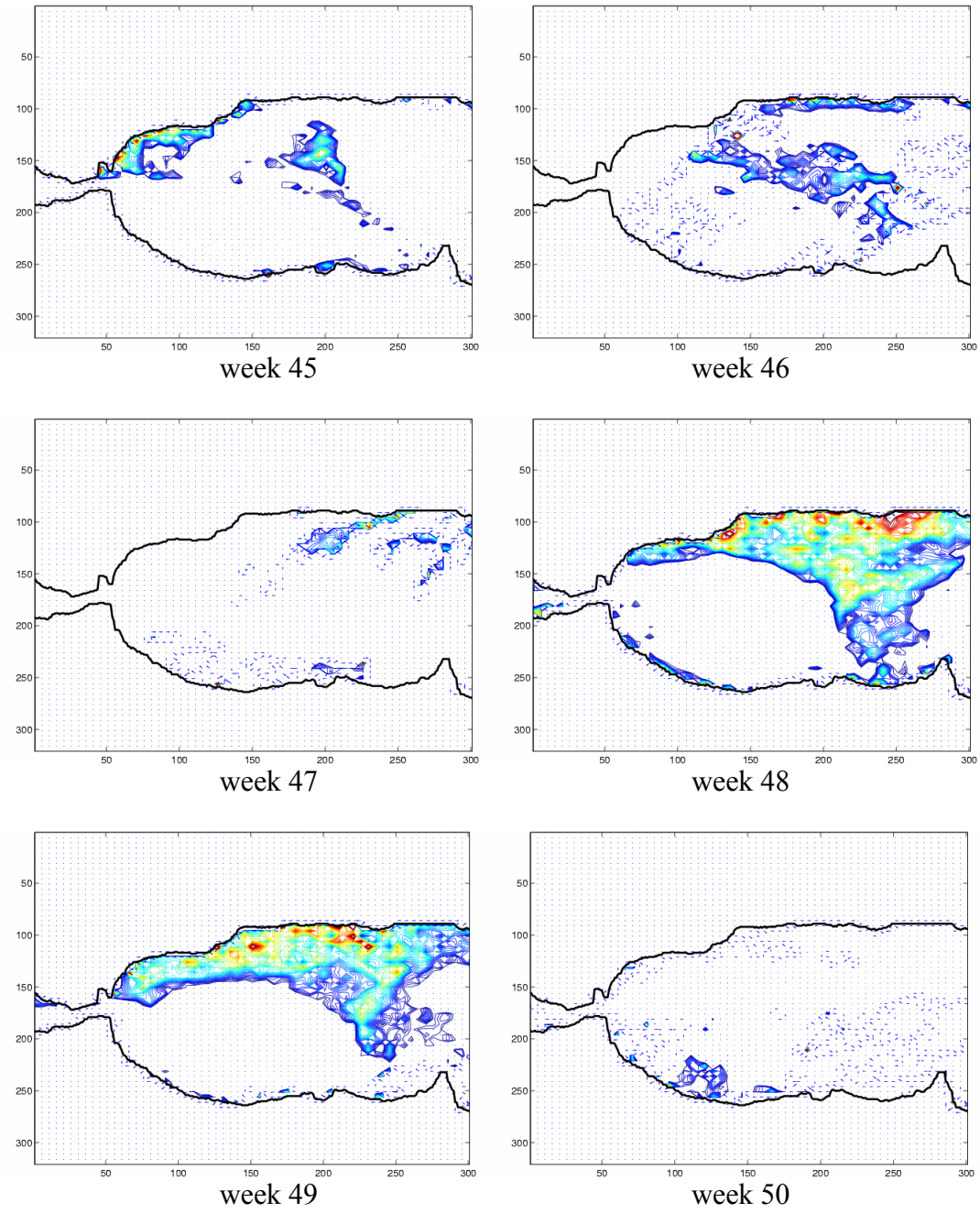

APPENDIX 15 (h) Alboran Sea
Spatial Gradient (*chl* range 1.0-1.9 mg m^{-3})

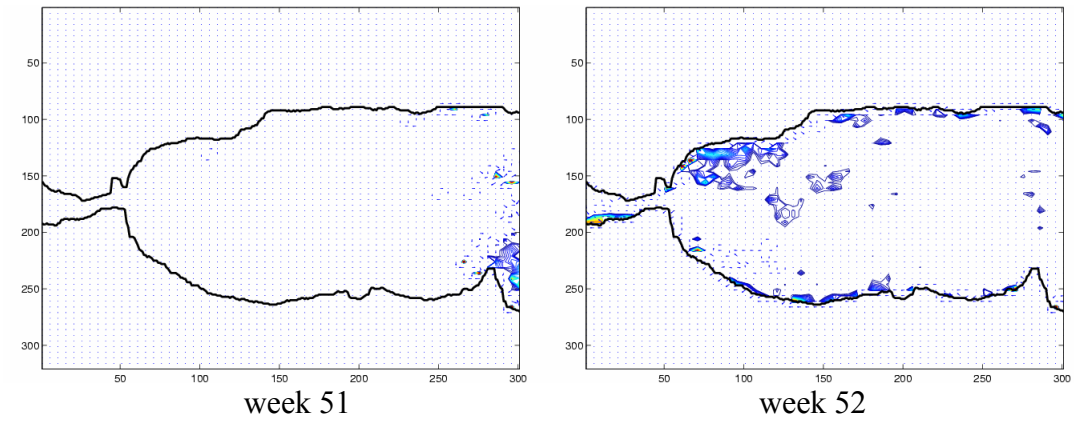

week 51 week 52

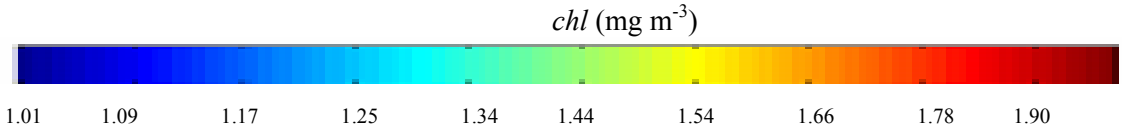

APPENDIX 16 (a) Al Hoceima National Park
Spatial Gradient (*chl* range 0.16-0.9 mg m^{-3})

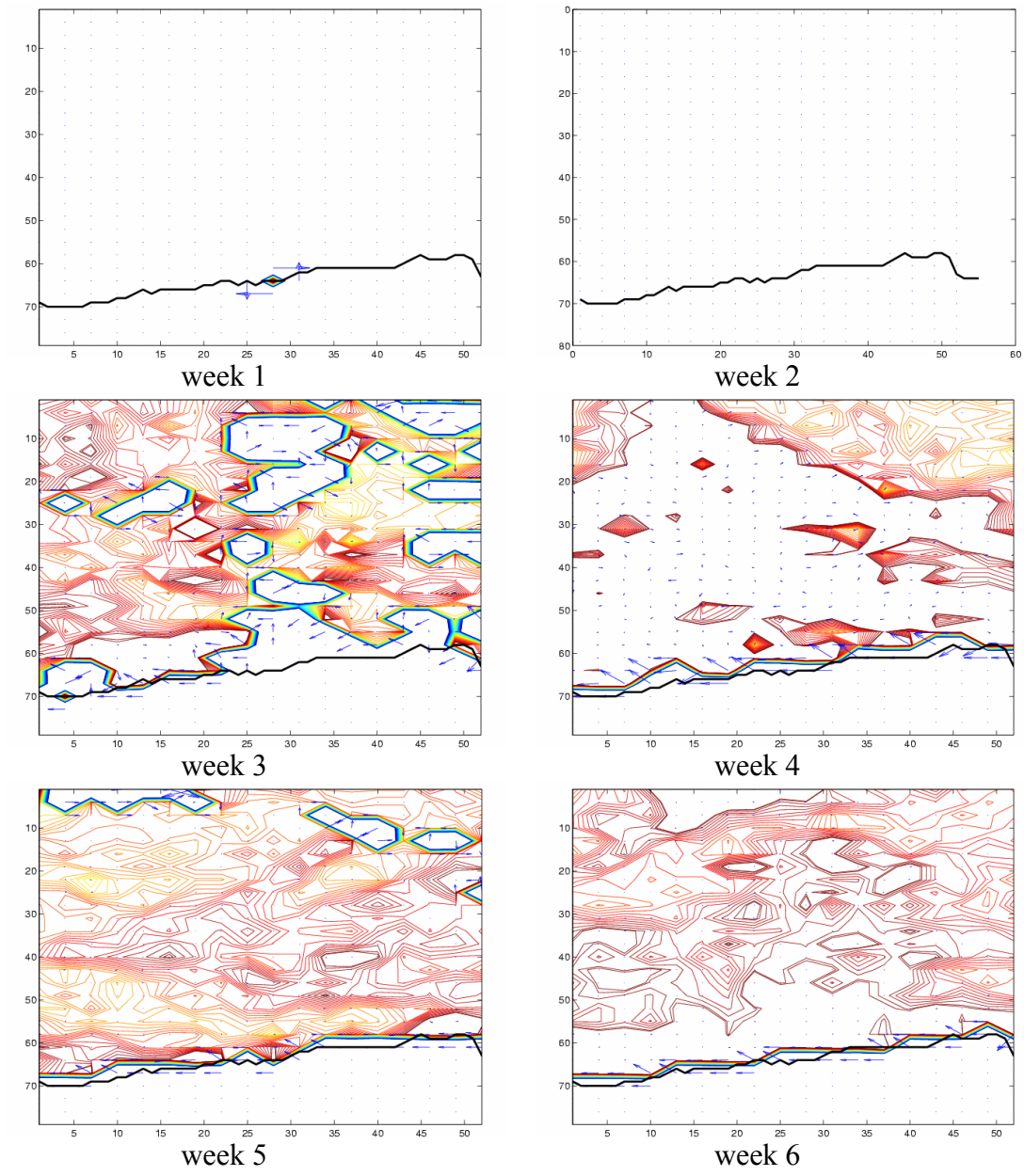

APPENDIX 16 (b) Al Hoceima National Park
Spatial Gradient (*chl* range 0.16-0.9 mg m^{-3})

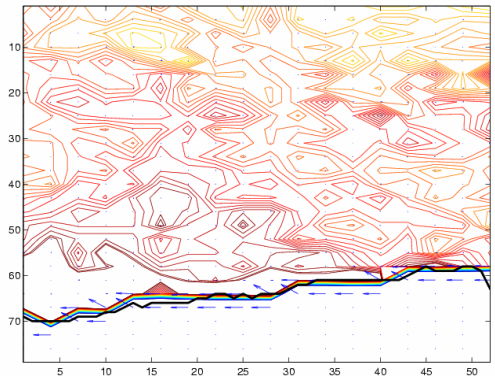

week 8

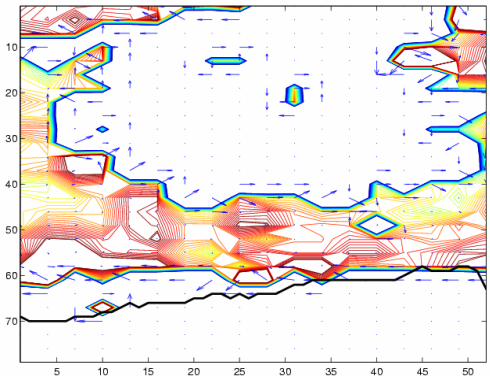

week 9

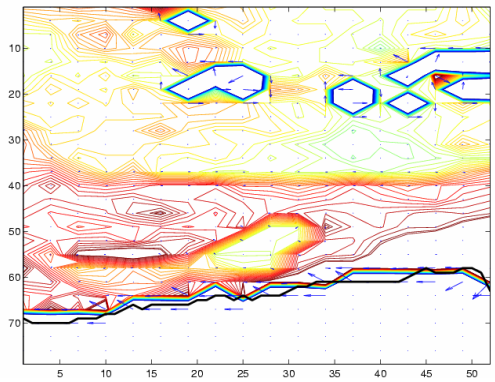

week 10

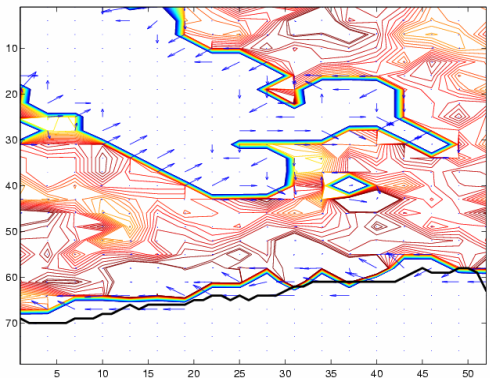

week 11

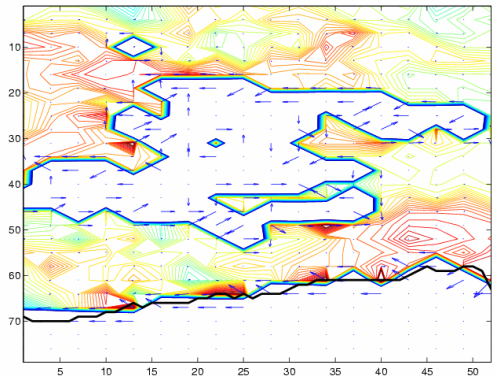

week 12

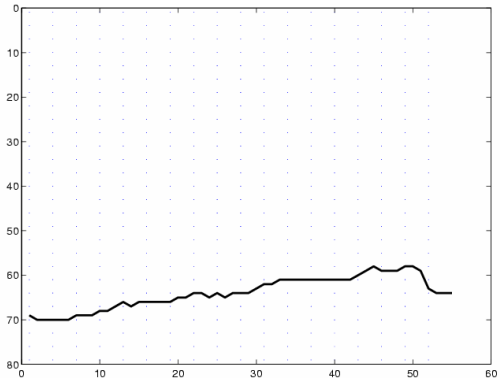

week 13

chl (mg m^{-3})

0.16 0.19 0.23 0.27 0.33 0.39 0.46 0.55 0.66 0.79

APPENDIX 16 (c) Al Hoceima National Park
Spatial Gradient (*chl* range 0.16-0.9 mg m^{-3})

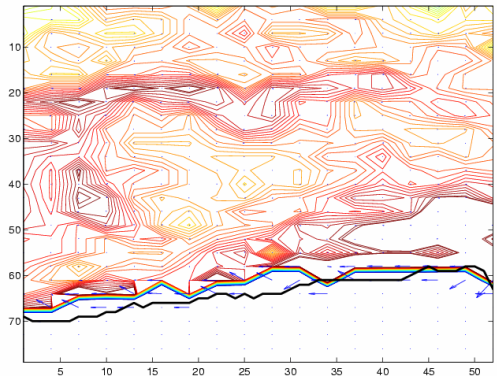

week 14

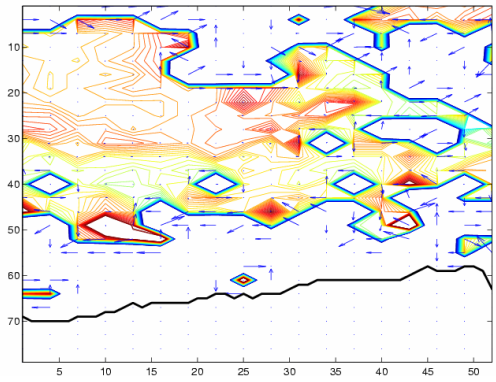

week 15

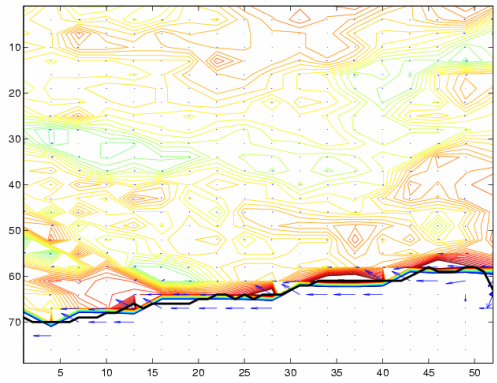

week 16

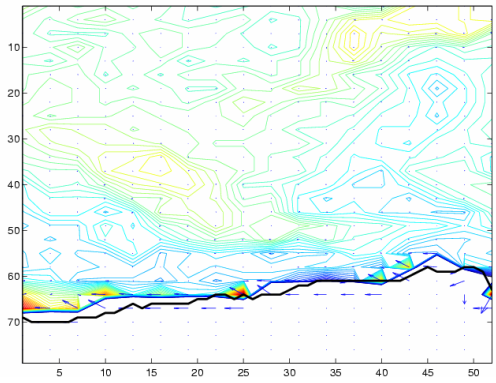

week 17

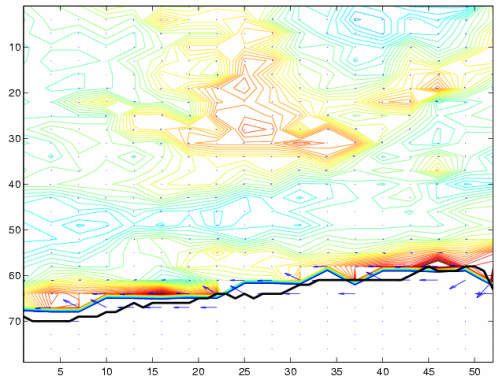

week 18

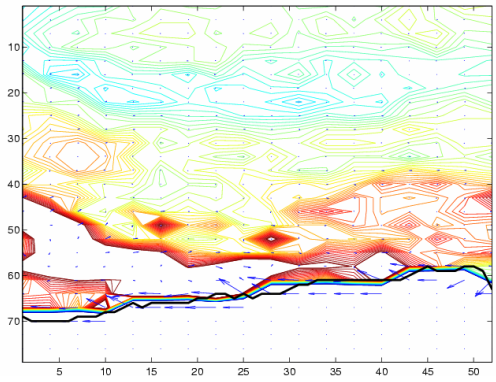

week 19

chl (mg m^{-3})

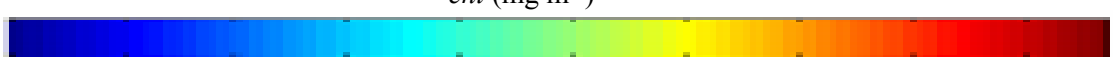

0.16 0.19 0.23 0.27 0.33 0.39 0.46 0.55 0.66 0.79

APPENDIX 16 (d) Al Hoceima National Park
Spatial Gradient (*chl* range 0.16-0.9 mg m^{-3})

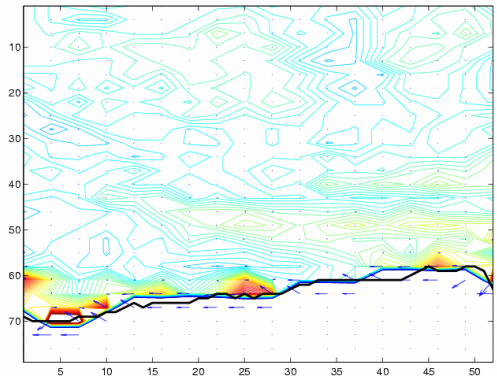

week 20

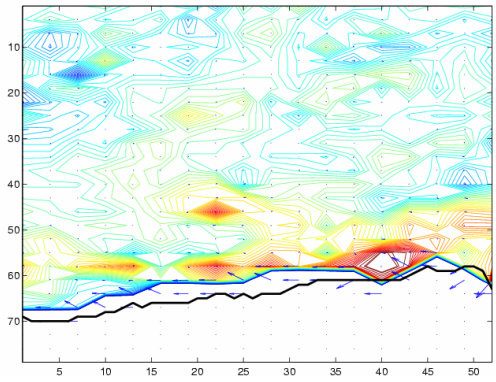

week 21

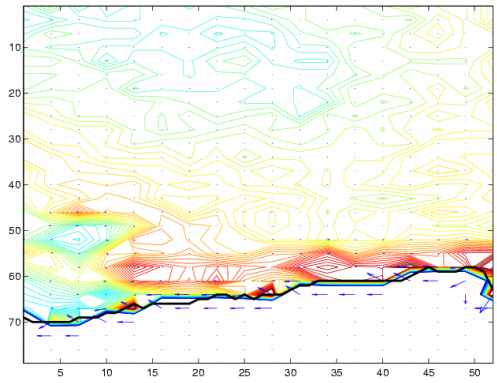

week 23

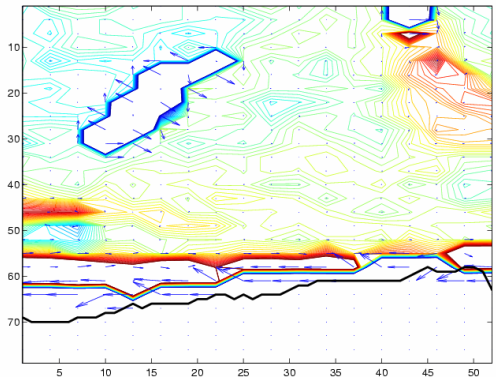

week 24

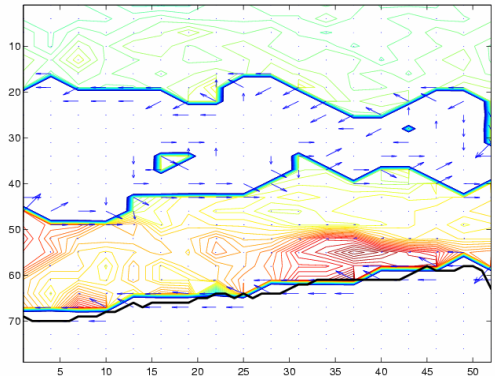

week 25

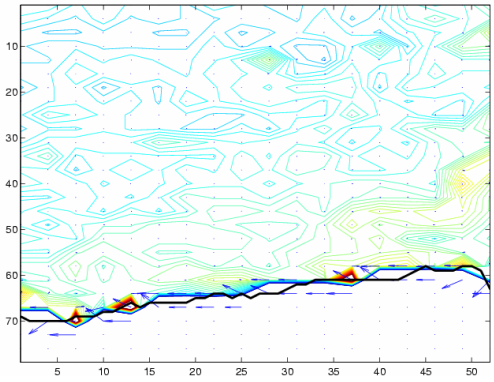

week 26

chl (mg m^{-3})

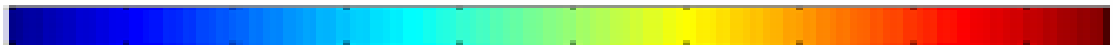

0.16 0.19 0.23 0.27 0.33 0.39 0.46 0.55 0.66 0.79

APPENDIX 16 (e) Al Hoceima National Park
Spatial Gradient (*chl* range 0.16-0.9 mg m^{-3})

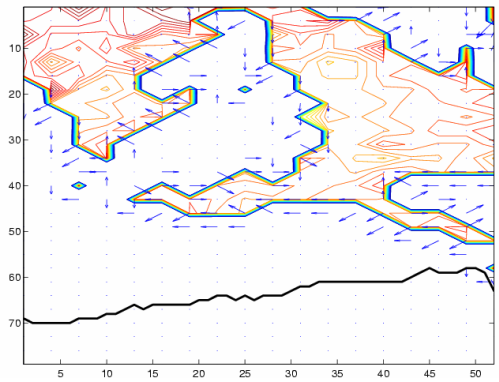

week 29

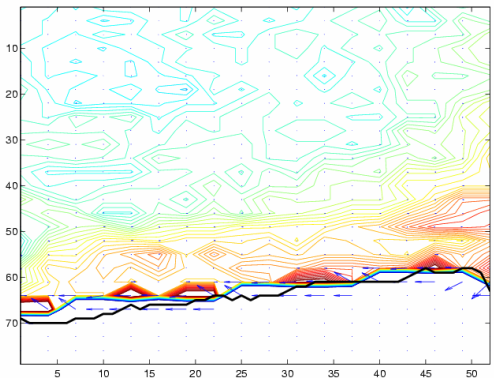

week 30

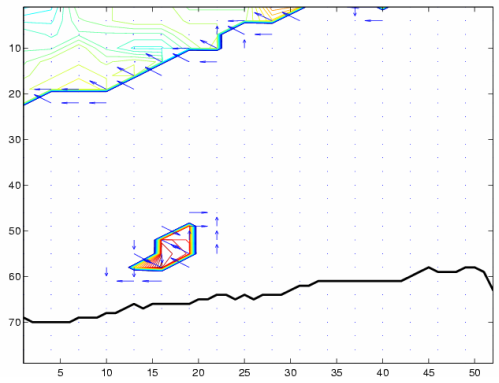

week 31

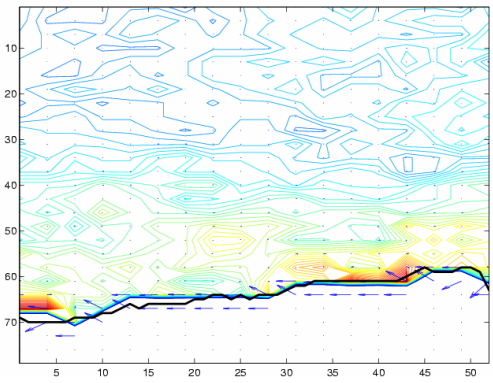

week 32

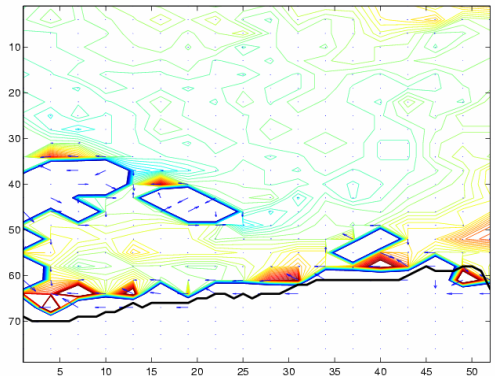

week 33

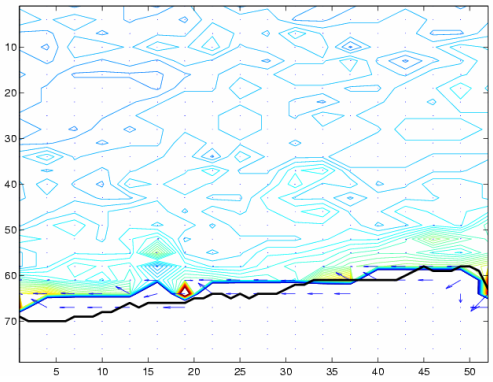

week 34

chl (mg m^{-3})

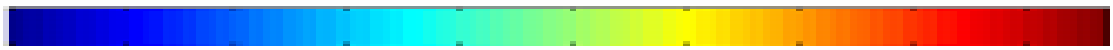

0.16 0.19 0.23 0.27 0.33 0.39 0.46 0.55 0.66 0.79

APPENDIX 16 (f) Al Hoceima National Park
Spatial Gradient (*chl* range 0.16-0.9 mg m^{-3})

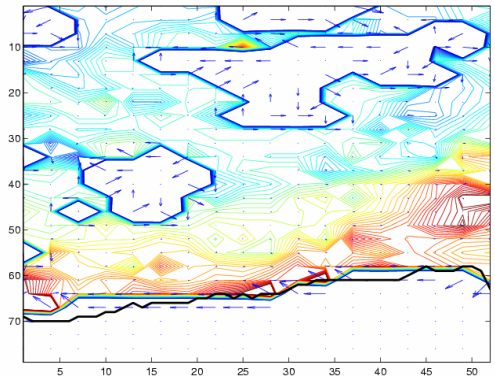

week 35

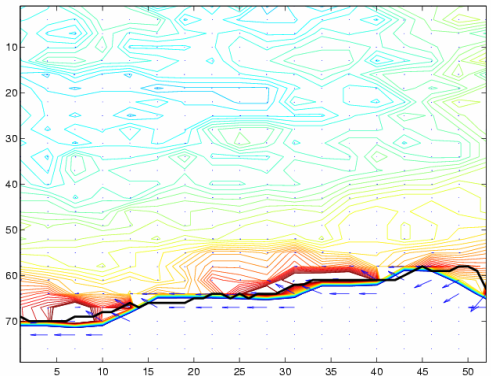

week 36

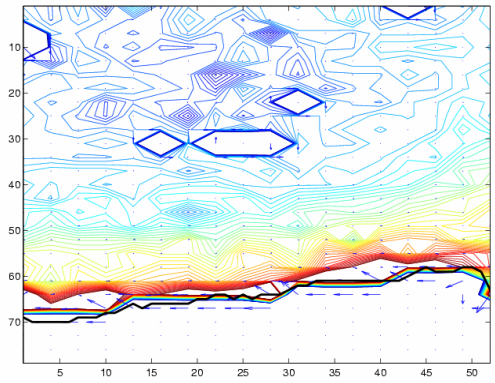

week 37

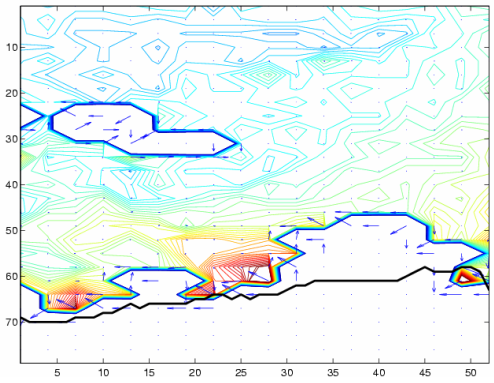

week 38

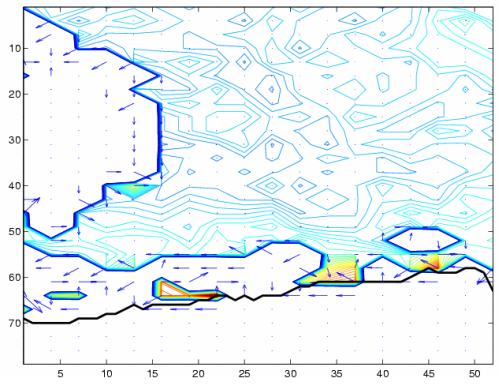

week 39

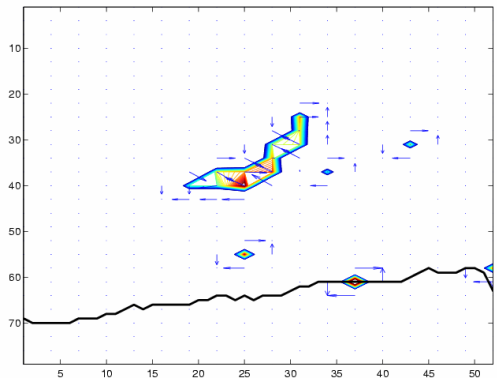

week 40

chl (mg m^{-3})

0.16 0.19 0.23 0.27 0.33 0.39 0.46 0.55 0.66 0.79

APPENDIX 16 (g) Al Hoceima National Park
Spatial Gradient (*chl* range 0.16-0.9 mg m^{-3})

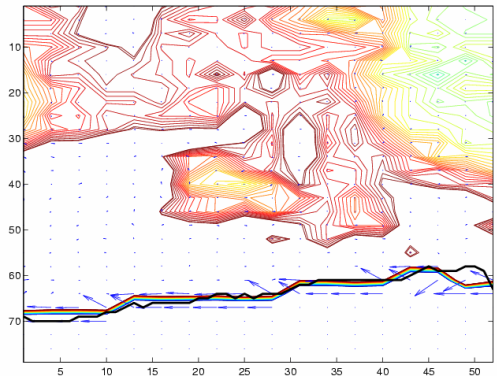

week 41

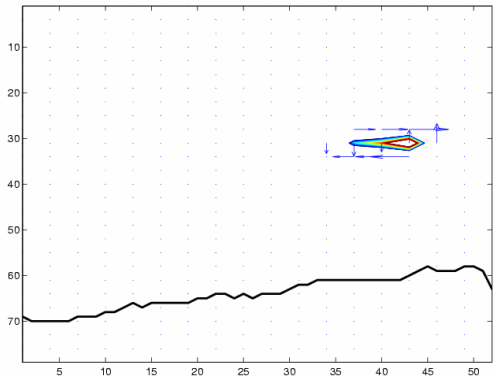

week 42

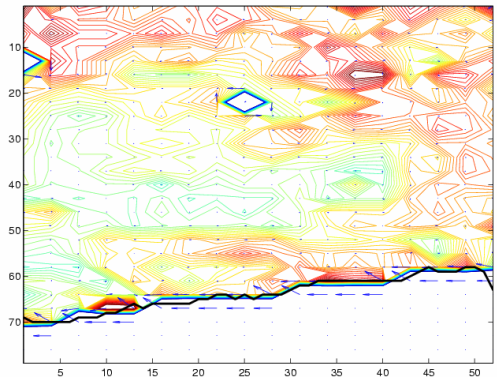

week 43

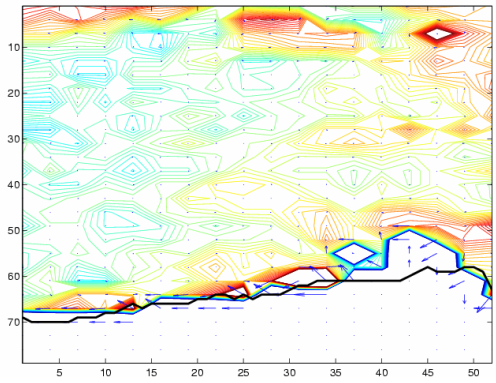

week 44

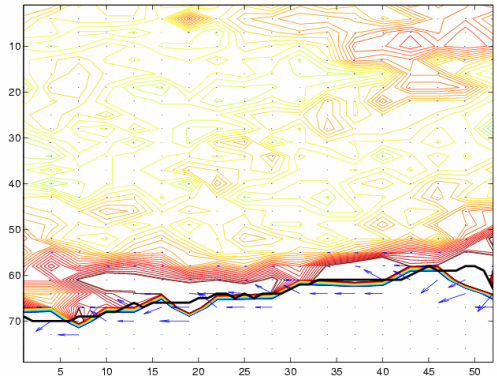

week 45

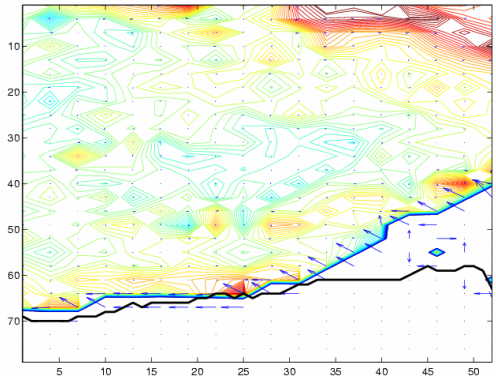

week 46

chl (mg m^{-3})

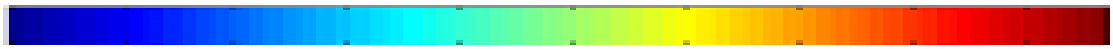

0.16 0.19 0.23 0.27 0.33 0.39 0.46 0.55 0.66 0.79

APPENDIX 16 (h) Al Hoceima National Park
Spatial Gradient (*chl* range 0.16-0.9 mg m^{-3})

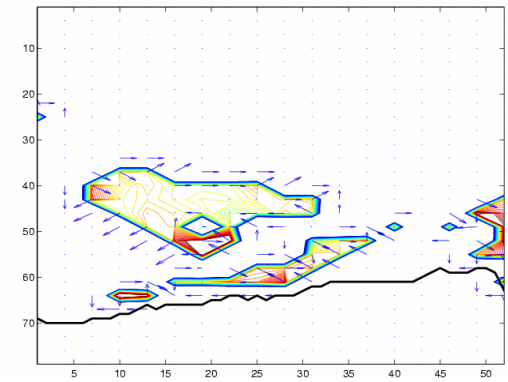

week 47

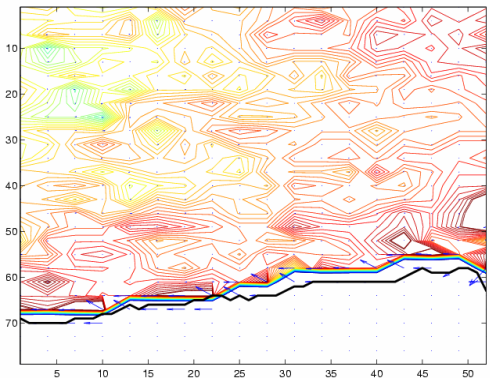

week 48

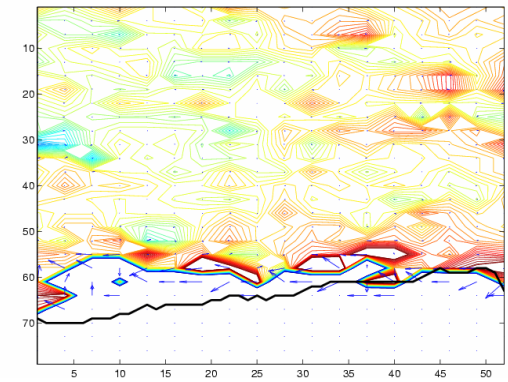

week 49

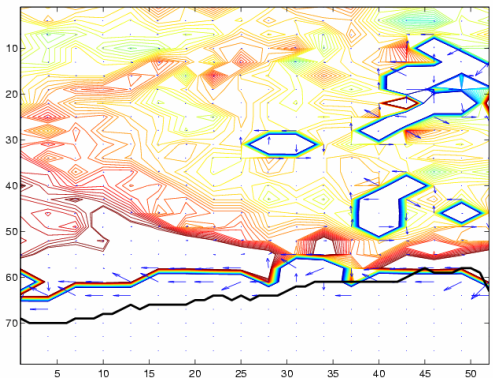

week 50

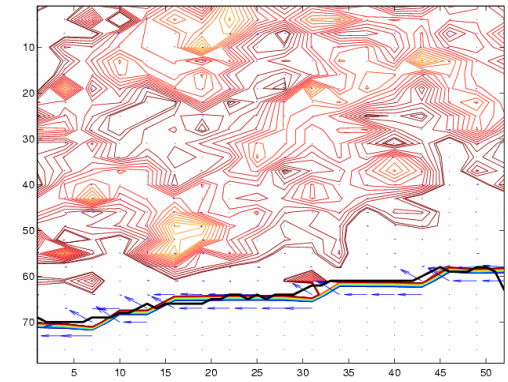

week 52

chl (mg m^{-3})

0.16 0.19 0.23 0.27 0.33 0.39 0.46 0.55 0.66 0.79

APPENDIX 17 (a) Al Hoceima National Park
Spatial Gradient (*chl* range 1.0-4.0 mg m^{-3})

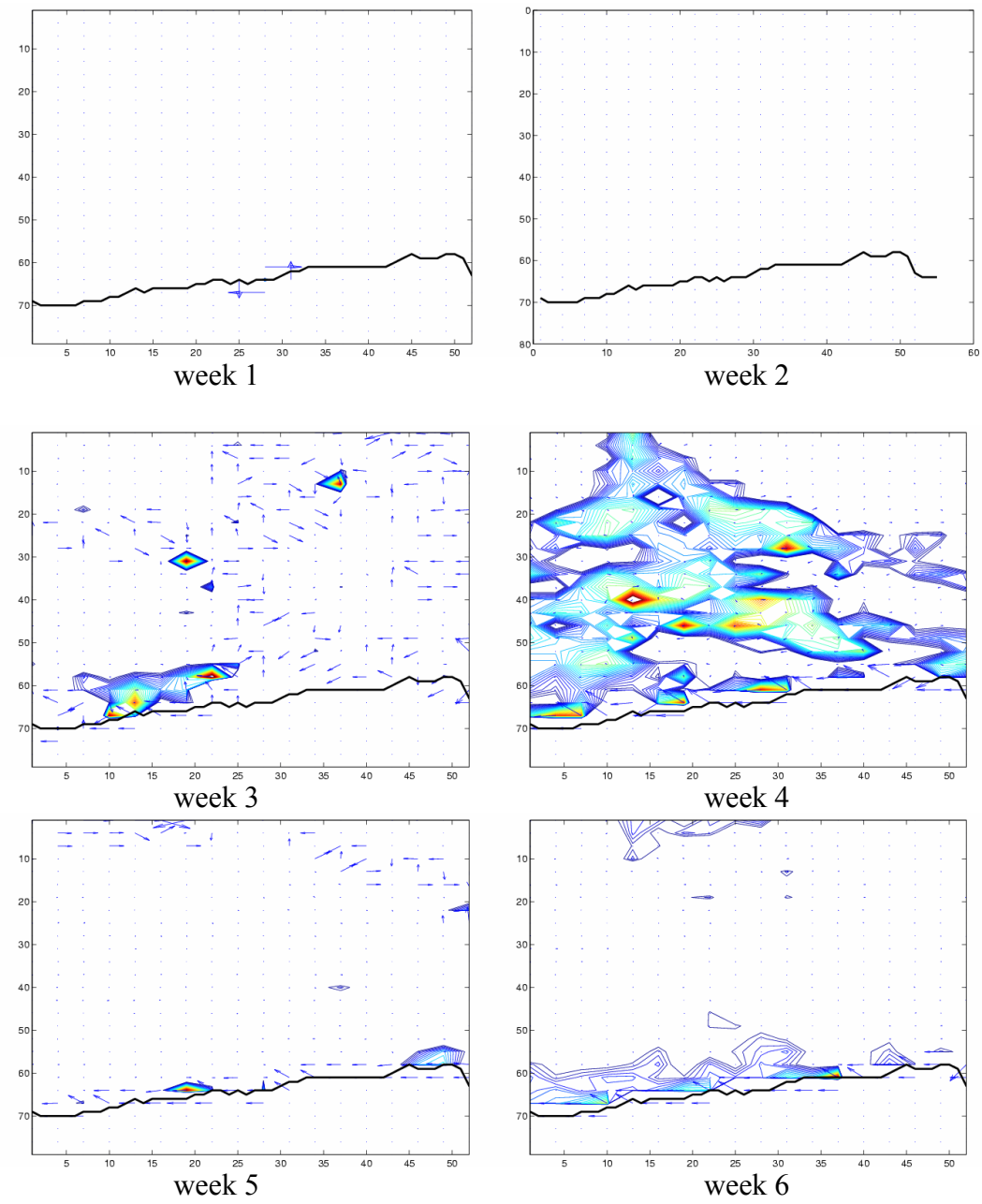

APPENDIX 17 (b) Al Hoceima National Park
Spatial Gradient (*chl* range 1.0-4.0 mg m^{-3})

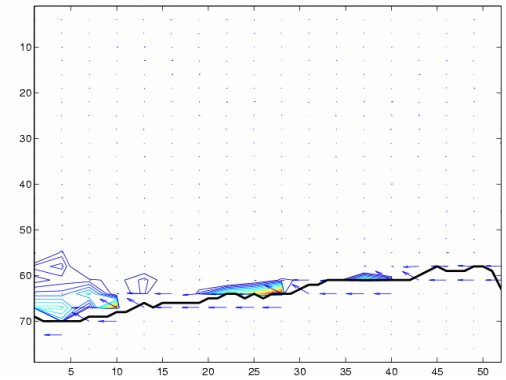

week 8

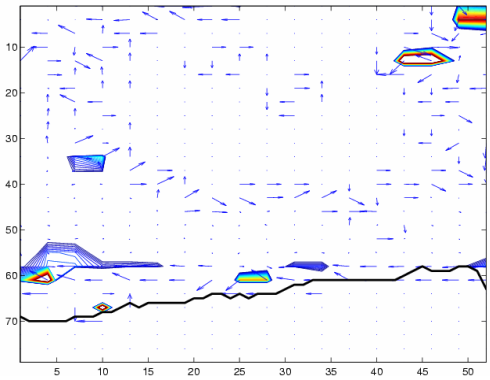

week 9

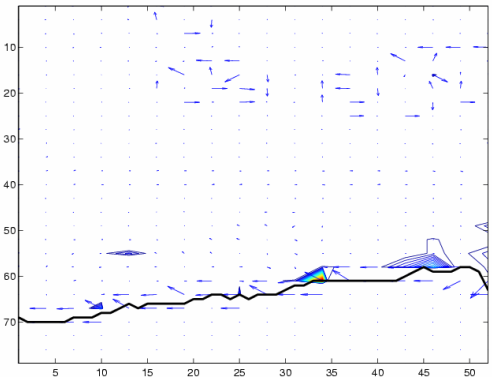

week 10

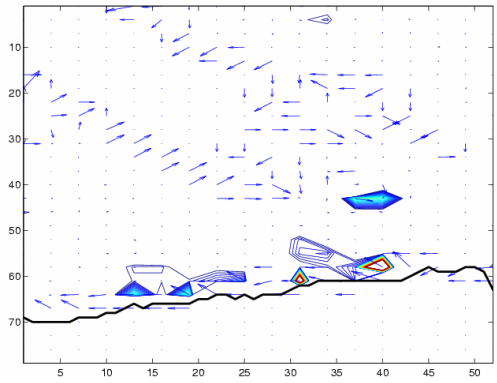

week 11

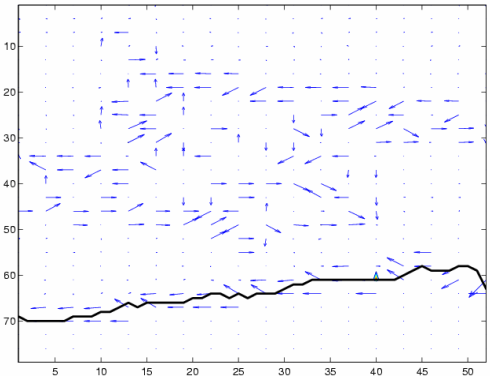

week 12

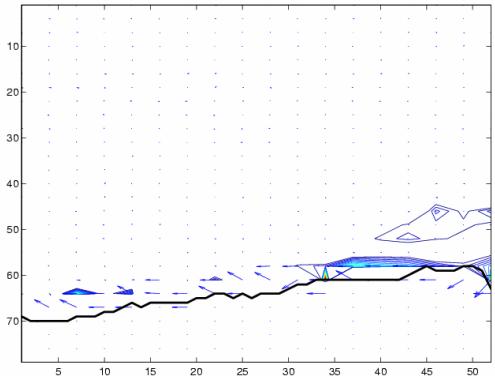

week 14

chl (mg m^{-3})

1.13 1.34 1.60 1.91 2.27 2.70 3.22 3.84

APPENDIX 17 (c) Al Hoceima National Park
Spatial Gradient (*chl* range 1.0-4.0 mg m^{-3})

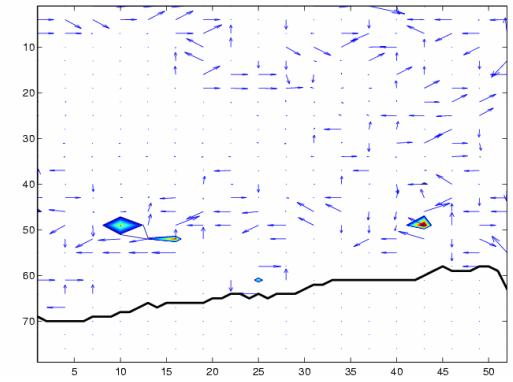

week 15

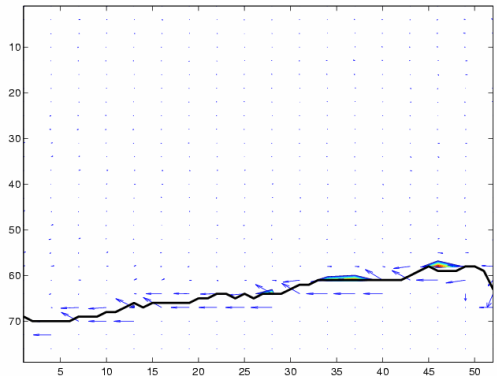

week 16

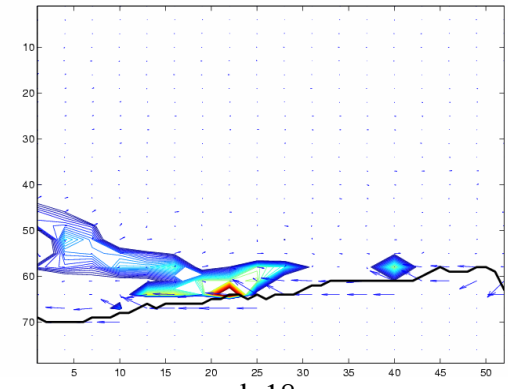

week 18

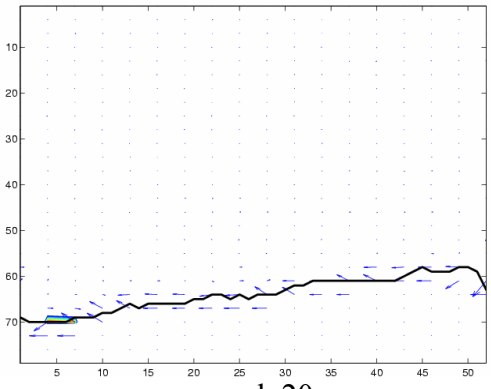

week 20

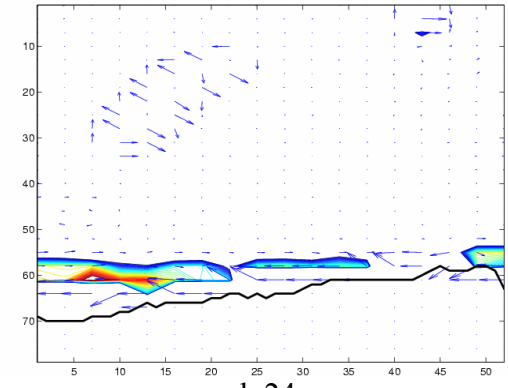

week 24

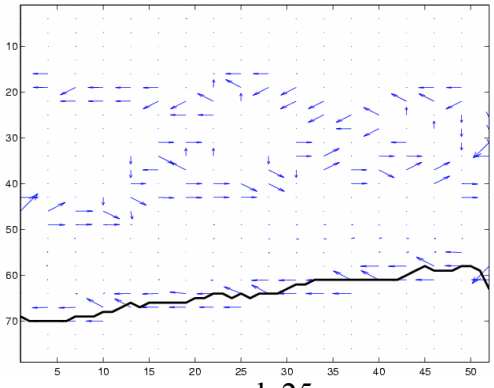

week 25

chl (mg m^{-3})

1.13 1.34 1.60 1.91 2.27 2.70 3.22 3.84

APPENDIX 17 (d) Al Hoceima National Park
Spatial Gradient (*chl* range 1.0-4.0 mg m^{-3})

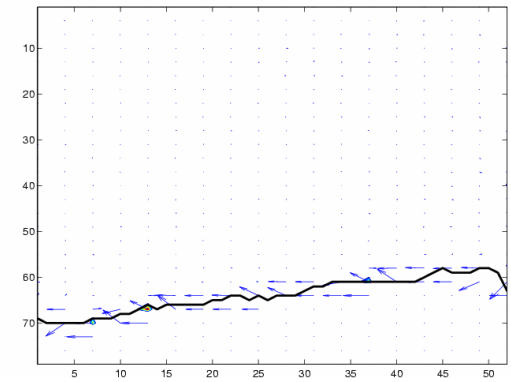

week 28

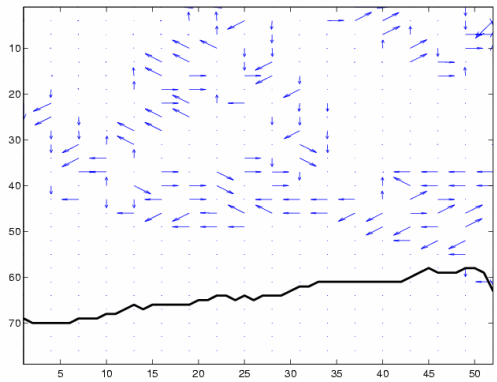

week 29

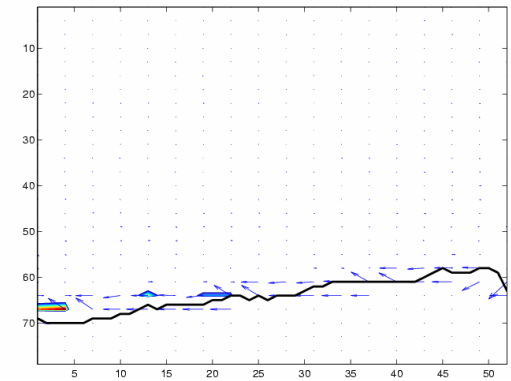

week 30

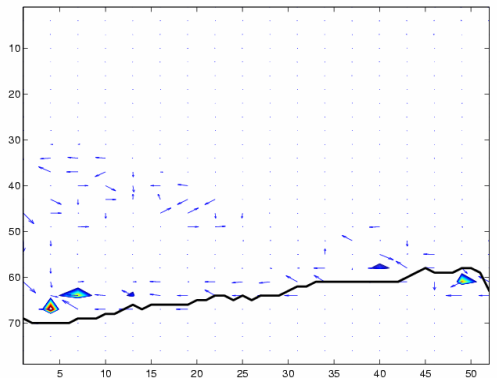

week 33

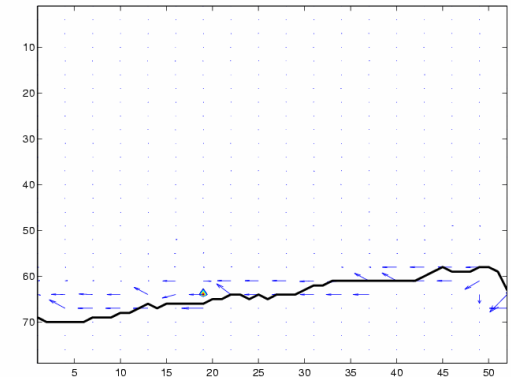

week 34

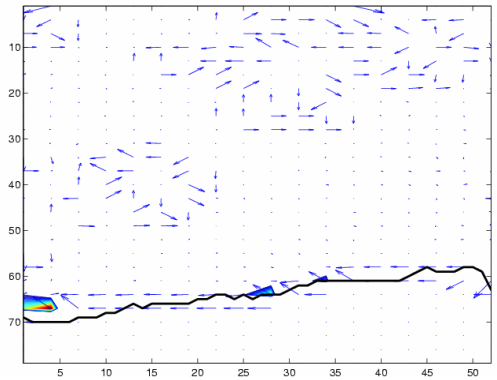

week 35

chl (mg m^{-3})

1.13 1.34 1.60 1.91 2.27 2.70 3.22 3.84

APPENDIX 17 (e) Al Hoceima National Park
Spatial Gradient (*chl* range 1.0-4.0 mg m^{-3})

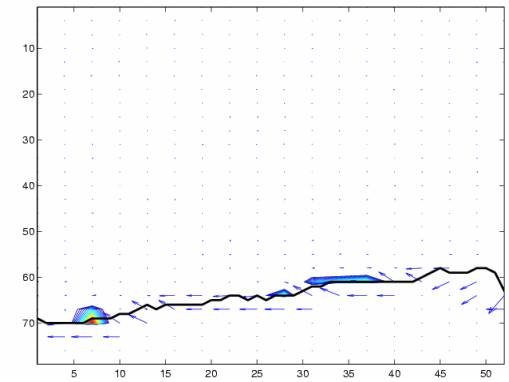

week 36

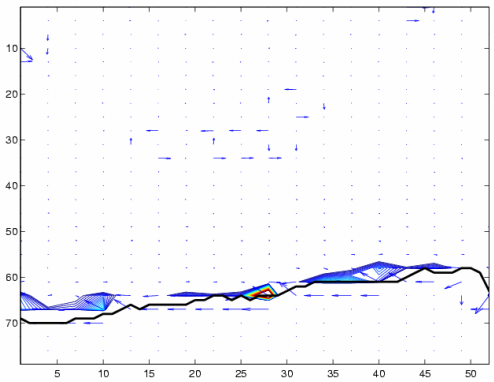

week 37

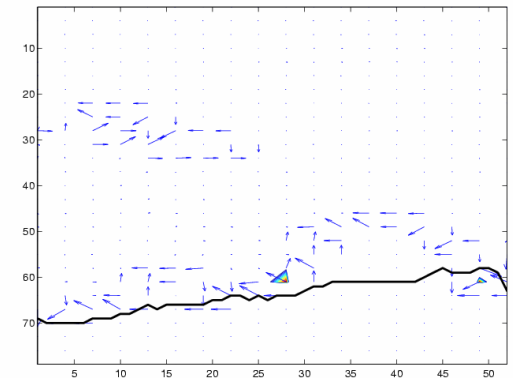

week 38

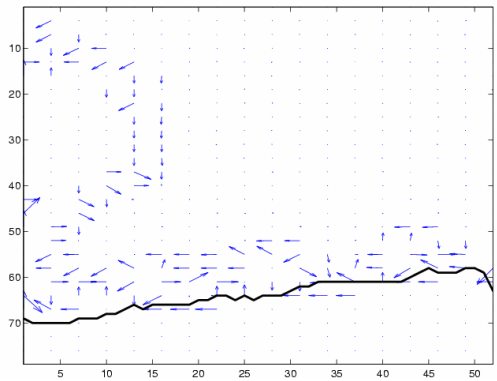

week 39

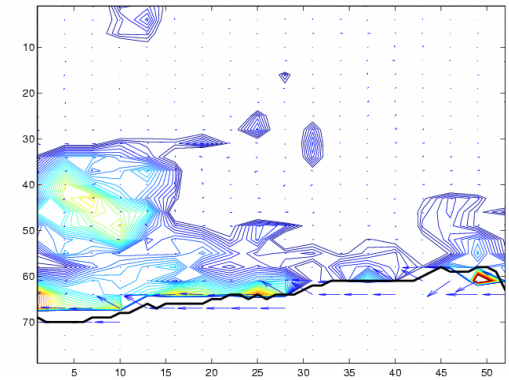

week 41

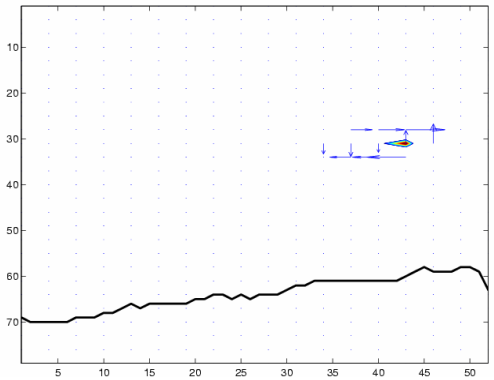

week 42

chl (mg m^{-3})

1.13 1.34 1.60 1.91 2.27 2.70 3.22 3.84

APPENDIX 17 (f) Al Hoceima National Park
Spatial Gradient (*chl* range 1.0-4.0 mg m^{-3})

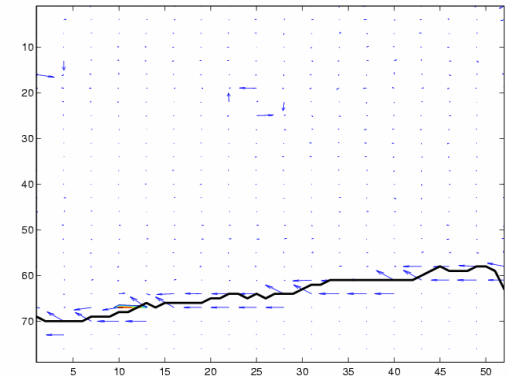

week 43

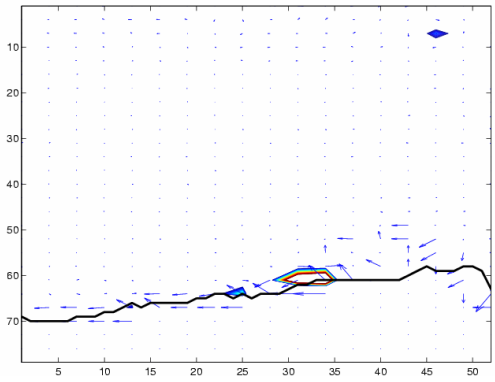

week 44

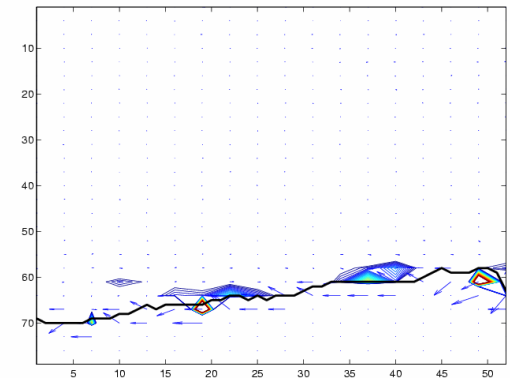

week 45

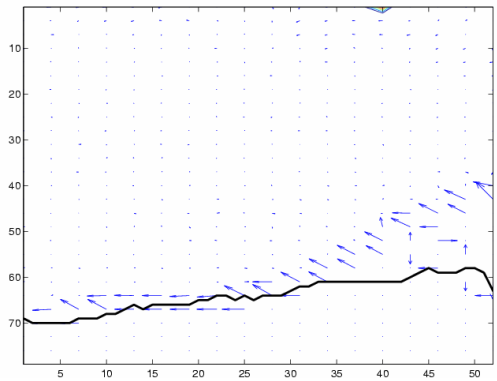

week 46

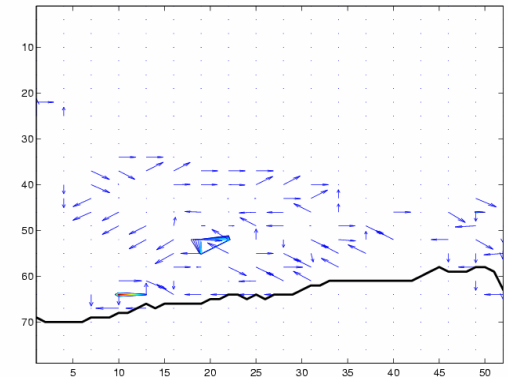

week 47

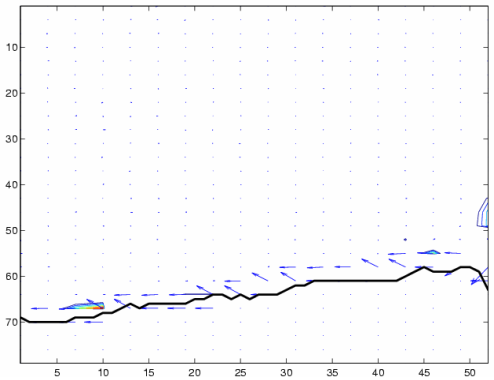

week 48

chl (mg m^{-3})

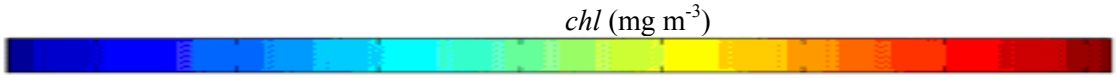

1.13 1.34 1.60 1.91 2.27 2.70 3.22 3.84

APPENDIX 17 (g) Al Hoceima National Park
Spatial Gradient (*chl* range 1.0-4.0 mg m^{-3})

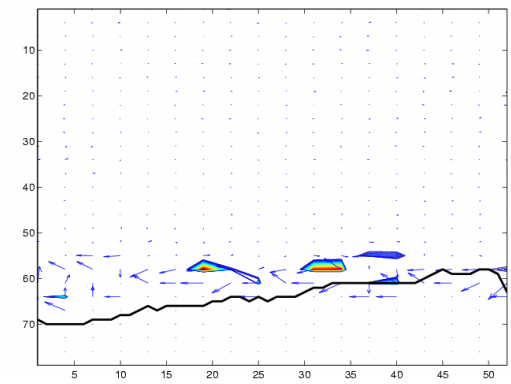

week 49

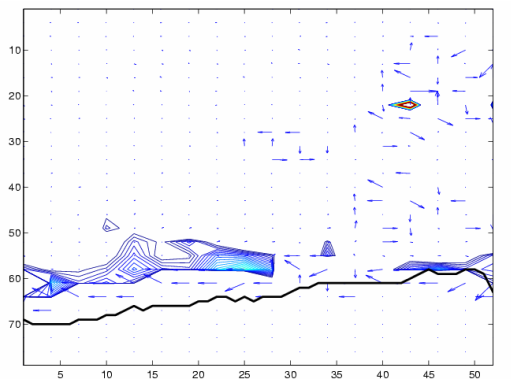

week 50

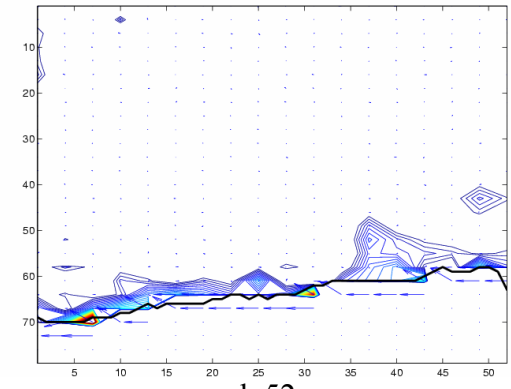

week 52

chl (mg m^{-3})

1.13 1.34 1.60 1.91 2.27 2.70 3.22 3.84

APPENDIX 18 (a) Gibraltar Strait
Sea Surface Temperature skin (SST skin) maps
(AVHRR data April-December 2002)

37.30 N, -5.87 E

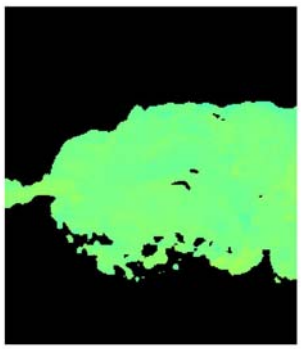

week 14

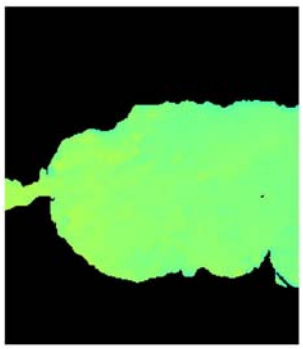

week 15

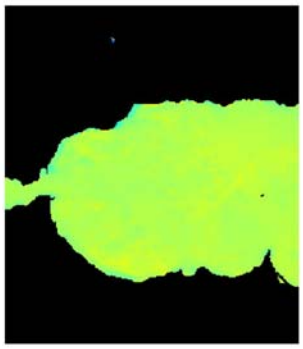

week 16

34.47 N, -2.75 E

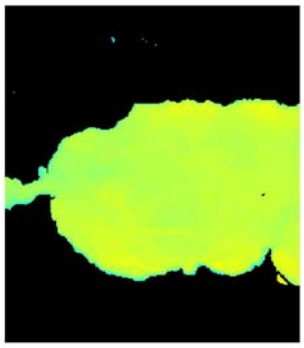

week 17

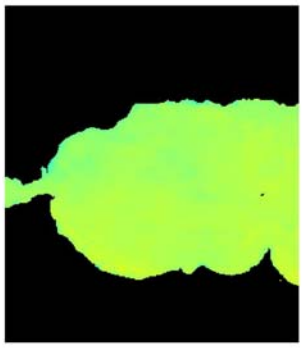

week 18

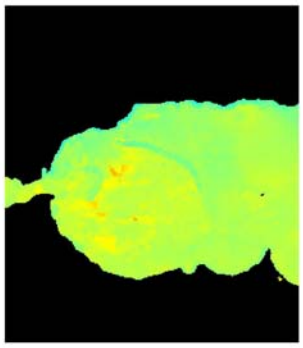

week 19

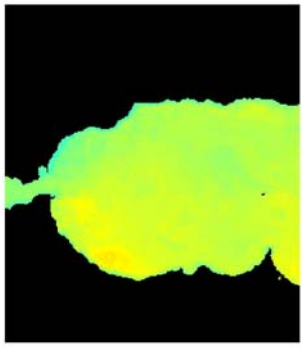

week 20

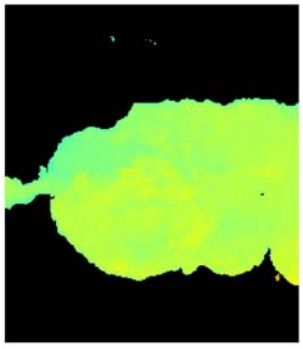

week 21

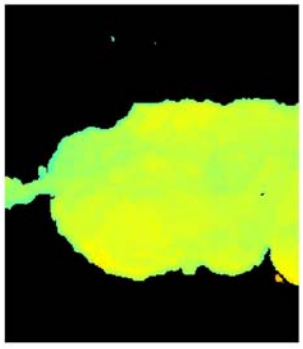

week 22

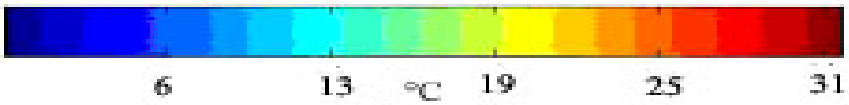

APPENDIX 18 (b) Gibraltar Strait
Sea Surface Temperature skin (SST skin) maps
(AVHRR data April-December 2002)

37.30 N, -5.87 E

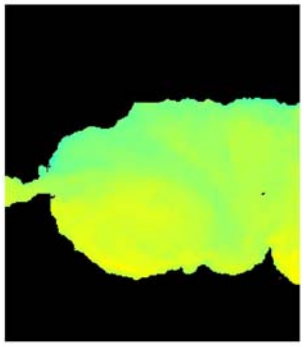

week 23

34.47 N, -2.75 E

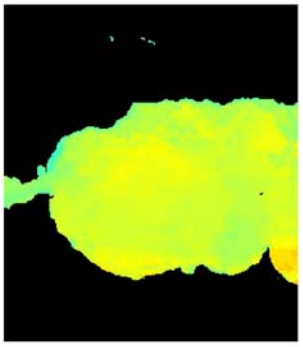

week 24

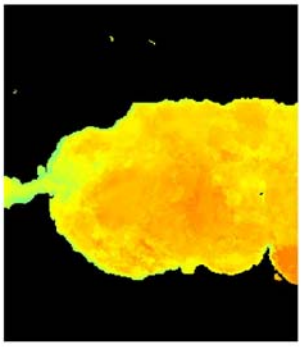

week 25

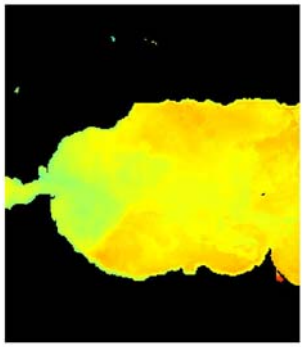

week 26

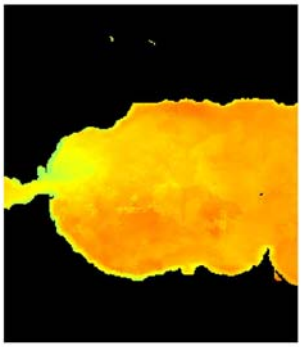

week 27

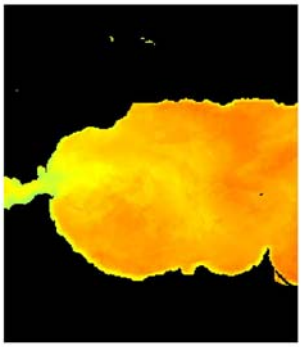

week 28

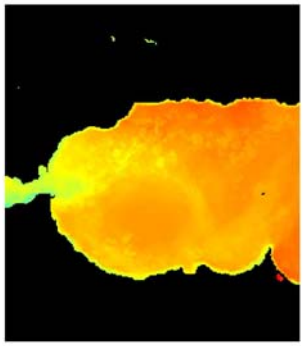

week 29

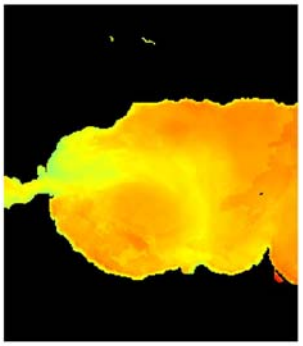

week 30

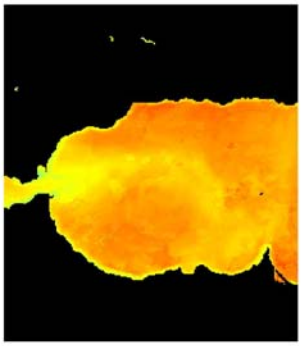

week 31

APPENDIX 18 (c) Gibraltar Strait
Sea Surface Temperature skin (SST skin) maps
(AVHRR data April-December 2002)

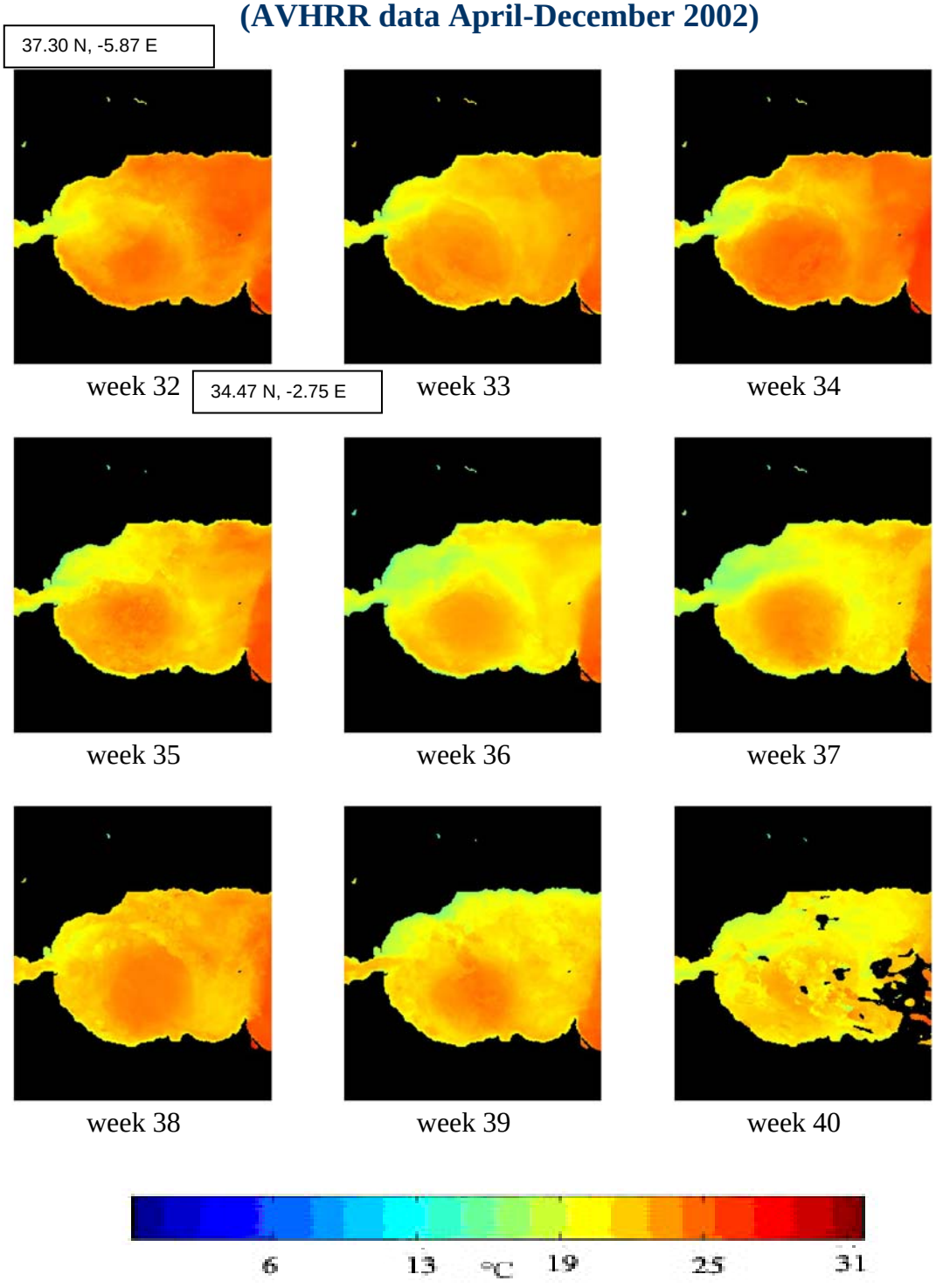

APPENDIX 18 (d) Gibraltar Strait
Sea Surface Temperature skin (SST skin) maps
(AVHRR data April-December 2002)

37.30 N, -5.87 E

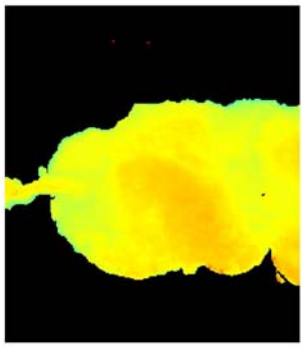

week 41

34.47 N, -2.75 E

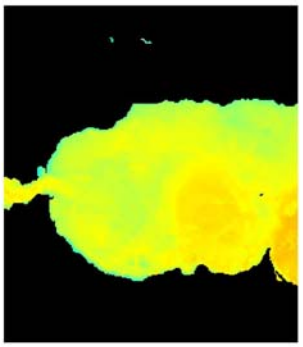

week 42

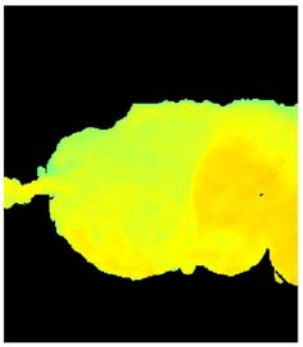

week 43

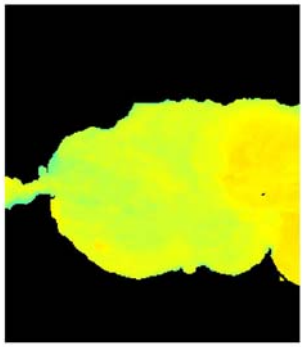

week 44

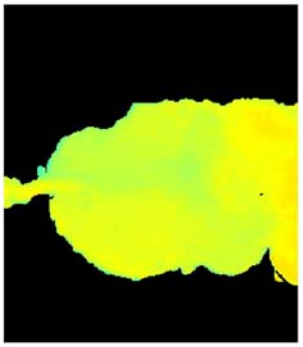

week 45

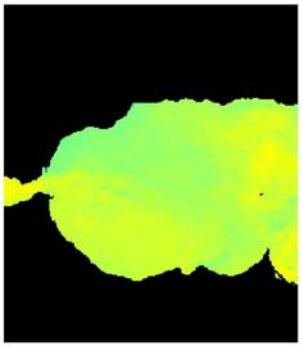

week 46

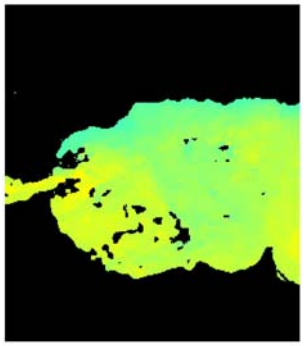

week 47

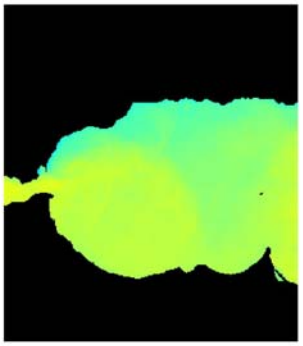

week 48

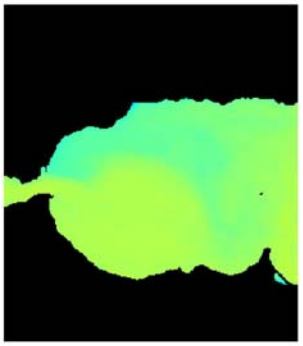

week 49

APPENDIX 18 (e) Gibraltar Strait
Sea Surface Temperature skin (SST skin) maps
(AVHRR data April-December 2002)

37.30 N, -5.87 E

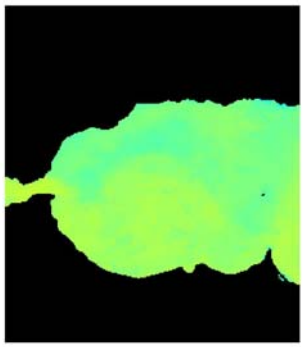

week 50

34.47 N, -2.75 E

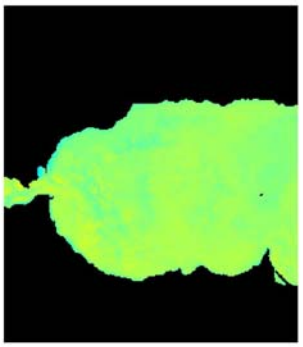

week 51

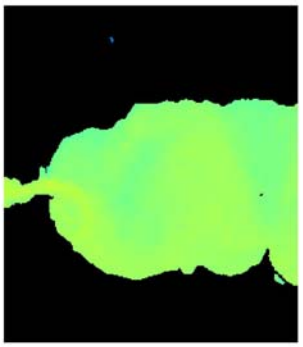

week 52

APPENDIX 19 (a) Al Hoceima National Park
Sea Surface Temperature skin (SST skin) maps
(AVHRR data April-December 2002)

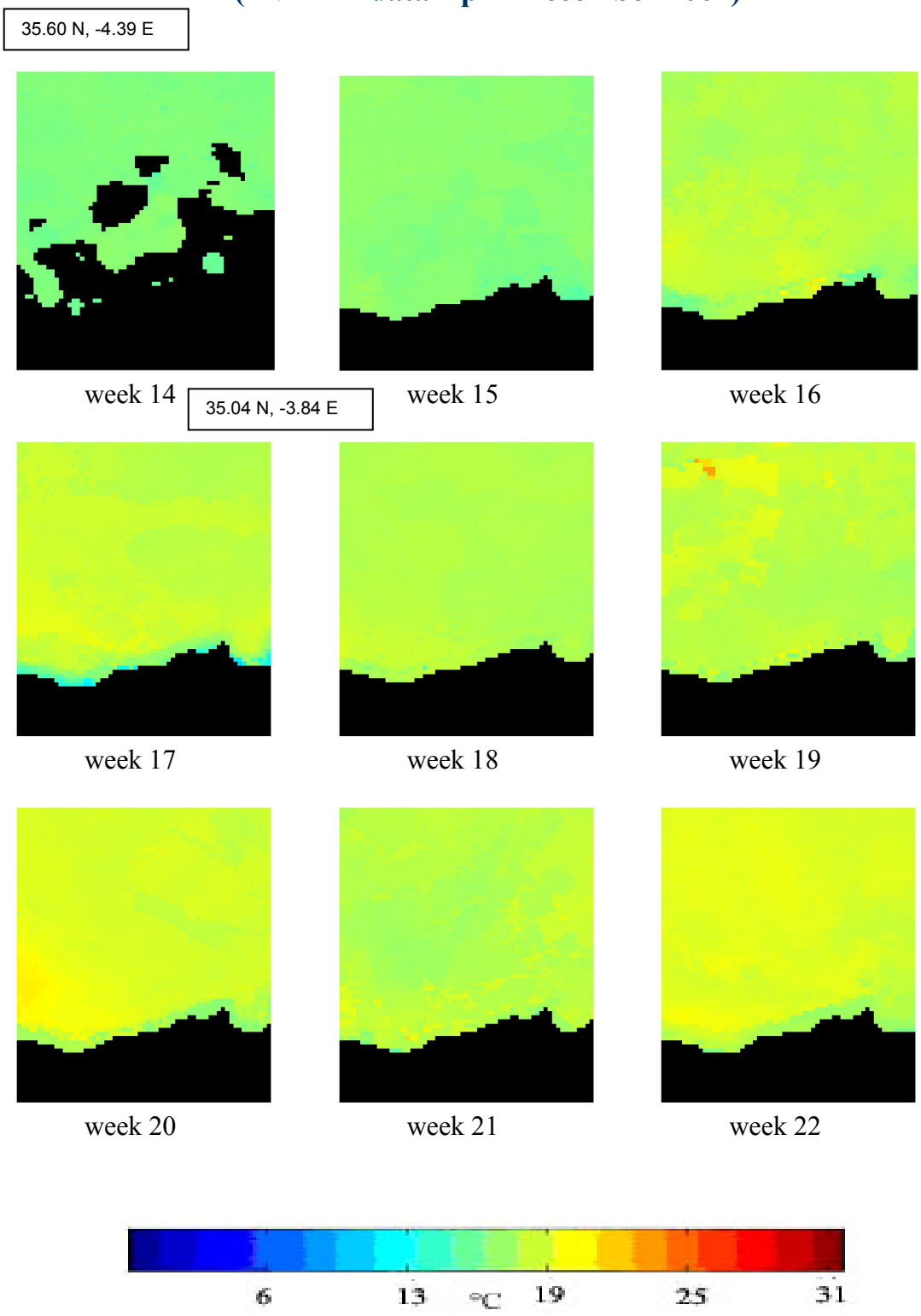

APPENDIX 19 (b) Al Hoceima National Park
Sea Surface Temperature skin (SST skin) maps
(AVHRR data April-December 2002)

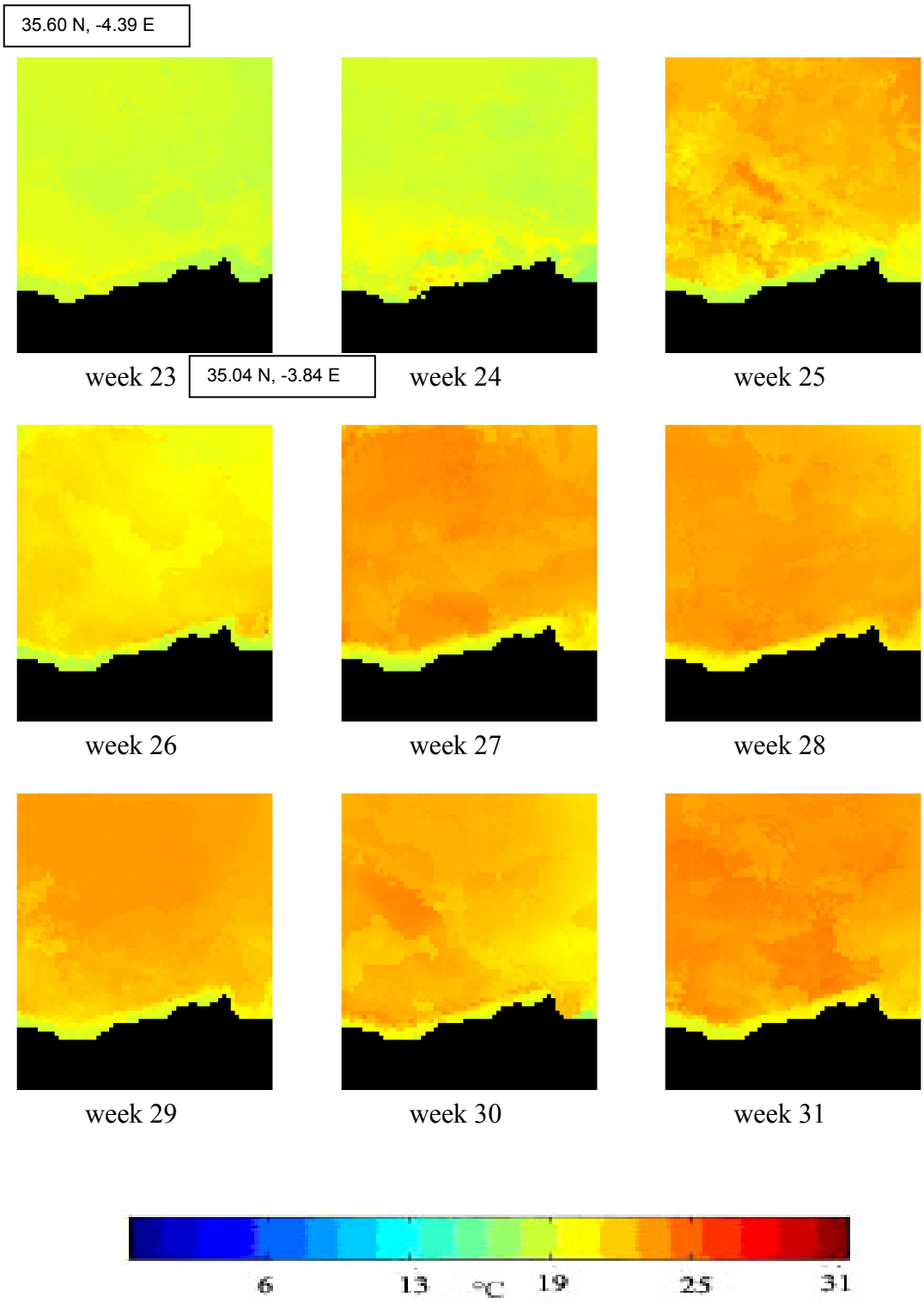

APPENDIX 19 (c) Al Hoceima National Park
Sea Surface Temperature skin (SST skin) maps
(AVHRR data April-December 2002)

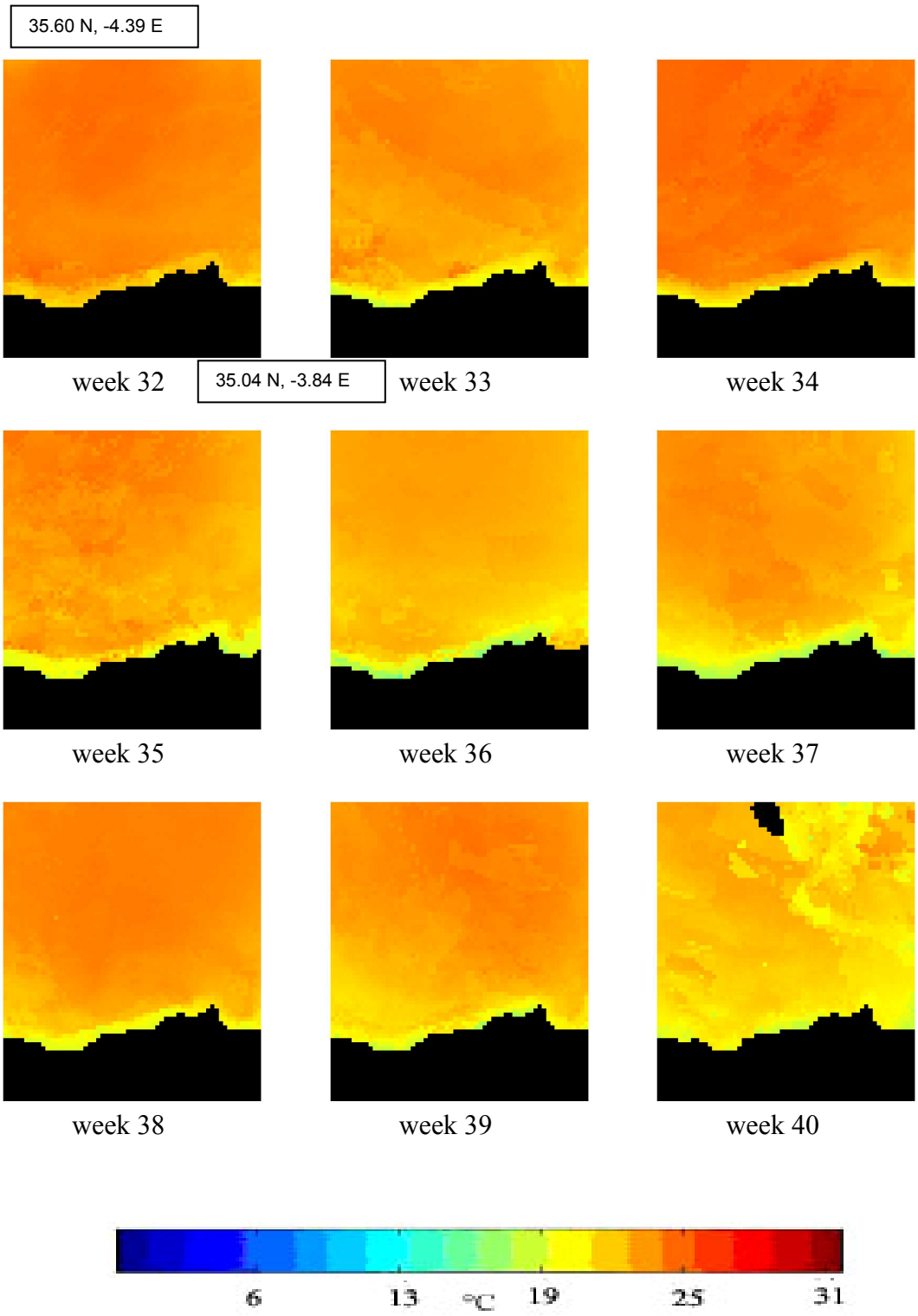

APPENDIX 19 (d) Al Hoceima National Park
Sea Surface Temperature skin (SST skin) maps
(AVHRR data April-December 2002)

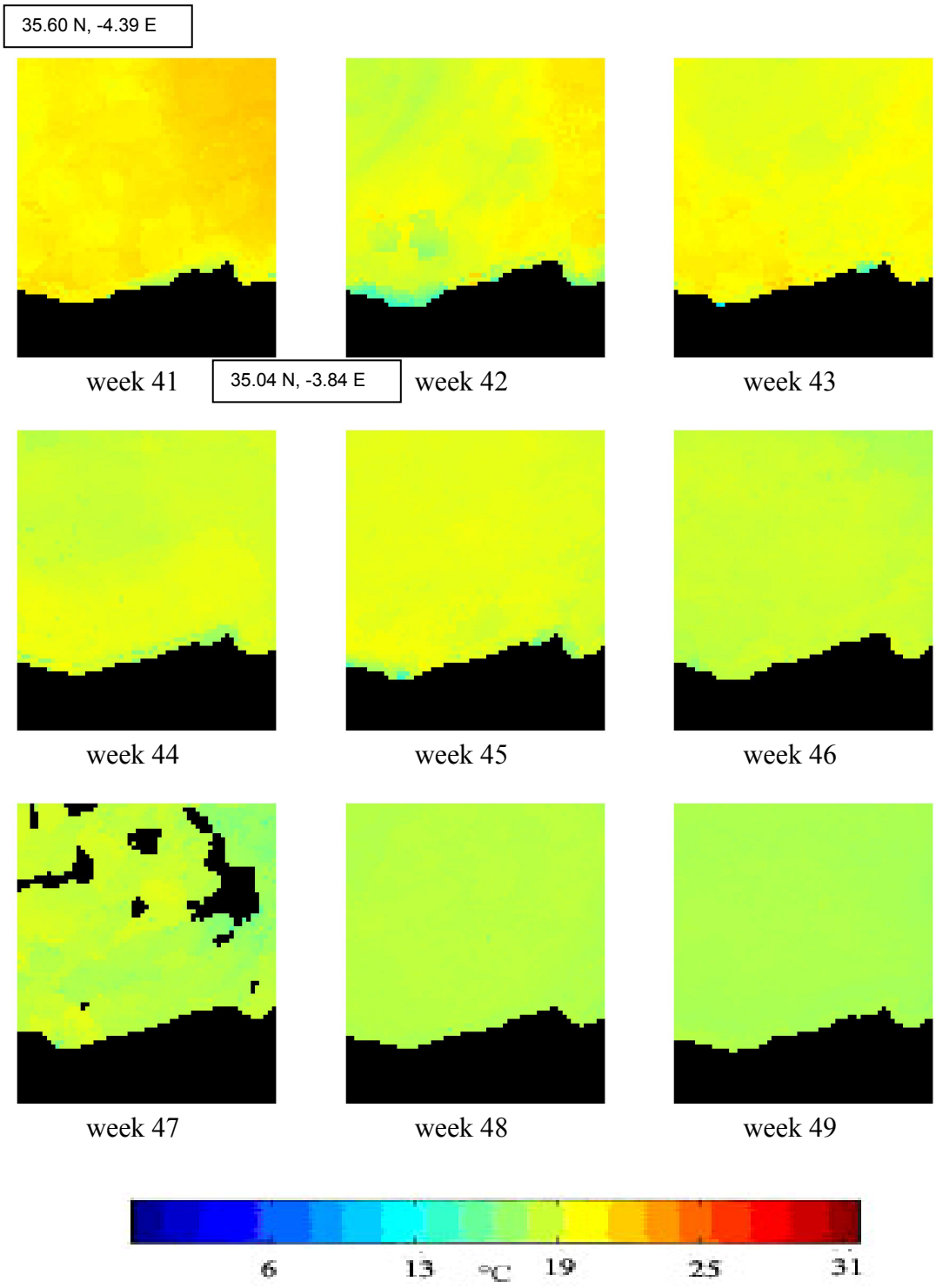

APPENDIX 19 (e) Al Hoceima National Park
Sea Surface Temperature skin (SST skin) maps
(AVHRR data April-December 2002)

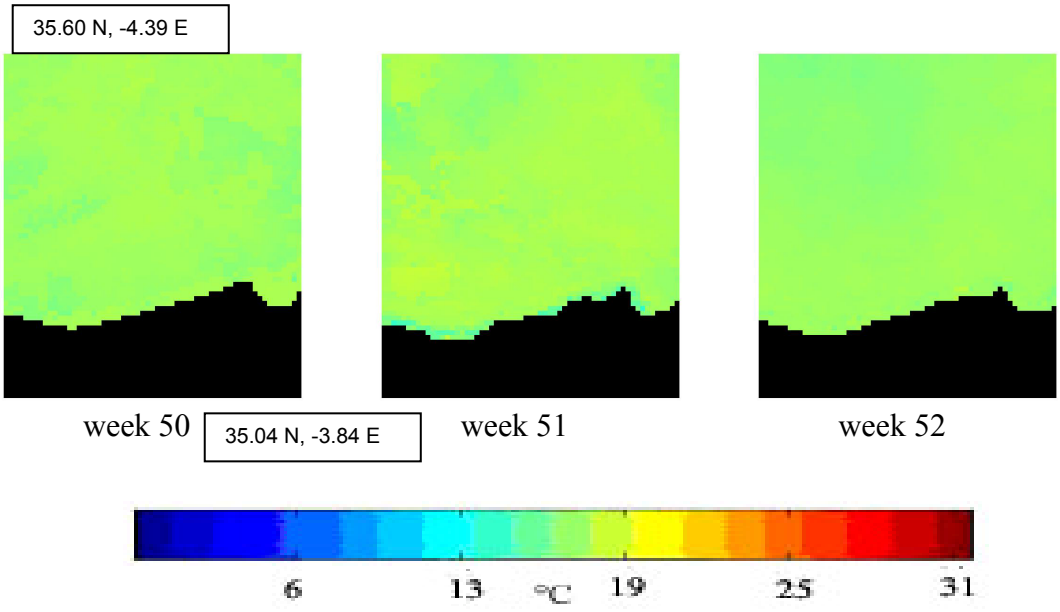

APPENDIX 20 (a) Malta Island
Chlorophyll (*chl*) maps (SeaWiFS data year 2002)

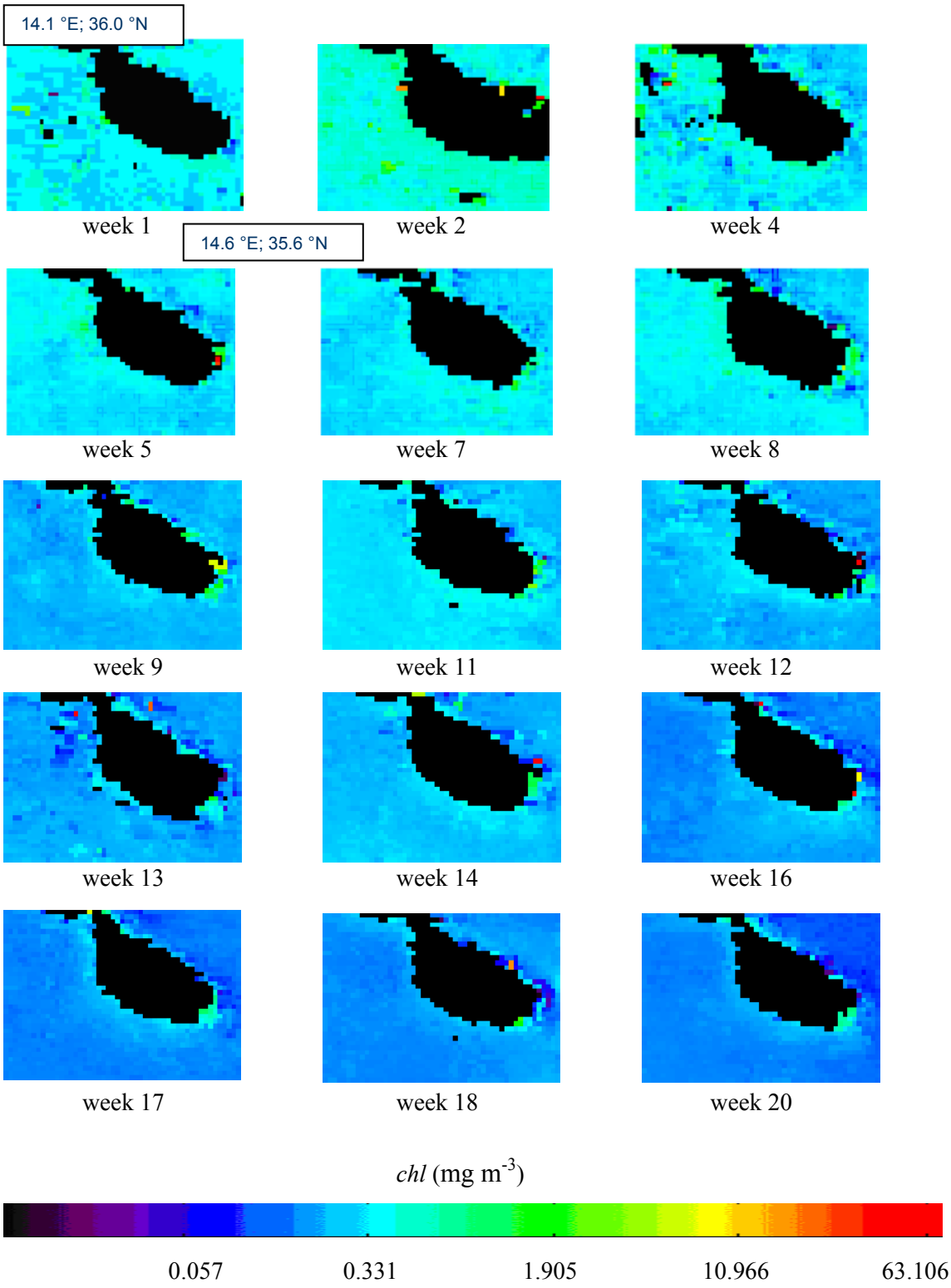

APPENDIX 20 (b) Malta Island
Chlorophyll (*chl*) maps (SeaWiFS data year 2002)

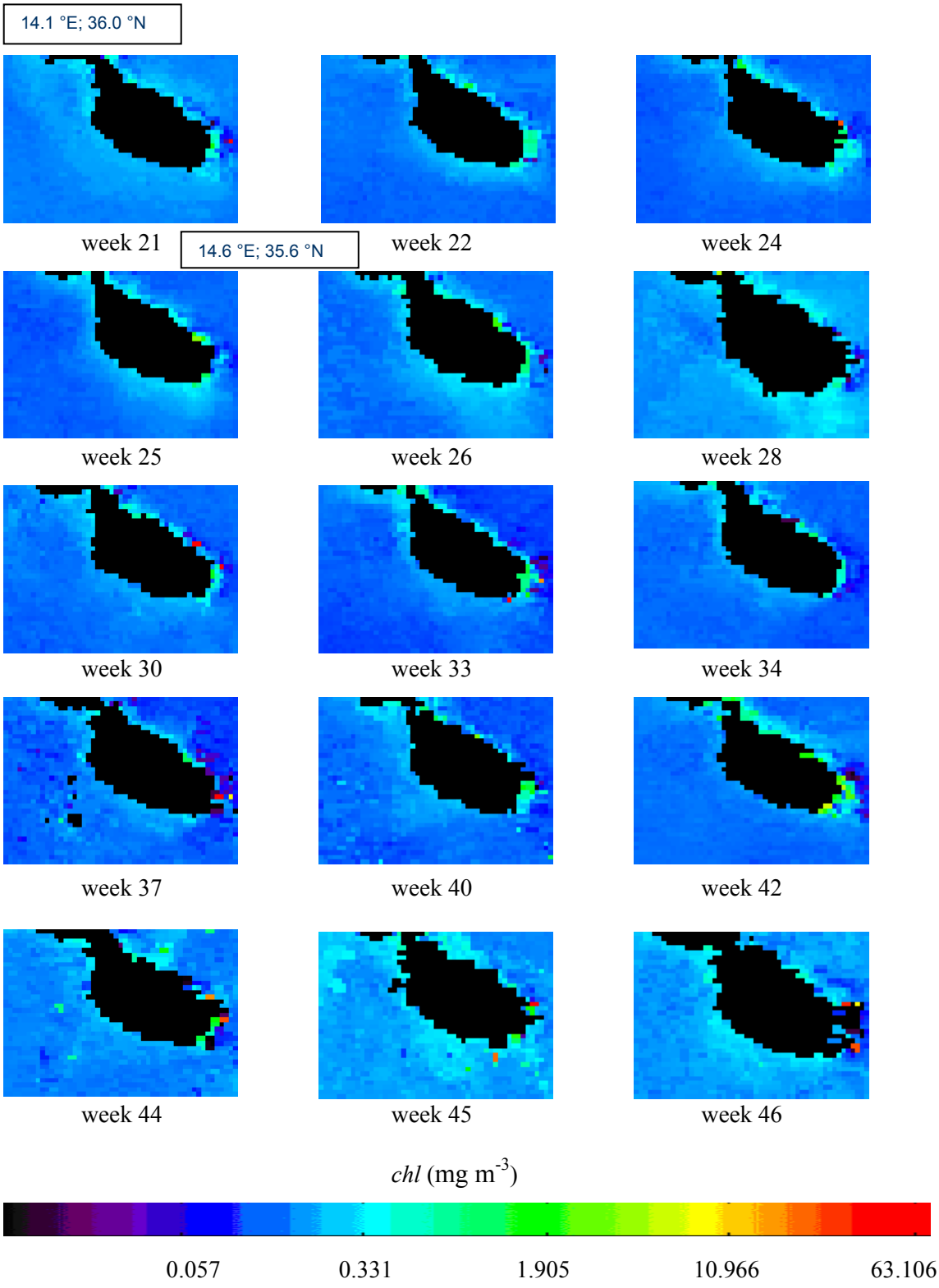

APPENDIX 20 (c) Malta Island
Chlorophyll (*chl*) maps (SeaWiFS data year 2002)

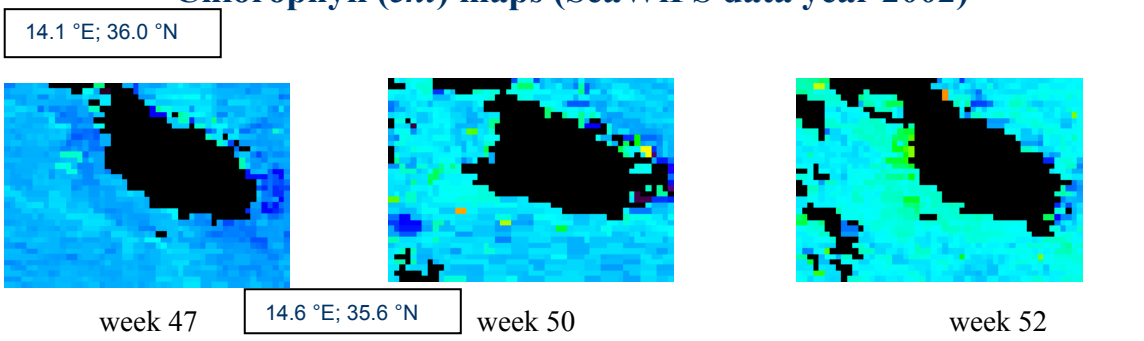

week 47 week 50 week 52

chl (mg m^{-3})

0.057 0.331 1.905 10.966 63.106

APPENDIX 21 (a)
Spatial Gradient (*chl* range 0.164-0.9 mg/m^3)

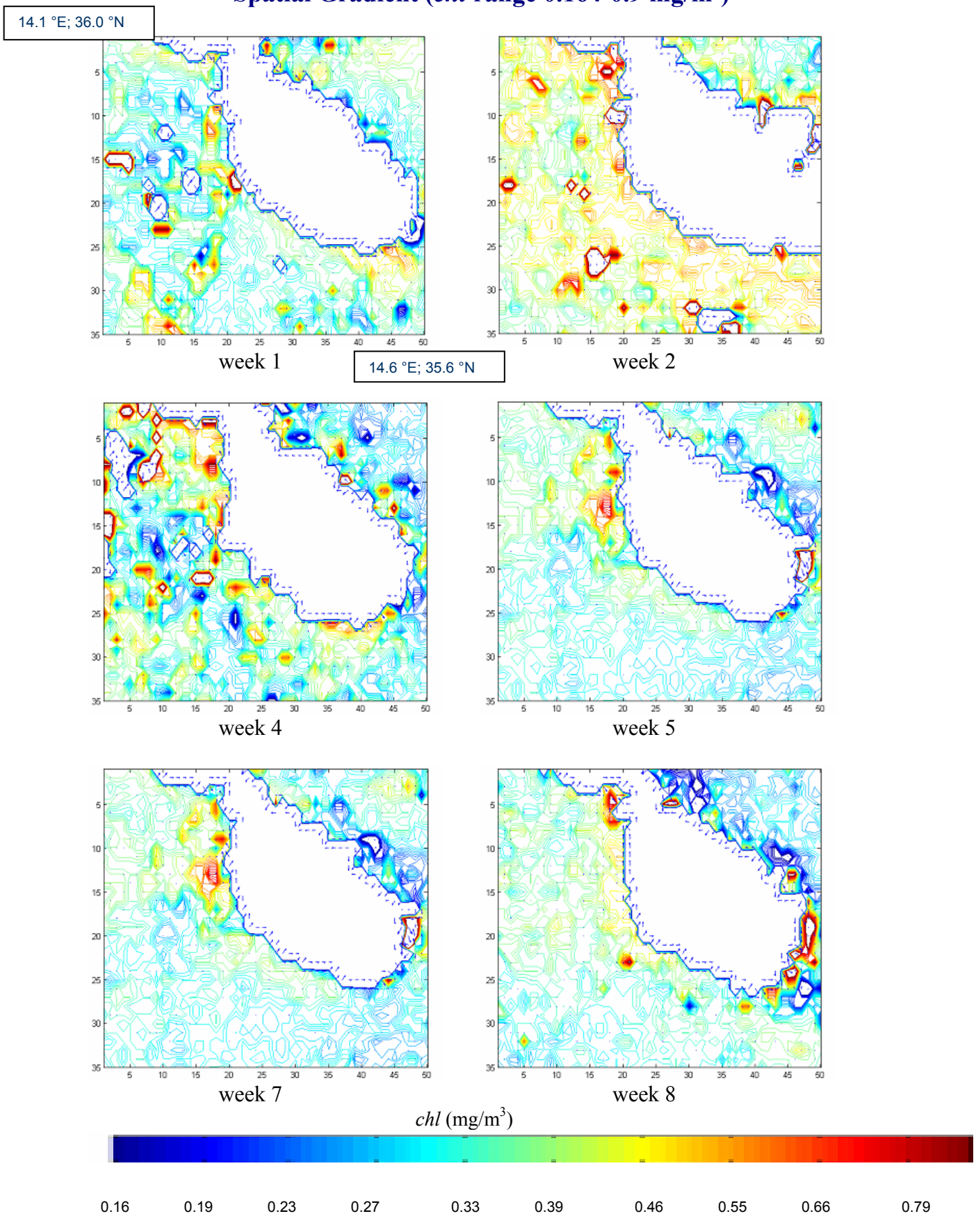

APPENDIX 21 (b)
Spatial Gradient (*chl* range 0.164-0.9 mg/m^3)

14.1 °E; 36.0 °N

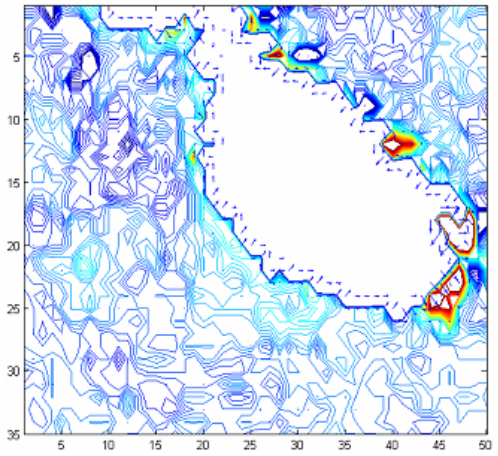

week 9

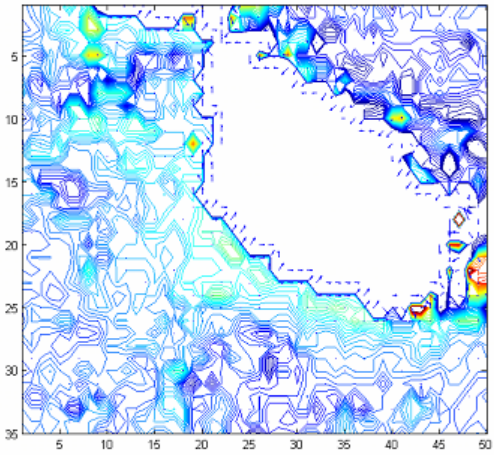

week 12

14.6 °E; 35.6 °N

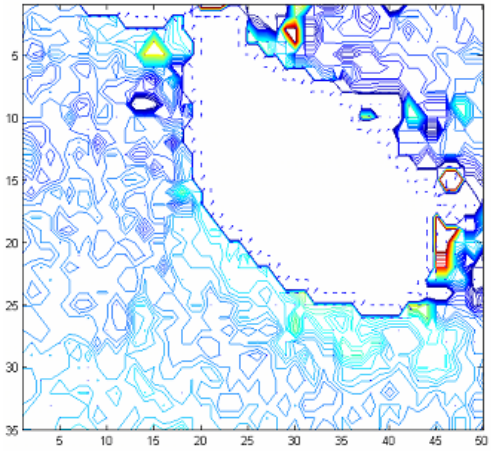

week 14

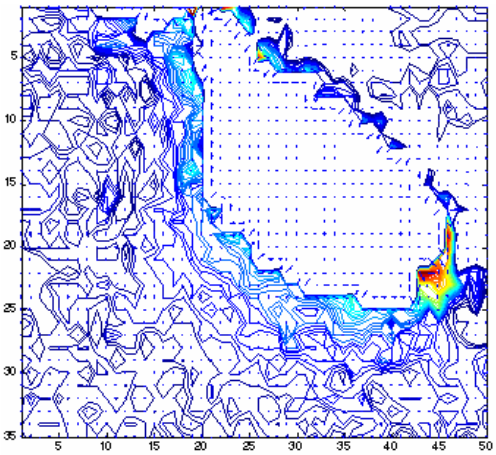

week 17

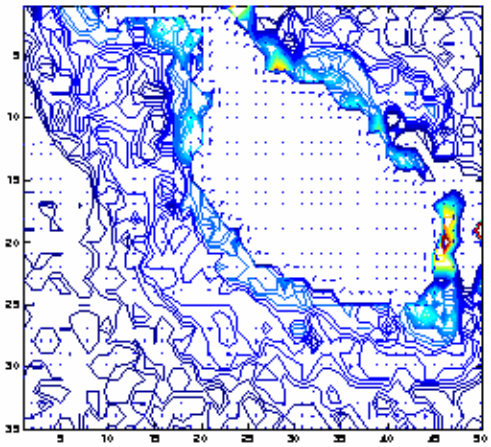

week 21

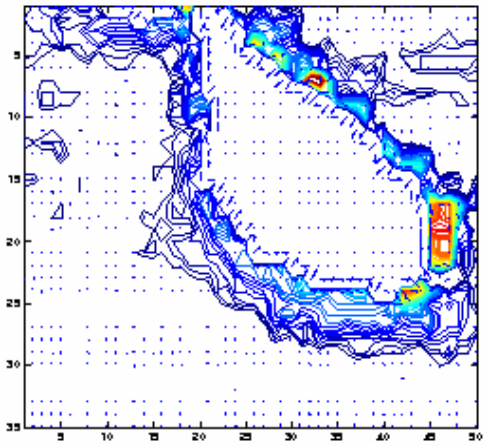

week 22

chl (mg/m^3)

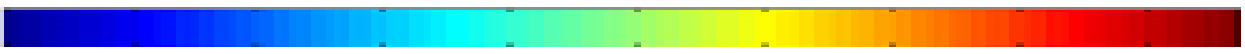

0.16 0.19 0.23 0.27 0.33 0.39 0.46 0.55 0.66 0.79

CV

APPENDIX 21 (c)
Spatial Gradient (*chl* range 0.164-0.9 mg/m^3)

14.1 °E; 36.0 °N

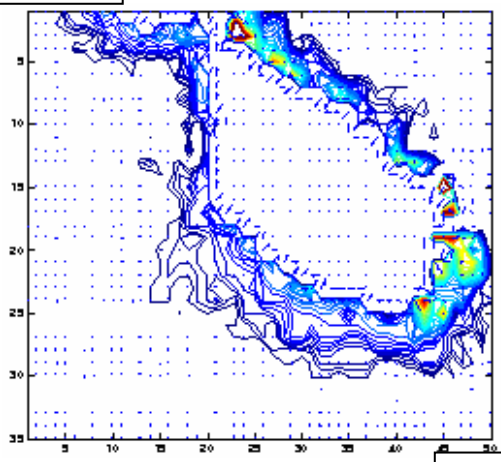

week 24

14.6 °E; 35.6 °N

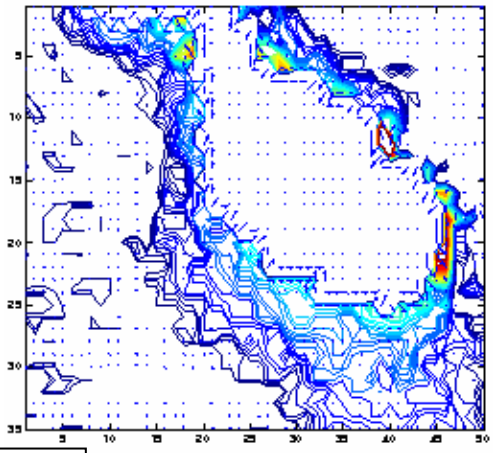

week 26

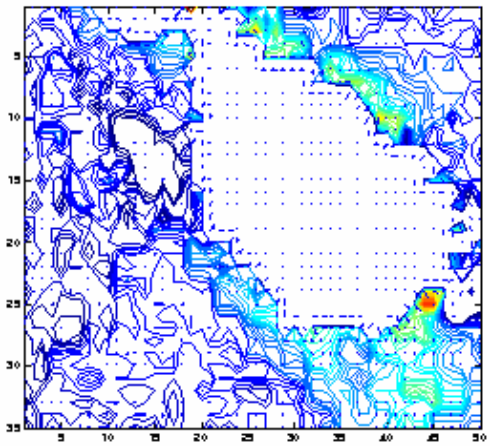

week 28

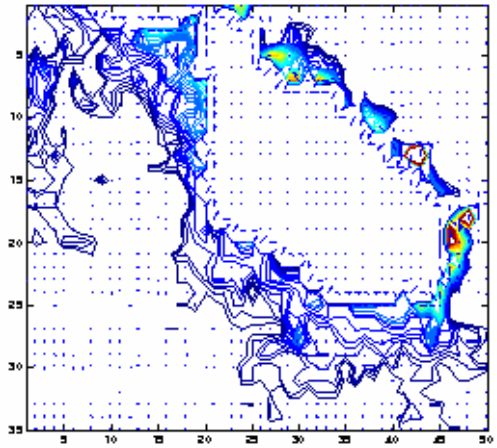

week 30

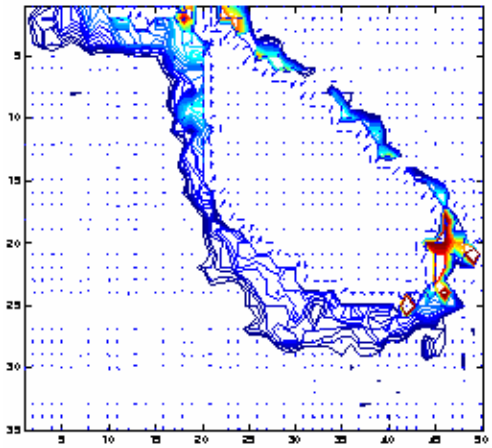

week 33

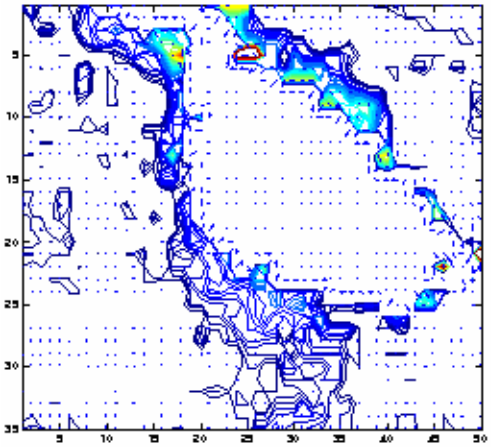

week 36

chl (mg/m^3)

0.16 0.19 0.23 0.27 0.33 0.39 0.46 0.55 0.66 0.79

CVI

APPENDIX 21 (d)
Spatial Gradient (*chl* range 0.164-0.9 mg/m^3)

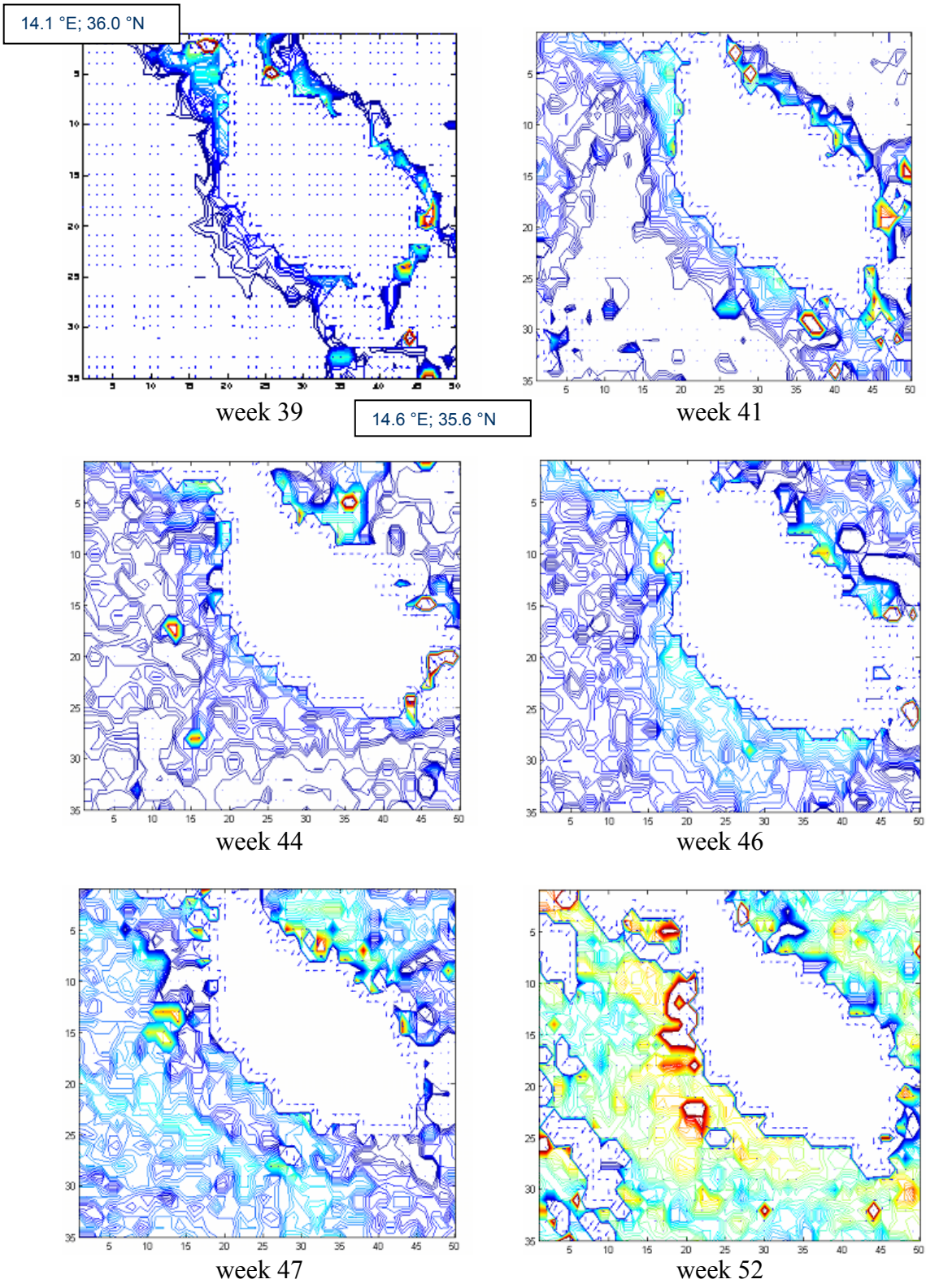

APPENDIX 22(a) Malta Island
Sea Surface Temperature skin (SST skin) maps
(AVHRR data April-December 2002)

14.1 °E; 36.0 °N

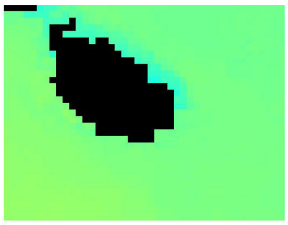

week 14

14.6 °E; 35.6 °N

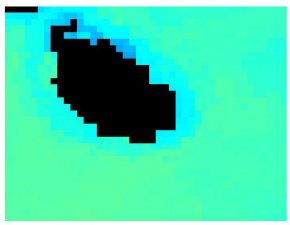

week 15

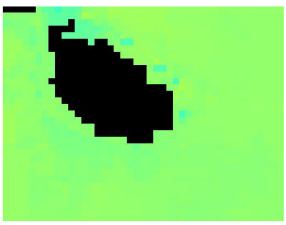

week 16

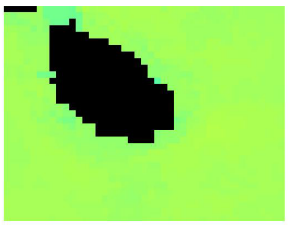

week 17

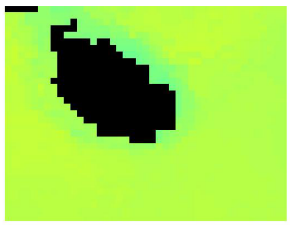

week 18

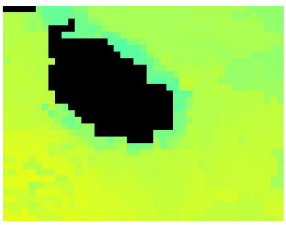

week 19

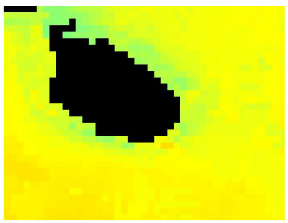

week 20

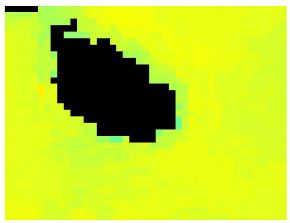

week 21

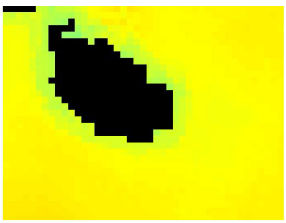

week 22

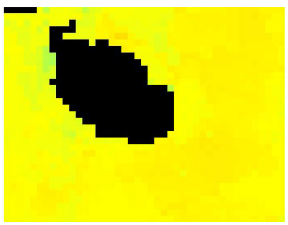

week 23

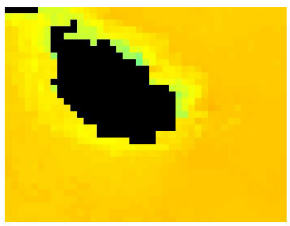

week 24

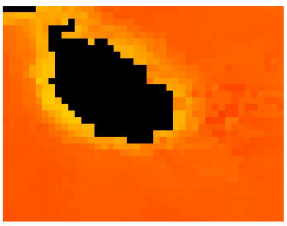

week 25

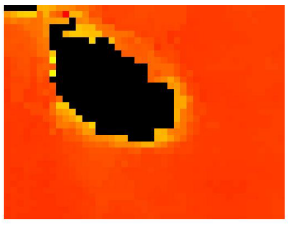

week 26

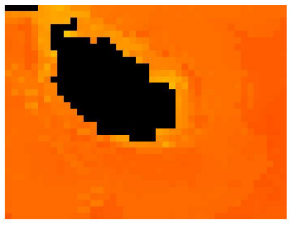

week 27

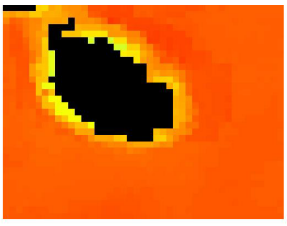

week 28

APPENDIX 22(b) Malta Island
Sea Surface Temperature skin (SST skin) maps
(AVHRR data April-December 2002)

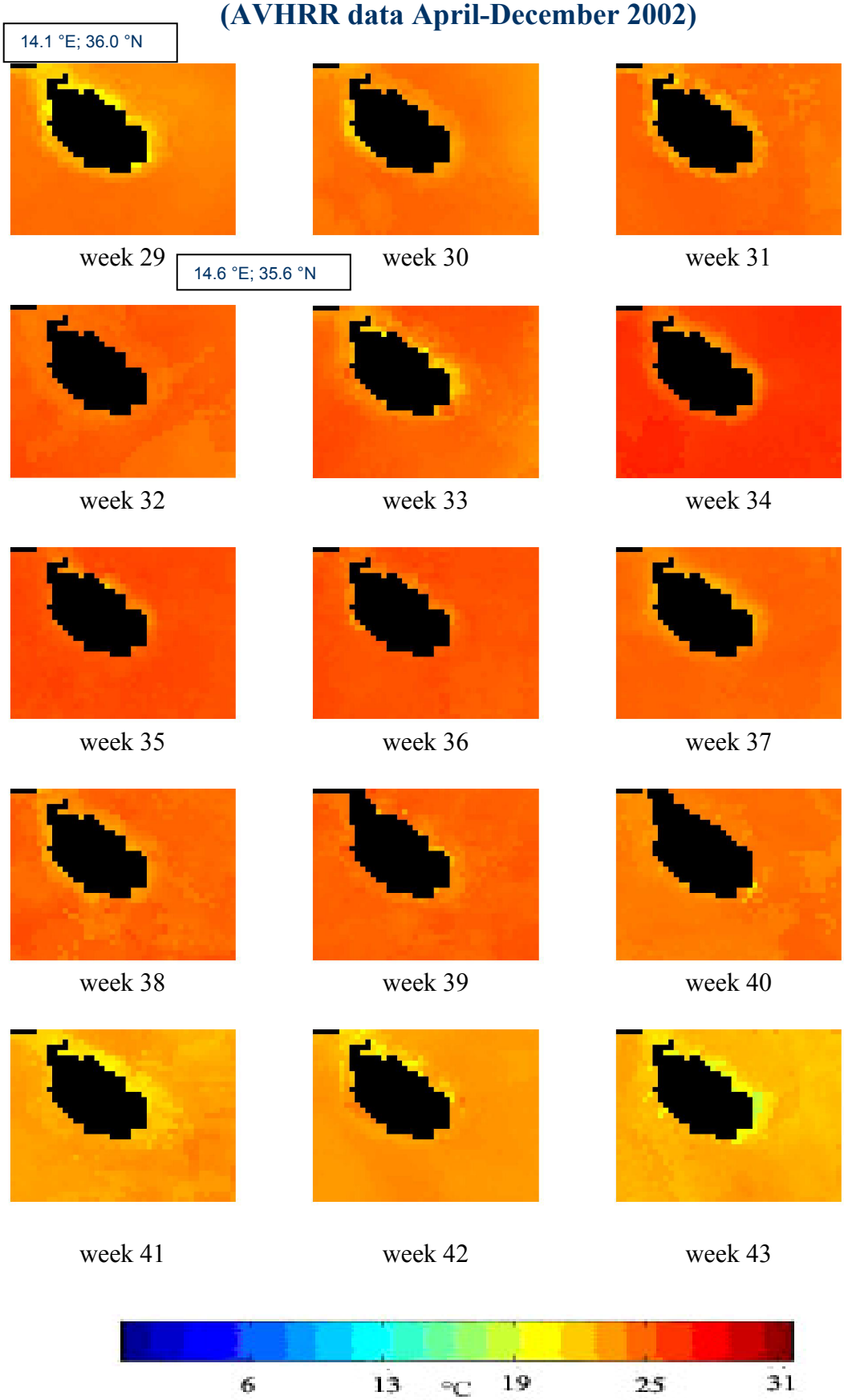

APPENDIX 22(c) Malta Island
Sea Surface Temperature skin (SST skin) maps
(AVHRR data April-December 2002)

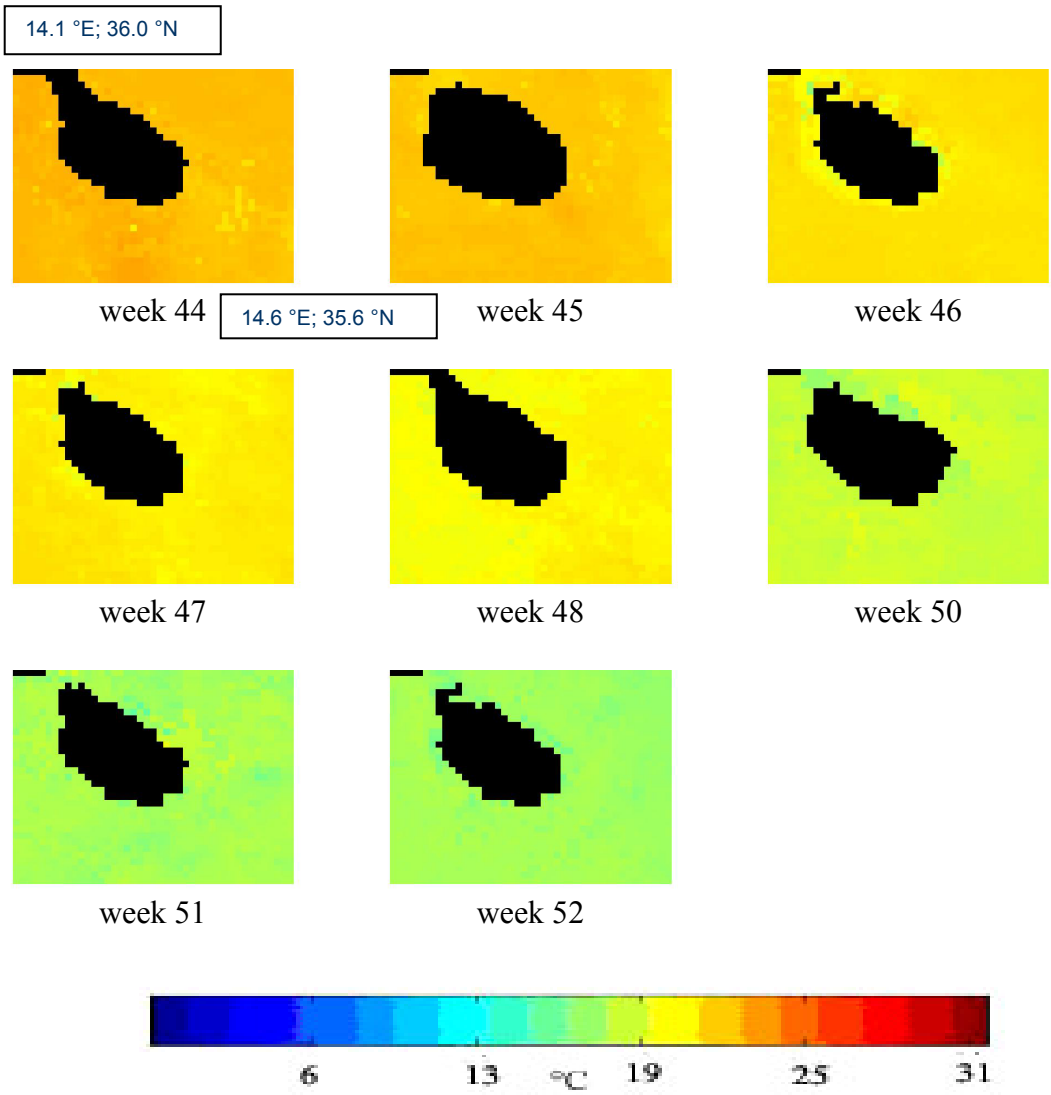

APPENDIX 23
LOCATIONS OF *IN SITU* SAMPLING STATIONS IN PORTOFINO MPA (dd: decimal degree)

Code	Maximum depth (m)	Latitude N (dd)	Longitude E (dd)
T1A	10	44.368	9.102
T1B	20	44.363	9.100
T1C	30	44.360	9.097
T1D	50	44.354	9.093
T1E	75	44.343	9.087
T1F	85	44.334	9.080
T1G	100	44.323	9.074
T2A	10	44.360	9.127
T2B	20	44.356	9.125
T2C	30	44.353	9.122
T2D	50	44.347	9.118
T2E	70	44.336	9.111
T2F	85	44.326	9.105
T2G	100	44.315	9.097
T3A	10	44.350	9.149
T3B	20	44.346	9.146
T3C	30	44.341	9.143
T3D	50	44.335	9.138
T3E	70	44.325	9.133
T3F	85	44.316	9.127
T3G	100	44.308	9.121
T4A	80	44.318	9.143
T4B	90	44.310	9.138
T4C	100	44.303	9.134
T5A	70	44.313	9.161
T5B	85	44.305	9.157
T5C	100	44.298	9.153
T6A	90	44.295	9.217
T6B	100	44.291	9.213
T6C	105	44.286	9.210
T6D	110	44.281	9.207
T7A	30	44.300	9.217
T7B	70	44.296	9.231
T8A	30	44.309	9.215
T8B	70	44.305	9.228

LIST OF REFERENCES

Abdulla A., Gomei M., Maison E., and Piante C., 2008. *Status of Marine Protected Areas in the Mediterranean Sea*. IUCN, Malaga and WWF, France, 152 pp.

Agnesi S., Di Nora T., Grech P., Manca Zeichen M., Mo G., Molinari A., Piccione M.E., Pirrotta K., Salvati E., Schembri P.J., Tunesi L., 2003. *Regional Project for the Development of Coastal protected Areas in the Mediterranean Region (MedMPA) – Activity MP2: Elaboration of Management Plan for the Marine Area of Rdum Majjiesa and Ras Raheb in Malta. Zoning Proposal for the Marine Protected Area from Rdum Majjiesa to Ras Raheb Cave*.

Agardy T., 1994. Advances in marine conservation: the role of marine protected areas. *Trend in Ecology and Evolution*, 9 (7): 267-270

Agardy, T.S. 1997. *Marine protected areas and ocean conservation*. Environmental Intelligence Unit, Landes R.G.Co., Austin, Texas: 240 pp.

Agardy T., 1999. Global experiences in marine protected area planning and lessons learned. In *C.I.E.S.M Workshop Series Scientific Design and Monitoring of Mediterranean Marine Protected Areas*, 8 (22), Porto Cesareo 21-24 October.

Agardy T., 2000. Information needs for marine protected areas: scientific and societal. *Bulletin of Marine Science,* 66(3): 875–888.

Aguilar A**.,** 1998. Current status of Mediterranean monk seal populations. In: *Meeting of experts on the implementation of the Action Plans for marine mammals* (monk seal and cetaceans) *adopted within MAP*. Arta, Greece, 29-31 October 1998. UNEP (OCA)/MED WG.146/4.

Aguilar A., 2000. Population biology, conservation threats and status of Mediterranean striped dolphins (*Stenella coeruleoalba*). *Journal of Cetacean Research and Management*, 2: 17-26.

Airoldi S., Azzellino A., Nani B., Ballardini M., Bastoni C., Notarbartolo di Sciara, G., Sturlese A., 1999. Whale watching in Italy: results of the first three years of activity. *European Research on Cetaceans* 13:153-156.

Allison G.W., Lubchenco J., Carr M.H., 1998. Marine reserves are necessary but not sufficient for marine conservation. *Ecological Applications*, 8 (1) suppl.: S79-S92.

Antoine D., Morel A., & André J.M., 1995. Algal pigment distribution and primary production in the eastern Mediterranean as derived from Costal Zone Color Scanner observations. *Journal of geophysical Research*, 100: 16193-16209.

Antoine, D., D'Ortenzio F., Hooker S.B., Bécu G., Gentili B., Tailliez D. and Scott A., 2008. Assessment of uncertainty in the ocean reflectance determined by three satellite ocean colour sensors (MERIS, SeaWiFS, MODIS) at an offshore site in the Mediterranean Sea (BOUSSOLE project). *Journal of Geophysical Research*, 113, C07013, doi:10.1029/2007JC004472.

Arnone R., 1994. The temporal and spatial variability of chlorophyll in the western Mediterranean. In *Seasonal and interannual Variability of the Western Mediterranean Sea*, *Coastal and Estuarine Studies*, Paul E. La Violette (ed.), American Geophysical Union, Washington, USA: 195-225.

Astraldi, M., and Manzella G., 1983. Some observations on current measurements on the East Ligurian shelf, Mediterranean Sea, *Cont. Shelf Res*., 2: 183–193.

Astraldi M. and Gasparini G.P., 1984. Correnti costiere nel Bacino Ligure. *Boll. Geof.*, **7**(1): 83.

Astraldi, M., and Gasparini G., 1986. La circolazione costiera nel Mar Ligure orientale, *Boll. Mus*. Ist. Biol. Univ. Genova, 52 suppl.: 317–331.

Astraldi M., Gasparini G. and Sparnocchia S., 1994. The Seasonal and Interannual Variability in the Ligurian-Provençal Basin. In *Seasonal and Interannual Variability of the Western Mediterranean Sea*, Paul E. La Violette (ed.), American Geophysical Union, Washington, USA: 93-113.

Astraldi M., Balopoulos S., Candela J., Font J., Gacic M., Gasparini G.P., Manca B. and Theocharis A., 1999. The role of straits and channels in understanding the characteristics of Mediterranean circulation. *Progress in Oceanography*, 4: 65-108.

Attwood C.G., Mann B.Q., Beaumont J., and Harris J.M., 1997. Review of the state of marine protected areas in South Africa. *South African Journal of Marine Science*, 18: 341-367.

Avella, F.J. and L.M. Gonzales. 1984. Monk seal (*Monachus*): A survey along the Mediterranean coast of Morocco. In: *The Monk Seals, proceedings of the Second International Conference*, La Rochelle, France, 5-6 October 1984. K. Ronald & R. Duguy eds.). *Ann. Soc. Sci. net. Charente-Maritime*, Fr., Suppl.: 60-78.

Badalamenti,F., Ramos A.A., Voultsiadou E., Sánchez Lizado J.L., D'Anna G., Pipitone C., Mas J., Ruiz Fernandez J.A., Whitmarsh D., Riggio S., 2000. Cultural and Socio-Economic Impacts of Mediterranean Marine Protected Areas. *Environmental Conservation* 27 (2): 110-125.

Baker J.L., 2000**.** *Guide to Marine Protected Areas*. Office for Coast and Marine Department for Environment and Heritage, South Australia, B.Sc. M.Env.St, 201 pp.

Barale V., McClain .R., and Malanotte-Rizzoli P., 1986. Space and time variability of the surface colour field in the Northern Adriatic Sea. *J. Geophys. Res*., 91: 12957-12974.

Barale V. and Folving S., 1996. Remote Sensing of coastal interactions in the Mediterranean region. *Ocean & Coastal Management*, 30 (2-3): 217-233.

Barale V, 1999. Integrated Geographical and Environmental Remotely-sensed data on marginal and enclosed basins: the Mediterranean case. In: *Marine and Coastal Geographical Information Systems*, Wright D. and Bartlett D. eds, Taylor and Francis, Philadelphia, USA., 177-187

Barale, V., Panigada, S., Zanardelli, M., 2002. Habitat preferences of fin whales (*Balaenoptera physalus*) in the northwestern Mediterranean Sea: a comparison between *in situ* and remote sensing data. *Proceedings of the 7th Thematic Conference 'Remote Sensing for Marine and Coastal Environments'*, Miami, FL, USA, 20-22/05/2002 (on CD-ROM, VERIDIAN, Ann Arbor, MI, USA, 2002).

Barale V., 2003. Environmental remote sensing of the Mediterranean Sea. *Journal of Environmental Sciences and Health*, A38(8): 1681-1688.

Barale V., Jaquet J.-M., Ndiaye M., 2008. Algal blooming patterns and anomalies in the Mediterranean Sea as derived from the SeaWiFS data set (1998-2003). *Remote Sensing of the Environment*, 112: 3300-3313.

Barozzi E., Bergamaschi L., Gonzalez E., 2002. *Nuovo calculus per studenti di Scienze, Matematica ed Ingegneria*. Libreria Progetto, Padova: pp. 517.

Batisse M. and de Grissac A.J., 1995. Marine Region 3: Mediterranean. In *A Global Representative System of Marine Protected Areas*. Great Barrier Reef Marine Park Authority, The World Bank, The World Conservation Union (IUCN): 77-104.

Bayed A. and P.C. Beaubrun, 1987. Les mammifères marins du Maroc: Inventaire préliminaire. *Mammalia*, Fr., 51: 437-446.

Bayed A. 1991. Etude Ecologique des Ecosystèmes de plages de sables fin de la côte atlantique marocaine. *Thèse Doc. en-sciences Biologiques*, Uni. Mohammed V, Faculté des Sciences Rabat.

Beaumont, J. 1997. Community participation in the establishment and management of marine protected areas: a review of selected international experience. *South African Journal of Marine Science*, 18: 333-340.

Bee Dagum E., 2002. *Analisi delle Serie storiche. Modellistica, Previsione e Scomposizione*. Sprinter-Verlag Italia, 302 pp.

Behrenfeld M.J., O'Malley R.T., Siegel D.A., McClain C.R., Sarmiento J.L., Feldman G.C., Milligan A.J., Falkowsky P.G., Latelier R.M., Boss E.S., 2006. Climate-driven trends in contemporary ocean productivity. *Nature*, 444 (7120):752-755.

Bellan-Santini, D., Lacazet, J.C. & Poizat, C., 1994. *Les biocénoses marines et littorales de Méditerranée, synthèse, menaces et perspectives*. Muséum Nationale d'Histoire Naturelle, Paris, 246 pp.

Bernstein R.L., 1982. Seasat Special Issue 1: Geophysical evaluation. *Journal of Geophysical Research*, 87 (C5).

Bérubé M., Aguilar A., Dendanto, D., Larsen F., Notarbartolo di Sciara G., Sears R., Sigurjonsson J., Urbàn R., Palsbøl, P. 1998. Population genetic structure of North Atlantic, Mediterranean Sea and Sea of Cortez fin whales, *Balaenoptera physalus* (Linnaeus, 1758); analysis of mitochondrial and nuclear loci. *Molecular Ecology* **7**:585-599.

Béthoux J. P., 1980. Mean water fluxes across sections in the Mediterranean sea, evaluated on the basis of water and salt budgets and of observed salinities. *Oceanologica Acta*, 3, 79-88.

Béthoux J. P., Gentili B. & Tailliez D., 1998. Warming and freshwater budget change in the Mediterranean since the 1940s, their possible relation to the greenhouse effect. *Geophysical Research Letters*, 25(7): 1023-1026.

Bianchi C.N. and Morri C., 2000. Marine Biodiversity of the Mediterranean Sea Situation, Problems and Prospects for future research. *Marine Pollution Bulletin*, 40 (5): 367-376.

Bianchi C.N. and Morri C., 2004. Climate change and biological response in Mediterranean Sea ecosystems: a need for broad-scale and long-term research. *Ocean Challenge* 13(2): 32-36

Bishop K., Dudley N., Phillips A., Stolton S., 2004**.** *Speaking a Common Language*. *The uses and performance of the IUCN System of Management Categories for Protected Areas*. IUCN.

Boero F., Briand F., & Micheli F., 1999. Executive summary. In *Scientific design and monitoring of Mediterranean marine protected areas*. F. Briand (Ed.), *CIESM Workshop Series* (8), 7–14. Available http://www.ciesm.org/publications/porto.html.

Böhm E., V. Banzon, E. D'Acunzo, F. D'Ortenzio, R. Santoleri, 2003. Adriatic Sea surface temperature and ocean color variability during the MFSPP, *Annales Geophysicae*, 137-149, 2003.

Bosc E., Bricaud A. and Antoine D., 2004. Seasonal and interannual variability in algal biomass and primary production in the Mediterranean Sea, as derived from 4 years of SeaWiFS observations. *Glob. Biogeochem. Cy*., 18, GB1005 doi:10.GB1005, 1029/2003GB0020034.

Boudouresque C.F., 1994. Intérêt économique des reserves marines. In: *Réhabilitation, Protection et Valorisation de l'Environment Marin à Marseile*, pp. 41-58. Délégation à l'Écologie, la Protection et la Mise en Valeur du Milieu Marine, Marseille.

Boudouresque C.F., 1996. Impact de l'homme et conservation du milieu marin en Mèditerranée. 2° édition. *GIS Posidonie publ.,* Marseille, France: 1-243.

Bricaud A., Bosc E. and Antoine D., 2002. Algal biomass and sea surface temperature in the Mediterranean Basin: Intercomparison of data from various satellite sensors, and implications for primary production estimates. *Remote Sensing of the Environment*, 81: 163– 178.

Brown C.W., Connor L. N., Lillibridge J.L., Nalli N.R. and Legeckis R.V., 2005. An introduction to satellite sensors, observations and techniques. In *Remote Sensing of Coastal Aquatic Environments*. Miller R.L *et al*. (eds), Springer, Dordrecht: 21-50.

Brown O.B., and Evans R.H., 1982. Visible and infrared satellite remote sensing: a status report. *Naval Research Reviews*, 29: 7-25.

Brown O.B., Evans R.H., Brown J.W., Gordon H.R., Smith R.C., Baker K.S., 1985. Phytoplankton blooming off the U.S. East coast: a satellite description. *Science*, 229: 163-67.

Buffoni G., P. Falco, A. Griffa, and E. Zambianchi, 1997. Dispersion processes and residence times in a semi-enclosed basin with recirculating gyres. An application to the Tyrrhenian Sea, *J. Geophys. Res*., 102 (C8): 18699–18713.

Bulgarelli B.and Mélin F., 2000. *SeaWiFS Data Processing Code, REMBRANDT v.1 Code Elements*. Ispra European Commission (I), EUR 19514 EN, 27 pp. Available at http://ies.jrc.cec.eu.int/documentation.html

Bunker A.F., 1972. Wintertime interactions of the atmosphere with the Mediterranean Sea. Journal of Physical Oceanography, 2: 225-238.

Buongiorno Nardelli B., Santoleri R., Marullo S., Guarracino M., 2007. La temperatura superficiale del Mar Mediterraneo negli ultimi 21 anni: analisi delle misure satellitari (Mediterranean Sea SST skin within the last 21 Years: Satellite Data Analyses). In *Clima e Cambiamenti Climatici: le attività di ricerca del CNR*, B. Carli, G. Cavarretta, M. Col acino, S. Fuzzi (eds.), 345-348.

CAMP (Coastal Area Management Programme for Malta), 2002. *A pilot study for the evaluation, designation and management of a Marine Protected Area: Rdum Majjiesa to Raheb Cave* (N.W. Coast of Malta). Final Report: pp. 70.

Carr M H, 2000. Marine protected areas: challenges and opportunities for understanding and conserving marine ecosystems. *Environmental Conservation* 27 (2): 106-109.

Carr M.H. & Reed D.C., 1993. Conceptual Issues Relevant to Marine Harvest Refuges: Examples from Temperate Reef Fishes. *Caadian Journal of Fisheries and Aquatic Scence,* 50: 2019-2080.

Carr M.H. and Raimondi P.T., 1999*b*. Marine protected areas as a precautionary approach to management. *California Cooperative Oceanic Fisheries Investigations Reports*, 40: 1-6.

Castellano M., Ruggieri N., Gasparini G.P., Locritani M., Cattaneo Vietti R., Povero P., 2008. LTER-AMP-Portofino (Mar Ligure): variabilità stagionale ed interannuale delle forzanti meteo-climatiche, delle variabili fisico-chimiche e biologiche del comparto pelagico. *VI° Convegno CoNISMa*, Lecce, Italy, 4-8 November.

Cattaneo Vietti, R., Sirigu A., and Tommei A., 1982. *Sea of Liguria*, Ed. Centro Studi Unione Camere di Commercio Liguri, Genova, 162 pp.

Cattaneo-Vietti R., and Tunesi L., 2007. *Le aree marine protette in Italia -Problemi e prospettive*. ARACNE editrice S.r.l., Roma.

Cruzado, A. 1985. Chemistry of Mediterranean waters. In *Western Mediterranean*. Oxford, R. Margalef (ed.), Pergamon Press, U.K, 126-147.

Clark J.R., 1992. *Integrated Management of Coastal Zones*. Food and Agriculture Organization of the United Nations (FAO), Fisheries Technical Papers No. 327, FAO, Rome.

Clark, G.L., Ewing G.C. and Lorenzen C.J., 1970. Spectra of backscattered light from the sea obtained from aircraft as a measure of chlorophyll concentration. *Science*, *167*: 1119–1121.

Clark C.W., Borsani J.F., Notarbartolo di Sciara G., 2002. Vocal Activity of *Balaenoptera physalus*, in the Ligurian Sea. *Marine Mammal Science*, 18 (1): 286-295.

Claustre H., Morel A., Hooker S.B., Babin M., Antoine D., Oubelkheir K., Bricaud A., Leblanc K., Quéguiner B., and Maritorema S., 2002. Is desert dust making oligotrophic waters greener? *Geophysical Research Letters*, 29, 1469, doi:10.1029/2001GL014056.

Colella S., 2006. La produzione primaria nel Mar Mediterraneo da satellite: sviluppo di un modello regionale e sua applicazione ai dati SeaWiFS, MODIS e MERIS. Thesis for the degree of Doctor of Philosophy, pp. 162.

Cotté C., Guinet C., Taupier-Letage I., Mate B., Petiau E., 2009. Scale-dependent habitat use by a large free-ranging predator, the Mediterranean fin whale. *Deep-Sea Research I*, 56:801-811.

Dagnino I., 1978. On the transport of sediments along the western border of the Ligurian Sea. *Atti II Congresso A.I.O.L.*: 223-226.

Day J.C., 2002. Zoning-lessons from the Great Barrier Reef Marine Park. *Ocean & Coastal Management*, 45: 139-156.

Dayton, P.K., Sala E., Tegner M.J., and Thrush S., 2000. Marine reserves: parks, baselines, and fishery enhancement. *Bulletin of Marine Science*, 66:617-634.

Davis F.W., Stoms D.M., Estes J.E., Scepan J., Scott J.M., 1990. An Information Systems Approach to the Preservation of Biological Diversity. *International Journal of Geographical Information Systems*, 4 (1), 55-78.

De Maio A., Moretti M., Sansone E:, Spezie G., Vultaggio M., 1975. Su la circolazione superficiale e profonda nel Golfo di Genova. *Ann. Ist. Univ. Nav. Napoli,* 43-44: 97-112.

De Vooys C.G.N., 1979. Primary production in aquatic environments. In: *SCOPE 13 The Global Carbon Cycle* (Bolin B., Degens E.T., Kempe S.S., and Ketner P. eds.), J. Wiley, N.Y.: pp. 259.

Devred E., Sathyendranath S., Platt T., 2007. Delineation of ecological provinces using ocean colour radiometry. *Marine Ecology Progress Series*, 346:1-13.

Doerffer R., Heymann K. and Schiller H., 2002. Case 2 water algorithm for the medium resolution imaging spectrometer (MERIS) on ENVISAT. In: *Proceedings of the ENVISAT validation workshop*, 9-13 December, ESA report.

Doerffer R. and Schiller H., 2007. The MERIS Case 2 water algorithm. *International Journal of Remote Sensing*, 28 (3 & 4): 517–535.

Doglioli A.M., A. Griffa, M. G. Magaldi, 2004. Numerical study of a coastal current on a steep slope in presence of a cape: the case of the Promontorio of Portofino**.** *J. Geophys. Res.*, **109**: C12033, doi10.1029/2004JC002422.

D'Ortenzio F., Marullo S., Ragni M., Ribera d'Alcalà M. & Santoleri R., 2002. Validation of empirical SeaWiFS algorithms for chlorophyll-α retrieval in the Mediterranean Sea. A case study for oligotrophic seas. *Remote Sensing of the Environment*, 82 (1): 79-94.

D'Ortenzio F. and Ribera d'Alcalà M., 2008. On the trophic regimes of the Mediterranean Sea. *Biosciences Discussions*, 5: 2959-2983.

Drago A. F. and S. Ferraro, 1994. Oscillazioni del livello del mare nel Porto di Malta (Sea Level Oscillations within the Malta Harbour). *Proc. 11th Congress of the Italian Association of Oceanography and Limnology,* Sorrento, Italy, 235–246.

Drago A. F., Sorgente . and Ribotti A., 2003. A high resolution hydrodynamic 3-D model simulation of the Malta shelf area. *Annales Geophysicae* 21: 323-344.

Earle M., 1996. Ecological interactions between cetaceans and fisheries. In *The Conservation of Whales and Dolphins: Science and Practice*, M.P. Simmonds and J.D. Hutchinson eds., John Wiley & Sons, Ltd., Chichester: 167-204.

Esposito A., and G. Manzella, 1982. Current circulation in the Ligurian Sea. In *Hydrodynamics of Semi-Enclosed Seas*, J. Nihoul (ed.), Elsevier Scientific Publishing Company, Amsterdam: 187–204.

Feldman G.C., 2003. *Summary and Samples of SeaWiFS Operational Data*. http://seawifs.gsfc.nasa.gov/SEAWIFS/SOFTWARE/DATA_PRODUCTS.html

Ferla M., 2003. Monitoraggio e previsione dell'Acqua Alta a Venezia. 7° Conferenza Nazionale delle Agenzie Ambientali, Milano, 24-26 November: 1-9.

Flos J., 1985. The driving Machine. In *Western Mediterranean*, Margalef, R. (ed.), Pergamon Press, Oxford:60-99.

Fontaubert, A.C. de, Downes D.R., and. Agardy T.S., 1996. *Biodiversity in the Seas: Implementing the Convention on Biological Diversity in Marine and Coastal Habitats*. IUCN Environmental Policy and Law Paper No. 32. A Marine Conservation and Development Report. IUCN, Gland, Switzerland, and Cambridge, UK.

Forcada J., 1995. Abundance of common and striped dolphins in the southwestern Mediterranean. *European Research on Cetaceans* 9:153-155.

Forcada, J., Aguilar A., Hammond P., Pastor X., Aguilar R., 1996. Distribution and abundance of fin whales (*Balaenoptera physalus*) in the western Mediterranean Sea during the summer. *Journal of Zoology*, London 238: 23-34.

Forcada J. and Hammond P., 1998. Geographical variation in abundance of striped and common dolphins of the western Mediterranean. *Journal of Sea Research* 39: 313-325.

Forney, K.A., 1999. Trends in harbour porpoise abundance off central California, 1986-95: evidence for interannual changes in distribution? *Journal of Cetacean Research and Management* 1: 73-80.

Francour P., Harmelin J.G, Pollard D., Sartoretto S., 2001. A review of marine protected areas in the northwestern Mediterranean region: siting, usage, zonation and management. *Aquatic conservation*: *Marine and Freshwater Ecosystems*, 11: 155-188.

Fraschetti S.,Terlizzi A., Micheli F., Benedetti-Cecchi L., Boero F., 2002. Marine protected areas in the Mediterranean Sea: Objectives, Effectiveness and Monitoring. *P.S.Z.N.: Marine Ecology*, 23, (Supplement 1): 190-200.

Fraschetti S., Terlizzi A., Bussotti S., Guarnieri G., D'Ambrosio P., Boero F., 2005. Conservation of Mediterranean seascapes: analyses of existing protection schemes. *Marine Environmental Research* 59: 309–332.

Fu ,G., Baith K.S. and McClain C.R., 1998. SeaDAS: The SeaWiFS Data Analysis System. *Proc. of the 4th Pacific Ocean Remote Sensing Conference*, Quingdao (China), 28-31 July: 73-79.

Garcia Charton J.A., Williams I.D., Pérez Ruzafa A., Milazzo M., Chemello R., Marcos C., Kitsos M.S. Koukouras & Riggio S., 2000. Evaluating the ecological effects of Mediterranean marine protected areas: habitat, scale and the natural variability of the ecosystems. *Environment Conservation,* 27: 159-178.

Garcia-Martinez J., Moya A., Raga J.A., Latorre A., 1999. Genetic differentiation in the striped dolphins *Stenella coeurleoalba* from European waters according to mitochondrial DNA (mtDNA) restriction analysis. *Molecular Ecology* 8: 1069-1073.

Gascard J.-C., 1978. Mediterranean deep water formation, baroclinic instability and oceanic eddies. *Oceanologica Acta*, 1 (3): 315-330.

Gascard, J.-C. and Richez, C. 1985. Water masses and circulation in the Western Alboran sea and the strait of Gibraltar. *Progress in Oceanography*, 15, 157-216.

GCOS, 2004. Implementation plan for the global observing system for climate in support of UNFCCC. GCOS-92,WMO/TD No 1219.

GESAMP (Joint Group of Experts on the Scientific Aspects of Marine environment Protection), 1997. *Marine biodiversity: patterns, threats and conservation needs*. Reports and studies No. 62, London, International Maritime Organisation.

Gordon H.R., D.K. Clarck, J.L. Mueller, W.A. Hovis, 1980. Phytoplankton pigments derived from the Nimbus-7 CZCS: initial comparisons with surface measurements. *Science*, 210: 63-66.

Gordon H. R. and Wang M., 1994. Retrieval of water-leaving radiance and aerosol optical thickness over the oceans with SeaWiFS: A preliminary algorithm. *Applied Optics*, 33: 443–452.

Gordon J. and Moscrop A., 1996 Underwater noise pollution and its significance for whales and dolphins. In *The Conservation of Whales and Dolphins: Science and Practice.* M.P. Simmonds and J.D. Hutchinson (eds.), John Wiley & Sons, Chichester: 281-319.

Gordon, J.C.D., Matthews J.N., Panigada S., Gannier A., Borsani J.F. and Notarbartolo di Sciara G., 2000. Distribution and relative abundance of striped dolphins, and distribution of sperm whales in the Ligurian Sea cetacean sanctuary: results from a collaboration using acoustic monitoring techniques. *Journal of Cetacean Research and Management* , 2: 27-36.

Gubbay S., 1995 (ed.). *Marine Protected Areas: Principles and Techniques for management*. Chapman and Hall.

Gray J.S., 1997. Marine biodiversity: patterns, threats and conservation needs. *Biodiversity and conservation*, 6: 153-175.

Grassle J.F., 1991. Deep Sea Benthic Biodiversity. *Bioscience* 41: 464-469.

Gregg W. W. and Casey N.W., 2004. Global and regional evaluation of the SeaWiFS chlorophyll data set. *Remote Sensing of Environment*, 93(4):463-479.

Harmelin J.G., 2000. Mediterranean marine protected areas: some prominent traits and promising trends. *Environmental Conservation*, 27 (2): 104-105.

Hela I., 1963. Surface currents of the Ligurian Sea. *Bull. Instr. Oceanogr.Monaco,* 60: 1-15.

Herburn G. W. and La Violette P. E. 1990. Related variations in the structure of the anticyclonic gyres in the Alboran sea. *Journal of Geophysical Research*, 95 (C2), 1599-1613.

Hyrenbach K.D., Forney K.A., Dayton P.K., 2000. Marine protected areas and ocean basin management. *Aquatic conservation: Marine and Freshwater Ecosystems*, 10: 437-458.

ICES, 2004. ICES response to EC request for information and advice about appropriate ecoregions for the implementation of an ecosystem approach in European waters, 27 pp.

ICRAM, 2002. Towards the Co-ordination of Scientific Research in marine Protected Areas. *International Workshop on the Development of a European Research Network*. AFRODITE-WS. Final Report, Rome, 1 – 4 July 2002, pp. 49.

IOC, 1998. Workshop on GOOS capacity building for the Mediterranean region, Valletta, Malta, November 26–29th 1997. IOC Workshop Report,140: 18pp.

IOCCG, 2000. Remote sensing of ocean colour in coastal, and other optically-complex, waters. In: *Reports of the International Ocean-Colour Coordinating Group*, Sathyendranath S. (ed.), No. 3, IOCCG, Dartmouth, Canada.

IUCN, 1980. *World Conservation Strategy – Living Resources Conservation for Sustainable Development*. IUCN, Gland, Switzerland.

IUCN, 1994. *Guidelines for Protected Area Management Categories*. CNPPA with the assistance of WCMC. IUCN, Gland, Switzerland and Cambridge, UK. x + 261pp.

IUCN/WCPA, 2007. Establishing networks of marine protected areas: A guide for developing national and regional capacity for building MPA networks. Non-technical summary report.

Jacques, G. et P. Tréguer. 1986. *Ecosystèmes pélagiques marins*. Masson (ed.) Paris: 243 pp.

Jacques G., 1990. L'oligotrophie du milieu pelagique de la Mediterranee occidentale:un paradigme que s'stompe?. *Bull. Soc. Zool. France*, 114 (3): 17-30.

Jacques G., 1994. Nouvelles vues sur le systeme pelagique de Mer Ligure. *Biol. Mar. Medit*., 1 (1): 65-82.

Johannessen J., Pinardi N., Le Traon P.Y., Robinson I., and Nittis K., 2002. *Marine Environment and Security for the European area-MERSEA strand 1*. 3rd EuroGOOS Conference, Athens.

Johnson R.A. and Wichern D.W., 1982. *Applied Multivariate Statistical Analysis*. Englewood Cliffs, N.J. (ed.), Prentice-Hall, Inc. 594 pp.

Jones P.J.S., 1994. A review and analysis of the objectives of marine nature reserves. *Ocean & Coastal Management*, 24: 149-178.

Kelleher G, 1999. *Guidelines for Marine Protected Areas*. IUCN, Gland, Switzerland and Cambridge, UK: xxiv+107pp.

Kelleher G., Kenchington R., 1992. *Guidelines for establishing marine protected areas***.** IUCN, Gland, Switzerland.

Kelleher, G., and Kenchington R., 1993. Political and social dynamics for establishing marine protected areas. In *Application of the Biosphere Reserve Concept to Coastal Marine Areas*. Price A. and Humphrey S., (eds.), Papers presented at the UNESCO/IUCN San Francisco Workshop of 14-20 August 1989. A Marine Conservation and Development Report. IUCN, Gland, Switzerland: 43-55.

Kelleher G. and Bleakely C., 1994. Coastal Marine Protected Areas. In: *Protecting Nature, Regional Reviews of protected Areas*, McNeely JA, Harrison J, Dingwall P (eds.). IUCN, IV th World Congress on National Parks and protected Areas, Caracas, Venezuela: 33-42.

Kelleher G., Bleakley C. and Wells S., 1995. *A Global Representative System of Marine Protected Areas*. 4 volumes. Great Barrier Reef Marine Park Authority, World Bank, and IUCN, Washington, D.C.

Kenney R.D., Payne P.M., Heinemann D.W., and Winn H.E., 1996. Shifts in northeast shelf cetacean distributions relative to trends in Gulf of Maine/Georges Bank finfish abundance. In *The Northeast Shelf Ecosystem: Assessment, Sustainability, and Management*, Sherman K.., Jaworski N.A., and Smayda T.J. (eds), Blackwell Science, Cambridge, Massachusetts, USA: 169-196.

Kenyon 1960. The Pacific walrus. *Oryx* 5: 332-340.

Ketchum, B.H. 1983. *Ecosystems of the World: 26 Estuaries and Enclosed Seas*. Amsterdam, Oxford, New York: Elsevier Scientific Publishing Company.

Kirkpatrick G., Millie D. F., Moline M. A., Schofield O., 2000. Absorption-based discrimination of phytoplankton species in naturally mixed populations. *Limnology and Oceanography* 42: 467-471.

Krattiger A.F., McNeely J.A:, Lessar W.H., Miller K, St. Hill R.Y., Senanayake R. (eds), 1994. Widening Perspecitives on Biodiversity. IUCN, Gland, Switzerland & International Academy of the Environment, Geneva , Switzerland.

La Violette P. E., 1994. Overview of the Major Forcings and Water Masses of the Western Mediterranean Sea. In *Seasonal and interannual Variability of the Western Mediterranean Sea*, *Coastal and Estuarine Studies*, P. E. La Violette (ed.), American Geophysical Union, Washington, USA: 1-11.

Lacombe H. and Tchernia P., 1972. *Caractères hydrologiques et circulation des eaux en Méditerranée. The Mediterranean Sea*. Stanley D. J.(ed.), Dowden, Hutchinson and Ross: 26-36.

Lacombe H., Gascard J. C., Gonella J. et Béthoux J. P., 1981. Response of the Mediterranean to the water and energy fluxes across its surface, on seasonal and interannual scales. *Oceanologica Acta*, 4 (2): 247-255.

Lacombe H. and Richez C., 1982. *The regime of the strait of Gibraltar. Hydrodynamics of semi-enclosed seas*. Nihoul J. C. J.(ed.), Elsevier: 13-74.

Laffoley D., 1995. Techniques for managing marine protected areas: Zoning. In*: Marine Protected Areas. Principles and techniques for management.* S. Gubbay ed., Chapman & Hall, London, 103-118.

Laist, D.W. 1996. Marine debris entanglement and ghost fishing: A cryptic and significant type of bycatch? In *Solving Bycatch: Considerations for Today and Tomorrow*. Alaska Sea Grant College Program Report 96-03. University of Alaska, Fairbanks: 33-39.

Laist, D.W., J.M. Coe, and K.J. O'Hara. 1999. Marine debris pollution. In *Conservation and Management of Marine Mammals*. J.R. Twiss, Jr., and R.R. Reeves (eds.), Smithsonian Institution Press, Washington D.C.: 342-366.

Lanoix F., 1974. Projet d'Alboran, étude hydrologique et dynamique de la mer d'Alboran. *Rapport technique,* 66*, NATO*, Bruxelles.

Lauriano G., Panigada S., Canneri R., Manca Zeichen M., Notarbartolo-di Sciara G., 2009. Abundance estimate of striped dolphins (*Stenella coeruleoalba*) in the *Pelagos* Sanctuary (NW Mediterranean) by means of line transect surveys. *Journal of Cetacean Research Management*, submitted.

Lévy M., Mémery L., Madec G., 1998. The onset of a bloom after deep winter convection in the North Western Mediterranean Sea: mesoscale process study with a primitive equation model. *Journal of Marine Systems*, 16: 7-21.

Liebig V. and Aschbacher J., 2005. Global Monitoring for Environment and Security - Europe's next space initiative takes shape. *E.S.A. Bulletin*, 123: 20-26.

Littaye A., Gannier A., Laran S., Wilson J.P.F., 2004. The relationship between summer aggregation of fin whales and satellite-derived environmental conditions in the northwestern Mediterranean Sea. *Remote Sensing of the Environment*, 90: 44-52.

Locritani M., Gambetta M., Gasparini G. P., Povero P., Castellano M., Carmisciano C., 2008. Condizioni idrografiche e dinamiche nell'Area Marina Protetta di Portofino durante il periodo estivo. *VI° Convegno CoNISMa*, Lecce, Italy, 4-8 November.

Longhurst A., 2007. Ecological geography of the sea. 2nd Edn., Elsevier Science Publishers, San Diego, California, USA, 552 pp.

Lourie S.A. and Vincent A.C.J., 2004. Using Biogeography to Help Set Priorities in Marine Conservation *Conservation Biology*, 18 (4): 1004.

MacGarvin, M., and Simmonds M.. 1996. Whales and climate change. In *The Conservation of Whales and Dolphins: Science and Practice.* M.P. Simmonds and J.D. Hutchinson, (eds.), John Wiley & Sons, Ltd., Chichester: 321-332.

Manca Zeichen M., Agnesi S., Mariani L., Tunesi L., 2001. Sea Surface Temperature (SST) and bentho-nectonic juveniles settlement of genus *Diplodus* within Portofino Marine Protected Area (Ligurian Sea). *Proceedings of the 5° Conferenza Nazionale. Federazione delle Associazioni Scientifiche per le Informazioni Territoriali e Ambientali* (*ASITA*), 9-12 ottobre, Rimini, 2: 989-996.

Mann K.H. and Lazier J.R.N, 2008. *Dynamics of Marine Ecosystems*. Blackwell Publishing, Malden, USA; pp. 489.

Manzella G.M.R., 1983. *The Ligurian Sea dynamics and its time evolution*, C.N.R. – I.S.D.G.M., Staz. Oceanografica La Spezia, T.R. 123: 55 pp.

Manzella G.M.R., Gasparini G.P., and Astraldi M., 1988. Water exchange between the eastern and western Mediterranean through the Strait of Sicily. *Deep Sea Research I*, 35: 1021-1035.

Manzella G.M.R., 1994. The seasonal variability of the water masses and transport through the Strait of Sicily. In *Seasonal and interannual Variability of the Western Mediterranean Sea*, *Coastal and Estuarine Studies*, Paul E. La Violette (ed.), American Geophysical Union, Washington, USA: 33-45.

Margalef R., 1985. *Western Mediterranean*, Pergamon Press, Oxford, 363 pp.

Marty J.-C., Chiaverini J., Pizay M.D. and Avril B., 2002. Seasonal and interannual dynamics of nutrients and phytoplankton pigments in the western Mediterranean Sea at the DYFAMED time-series station (1991-1999). *Deep Sea Research II*, 49:1965-1985.

Marullo S., D'Ortenzio F., Ribera D'Alcalà M., Ragni M., Santoleri R., Vellucci V., Luttazzi C., 2004. Validation of MERIS Ocean Color Algorithms in the Mediterranean Sea. *Proceedings of MERIS User Workshop* (ESA SP-549), 10-13 November 2003, ESA-ESRIN, Frascati, Italy. Editor: H. Lacoste. Published on CDROM., p.7.1.

May R.M., 1988. How many species are there. *Science*, 21 (4872): 1441-1449.

McClain E.P., Pichel W.G. and Walton C.C., 1985. Comparative performance of AVHRR-based multichannel sea surface temperatures. *Journal of Geophysical Research*, 90: 11 587-11 601.

McClain C. R., Feldman G.C., Hooker S.B., 2004. An overview of the SeaWiFS project and strategies for producing a climate research quality global ocean bio-optical time series. *Deep-Sea Research II*, 51: 5–42.

MEDATLAS Consortium, 1997. A composite quality checked hydrographic data set for the Mediterranean sea. *IFREMER*, Brest.

Mélin F., Bulgarelli B., Gobron N., Pinty B. & Tacchi, R., 2000. *An integrated tool for SeaWiFS operational processing*, European Commission, EUR 19576 EN.

Mifsud C.R., Stevens T.D. and Baldacchino A.E., 2003. *Strategic Action Plan for the Conservation of Maltese Coastal and Marine Biodiversity*, 348 pp.

Miller, A. R., 1983. The Mediterranean sea: a physical aspect. In *Estuaries and enclosed seas.* Ketchun B. H. (ed.), Elsevier, New-York: 219-283.

Miller, C.B., 2004. *Biological Oceanography*. Blackwell Science, Oxford, 392 pp.

Millot, C., 1990. The Gulf of Lions' hydrodynamics. *Continental Shelf Research*, 10 (9-11): 885-894.

Millot C., 1991. Mesoscale and seasonal variabilities of the circulation in the Western Mediterranean. *Dynamics of Atmospheres and Oceans*, 15: 179-214.

Millot C., 1999. Circulation in the Western Mediterranean Sea. *J. Mar. Syst*., 20: 423-442.

Millie D. F., Schofield O., Kirkpatrick G. J., Johnsen G., Tester P. A. and Vinyard B. T., 1997. Phytoplankton pigments and absorption spectra as potential 'Biomarkers' for harmful algal blooms: A case study of the Florida red-tide dinoflagellate, Gymnodinium breve. *Limnol. Oceanogr*. 42: 1240-1251.

Minas H. J., B. Coste, P. Le Corre, M. Minas and Raimbault P., 1991. Biological and geochemical signatures associated with the water circulation through the Strait of Gibraltar and in the Western Alboran Sea. *J. Geophys. Res.*, 96(C5), 8755–8771.

Mobley C.D., 1994. *Light and Water; Radiative Transfer in Natural Waters*. Academic Press, San Diego: pp. 579.

Molcard, A., N. Pinardi, M. Iskandarani, and D. Haidvogel, 2002. Wind driven general circulation of the Mediterranean Sea simulated with a Spectral Element Ocean Model. *Dyn. Atmos. Oceans*, 35 (2): 97–130.

Morel A., 1972. The hydrological characteristics of the water exchanged between the eastern and the western basins of the Mediterranean. In: *Oceanography of the Strait of Sicily, Saclantcen Conference Proceedings* 7: 11-37, Saclant Undersea Research Centre, La Spezia, Italy.

Morel A., and Prieur L., 1977. Analysis of variations in ocean colour. *Limnology and Oceanography*, 22: 709-722.

Morel A., 1988. Optical modelling of the upper ocean in relation to its biogenous matter content (case 1 waters). *J. Geophys. Res.*, 93: 10749-10768.

Morel A. and André J.M., 1991. Pigment distribution ad primary production in the western Mediterranean as derived and modelled from Coastal Zone Color Scanner observations. *J. Gephys. Res*., 96:12685-12698.

Morel A. and Antoine D., 2000. Pigment Index Retrieval in Case I Waters. *ESA Document PO-TN-MEL-GS-0005*: 1-26.

Morri C., Bianchi C.N., Damiani V., Peirano A., Romeo G., Tunesi L., 1986. The marine environment between Punta della Chiappa and Sestri Levante (Ligurian Sea): ecotipological outline and proposal of a biocenotic map. *Proceeedings of the VIII Meeting of Gruppo di Ecologia di Base "G. Gadio"*: 213-231.

Moulin C., Gordon H. R., Chomko R. M., Banzon V. F. and Evans R. H., 2001. Atmospheric correction of ocean color imagery through thick layers of Saharan dust, Geophys. *Research Letters*, 28: 5–8.

Nair A., Sathyendranath S., Platt T., Morales J., Stuart V., Forget M-H., Devred E., Bouman H., 2008. Remote sensing of phytoplankton functional types. *Remote Sensing of the Environment*, 112:3366-3375.

National Research Council (NRC), 2001. *Marine Protected Areas. Tools for sustaining Ocean Ecosystems*. Report of National Academic Press, Washington DC: pp. 288.

National Oceanic and Atmospheric Administration (NOAA), 2003. *Marine Protected Area (MPA) process review: case studies of five MPAs establishment processes*. Prepared by the National Marine Protected Areas Centre in cooperation with the National Oceanic and Atmospheric Administration Coastal Services Centre.

Notarbartolo di Sciara G., 1994. La cetofauna del bacino corso-ligure-provenzale: rassegna delle attuali conoscenze. *Biologia Marina Mediterranea*, 1 (1): 95-98.

Notarbartolo di Sciara G., 2002. Cetacean Species Occurring in the Mediterranean and Black Seas. In *Cetaceans of the Mediterranean and Black Seas: state of knowledge and conservation strategies*, Notarbartolo di Sciara G. (ed.), A report to the ACCOBAMS Secretariat, Monaco, Section 3, 17 pp.

Notarbartolo di Sciara G., Zanardelli M., Jahoda M., Panigada S., Airoldi S., 2003. The fin whale *Balaenoptera physalus* (L. 1758) in the Mediterranean Sea. *Mammal Review*, 33: 105-150.

Notarbartolo di Sciara G., 2005. Scoping meeting to support Mediterranean States to meet the 2012 WSSD target on networks of Mediterranean MPAs. Report of the Meeting, Livorno, 6-8 December 2004. IUCN - World Commission on Protected Areas, 13 pp.

Notarbartolo di Sciara G., Agardy T., Hyrenbach D., Scovazzi T., Van Klaveren P. 2008. The *Pelagos* sanctuary for Mediterranean marine mammals. *Aquatic Conservation*: *Marine and Freshwater Ecosystems*, 18:367-391.

Orsi Relini L., Relini G., Palandri G., Relini M., Garibaldi F., Cima C., Torchia G., and Costa C., 1998. Notes on ecology of the Mediterranean krill, a mirror of the behaviour of Mediterranean fin whales. *European Research on Cetaceans* 12, 119.

O'Reilly J. E., Maritorena S., Mitchell B.G., Siegel D.A., Carder K.L., Kahru M., Garver S.A., McClain C.R., 1998. Ocean colour algorithms for SeaWiFS. *Journal of Geophysical Research* , 103, 24937–24953.

O'Reilly J.E., Mueller J.L., Mitchell B.G., Kahru M., Chavez F.P., Strutton P., Cota G.F., Hooker S.B., McClain C.R., Carder K.L., Muller-Karger F., Harding L., Magnuson A., Phinney D., Moore G.F., Aiken J., Arrigo K.R., Letelier R. and Culver M., 2000. SeaWiFS Postlaunch Calibration and Validation Analyses Part 3. Hooker S.B. and Firestone E.R. (eds.), *SeaWiFS Postlaunch Technical Report Series*, *NASA Technical Memorandum* 2000-2067892, Vol. 11.

O'Shea, T.J. 1999. Environmental contaminants and marine mammals. In *Biology of Marine Mammals*. J.E. Reynolds, III, and S.A. Rommel, eds., Smithsonian Institution Press, Washington D.C.: 485-563.

Ovchinnikov I.M., 1974. On the water balance of the Mediterranean sea. *Oceanology*, 14 (2): 198-202.

Palumbi, S., 2001. Genetics, Marine Dispersal Distances and the Design of Marine Reserve Networks. In *The Scientific Theory of Marine Reserves – AAAS Session: Science and the Biosphere*, Department of Organismic and Evolutionary Biology, Harvard University, US. http://compassonline.org/AbstractsScienceTheory.htm

Panigada S., Notarbartolo di Sciara G., Zanardelli Panigada M., Airoldi S., Borsani J.F., Jahoda M. 2005. Fin whales (*Balaenoptera physalus*) summering in the Ligurian Sea: distribution, encounter rate, mean group size and relation to physiographic variables. *Journal of Cetacean Research and Management* 7: 137–145.

Pavan G., Hayward T. J., Borsani J. F., Priano M., Manghi M., Fossati C., and Gordon J., 2000. Time patterns of sperm whale codas recorded in the Mediterranean Sea 1985–1996. *J. Acoust. Soc. Am.* 107 (6):3487-3495.

Pearce A. & Pattiaratchi C., 1997. Applications of satellite remote sensing to the marine environment in Western Australia. *Journal of the Royal Society of Western Australia*, 80: 1-14.

Pérès, J.M., and Picard, J. 1964. *Nouveau manuel de bionomie benthique de Méditerranée*: Station marine d'Endoume. Marseille.

Perkins H. and Pistek P., 1990. Circulation in the Algerian basin during June 1986. *Journal of Geophysical Research*, 95 (C2): 1577-1585.

Perrin, W.F., Donovan G.P., and Barlow J., eds., 1994. Gillnets and cetaceans. International Whaling Commission, Cambridge, UK. *Report of the International Whaling Commission*, (Special Issue 15).

Phillipe M. and Harang L., 1982. Surface temperature fronts in the Mediterranean Sea from infrared satellite imagery. In *Hydrodynamics of Semi-Enclosed Seas*, J.C.J. Nihoul (ed.) Elsevier, Amsterdam: 91-128.

Pinardi, N. and Coppini, G., 2010. Operational oceanography in the Mediterranean Sea: the second stage of development In: Mediterranean ocean forecasting system towards environmental predictions-the results. *Ocean Science*, 6: 263–267.

Pinardi N., Allen I., Demirov E., De Mey P., Korres G., Lascaratos A., Le Traon P.Y., Maillard C., Manzella G. and Tziavos C., 2003. The Mediterranean ocean forecasting system: first phase of implementation (1998–2001), *Annales Geophysicae*, 21: 3–20.

Planes S., Galzin R., García-Rubies A., Goñi R., Harmelin J.G., Le Diréach L., Lenfant P & Quetglas A., 2000. Effects of Marine Protected Areas on Recruitment Processes with Special Reference to Mediterranean Littoral Ecosystems. *Environmental Conservation*, 27(2):126-143.

Pinnegar J.K., Polunin N.V.C., Francour P, Badalamenti F., Chemello R., Harmelin-Vivien M-L., Hereu B., Milazzo A., Zabala M., D'Anna G., Pipitone C., 2000. Trophic Cascades in Benthic Marine Ecosystems: Lessons for Fisheries and Protected Area Management. *Environmental Conservation*, 27(2): 179-200.

Polunin, N.V.C., 1983 Marine Genetic-Resources and the Potential Role of Protected Areas in conserving them. *Environmental Conservation*, 10 (1): 31-41.

R Development Core Team, 2004. *R: A language and environment for statistical computing. R Foundation for Statistical Computing*. Vienna, Austria, ISBN 3-900051-07-0. Available at http://www.R-project.org

Ramade, F. 1990. *Conservation des ecosystemes mediterraneens: Enjeux et perspectives*. Fascicules du Plan Bleu No 3. Paris: Economic.

Ramos A. A., 1999. Marine protected areas: conservation of biodiversity and enhancement of fisheries. In *C.I.E.S.M Workshop Series Scientific Design and Monitoring of Mediterranean Marine Protected Areas,* 8 (22), Porto Cesareo 21-24 October.

Ray G.C., 1999. Coastal-marine protected areas: agonies of choice. *Acquatic Conservation: marine and freshwater ecosystems* 9: 607-614.

Reeves, R.R. 2000. The Value of Sanctuaries, Parks, and Reserves (Protected Areas) as Tools for Conserving Marine Mammals. *Final Report to the Marine Mammal Commission*, contract number T74465385. Marine Mammal Commission, Bethesda, MD: 50 pp.

Richardson, W.J., C.R. Greene, Jr., C.I. Malme, and D.H. Thomson, 1995. *Marine mammals and noise*. Academic Press, San Diego.

Richardson L.L.(ed.) and LeDrew E.F. (ed.), 2006. *Remote Sensing of Acquatic Coastal Ecosystems Processing*. Springer, Dordrecht, Netherlands, pp. 325.

Roberts C.M., 1997. Ecological advice for the global fisheries crisis. *Trends in Ecology and Evolution*, 12: 35-38.

Roberts C.M., Andelman S., Branch G., Bustamante R. H., Castilla J. C., Dugan J., Halpern B.S., Lafferty K.D., Leslie H., Lubchenco J., Mcardle D., Possingham H.P., Ruckelshaus M., and Warner R.R., 2003. Ecological criteria for evaluating candidate sites for marine reserves. *Ecological Applications,* 13(1) Supplement*,* 199–214.

Robinson I.S., 1985. *Satellite Oceanography, An Introduction for Oceanographers and Remote Sensing Scientists*. Ellis Horwood Ltd., Chichester, UK.

Robinson I.S., 2004. *Measuring the Oceans from Space. The Principles and methods of satellite oceanography*. Praxis Publishing Ltd., Chichester, UK; pp. 669.

Robinson, A.C., and T.E. Dennis. 1988. The status and management of seal populations in South Australia. In *Marine Mammals of Australia: Field Biology and Captive Management*, M.L. Augee (ed.), Royal Zoological Society of New South Wales, Mosman: 87-110.

Rodrigues A.L., Andelman S.J., Bakarr M.I., Boitani L., Brooks T.M., Cowling R.M., Fishpool L.D.C., da Fonseca G.A.B., Gaston K.J., Hoffmann M., Long J.S., Marquet P.A., Pilgrim J.D., Pressey R.L., Schipper J., Sechrest W., Stuart S.N., Underhill L.S., Waller R.W., Watts M.E.J. and Yan X., 2004. Effectiveness of the global protected area network in representing species diversity. *Nature*, 428, 640–643.

Salm R.V. and Clark J., 1984. *Marine and Coastal Protected Areas: A guide for Planners and Managers.* IUCN, Gland, Switzerland, 302 pp.

Salm R.V., and Dobbin J.A., 1993. Planning, Management, and Administrative Processes for Marine Protected Areas. In *Application of the Biosphere Reserve Concept to Coastal Marine Areas*. Price A. & Humphrey S. (eds.), UICN/UNESCO, Gland, Switzeland: 57-65.

Salm R.V., Clark J. and Siirila E., 2000. *Marine and Coastal Protected Areas: A guide for Planners and Managers.* IUCN, Washington DC: xxi + 371 pp.

Salmona P, Verardi D, 2001. The marine protected area of Portofino, Italy: a difficult balance. *Ocean & Coastal Management*, 44: 39-60.

Sánchez-Jerez P., Cebrian C.B. and Espla A.A.R., 1999. Comparison of the epifauna spatial distribution in *Posidonia oceanica*, *Cymodocea nodosa* and unvegetated bottoms: Importance of meadow edges. *Acta Oecologia*, 20: 391-405.

Sánchez Lizaso J.L., Goñi R., Reñones O., Garcia Charton J.A., Galzin R., Bayle J.T., Sanchez Jerez P., Pérez Ruzafa A. & Ramos A.A., 2000. Density dependence in marine protected populations,: a review. *Environmental Conservation*, 27(2): 144-158.

Santoleri R., Bohm E., Schiano M.E., 1994. The Sea Surface Temperature of the Western Mediterranean Sea: Historical Satellite Thermal Data. In *Seasonal and interannual Variability of the Western Mediterranean Sea*, *Coastal and Estuarine Studies*, Paul E. La Violette (ed.), American Geophysical Union, Washington, USA: 155-176.

Scheffer, V.B., C.H. Fiscus, and E.I. Todd. 1984. History of scientific study and management of the Alaskan fur seal, *Callorhinus ursinus*, 1786-1964. *NOAA Technical Report* NMFS SSRF-780: 70 pp.

Schiller, H and Doerffer, R., 2005. Improved determination of coastal water constituent concentrations from MERIS data. *IEEE Trans. Geosci. Remote Sens*., 43: 1585-1591.

Schofield O., Gryzmski J., Bissett P., Kirkpatrick G., Millie D. F., Moline M. A. and Roesler C. 1999. Optical monitoring and forecasting systems for harmful algal blooms: Possibility or pipedream? *J. Phycol*.. 35: 125-145.

Schofield O., Bissett P. W., Frazer T. K, Iglesias-Rodriguez D., Moline M.A., Glenn S., 2003. *Development of Regional Coastal Ocean Observatories and the Potential Benefits to Marine Sanctuaries*. In: Science,Technology and Managment in the US National Marine Sanctuary Program (J. Lindholm, ed). *Marine Technology Society Journal*, 37: 54-67.

SeaWiFS, 2000. Ocean colour algorithm evaluation. URL http://seawifs.gsfc.nasa.gov/SeaWiFS/RECAL/R3/OC4_reprocess.html.

SIAM database, http://estaxp.santateresa.enea.it/www/siams/prov102.html.

Siegel D. A., Wang M., Maritorena S. and Robinson W., 2000. Atmospheric correction of satellite ocean color imagery: The black pixel assumption. *Applied Optics*, 39: 3582– 3591.

Siegel D.A., Thomas A.C., Marra J., 2004. Views of ocean processes from the Sea-viewing Wide Field-of view Sensor mission: introduction to the first special issue. *Deep-Sea Research II*, 51: 1–3.

Sorgente R., Drago A. F., and Ribotti A., 2003. Seasonal variability in the Central Mediterranean Sea circulation. *Annales Geophysicae*, 21: 299–322

Sournia A., 1973. La production primaire planctonique en Mediterranee. Essai de mise a jour. *Bull. Et. Comm. Medit*., 5, 1–128.

Sparnocchia S., Manzella G.M.R. and La Violette P.E. 1994. The interannual and seasonal variability of the MAW and LIW core properties in the Western Mediterranean sea. *Seasonal and interannual variability of the Western Mediterranean sea*. La Violette P. E. (ed.), American Geophysical Union, Washington D.C.: 177-194.

Sparnocchia S., Gasparini G.P., Astraldi A., Borghini M., and Pistek P., 1999. Dynamics and mixing of the Estern Mediterranean outflow in the Tyrrhenian Sea. *Journal of Marine Systems*, 20: 301-317.

Spellerberg I.F. (ed), 1996. *Conservation Biology*. Longman, England: 242 pp.

Steele J., 1998. Regime shifts in marine ecosystems. *Ecol. Appl*., 8 (1):S33-S36.

Stevens T., 2002. Rigor and Representativeness in Marine Protected Area Design. *Coastal Management*, 30: 237-248.

Stocchino C. and Testoni A., 1977. Nuove osservazioni sulla circolazione delle correnti nel Mar Ligure. Progetto finalizzato “Oceanografia e fondi marini”. *Ist. Idogr. Mar. Genova*, F.C. 1076: 1-13.

Stocker M., 2002. Ocean Bio-Acoustics and Noise Pollution: fish, mollusks and other sea animals’ use of sound, and the impact of anthropogenic noise in the marine acoustic environment. *The Journal of Acoustic Ecology*, 3 (2): 16-29.

Sturm B. & Zibordi G., 2002. SeaWiFS atmospheric correction by an approximate model and vicarious calibration. *International Journal of Remote Sensing*, 23 (3): 489-501.

Sverdrup H.U., 1953. On conditions for the vernal blooming of phytoplankton. *Journal du Conseil international pour l’exploration de la mer*, 18: 287-295.

Szekely G. J. and Rizzo M. L., 2004. *The energy package, Version 1.0.1*. License GPL 2.0 or later Available at http://cran.r-project.org/

Tait H.I., 1985. The physical oceanography of the Tyrrenian and Ligurian Seas. *Proceedings 6° AIOL Workshop*: 49-84.

Tamburini C., Garcin J., Bianchi A., 2003. Role of deep-sea bacteria in organic matter mineralization and adaptation to hydrostatic pressure conditions in the NW Mediterranean Sea. *Aquatic Microbial Ecology*, 32: 209-218.

Tassan S., 1994. Local algorithms using SeaWiFS data for the retrieval of phytoplankton, pigments, suspended sediment and yellow substance in coastal waters. *Applied Optics*, 33 (12): 2369-2378.

Ticco P.C., 1995. The use of marine protected areas to preserve and enhance marine biological diversity: A case study approach. *Coastal Management* 23: 309-314.

Tintoré J.D., La Violette P.E., Blade I. and Cruzado A., 1988. A study of an intense density front in the Eastern Alboran sea : the Almeria-Oran front. *Journal of Physical Oceanography*, 18: 1384-1397.

Tomasevich J., 1942. *International agreements on conservation of marine resources*. Food Research Institute, Stanford University, California.

Tortonese E., 1985. Distribution and ecology of endemic elements in the Mediterranean fauna (fishes and echinoderms). In *Mediterranean Marine Ecosystem*, Moraitou-Apostolopou M., Kiortsis V., eds. Plenum Press Publ., New York: 57-83.

Tunesi L. and Diviacco G., 1993. Environmental and socio-economic criteria for the establishment of marine coastal parks. *Intern.J. Environmental Studies*, 43: 253-259.

UNEP, 1992. *Convention on Biological Diversity*. Environmental Law and Institutions programme activity centre, UNEP.

UNEP, 1995. Global Biodiversity assessment. University Press, Cambridge, UK.

UNEP, MAP, RAC/SPA, 2003. Regional Project for the Development of Marine and Coastal Protected Areas in the Mediterranean Region (MedMPA), First Annual Report: 49 pp.

United National Educational, Scientific, and Cultural Organization (UNESCO), 1988. *Reports in Marine Science* No. 49. Paris.

Vidal M., Vila G., Emelianov M., López-Jurado J. L., Latasa M. and Salat J., 2007. Nutrient distribution during the spring bloom following the unusual winter 2005 deep mixing event in NW Mediterranean. *Geophysical Research Abstracts*, Vol. 9, 06990, SRef-ID: 1607-7962/gra/EGU2007-A-06990.

Volpe G., Santoleri R., Vellucci V., Ribera d'Alcalà R., Marullo S. and D'Ortenzio F., 2007. The colour of the Mediterranean sea: global versus regional bio-optical algorithms evaluation and implication for satellite chlorophyll estimates. *Remote Sensing of the Environment*, 107:625-638.

Warn-Varnas A., Sellshops J., Haley Jr. P.J., Leslie W.G., and Lozano C.J., 1999. Strait of Sicily water masses. *Dyn. Atmosph. Oceans*, 29h: 437-469.

Whitehead, H., Reeves R.R., and Tyack P.L., 2000. Science and the conservation, protection, and management of wild cetaceans. In *Cetacean societies: field studies of dolphins and whales.* J. Mann, R.C. Connor, P.L. Tyack, and H. Whitehead (eds.), University of Chicago Press, Chicago, IL: 308-332.

WWF/IUCN, 1998. *Creating a sea change. The WWF/IUCN Marine Policy*. WWF and IUCN, Gland, Switzerland. 65pp.

Zanardelli M., Panigada, S., Airoldi S., Borsani J. F., Jahoda M., Lauriano G, Notarbartolo di Sciara, G., 1998. Site fidelity, seasonal residence and sex ratio of fin whales (*Balaenoptera physalus*) in the Ligurian Sea feeding grounds. *European Research on Cetaceans,* **12**: 124.

Zodiatis G., Lardner R., Georgiou G., Demirov E.,Manzella G. and Pinardi N., 2003. An Operational European Global Ocean Observing System for the Eastern Mediterranean Levantine Basin: The Cyprus Coastal Ocean Forecasting and Observing System. *MTS Journal,* 37(3):115-123.